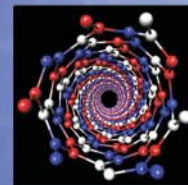
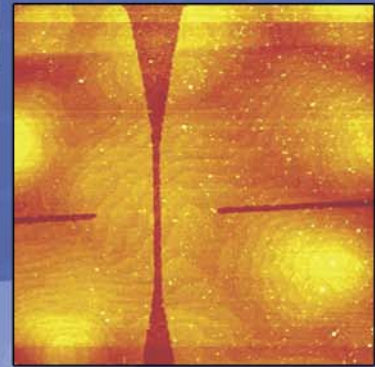
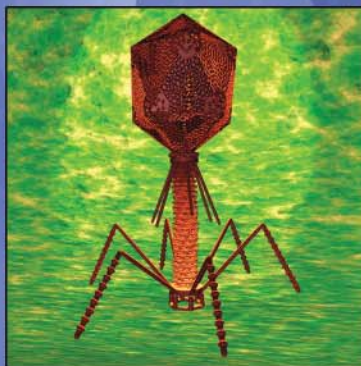
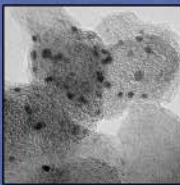
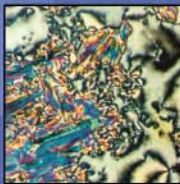
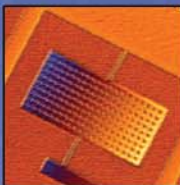
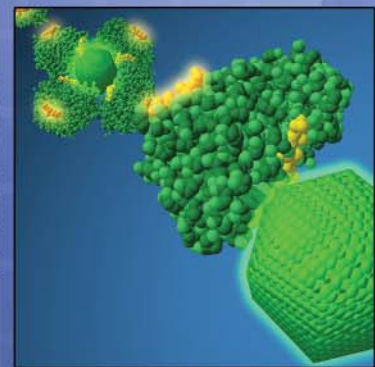
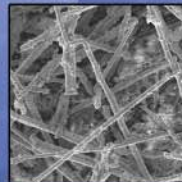
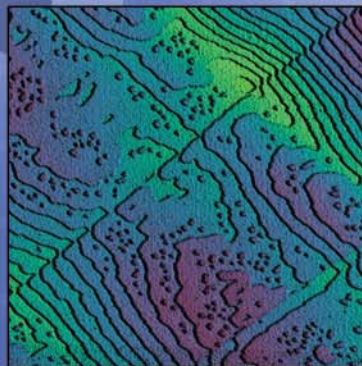
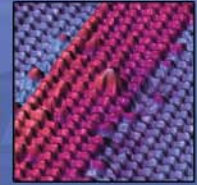
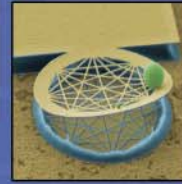


THE NAVY'S CORPORATE LABORATORY

2004

NRL REVIEW



NAVAL RESEARCH LABORATORY
Washington, DC 20375

General information on the research described in this *NRL Review* can be obtained from the Public Affairs Office, Code 1030, (202) 767-2541. Information concerning Technology Transfer is available from the Technology Transfer Office, Code 1004, (202) 767-7230. Sources of information on the various educational programs at NRL are listed in the chapter entitled "Programs for Professional Development."

For additional information about NRL, the *Fact Book* lists the organizations and key personnel for each division. It contains information about Laboratory funding, programs, and field sites. The *Fact Book* can be obtained from the Technical Information Services Branch, Code 3430, (202) 404-4963. The web-based *NRL Major Facilities* publication, which describes each NRL facility in detail, can be accessed at <http://www.nrl.navy.mil>.

NRL REVIEW STAFF	
Senior Science Editor	John D. Bultman
Coordinator	Jonna Atkinson
Consultant	Kathy Parrish
Design, Layout, and Graphic Support	Jonna Atkinson, Donna Gloystein, Jan Morrow, and Suzanne Guilmineau
Editorial Assistance	Maureen Long
Historical Update	David van Keuren
Photographic Production	Gayle Fullerton and Michael Savell

REVIEWED AND APPROVED

NRL/PU/3430--04-471

May 2004



David M. Schubert, Captain, USN
Commanding Officer

On the Cover: NRL has established an Institute for Nanoscience to conduct multidisciplinary research at the intersection of the fields of materials, electronics, and biology at the nanometer length scale. The Institute serves as NRL's nucleus of collaborative activity in this rapidly evolving research area. The images on the cover portray actual nanoscience research carried out and fabricated at NRL.



Mission

To conduct a broadly based multidisciplinary program of scientific and advanced technological development directed toward maritime applications of new and improved materials, techniques, equipment, systems, and ocean, atmospheric, and space sciences and related technologies.

The Naval Research Laboratory provides primary in-house research for the physical, engineering, space, and environmental sciences; broadly based applied research and advanced technology development programs in response to identified and anticipated Navy and Marine Corps needs; broad multidisciplinary support to the Naval Warfare Centers; and space and space systems technology, development, and support.

FEATURES

VIEW FROM THE TOP



NRL'S INVOLVED!

- 3 Our People Are Making a Difference
- 6 NRL's Contributions to Operation Iraqi Freedom
- 10 Nanoscience Research Laboratory Opens at NRL
- 12 NRL Rededicates its Newly Refurbished Pier
- 14 NRL Donates *Clementine* Spacecraft to National Air and Space Museum



THE NAVAL RESEARCH LABORATORY

- 17 NRL – Our Heritage
- 18 2003 in Review
- 22 NRL Today
- 43 Looking Ahead

ARTICLES



FEATURED RESEARCH

- 51 New Horizons in Cathodic Protection Design
V.G. DeGiorgi, E.A. Hogan, and S.A. Wimmer
- 59 Propagation of High-Energy Lasers in a Maritime Atmosphere
P. Sprangle, J.R. Peñano, A. Ting, and B. Hafizi
- 69 Fabrication of a Fast Turn-off Transistor by Wafer Bonding
K.D. Hobart, F.J. Kub, and J.M. Neilson
- 77 Applications of Time-Reversal to Underwater Acoustics
J.F. Lingeitch, C.F. Gaumond, D.M. Fromm, and B.E. McDonald
- 87 WindSat – Remote Sensing of Ocean Surface Winds
P.W. Gaiser



ACOUSTICS

- 97 Passive Swimmer Detection
S. Stanic, C.K. Kirkendall, A.B. Tveten, and T. Barock
- 98 Passive Acoustic Ranging by Multimode Waveguide Interferometry
A. Turgut, M.H. Orr, and B.H. Pasewark

6



10



12



14





ATMOSPHERIC SCIENCE AND TECHNOLOGY

- 103** Real-Time, High-Resolution, Three-Dimensional Cloud and Wind Data Assimilation Technology for the Battlespace Environment
Q. Zhao, J. Cook, P. Harasti, and J. Strahl
- 105** NRL Ionosphere Model: SAMI3
J. Huba and G. Joyce
- 106** The High Frequency Active Auroral Research Program
E.J. Kennedy, P. Rodriguez, and C.A. Selcher
- 109** Advances in Upper Atmosphere Forecasting: NOGAPS-ALPHA
J.P. McCormack, L. Coy, S.D. Eckermann, D.R. Allen, T. Hogan, and Y.-J. Kim



CHEMICAL/BIOCHEMICAL RESEARCH

- 115** Navy Cyanide Test Kit (NACTEK)
J.R. Deschamps
- 116** Water-Soluble Carbon Nanotubes
O.-K. Kim, J. Je, J.W. Baldwin, S. Kooi, P.E. Pehrsson, and L.J. Buckley
- 118** Neuronal Network Biosensor for Environmental Threat Detection
K.M. Shaffer, S.A. Gray, S.J. Fertig, J.V. Selinger, T.J. O'Shaughnessy, N.V. Kulagina, D.A. Stenger, and J.J. Pancrazio
- 121** Self-Cleaning Catalytic Filters Against Pesticides and Chemical Agents
A. Singh, Y. Lee, and W.J. Dressick



ELECTRONICS AND ELECTROMAGNETICS

- 125** UHF Delta-Sigma Waveform Generator
R.M. White, B.H. Cantrell, J.P. McConnell, and J.J. Alter
- 127** Unmanned Aerial Vehicle (UAV) Radar
D.W. Baden, E.M. Kutrzyba, A.P. Desrosiers, J.O. Alatishe, S. Talapatra, and M.G. Parent
- 129** The NRL 94 GHz High-Power WARLOC Radar as a Cloud Sensor
W.M. Manheimer, A.W. Fliflet, K. St. Germain, G.L. Linde, W.J. Cheung, V. Gregers-Hansen, M.T. Ngo, and B.G. Danly
- 132** Coupled Quantum Dots for Quantum Computing
T.L. Reinecke, Y. Lyanda-Geller, M. Bayer, and A. Forchel



INFORMATION TECHNOLOGY AND COMMUNICATIONS

- 137** Energy-Aware Broadcasting and Multicasting in Wireless Ad Hoc Networks
J.E. Wieselthier, G.D. Nguyen, and A. Ephremides
- 140** Netcentric Multi-INT Fusion Targeting Initiative (NCMIFTI)
D.C. Linne von Berg, M.R. Kruer, J.N. Lee, M.D. Duncan, J.G. Howard, F. Olchowski, and R.A. Patten
- 143** Real-Time Exploitation and Dissemination of Tactical Reconnaissance Imagery During Operation Iraqi Freedom for Ground and Maritime Operations
J.N. Lee, D.C. Linne von Berg, M.D. Duncan, M.R. Kruer, and R.A. Patten
- 144** Volume Sensor for Shipboard Damage Control
S.L. Rose-Pehrsson, J.C. Owrutsky, D.T. Gottuk, D.A. Steinhurst, C.P. Minor, J.P. Farley, and F.W. Williams
- 148** Control Algorithms for UUV Teams Using Acoustic Communications
P. McDowell and B. Bourgeois



MATERIALS SCIENCE AND TECHNOLOGY

- 153** Qualification of Copper Water Heat Pipes for Space Application
K. Cheung
- 156** GelMan: A Physical Model for Measuring the Response to Blast
K.E. Simmonds, P. Matic, M. Chase, and A. Leung
- 158** Rapid Prototyping of Conformal Antenna Structures
A. Piqué, R.C.Y. Auyeung, M.W. Nurnberger, D.J. Wendland, C.B. Arnold, A.R. Abbott, and L.C. Schuette
- 160** Carbon Nanotube Networks: A New Electronic Material
E.S. Snow, J. Novak, M.D. Lay, and E.J. Houser



OCEAN AND ATMOSPHERIC SCIENCE AND TECHNOLOGY

- 165** Drag Coefficient, Surface Roughness, and Reference Wind Speed
P.A. Hwang
- 167** An Approach for Coupling Diverse Geophysical and Dynamical Models
J.D. Dykes, R.A. Allard, C.A. Blain, B. Estrade, T. Keen, L. Smedstad, A. Wallcraft, M. Bettencourt, and G. Peggion
- 170** Airborne Sea-Surface Topography in an Absolute Reference Frame: Applications to Coastal Oceanography
J. Brozema, V. Childers, and G. Jacobs
- 172** New Observations of Hydroxyl from the Space Shuttle by NRL's SHIMMER
J.G. Cardon, C.R. Englert, M.H. Stevens, R.R. Conway, J.M. Harlander, and F.L. Roesler



OPTICAL SCIENCES

- 177** Development of the Fiber Optic Wide Aperture Array: From Initial Development to Production
A. Dandridge, A.B. Tveten, and C.K. Kirkendall
- 179** High-Resolution Distributed Fiber Optic Sensing
C.K. Kirkendall, R.E. Bartolo, A.B. Tveten, and A. Dandridge



REMOTE SENSING

- 185** Unattended Ground Sensor Network
J. Heyer and L.C. Schuette
- 186** Measurement of Ocean Wave Spectra and Surface Slopes by Polarimetric SAR
D.L. Schuler and J.S. Lee
- 188** The Lowest Frequency Detection of the Black Hole at the Center of Our Galaxy
M.E. Nord, T.J.W. Lazio, N.E. Kassim, W.M. Goss, and N. Duric
- 191** High-Resolution Infrared Ocean Imagery
G.O. Marmorino, G.B. Smith, and G.J. Lindemann



SIMULATION, COMPUTING, AND MODELING

- 195** Human System Interface Assessment of the Sonar Workstation During the USS *Nicholson* Integrated Undersea Warfare Sea Test
J.A. Ballas and B. McClimens

- 197 Autonomous Navigation Control of UAVs Using Genetic Programming
C.K. Oh, G. Cowart, and J. Ridder
- 199 Electronics and Physics of Left-Handed Materials and Circuits
C.M. Krowne
- 201 Real-Time Wave, Tide, and Surf Prediction
R.A. Allard, J. Christiansen, T. Taxon, S. Williams, and D. Wakeham



SPACE RESEARCH AND SATELLITE TECHNOLOGY

- 207 Tactical Microsatellite Experiment (TacSat-1)
M. Hurley
- 209 The Microelectronics and Photonics Test Bed (MPTB): The First Six Years
K.A. Clark, M.S. Johnson, and A.B. Campbell
- 212 Rapid Satellite Payload Development for TacSat-1
C.M. Huffine

AWARDS



SPECIAL AWARDS AND RECOGNITION

- 217 Special Awards and Recognition
- 234 Alan Berman Publication and Edison Patent Awards

PROGRAMS



PROGRAMS FOR PROFESSIONAL DEVELOPMENT

- 241 Programs for NRL Employees — Graduate Programs, Continuing Education, Professional Development, Equal Employment Opportunity (EEO) Programs, and Other Activities
- 244 Programs for Non-NRL Employees — Recent Ph.D., Faculty Member, and College Graduate Programs, Professional Appointments, College Student Programs, and High School Student Programs

GENERAL INFO



GENERAL INFORMATION

- 249 Technical Output
- 250 Key Personnel
- 251 Contributions by Division, Laboratories, and Departments
- 254 Subject Index
- 257 Author Index
- 258 Employment Opportunities



View from the Top

a message from the Captain and the Director of Research

What an important time it is for Naval research. Our Navy and Marine Corps face ever-greater challenges as we confront global terrorism and the enormous task of rebuilding Iraq. The technology needs of our sailors and marines are dynamic and urgent; they must be armed with the right technology to generate awesome effects in precision, speed, and lethality, while remaining safe from terrorist and insurgent attack. As it has throughout its 80 year history, the Naval Research Laboratory is delivering the new technologies that will help meet these challenges.

In his recently released "CNO Guidance for 2004," Admiral Vern Clark, Chief of Naval Operations, focused on a strategy of "Accelerating Our Advantages." ADM Clark noted that in 2003, the Navy demonstrated its value by projecting decisive, joint power across the globe. Our task in 2004 is to accelerate the advantages the Navy brings the nation.

Operations Enduring Freedom and Iraqi Freedom demonstrated more than just combat excellence; they demonstrated the important

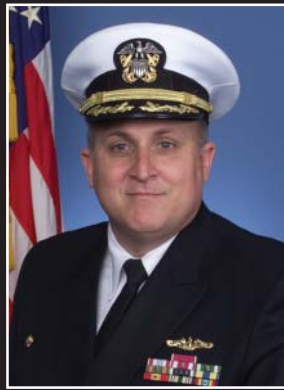
benefits of the latest technology in surveillance and attack, and, most importantly, they reaffirmed the genius of our people contributing their utmost to mission accomplishment.

Operations Enduring Freedom and Iraqi Freedom provided a great opportunity to dissect, study, and analyze some of the effects and limiting factors of how we fight. These operations showcased the new capabilities of our armed forces, including many NRL-developed technologies that significantly contributed to these operations. In discussing the Navy's *Sea Strike* initiative, the CNO singled out NRL's Shared Reconnaissance Pod (SHARP) as a system that "arrived in the Fleet and showed us the power of these new knowledge dominance technologies." Other recent NRL technologies have also proven their worth in battle: the Tactical Air Reconnaissance Pod System-Completely Digital (TARPS-CD) that enables our fighter aircraft to use near real-time digital imagery to evaluate the effectiveness of their bombing strikes; Specific Emitter Identification technology that allows ships, aircraft, and submarines to uniquely identify and track ships; the Dragon Eye small un-

manned aerial vehicle that can be carried in a marine's backpack and allows ground forces to see over the next hill; atmospheric and ocean models that allow our forces to more effectively find and neutralize sea mines and to predict and avoid dust storms in the desert; and chemical, biological, and nuclear sensors that can warn our troops in the event of an attack from weapons of mass destruction.

In December 2003, NRL had the opportunity to host the Honorable Gordon England, Secretary of the Navy; the Honorable John Young, Assistant Secretary of the Navy for Research, Development, and Acquisition; several senior flag officers from the Navy and Marine Corps; and senior officials from other government agencies for a series of technology demonstrations designed to showcase new capabilities for Marines re-deploying to Iraq in 2004. NRL technologies included a sniper detection system; an early warning radar system for detecting rocket propelled grenades, "stinky paints" for tagging and deterring terrorists, a dust abatement system to prevent damage to helicopters landing in the desert, an infrared missile countermeasure for aircraft, and sensitive explosive detection sensors. The demonstrations were very well received by Secretary England and his delegation. The projects shown have the potential to significantly enhance the safety of our marines as they return to a very treacherous environment in Iraq this year. The CNO has stated, "our lessons learned to date indicate that the capabilities-based investment strategies, new warfighting concepts, and enabling technologies we are pursuing in our *Sea Power 21* vision are on the right vector."

Deployment-ready technologies are the products of NRL's sustained investment in basic science. Our potential to conduct research has been



CAPT David M. Schubert
USN



Dr. John A. Montgomery
Director of Research

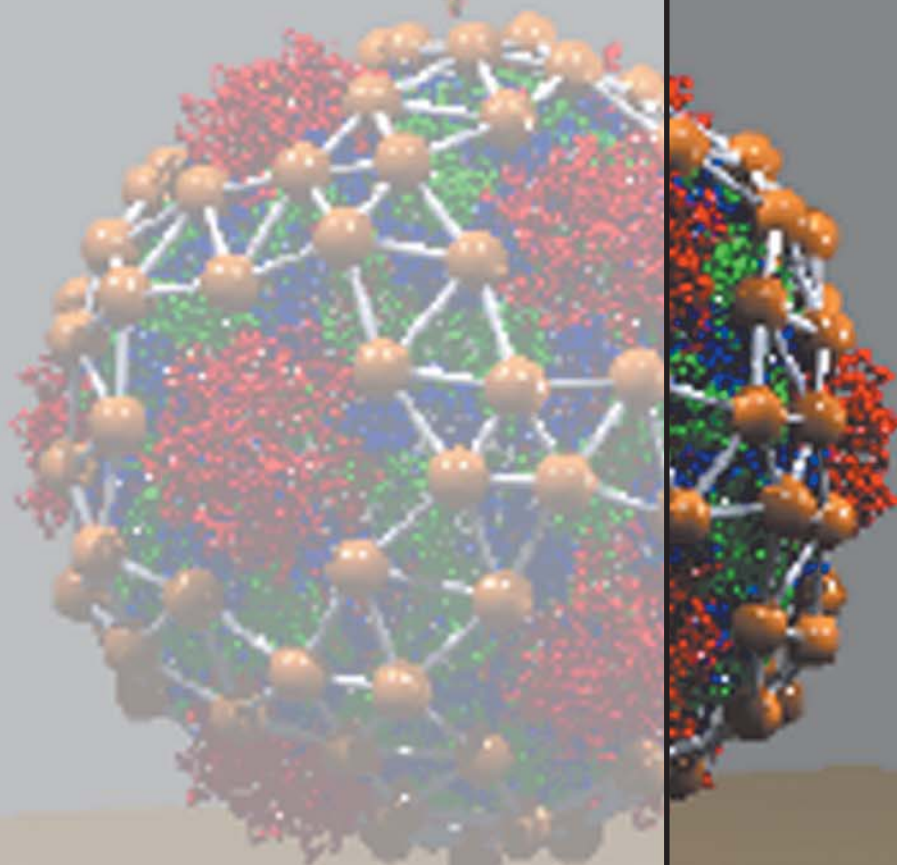
significantly bolstered by the establishment of NRL's Institute for Nanoscience, which opened in October 2003. This world-class nanoscience center will host NRL scientists and their collaborators from other world-class laboratories. Collaborative interest has already been expressed by leading academic institutions both here and abroad. Our Institute for Nanoscience will allow the Laboratory to move to the forefront of new research in materials, electronics, and biomolecular science.

NRL's overall research program remains broadly based and world class. Recruiting new talent is a key to future success, and we continue to draw top postdoctorate candidates to replenish our research staff. The future is indeed bright for our Naval services, and the way to that future is being illuminated by the extraordinary contributions of the men and women of the Naval Research Laboratory.

Two handwritten signatures in black ink. The top signature is 'DMSchubert' and the bottom signature is 'John A. Montgomery'.



NRL'S INVOLVED!



ELECTRONIC CIRCUIT ON A PLANT VIRUS

This model represents a plant virus being used as a scaffold to build an electronic circuit with the electrical measurement being done by STM. The gold-colored STM tip makes contact at the top of the virus shell. The virus is a 30-nm icosahedral particle upon which we have been able to build a conductive network using conducting molecules.



- 3** Our People Are Making a Difference
- 6** NRL's Contributions to Operation Iraqi Freedom
- 10** Nanoscience Research Laboratory Opens at NRL
- 12** NRL Rededicates its Newly Refurbished Pier
- 14** NRL Donates *Clementine* Spacecraft to National Air and Space Museum

Our People Are Making a DIFFERENCE

The *NRL Review* dramatically illustrates the range of research capabilities that have been and are being developed to provide the Naval Research Laboratory with the world-class technologies for which we are known. However, these capabilities, no



matter how expensive and complex, are of no value without the highly motivated people who work here. It is these people who make the Laboratory the renowned institution that it is, who provide the ideas and sustained efforts to make these innovative research capabilities “come to life.” In this section, we highlight some of these special people.



Dr. Simon W. Chang

Dr. Simon W. Chang is the new Superintendent of NRL's Marine Meteorology Division, located in Monterey, California. Dr. Chang relocated to Monterey in May 2003 from the Office of Naval Research, where he was a program manager in the Processes and Prediction Division of the Atmosphere, Ocean, and Space Department. However, Dr. Chang is not a newcomer to the NRL research family. His association with the Laboratory goes back to 1978, when he worked as a contractor in the Remote Sensing Division until joining the ranks of NRL federal employees in 1983. Dr. Chang also served NRL as a Branch Head in the Marine Meteorology Division from 1994 to 1996, so he brings an insider's knowledge of NRL along with his other experiences in DOD, the private sector, and academia to the challenges of his new position. “It has been very exciting to return to Monterey and see how initiatives I started as a Branch Head have blossomed into much larger programs and how people that I hired have matured into key members of the Division. During the time I was away from Monterey, the Division has successfully diversified both their funding and customer base. Efforts like the recent support of Operation Iraqi Freedom provided directly from NRL continue to show the relevance of this Division in providing warfighter support. We are all facing challenging times, but I am confident that we have the world-class expertise to adapt our research to meet these new directions and continue our long history of transitioning science and technology to support the operational missions of DOD.”

Dr. Francis Klemm

Dr. Francis Klemm joined NRL in 1975 as an aerospace engineer in what is now the Offboard Countermeasures Branch of the Tactical Electronic Warfare Division. He has been involved in the development of numerous decoy systems, initially designing decoy vehicles. With on-the-job training, he became an efficient microwave systems engineer. In 1985, Dr. Klemm became the Branch Head of the Offboard Countermeasures Branch. As Branch Head, he fielded operational decoy systems used off the coasts of Kuwait and Bahrain and on aircraft operating over Iraq. In August 2003, he was selected as the Division Superintendent of the Tactical Electronic Warfare Division. “I have seen, experienced, and participated in so many different and interesting things at the Lab — more than I could have imagined when I joined NRL over 25 years ago. The Lab has become a second home to me, and the people a second family. I look forward to coming to work every day knowing that there will be a new and different challenge and that I have an opportunity to make a difference. I consider it a great honor to serve my nation by being a member of this Laboratory — a place where R&D and S&T make a difference.”



Research capabilities, no matter how expensive



and complex, are of no value without the highly motivated people who work at NRL.



Dr. Fran Ligler

Dr. Fran Ligler is currently the Navy's Senior Scientist for Biosensors & Biomaterials, though at various times her duties have also included Deputy Head of the Center for Bio/Molecular Science & Engineering and Head of two different CBMSE Branches. She is best

known for pioneering the development of ultrasensitive detection systems based on optical biosensor technology. With her colleagues in CBMSE, she demonstrated the use of biosensors to identify biological warfare agents, monitor environmental pollutants, analyze food safety, diagnose infectious disease, and detect explosives. Four of the biosensors developed by Dr. Ligler and her colleagues are commercially available, and two more systems are under commercial development. Dr. Ligler's wide range of collaborations include the demonstration of liposome encapsulation of hemoglobin as a blood substitute, integration of biological molecules into optoelectronic devices (biosensors), thin film biomaterials for metal detection, microfluidics fabrication, and proteomic analysis of marine bacteria. She led a consortium including industry and four DOD labs that produced and tested sensors for botulinum toxin and anthrax during Desert Storm and headed the U.S. delegation to NATO Panel 33 on Biosensors. She cofounded a network of women scientists at NRL that initiated a labwide mentorship program, created opportunities for undergraduate research at NRL, and has mentored numerous, highly successful graduate students and postdoctoral fellows. "NRL offers unparalleled opportunities to explore new science and technology in the company of one of the finest groups of people on the planet."

Mr. Dale C. Linne von Berg

Mr. Dale C. Linne von Berg is a research electrical engineer and Head of the Optical Systems Section in the Optical Sciences Division. This section develops advanced EO/IR sensors, airborne reconnaissance systems, and real-time image exploitation stations.



The real-time reconnaissance systems that Mr. Linne von Berg has helped develop include the F-14 Tactical Airborne Reconnaissance Pod System Full Capabilities (TARPS-FCAP), the F/A-18 Shared Reconnaissance Pod (SHARP), and the Navy Input Station (NAVIS), all of which were utilized in Operation Iraqi Freedom. Currently, he is working on programs providing real-time multi-INT fusion targeting and simultaneous command and control of multiple UAVs from the NRL P3. "NRL is a wonderful place to work because of its unique working environment and the unparalleled quality and dedication of its staff. I believe these attributes are interrelated and are a result of the support and philosophy provided by NRL. The NRL philosophy encourages a working environment where the exchange of new ideas is expected. It supports the pursuit and defense of the technical right answer. It allows scientists and engineers the freedom to develop applied capabilities that address relevant national needs, as well as to establish long-term research initiatives that will develop tomorrow's advanced technology. The realization of this philosophy is what makes working at NRL so rewarding and I am very proud to be a part of it."

Our People Are Making a



DIFFERENCE



Dr. Elaine Oran

Dr. Elaine Oran is a Senior Scientist for Reactive Flow Physics in the Laboratory for Computational Physics and Fluid Dynamics, an interdisciplinary group doing research in a broad range of basic and applied research in fluid and particle dynamics, reactive

flows, computational methods, and computer science and architectures. “My own small part of LCP&FD comprises work ranging from astrophysics (explosions on cosmological scales) down to the behavior of fluids and molecules in micro- and nanochannels. What I have loved about NRL is that anything is possible. If I’ve had an idea, no one has stopped me from trying it. Instead, I have almost always been actively encouraged. It is also wonderful to be in an environment where we are rewarded rather than demeaned for collaborations and interdisciplinary research. This is a far cry from situations I have seen at other laboratories and universities. The grass is definitely greener here.”

Dr. Karen Swider Lyons

Dr. Karen Swider Lyons is a Materials Research Engineer in the Surface Chemistry Branch of the Chemistry Division. She is passionately devoted to the study and development of power sources for military, government, and commercial purposes.

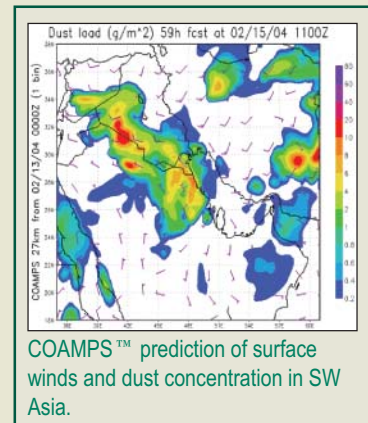


She is funded by DOE’s FreedomCAR program to develop new, low-cost catalysts for polymer fuel cells. She also has NRL funding to research microbattery and energy harvesting devices. In addition, she serves in numerous roles outside of NRL, as a consultant to DARPA and on national panels. “We have a relatively small effort in power sources at NRL, compared to most DOE laboratories, but nonetheless, NRL is a great place to do research in this field. I feel privileged to have the resources to do state-of-the-art research on materials and materials systems within NRL. As a government employee, I can be involved in an advisory role on systems integrations programs. We work closely with our end-users to make sure that we are on target with our goals. It is a great opportunity and experience to be involved in something that can have a tremendous impact both on military and commercial sectors.”

NRL's Contributions to Operation Iraqi Freedom

The outbreak of hostilities on March 19, 2003 between the United States-led international coalition and the military forces of Sadaam Hussein brought the Naval Research Laboratory to the war front. Numerous Laboratory-developed technologies and systems were deployed during the conflict, and they played an important contributory role in the ensuing victory. Operation Iraqi Freedom (OIF) demonstrated once again the significant role that R&D, particularly NRL R&D, can play in giving the American armed forces that critical edge that saves lives while winning battles.

U.S. and allied forces were provided daily localized weather and predictions from the NRL-developed Navy Operational Global Atmospheric Prediction System (NOGAPS), the NRL Aerosol Analysis and Prediction System (NAAPS), and the Coupled Ocean/Atmosphere Prediction System (COAMPS™). Together, these NRL systems provided high-resolution analyses and forecasts to help evaluate the effects of wind variability on munitions targeting, probable atmospheric effects on aircraft detection and ranging systems (through target acquisition weather software), and impacts of visibility on carrier operations. NRL enhanced imagery of MODIS (Moderate Resolution Imaging Spectroradiometer) data from Earth-observing satellites were used along with NRL aerosol prediction models to provide real-time assessments of atmospheric dust conditions and forecasts of dust concentration and movement in operational areas.



The Marine Meteorology Division's dust analysis and prediction efforts, along with the Chemistry Division's dust abatement techniques, produced a significant impact on Allied military effectiveness in the desert environment. American helicopter operations in Iraq during Operation Iraqi Freedom were severely impacted by poor visibility during landings and by intake of dust and sand, leading to engine failure. In response, NRL chemists developed an inexpensive, polysaccharide-based, polymeric solution that could be sprayed onto the sand, solidifying it during helicopter landings and takeoffs. Current efforts are directed at developing a liquid form of the solution that can be dispersed from helicopters in the combat setting.

Operation Iraqi Freedom demonstrated once again the significant role that R&D, particularly NRL R&D, can play in giving the American armed forces that critical edge that saves lives while winning battles.

A team of scientists from the Marine Geosciences Division made a quick turnaround in custom software development for the 5th Special Forces Group in Baghdad. Responding to an urgent call for assistance from the Special Forces, researchers with the Digital Mapping, Charting, and Geodesy Analysis Program (DMAP) developed software to read data from an existing Geographical Information System (GIS) database, convert data points to latitude-longitude coordinates, and make the converted data congruent with established mapping applications. The NRL team took components from NRL's Geospatial Information Database (GIDB) system and incorporated them into new software that met the unique requirements of the Special Forces. The result was a small, easy-to-use program, posted on the NRL GIS server at Stennis Space Center, that moved intelligence data from the original database to a mapping application upon download by U.S. forces. Major Altrus Campbell of the 5th Special Forces Group (Airborne) commented of the NRL work, "It works like a charm. It has already allowed us to confirm some of the enemy's tactics, techniques, and procedures ... Once again, thank you ... for all of your help. Believe me when I say that your work will help us save lives."



NRL's Oceanography Division was also a critical player in support of the Allied operating forces. The Laboratory's coastal ocean prediction model, NCOM (Navy Coastal Ocean Model), produced twice daily sea-state prediction reports

for the waters contiguous to Iraq. The reports were posted to the NRL Stennis SIPRNet website for access by on-scene Naval operators in the Persian Gulf. NRL oceanographers, using the NRL ADCIRC (Advanced Circulation) Model, produced a tidal currents and elevation model for the northern Persian Gulf and the Iraqi coastline. The model produced daily 48-hour forecasts, in 3-hour increments, for water elevation and tidal currents. Oceanographers also carried out high-resolution tidal modeling for

the complicated approach and waterway system of the Iraqi coast. Other NRL input to the Allied forces included data on horizontal and vertical water visibility for the northern Gulf waters, using the SeaWiFS and NASA MODIS satellites, and wave height forecasts along the Iraq/Kuwait coastlines delivered by NRL's SWAN (Shallow Waves Nearshore) prediction model. The AN/UQN-4A Bottom Sediment Classifier, produced by NRL's Marine Geosciences Division, was installed on the USS *Dextrous*, a mine countermeasures (MCM) mine hunter/sweeper, to assist mine hunting operations in the Persian Gulf.





The Optical Sciences Division provided Allied forces digital reconnaissance systems for use in the conflict. The full-capability TARPS-CD (Tactical Air Reconnaissance Pod System-Completely Digital) system was deployed on the USS *Harry S. Truman* and Air Wing CVW-3 of F-14 squadron VF-32 from December of 2002. The NRL system on-board the F-14 fighters supplied real-time high-resolution images to Allied troops in northern Iraq through tactical radios, a likely first for ground forces. The NRL-developed



The shared reconnaissance pod (SHARP) on F-18F Super Hornet during trials.

SHARP (Shared Reconnaissance Pod) system was also deployed to the Gulf on F-18 Super Hornets. TARPS-CD and SHARP

capabilities included visible and infrared digital camera systems, in-cockpit image review and exploitation, geocoordinate determination, and image annotation. NRL also developed ground stations used on two carriers in OIF to exploit the imagery acquired by these systems on F-14's and F/A-18's.

Another reconnaissance system, the Tactical Electronic Warfare Division's Dragon Eye, was also used in Iraq. Dragon Eye consists of an

expendable, man-portable, 5.5 lb, hand-launched air vehicle and a miniature Ground Control Station (GCS) to provide command and control and receive the aircraft's video and GPS position. The unit can fly 60 minutes at 40 knots airspeed at a mission altitude of 300 to 500 feet, using an electric propulsion system. With either a day- or lowlight camera in its nose, it can provide ground troops reconnaissance and threat detection intelligence. Dragon Eye was deployed with the 1st Marine Expeditionary Force in Iraq. A post-Operation Iraqi Freedom review from the First Marine Division (as reported in the *Wall Street Journal*) noted that on-site intelligence provided by Dragon Eye proved to be a conspicuous bright spot in overall intelligence gathering.

NRL also helped provide Allied troops with reliable and secure communications on the battle front. The Information Technology Division used commercial Ku-band satellites and cutting-edge networking technologies on-board an experimental high-speed catamaran, *Joint Venture*, as a platform for advanced communications for the U.S. Navy, Marine Corps, and Army. The *Joint*



Dragon Eye – an expendable, man-portable, 5.5 lb, hand-launched air vehicle and a miniature Ground Control Station (GCS) to provide command and control and receive the aircraft's video and GPS position.

Venture supported standard military communications channels as well as advanced data, voice, and video applications. NRL's Multicast Dissemination Protocol (MDP), which provides highly reliable and efficient transport service for network multicast protocol, was deployed with



The catamaran, *Joint Venture* (HSV-X1), is an experimental high speed vessel used by the U.S. military as a test platform for emerging technologies.

the U.S. Army's 4th Infantry Division in Iraq. MDP was also integrated into the Navy Information and Screening and Delivery Subsystem for transmission of messaging and email to U.S. submarine forces. The Multi-Mission Advanced Tactical Terminal, Improved Data Modem, and Joint Combat Information Terminal, developed by the Naval Center for Space Technology (NCST) for improved battlefield communications, were also put into use by Allied operating forces during the Iraqi war. In addition, NRL contributed to the war effort by providing Specific Emitter Identification (SEI) technology for identifying the radar signatures of Iraqi transmitters. This technology saw use on both U.S. and Allied military platforms.

Other Laboratory contributions included the AN/ALE-50 Advanced Airborne Expendable Decoy, developed by the Tactical Electronic Warfare Division to protect American military aircraft from anti-aircraft missiles. The Radar Division contributed the AN/SPQ-9B Sea Skimmer Detection Radar to protect U.S. Navy and

Allied ships from sea-skimming missiles in the Persian Gulf littoral environment.

Finally, the NRL-developed Surface Acoustic Wave (SAW) chemical agent detector and the Contaminant Transport Analyst (CT-Analyst) was prepared for the Baghdad region prior to Operation Iraqi Freedom for the detection of chemical weapons and threats. The SAW uses surface wave technology to detect the presence of chemical agents through the use of deployable handheld and UAV (unmanned aerial vehicle) carried detectors. CT-Analyst is an NRL-developed operational, instantaneous emergency assessment system for airborne contaminants and Weapons of Mass Destruction (WMD) threats in the urban environment. It was transferred to the Naval Central Command (NAVCENT) through ONR for use if necessary during the conflict.



Numerous other NRL-developed technologies and operating techniques were used during Operation Iraqi Freedom. By one count, 44 different NRL technologies were deployed in some fashion during the conflict. It is a record befitting the Navy's corporate laboratory and one of the country's leading centers for scientific research and development.

Major Altrus Campbell of the 5th Special Forces Group (Airborne) commented of the NRL work, "It works like a charm. It has already allowed us to confirm some of the enemy's tactics, techniques, and procedures ... Once again, thank you ... for all of your help. Believe me when I say that your work will help us save lives."



NANOSCIENCE RESEARCH LABORATORY OPENS AT NRL

The U.S. Navy, known for its enormous aircraft carriers and nuclear submarines, now has the opportunity to exploit the world of the very small for its next generation of technology. Future technology will be increasingly based upon materials and devices fabricated at the atomic scale (measured in nanometers – billionths of a meter). And because it understands both nanoscience and the needs of the Navy, NRL is uniquely positioned to bring that knowledge to bear to benefit our warfighters and our nation.

Toward increasing that understanding, NRL has established an Institute for Nanoscience to conduct multidisciplinary research at the intersection of the fields of materials, electronics, and biology at the nanometer-length scale. The Institute serves as NRL's nucleus of collaborative activity in this rapidly evolving research area.

In support of this new initiative, NRL has constructed a major new facility at its Washington, DC, location. The new facility, opened in October 2003, is administered by the Institute Director. It houses approximately 5,000 square feet of Class 100 fabrication clean rooms and an equal area of specialized, acoustically quiet and ultraquiet laboratory space to carry out research in this demanding regime, under very carefully controlled conditions. Here, postdoctoral students, scientists, and developers can learn firsthand from the scientists who developed the material, equipment, or technique.

Dr. Gary Prinz, Director, Institute of Nanoscience
nanoscience@nrl.navy.mil — <http://nanoscience.nrl.navy.mil>

Dedication of the NRL NANOSCIENCE RESEARCH LABORATORY October 22, 2003

RIBBON-CUTTING CEREMONY — CAPT David Schubert, NRL Commanding Officer; Dr. Stephen Lubard, Director of Science and Technology for the Office of Naval Research; Dr. Gary Prinz, Director of the Institute for Nanoscience; and Dr. John Montgomery, NRL Director of Research, officially open the Nanoscience Research Laboratory.



WELCOMING REMARKS — CAPT David Schubert welcomes VIPs, distinguished guests, and friends to the building dedication ceremony.



RESEARCH NETWORK — Dr. Stephen Lubard and Dr. Gary Prinz.



FROM PLAN TO INSTITUTE — Dr. Gary Prinz greets Dr. Timothy Coffey, former NRL Director of Research. Both were members of the management team that devised the plan to establish a nanoscience institute at the Laboratory.



RESEARCH COLLEAGUES — Dr. Bhatka Rath and Dr. Fred Saalfeld.



NANOSCIENCE RESEARCH AT NRL — Dr. John Montgomery, Dr. Fred Saalfeld, former Director of Science and Technology for the Office of Naval Research, with his wife, Liz, during the Nanoscience Research Laboratory tour.



PAST AND PRESENT LEADERS — Mr. Stephen Harrison, Director of NRL's Research and Development Services Division, Dr. Timothy Coffey, CAPT David Schubert, and Dr. Gary Prinz.



NANOCHEMISTRY — Dr. Richard Colton, head of the Chemistry Division's Surface Chemistry Branch, demonstrates the fieldable BARC sensor to Dr. Fred Saalfeld and his wife.



NEXT GENERATION TECHNOLOGY — Dr. Andy McGill from the Materials Science and Technology Division, and Dr. Lloyd Whitman from the Chemistry Division.



GUIDED TOURS — Dr. Gary Prinz gives an informative tour of the new Nanoscience Research Laboratory building, explaining its advanced laboratory specification capabilities and flexibility.

NRL Rededicates its Newly Refurbished Pier

RADM Jay Cohen, Chief of Naval Research, given special thanks



NRL PIER REDEDICATION – RADM Jay Cohen, Chief of Naval Research, CAPT David Schubert, NRL Commanding Officer, and Dr. John Montgomery, NRL Director of Research, jointly snip the ribbon, officially reopening the NRL Pier.



NRL SUPPORT – At the back of Building 43, facing the NRL pier, NRLers gather for the pier reopening and rededication.



CHIEF OF NAVAL RESEARCH – RADM Cohen commends NRL Director of Research and Commanding Officer, Dr. Montgomery and CAPT Schubert, on NRL's dedication to pursuing excellence in research and technology to support the Navy, the Marine Corps, and the Nation.

The Laboratory rededicated its newly refurbished pier in a ribbon-cutting ceremony held on October 6, 2003. The pier had not been usable and was in need of repair for a number of years.

RADM Jay Cohen, Chief of Naval Research, was recognized at the dedication ceremony by CAPT David Schubert, NRL Commanding Officer, and Dr. John Montgomery, NRL Director of Research, on behalf of NRL for “his unwavering support of the Naval Research Laboratory and sponsorship of this refurbishment.”

The two plaques mounted at the foot of the pier, give special thanks to RADM Cohen and present a brief historical background of USNS *Josiah Willard Gibbs*.

The pier, a 730-foot long timber structure, was built in 1942 to serve as a mooring for cargo and passenger boats. For a period of time, a ferry transported NRLers to and from Alexandria. However, the ferry service ended in 1961, when the Woodrow Wilson Bridge opened.

In the late 1960s, NRL acquired the oceanographic research vessel, USNS *J. Willard Gibbs*, to carry out programs in acoustic and oceanographic research. The NRL pier was the home base for the *Gibbs*. The ship's quarterdeck sign was found during the renovation of Building A-59 and placed at the entrance to the pier.

Following the dedication ceremony and ribbon cutting, NRLers were invited to tour and ride the Office of Naval Research (ONR) Afloat Lab and join colleagues and friends for the first Picnic on the Pier since its closure.



SPECIAL THANKS AND HISTORICAL BACKGROUND – These two placques, mounted at the foot of the pier, give special thanks to RADM Cohen and present a brief historical background of USNS *Josiah Willard Gibbs*.



ONR AFLOAT LAB – The YP-679 arrives at the NRL pier for the rededication ceremony held October 6, 2003.



ONR/NRL LEADERSHIP – NRL Director of Research and Commanding Officer, Dr. John Montgomery and CAPT David Schubert, and Chief of Naval Research, RADM Jay Cohen, are among the first visitors on the ONR Afloat Lab at the NRL pier rededication.

ONR's Afloat Lab

Discovery to Deployment Powered by Naval Research

The Office of Naval Research's Afloat Lab is a test platform for new technologies intended for shipboard use. Formerly classified as the Yard Patrol craft and used to train midshipmen, the Afloat Lab has the same machinery, electronics, and navigation systems as the Navy's large ships, which makes it an ideal test platform.

The vessel provides a realistic shipboard environment for an innovative self-healing communications network that can route around breaks and allows critical shipboard systems to keep functioning. The Afloat Lab takes its nickname, the "Starfish," for this technology because it functions like a real starfish that relies on radial nerves running the length of each ray and connecting to other radial nerves through a nerve ringing the body. In addition to this namesake technology, the Afloat Lab features other working demonstrations and exhibits to give visitors a sample of cutting edge Navy science and technology.



DRAGON EYE – NRL's Dragon Eye exhibit showcases the unmanned air vehicle and its capabilities.



SIMDIS – An exhibitor demonstrates the toolset that provides interactive display and analysis of a specified location.



PICNIC ON THE PIER – Many NRLers join colleagues and friends for the first picnic on the pier since its closure for a number of years.



NRL Donates *Clementine* Spacecraft to National Air and Space Museum



The engineering model of the *Clementine* satellite hangs at the National Air and Space Museum and is part of the largest collection of historic air and spacecraft in the world.

The Naval Research Laboratory donated the engineering model of the *Clementine* satellite for display at the Smithsonian Institution's National Air and Space Museum in Washington, DC. *Clementine* is known for taking approximately two million photographs of the Moon's surface during the 1990s. The display of the engineering model of the satellite was marked with a ceremony held on January 22, 2003.

Clementine was developed by NRL as a project jointly sponsored by NASA and the Ballistic Missile Defense Organization. It was launched in January 1994 to space qualify lightweight imaging sensors and component technologies for the next generation of Department of Defense spacecraft. The images returned by *Clementine* were the first high-resolution images of the Moon collected since the *Apollo* lunar landing in 1972. In addition to taking several million photos of the Moon, *Clementine* was significant in finding evidence of water ice on the lunar surface.

Clementine was a "fast-track" program from its inception. The work on the spacecraft was completed in just 22 months, less than half the time usually required to build a spacecraft like *Clementine*. And with the spacecraft and launch vehicle costing \$75 million, it was built at about one-fifth the usual cost. The Lawrence Livermore National Laboratory developed the sensor suite used in the spacecraft, and other federal agencies provided support. *Clementine* showed the capabilities of the national laboratories, working with DOD, NASA, industry, and international space organizations, to integrate, execute, and operate meaningful space missions at low cost.

MEMS “PADDLE RESONATOR”

Scanning electron micrograph of a microelectromechanical system (MEMS) “Paddle Resonator” image using a laser Doppler vibrometer microscope (LDVM). The “blue” edge is moving toward the observer, and the “yellow” edge is moving away in this mode of vibration. The paddle dimensions are $50 \times 147 \text{ mm}$, wire dimensions are $4.17 \times 51 \text{ mm}$, and dots are $5 \times 5 \text{ mm}$. Displacement of the edges is at most 1 nm.



17 NRL – Our Heritage

18 2003 in Review

22 NRL Today

43 Looking Ahead

NRL — OUR HERITAGE

Today, when government and science seem inextricably linked, when virtually no one questions the dependence of national defense on the excellence of national technical capabilities, it is noteworthy that in-house defense research is relatively new in our Nation's history. The Naval Research Laboratory (NRL), the first modern research institution created within the United States Navy, began operations in 1923.

Thomas Edison's Vision: The first step came in May 1915, a time when Americans were deeply worried about the great European war. Thomas Edison, when asked by a *New York Times* correspondent to comment on the conflict, argued that the Nation should look to science. "The Government," he proposed in a published interview, "should maintain a great research laboratory....In this could be developed...all the technique of military and naval progression without any vast expense." Secretary of the Navy Josephus Daniels seized the opportunity created by Edison's public comments to enlist Edison's support. He agreed to serve as the head of a new body of civilian experts—the Naval Consulting Board—to advise the Navy on science and technology. The Board's most ambitious plan was the creation of a modern research facility for the Navy. Congress allocated \$1.5 million for the institution in 1916, but wartime delays and disagreements within the Naval Consulting Board postponed construction until 1920.

The Laboratory's two original divisions—Radio and Sound—pioneered in the fields of high-frequency radio and underwater sound propagation. They produced communications equipment, direction-finding devices, sonar sets, and perhaps most significant of all, the first practical radar equipment built in this country. They also performed basic research, participating, for example, in the discovery and early exploration of the ionosphere. Moreover, the Laboratory was able to work gradually toward its goal of becoming a broadly based research facility. By the beginning of World War II, five new divisions had been added: Physical Optics, Chemistry, Metallurgy, Mechanics and Electricity, and Internal Communications.

The War Years and Growth: Total employment at the Laboratory jumped from 396 in 1941 to 4400 in 1946, expenditures from \$1.7 million to \$13.7 million, the number of buildings from 23 to 67, and the number of projects from 200 to about 900. During WWII, scientific activities necessarily were concentrated almost entirely on applied research. New electronics equipment—radio, radar, sonar—was developed. Countermeasures were devised. New lubricants were produced, as were antifouling paints, luminous identification tapes, and a sea marker to help save survivors of disasters at sea. A thermal diffusion process was conceived and used to supply some of the ^{235}U isotope needed for one of the first atomic bombs. Also, many new devices that developed from booming wartime industry were type tested and then certified as reliable for the Fleet.

NRL Reorganizes for Peace: Because of the major scientific accomplishments of the war years, the United States emerged into the postwar era determined to consolidate its wartime gains in science and technology and to preserve the working relationship between its armed forces and the scientific community. While the Navy was establishing its Office of Naval Research (ONR) as a liaison with and supporter of basic and applied scientific research, it was also encouraging NRL to broaden its scope and become, in effect, its corporate research laboratory. There was a transfer of NRL to the administrative oversight of ONR and a parallel shift of the Laboratory's research emphasis to one of long-range basic and applied investigation in a broad range of the physical sciences.

However, rapid expansion during the war had left NRL improperly structured to address long-term Navy requirements. One major task—neither easily nor rapidly accomplished—was that of reshaping and coordinating research. This was achieved by transforming a group of largely autonomous scientific divisions into a unified institution with a clear mission and a fully coordinated research program. The first attempt at reorganization vested power in an executive committee composed of all the division superintendents. This committee was impracticably large, so in 1949, a civilian director of

research was named and given full authority over the program. Positions for associate directors were added in 1954.

The Breadth of NRL: During the years since the war, the areas of study at the Laboratory have included basic research concerning the Navy's environments of Earth, sea, sky, and space. Investigations have ranged widely—from monitoring the Sun's behavior, to analyzing marine atmospheric conditions, to measuring parameters of the deep oceans. Detection and communication capabilities have benefitted by research that has exploited new portions of the electromagnetic spectrum, extended ranges to outer space, and provided a means of transferring information reliably and securely, even through massive jamming. Submarine habitability, lubricants, shipbuilding materials, firefighting, and the study of sound in the sea have remained steadfast concerns, to which have been added recent explorations within the fields of virtual reality, superconductivity, and biomolecular science and engineering.

The Laboratory has pioneered naval research into space—from atmospheric probes with captured

V-2 rockets, through direction of the *Vanguard* project (America's first satellite program), to inventing and developing the first satellite prototypes of the Global Positioning System. Today, NRL is the Navy's lead laboratory in space systems research, fire research, tactical electronic warfare, microelectronic devices, and artificial intelligence.

The consolidation in 1992 of NRL and the Naval Oceanographic and Atmospheric Research Laboratory, with centers at Bay St. Louis, Mississippi, and Monterey, California, added critical new strengths to the Laboratory. NRL now is additionally the lead Navy center for research in ocean and atmospheric sciences, with special strengths in physical oceanography, marine geosciences, ocean acoustics, marine meteorology, and remote oceanic and atmospheric sensing. The expanded Laboratory is focusing its research efforts on new Navy strategic interests and needs in the post-Cold War world. Although not abandoning its interests in blue-water operations and research, the Navy is also focusing on defending American interests in the world's littoral regions. NRL scientists and engineers are working to give the Navy the special knowledge and capabilities it needs to operate in these waters.

2003 IN REVIEW

During the last year, science and technology contributions from the Naval Research Laboratory have continued to bolster the nation's defensive efforts at home and abroad. Work done by the Laboratory's Optical Sciences Division made major contributions to *Operation Iraqi Freedom*. The Tactical Air Reconnaissance Pod System-Completely Digital (TARPS-CD) system was deployed on the USS *Harry S. Truman* and Air Wing CVW-3 with F-14 squadron VF-32. The Full Capability (F-CAP) version of the system used during the war helped provide real-time high-resolution images to alliance ground forces in Northern Iraq. Additionally, the Shared Airborne Reconnaissance Pod (SHARP), a dual-band electro-optical/infrared (EO/IR) reconnaissance system prototyped by NRL, was used by squadron VFA-41 flying F-18 Super Hornet aircraft from aboard the USS *Nimitz*. The supporting carrier-based image-screening and exploitation stations used on the F-CAP and SHARP deployments were built with NAVIS (Navy Input Station) technology developed by NRL.

An experimental high-speed catamaran was used jointly by the U.S. Navy, Marine Corps, and Army as a test platform for new communications

technology during *Operation Iraqi Freedom*. The catamaran was equipped with a state-of-the-art communications system and an interoperable C4I operations center designed and installed by a team from the Navy Warfare Development Center, the Space and Naval Warfare Systems Command, and NRL. The Laboratory's Satellite and Wireless Networking Section of the Information Technology Division used commercial Ku-band satellites and cutting-edge networking technologies on the catamaran to support communications channels, as well as advanced data, voice, and video applications. Flexible, reliable C-4I systems support time-critical operations and offer the possibility of an at-sea Joint Operations Center (JOC) during wartime. The JOC Line of Sight Communications system uses the Joint Combat Information Terminal developed by NRL's C4I Branch of the Naval Center for Space Technology.

Laboratory scientists have created a software tool called CT-Analyst that can assess airborne chemical, biological, or radiological threats with greater accuracy and speed than previously possible. The innovation has potential for both military and homeland security use. NRL's new Contaminant

Transport Analyst uses a new “dispersion nomograph” technology that runs on Macintosh, Windows, and Unix systems. Entire series of potential scenarios based on different locations of contaminant sources and changing wind conditions can be computed and displayed in a few seconds. The technology is 80 to 90 percent as accurate as state-of-the-art three-dimensional computational fluid dynamics models and can provide results 100 to 10,000 times faster than real time. It is also designed for urban settings where tall buildings may be present. The most complicated computing work is done before the emergency happens, and the data are condensed into tables (dispersion nomographs) that can be recalled quickly in an emergency to provide information on source location and plume dispersion patterns.

In a demonstration for the Chicago Office of Emergency Management and Communications, NRL researchers demonstrated a suite of technologies that could be useful in crisis situations. The demonstration featured the NRL-developed InfraLynx communications van technology, Software Definable Radio (SDR)-Pathfinder, and robotics and plume modeling technologies. InfraLynx includes satellite, video, and data communications, video streaming, cell phone and traditional telephone communications, and microwave relay collocated in a mobile communications van. SDR-Pathfinder provides a cross-banding capability for radios operating at different frequencies. NRL's Navy Center for Artificial Technology added its “Magnetot” mobile robot to the mix for use as an autonomous platform. Video camera and microwave communications send images from the emergency scene back to emergency management personnel. Other NRL researchers demonstrated the utility of a plume model developed by the Laboratory for Computational Physics and Fluid Dynamics in predicting the dispersal of contaminants in an area with tall buildings. The demonstration was funded under a grant from the National Institute of Justice.

In other work, a team of scientists at NRL fabricated three-dimensional tissue using a unique laser transfer process. The team designed tissue with a computer and then placed living cells in the design-specified locations, using a laser to guide the deposition process. With this technique, scientists have the ability to rapidly build engineered tissue constructs cell-by-cell, layer-by-layer, to simulate or facilitate native structured tissue. The NRL team has already transferred human bone-forming cells, mouse muscle cells, and rat heart cells onto polymer gels. This process may someday be used for instant wound repair.

In the field of nanoelectronics, Laboratory researchers have applied a technique called a crossed-wire tunnel junction to see how charges move across molecules in contiguity with two different metals on opposite sides. The technique varies the nature of the metal-molecule contact to explore how it affects the transmission of electrical charges. The NRL approach demonstrated that a molecule can behave like a molecular *diode* when it is chemically linked at one end, while it exhibits the characteristics of a molecular *wire* when linked at both ends. The research also shows that it should be possible to make a nanoelectronic device using a very small number of molecules and the function of the device would still be representative of the function of a single molecule. In other work, Laboratory scientists discovered that the right combination of materials can spontaneously form a three-dimensional lattice of wires only a few nanometers across. In this research, the nanowires were composed of the compound semiconductor indium arsenide. This was created when a special crystal was grown containing alternating layers of indium arsenide and gallium arsenide only a few atoms thick. The unusual nanostructure was discovered while researchers in the Electronics Science and Technology and Chemistry Divisions were attempting to create new infrared detectors. Current research focuses on exploring what interesting optical and electrical properties the nanowire lattice may possess.

Laboratory researchers have had success in discovering a new approach for producing carbon nanotubes for use in electronics and bio-chemical sensors. Avoiding problems encountered by earlier researchers, the NRL team has found that atomic-level problems of position and orientation control in nanotube construction can be avoided by using random networks of single-wall carbon nanotubes. The networks have proven to be chemically and mechanically robust and can be patterned into electronic devices by using conventional photolithographic techniques. In the fabrication process, problems of position and structural control are avoided because the device properties are determined by the averaged properties of the individual carbon nanotubes. At the right density, the network behaves like a semiconducting thin film that maintains the functionality and sensitivity found in individual semiconducting carbon nanotubes.

Scientists at NRL have also been busy developing advanced composite materials for electronics applications. Research and development programs at the Laboratory have progressed from initial observations of bio/molecular self-assembly in diacetylenic lipids to the modification of 500-nm

hollow cylinders. These micro-sized cylinders have recently been used in electronic composites for cross-talk reduction in the Navy NULKA decoy, an active, off-board, ship-launched decoy that counters radar-guided antiship cruise missiles. The new composites contain advanced bio/nanoparticles with dielectric properties that give high isolation with a large bandwidth. The final product is a composite that weighs less than half as much as its predecessor coating, leading to improvements in decoy “dwell” time and performance.

In space science research, Laboratory investigators have discovered new features of the Milky Way Galaxy that challenge the established understanding of the magnetic field at the Galaxy’s center. Using the National Science Foundation’s Very Large Array radio telescope, NRL astronomers detected filament-like structures with a wide variety of spatial orientations. The NRL study triples the number of such filaments that have been discovered and shows that they do not all point in the same direction, as previously believed. Rather, the new information suggests that the magnetic field at the Galaxy’s center is more like a bowl of spaghetti than a well-ordered bar magnet. The data came from collecting radio waves with a wavelength of approximately 1 m.

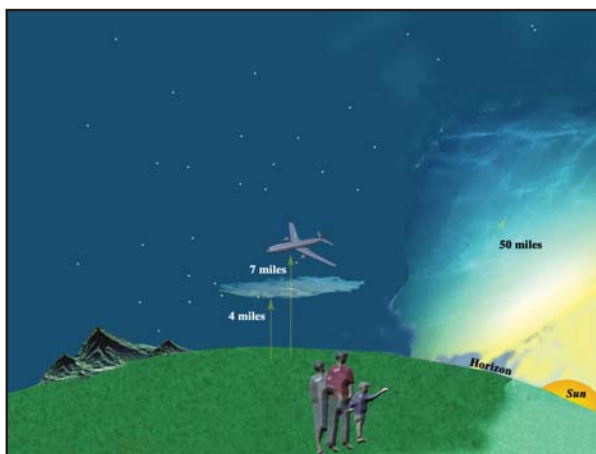
NRL researchers have also discovered that exhaust from NASA’s Space Shuttle can travel to the Arctic in the Earth’s thermosphere where it forms ice to create some of the Earth’s highest clouds. The Space Shuttle exhaust is 97 percent water vapor. The clouds produced by this water vapor settle to 82-km altitude in the atmosphere’s mesosphere. The polar mesospheric clouds are too thin to be seen by the

naked eye in daylight, but they shine at night when the Sun’s rays hit them from below the horizon when the lower atmosphere is bathed in darkness. The data from which these observations were made came from NRL’s Middle Atmosphere High Resolution Spectrograph Investigation (MAHRSI), launched on the Space Shuttle in August 1997.

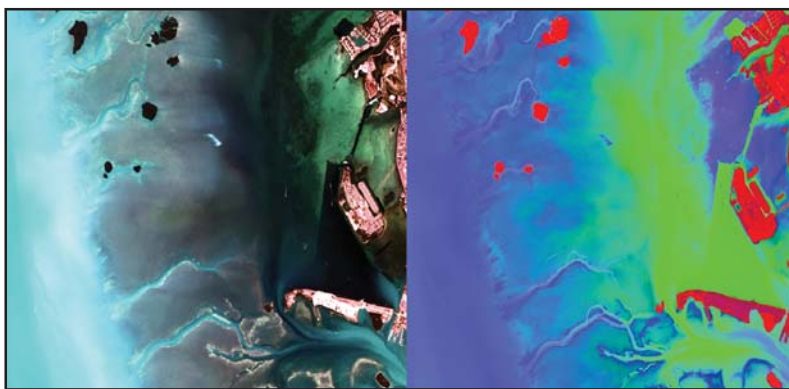
In other atmospheric work, NRL scientists have conducted a field study to investigate the properties and effects of natural and man-made dust and pollution from Asia that are carried by the wind to the west coast of the United States. In the spring, strong winds over the Takla Makan and Gobi deserts of China and Mongolia generate massive dust storms. The dust can be lofted high into the air and be carried downwind across China, Korea, and Japan, mixing with other particulate matter and pollution along the way. Under the right atmospheric conditions, the dust plume can reach the United States and have a significant effect on the atmosphere, both locally and regionally. It may degrade air quality, reduce visibility, reflect and absorb sunlight and infrared energy, and possibly alter weather patterns. The NRL work is an attempt to use various ground, sea, and air-based platforms to measure the properties and effects of the aerosols and to test the predictability skill of NRL’s global aerosol forecast model.

The Naval Research Laboratory’s WindSat microwave radiometer was launched this year on a Titan II rocket from Vandenberg Air Force Base. The polarimetric radiometer will provide meteorological information on wind speed and direction at or near the surface of the ocean. WindSat was developed by the Laboratory under sponsorship of the National Polar-orbiting Operational Environmental Satellite System. The NRL experiment will demonstrate the viability of using polarimetry to passively measure the wind vector from space and thus provide tactical information to Navy units. WindSat will extract brightness temperature data from the microwave energy emitted by the ocean—which is related to wind speed and direction—and generate information that can be downlinked to Navy users in real time.

In the ocean sciences, Laboratory researchers have developed new algorithms and tools for characterizing the optical constituents of coastal waters based on satellite observations. Using these algorithms, they have created an optical water mass classification system to identify and track coastal features. The classification system can be automatically applied to satellite imagery and will facilitate estimates of the transport of dissolved and particulate material in the water. Sunlight strikes the ocean surface, penetrates the water column, interacts with



Because of their high altitude near the edge of space noctilucent clouds shine at night when the Sun’s rays hit them from below, while the lower atmosphere is bathed in darkness. They typically form in the cold, summer polar mesosphere and are made of water ice crystals. Artist rendition created by Suzanne Guilmineau, Technical Information Services Branch.



True-color RGB image (left) taken from hyperspectral data collected over the Florida Keys. ORASIS-produced false-color image (right). The ORASIS data are color-classified to correlate with land (red), shallow water (green), and deeper water (blue). The enhanced image reveals that the actual water depth is the opposite of what the true-color image suggests.

dissolved and particulate matter, and is then reflected out. The quantity and quality of the light reflected from the ocean varies over time and space and represents the “ocean color signature” of the water, which can be measured by satellite sensors. The new NRL-produced algorithms provide researchers a tool for monitoring geochemical and optical processes in the ocean and for measuring the impact of human activity on the coastal zone.

Finally, the Naval Research Laboratory has become a lead center for the study of methane hydrates. Gas hydrates, ice-like mixtures of hydrocarbon gas (mainly methane) and water, are found within arctic permafrost and within ocean sediments located along continental margins. The methane hydrates are generated when water and methane lie within a particular pressure-temperature regime. They are a vast new potential fuel reservoir encompassing 300,000 trillion cubic feet of world reserves. Additionally, combustion of methane produces significantly less carbon dioxide than does that of oil and coal. Hydrate research at NRL is addressing issues such as seafloor instabilities related to methane hydrates that can lead to slope failures and impact Navy systems; the impact of hydrates on undersea navigation and geoaoustic anomalies; and the potential for using methane hydrates to power Navy systems or to fuel unmanned underwater vehicles. The Laboratory has established collaborations with the U.S. and Canadian Geological Surveys, the National Energy Technology Laboratory, the Japan National Oil Corporation, and several universities to conduct methane hydrate research.

NRL’s achievements in technology transfer to the private sector were also recognized with awards

in 2003. In May 2003, at the Annual Meeting of the Federal Laboratory Consortium (FLC), NRL received an award for Excellence in Technology Transfer. This award was presented to Jeffrey Bowles of NRL’s Remote Sensing Division to recognize his exemplary work that led to the successful transition and licensing of NRL’s Optical Real-time Adaptive Spectral Identification System (ORASIS) to Advanced Power Technology, Inc. (APTI). This system is a software application for the analysis and compression of hyperspectral images based on a patented algorithm developed by researchers at NRL. Hyperspectral images are composite images made up of multiple pictures of a “scene” taken at different wavelengths. Examples of scenes include a view of the Earth’s surface taken from an aircraft or satellite, a medical image recorded using a fiber optic probe, or images of industrial processes that can be used for automation or quality control. ORASIS mathematically identifies constituent components and maps their abundances within the image. The main advantages of ORASIS over other methods currently available are its real-time capability and the ease of use. Moreover, ORASIS is superior to other products for detecting a small amount of a specific component within a scene. This makes it particularly useful in applications such as search and rescue.

Using ORASIS, APTI is selling value-added Earth image analysis products and services such as customized maps and systems for remote sensing data collection and analysis. APTI’s Earth image products will be used for oil, gas, and mineral exploration; environmental assessment; crop analysis for optimizing irrigation and fertilization; and military remote sensing.

NRL TODAY

ORGANIZATION AND ADMINISTRATION

The Naval Research Laboratory is a field command under the Chief of Naval Research, who reports to the Secretary of the Navy via the Assistant Secretary of the Navy for Research, Development and Acquisition.

Heading the Laboratory with joint responsibilities are CAPT David M. Schubert, USN, Commanding Officer, and Dr. John A. Montgomery, Director of Research. Line authority passes from the Commanding Officer and the Director of Research to three Associate Directors of Research, the Director of the Naval Center for Space Technology, and the Associate Director for Business Operations. Research divisions are organized under the following functional directorates:

- Systems
- Materials Science and Component Technology
- Ocean and Atmospheric Science and Technology
- Naval Center for Space Technology.

NRL operates as a Navy Working Capital Fund (NWCF). All costs, including overhead, are charged to various research projects. Funding in FY03 came from the Chief of Naval Research, the Naval Systems Commands, and other Navy sources; government agencies, such as the U.S. Air Force, the Defense Advanced Research Projects Agency, the Department of Energy, and the National Aeronautics and Space Administration; and several nongovernment activities.

PERSONNEL DEVELOPMENT

At the end of FY03, NRL employed 2921 persons—36 officers, 78 enlisted, and 2807 civilians. In the research staff, there are 838 employees with doctorate degrees, 372 with masters degrees, and 569 with bachelors degrees. The support staff assists the research staff by providing administrative, computer-aided design, machining, fabrication, electronic construction, publication and imaging, personnel development, information retrieval, large mainframe computer support, and contracting and supply management services.

Opportunities for higher education and other professional training for NRL employees are available through several programs offered by the

Employee Relations Branch. These programs provide for graduate work leading to advanced degrees, advanced training, college course work, short courses, continuing education, and career counseling. Graduate students, in certain cases, may use their NRL research for thesis material.

For non-NRL employees, several postdoctoral research programs exist. There are also agreements with several universities for student opportunities under the Student Career Experience Program (formerly known as Cooperative Education), as well as summer and part-time employment programs. Summer and interchange programs for college faculty members, professional consultants, and employees of other government agencies are also available.

For more information, see the *NRL Review* chapter, "Programs for Professional Development."

NRL has active chapters of Women in Science and Engineering, Sigma Xi, Toastmasters International, and the Federal Executive and Professional Association. Three computer clubs meet regularly—NRL Microcomputer User's Group, NeXT, and Sun NRL Users Group. An amateur radio club, a drama group (the Showboaters), and several sports clubs are also active. NRL has a Recreation Club that provides sports leagues and swim, whirlpool bath, gymnasium, and weight-room facilities. The Recreation Club offers classes in martial arts, aerobics, swimming, and water walking.



RADM Jay M. Cohen, CAPT David M. Schubert, and Dr. John A. Montgomery participate in a ribbon-cutting ceremony held on October 6, 2003, to celebrate the NRL Pier Refurbishment and Rededication.

The Community Outreach Program traditionally has used its extensive resources to foster programs that provide benefits to students and other community citizens. Volunteer employees assist with and judge science fairs, give lectures, and serve as tutors, mentors, coaches, and classroom resource teachers. The program sponsors African American History Month art and essay contests for local schools, student tours of NRL, a student Toastmasters Youth Leadership Program, an annual holiday party for neighborhood children in December, and a book donation program for both students and teachers. Through the Community Outreach Program, NRL has active partnerships with four District of Columbia public schools.

NRL has an active, growing Credit Union. Since its creation in 1946, NRL Federal Credit Union (NRL FCU) has grown to more than \$300 million in assets and serves about 22,000 NRL employees, contractors, select employee groups, and their families. NRL FCU is a leader in providing innovative financial services such as a dynamic home page, Online Access (Internet home banking) with bill payer, and estatements. Focusing on the credit union philosophy of *People Helping People*, NRL FCU offers a wide array of no-fee services plus financial education and assistance. NRL FCU Financial Services, LLC (NFFS), a wholly owned subsidiary of NRL Federal Credit Union, has \$18 million in assets under management. NFFS offers full-service investment and brokerage services. For information about membership or any financial service, call (301) 839-8400 or click on www.nrlfcu.org.

Public transportation to NRL is provided by Metrobus. Metrorail service is three miles away.

SCIENTIFIC FACILITIES

In addition to its Washington, D.C., campus of about 130 acres and 85 main buildings, NRL maintains 11 other research sites, including a vessel for fire research and a Flight Support Detachment. The many diverse scientific and technological research and support facilities are described in the following paragraphs.

RESEARCH FACILITIES

Institute for Nanoscience

The revolutionary opportunities available in nanoscience/nanotechnology have led to a National Nanotechnology Initiative. NRL has been a major contributor to the science of nanostructures and is making a commitment to expand that effort. The NRL Institute for Nanoscience has been established

with a \$10 million annual budget in core research funds. The mission of the Institute for Nanoscience is to conduct highly innovative, interdisciplinary research at the intersections of the fields of materials, electronics, and biology in the nanometer-size domain. The Institute will exploit the broad multidisciplinary character of the Naval Research Laboratory to bring together scientists with disparate training and backgrounds to pursue common goals at the intersection of their respective fields at this length scale. The objective of the Institute's programs is to provide the Navy and DOD with scientific leadership in this complex, emerging area and to identify opportunities for advances in future Defense technology.

Its current research program emphasizes multidisciplinary, cross-division efforts in nano-assembly, nanochemistry, nanophotonics, nano-electronics, and nanomechanics.

Radar

NRL has gained worldwide renown as the "birthplace of radar" and, for a half-century, has maintained its reputation as a leading center for radar-related research and development. A number of facilities managed by NRL's Radar Division continue to contribute to this reputation.



The WARLOC radar system is located at NRL's CBD. This site overlooks the Chesapeake Bay, making it ideal for research related to Naval applications. The radar system is housed in two transportable shelters. A larger shelter houses the gyro-klystron amplifier and its power supply and modulator. An integral part of this shelter is the antenna support structure that provides a rigid platform for the precision pedestal and the 6-ft Cassegrain antenna. The smaller shelter contains receivers, waveform generators, the antenna controller, and the real-time signal processing computer.

A widely used major facility is the Compact Antenna Range (operated jointly with the Space Systems Development Department) for antenna design and development, as well as radar cross section measurements. The range is capable of simulating farfield conditions from 1 to 110 GHz, with a quiet zone of approximately 7 ft in diameter and 8 ft in length. Instrumentation covers from 1 to 95 GHz. Another strong division capability is in the Computational Electromagnetics (CEM) Facility, which has capabilities for complex electromagnetic modeling, including radar target and antenna structures. The Radar Signature Calculation Facility within this group produces detailed computations of radar cross sections of various targets, primarily ships. The CEM facility includes multiple-CPU supercomputers that are also used to design phased array radar antennas. There is tremendous synergism between the CEM group and the Compact Range Facility. This provides the ability to design in the CEM environment, test in the compact range, and have immediate feedback between the theoretical and experimental aspects to shorten the development cycle for new designs.

In connection with airborne radar, the division operates a supercomputer-based Radar Imaging Facility and an inverse synthetic aperture radar (ISAR) deployed either in the air, on the ground, or aboard ship for radar-imaging data collection. A P-3 aircraft equipped with the AN/APS-145 radar and cooperative engagement capability is also available for mounting experiments.

In connection with ship-based radar, the division operates a Radar Test Bed Facility at the Chesapeake Bay Detachment (CBD), Randle Cliffs, Maryland. Radars for long-range air search, point defense, and surface search functions are available. The point defense radar, with its large (4 ft × 8 ft) X-band phased array antenna, and the AN/SPQ-9B ADM systems are designed to be mobile so that testing is not limited to this specific environment. The CBD facility also features the newly developed WARLOC. This high-power coherent millimeter-wave radar operating at 94 GHz is now fully operational. The transmitter is capable of producing 10 kW of average power, with a variety of waveforms suitable for precision tracking and imaging of targets at long range. Waveforms with a bandwidth of 600 MHz can be transmitted at full power. A 6-ft Cassegrain antenna is mounted on a precision pedestal and achieves 62 dB of gain.

The division also operates the microwave microscope, a high-resolution (2-cm) capability for investigating backscatter from both surface and volumetric clutter. The division provides direct technical support and has direct access to data from



NRL's Ship Motion Simulator is located at the Chesapeake Bay Detachment, Randall Cliffs, Maryland.

the AN/TPS-71, the Navy's relocatable over-the-horizon radars. Concepts and engineering developments in connection with target identification are explored by using an experimental Cooperative Aircraft Identification system.

Information Technology

The Information Technology Division (ITD) is at the forefront of DOD research and development in artificial intelligence, telecommunications, computer networking, human-computer interaction, information security, parallel computation, and computer science.

The division maintains local-area computer networks to support its research and hosts metropolitan-area testbeds for advanced high-performance fiber-optic network research. These networks make hundreds of high-performance computers across DOD available to local and remote users. The ITD research networks connect to NRL's internal network via high-speed links ranging from links on the NASA Science Internet (NSI); to OC-12c (622 Mbps) on DREN/S-DREN; to multiple OC-192 (9.6 Gbps) on ATDnet. The ATDnet is a metropolitan ATM network that supports advanced network research on multiple wavelengths, each with 10 Gbps capability. Other major partners include the National Security Agency, the Defense Information Systems Agency, the Defense Advanced Research Projects Agency, the Defense Intelligence Agency, and the National Aeronautics and Space Administration. Research on ATDnet includes introduction and testing of new networking protocols; wave division multiplexing to greatly increase network capacity; and the evolution to all-optical networks, with switching at the optical layer. Research on the high-

end computational assets and networks results in close association with applications that demand these leading-edge capabilities and has allowed ITD to achieve significant results in a number of areas. These include current efforts in pushing the state of the art in motion imagery with progressive scan in high-definition TV (HDTV) where 1.5 Gbps data streams are needed to handle the raw output. The Motion Imagery Laboratory (MIL) continues at the leading edge of technology to provide the environment for experiments in the convergence of the progressive video, high-performance computing, very large data sets at hundreds of terabytes, and high-speed networking that allows the user to be enveloped in the data presentation with a capability for real-time manipulation.

The Defense Research and Engineering Network (DREN) is a high-speed continental United States network that connects the four Major Shared Resource Centers (MSRCs) and 19 Distributed Centers (DCs) of DDR&E's High Performance Computing Modernization Program (HPCMP) as well as a number of user organizations that use HPCMP resources.

As one of 19 Distributed Centers in the HPCMP, ITD's Center for Computational Science supports a range of shared resources, including massively parallel computer systems and high-performance networks. Current systems include an SGI Origin3800 with 128 processors and 128 gigabytes of memory. During FY03, another first-of-a-kind machine was introduced, an SGI Altix with 128 next-generation Intel IA64 processors. The Altix is the first successful attempt to use Linux as the basis of a true supercomputer with a single system image. At the end of FY02, a first-of-a-kind Multi-Threaded Architecture (MTA) from Cray Systems

was delivered as part of the NRL Distributed Center's leading-edge work in HPC. The Cray MTA is a 40-processor machine with 160 gigabytes of memory capable of executing across 128 threads for each of its 40 processors. The CCS also has more than 12.5 terabytes of on-line shared rotating disk as well as robotic storage systems for fileserving and archiving that hold 300 terabytes of multimedia data but are scalable to over a Petabyte. The Center manages the NRL local-area network, NICEnet, which has transitioned from the older FDDI and shared Ethernet local-area networks to a fully switched environment based on ATM backbones. It also provides both high-speed mid-Atlantic Cross-roads (MAX)/University of Maryland Ethernet and ATM to the users' desktops. The goal is to provide digital transparency of resources with security across the information infrastructure—from globally available archives, to the computational engines, to the networks that bring it all together at 10 Gbps directly to the desktops of the most demanding users. NICEnet provides external connections to other networks and to the Internet.

Division facilities include an Information Security Engineering Laboratory, a Robotics Laboratory, an Immersive Simulation Laboratory, an Audio Laboratory, and a high-data-rate multimedia satellite transmission facility.

The Integrated Communications Testing (ICT) Laboratory houses research facilities for multiple projects. Its primary role is to serve as a platform for researching, testing, and evaluating new protocols and technologies for high-speed terrestrial networks. At the present time, it is heavily used for experimenting with networking technologies that benefit the Joint Forces Command (JFCOM) Modeling and Simulation (M&S) community. It



The 128-processor Silicon Graphics Origin3800 system, currently with 128 Mbytes of RAM, the first production unit in the world with R14000 processors, was brought on-line in mid FY01. The NRL Center for Computational Science, as a Distributed Center of the DOD High Performance Computing Modernization Program, provides such systems (at no cost) for anyone approved by the Program Office.

houses a large base of networking gear that can be used to reproduce large nationwide networks or small specialized networks. The ICT Lab also contains equipment capable of injecting “real-world” conditions into test environments. The test gear ranges from commercial-grade equipment to specialized software tools developed at NRL. The ICT Lab is connected into the NRL networking infrastructure such that connections across the DREN and other nationwide networks are possible to facilitate collaborative efforts with other DOD/government facilities. Protocol testing of network cryptographic gear is routinely done in the ICT Lab in conjunction with other affiliated facilities. By using its large base of equipment and rapidly configurable nature, the ICT Lab also serves as a debugging environment for many other projects such as JTF WARNET, Fleet Battle Experiments, and Dragon Warrior. These projects, once proven in the laboratory, are deployed at reduced risk to their execution schedule. A wireless networking testbed is being used to develop Mobile Ad Hoc Networking (MANET) standards that can meet a wide range of military and commercial needs.

The Virtual Reality (VR) Laboratory provides the facilities and expertise to allow NRL scientists to use virtual reality in a variety of scientific investigations. Research areas include shipboard firefighting; simulation-based design; command and control; and scientific visualization. A number of high-speed graphics workstations, including Onyx Reality Engine 2 and Infinite Reality computers, and a variety of VR peripherals comprise the VR Lab computer equipment inventory.

Current VR technologies available include desktop VR systems, head-mounted displays (HMDs), the Responsive Workbench, and the surround-screen Immersive Room. The Responsive Workbench is an interactive 3-D tabletop environment that displays computer-generated, stereographic images on the workbench surface for use in battlespace situation awareness, simulation-based design, and other applications. The surround-screen Immersive Room is a multiuser, high-resolution 3-D visual and audio environment that projects computer-generated images onto three walls and the floor to create an immersive, large-scale, shared virtual environment. It uses an SGI Onyx RE2 so scientists can interact and control their super-computing calculations in real time.

The NEWAVE facility has been developed as a multiscreen distributed simulation laboratory and viewport. Powered by SGI and Pentium workstations and linked to the NRL HPC Distributed Center with ATM/SONET networking, the facility is capable of handling high-performance computing,

graphics, and distributed simulation. It is a multipurpose facility that can be used for virtual prototyping, warfare analysis, wargaming, and many other applications.

NRL has owned and operated a Ship Motion Simulator (SMS) since 1943. This facility is currently located at the NRL Chesapeake Bay Detachment. Originally developed to provide gunnery practice for sailors, the SMS has been used more recently to test radar and satellite receiving systems. A roll motion of up to 28 degrees (14 degrees to port and 14 degrees to starboard) can be applied to the roll axis. The pitch axis has a fixed motion of 10 degrees (5 degrees to stern and 5 degrees to bow). Periods along both the pitch and roll axes are variable—from a slow 20-s to a brisk 8-s per cycle.

A 7-ft × 12-ft operations van (Connex box) was recently mounted on the SMS following structural modifications to the platform. The van can accommodate four to five experimenters and subjects. A work area provides adequate space for computer monitors and support hardware. Climate control is maintained by a heat pump. The integrated van/SMS system is designed to be a permanent NRL facility for evaluating the impact of shipboard motion on human performance. This research was sponsored by Aviation Medicine, Code 341, and Virtual Environment Technologies, Code 342, at the Office of Naval Research.

The Advanced Information Technology Branch is procuring a one-person three degrees-of-freedom motion platform for vestibular research to be housed at NRL-DC. NRL has also contributed to the design of a single degree-of-freedom motion simulator being developed with ONR funding. The point of contact for the Ship Motion Simulator and the vestibular motion platform is Dr. Roger Hillson, Code 5580, NRL.

Optical Sciences

The Optical Sciences Division has a broad program of basic and applied research in optics and electro-optics. Areas of concentration include infrared materials and fibers, organic electro-optics, optical signal and information processing, fiber-optic sensors, surveillance and reconnaissance, integrated optical devices, and laser development.

The division occupies some of the most modern optical facilities in the country. This includes an Ultralow-loss, Fiber-Optic Waveguide Facility using high-temperature infrared glass technology. There is also a Focal-Plane Evaluation Facility to measure the optical and electrical characteristics of infrared focal-plane arrays being developed for advanced Navy sensors. The IR Missile-Seeker Evaluation Facility



The NRL Tactical Directed Infrared Countermeasure (TADIRCM) system and the QF-4 drone aircraft on which TADIRCM was successfully live-fire tested. TADIRCM protects aircraft by detecting, tracking, and jamming heat-seeking anti-air missiles with infrared laser radiation.

performs open-loop measurements of the susceptibilities of IR tracking sensors to optical countermeasures. The Large-Optic, High-Precision Tracker system is used for atmospheric transmission and target signature measurements. The Infrared Test Chamber is an ultradry test chamber used to measure the IR signatures of new surface treatments, scale models, and components used for signature control on ships, aircraft, and missiles. A UHV multichamber deposition apparatus for fabrication of electro-optical devices is interfaced to a surface analysis chamber equipped with UPS, XPS, AFM, and STM. Other scanning probe facilities are equipped with Atomic Force and Magnetic Force Microscopes.

There are several fiber-optic sensor facilities with fiber splicers, an acoustic test cell, a three-axis magnetic sensor test cell, equipment for evaluating optical fiber coatings, and various computers for concept analysis. The Digital Processing Facility is used to collect, process, analyze, and manipulate infrared data and imagery from several sources. The Emittance Measurements Facility performs measurements of directional hemispherical reflectance. An extensive set of laboratories exists to develop and test new laser and nonlinear frequency conversion concepts and to evaluate nondestructive test and evaluation techniques.

Electronic Warfare

The scope of the Tactical Electronic Warfare (TEW) Division's program for electronic warfare (EW) research and development covers the entire electromagnetic spectrum. The program includes basic technology research and advanced developments and their applicability to producing EW products. The range of ongoing activities includes components, techniques, and subsystems develop-

ment as well as system conceptualization, design, and effectiveness evaluation. The focus of the research activities extends across the entire breadth of the battlespace. These activities emphasize providing the methods and means to counter enemy hostile actions—from the beginning, when enemy forces are being mobilized for an attack, through to the final stages of the engagement. In conducting this program, the TEW Division has an extensive array of special research and development laboratories, anechoic chambers, and modern computer systems for modeling and simulation work. Dedicated field sites and an NP-3D EW flying laboratory allow for the conduct of field experiments and operational trials. This assembly of scientists, engineers, and specialized facilities also supports the innovative use of all Fleet defensive and offensive EW resources now available to operational forces through the Naval Fleet/Force Technology Innovation Office.

Laboratory for Structure of Matter

This laboratory investigates the atomic arrangements in materials to improve them or facilitate the development of new substances. Various diffraction methodologies are used to make these investigations. Subjects of interest include the structural and functional aspects of energy conversion, ion transport, device materials, and physiologically active substances such as drugs, antibiotics, and antiviral agents. Theoretical chemistry calculations are used



NRL developed Dragon Warrior, a 325-lb tactical unmanned air vehicle (UAV) helicopter for expeditionary use by the Marines. Primary missions include reconnaissance, surveillance, and targeting acquisition (RSTA). The vehicle could also perform communications relay missions at distances of up to 50 nmi from its ground station. Because it is a helicopter, it requires no improved ground site other than a clearing. With autonomous flight capability, it requires no direct pilot input. Instead, the vehicle offers the options of using a pre-programmed flight plan or allowing operator guidance via GPS waypoint navigation.



SMART 6000 CCD X-ray detector, which detects the X-ray scattering pattern of interest, is shown mounted on a platform goniometer. The scattering patterns are used to determine the geometric arrangements of molecules in their crystallographic form.

to complement the structural research. A real-time graphics system aids in modeling and molecular dynamics studies. The facilities include three x-ray diffraction units, two being state-of-the-art facilities, and an atomic force microscope.

Chemistry

NRL has been a major center for chemical research in support of naval operational requirements since the late 1920s. The Chemistry Division continues this tradition. It is pursuing a broad spectrum of basic and applied research programs focusing on controlled energy release (fuels, fire, combustion, countermeasure decoys, explosives), surface chemistry (corrosion, adhesion, tribology, adsorbents, film growth/etch), advanced materials (high-strength/low-weight structures, drag reduction, damping, polymers, thin films, nanostructures), and advanced detection techniques (environment, chemical/biological, surveillance). Facilities for research include:

Chemical analysis facilities, with a wide range of modern photonic/electronic, magnetic- and ionic-based spectroscopic/microscope techniques for bulk and surface analysis;

Synchrotron Radiation Facility, with intense, monochromatic X-ray photon beams tunable from 10 eV to 12 KeV available from four beam lines developed by NRL at the National Synchrotron Light Source at the Brookhaven National Laboratory. Environmental target chambers span a pressure range from 10^{-12} to 10^5 atm and temperatures from 10 to 1500 K;

Nanometer measurement/manipulation facility, which includes fabrication and characterization capability based on scanning tunneling microscopy/spectroscopy, atomic force microscopy, and related techniques;

Materials synthesis/property measurement facility, with special emphasis on polymers, surface-film processing, and directed self assembly.

Commensurate support has been devoted to survivorability of the new classes of ships, DDX, LUN21, LPD17, and LHA(R); and

Marine Corrosion Test Facility, located on Fleming Key at Key West, Florida, offers an ocean-air environment and clean, unpolluted, flowing seawater for studies of environmental effects on materials. Equipment is available for experiments



Femtosecond laser system for ultrafast dynamics; nonlinear mixing techniques are used to generate femtosecond pulses over a wide spectral range (mid infrared to deep ultraviolet) to investigate dynamic processes in molecules and materials. Recent studies include photochemistry and vibrational energy dynamics of ions in solution and in reverse micelles.

involving weathering, general corrosion, fouling, and electrochemical phenomena as well as coatings, cathodic protection devices, and other means to combat environmental degradation.

Materials Science and Technology

NRL has capabilities for X-ray and electron-diffraction analyses and for electron and Auger spectroscopy. Scanning, transmission, and combined scanning-transmission electron microscopes are used to study surface and/or internal microstructures. The division has a secondary ion mass spectrometer for surface analysis that significantly extends the diagnostic capability of the technique. A high-resolution, reverse-geometry mass spectrometer is used to probe reactions between ions and molecules. The Laboratory has a fully equipped fatigue and fracture laboratory and hot isostatic press facilities. The Laboratory's cryogenic facilities include dilution refrigerators and superconducting magnetic sensors for measuring ultrasmall magnetic fields. Also available are two molecular beam epitaxy devices for growing thin films. Division facilities include:

Molecular Beam Epitaxy: As well as other materials synthesis and processing equipment, an up-to-date fatigue and fracture laboratory and state-of-the-art diagnostic equipment, including electron microscopes, spectrometers, and electron and X-ray diffraction equipment, are being used to fabricate and characterize thin films and other materials.

Trace Element Accelerator Mass Spectrometry (TEAMS) – 3 MV Tandem Pelletron Accelerator Facility: Used for standard materials analysis such as

Rutherford backscattering, for MeV-energy ion implantation, and for accelerator mass spectrometry (AMS). AMS measures trace elements in parallel with 3-D imaging at 10- μm lateral resolution (0.01 μm in depth) to 10-ppt sensitivity, and isotopes for sample dating and forensics.

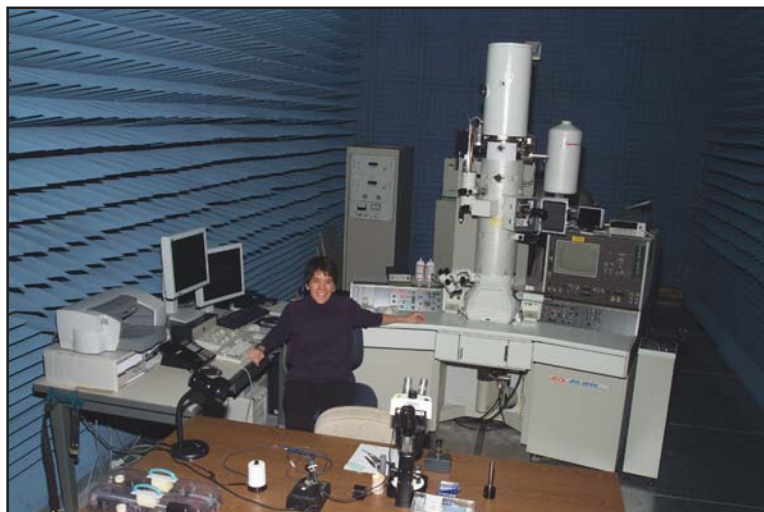
Laser Facilities: Pulses of up to several joules are available from one system, while time resolutions down to 30 femtoseconds are produced by another. Synchronized Q-switched oscillators are configured for pump-probe experiments.

Thin-Film Preparation Facilities: The division has several major capabilities for preparation of thin films of advanced materials, such as high-temperature superconductors and active dielectrics. These include ion-assisted evaporation (which produces dense, adherent films), various dc plasma sources (which can etch as well as deposit films), and pulsed laser deposition (for production of chemically complex films).

Ion Implantation Facility: The facility consists of a 200-keV ion implanter with specialized ultrahigh vacuum chambers and associated in situ specimen analysis instrumentation.

Physical Property Measurement: Laboratories have a complete array of physical property measurement facilities (including magnetometers, electromagnetic (EM) sensors, a tunneling electron microscope (TEM), and a scanning electron microscope (SEM)) to study the properties of materials over a wide range of temperature (cryogenic to 1000 °C), pressure (vacuum to 20 kbar) frequency (dc to infrared), and magnetic fields (0 to 10 tesla).

Material Synthesis and Processing: Laboratories have a variety of facilities for material synthesis and



The new high-resolution transmission electron microscope allows visualization and quantitative analysis of the sub-nanometer-scale structure and composition of new materials.

processing including chemical methods, pulsed laser deposition, ion implantation, clean rooms for patterning films, vacuum to high pressure furnaces, and arc melting.

Laboratory for Computational Physics and Fluid Dynamics

The Laboratory for Computational Physics and Fluid Dynamics (LCP & FD) maintains a very powerful collection of computer systems. There are currently a total of 150 parallel SGI processors, 272 clustered x86 processors, 72 clustered Alpha processors, and several other support systems.

The individual systems are composed of a 64 R12K processor SGI Origin 2000, a 32 R10K processor Origin 2000, an 18 R10K processor Power Challenge, and an 8 R12K processor Origin. There are two x86 clusters, a 16 Athlon processor cluster, and a 256 Pentium 4 processor cluster, both with Myrinet interconnect. The Alpha cluster is a collection of 21264 processor Linux systems well coupled with Myrinet high-speed switched interconnect.

Each system has on the order of 200 gigabytes of disk space for storage during a simulation, and at least 256 megabytes of memory per processor. All unclassified systems share a common disk space for home directories as well as almost 250 gigabytes of AFS space that can be used from any AFS-capable system throughout the allowed Internet.

The AFS capability also allows access to other storage systems including NRL's multiresident AFS (MRAFS) system, which automatically handles archival to a multiterabyte tape archival system.

Plasma Physics

The Plasma Physics Division is the major center for in-house Navy and DOD plasma physics research. The division conducts a broad experimental

and theoretical program in basic and applied research in plasma physics, which includes laboratory and space plasmas, pulsed-power sources, plasma discharges, intense electron and ion beams and photon sources, atomic physics, laser physics, advanced spectral diagnostics, plasma processing, nonlinear dynamics and chaos, and numerical simulations. The facilities include an extremely high-power laser—Pharos III—for the laboratory simulation of space plasmas and nuclear weapons effects studies and two short-pulse high-intensity lasers, the Table-Top Terawatt (T^3) laser and the new Ti:Sapphire Femtosecond Laser (TFL) to study intense laser-plasma, laser-electron beam, and laser-matter interactions. The division also has an 11-m³ space chamber capable of reproducing the near-Earth space plasma environment and a Large Area Plasma Processing System (LAPPS) facility to study material modification such as surface polymerization or ion implantation. The division has developed a variety of pulsed-power sources to generate intense electron and ion beams, powerful discharges, and various types of radiation. The largest of these pulsers—GAMBLE II—is used to study the production of megampere electron and ion beams and to produce very hot, high-density plasmas. Other generators are used to produce particle beams that are injected into magnetic fields and/or cavities to generate intense microwave pulses. A large array of high-frequency microwave sources (2.45, 35, and 83 GHz) are available to conduct research on microwave processing of advanced ceramic materials. In particular, the division added a 15-kW, continuous wave, 83 GHz gyrotron to its facility for research on high-frequency microwave processing of materials. The Russian-made gyrotron produces a focused, high-intensity millimeter-wave beam (10^3 – 10^5 W/cm²) that has unique capabilities for rapid, selective heating of a wide range of nonmetallic materials. The new gyrotron-based



The NRL Electra system is used to develop high-energy high-repetition-rate KrF laser technology. The Electra 30-cm aperture electron-beam-pumped amplifier is shown in the photograph. A portion of the recirculating system that cools the laser gas can be seen at the top. This amplifier is capable of a 5 Hz repetition rate and is expected to produce more than 500 J of laser light per pulse.

system will be used to investigate the application of such beams to important areas of material processing, including coating of materials, soldering and brazing, and treatment of ceramics, semiconductors, and polymers.

A major 3 kJ KrF laser facility (Nike) opened in June 1995. This facility is made up of 56 laser beams and is single-pulsed (4-ns pulse). This facility provides intense radiation for studying inertial confinement fusion (ICF) target heating at short wavelengths (0.25 μm) and high-pressure physics.

Electronics Science and Technology

The Electronics Science and Technology Division conducts a multidisciplinary basic and applied research program to exploit the creation/discovery/invention of new enabling materials, components, and techniques in electronics. In-house efforts include research and development in solid-state electronics; electronic materials including growth, theory, and characterization of semiconductors, heterostructures, and superconductors; surface and interface science; microwave and millimeter-wave components and techniques; microelectronic device research and fabrication; nanoelectronics science and technologies; vacuum electronics; power electronics; device and process modeling and simulation; and cryoelectronics.

In addition to specific equipment and facilities to support individual science and technology programs, the division operates the Compound Semiconductor Processing Facility (CSPF), the Laboratory for Advanced Materials Synthesis

(LAMS), the Epicenter, the Vacuum Electronics Fabrication Facility (VEFF), the Ultrafast Laser Facility (ULF), the Wafer Bonding Facility (WBF), the Power Device Characterization Facility (PDCF), and the Space Solar Cell Characterization Facility (SSCCF).

The CSPF is dedicated to processing compound semiconductor devices and circuits, to providing micro- and nanofabrication processing support, and to selectively serve the hands-on fabrication needs of individual division and NRL scientists. The LAMS uses metallorganic chemical vapor deposition to synthesize a wide range of thin films, particularly wide bandgap semiconductors such as GaN and related alloys. The Epicenter (a joint activity of the Electronics Science and Technology, Materials Science and Technology, Optical Sciences, and Chemistry Divisions) is dedicated to the growth of multilayer nanostructures by molecular beam epitaxy (MBE). Current research involves the growth and etching of conventional III-V semiconductors, ferromagnetic semiconductor materials, 6.1 \AA III-V semiconductors, magnetic materials, and II-VI semiconductors. The structures grown in this facility are analyzed via in situ scanning tunneling microscopy and angle-resolved electron spectroscopy. The Ultrafast Laser Laboratory is optimized for the characterization of photophysical and photochemical processes in materials on a timescale of tens of femtoseconds. It includes a synchronously pumped dye laser system for simulating the effects of charge deposited in semiconductors characteristic of space radiation. The Wafer Bonding Facility is a Class 100 clean room facility for conducting research on the



Molecular beam epitaxial growth of nanostructures using high vacuum, chamber-to-chamber sample transfer.

fabrication of high-voltage wafer-bonded power devices and the development of novel high-performance wafer-bonded substrates for epitaxial growth of both narrow bandgap and wide bandgap material layers. The Power Device Characterization Facility characterizes the performance and reliability of silicon and SiC power devices. The SSCCF studies the effect of particle irradiation on new and emerging solar cell technologies for space applications. The VEFF provides electrical and mechanical design, fabrication, assembly, modification, and repair, as well as processing services for vacuum electronic devices.

Bio/Molecular Science and Engineering

The Center for Bio/Molecular Science and Engineering conducts research and development using biotechnological approaches to support the Navy, DOD, and the nation at-large. Studies are currently underway to investigate biomaterial development (for electronic and structural applications), environmental quality (including pollution cleanup and control), and chemical/biological warfare defense. Other program areas of interest include optical biosensors, nanoscale manipulations, genomics and proteomics, controlled sustained release, bio/molecular and cellular arrays, surface modification and patterning, energy harvesting and microbatteries, advanced materials from self-assembly, and liquid-crystal-based electro-optic materials.

The staff of the Center is an interdisciplinary team with expertise in bio- and surface chemistry, biophysics, genetic engineering, cell biology, advanced organic synthesis, solid-state and theoretical physics, and electronics and materials engineer-

ing. In addition, the Center has collaborations throughout the Laboratory, with other government laboratories, at universities, and in industry.

The Center occupies laboratories and offices in Buildings 30 and 42. These modern facilities include general laboratories for research in chemistry, biochemistry, molecular biology, and physics. Specialized areas include a 600-ft² Class-1000 clean room, an advanced electron microscope facility, and a scanning probe microscope laboratory. Instrument rooms provide access to a variety of spectrophotometers and other equipment used in biochemical or physical analyses of biomaterials. Additional laboratories accommodate an X-ray diffraction instrument, a liquid crystal fabrication facility, and equipment for advanced electronics, microarrays, and biosensor programs. The Center has recently added a plastic microfabrication facility that enables fabrication of microfluidic and microoptical systems in polymers.

Acoustics

The Acoustics Division has three integrated structural acoustic facilities—two pools (including one with a sandy bottom) and a large in-air, semi-anechoic laboratory—that support research in submarine target characteristics for antisubmarine warfare, submarine acoustic design and quieting, sensors for hull-mounted sonars, mine detection and identification, torpedo quieting, and noise control in the interior of air and submarine structures. Scaled submarine targets, real mines, sensors mounted on hull simulators, underwater buried objects, actual torpedoes, small aircraft fuselages, and satellite payload launch fairings can all be examined with advanced nearfield holographic and scanning 3-D



Plastic microfabrication facility with minimill and molding machine for high-resolution molding of plastic components used in biosensors.



The Bottomed Vertical Line Array (BVLA) provides an autonomous system for collecting 64 channels of acoustic data for a total record time of 80 hours. The system can be controlled remotely from the ship and can telemeter data for shipboard analysis. The system can also be deployed in an L-shaped configuration, using 32-channel vertical and horizontal arrays.

laser vibrometer systems to measure and visualize the sound fields near a structure, the vibrations of the structure itself, the resulting farfield and interior sound fields, and the physics of the sound-structure-fluid interactions.

The division operates state-of-the-art laboratories equipped to study the structural dynamics and performance of high-Q oscillators and other micro-mechanical systems. A number of laser Doppler vibrometers permit spatial mapping of the complex vibratory motion of the micro-oscillators. Nano-structures are probed with a super-resolution nearfield scanning optical microscope (NSOM), allowing the monitoring of modes with a spatial resolution of 100 nm. These unique databases can be used to identify and analyze modes of vibration and loss mechanisms with a view toward pushing the Q to still higher levels and for designing optimum oscillator coupling for micro- and nano-oscillator array applications. In addition, the viscoelastic properties of thin films can be studied by depositing them on portions of the oscillator. The laboratory includes the ability to measure many of these mechanical and electrical properties down to 370 mK.

The Acoustics Division Salt Water Tank Facility is designed to provide a controlled environment for studying a variety of complex ocean processes under saline conditions, especially the study of the acoustics of bubbly media. Instrumentation includes acoustic sources, amplifiers, hydrophones, environmental sensors, a Digital Holographic Imaging

System, high-speed digital cameras, and a LabVIEW-based data acquisition system.

The division operates several sound sources for the generation and reception of sound in at-sea experiments. Sound sources include three XF-4 units, one ITC 2077 source that can be operated while being towed by a ship, two battery-operated organ-pipe sources that can project single tones from off-board moorings, and a towable, directional source array for active sonar studies consisting of 10 individually controllable elements, at frequencies 2.5 to 5 kHz. In addition, the division has several battery-operated rubidium-clock-controlled, programmable sound source moorings that can transmit sounds having arbitrary waveforms.

The division has a 64-channel broadband source-receiver array with time-reversal mirror functionality. Projects involving scanning focused acoustic fields and phase conjugation for multistatic sonar will use the new array to test and study time reversal methods. The transducers for the array are 6-in. spheres that operate over a 500 to 3500 Hz frequency band.

The division has several acoustic receiving arrays for at-sea experiments. For continuous, long-duration (10- to 24-day) acoustic measurements, a unique autonomous acoustic data acquisition suite has been developed. Acoustic sources controlled via rubidium clocks generate programmable waveforms at 300 and 500 Hz. Three independent autonomous 32-channel vertical arrays and a 96-channel horizontal array controlled with rubidium clocks acquire

and store 24-bit data up to 900 Hz at a 4 kHz sample rate for 18 to 22 days. As presently configured the systems operate to water depths of 500 m. These systems acquire data with rubidium-clock sampling accuracy. The division also has unique, self-recording digital acquisition buoy systems (DABS) that are used to obtain multichannel (up to 128) acoustic data in the 10 Hz to 5 kHz regime. These systems provide up to 250 Gbytes of data on a single 15-in. reel of 1-in. tape.

The Acoustics Division has a satellite-linked buoy system with underwater receive arrays designed to collect acoustic and oceanic data, unattended, for periods of up to 1 month. The system currently can handle 64 channels of acoustic data (distributed on one or two arrays), and can implement onboard signal processing prior to data transmission. Two-way satellite communication is supported, providing a high-speed data link (up to 1.5 Mbps) for data transfer from the buoy to shore, and a low-speed command and control link to remotely control buoy functions. The system also contains high-speed (up to Mbps) line-of-sight communications utilizing a GPS-linked directional antenna.

The division conducts research to understand the channel capacity of multinode underwater acoustic communications networks. The research is conducted in the 1 to 10 kHz and 10 to 20 kHz frequency bands using four 8-channel acoustic communications data acquisition systems or modems.

A narrowbeam 200 and 350 kHz backscattering system is used to study internal wave and larger scale turbulent processes. The system is used to estimate the magnitude of the randomization of the sound speed field by a variety of fluid processes. It consists of a deck-mounted towing assembly, power and signal amplifiers, and a real-time display and digital data acquisition system. In addition, a 25 kW narrowbeam radar is used to detect the surface manifestation of fluid processes including internal waves and fronts.

The division operates high-frequency (up to 600 kHz) acoustic measurement systems to obtain scattering, target strength, and propagation data using bottom moored instrumentation towers and a high-speed, remotely operated vehicle. These data are used to simulate the performance of weapons and mine countermeasure sonars.

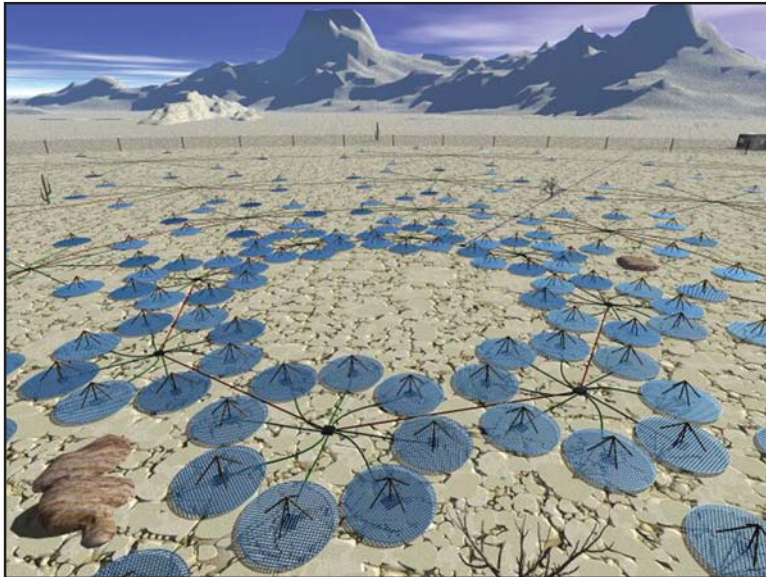
The Tactical Oceanography Simulation Laboratory (TOSL) is a modeling and simulation architecture consisting of a set of tools for processing climatology and real-time environmental data and applying energy propagation models to those data. TOSL features a high-performance computational

capability to provide calculations in support of training, war games, operations rehearsal, and other distributed simulation functions. TOSL is coupled via Ethernet and SIPRNET with the Tactical Oceanography Wide Area Network (TOWAN) repository of environmental data, which allows full participation in a distributed simulation environment.

Remote Sensing

The Remote Sensing Division conducts a program of basic research, science, and applications to develop new concepts for sensors and imaging systems for objects and targets on Earth, in the near-Earth environment, and in deep space. The research, both theoretical and experimental, leads to discovery and understanding of the basic physical principles and mechanisms that give rise to background environmental emissions and targets of interest and to absorption and emission mechanisms of the intervening medium. Accomplishing this research requires the development of sensor systems technology. The developmental effort includes active and passive sensor systems used for study and analysis of the physical characteristics of phenomena that evolve from naturally occurring background radiation, such as that caused by the Earth's atmosphere and oceans, and man-made or induced phenomena, such as ship/submarine hydrodynamic effects. The research includes theory, laboratory, and field experiments leading to ground-based, airborne, or space systems for use in remote sensing, astrometry, astrophysics, surveillance, nonacoustic ASW, meteorological/oceanographic support systems for the operational Navy, and the environmental/global climate change initiatives. Special emphasis is given to developing space-based platforms and exploiting existing space systems.

The Remote Sensing Division conducts airborne hyperspectral data collections for characterization of the environment. Hyperspectral data are series of pictures, taken simultaneously, of a scene at many different wavelengths (colors). The sensors are built and calibrated in-house, although they rely heavily on commercial off-the-shelf elements. The most recent sensor was specifically designed for use over ocean areas. It covers the 400 to 1000-nm wavelength range with 128 different wavelengths (channels). The sensor consists of a standard video camera lens, a grating spectrograph, and a 1024 × 1024 pixel charge-coupled device (CCD). The spectrograph and CCD are specially designed to achieve high sensitivity in the blue end of the spectrum to optimize water-penetrating measurements. This makes possible measurements such as the determination of the ocean bottom type (coral, sea grass,



Artist concept of the future Low Frequency Radio Array (LOFAR) telescope.



The Navy Prototype Optical Interferometer (NPOI) is used for both operational astrometry and for development of distributed aperture imaging techniques.

sand, rock, etc.) to water depths of as much as 20 m (in clear water), and the identification of material in the water column (phytoplankton, sediments, colored dissolved organic matter, etc.). The sensor is very compact and can be flown at heights of 8000 to 10,000 ft, simply “looking” out of a hole in the bottom of the airplane. At ground speeds of 90 kts, the data can still be collected digitally and stored on computer. They are then processed in a ground system operating on a standard personal computer.

Proper interpretation of the hyperspectral data requires calibration of the sensor. This means both radiometric and spectral calibration. The latter plays a critical role in the successful correction of the data for atmospheric effects. The Remote Sensing Division operates an Optical Calibration Facility to perform these calibrations. NIST radiometric standards are transferred to a large integrating sphere. The integrating sphere has 10 precisely controlled quartz-halogen lamps to enable linearity measurements. A set of gas emission standards provides wavelength calibration. As a result, the complete process of data collection through data analysis can be handled in-house.

To validate the results of airborne hyperspectral sensing and to support interpretation of the physical processes they reveal, the Remote Sensing Division has developed a Profiling Optics Package. This system measures the inherent optical properties of water (absorption, attenuation, and scattering) in the 400 to 700-nm range, and collects water samples for various laboratory measurements. The package was built around a Seabird Rosette frame and includes a WETLabs Histar meter to measure water absorption and attenuation at 103 wavelengths; an unfiltered WETLabs ac9 meter to measure water absorption and attenuation at nine wavelengths; a filtered WETLabs ac9 meter to measure colored dissolved organic matter (CDOM) absorption and attenuation at nine wavelengths; a HOBILabs Hydrosat to measure backscattering of water in six wavelengths; a WETLabs WetStar fluorometer to measure stimulated fluorescence of chlorophyll; a Seabird CTD to measure conductivity (salinity), temperature, and depth; and eight sample bottles to collect up to 20 liters of water. Data from each sensor are collected and archived inside a WETLabs Super MODAPS instrument. They are then transmitted to the surface via an armored sea cable, where they are stored on a computer disk. The package has a maximum depth rating of 300 meters, although it is usually operated in coastal waters of less than 50 meters.

The Navy Prototype Optical Interferometer (NPOI), a major facility of the Remote Sensing Division, is actually two collocated instruments for making high-angular-resolution optical measurements of

stars. Light from widely separated individual siderostats is combined simultaneously to synthesize the angular resolution of a telescope tens to hundreds of meters in diameter. Four siderostats are placed in an array with extremely accurate metrology to enable very-high-precision measurements of stellar positions (wide-angle astrometry). These measurements are used by the U.S. Naval Observatory to refine the celestial reference frame, determine Earth rotation parameters, and thus satisfy Navy requirements for precise time and navigation data. They also provide determinations of basic astrophysical parameters, such as stellar masses and diameters. Additional relocatable siderostats can be placed out to distances of 250 m from the array center and used to construct very-high-resolution images of stars. These images provide fundamental astrophysical information on stellar structure and activity. When complete, the NPOI will be the most advanced high-resolution imaging optical interferometer in the world.

To validate numerical and theoretical efforts ongoing within the Remote Sensing Division, extensive hierarchical-coupled experiments are carried out in the Free-Surface Hydrodynamics Laboratory. This laboratory is used to study free-surface turbulence interactions, wave-generation phenomena, jet-flow phenomena, vorticity dynamics, and free-surface/surfactant interactions. Emphasis is placed on those processes that determine the fluxes of heat, mass, and momentum across the air-sea interface. State-of-the-art diagnostic tools are available, such as Langmuir film balance to measure the properties of surface films, hot-wire and laser-Doppler anemometry, and the new quantitative flow techniques of laser speckle, particle tracking, and particle image velocimetry. The laboratory is also equipped with an IR camera with a 20×10^{-3} K resolution. These experimental diagnostic techniques use high-powered lasers, high-tolerance optical lenses, and extensive ultra-high-resolution video-imaging hardware and PC-based computerized systems. Further computational assets consist of powerful graphical computer work stations, the NRL Connection Machine, and other off-site Cray supercomputer systems.

The Airborne Polarimetric Microwave Imaging Radiometer (APMIR) is a state-of-the-art multichannel microwave radiometer system being designed and built by the Remote Sensing Division. APMIR is being developed in response to the emerging need for extensive airborne calibration and validation of spaceborne remote sensing assets: the SSMIS, WindSat, and CMIS spaceborne microwave imaging systems. APMIR will cover five frequency bands: 5-7, 10.7, 18.7/19.35, 22.23/23.8, and 37.0 GHz. Frequency agility allows for frequency matching to each

of the spaceborne systems of interest. The 10.7, 18.7/19.35, and 37.0 GHz channels are fully polarimetric, and will thus measure the ocean surface wind speed and direction. The 5 to 7 GHz channel simultaneously observes several frequencies, providing sensitivity to sea surface temperature; the means to separate rain effects from surface effects; and protection from radio frequency interference (RFI). The 22.23/23.8 GHz channels respond to the atmospheric water vapor in the column below the aircraft, while the 18.7/19.35 and 37.0 GHz channels are sensitive to both ocean surface and cloud parameters. The APMIR system will be mounted in the bomb bay of the NRL P-3 aircraft and flown at altitudes ranging from 500 to 25,000 ft over the ocean.

Oceanography

The Oceanography Division is the major center for in-house Navy research and development in oceanography. It is known nationally and internationally for its unique combination of theoretical, numerical, experimental, and remotely sensed approaches to oceanographic problems. The division modeling focus is on a truly integrated global-to-coastal modeling strategy, from deep water up to the coast including straits, harbors, bays, and inlets. This requires emphasis on both ocean circulation and wave/surf prediction, with additional emphasis on coupling the ocean models to biological, optical, and sediment models. This modeling is conducted on the Navy's and DOD's most powerful vector and



SEPTR is the prototype of a trawl-resistant, bottom-mounted ADCP system that includes a pop-up profiling float for real-time observation and reporting. After a successful test in the Adriatic Sea in May 2003, SEPTR is being winched aboard SACLANT's research vessel *Alliance*. NRL and SACLANT have just entered into a Cooperative Agreement for final engineering development of SEPTR and for deployment of several in a real-time environmental assessment system.

parallel-processing machines. To study the results of this intense modeling effort, the division operates a number of highly sophisticated graphic systems to visualize ocean and coastal dynamic processes. The seagoing experimental programs of the division range worldwide. Unique measurement systems include a wave measurement system to acquire in situ spatial properties of water waves; a salinity mapper that acquires images of spatial and temporal sea surface salinity variabilities in littoral regions; an integrated absorption cavity, optical profiler system, and towed optical hyperspectral array for studying ocean optical characteristics; and self-contained bottom-mounted upward-looking acoustic Doppler current profilers for measuring ocean variability. Specifically, NRL is working jointly with NATO's SACLANT Research Center for development and deployment of the SEPTR instrument. This is a trawl-resistant, bottom-mounted ADCP system that includes a pop-up profiling float for real-time observation and reporting.

In the laboratory, the division operates an environmental scanning electron microscope for detailed studies of biocorrosion in naval materials. The division's remote sensing capabilities include the ability to analyze and process multi/hyperspectral, IR, SAR, and other satellite data sources. The division is a national leader in the development and analysis of Sea WiFS data for oceanographic processes and naval applications in littoral areas.

Marine Geosciences

The Marine Geosciences Division is the major Navy in-house center for research and development in marine geology, geophysics, geodesy, geoacoustics, geotechnology, and geospatial information and systems. The division has unique suites of instrumentation and facilities to support laboratory and field experimental programs.

The instrumentation used in the field experiments is deployable from ships, remotely operated and unmanned vehicles, and airborne platforms and by divers. Instrumentation includes an integrated airborne geophysical sensor suite with gravity, magnetic, and sea/ice/land topographic profiling sensors, all based on cm-level KGPS aircraft positioning. Seafloor and subseafloor measurements use the Deep-Towed Acoustic Geophysical System (DTAGS—220 to 1000 Hz); chirp sub-bottom profiler; high-resolution sidescan sonars (100 and 500 kHz); the Acoustic Seafloor Characterization System (ASCS-15, 30, and 50 kHz); an optically pumped marine magnetometer; several gravimeters; the In Situ Sediment Acoustic Measurement System (ISSAMS); underwater stereo photography; and

nearshore video imaging systems. ISSAMS has specialized probes that measure acoustic compressional and shearwave velocities and attenuation, sediment shear strength, and electrical conductivity in surficial marine sediments.

Five instrumented, 8-ft long, 2220-lb, mine-like cylinders are used to gather impact burial data (one system) and scour and sand wave burial data (four systems) for validation of mine burial prediction models.

Laboratory facilities include sediment physical, geotechnical, and geoaoustic properties and sediment core laboratories. The Electron Microscopy Facility is the focal point for research in microscale biological, chemical, and geological processes. The key instrumentation includes a 300 kVa transmission electron microscope with environmental cell. The environmental cell allows hydrated and gaseous experiments.

A high-resolution industrial CT scanner is a recent addition to the laboratory. It will be used for investigating volumetric heterogeneity of sediments.

The Moving Map Composer Facility is used to design and write mission-specific map coverages for F/A-18 and AV-8B tactical aircraft onto militarized optical disks. The National Imagery and Mapping Agency also uses this state-of-the-art computer facility to update the compressed aeronautical chart library on CD for distribution. The Geospatial Information Data Base (GIDB) capability provides Internet access to the Digital Nautical Chart data, mapping data, imagery, and other data types such as video and pictures. This development tool can be used for planning, training, and operations.

Marine Meteorology

The Marine Meteorology Division is located in Monterey, California. NRL-Monterey (NRL-MRY) serves the Navy's needs for basic research in atmospheric sciences. It develops meteorological analysis and prediction systems and other products to support global and tactical operations.

NRL-MRY is collocated with Fleet Numerical Meteorology and Oceanography Center (FNMOC), the Navy's operational center of expertise in numerical weather prediction. This provides NRL-MRY with efficient access to a variety of classified and unclassified computer resources and databases to support development and transition of operational analysis and prediction systems. In addition, interfaces to the Defense Research and Engineering Network provide access to the DOD High Performance Computing resources. NRL-MRY has established the Daley Supercomputer Resource

Center, the Bergen Data Center, and the Geostationary Satellite/Radar Processing Center to support research and development requirements. The Daley Geostationary Supercomputer is an Origin2000 128-processor supercomputer that contains high-performance computer workstations, an 8-terabyte (expandable to 24-terabyte) Storage Area Network. It is used to conduct numerical weather prediction experiments, process and analyze satellite data, perform simulation studies, and demonstrate tactical weather products. The Bergen Data Center has a 24-terabyte capacity data center with a hierarchical storage management capability to provide archival and easy retrieval of research data sets.

State-of-the-art satellite/radar receiving and processing systems allow local collection of real-time geostationary data globally from four different satellites for applications research in support of Navy and Joint Typhoon Warning Center operations. The system also records and processes real-time CONOS weather radar data. This capability has allowed NRL-MRY to take the lead in developing meteorological applications of satellite data for the FMQ-17, which is installed at the Navy's regional meteorological/oceanographic (METOC) centers, and of radar data for the future shipboard thru-the-sensor tactical radar systems.

Space Science

The Space Science Division conducts and supports a number of space experiments in the areas of upper atmospheric, solar, and astronomical research aboard NASA, DOD, and other government-agency space platforms. Division scientists are involved in major research thrusts that include remote sensing of the upper and middle atmospheres, studies of the solar atmosphere, and astronomical radiation ranging from the ultraviolet through gamma rays and high-energy particles. In support of this work, the division maintains facilities to design, construct, assemble, and calibrate space experiments. A network of computers, workstations, image-processing hardware, and special processors is used to analyze and interpret space data. The division's space science data acquisition and analysis efforts include: data analyses of the Oriented Scintillation Spectrometer Experiment (OSSE) for NASA's Compton Observatory; observation of the Sun's interaction with the Earth's upper atmosphere through the Solar Ultraviolet Spectral Irradiance Monitor (SUSIM) experiment in support of NASA's Upper Atmosphere Research Satellite (UARS); observation and analysis of solar flares using the Bragg Crystal Spectrometer (BCS) on the

Japanese Yohkoh space mission; and observation and analysis of the evolution and structure of the solar corona from the disk to 0.14 AU. This latter effort involves acquiring and analyzing data from the Large-Angle Spectrometric Coronagraph (LASCO) and the Extreme Ultraviolet Imaging Telescope (EIT) on the Solar Heliospheric Observatory satellite. In each of these missions, NRL maintains a complete database of spacecraft observations and control over acquisition of data from new observations. These data are available to qualified investigators at DOD and civilian agencies. In addition, the division has a sounding rocket program that affords the possibility of obtaining specific data of high interest and of testing new instrument concepts. These include the general area of high-resolution solar and stellar spectroscopy, extreme ultraviolet imagery of the Sun, and high-resolution, ultraviolet spectral-imaging of the Sun.

In addition, selected celestial and atmospheric targets in the ultraviolet and X-ray bands are observed by three Advanced Research and Global Observation Satellite (ARGOS) experiments—Global Imaging of the Ionosphere (GIMI), High-Resolution Airglow and Auroral Spectroscopy (HIRAAS), and Unconventional Stellar Aspect (USA). ARGOS was successfully launched on February 23, 1999. As part of this program, NRL has established collaborative programs to make use of the ARGOS data for validating various upper-atmosphere models, for studying the response of the thermosphere and ionosphere to solar and geomagnetic forcing, for testing and evaluating operational space weather sensors and algorithms, and for studying time-dependent phenomena in X-ray sources.

Optical calibration facilities, including clean rooms, are maintained to support these activities. These calibration facilities are routinely used by outside groups to support their own calibration requirements.

Space Technology

In its role as a center of excellence for space systems research, the Naval Center for Space Technology (NCST) designs, builds, analyzes, tests, and operates spacecraft and identifies and conducts promising research to improve spacecraft and their support systems. NCST facilities that support this work include large and small anechoic radio frequency chambers, clean rooms, shock and vibration facilities, an acoustic reverberation chamber, large and small thermal/vacuum test chambers, a spacecraft robotics engineering and control system interaction laboratory, satellite command and control ground stations, a fuels test facility, and modal analysis test facilities. Also, the Center maintains and operates a number of electrical and electronic development laboratories and fabrication facilities for radio frequency equipment, spacecraft power systems, telemetry, and command and control systems, and includes an electromagnetic interference-electromagnetic compatibility test chamber. NCST has a facility for long-term testing of satellite clock time/frequency standards under thermal/vacuum conditions linked to the Naval Observatory; a 5-m optical bench laser laboratory; and an electro-optical communication research laboratory to conduct research in support of the development of space systems.



Naval Center for Space Technology Optical Test Facility at the Midway Research Center, Stafford County, Virginia. Large dome on the left houses a 1-m telescope with active laser transmit and receive capability. Smaller dome and trailer in background is a self-contained transportable 16-in. telescope that has been used as a passive optical tracker and a laser communications receiver.

RESEARCH SUPPORT FACILITIES

Exhibits/Multimedia Office

This office designs and develops full-sized and portable displays and posters for technical conferences and symposia, briefings on Capitol Hill, at DOD installations, Laboratory special events, and public events. The NRL booth at trade shows and technical conferences provides a platform for scientists and engineers to market research projects and also enhances NRL's technology transfer efforts.

The Exhibits Office also designs and develops static displays for buildings, i.e., wall arrangements, division research highlights, and award panels and cases. The static displays found in Buildings 72, 43, 226, 28, 222, and Quarters A are maintained by the Exhibits Office. Other available services include assistance in presentation development (research, writing, layout, design, photo/video archival searches, and finalized vugraph/computer presentation products) and acting as a translator between the researcher and the artist to assist researchers in developing an artist's concept that visually explains the research.

This office produces, directs, and develops multimedia products (CD-ROMs, videos, and films) to enhance exhibits at trade shows and to directly support Laboratory presentation capabilities needed for briefings to existing sponsors, potential sponsors, Congressional representatives, and for recruitment and special events. The most recent "A Tour of NRL" has won four international awards.

Technical Information Services

The Technical Information Services Branch combines publications, graphics, photographic, multimedia, and video services into an integrated organization. Publication services include writing, editing, composition, publications consultation and production, and printing management. Quick turnaround digital black-and-white and color copying/printing services are provided. The primary focus is to use digital publishing technology to produce scientific and technical reports that can be used for either print or Web. Graphic support includes technical and scientific illustrations, computer graphics, design services, photographic composites, display panels, sign making, and framing. The NovaJet Pro 600e and HP Designjet 5500ps printers offer exceptional color print quality up to 600 dpi. They produce large-format indoor and outdoor posters and signs up to 48 inches wide. Lamination and mounting are available. Photographic services include digital still camera coverage



The Technical Information Services Branch has a new HP Designjet 5500ps large format printer and Seal laminator to help you with your poster sessions.

for data documentation, both at NRL and in the field. Photographic images are captured with state-of-the-art digital cameras and can be printed on a variety of digital media. Photofinishing services provide automatic and custom printing from digital files on a new digital minilab. Quick-service color prints are also available. Video services include producing video reports of scientific and technical programs. Digital video editing equipment is available to support video production and produce QuickTime movies.

Administrative Services

The Administrative Services Branch is responsible for collecting and preserving the documents that comprise NRL's corporate memory. Archival documents include personal papers and correspondence, laboratory notebooks, and work project files—documents that are appraised for their historical or informational value and considered to be permanently valuable. The branch provides records management services, training, and support for the maintenance of active records, including electronic records and e-mail, as an important information resource. The Administrative Services Branch is responsible for NRL's postal mail services and NRL's Forms and Reports management programs (including electronic forms). The Administrative Services Branch also compiles and publishes the NRL Code Directory and Organizational Index and provides NRL Locator service.

Ruth H. Hooker Research Library

The Ruth H. Hooker Research Library offers a full range of traditional library services to support the research program of the Naval Research Laboratory. In addition, it is actively engaged in developing

the NRL Digital Library that is available 24-hours-a-day, 7-days-a-week from any of the NRL sites (including ONR headquarters) and through NRL dial-up facilities. The “portal” to the NRL Digital Library, InfoWeb, is located at <http://infoweb.nrl.navy.mil>. InfoWeb provides desktop access to more than 2,500 research journals and hundreds of technical databases and reference tools including Science Citation Index (part of Web of Science) and INSPEC. A key InfoWeb service is TORPEDO *Ultra* v.2, which hosts more than 1,500 licensed journals (nearly 2.5 million articles), and thousands of NRL publications, such as technical reports, press releases, and NRL-authored journal articles/conference proceedings. TORPEDO *Ultra* v.2 is the only known system that permits integrated searching, browsing, display, and printing of scientific journals from multiple publishers along with agency publications. Many of the online services (including the library catalog, Web of Science, and INSPEC) have been enhanced to link directly from the bibliographic citation to the full-text article, either in TORPEDO or on a publisher’s web site.

FIELD STATIONS

NRL has acquired or made arrangements over the years to use a number of major sites and facilities for research. The largest facility is located at the Stennis Space Center (NRL-SSC), in Bay St. Louis, Mississippi. Others include a facility at the Naval Postgraduate School in Monterey, California (NRL-MRY), and the Chesapeake Bay Detachment (CBD) in Maryland. Additional sites are located in Maryland, Virginia, Alabama, and Florida.

Flight Support Detachment (NRL FSD)

Located at the Naval Air Station Patuxent River, Lexington Park, Maryland, the Flight Support Detachment (NRL FSD) is manned by approximately 11 officers, 70 enlisted personnel, and four civilians. NRL FSD is currently responsible for the maintenance and security of four uniquely configured P-3 Orion turboprop research aircraft. The FSD conducts numerous single-aircraft deployments around the world in support of a wide range of scientific research projects.

In FY03, NRL FSD provided flight support for diverse research programs including: the Bow Echo and Mesoscale Convective Vortices Experiment (BAMEX) in conjunction with the National Center for Atmospheric Research and NOAA to advance severe storm prediction capabilities; Cooperative Engagement Capability (CEC), an airborne suite to test USN Aegis Cruiser systems; Airborne Geo-



The Electra Doppler Radar (ELDORA) (located on the tail) and a laser (mounted to the side of the fuselage of Researcher 587) were used to collect atmospheric data in the skies over the midwest from the Bow Echo and Mesoscale Convective Vortices Experiment (BAMEX).

graphical Sensor Suite (AGSS), involving data and gravimeter testing to detect variations in the ocean floor; Integrated Electronic Warfare System (IEWS), a system that simulates radar of various surface and airborne platforms. NRL FSD’s flight safety record spans more than 40 years and includes over 62,000 mishap-free flight hours.

Chesapeake Bay Detachment (CBD)

CBD occupies a 168-acre site at Randall Cliffs, Maryland, and provides facilities and support services for research in radar, electronic warfare, optical devices, materials, communications, and fire research. A ship-motion simulator (SMS) is used to test and evaluate radar, satellite communications, and line-of-sight RF communications systems under dynamic conditions (various sea states). The SMS can handle up to 12,000 lb of electronic systems. A roll motion of up to 30 deg (15 deg to port and 15 deg to starboard) can be applied to this axis. The pitch axis has a fixed motion of 10 deg (5 deg to stern and 5 deg to bow). Periods along both axes, pitch and roll, are variable—from a slow 32-s to a brisk 4-s rate. Variable azimuth motion can also be added to the pitch and roll action. Synchronized positioning information ($\times 1$ and $\times 36$) is available for each of the three axes of the SMS.

Because of its location high above the western shore of the Chesapeake Bay, unique experiments can be performed in conjunction with the Tilghman Island site, 16 km across the bay from CBD. Some of these experiments include low clutter and generally low-background radar measurements. By using CBD’s support vessels, experiments are performed that involve dispensing chaff over water and radar target characterizations of aircraft and ships. Basic



Broadband source array and receiving system being prepared for deployment. It is used by the High Frequency Acoustics Section to measure acoustic coherence links in very shallow water.

research is also conducted in radar antenna properties, testing of radar remote-sensing concepts, use of radar to sense ocean waves, and laser propagation. CBD also hosts facilities of the Navy Technology Center for Safety and Survivability, which conducts fire research on simulated carrier, surface, and submarine platforms.

Stennis Space Center (NRL-SSC)

The NRL Detachment at Stennis Space Center, Mississippi (NRL-SSC) consists of NRL's Oceanography Division and portions of the Acoustics and Marine Geosciences Divisions. NRL-SSC, a tenant activity at NASA's John C. Stennis Space Center (SSC), is located in the southwest corner of Mississippi, about 50 miles northeast of New Orleans, Louisiana, and 20 miles from the Mississippi Gulf Coast. Other Navy tenants at SSC include the Naval Meteorology and Oceanography Command, the Naval Oceanographic Office, the Navy Small Craft Instruction and Training Center, the Special Boat Team-Twenty-two, and the Human Resources Service Center South East. Other Federal and State agencies at SSC involved in marine-related science and technology are the National Coastal Data Development Center, the National Data Buoy Center, the U.S. Geological Survey, the Environmental Protection Agency's Gulf of Mexico Program and Environmental Chemistry Laboratory, the Center for Higher Learning, University of Southern Mississippi, and Mississippi State University.

The Naval Meteorology and Oceanography Command and the Naval Oceanographic Office are

major operational users of the oceanographic, acoustic, and geosciences technology developed by NRL researchers. The Naval Oceanographic Office operates the Major Shared Resource Center (MSRC), one of the nation's High Performance Computing Centers, which provides operational support to the warfighter and access to NRL for ocean and atmospheric science and technology.

The Acoustics, Marine Geosciences, and Oceanography Divisions occupy more than 175,000 ft² of research, computation, laboratory, administrative, and warehouse space. Facilities include the dual-use analysis center, sediment core laboratory, transmission electron microscope moving-map composer facility, underwater navigation control laboratory, computed tomography scanning laboratory, visualization laboratory, ocean color data receipt and processing facility, environmental microscopy facility, maintenance and calibration systems, environmental modeling and simulation high-speed network, and numerous laboratories for acoustic and oceanographic computation, instrumentation, analysis, and testing, including the TOWAN database. Special areas are available for constructing, staging, refurbishing, and storing sea-going equipment.

Marine Meteorology Division (NRL-MRY)

NRL's Marine Meteorology Division (NRL-MRY) is located in Monterey, California, on the grounds of the Naval Postgraduate School (NPS) Annex, which is about a mile from the NPS main campus. The NRL facility is collocated with the Navy's operational Fleet Numerical Meteorology and Oceanography Center (FNMOC) and with a NOAA National Weather Service Forecast Office (NWSFO). The NPS Annex campus, which covers approximately five acres, comprises four primary buildings—one occupied exclusively by NOAA, one that houses both the NRL and FNMOC super-computer/operational facilities, and two large buildings containing office space, computer laboratories, and conference facilities that are shared by FNMOC and NRL-MRY personnel. The site also provides warehouse space and recreational facilities. NRL-MRY occupies approximately 30,000 ft² in shared buildings. This includes not only office space, but also a small library, the Daley Supercomputer Resource Center, the Bergen Data Center, the Geostationary Satellite/Radar Processing Facility, and space for the hardware supporting the Navy Integrated Tactical Environmental System (NITES), the Coupled Ocean/Atmosphere Mesoscale Prediction System-On Scene (COAMPS-OS™), and the Master Environmental Laboratory.

NRL-MRY is dedicated to advancing fundamental scientific understanding of the atmosphere, including the air-sea interface, and to applying those scientific discoveries in the development of innovative objective weather prediction systems. FNMOC is the Navy's central facility for the production and distribution of numerical weather prediction products in support of Navy operations around the globe, as well as to other defense-related activities. Fleet Numerical and the Navy's regional METOC Centers are the primary customers for the numerical weather prediction systems that are developed by NRL-MRY. This collocation of the scientific developer with the operational customer offers advantages for the successful implementation of new systems and system upgrades, and for the rapid infusion of new research results from the community at large. NRL-MRY has efficient access to FNMOC's large classified vector supercomputer and other systems. This allows advanced development to take place using the real-time on-site global atmospheric and oceanographic databases. Collocation also offers the opportunity for FNMOC scientists to team with NRL-MRY scientists during the transition and implementation process, and NRL-MRY scientists remain readily available for consultation on any future problems that arise.

NRL-MRY benefits from the opportunities provided by NPS for continuing education and

collaborative research with the Department of Meteorology and Oceanography.

Midway Research Center

The Midway Research Center (MRC) is located on a 162-acre site in Stafford County, Virginia. Located adjacent to the Quantico Marine Corps' Combat Development Command, the MRC has 16,000 ft² of operations and administration area. Instruments include three precision 18.5-m-diameter parabolic antennas housed in 100-ft radomes, a fast-tracking 1-m telescope currently used for satellite laser ranging, and a transportable 16-in. telescope capable of passive optical tracking and laser communications. The MRC, under the auspices of the Naval Center for Space Technology, provides NRL with state-of-the-art facilities dedicated solely to space-related applications in naval communications, navigation, and basic research.

Research Platforms

Mobile research platforms contribute greatly to NRL's research. These include six P-3 Orion turboprop aircraft and one ship, the ex-USS *Shadwell* (LSD-15), berthed in Mobile Bay, Alabama. The ex-USS *Shadwell* is used for research on aboard-ship fire-suppression techniques.

LOOKING AHEAD

To provide preeminent research for tomorrow's Navy, NRL must maintain and upgrade its scientific and technological equipment to keep it at the forefront of modern research facilities. The physical plant to house this equipment must also be state of the art. NRL has embarked on a Corporate Facilities Plan to accomplish these goals. This plan and future facility plans are described below.

THE CORPORATE FACILITIES INVESTMENT PLAN (CFIP)

The CFIP is a capital investment plan that uses both Congressionally approved military construction (MILCON) and Laboratory overhead funds to provide modern, up-to-date laboratory facilities for NRL. Past MILCON projects have included the Electro-Optics Building at NRL-DC, the Ocean Acoustics Research Laboratory at NRL-SSC, and the

Nanoscience Research Laboratory at NRL-DC. Future MILCON projects include an Autonomous Vehicles Research Building in the FY06 time frame.

To complement these efforts, overhead funds have been used to renovate and upgrade laboratory and support areas in several existing buildings. Modern laboratory facilities have recently been provided for the Center for Bio/Molecular Science and Engineering, the Materials Science and Technology Division, the Remote Sensing Division, the Acoustics Division, the Information Technology Division, and the Radar Division.

In parallel with efforts to upgrade laboratory buildings to the most modern standards, those buildings that were built during World War II and do not lend themselves to renovation are being demolished. This will provide space for the construction of future MILCON buildings, and it will also reduce the Laboratory's overhead costs.

The manipulation and measurement of materials with nanometer dimensions is very difficult. One must be able to reliably and precisely locate structures of nanometer dimensions in much larger areas. Furthermore, the measurement of nanostructure properties is difficult simply because not many atoms/molecules are present. Vibrations and thermal/humidity/pressure fluctuations in the environment can cause major problems in positioning a tool. Good signal-to-noise ratios require electromagnetic and acoustic interference-free environments. Airborne contamination can readily cover a nanostructure. A new Nanoscience Research building has been constructed that controls these sources of “noise”; it became available for use in January 2004. There is 5000 ft² of Class 100 clean room for device fabrication; 4000 ft² of “quiet” space with temperature controlled to 0.5 °C, acoustic isolation at the NC35 standard (35 dB at 1 kHz), and vibration isolation to <3 m/s rms 10-100 Hz. There are also 1000 ft² of “ultra-quiet” space with temperature controlled to 0.1 °C and acoustic isolation at the NC25 standard (25 dB at 1 kHz).

Ruth H. Hooker Research Library

The Ruth H. Hooker Research Library has encouraged “Innovation for Research” for many years, becoming a world-class research library. This is exemplified by first-of-its-kind systems such as InfoNet, InfoWeb, and TORPEDO *Ultra*. These custom systems, combined with the aggressive licensing of online resources for all NRL sites, dramatically increase resources available at the researcher’s desktop. Plans for FY04 include the release of the NRL Honors and Awards Database (which will help researchers discover and apply for scholarly awards), the NRL Online Bibliography (containing references and full text links to all scholarly work created by NRL authors over the past 30 years), improved full-text linking schemes (to permit linking to all articles available online from within several bibliographic databases), and cross-database searching (searching multiple bibliographic databases from various providers with a single search). In addition, desktop access to journals will continue to grow with more back issues available online and more professional society titles being added. Finally, the NRL Library is working closely with the Naval research community to jointly expand access to portions of the NRL Digital Library and expand the volume of content available within.

The Information Technology Division’s Center for Computational Science (CCS) operates scalable, massively parallel Global Shared Memory (GSM) computer systems, including a 128-processor SGI Origin3800 with cache-coherent Non-Uniform Memory Access (ccNUMA) architecture. Resources include an experimental multi-threaded architecture (MTA) high-performance computer with 40 processors. Recent additions for FY03 include a 128-processor SGI Altix, also a ccNUMA machine, based on the leading-edge Intel IA64 architecture. Altix is particularly interesting as it is the first HPC machine to run a single system image across 128 processors using a commercially available LINUX operating system (Red Hat). These systems comprise the Distributed Center (DC) at NRL whose hardware is funded by the DOD High Performance Computing Modernization Program (HPCMP). The systems are used in the innovative exploration and evaluation of MPP technology for solving significant militarily relevant problems relating to computational and information science. The systems allow leading-edge research in support of heterogeneous parallel processing applications by the Navy and DOD science and technology communities.

Chemistry

Force Protection/Homeland Defense (FP/HD) has been a focus of the Chemistry Division since September 11, 2001, especially in the development of improved detection techniques for chemical, biological, and explosive threats. In conjunction with technologies contributed by other divisions, Chemistry Division staff will be major contributors to the definition and development of new technology systems. In a parallel and complementary multidivisional program, the Chemistry Division will be a major contributor to the NRL Nanoscience Research Institute. Nanoscience complements FP/HD in that nanoscience is expected to provide dramatic improvements to chemical/biological detection, protection, and neutralization. Chemistry will approach the nanoscale from the bottom-up—building smaller atoms and molecules into nanostructures with new properties, and developing the directed assembly of nanostructures into hierarchical systems. The new NRL Nanoscience building is linked directly into the Chemistry building to provide both controlled access and auxiliary space for work not requiring a “low noise” environment.

Plasma Physics

The Plasma Physics Division has set up a Large Area Plasma Processing System (LAPPS) facility to investigate a new technique for producing plasmas for plasma processing. Applications include production of large-area flat-screen displays or elements for phased arrays or materials modification such as surface polymerization or ion implantation. The system is based on low-energy electron beam ionization of a background gas to produce the desired plasma. The system may have advantages over existing techniques for production of large-area (square meter) plasmas, efficiency of plasma production, and control of reactive species.

Electronics Science and Technology

The division is considerably enhancing the capabilities of the Compound Semiconductor Processing Facility (CSPF) and expanding activities in the nanoelectronics, wafer bonding, heterostructures, optoelectronics, and vacuum electronics integration areas. The CSPF has absorbed the nanoprocessing, deep etching, and electron beam nanowriter capabilities of the Nanoelectronics Processing Facility (NPF), which was disestablished in 2003. The Laboratory for Advanced Materials Synthesis (LAMS) will install a number of in situ growth diagnostics to aid in the growth of custom, high-quality semiconductor layers and heterostructures and will implement an updated computer control capability for the growth of complex structures. The Silicon Carbide Processing Laboratory (SCPL) will be established in 2004 to serve the needs of the division's power electronics research activities.

Acoustics

NRL's Salt Water Tank Facility provides a controlled environment for studying complex bubble-related processes found in the ocean. It is an experimental pool facility for studies of underwater acoustics, fluid dynamics, and air-sea interface environmental topics under saline conditions. This facility is currently being used to study the acoustics of bubbly media, including bubble entrainment and ambient noise generation, scattering from bubbly structures, and propagation through bubbly media. Future studies include the interaction of bubbles with turbulent fluid flows, bubble coalescence and dissolution, effects of surfactants and contaminants, and bubble-related gas exchange across the air-sea interface.

Remote Sensing

The Remote Sensing Division has developed and installed 74 MHz receivers on the National Radio Astronomy Observatory's Very Large Array (VLA), thereby producing the world's highest angular resolution and most sensitive astronomical interferometric array operating below 150 MHz. In contrast to the VLA's maximum baseline of 35 km, all previous astronomical interferometers operating below 150 MHz had baselines less than 5 km because ionospheric structure had been thought to impose phase variations that would corrupt the interferometric imaging. Work in the Remote Sensing Division has shown that radio astronomical techniques can now remove the ionospheric phase variations and extend interferometer baselines to arbitrary lengths. In its first year of operation, the NRL/NRAO 74 MHz system has been used for a variety of innovative observations with encouraging initial results in solar system, Galactic, and extragalactic astrophysics. The success of the NRL/NRAO 74 MHz system indicates that it is possible to open a new high-resolution, high-sensitivity astronomical window by going to an even larger, more sensitive system. The Remote Sensing Division, in collaboration with the Netherlands Foundation for Research in Astronomy, is currently designing a follow-on instrument, the Low Frequency Array (LOFAR). LOFAR will be a fully electronic, broadband array operating in the 15 to 150 MHz range, with a collecting area of 1 square km at 15 MHz and a maximum baseline of 500-km resolution and sensitivity over the state of the art.

The Remote Sensing Division is also developing other new facilities-class sensors including the Navy Ultrawideband Synthetic Aperture Radar (NUSAR). NUSAR is a fully capable high-resolution (less than 1-m impulse response) synthetic aperture radar system made to be operated from light aircraft. It is fully polarimetric and can operate as an along-track interferometer. Its frequency range will be expandable, and ultimately it will operate from VHF to X-band.

Ocean Research Laboratory

NRL's Ocean Research Laboratory is a 52,000 ft² building that houses the Oceanography Division of the Ocean and Atmospheric Science and Technology Directorate. The building contains office space, oceanographic laboratories, staging areas, a small machine shop, electronic and secure laboratories, and visualization and computing facilities for research and development in ocean science and remote sensing.

Marine Geosciences

The Marine Geosciences Division has greatly enhanced the capabilities and quality of seafloor sediment fabric analyses through completion of installation and staff training for its High-Resolution Industrial CT Scanner. The CT Scanner is a powerful tool for investigating volumetric heterogeneity of materials. By using X rays at energies from 10 to 225 kV and 0-1 mA, the scanner can image single- or multi-phase media with resolving power as fine as 10- μ m voxel size with the microfocus system. The system is capable of rendering and storing real-time radiographic images, reconstructing the images in three dimensions, and processing the images to fit a wide range of project applications.

Vacuum Ultraviolet Space Instrument Test Facility

The Space Science Division facilities include an ultraclean solar instrument test facility in Building A-13 on the main NRL campus. The facility is designed to satisfy the rigorous contamination requirements of state-of-the-art solar spaceflight instruments. The facility has a 400-ft² Class 10 clean room and a large Solar Coronagraph Optical Test Chamber (SCOTCH). This completely dry-pumped, 550-ft³ vacuum chamber is maintained at synchrotron levels of cleanliness. Solar instrumentation up to 1 m in diameter and 5 m in length can be physically accommodated in the chamber. The instrument's optical performance is probed and calibrated with a variety of visible and XUV sources mounted on the chamber's 11-m beamline. The optical testing and characterization of the Large-Angle Spectrometric Coronagraph (LASCO) instrument for the European Space Agency's Solar Heliospheric Observatory satellite were conducted in this chamber. Coronagraph stray-light characterization was carried out by mounting a set of baffles in the main beamline, illuminating the instrument with a simulated solar beam, and measuring the residual radiation. A stray light background measurement of 10⁻¹² was successfully measured in the LASCO C3 channel. Coronagraph calibration was carried out by installing back-illuminated calibrated opals in front of the instrument entrance aperture. Instrument polarization properties were analyzed by using a variety of polarizers installed in a wheel located between the opal and the instrument. The wheel was remotely controlled from outside the chamber. Instrument Mueller matrices were verified with a 12-in. diameter, two-plate partial polarizer. Calibration and focus of XUV solar instrumentation are accomplished by exposing the instrument to an

XUV windowless collimator at the end of the tank. The facility also has a small thermal bake/vacuum test chamber used for vacuum conditioning and thermal testing of spaceflight components and subassemblies. Both the SCOTCH and the small test chamber are instrumented with temperature-controlled quartz-crystal monitors and residual gas analyzers for real-time, quantitative measurements of volatile contamination.

REHABILITATION OF SCIENTIFIC FACILITIES

Specialized facilities are being installed or upgraded in several of the research and support divisions.

Flight Support Detachment

NRL's Flight Support Detachment (FSD) has continued to improve both capabilities and diversity among its aircraft platforms. Aircraft 153442 has undergone extensive modifications with Lockheed Martin to install a "rotodome" antenna and full AEW radar system. The aircraft is currently supporting the Navy's Theater Air Defense programs and providing a testbed for advanced EW radar research. Additionally, all aircraft have completed extensive bomb-bay design improvements that will allow the aircraft to carry more diverse scientific payloads. The Electra Doppler Radar (ELDORA) and a laser were installed on aircraft 154587 during an extensive modification for the BAMEX project, and will be used in upcoming atmospheric research projects. These upgrades and modifications will ensure that NRL will have the finest airborne research capabilities well into this century.

Radar

In FY03 we began to assemble the Advanced Multifunction Radio Frequency Concept (AMRFC) Testbed Facility at the Chesapeake Bay Detachment (CBD). The goal of the AMRFC Program is to demonstrate the integration of many shipboard RF functions, including radar, communications, and electronic warfare (EW) that use a common set of broadband array antennas, as well as common signal and data processing, signal generation, and display hardware. The AMRFC Testbed operates in the nominal 6 to 18 GHz frequency range, and a demonstration is currently planned for FY04 at CBD. The RF functions to be demonstrated include multiple line-of-sight Common Data Link (CDL) communication links, satellite communication links utilizing a commercial Ku-band satellite as well as a military satellite, High Probability of Intercept-

Precision Direction Finding (HPOI-PDF) and High Gain High Sensitivity (HGHS) electronic surveillance (ES) functions, coherent and noncoherent electronic attack (EA) techniques, navigation radar, and an in situ calibration function. The testbed facility is constructed from a network of several $20 \times 8 \times 8$ -ft standard connex shipping containers, and the transmit and receive arrays are embedded into a radar-absorbing structure (RAS) similar to the topside superstructure of future Navy vessels.

Information Technology

The Information Technology Division continues to transition stable technology from high-performance network testbed activities into the NRL local area network. This effort includes support of ATM technology at stream rates of 622 Mbps (OC12c) and 2.5 Gbps (OC48) across the enterprise with demonstrations and technology integration to allow first use of 10 Gbps single streams and higher. The current computing architectures, the SGI Origin3800 and the SGI Altix and Cray MTA, are continuously undergoing upgrade and evaluation of both hardware and software. The NRL CCS works closely with the DOD HPC community and the HPC vendors to provide insight, balance, and value-added capabilities within the MPP testbed infrastructure.

Personnel who work in the Integrated Communications Testing (ICT) Laboratory have extensive knowledge of multiprotocol interactions and are poised to help in future Navy/DOD network research, evaluation, and integration efforts. The ICT facility will be involved in future work providing a transition between high-performance fiber optic technologies and tactical networking.

Plasma Physics

A single-shot, short-pulse (400 fs), high-intensity Table-Top Terawatt (T^3) laser has been recently upgraded for operation with two independently timed beams, one with up to 15 TW and 3×10^{19} W/cm², and the other up to 2 TW for intense laser-matter interaction studies, including particle acceleration. A new 10 Hz ultrashort-pulse (40 fs),

Ti:Sapphire Femtosecond Laser (TFL) system is now operational at 1 TW. These lasers comprise a facility to do fundamental physics experiments in intense laser-plasma interactions, intense laser-electron beam interactions, and intense laser-matter interactions.

The division is building a repetitively pulsed (5 pps) krypton fluoride (KrF) laser called Electra. Electra will develop the technologies needed for inertial fusion energy (IFE). A laser for a power plant would have to fire five times per second, run for several years, and meet stringent cost and efficiency requirements. Electra will develop the technologies that can meet these requirements. It will have a laser output of around 400 to 700 joules. The size of Electra was chosen to be large enough to be scalable to a power plant size, but small enough to be flexible.

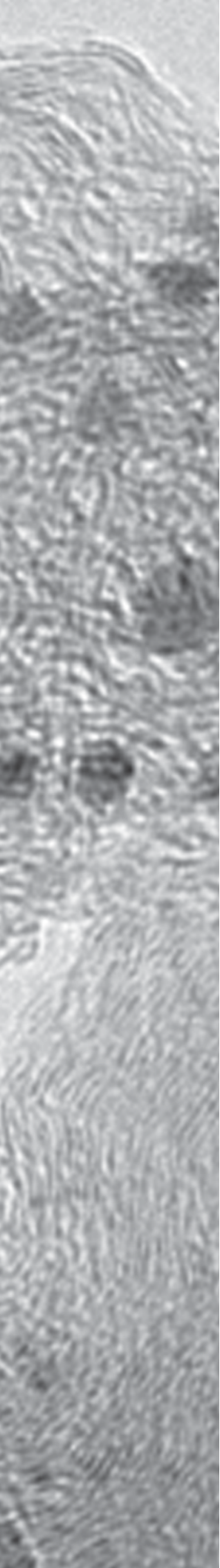
The Plasma Physics Division will be bringing on line the new Mercury pulsed-power generator in FY04. The facility is located in renovated space in Building 256. Mercury is an inductively isolated, voltage-adder device that will be capable of producing a 6-MV, 375-kA, 50-ns electrical power pulse for driving electron beam and ion beam diodes. The new facility will support ongoing radiographic source development for the Department of Energy and nuclear weapons effects simulation for the Defense Threat Reduction Agency.

Electronics Science and Technology

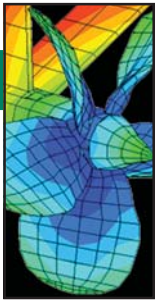
The Electronics Science and Technology Division continues to upgrade and expand its capabilities in nanofabrication science, solar cell characterization, and ultrafast lasers. The Compound Semiconductor Processing Facility (CSPF) will be enhanced with a new capability for chlorine-chemistry inductively coupled plasma etching and an e-beam writer with a wide range of pattern writing ability. The Epicenter will be enhanced with a new AsBr₃ etching source that can be used in the MBE environment. The Space Solar Cell Characterization Laboratory has moved into Building 208 and is being upgraded. The Silicon Carbide Processing Laboratory (SCPL) will be created in 2004 through an absorption and rehabilitation of existing capabilities within the division.

BIO-AEROGEL NANOCOMPOSITE

Transmission electron micrograph of a bio-aerogel nanocomposite. When attached to a 10-nm gold particle (dark spot), the protein cytochrome-c (gray globule) remains functional after incorporation into a silica aerogel host (fine mottled gray region).



- 51** New Horizons in Cathodic Protection Design
V.G. DeGiorgi, E.A. Hogan, and S.A. Wimmer
- 59** Propagation of High-Energy Lasers in a Maritime Atmosphere
P. Sprangle, J.R. Peñano, A. Ting, and B. Hafizi
- 69** Fabrication of a Fast Turn-off Transistor by Wafer Bonding
K.D. Hobart, F.J. Kub, and J.M. Neilson
- 77** Applications of Time-Reversal to Underwater Acoustics
J.F. Lingeitch, C.F. Gaumont, D.M. Fromm, and B.E. McDonald
- 87** WindSat — Remote Sensing of Ocean Surface Winds
P.W. Gaiser



NEW HORIZONS IN CATHODIC PROTECTION DESIGN

V.G. DeGiorgi, E.A. Hogan, and S.A. Wimmer
Materials Science and Technology Division

Computational modeling is a well-established practice in many engineering fields. In the past decade, NRL has applied computational methods, specifically boundary element techniques, to shipboard electrochemical corrosion problems. Boundary element computational methods have been demonstrated as predictive tools for on-hull potential profiles. Hull geometries investigated include U.S. Navy CG hull class cruiser and CVN aircraft carrier. Accuracy was measured by comparison with physical scale model experimental results. These analyses, as well as a series of parametric studies examining basic assumptions, are presented as a review of the validation of boundary element methods for designing shipboard ICCP (Impressed Current Cathodic Protection) systems.

INTRODUCTION

As all sailors know, paint chips and metal corrode when exposed to salt water and the damp harsh marine environment. This is an age-old truth that the U.S. Navy faces. We have a much better understanding today of the nature of corrosion, ways of reducing if not eliminating it, and a host of new tools for design and evaluation. In some instances, advancing technologies have provided a new twist to older methods of corrosion prevention. Cathodic protection (CP) is a method that has been used since the early 1800s to prevent the corrosion of maritime structures such as ships. CP takes advantage of the natural electromotive characteristics of a metal to prevent corrosion. Electrochemical corrosion can be prevented if the potential, or voltage, on a metal is altered past a certain value. This value is unique to each metal. Altering the potential requires the addition of electrons from a source, either from another metal (referred to as sacrificial), or from an active source like a power supply. In a case of two metals combined in one structure, CP is obtained by adding, as the source of electrons, a second metal (anode) that is more electrochemically active than the metal to be protected (cathode). Sir Humphrey Davy in 1824 was the first to use cathodic protection by sacrificial anodes. This was to protect copper sheathing on British Navy hulls by using zinc, tin, or iron. This technique of sacrificial CP is still used. More commonly today, steel is protected with zinc sacrificial anodes. This method of protection for ship hulls requires periodic anode inspection and replacement. For large hulls, it requires a large quantity of sacrificial material that significantly increases the weight of the hull. These limitations have led to the

development of Impressed Current Cathodic Protection (ICCP) systems in which anode current is supplied by a power supply rather than by a sacrificial metal. Because the system now actively controls the corrosion, anodes can be made from noble metals to minimize deterioration, fewer anodes are required because of the increased output capabilities, and feedback control can be included to closely monitor the hull protection levels.

ICCP systems provide good protection against corrosion when they are designed well. The key to a well functioning system is the proper location of all components on the complex hull geometry. Until 1986, ICCP systems were designed empirically and often resulted in hulls that were overpolarized, underpolarized, or contained regions of both, and systems were not designed for the operational life-cycle of the ship. Either polarization extreme can be detrimental to the structure. Overpolarization will cause excess gas evolution and may lead to disbondment of coatings or embrittlement of high-strength materials. Underpolarization means the material may freely corrode.

In this article we discuss two methodologies for determining optimal component locations and for designing optimal ICCP systems. The first is experimentally based and is presently in use by the U.S. Navy. The second, which is under development, relies on computational analyses. The computational analyses method relies heavily on validation using experimental results.

SHIP HULL CATHODIC PROTECTION SYSTEMS — A BASIC INTRODUCTION

Understanding how CP works on ships involves consideration of the ship as an electrochemical system.

Cathodes (hull/propeller) are protected regions, and anodes are either discrete bits of sacrificial metal or electron source points dispersed along the underwater hull at various intervals. For a ship at sea, the wetted surface area of the hull and the appendages (like bilge keel, rudder, and propeller) are the cathodes that require CP. In a new hull state, typically only the propellers and small regions on the hull where the coatings may not be adequate (including small breaks in the paint, which are referred to as paint holidays) require protection. New coatings are usually good dielectric materials and will require little protection. Over time, during the life-cycle of the ship, the coatings will degrade, adsorb moisture, and ultimately expose additional metal surfaces that require increasing levels of protection. Otherwise, corrosion will occur.

A typical ICCP system consists of nonsacrificial noble anodes connected to power supplies, reference cells to monitor hull potential state, and a controller to adjust the current output of the anodes. Anodes must be located so that the current distribution can be uniformly maintained at all points along the underwater hull. Reference cells must be placed at locations that can sense representative regions of the hull and respond effectively as hull state changes. The identification of both anode and reference cell locations is complicated by complex hull geometries and multiple reference control points (zones). A zone is defined as a single controller with input from a reference cell, controlling the output of one or more power supplies through their electrically associated anodes. Because of the size and complexity of the Navy vessel, multiple zones are required to adequately protect the diverse geometric areas of the hull. The U. S. Navy design criteria requires that the potential of

a ship hull be maintained at -0.85 V vs an Ag/AgCl reference cell, $\pm 0.05\text{ V}$.

Experiment-based Design

Physical Scale Modeling (PSM) is an experiment-based ICCP design technique developed by the NRL Center for Corrosion Science and Engineering in 1986. However, the potential and current distribution theory behind this PSM approach was originally defined by Waber and Fagen¹ for scaled electroplating methods that are directly applicable to ICCP design. PSM uses near-exact scale models and scaling factors based on the physics of electrochemical response to provide information on current and potential values on the structure. The models are described as “near-exact” because of the limitations in size and number of components that can be placed on the scaled hull. There is also a limit to the amount of instrumentation that can be attached to the scaled hull. These limitations are defined by the fact that the models are scaled replicas. As much detail as possible is included in the model, but it is not possible to include all features found on a ship. The models, ranging in length from 0.6 to 3.0 m (Figure 1), with a close-up of an aft section shown in Fig. 2, are used along with a scaled electrolyte to provide equivalent ohmic paths. Figure 3 shows a typical ship model with instrumentation in the tank testing facility. These models have been used to design ICCP systems on more than 13 classes of ships. Keeping in mind that experimental techniques, like computational techniques, require validation, the NRL Center for Corrosion Science and Engineering has provided such validation through comparisons with ship data obtained during sea trials.²



FIGURE 1
Typical models.



FIGURE 2
Details of aft end geometry.

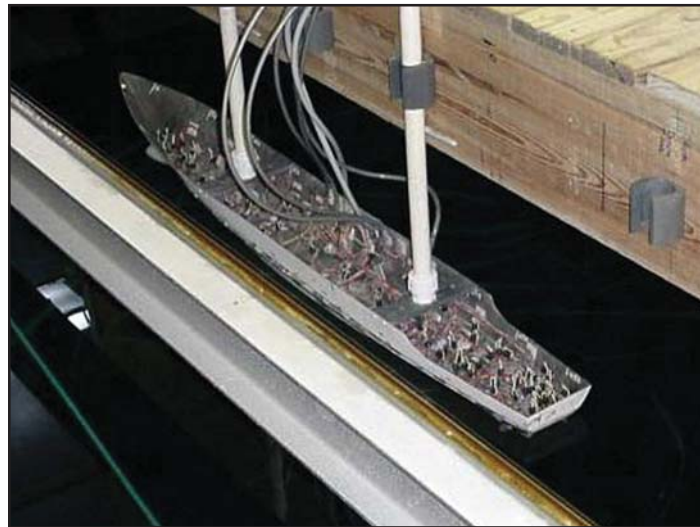


FIGURE 3
Typical model shown in the test tank facility at NRL Center for Corrosion Science and Engineering.

The PSM method has provided the U.S. Navy the ability to effectively design ICCP component placement, life-cycle performance, and various failure modes under both static (dockside) and dynamic (underway) operational conditions for a variety of ship and system configurations. PSM can directly address difficult geometries, areas of restricted flow, protective coatings degradation, advances in ICCP design technologies (i.e., use of digital comptrollers — hardware and software, advanced control algorithms), and complex interaction of power supplies and control algorithms (i.e., zone behavior). The Navy has extensively used PSM as performed by the NRL Center for Corrosion Science and Engineering. Design criteria have been established, and PSM is currently the accepted standard technique for design of U.S. Navy ICCP systems.³ But although PSM provides a valuable tool for today's design engineer, NRL researchers have determined that it may not answer all the needs of the design engineer for tomorrow's Navy.

NRL researchers considered various methods to supplement PSM. They determined that computational modeling could potentially provide the ICCP design engineer with the additional information required in the detailed design of the next generation of these complex systems. Computational modeling allows the designer the freedom to evaluate numerous “what-if” scenarios such as changes in system design, changes in hull geometry, ranges of environmental conditions, and variations in numerous other factors. Computational modeling-based evaluations of complex systems provides the ability to identify and evaluate system problems before a hull design is finalized. Computational modeling also allows systems

to be evaluated based on multiple, and sometimes conflicting, system requirements. Studies can lead to a better understanding of how systems respond under changing conditions. These capabilities meet many of the design requirements for tomorrow's Navy. NRL has focused on developing a validated computational modeling technique for CP systems.

COMPUTATIONAL ANALYSIS

Computational modeling is an established practice in many engineering fields. The ability to develop models has provided the engineer a valuable tool, and changes in design or performance requirements can be easily evaluated without having to resort to the lengthy process of building and testing prototypes. Engineers are now comfortable with using computational methods to design and evaluate “what-if” scenarios and are confident of the accuracy of the computational techniques applied. The key to the confidence in computational modeling in diverse fields (such as nuclear power plant design and automotive design) is the validation process.

Initial computational work on maritime CP systems⁴ involved evaluation of the applicability of computational methods, with the first step being to determine the governing equation. For the case of corrosion on a structure submerged in an electrolyte, this is LaPlace's equation:

$$k\nabla^2\Phi = 0, \quad (1)$$

where Φ is the electric potential and k is the conductivity of the electrolyte. The equation models steady

state conditions and does not address corrosion initiation. Introductory work emphasized the feasibility of applied computational methods to shipboard CP systems. The computational technique most appropriate for the problem of ship hull ICCP systems is the boundary element method. In this type of analysis, a “mesh” is created that is a geometric representation of the interface surface defining the boundary between the structure and the electrolyte. Figure 4 is a full ship computational model of the CVN Nimitz-class aircraft carrier. The mesh details are hidden in this figure, which shows the geometric complexity and indicates region of coating damage for the 15% damage condition. Figure 5 is a detailed view of the aft portion of a ship hull mesh, with calculated potential values superimposed. The interface surface is represented by the underwater portion of the ship hull. The electrolyte is defined as a uniform solution of constant properties and is a reasonable representation of the ocean. Boundary condition equations are used to define the water surface and the response of materials exposed to seawater. The basic material response used in the computational model is the polarization response. The polarization response is the voltage

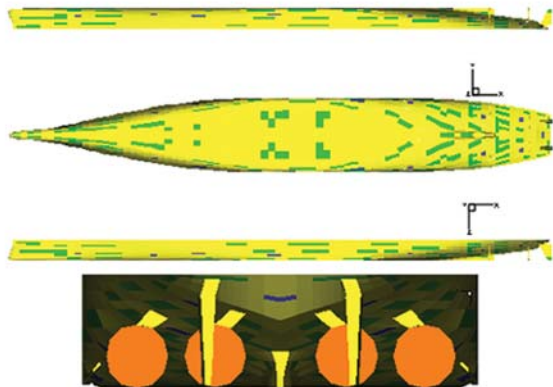
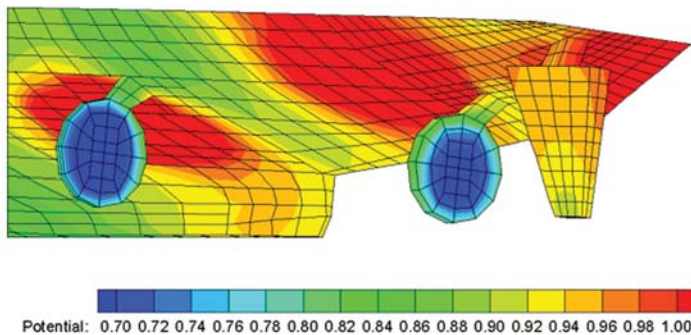


FIGURE 4 Computational model representation of the CVN Nimitz-class aircraft carrier. Green indicates locations of coating damage. Mesh details are hidden. Full ship model.



(potential)-current relationship for a material in the defined electrolyte. Once a defining mesh is created with boundary conditions defined and material properties assigned, numerical techniques, based on Laplace’s equation, are used to solve for the potential and current on the structure and in the surrounding electrolyte.

NRL researchers have conducted both preliminary and more detailed system performance investigations comparing this analysis methodology with PSM to evaluate the validity of the technique. Reference 5 summarizes this multiple-year effort. Results of these evaluations have led to further work that examined material and boundary condition assumptions. Increasing confidence of the community in the application of boundary element methods to shipboard ICCP system calculations has led to questions that require more and more detailed models. In addition, advances in control systems and the complexity of the next-generation ICCP system have increased the need for accurate prediction of system performance under many different operating conditions.

SHIP ANALYSES

The U.S. Navy’s Ticonderoga class of ships are quick-response vessels (cruisers). These vessels are also known as the CG class. These were the first ship CP systems to be modeled by using computational techniques. The Cruiser’s CP systems are relatively simple. Three different systems have been computationally analyzed: one control point (single-zone) system with six anodes, and two dual control point (two-zone) systems with either six or seven anodes, respectively. The first goal of the CG hull series of analyses was to determine the feasibility of using commercial boundary element codes that used Laplace’s equation as the general framework for solving the boundary conditions.

The CG hull series of analyses were highly successful in that comparison with PSM-based experimental results with calculated values were very good. For instance, calculated and experimental values of total current for minimum damage in static water (dockside) conditions were 64.0 amps (A) and 64.9 A, respectively,

FIGURE 5 Details of boundary element mesh of CVN Nimitz-class ship. Calculated potential (V) contours for minimum damage static water conditions are shown. Boundary element model uses smooth disk representations for propellers.

with a difference of only 1.4%. A detailed review of results determined that the accuracy of computational data is directly related to the accuracy of the input polarization response data. However, even with poor material polarization curves, ICCP performance trends were similar in behavior. It was also observed that the computational mesh could be used for basic system design and response work, although not for validation of a design. In addition to basic feasibility studies, the CG hull was used for analyses that evaluated basic modeling assumptions. Specifically, mesh refinement, internal program parameters, variations of environmental conditions, and methods for modeling small regions of paint damage were examined.⁶ All of the findings of these studies were relevant to establishing rigorous computational design parameters. By reviewing the results, appending more precise information, and supplementing the code, the analyst is learning about how to construct a computational model that will provide accurate results.

Finally, a question was raised that must be answered. Can we take what we have learned from the CG hull analyses and use the model building information as guidelines for creating a model of an entirely different hull form? The CVN Nimitz-class Carrier was the next hull chosen for analysis; it was selected because it was as different from the Ticonderoga Cruiser class in geometry as possible. The existing CVN CP system was large, with 17 anodes. It had three zones, with a total amperage output of 1800 A, as compared to the CG ICCP systems, which were either a single-zone 450 A system or a two-zone 600 A system. The computational analyst went about creating the boundary element mesh of the CVN hull, keeping in mind all of the lessons learned from the CG hull class.

Even with the most powerful computers available, it is not possible to include all physical features on a computation in a timely manner. Computational modeling always consists of compromises. The analyst has to determine which features to include and how large the model can be. Model size relates to computer capability (memory and storage), run times,

and costs. The result is that any computational analysis involves some simplifying assumptions, and the CVN model was created so that it pushed the limit of available computer memory. As computer systems have become more powerful, NRL researchers have added more details to this model. Figure 6 calculates potential values for the latest CVN hull mesh. The mesh is hidden in this figure. This model includes detailed propeller geometries — features that were absent in the original computational model.

The CVN boundary element mesh, as originally defined, relied on symmetry and also used solid disks to represent the propellers. These geometric simplifications were mandated by computer resources available at the time. Despite these simplifications, the calculated results showed very good agreement within experimental values. The primary products of a computational analysis are the potential map of the hull surface and the anode current required to maintain the reference potential at target values. The computational method supplies potential values at all points on the hull, whereas the experimental data are available only at discrete points. Therefore, potential profiles along longitudinal sections of the hull were compared individually rather than mapping the potential distribution across the entire surface. For all combinations of coatings damage and static/dynamic flow conditions considered, the computational results closely resembled the PSM experimental profiles in both shape and magnitudes. Reference 7 shows these comparisons in considerable detail. Where discrepancies have occurred between the computational and PSM results, such as the condition of 15% coatings damage under both static and dynamic flow conditions, the computational model underpredicted current requirements by 14.1% for the static case and by 6.5% for the dynamic case. Two possible sources of the variation in calculated and experimental results were insufficiencies in the material polarization response curves and oversimplification of the critical geometric details, such as the propeller mesh.

The material response curves can be very complex in nature when describing the actual behavior of

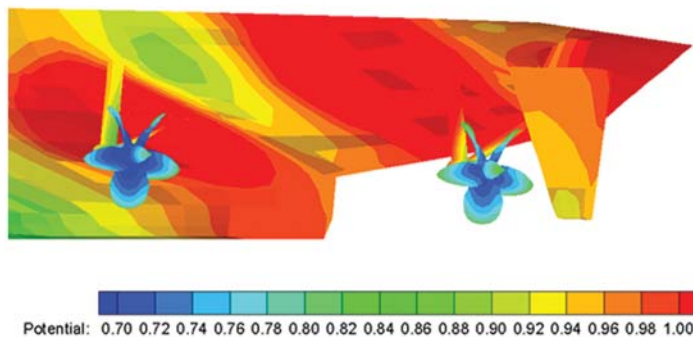


FIGURE 6

CVN Nimitz-class aircraft carrier, showing calculated potential (V) contours for 15% coating damage static (dockside) water conditions. Boundary element model uses detailed representations of propellers. Mesh is not shown in this figure.

metals on a hull. Insufficiencies could have been related to, but not limited to, time-based cathodic film formation, the lack of incorporation of a “mixed potential” materials response, and variations of the polarization behavior based on the spatial relationship between cathode location and the anodes. These are material electrochemistry issues that cannot be addressed by the computational code as it is now written, but are areas identified for future work.

The geometric modeling details can be addressed because of advances in computational capabilities. The most recent CVN model incorporates detailed representations of the propeller and shaft assemblies. Two propeller representations actually have been created for the CVN model, one for the static case and one for the dynamic flow condition. Figure 7 shows the aft mesh details with the potential contours for 15% coatings damage and static water conditions. Individual propeller blades are included in the representation. The second model, shown in Fig. 8, is used for ship underway conditions. It shows a fast spinning propeller mesh, which gives the model a dynamic materials response, and current shielding properties representative of a rotating propeller. As can be seen by comparing the contour maps in Figs. 5 and 6, the two different geometries resulted in very different potential profiles on the supporting struts. Detailed models, such as the ones shown here, provide the designer the ability to look both at overall response and in detail at smaller regions of interest.

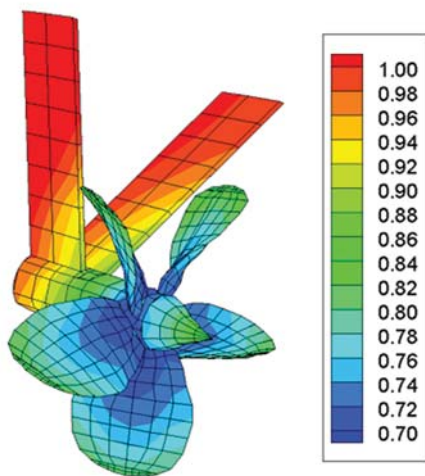


FIGURE 7
Detail of propeller of CVN Nimitz-class aircraft carrier showing calculated potential (V) contours for 15% coating damage static (dockside) water conditions. Boundary element model uses detailed representations of propellers.

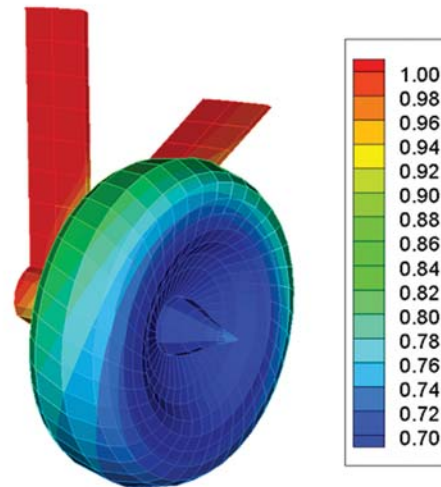


FIGURE 8
Detail of propeller of CVN Nimitz-class aircraft carrier showing calculated potential (V) contours for 15% coating damage dynamic (ship underway) water conditions. Boundary element model uses detailed representations of propellers.

GUIDELINES FOR USE OF BOUNDARY ELEMENT METHODS

Computational model results can be evaluated at two levels. One is concerned only with relative response behaviour, i.e., what can be determined about the performance of a known ICCP system on a specific hull. At the second level, the analyst is concerned with both detailed analyses that provide highly accurate results and advanced life-cycle analyses. Evaluation at this higher level is what is required for the development of an engineering design methodology. By rigorously exercising the commercial code up to this second level, NRL researchers have developed a set of guidelines to assist the development of new models.⁵ The guidelines are:

- A more refined model is needed than is traditionally associated with boundary element techniques.
- Accurate modeling of relatively small-scale features, such as bilge keels, struts, propeller, and shaft are necessary.
- The accuracy of computational results is directly dependent on the accuracy and appropriateness of the polarization data used as material characterization input data.
- Preliminary design and trend studies can be successfully completed using less than optimum polarization data. Trends in performance can be determined even though magnitudes will be suspect.
- Variations in seawater conductivity that correspond to changes in deployment region can be

significant to system performance and should be incorporated into the design basis.

- Modeling damaged paint as totally bare metal is a conservative approach. The selection of appropriate cathodic sites within the mesh that are representative of the hull structure and known damage profiles is essential to an accurate analysis.
- Modeling paint as a perfect dielectric material is acceptable, depending on the accuracy of results required.

These guidelines are part of the development of a design methodology that will allow the Navy community to apply computational methods to CP system design with confidence.

SUMMARY

Corrosion is a problem that is of great concern for all maritime structures, including U.S. Navy ships. CP systems are a necessary defense against corrosion and are one of the principal tools used to minimize coatings degradation over time. Past empirical design methodologies used for shipboard CP systems (design rules, past practices, or designer expertise) were seriously deficient and were not applicable to the new ship designs, new materials, and changing deployment environments. The U.S. Navy needed something better than the status quo, and NRL responded. NRL, with the support of the Naval Sea Systems Command, developed a physics/electrochemical-based experimental methodology for the PSM ICCP design that has been the standard technique for 17 years. Looking toward the future and building on the PSM expertise, NRL has led research efforts in applying computational techniques to this problem. The development of computational methodology is underway, and work to date has shown the capability of computational methods. But this effort is far from complete. NRL has developed the skeletal framework for a comprehensive computational design methodology that goes beyond ICCP design and one that can support future U.S. Navy requirements. The work that has been presented here is part of an ongoing research project that closely links computa-

tional with experimental validation. The ultimate goal is to provide the U.S. Navy with a robust design tool that can be used with confidence on existing and new designs, including evaluations of new materials and advanced electronic control systems. Paint will probably always chip and metal will corrode. If left unchecked, corrosion will ultimately result in the removal of a ship from service. Advances in technology, such as the application of computational methods to ICCP system design, are part of the U.S. Navy's next generation of tools for corrosion control.

ACKNOWLEDGMENTS

The authors acknowledge Dr. Alexis Kaznoff and Mr. E. Dail Thomas, Naval Sea Systems Command, for their long-standing support of this effort. In addition, the authors thank Mr. Keith E. Lucas, NRL Code 6130, for his support and assistance to their research efforts.

[Sponsored by NAVSEA]

References

- ¹ J.T. Waber and B. Fagen, "Mathematical Studies of Galvanic Corrosion," *J. Electrochem. Soc.* **103**(1), 64-72 (1956).
- ² A.R. Parks, E.D. Thomas, and K.E. Lucas, "Verification of Physical Scale Modeling with Shipboard Trials," *Corrosion 90*, Paper 370, National Association of Corrosion Engineers (1990).
- ³ K.E. Lucas, E.D. Thomas, A.I. Kaznoff, and E.A. Hogan, "Design of Impressed Current Cathodic Protection Systems for the U.S. Navy," *Designing Cathodic Protection Systems for Marine Structures and Vehicles*, American Society for Testing and Materials, Special Technical Publication (STP) **1370**, H.P. Hack (ed.), 17-33 (1999).
- ⁴ R.A. Adey and S.M. Niku, "Computer Modeling of Corrosion Using the Boundary Element Method," *Computer Modeling in Corrosion*, American Society for Testing and Materials, Special Technical Publication (STP) **1154**, R.S. Munn (ed.), 248-264 (1992).
- ⁵ V.G. DeGiorgi, E. Hogan, K.E. Lucas, and S.A. Wimmer, "Computational Modeling of Shipboard ICCP Systems," *J. Corrosion Sci. and Eng.* (<http://www2.umist.ac.uk/corrosion/JCSE/>), **4**, Paper 3 (2003).
- ⁶ V.G. DeGiorgi, A. Kee, K.E. Lucas, and E.D. Thomas, "Examination of Modeling Assumptions for Impressed Current Cathodic Protection Systems," in *Proceedings of the Corrosion '99 Research Topical Symposium, Cathodic Protection: Modeling and Experiment*, National Association of Corrosion Engineers, 1-16 (1999).
- ⁷ V.G. DeGiorgi, E.D. Thomas, and K.E. Lucas, "Scale Effects and Verification of Modeling of Ship Cathodic Protection Systems," *Eng. Anal. Bound. Elements* **22**, 41-49 (1998).

THE AUTHORS



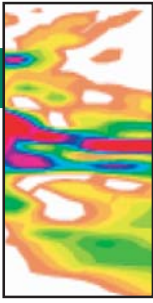
VIRGINIA G. DeGIORGI is Head of the System Design and Integration Section in the Multifunctional Materials Branch. Dr. DeGiorgi received her B.S. and M.E. degrees from the University of Louisville in 1980. She then went to work for Westinghouse Electric Corp. nuclear steam generator division. She completed her Ph. D. work at Southern Methodist University, Dallas, in 1986. She joined NRL soon afterward. In addition to her research at NRL, she is serving part-time at ONR as a program manager. She served two years on the Office of Naval Research's TechSolutions program, a Fleet-focused initiative for the rapid transition of technology. She is currently serving part-time as a program manager on the Office of Naval Research's Swampworks program.



ELIZABETH A. HOGAN is a physical scientist for the Materials Science and Technology Division. She is a graduate of UCLA and has more than 18 years of experience in conducting research and engineering efforts in the area of materials selection and cathodic protection design for marine applications. Her primary research focus is in the area of physical scale modeling for the design of Impressed Current Cathodic Protection systems and associated electric field analysis. Additionally, she has been conducting nickel alloy crevice corrosion research and ballast tank corrosion sensor development. Her past engineering research efforts have included studies to evaluate the effects of chlorination on marine materials, characterization of coatings for thermal insulation effectiveness, and assessment of seawater reference half-cell technology.



STEPHANIE A. WIMMER received her Ph.D. from the Naval Architecture and Marine Engineering Department, University of Michigan, in 1998. She holds a dual M.S.E. from the Aerospace Department and the Naval Architecture and Marine Engineering Department in 1997. She received her B.S. in Ocean Engineering from the Civil Engineering Department at Texas A&M University in 1993. Prior to joining NRL in 2002, she worked as a contractor with Nova Research, Inc. Before coming to NRL, she was a postdoctorate associate in the Science-Based Materials Modeling Department at Sandia National Laboratories, California. Her research interests include marine structural mechanics, damage mechanics and prognostics, numerical simulations (finite-element, mesh-free, and large systems), computational modeling of crack propagation using decohesion theories, computational simulations of electrochemical systems, and anisotropic material response evaluation.



PROPAGATION OF HIGH-ENERGY LASERS IN A MARITIME ATMOSPHERE

P. Sprangle, J.R. Peñano, and A. Ting
Plasma Physics Division

B. Hafizi
Icarus Research, Inc.

The free electron laser (FEL) is potentially capable of producing high average power at high efficiency without the conventional thermal management and waste issues associated with other laser systems. In addition, the operating wavelength of the FEL can be chosen for optimized propagation in a maritime environment. These unique features make the FEL a leading candidate for naval directed-energy applications. This article addresses the key physical processes that affect the propagation of FEL beams and discusses the optimum choice of wavelength for propagation in a maritime environment. A number of physical processes affect the propagation of high-energy lasers in air. These include molecular and aerosol absorption/scattering, thermal blooming, turbulence, and other nonlinear processes. HELCAP is a fully 3-D, time-dependent simulation code used to model high energy laser (HEL) propagation in a maritime atmosphere. The laser power delivered to a distant target vs transmitted laser power is shown for a specific maritime atmosphere.

INTRODUCTION

One of the Navy's primary interests in a laser-based directed energy weapon (DEW) system arises from the need for antiship cruise missile and tactical air defense. The Navy is currently considering two main classes of laser systems for DEW applications. These are the free electron laser (FEL) and the solid-state diode pumped laser. The FEL can be designed to operate over a wide range of wavelengths and is capable of generating high average power at high efficiency.¹ Diode pumped solid-state lasers can operate at a limited number of discrete wavelengths and, in principle, can be compact and efficient. The Navy's future all-electric-ship can make available a significant amount of electrical power for a laser-based system. The major elements of this system, which are presently being studied and evaluated, include the high average power laser source, beam control, atmospheric propagation, and lethality.

This article addresses key physical processes associated with the propagation of high-average power laser beams in a maritime environment. A number of physical processes affect and limit the amount of laser energy that can be delivered to a target. These effects are interrelated and include thermal blooming, turbulence, and molecular/aerosol absorption and scattering. These processes affect the

laser intensity profile by modifying the refractive index of the air, which causes the laser beam wavefront to distort. Wavefront distortion results in enhanced transverse laser beam spreading, and can severely limit the amount of energy that can be propagated. The maritime environment is particularly challenging for high energy-laser (HEL) propagation because of its relatively high water vapor and aerosol content. In the infrared regime, water molecules and aerosols constitute the dominant source of absorption and scattering of laser energy, and represent a limitation for HELs propagating in a maritime atmosphere.

Absorption and scattering of laser energy by molecules, water vapor, and aerosols is a strong function of wavelength.² Therefore, the choice of laser wavelength is critical for maximizing the laser energy that can be delivered to a target. One of the major advantages of using an FEL for the DEW system, besides its potential for high average power and efficiency, is its ability to operate at a predetermined wavelength. Absorption of laser energy causes local heating of the air. The resulting local reduction in both the air density and refractive index causes the laser beam to undergo thermal blooming, i.e., defocusing. This deleterious process can be significantly reduced by choosing an operating wavelength in an atmospheric window where the absorption is low. Figure 1 shows the extinction coefficient, i.e., sum of scattering

and absorption, as a function of wavelength. As shown in Fig. 1, there are several molecular transmission windows in the infrared wavelength range near 1, 1.6, and 2.2 μm .

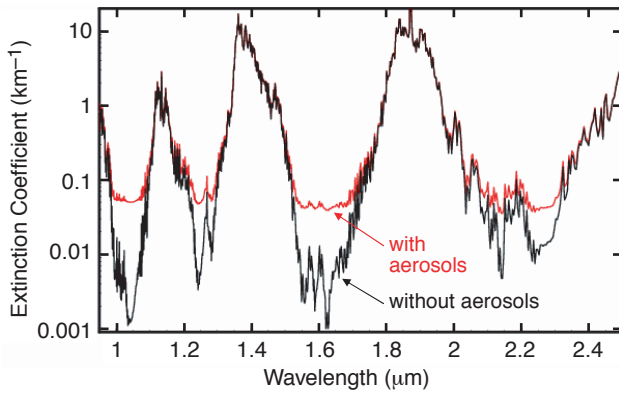


FIGURE 1 Extinction coefficient of air with (red) and without (black) aerosols vs wavelength for a midlatitude summer (MLS) Navy maritime environment with 50-km visibility. The extinction coefficient was generated using MODTRAN.

In a maritime environment, water vapor absorption plays a major role in determining optimal wavelength. Water vapor has a transmission window centered at 1.045 μm , which is sufficiently broad to permit the propagation of a train of ultrashort pulses characteristic of FELs (Fig. 2). That is, the spectral width associated with the FEL pulses lies well within the water vapor window at 1.045 $\mu\text{m} \pm 0.004 \mu\text{m}$, as shown in Fig. 3. The detailed line structure within the atmospheric windows at 1.6 μm and 2.2 μm results in a higher effective absorption for ultrashort FEL pulses. It should be noted that there are diode-pumped solid-state lasers based on neodymium-doped lithium yttrium fluoride (Nd:YLF) crystals that lase at 1.047 μm and, in principle, can also operate within the water vapor window.

The physical processes described above are modeled using the propagation code HELCAP (High Energy Laser Code for Atmospheric Propagation).

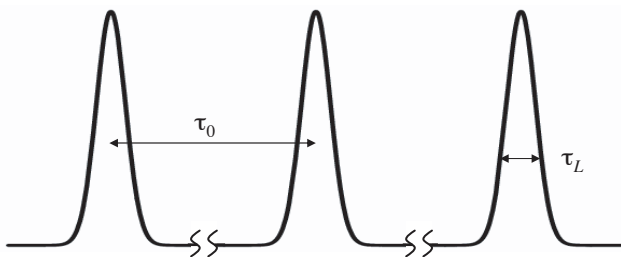


FIGURE 2 Schematic diagram of a pulse train characteristic of an FEL. The duty factor of the pulse train is τ_L/τ_0 .

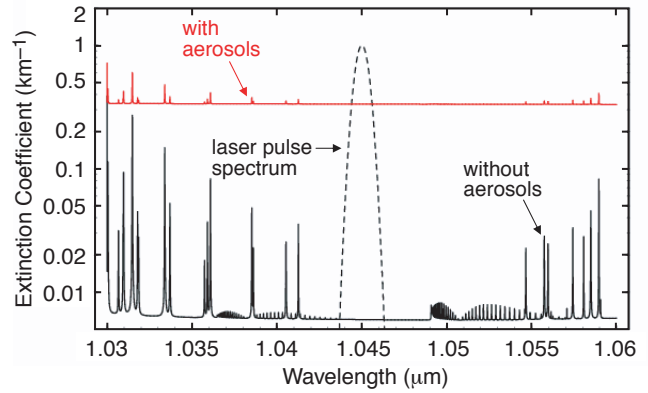


FIGURE 3 Extinction coefficient vs wavelength with (red) and without (solid black) aerosols showing in detail the transmission window near $\sim 1 \mu\text{m}$. The extinction coefficient was generated using PLEXUS/FASCODE 3 for the same maritime environment as Fig. 1. The dashed curve is a sketch of the spectrum of an ultrashort laser pulse. Note that the continuum absorption at $\sim 1.045 \mu\text{m}$ is $\sim 6 \times 10^{-3} \text{ km}^{-1}$, which is somewhat higher than the absorption coefficient calculated using MODTRAN 4.

HELAP is a 4-D (3-D space + time) computer simulation developed at NRL that models the propagation of HEL beams through air affected by a variety of linear and nonlinear processes. The code self-consistently solves a set of coupled nonlinear equations for the laser beam and surrounding air medium. The present version of HELCAP includes thermal blooming, molecular and aerosol absorption/scattering, turbulence, Kerr focusing, ionization, stimulated rotational Raman scattering, laser energy depletion due to ionization, collisions, and quantum saturation effects. Not all of these processes are important in the parameter regime of interest here. However, the capability exists to model the propagation of laser pulses with much higher intensities for a number of other applications.

ATMOSPHERIC HEL PROPAGATION

In this section we discuss key processes that affect atmospheric propagation of FELs in general, and present the physical model that forms the basis for the HELCAP propagation code. For the parameter regime considered here, key physical processes are thermal blooming, turbulence, and molecular/aerosol absorption and scattering. HELCAP models all of these processes in a fully time-dependent manner. In addition, it has the capability to model transient thermal blooming effects and propagation through stagnation points, i.e., regions of vanishing wind velocity where thermal blooming is enhanced.

In the HELCAP model, the laser electric field $\mathbf{E}(x, y, z, t)$ is written as $\mathbf{E}(x, y, z, t) = A(x, y, z, t) \exp(i(k_0 z - \omega_0 t)) \hat{\mathbf{e}}_x/2 + c.c.$, where A is the complex laser

amplitude, i.e., amplitude and phase, k_0 is the carrier wavenumber, ω_0 is the carrier frequency, z is the propagation coordinate, $\hat{\mathbf{e}}_x$ is a transverse unit vector in the direction of polarization, and *c.c.* denotes the complex conjugate. The spatial rate of change of the complex laser amplitude is found to be^{3,4}

$$\frac{\partial A}{\partial z} = \frac{1}{2} \left[\frac{i}{k_0} \nabla_{\perp}^2 - 2ik_0(\delta n_{TB} + \delta n_T + \delta n_A) - \alpha - \beta \right] A, \quad (1)$$

where $k_0 = n_0\omega_0/c$, n_0 is the ambient refractive index of air; c is the vacuum speed of light; δn_{TB} , δn_T , and δn_A represent the change in the refractive index due to thermal blooming, turbulence, and aerosols, respectively; α is the molecular/aerosol absorption coefficient; and β is the molecular/aerosol scattering coefficient. In calculating the aerosol contributions to α and β , the size distribution and type of aerosol must be considered. Here, we use absorption and scattering coefficients generated using the “maritime” aerosol model of the atmospheric transmission codes MODTRAN and FASCODE. The extinction coefficient refers to the sum $\alpha + \beta$.

Equation (1) for the laser amplitude is self-consistently coupled to models for the atmospheric medium through various source terms appearing on the right-hand side of the equation. In what follows, we describe the models for the various terms.

Thermal Blooming

Propagation of a laser beam in the atmosphere results in a small fraction of the energy being absorbed by the air. The absorbed energy locally heats the air and leads to a decrease in the air density. The resulting change in the refractive index is given by $\delta n_{TB} = (n_0 - 1) \delta\rho/\rho_0$ where ρ_0 and $\delta\rho$ are the ambient and perturbed air mass density, respectively. This refractive index variation caused by the local heating of the air leads to a defocusing or spreading of the laser beam known as thermal blooming.

The perturbed air mass density may be calculated by using a hydrodynamic description of air. Analysis of thermal blooming starts with the fluid equations for continuity, momentum, and energy, as well as the ideal gas law. The HELCAP code solves a general set of coupled, linearized fluid equations for the perturbed air density and temperature change caused by the laser. The source term for the perturbed air mass density is the rate at which laser energy density is absorbed, $\alpha\langle I \rangle$, where α is the total effective absorption coefficient and $\langle I \rangle = (c/8\pi)\langle |A|^2 \rangle$ is the average laser intensity. Thermal blooming is a sensitive function of the heating mechanisms present in air.

Aerosol heating also affects thermal blooming by heating the surrounding air by a number of mechanisms.

Molecular Absorption

Molecular absorption of laser energy occurs at discrete but closely spaced lines (wavelengths). For example, Fig. 3 shows the absorption of air near the 1- μm transmission window. The absorbed laser energy goes into exciting the rotational and vibrational modes of the air molecules. The rotational/vibrational energy goes into heating the air through collisional processes that take place on a molecular collision time scale of ~ 100 ps – 200 ps. Thermal blooming occurs on a much longer, hydrodynamic, millisecond time scale.

Although nitrogen and oxygen are by far the most abundant molecules comprising air, they have no permanent electric dipole moments and are, therefore, relatively free of absorption lines in the infrared. Polar molecules such as H_2O , on the other hand, have permanent dipole moments and are typically strong absorbers in the infrared (IR) regime. The vibrational-rotational transitions in these molecules absorb in the mid-IR, while their rotational transitions lie in the far-IR. For HEL propagation in the maritime environment, water molecules are by far the most important IR absorbers at low altitudes. Ultrashort laser pulses have spectral widths sufficiently broad to generally overlap a number of absorption lines. The effective absorption coefficient $\bar{\alpha}_M$ is obtained by taking the appropriate overlap integral of the laser pulse spectrum and the absorption spectrum.

In the atmospheric window near 1 μm , the molecular absorption for an ultrashort laser pulse is determined mainly by the continuum absorption, as shown in Fig. 3. However, there is still a need for experiments to accurately determine the continuum absorption coefficient.

Turbulence

Turbulence affects the propagation of a laser beam through fluctuations in the refractive index caused by thermal fluctuations in the air. These fluctuations are inherent in the air and are not induced by the laser. Hence, unlike thermal blooming, the effect of turbulence on the laser propagation is independent of laser intensity. Modeling of turbulence is implemented by introducing fictitious phase screens at regular intervals along the propagation path. The screens randomize the phase of the laser field and represent the cumulative effect of turbulence on propagation between the two phase screens.

The Fourier transform of the fluctuating part of the refractive index due to turbulence can be expressed in terms of the spectral density function $\Phi_n(k_\perp, z)$, where $k_\perp = (k_x^2 + k_y^2)^{1/2}$ is transverse wavenumber. The modified von Karman spectral density function is given by $\Phi_n(k_\perp, z) = 0.033C_n^2 ((2\pi/L_0)^2 + k_\perp^2)^{-11/16} \exp[-k_\perp^2 \ell_0^2/35]$, where C_n^2 is the refractive index structure constant, L_0 is the outer scale length, and ℓ_0 is the inner scale length. Typical values for the inner and outer scale lengths are 1 and 100 m, respectively.

Turbulence can lead to both spreading and wandering of the laser beam. For an initially collimated beam with spot size (radius) w_0 propagating over a distance L , the increase in the laser spot size due to turbulence is given by $\rho_{spread} = (\lambda/\pi \rho_c)L$, where the transverse coherence length is given by $\rho_c \approx 0.158 \lambda (\lambda^{1/3} / C_n^2 L)^{3/5}$. Turbulence also causes the collimated beam centroid to wander transversely by the average amount, $\rho_{wander} \approx 1.14[C_n^2 L^3 / (2w_0)^{1/3}]^{1/2}$. The ratio of the beam wander to the beam spread is $\rho_{wander}/\rho_{spread} \approx 0.5$ and is relatively insensitive to laser and atmospheric parameters.

Adaptive optics can be used to correct for wavefront distortions due to turbulence, which is a process independent of intensity. Thermal blooming, however, is a highly nonlinear process and can only be modestly mitigated by conventional adaptive optics techniques. To correct for thermal blooming distortions, both the wavefront as well as the intensity of the transmitted laser beam must be compensated.

Maritime Aerosols

Aerosol scattering and absorption can play a significant role in limiting the laser energy that can be delivered to a target. Maritime aerosols consist of water droplets distributed over a wide range of radii ($R_A \sim 0.01$ to $10 \mu\text{m}$) and densities ($n_A \leq 10^3 \text{ cm}^{-3}$). The average water content of aerosols is typically far less than that of humid air. For example, at a temperature of 30°C and relative humidity of 50%, the water vapor mass density is $\rho_{wv} \sim 1.5 \times 10^{-5} \text{ g/cm}^3$, while the average mass density of maritime aerosols is typically far less, $\leq 10^{-9} \text{ g/cm}^3$. For oceanic water, the absorption coefficients are $\alpha_w \sim 7, 20,$ and 50 cm^{-1} at the wavelengths $\lambda \sim 1.045, 1.625,$ and $2.264 \mu\text{m}$, respectively. For pure water, note that the absorption coefficients are somewhat less than for oceanic water. Unlike water vapor, there are no absorption windows for liquid water since the molecular collision frequency is $\sim 10^3$ higher in liquids.

Although the average water mass density of maritime aerosols is small, it can have a large effect on the scattering of laser radiation. In the Rayleigh limit,

the laser wavelength is large compared to the aerosol radius $\lambda \gg R_A$, and the scattering coefficient is proportional to $R_A^6 \sim N_w^2$, where N_w is the number of water molecules in the aerosol. This is a factor of N_w larger than molecular Rayleigh scattering for the same number of water molecules. In the Mie limit, the laser wavelength is small compared to the aerosol radius $\lambda \ll R_A$, and the scattering coefficient is proportional to $R_A^2 \sim N_w^{2/3}$. The number of water molecules in an aerosol is large, e.g., for $R_A = 0.1 \mu\text{m}$, $N_w \sim 10^8$ water molecules. The aerosol scattering coefficient in the wavelength range of interest can be as large as $\beta_A \sim 0.2 \text{ km}^{-1}$.

The rate at which laser energy is absorbed determines the degree of thermal blooming. The thermal blooming source term can be written as $\alpha \langle I \rangle = \bar{\alpha}_M \langle I \rangle + \gamma_{AC}$. The molecular absorption coefficient $\bar{\alpha}_M$ is given by an overlap integral of the molecular absorption coefficient and the laser pulse spectrum, and is a sensitive function of the laser wavelength and pulse length. The aerosols absorb laser energy. The heated aerosols transfer part of their thermal energy to the surrounding air through conduction; this contribution is contained in γ_{AC} . The time scale for heat conduction from the aerosol into the surrounding air is given by $\tau_c \sim \ell^2 / D$, where D is the diffusion coefficient and ℓ is on the order of the interaerosol spacing.

SIMULATIONS OF HEL PROPAGATION IN A MARITIME ATMOSPHERE

In this section we present results of numerical simulations of the propagation of a high-energy laser beam through a maritime environment. For the present study, the HELCAP simulation solves Eq. (1) for the laser envelope and self-consistently tracks the nonlinear response of air. We consider the propagation of FEL pulse trains with wavelengths in the 1.045, 1.625, and 2.264- μm transmission windows. The pulse trains used in the HELCAP simulations are composed of Gaussian pulses with intensity $I = I_{peak} \exp[-(t - z/c)^2 / \tau_L^2] \exp(-2r^2/w_0^2)$, pulse duration τ_L , pulse separation τ_0 , and initial spot size w_0 . The average intensity associated with this pulse train is given by $\langle I \rangle = \sqrt{\pi} I_{peak} \tau_L / \tau_0$. The focusing geometry is illustrated in Fig. 4(a).

We consider a specific maritime atmosphere that is representative of moderate propagation conditions. The atmosphere is characterized by an average aerosol mass density of 10^{-9} g/cm^3 and a uniform wind. Table 1 lists the absorption and scattering coefficients used in the simulations. These coefficients are consistent with the ‘‘maritime’’ atmospheric model used in FASCODE. The ambient air tempera-

ture is assumed to be 296 K. The turbulence is characterized by index $C_n^2 = 10^{-16} \text{ m}^{-2/3}$, inner scale length $\ell_0 = 1 \text{ cm}$, and outer scale length $L_0 = 100 \text{ m}$.

Figure 4(b) shows the results of several simulations for propagation of a high average power FEL beam in the 1.045, 1.625, and 2.264- μm transmission windows. The figure plots P_{target} vs laser wavelength, where the quantity P_{target} is a figure of merit representing the average power at the target range within a given area centered about the peak. The results indicate that the power delivered to the target is highest when propagating in the 1.625- μm transmission window compared to the 1.045 and 2.264- μm windows. In the 2.264- μm transmission window, the large molecular absorption severely limits the power delivered.

Figure 5 plots the normalized average power on the target vs power at the transmitter for the 1.045

and 1.625- μm wavelengths. For lower transmitted powers, the power delivered on target at 1.625- μm is slightly greater than for 1.045- μm because of the lower scattering coefficient at 1.625- μm . However, because of the higher molecular absorption at 1.625- μm , thermal blooming significantly decreases the efficiency of this wavelength at higher power levels.

Figure 6 plots laser intensity vs time and transverse coordinate x at the target range for 1.045 and 1.625- μm wavelengths. Note the deflection of the trailing parts of the beam into the wind due to the time-dependent nature of the thermal blooming process.

Figure 7 shows the cross-sectional plots of average laser intensity on target for the three wavelengths of interest. The beam cross sections for the 1.045 and 1.625- μm wavelengths show a relatively well-focused beam with little deflection. However, the 2.264- μm

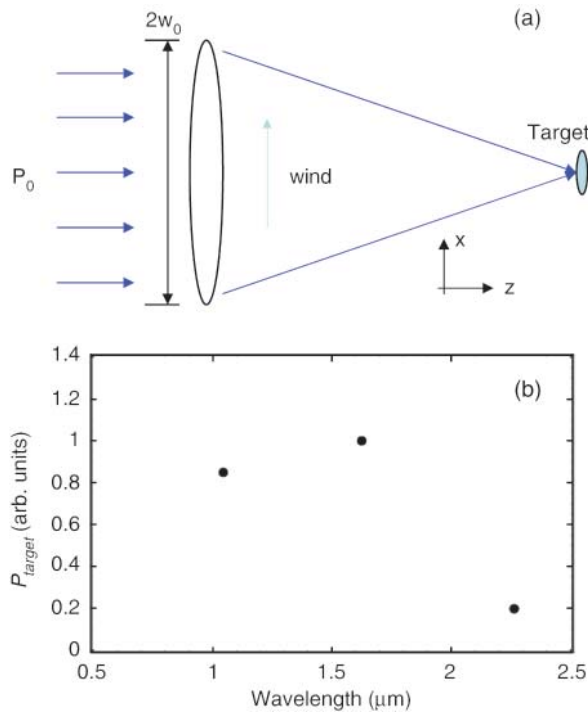


FIGURE 4

(a) Schematic illustration of the focusing geometry used in the simulations. The atmosphere is characterized by an average aerosol mass density of 10^{-9} g/cm^3 , turbulence with index $C_n^2 = 10^{-16} \text{ m}^{-2/3}$, and scale lengths $\ell_0 = 1 \text{ cm}$ and $L_0 = 100 \text{ m}$, and a uniform wind. The absorption and scattering coefficients used in the simulations are listed in Table 1. (b) Simulation results showing average power in arbitrary units within the target area for laser wavelengths $\lambda = 1.045, 1.625, \text{ and } 2.264 \text{ } \mu\text{m}$.

Table 1. Values of the Molecular and Aerosol Absorption Coefficients, and Aerosol Scattering Coefficients Used in the Numerical Simulations for Propagation at 1.045, 1.625, and 2.264- μm Wavelengths. Coefficients were Obtained using the Standard Maritime Atmospheric Model of MODTRAN. (Courtesy of Dan Leslie, Trex Enterprises.)

Wavelength (μm)	Molecular Absorption Coefficient (km^{-1})	Aerosol Absorption Coefficient (km^{-1})	Aerosol Scattering Coefficient (km^{-1})
1.045	0.001	0.0032	0.32
1.625	0.002	0.0035	0.27
2.264	0.01	0.0032	0.22

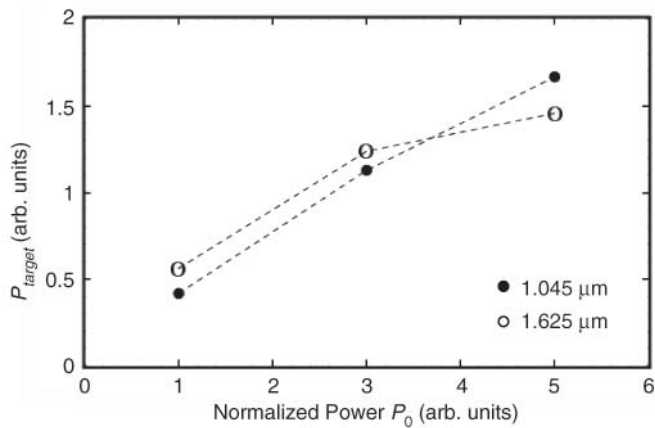


FIGURE 5 Average power on target vs normalized laser power at the transmitter P_0 for wavelengths $\lambda = 1.045 \mu\text{m}$ (filled circles) and $\lambda = 1.625 \mu\text{m}$ (open circles).

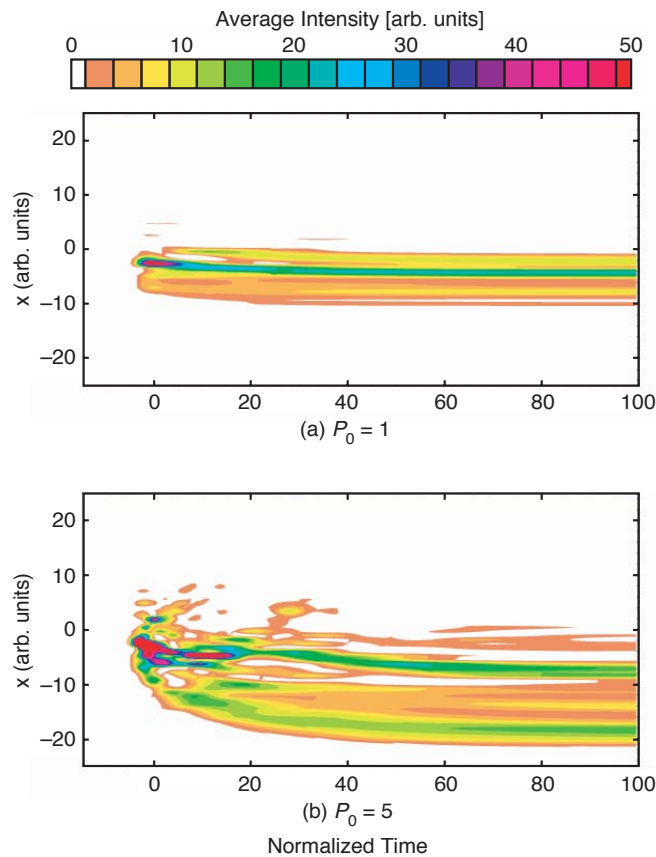


FIGURE 6 Average laser intensity on target vs time and transverse position x for $\lambda = 1.625 \mu\text{m}$ and initial ($z = 0$) normalized power. Other parameters are identical to those of Fig. 5.

wavelength beam shows severe distortion due to thermal blooming and a much lower intensity on target. The characteristic crescent shaped caused by blooming is not discernible because of the turbulence present in these examples.

DISCUSSION AND CONCLUSIONS

Laser-based directed energy weapons are envisioned to be an integral part of future Navy vessels.

The free electron laser, in particular, is especially suited for maritime applications. It can be designed to operate over a wide range of wavelengths and is capable of generating high average power at high efficiency.

In this article we discussed and analyzed the key physical processes that affect the propagation of high-energy lasers in a maritime environment. These processes include thermal blooming, turbulence, and molecular/aerosol absorption and scattering. Aerosol

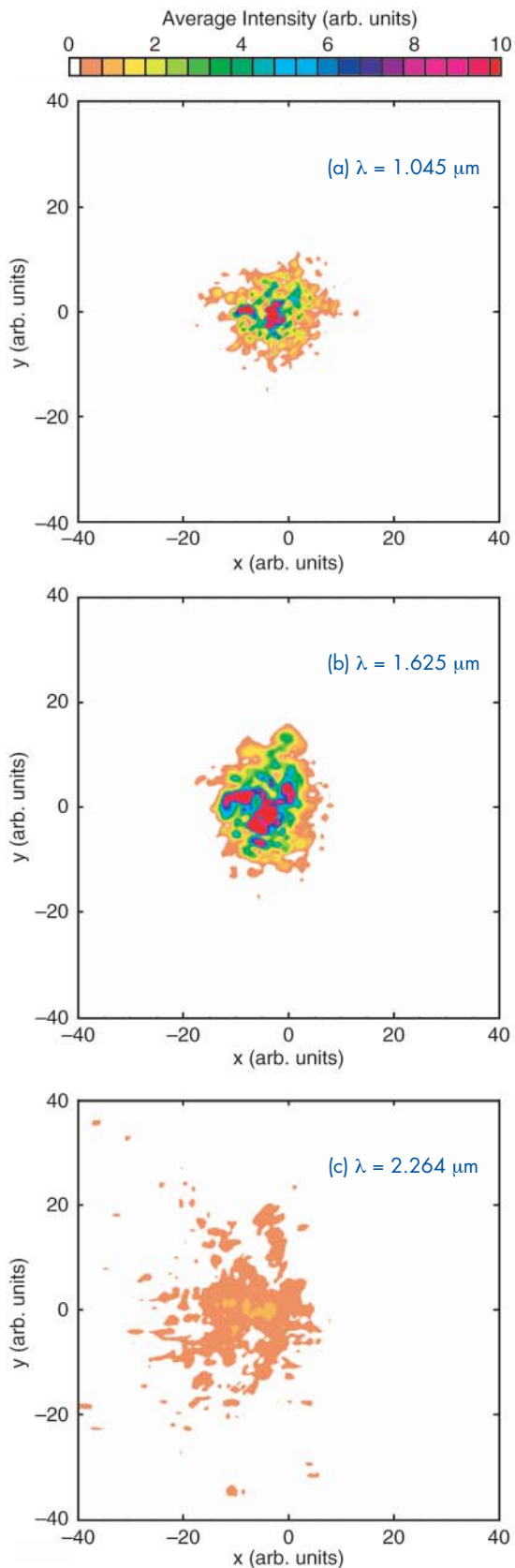


FIGURE 7
Cross sectional plots of average laser intensity on the target, corresponding to the simulations discussed in Fig. 4.

scattering and absorption as well as water vapor absorption can be a major limitation for HEL propagation in a maritime environment.

Using the HELCAP code, we performed full-scale simulations of propagation in the atmospheric transmission windows near 1.045, 1.625, and 2.264- μm .

ACKNOWLEDGMENTS

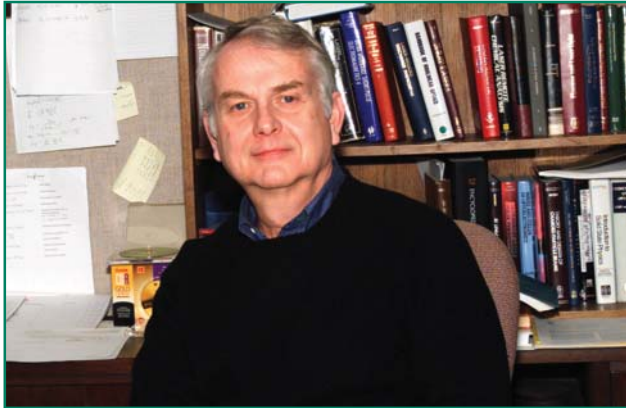
The authors thank John Albertine and Wallace Manheimer for useful discussions.

[Sponsored by NAVSEA, JTO, and ONR]

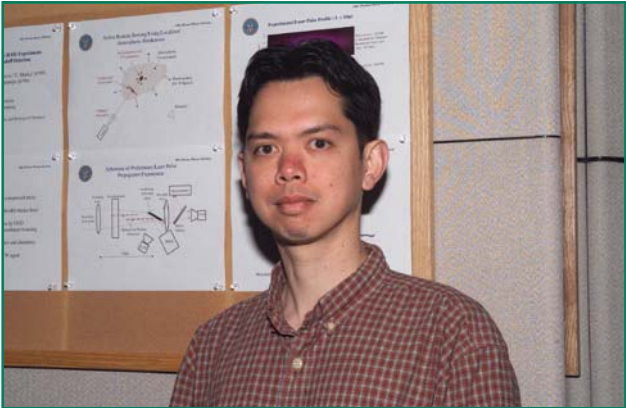
References

- ¹ G.R. Neil, C.L. Bohn, S.V. Benson, G. Biallas, D. Douglas, H.F. Dylla, R. Evans, J. Fugitt, A. Grippo, J. Gubeli, R. Hill, K. Jordan, G.A. Krafft, R. Li, L. Merminga, P. Piot, J. Preble, M. Shinn, T. Siggins, R. Walker and B. Yunn, "Sustained Kilowatt Lasing in a Free-Electron Laser with Same-Cell Energy Recovery," *Phys. Rev. Lett.* **84**, 662 (2000).
- ² F.G. Smith (editor), *The Infrared and Electron-Optical Systems Handbook*, Vol. 2, Environmental Research Institute of Michigan, Ann Arbor, MI, and SPIE Optical Engineering Press, Bellingham, WA (1993).
- ³ P. Sprangle, J.R. Peñano and B. Hafizi, "Propagation of Intense Short Laser Pulses in the Atmosphere," *Phys. Rev. E* **66**, 046418 (2002)
- ⁴ P. Sprangle, J.R. Renano, A. Ting, B. Hafizi, and D.F. Gordon, "Propagation of Short, High-Intensity Laser Pulses in Air," *J. Dir. Energy* **1**, 73 (2003).

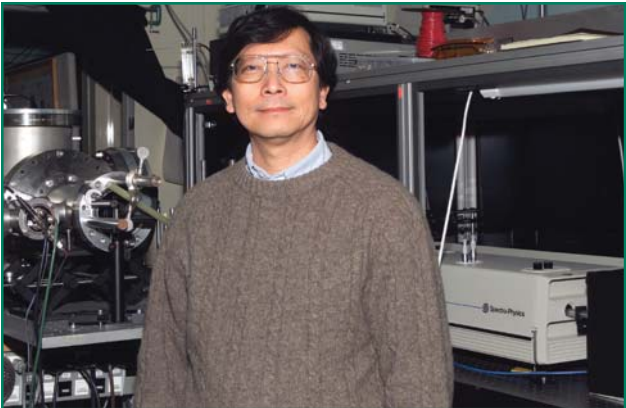
THE AUTHORS



PHILLIP SPRANGLE received his Ph.D. in applied physics from Cornell University in 1973. He is Chief Scientist and Head of the Beam Physics Branch at NRL. His primary research areas include atmospheric laser propagation, free electron lasers, nonlinear optics, and laser acceleration physics. Dr. Sprangle is a fellow of the American Physical Society and the IEEE. He is winner of the International Free Electron Laser Prize (1991), E.O. Hulburt Science and Engineering Award (1986), Sigma Xi Pure Science Award (1994), as well as numerous publication awards. Dr. Sprangle has published more than 200 refereed scientific articles (28 letters), has presented more than 180 invited lectures, review talks, and keynote addresses at conferences and universities, and holds 12 U.S. invention patents.



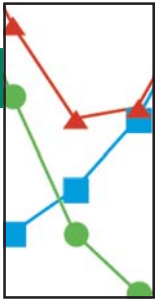
JOSEPH R. PEÑANO received B.S. and Ph.D. degrees in physics from the University of California, Los Angeles in 1991 and 1998. He joined NRL as a research physicist in the Beam Physics Branch in 2001. His present research interests include laser-plasma interactions, laser-driven accelerators, nonlinear optics, radiation sources, and directed-energy countermeasures. His most recent publications have dealt with modulation instabilities in plasma channels, channel-guided laser wakefield accelerators, superluminal propagation of laser pulses, and atmospheric propagation of high-intensity ultrashort laser pulses. He is the chief developer of the HELCAP laser propagation code. Prior to joining NRL, he was employed by LET Corp. He also held a National Research Council (NRC) postdoctoral fellowship at NRL, working on modeling space and ionospheric plasmas.



ANTONIO TING received his Ph.D. degree in physics from the University of Maryland in 1984 and also holds B.S. and M.S. degrees in physics from the National Taiwan University. He is a senior research physicist in the Beam Physics Branch and is the experimental group leader of the high field physics laboratory of the NRL Table Top Terawatt Lasers. He conducts research in intense ultra-short pulse laser interactions with air, plasmas, and electron beams. He worked at NRL as a contractor in 1985 and later joined in 1988. Prior to that, he was a research associate at the College of William and Mary and at Dartmouth College. He is a Fellow of the American Physical Society, and has twice won the Alan Berman publication award. He has published more than 75 articles and letters in refereed scientific journals, and he holds three U.S. invention patents.



BAHMAN HAFIZI received B.Sc. and Ph.D. degrees in physics from Imperial College, London, in 1974 and 1978. He is currently president of Icarus Research, Inc. He previously worked as a research associate in the Department of Astro-Geophysics at the University of Colorado and as a staff scientist for Science Applications International Corporation. His current research areas of interest include propagation of ultraintense laser pulses, laser-driven electron accelerators, laser-plasma interactions, and nonlinear optics. He has also worked on advanced sources of electromagnetic radiation and ultrabroadband sources, with application to imaging, lithography, and remote sensing. He is an Associate of the Royal College of Science and a member of the American Physical Society, the European Physical Society, and the IEEE.



FABRICATION OF A FAST TURN-OFF TRANSISTOR BY WAFER BONDING

K.D. Hobart and F.J. Kub

Electronics Science and Technology Division

J.M. Neilson

Consultant, JSMN

A new power switching transistor is presently under development to meet Navy goals for future electric power requirements. These high speed or fast turn-off (FTO) power switching devices are extremely efficient and versatile. It is envisioned that many aspects of Navy propulsion, weaponry, and power distribution demands will be met with solid-state electronic components, thereby reducing the size and weight of the associated systems. The realization of the prototype devices has been made possible through a low-temperature wafer bonding process developed at NRL that allows arbitrary joining of functional power electronic device wafers. The result is a variety of high voltage structures with active device components on the top and bottom to control charge within the volume of the transistor. Specific examples of 3.3 kV FTOs show that energy loss incurred during power switching transients is significantly reduced.

INTRODUCTION

The Navy's transformation to a fleet that is significantly more dependent on electric power as the primary means of providing energy for propulsion and weapons has placed significant emphasis on developing extremely efficient, high-voltage solid-state switching devices. Additionally, the increased magnitude of shipside electric power has generated new challenges in power distribution that are difficult to meet with conventional methods. A new class of electronic devices is presently under development to address the needs of the Navy's Advanced Electrical Power Systems program. One of the prime objectives of the program is to devise new power switching devices, dubbed Fast Turn-Off transistors or FTOs¹⁻³ that have significantly lower energy loss and higher switching frequencies than conventional power switches. Faster power switching devices are desirable on Navy platforms for several reasons: First, as switching frequencies increase, the physical size and weight of passive components used in power conditioning systems are reduced. Secondly, the higher switching frequencies make it easier to filter harmonics, which improves both silent operation of Navy vessels and electrical power quality. Thirdly, the FTO is projected to reduce switching loss by a factor of 5-10 and thereby improve efficiency of power systems. The FTO concept is particularly relevant to very high voltage devices required to meet new system de-

mands in which the shear volume of charge in the transistor becomes significant and faster switching becomes more difficult. The FTO will extend the useful voltage range of silicon power devices until a suitable replacement technology is qualified (e.g., silicon carbide-based electronics). To speed the development of FTOs, NRL has developed an advanced wafer bonding technology and has demonstrated a new double-side power switching device that shows dramatic improvement in performance over the state-of-the-art.⁴

BIPOLAR VS UNIPOLAR TRANSISTORS

There are many types of power switching transistors, and each application draws on the best properties of a particular design. For high voltage applications, only devices from the family of "bipolar" type transistors can obtain sufficiently low voltage drop in the "on" state while also supporting high voltage in the "off" state. The low voltage drop in bipolar transistors is achieved by high levels of charge injection consisting of *both* electrons and holes into the thick portion of the device designed for high voltage stand-off. The bipolar device is compared to a unipolar transistor in which only one type of charge carrier (typically electrons) is responsible for conduction. Unipolar devices are not considered useful for high voltage because of their large voltage drop in the on state. The key challenge in any of these transistors is to remove

the stored charge as quickly as possible and thus make the transition from the on to the off state efficiently. To achieve efficient switching, the current must cease immediately when the transistor is turned off. While this is the case in unipolar devices, it is typically not possible in bipolar devices because of the long transit time of charge carriers in the thick stand-off region of the device. The ideal power transistor would combine the low voltage drop of a high voltage bipolar device and the fast turn-off capabilities of a unipolar transistor.

FTO OPERATION

The FTO closely approximates the ideal switch and improves on the fundamental trade-offs between blocking voltage, forward voltage drop, and switching loss. The key feature is the additional gate control on the bottom of the transistor to manipulate the injection of charge into the volume of the device. The top and bottom MOS (metal oxide semiconductor) gates (G1 and G2 in Fig. 1) together control the current flow through the external cathode and anode connections of the transistor (in this case E1 and E2, respectively, in Fig. 1). When a voltage is applied to the top gate G1, an electron channel is created that allows charge injection (of electrons) into the n-base region of the internal p-n-p transistor. This sets up a chain reaction in the p-n-p transistor, and holes are also injected into the base from the bottom emitter E2, which is forward biased (when wired as the anode). In this case, *both* electrons and holes are strongly injected into the base. This is described as “conductivity modulation” because the basic conductivity properties of the semiconductor are modified and the concentration of charge is 1000–10,000 times

larger than when no charge is injected. With the base of the transistor in conductivity modulation, the total resistance across the device becomes extremely low. Consequently, the forward voltage drop decreases from around 500 V to approximately 3 V. Since the conductivity of unipolar devices cannot be modulated, their usefulness is limited to less than 1000 V for silicon and <3000 V for silicon carbide.

TURN-OFF TRANSIENT

The disadvantage of conductivity modulation is that the large quantity of stored charge in the base requires relatively long times to remove. The transistor is turned off by removing the voltage signal to the top gate G1 (Fig. 2, green gate trace). This begins the turn-off process by extinguishing the electron channel and halting electron injection into the base. Because of their long lifetime and low mobility, holes exit much more slowly. This results in a current “tail” during the turn-off transient and is responsible for significant energy loss. Figure 2 shows how current and voltage across FTO affect the energy loss: anytime both voltage *and* current are simultaneously present across the transistor, power in the form of heat must be dissipated to the ambient. In the “on” state, there is always a small loss associated with the forward voltage drop of the transistor. In the “off” state, energy loss is negligible. During switching transients, the energy loss can be very high because of the finite time it takes to establish the high voltage (turn-off) or high current (turn-on). The higher the switching frequency, the larger the energy loss associated with the transient. Therefore, the switching frequency is fundamentally limited by how much energy loss, or heat, can be removed from the transistor. While significant advances in power switching transistor technology have been made in recent years, high voltage power transistors are presently limited to relatively low switching frequencies (tens of kHz).

The turn-off loss of a power transistor is controlled by the internal device physics. Much has been done in the recent past to improve the turn-off capability of high-voltage bipolar switching transistor such as IGBTs (insulating gate bipolar transistors). The internal physics still limits the carrier behavior. As the voltage rating of a transistor increases, the number of options becomes limited. For instance, the turn-off loss is improved by lifetime “killing” in which high-energy protons or electrons are implanted throughout the bulk of the transistor, creating slight lattice damage and carefully reducing the lifetime of electrons and holes. The downside of this approach is that the damage also produces undesirable leakage current and also increases the forward voltage drop.

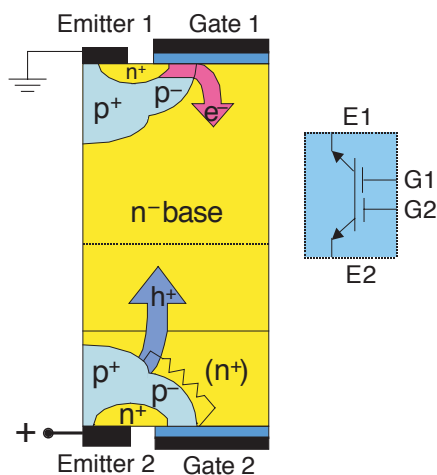


FIGURE 1 Cross section of Fast Turn-Off transistor (left) and schematic symbol (right).

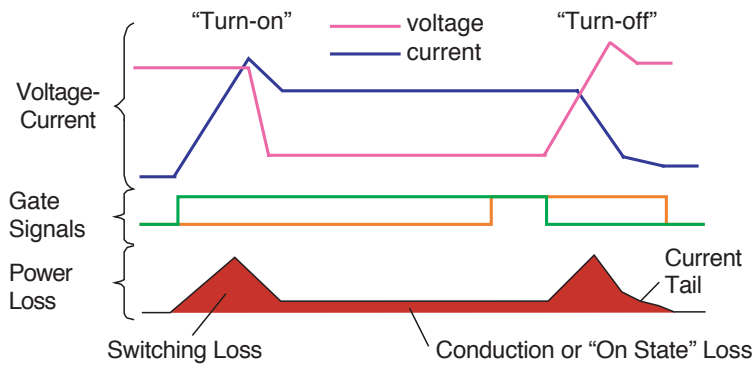


FIGURE 2

Current and voltage waveforms for FTO transistor. The red area represents the power loss that must be dissipated as heat to the ambient. The top gate (green) controls the primary current, and the secondary or bottom gate (orange) controls the current tail.

The second gate of the FTO allows the internal physics of the transistor to be manipulated to achieve very fast and efficient turn-off. The FTO improves the turn-off process by activating the bottom gate (G2) prior to turn-off (Fig. 2, orange gate trace). The effect is to reduce the injection of hole charge into the base and immediate extinction of hole injection once the transistor is switched off. As described below, the tail current is completely eliminated by the proper timing of G2, thereby implementing the performance of a unipolar device during transient operation.

POWER SWITCHING CIRCUITS AND APPLICATIONS

IGBTs are the preferred device for high-voltage continuous power applications where the magnitude and phase of the power delivered to the load is controlled through pulse-width modulation (PWM). Such applications include motor controllers (e.g., for propulsion), voltage converters, and solid-state transformers. For pulse power applications such as pulsed weapons systems, various thyristor designs are favored for their high peak current and very fast turn-on rate (di/dt). Thyristors are current controlled devices. From this standpoint, they are less attractive than IGBTs, which are voltage controlled, thus simplifying the driver circuitry. The FTO is designed to be a more efficient replacement for IGBTs in motor controller and voltage converter circuits and is essentially a symmetrical, bidirectional IGBT (Fig. 1). The symmetric nature of the FTO and the ability to precisely control stored charge in the volume of the device allows the number of components in the basic PWM switching circuit element to be reduced. This is called a “half-bridge” or “phase leg” since it controls one of many phases necessary to energize the windings of large electric motors (Fig. 3). Simplifying the basic architecture to a circuit composed entirely of FTOs significantly impacts switching performance. The benefit comes in reduced switching energy loss.⁵ The ability to control stored charge in the volume of the device is the key advantage because excess stored charge is the primary cause of energy loss during a

switching transient. Since the total loss increases as the device is cycled on and off, the switching frequency is limited by the amount of dissipated power that can be effectively removed from the transistor. Reducing energy loss and increasing switching frequency are the main goals of the FTO program because the size and weight of passive components associated with the power module decrease as the switching frequency increases (both the inductance L and the capacitance C scale inversely with frequency). With present technology, the sheer size of passive components (inductors, capacitors, transformers) precludes the introduction of certain capabilities due to size and weight restrictions. This article describes the fabrication, operation, and performance of a high-voltage FTO and shows that switching losses are significantly reduced.

FTO TRANSISTOR FABRICATION

Fabrication of the FTO depends on the unique low-temperature wafer bonding process developed at NRL, which allows the joining of fully functional device wafers. Significant research was performed to understand both the physical and electrical influences

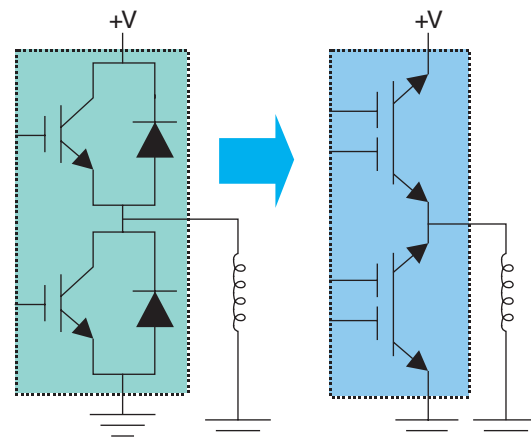


FIGURE 3

Standard “half-bridge” circuit configuration (left) and compact half-bridge using FTO (right).

of the wafer bonding process on electronic devices. The specific objectives of that work were to understand the mechanisms necessary to achieve an electrically benign bonded interface;⁶ generate sufficient mechanical stability for the fabrication of reliable power devices;⁷ and determine methods to eliminate voids or bubbles at the bonded interface.⁸ One of the key technology developments was the creation of NRL's Wafer Bonding Laboratory, which is devoted to the science and technology of wafer bonding.

To achieve the FTO structure shown in Fig. 1, fully fabricated IGBT wafers with only slight modifications were purchased from Dynex Semiconductor. The 100-mm diameter wafers containing 1-cm² IGBTs rated for 3.3 kV were carefully thinned from the backside and polished by CMP (chemical mechanical polishing). Using NRL's commercial alignment and bond tools, top and bottom IGBTs were joined by direct wafer bonding (the dashed line in the device cross section of Fig. 1 indicates the position of the bonding interface). In the wafer bonding process, the smooth backside silicon surface of the IGBT wafer is treated with a highly dilute hydrofluoric acid solution that removes (etches) the native silicon dioxide and leaves the silicon surface hydrogen-terminated and fully passivated against further oxidation. When the two wafers are carefully joined in clean room conditions, long-range van der Waals bonds between the surface hydrogen atoms pull the wafer surfaces together with sufficient force to maintain the wafers in the aligned and joined position. Annealing the wafers at a low temperature of 400°C for 4 hours significantly increases the strength of the bond by desorbing hydrogen from the interface and forming bridging silicon bonds across the interface. At this point the wafers are ready for "back end" processing, which includes additional metal depositions to improve solder adhesion during the packaging process. The transistor described thus far is fully symmetrical; however, there are also advantages for creating an asymmetrical structure that can block voltage in only one direction but can pass current in both directions. The benefit this structure is faster turn-off, which is achieved by incorporating an

additional n-type region, or "buffer layer" on the bottom of the transistor (as shown by the lower n⁺ layer in Fig. 1). The primary effect of the buffer is to reduce the lateral series resistance in the n-base adjacent to the bottom p-region (see Fig. 1). As described below, this has a significant effect on the transistor properties.

Advanced packaging techniques incorporating several novel features were used to improve reliability and reduce parasitic inductance of the module. Figure 4 shows a schematic cross section of the packaged module. The FTO die is soldered to a copper/aluminum nitride/copper substrate. The aluminum nitride is highly insulating to support high anode voltages and also has high thermal conductivity to reduce thermal resistance to the cold plate. The copper on one side of the substrate was patterned to allow connection of the individual gate and emitter contacts on the bottom of the FTO. The perforated alumina/tungsten/nickel ThinPak⁹ lid, which is also patterned to pick up the emitter and gate pads, is soldered onto the top of the FTO and is then soldered to the external copper lugs. This arrangement eliminates the less reliable wire bonds typical of conventional packages while also reducing the parasitic inductance. Once the transistor and ThinPak lid are mounted, the entire module is hermetically sealed with epoxy. Overall this packaging technology is highly robust. The ThinPak lid also solves the key problem in implementing double-side cooling, which is extremely desirable for high-performance switching transistors.

TRANSISTOR CHARACTERIZATION

Static Characterization

The key static characteristics for power transistors are the forward voltage drop (and its temperature dependence), the blocking or breakdown voltage, and the leakage current during the blocking condition. Figure 5 shows the blocking voltage characteristics of several wafer-bonded FTOs. Excellent blocking capability is observed up to the design value of 3.6 kV. No degradation in the breakdown voltage or excess leakage current is observed as the electric field

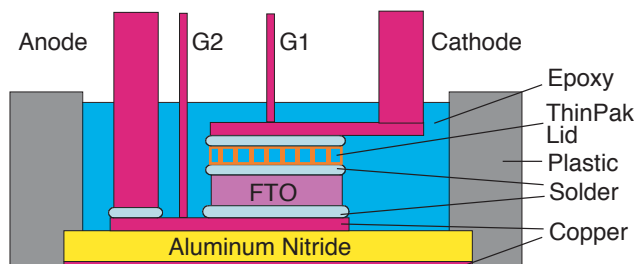


FIGURE 4 Packaged FTO module using ThinPak lid and aluminum nitride substrate.

penetrates the bond interface, which occurs for voltages of 1200–1400 V. Figure 6 shows the forward current-voltage characteristics for an FTO transistor and is compared to a conventional (single-gate) IGBT. The two operational modes of the FTO are shown: (1) when only the top gate (G1) is conducting, and (2) when both gates are conducting. First, when operating in the conventional mode (G2 OFF), the forward voltage drop of the FTO is approximately 40% lower than the comparable state-of-the-art 3.3 kV IGBT. Second, when the bottom gate is activated (G2 ON) and conductivity modulation is disrupted, the forward drop significantly increases. A sharp increase in

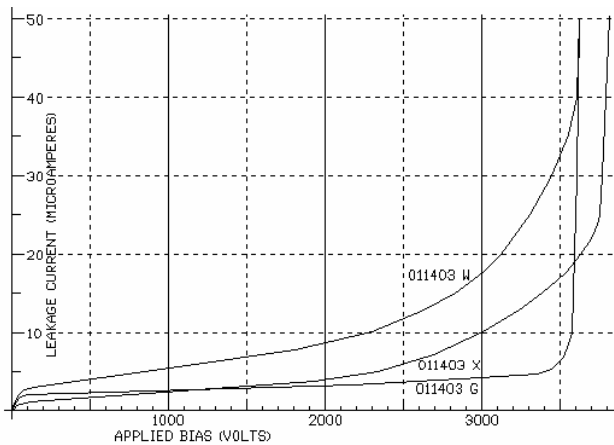


FIGURE 5
Blocking voltage characteristics for several FTOs.

current occurs at 50 A; this indicates that conductivity modulation, while delayed, still occurs in the device. The resurgence of conductivity modulation is the result of a voltage drop of approximately 0.7 V across the n-base adjacent to the lower p-region (and shown by the resistor in Fig. 1). The voltage drop allows the p-n junction to become forward biased, leading to strong hole injection into the base. To improve the ability to control hole injection from the lower p-region, transistors with n-buffer layers were fabricated. The n-buffer, which locally increases the conductivity of silicon by approximately 100, acts to decrease the parasitic resistor in the n-base and leads to more ideal transistor characteristics. Figure 7 shows the current-voltage characteristics of an FTO fabricated with a buffer layer. There is a small increase in the forward voltage drop in the conventional mode of operation (G2 OFF) resulting from slightly lower hole injection across the buffer layer. With both gates conducting (G2 ON), however, the current voltage characteristic is linear or purely resistive, indicating that the bottom gate has completely halted hole injection and thus conductivity modulation. With the bottom gate, G2, activated, the device now resembles a unipolar transistor since only one carrier type (electrons) is present. The ability to switch a power transistor between bipolar and unipolar modes of operation is significant: the bipolar mode is required for low voltage drop, and as shown below, the unipolar mode is extremely advantageous for efficient switching operation. Finally, Fig. 8 shows the forward current

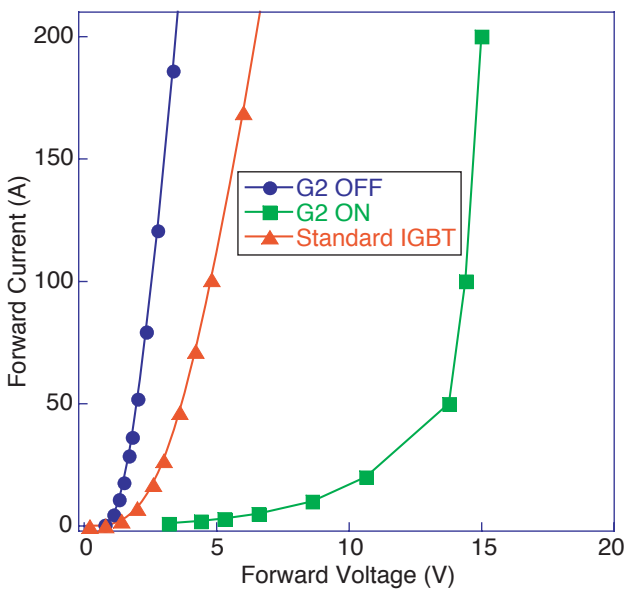


FIGURE 6
Forward current-voltage characteristics of FTO showing conventional forward behavior (G2 OFF) and control of current with aid of backside gate (G2 ON). Conventional IGBT characteristics are shown for reference.

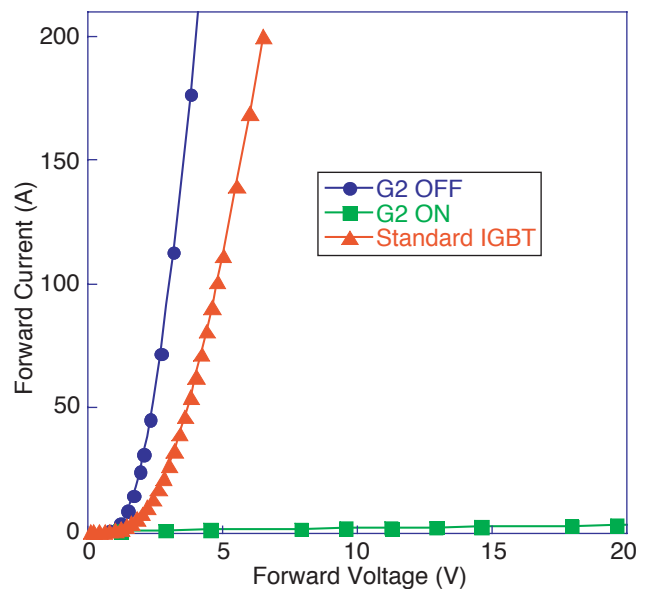


FIGURE 7
Forward current-voltage characteristics of a FTO transistor with n-buffer layer. Conventional IGBT characteristics are shown for reference.

voltage characteristic at room temperature and 125 °C. The desired behavior is observed: as the temperature increases, the forward voltage drop increases. This prevents any one transistor or portion of a transistor from becoming overheated due to thermal runaway. In high current applications where many transistors are paralleled, it is critical that the forward voltage drop have a positive temperature coefficient for reliable operation.

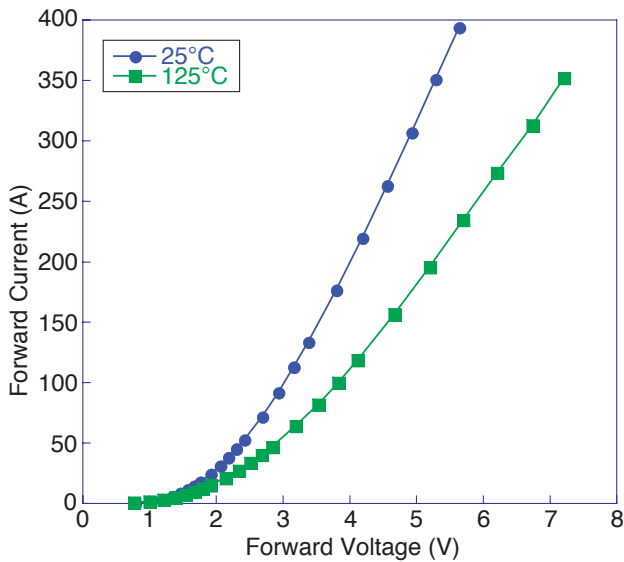


FIGURE 8 FTO temperature behavior of forward current-voltage characteristic. The observed positive temperature coefficient is desired for paralleling of devices in high current applications.

Turn-off Characterization

Transistor turn-off is evaluated by pulsing current from a charged capacitor bank through an inductor to simulate the inductive load of a motor. This transient analysis was carried out on FTOs at currents up to 100 A and voltages up to 2400 V. Figure 9 shows a typical turn-off transient characteristic in which the bottom gate of the FTO is always off, and thus the transistor is operating in the conventional mode. At the beginning of the pulse cycle, Gate 1 is on and the transistor is conducting. When the target current is reached, Gate 1 is turned off. At this point, the current ceases and the high voltage is supported across the thick n-base region, which is now mostly depleted of charge carriers. The tail current (red trace) that follows the switching event is due to the slow removal of holes from the n-base and accounts for all of the switching loss (pink trace). It is customary to integrate switching power loss over the switching event to generate a total energy loss value for the given switching conditions. Figure 10 shows similar switching conditions,

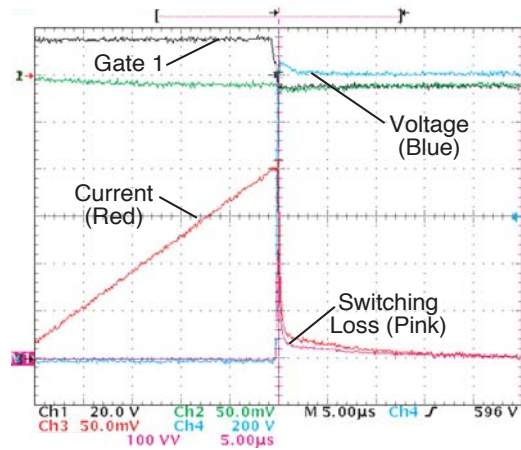


FIGURE 9 FTO transient waveform under normal operation showing turn-off behavior initiated by the Gate 1 signal. Switching conditions: 20 A and 1200 V.

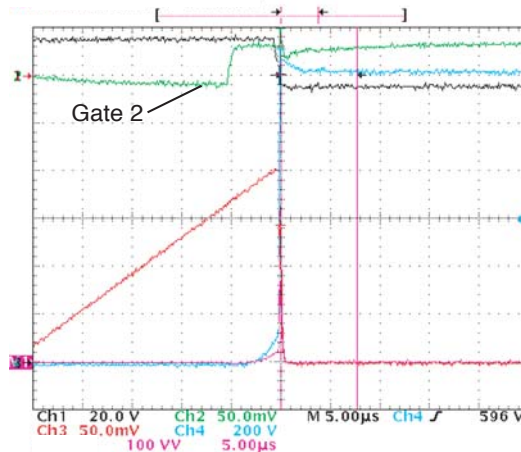


FIGURE 10 FTO transient waveform optimized for minimum switching loss by triggering Gate 2 signal 6 μs prior to turn-off. The tail current is eliminated.

however with the bottom gate activated 6 μs prior to the turn-off initiated by the top gate. The tail current is completely eliminated, and the total switching loss is reduced by 80%. If the Gate 2 signal is activated too far in advance of deactivating the Gate 1 signal, the forward voltage drop of the transistor begins to increase rapidly. The beginning of this can be seen in Fig. 10, where the voltage trace (blue) begins to rise prior to the switching event due to the transition to a unipolar transistor. Figure 11 shows how this “pre-switch” as well as the tail or “post-switch” energy loss components contribute to the total energy loss. Overall, these results represent better than a factor of three improvement over the fastest devices available today while maintaining greater than 40% lower forward voltage drop.

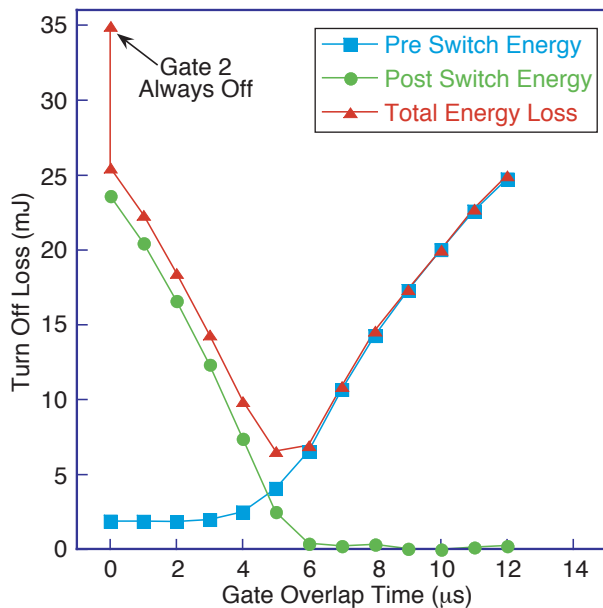


FIGURE 11
Components of turn-off loss that contribute to total energy loss. An optimum value exists at 5–6 μs for which the turn-off loss is substantially reduced.

SUMMARY

The development of a new high-voltage power switching transistor that combines off-the-shelf parts and a novel direct wafer bonding process is presented. The development program has led to the demonstration of a device with significantly enhanced performance and efficiency. The transistor has lower forward voltage drop and significantly lower switching loss than high voltage state-of-the-art power transistors. The bidirectional nature of the transistor allows for unique compact circuit topologies that additionally improve performance.

ACKNOWLEDGMENTS

The authors thank Kenneth Brandmier of Silicon Power Corporation, Malvern, PA, for packaging expertise; Peter Waind of Dynex Semiconductor, UK, for process design modifications and helpful discussions.
[Sponsored by ONR]

References

- ¹ E.J. Kub, V. Temple, K. Hobart, J. Neilson, "Methods for Making Semiconductor Device by Low Temperature Direct Bonding," U.S. Patent #6,194,290, issued February 27, 2001.
- ² E.J. Kub, V. Temple, K. Hobart, and J. Neilson, "Advanced Methods for Making Semiconductor Devices by Low Temperature Direct Bonding," U.S. Patent #6,153,495, issued November 28, 2000.
- ³ E.J. Kub, V. Temple, K. Hobart, and J. Neilson, "Devices Formable by Low Temperature Direct Bonding," U.S. Patent #6274892, issued August 14, 2001.
- ⁴ K.D. Hobart, E.J. Kub, M. Ancona, J.M. Neilson, K. Brandmier, P. Waind "Characterization of a Bi-Directional Double-Side, Double-Gate IGBT Fabricated by Wafer Bonding," *Proceedings of the 13th International Symposium on Power Semiconductor Devices and ICs*, Osaka, Japan, June 4–8, 2001, pp. 125–128.
- ⁵ J.M. Neilson, E.J. Kub, K.D. Hobart, K. Brandmier, and M. Ancona, "Double-Side IGBT Phase Leg Architecture for Reduced Recovery Current and Turn-On Loss," *Proceedings of the 14th International Symposium on Power Semiconductor Devices & ICs*, 2002, pp. 141–144.
- ⁶ E.J. Kub, K. D. Hobart, and C.A. Desmond, "Electrical Characterization of Low-Temperature Direct Silicon-Silicon Bonding for Power Device Applications," in *Semiconductor Wafer Bonding: Science, Technology and Applications IV*, edited by U. Goesele, H. Baumgart, T. Abe, C. Hunt, and S. Iyer, *Proceedings*, Vol. 97-36, The Electrochemical Society, Inc. 1998, pp. 466–472.
- ⁷ C.A. Desmond, K.D. Hobart, E.J. Kub, G. Campisi, and M. Weldon, "Low Temperature Atmospheric Silicon-Silicon Wafer Bonding for Power Electronics," in *Semiconductor Wafer Bonding: Science, Technology and Applications IV*, edited by U. Goesele, H. Baumgart, T. Abe, C. Hunt and S. Iyer, *Proceedings*, Vol. 97-36, The Electrochemical Society, Inc. 1998, pp. 459–465.
- ⁸ R.H. Esser, K.D. Hobart, E.J. Kub, "Directional Diffusion and Void Formation at Si(100) Bonded Wafer Interfaces," *J. Appl. Phys.* **92**(4), 2297-2303 (2002).
- ⁹ V. Temple, "ThinPak Package for Power Modules and Hybrids," PCIM Europe, November 2000, p. 18.

THE AUTHORS



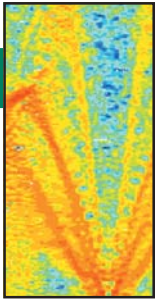
KARL D. HOBART received his B.S. degree in physics from the University of Illinois in 1984 and M.S. and Ph.D. degrees in electrical engineering from the University of Delaware in 1987 and 1990, respectively. In 1993 he joined SFA, Inc., as an on-site contractor at NRL where he led an effort for the growth, fabrication, and characterization of microwave power SiGe heterojunction transistors. In 1995, Dr. Hobart joined the Microelectronics Device Physics Section where his interests presently lie with wafer bonding technology for power electronic devices and alternative substrates. Dr. Hobart is head of the High Power Devices Section in the Power Electronics Branch. He has been an author or co-author on more than 60 technical articles and holds 14 patents.



FRITZ J. KUB received his B.S. degree from South Dakota State University in 1972, the M.S.E.E. degree from the University of Minnesota in 1974, and the Ph.D. degree in electrical engineering from the University of Maryland, College Park, in 1985. Since 1985, he has worked at NRL in the Power Electronics Branch. His research interests include power electronic devices, novel material systems made using wafer bonding, and analog signal processing circuits. He is manager of the NRL Power Electronics Science and Technology Program. He initiated the formation of the Naval Electrical Power Advisory Council (NEPAC) in 1998. He has received four NRL Technology Transfer Awards. He has served on the International Symposium on Power Semiconductor Devices in 2003 and Imager and Sensor Subcommittee of the International Solid State Circuits Conference from 1994 to 2002. He has authored more than 100 publications and has been awarded 25 patents.



JOHN M. NELSON received his B.S. degree in physics in 1955 from Albright College, Reading, Pennsylvania, and the M.S. degree in physics in 1962 from the University of Pennsylvania, Philadelphia, Pennsylvania. From 1958 to 1998 he was employed by RCA, GE, and the Harris Corporation, doing design, processing, and applications work on power semiconductor devices. Among the devices he has worked on are rectifiers, thyristors, bipolar transistors, MOSFETs, IGBTs, and MCTs. Since retiring from the Harris Corporation in 1998, he has been doing consulting work on the design and fabrication of power semiconductor devices.



APPLICATIONS OF TIME-REVERSAL TO UNDERWATER ACOUSTICS

J.F. Lingeitch, C.F. Gaumont, D.M. Fromm, and B.E. McDonald

Acoustics Division

The rapidly developing field of time-reversal acoustics is yielding results as robust and productive in large-scale ocean experiments as in table-top laboratory experiments. The operative physical principle is that acoustic waves can be turned around (time-reversed) and sent back to their source, no matter how complex the environment. Thus, unlike conventional sonar signals that disperse as they propagate away from their source, a time-reversal mirror can focus sound energy in the ocean. In practice, time-reversal mirrors are realized by constructing an array of collocated source and receiver elements. The Naval Research Laboratory has developed and deployed a source-receive array (SRA) that is being used to test time-reversal methods on problems of interest to the Navy. These experiments seek to enhance the target echo levels relative to conventional sonar by using time-reversal processing. By putting more energy on the target and keeping it away from the ocean boundaries, these techniques promise significant increases in echo-to-reverberation level.

INTRODUCTION

A time-reversal mirror (TRM) is an array of source-receiver elements that can be precisely controlled to project a desired acoustic wavefront. The Naval Research Laboratory has recently purchased a 64-element source-receive array (SRA) to test time-reversal methods on problems of interest to the Navy, including antisubmarine warfare, acoustic detection methods, remote bathymetry mapping, geo-acoustic inversion, and underwater communications. Time-reversal mirrors are an active area of investigation for these problems because of their capability for focusing acoustic energy in heterogeneous propagation environments such as shallow-water continental shelf areas in the ocean.

Acoustic propagation in shallow water is complicated by strong interactions with both the surface and the bottom, leading to extended multipath echoes. In addition, inhomogeneities in the water column distort the propagation paths. For these reasons, simple beam steering is not effective for ensonifying a desired location when it is away from the vicinity of the array. Time-reversal (phase conjugation) techniques have been demonstrated to focus acoustic energy in the ocean up to 30-km away by using a probe source. This method requires positioning a probe source at the desired focal point and measuring the propagated acoustic field from the probe source to the TRM. The measured signal on the TRM is then time-reversed and retransmitted from each element of the array. The new signal propagates through the waveguide and is

observed to focus both spatially and temporally at the probe source location.

One key advantage of time-reversal techniques is that they require no a priori knowledge of the ocean propagation environment. The method is applicable to areas with variable ocean bathymetry, range-dependent sound speed, and geo-acoustic properties. Time-reversal focusing follows from the fact that when a solution of the linear wave equation is played backwards in time, wavefronts will retrace their paths. Attenuation and time variability of the ocean will degrade the reversibility of acoustic waves by a TRM, but recent observations have shown that the time scale of the focal smearing ranges from many hours for frequencies below 1 kHz to tens of minutes at 3.5 kHz.

The Naval Research Laboratory conducted an at-sea time-reversal experiment during May/June 2003 (TREX-03) on the New Jersey continental shelf near the Hudson Canyon. Figure 1 shows the 64-channel SRA during one of its deployments from the R/V *Endeavor*. The transducers are 6-in. spheres, spaced evenly at 1.25-m intervals along the 80-m aperture of the array. The array is deployed in a vertical configuration by suspending it from the stern of the ship. It is being modified for autonomous bottom-moored deployments in future experiments. The bandwidth of the array is 500–3500 Hz; each element is an independently controllable source/receiver so that the array can be used to implement a TRM. The R/V *Oceanus* was also on-site for a portion of the experiment to deploy an NRL echo repeater.



FIGURE 1
Deployment of the NRL 64-channel SRA from the stern of the R/V *Endeavor* during the TREX-03 time-reversal experiment.

Below we describe several applications of time-reversal to ocean acoustics that are being studied at NRL. The first is a rapid wide-area bathymetry mapping technique with a TRM. This technique uses the reverberation from a TRM that is focused near the seafloor to construct a map of the azimuthal variation in bathymetry. Time-reversal techniques are also being applied to enhance the performance of active sonar systems in acoustic detection problems. The multiple guide source (MGS) method uses the principle of time-reversal with in situ data to generate a detector that is matched to the local propagation. Broadband time-reversal operator decomposition (DORT) is a processing technique based on the mathematical decomposition of acoustic data that is designed to separate scatterers at different depths into different beams. We are also exploring applications of time-reversal to develop an “acoustic searchlight” device that could be used to acoustically sweep large regions of the ocean floor for partially buried mines. To make this method practical, we are studying ways to focus a TRM in an unknown environment without using a probe source.

CONTROLLED REVERBERATION AS A BATHYMETRY PROBE

In ocean acoustic experiments, boundary reverberation (echo) is usually a source of interference to be mitigated. Time-reversal techniques, however, can control the locations where reverberation originates and use it to explore the environment. Figure 2 illustrates how this is done. Parameters are descriptive of actual ocean experiments performed in the Mediterranean by the NATO Undersea Research Center with NRL participation. First, a probe source of modest amplitude

placed 1 m above the ocean bottom emits a pulse of a few milliseconds duration that is recorded on a vertical SRA 5 km away. The SRA time-reverses the signal, amplifies it, and retransmits it in all directions. As illustrated in Fig. 3, the returning signal along the path back toward the probe source focuses tightly, ensonifying the bottom near the probe source location. In other directions, however, the focus is shifted by sloping bathymetry (green area of Fig. 2). The broken blue circle in Fig. 2 illustrates where the focal region would occur if the ocean bottom were flat.

The reverberant return to the SRA (unfilled blue arrows in Fig. 2) arrives at different times from different directions because of the bathymetric focal shift. If the returns from the reverberating annulus are analyzed by an appropriate horizontal array, the two-way travel time variation with direction can be extracted. A basic result from waveguide propagation theory then allows the travel time differences to be inverted to yield the bathymetric variation within the green band of Fig. 2.

This method, while still in the developing stages, has the potential of yielding bathymetric variation over many square kilometers of ocean in a matter of seconds in regions of unknown or shifting bathymetry. Traditional swath bathymetry from a moving ship would take many hours to complete.

MULTIPLE GUIDE SOURCES

Multiple Guide Sources (MGS) is a new technique for improving sonar detection in shallow-water environments. It is designed to compensate for the effects of channel spreading (the dispersion of sound as it propagates through the waveguide) by using a set of experi-

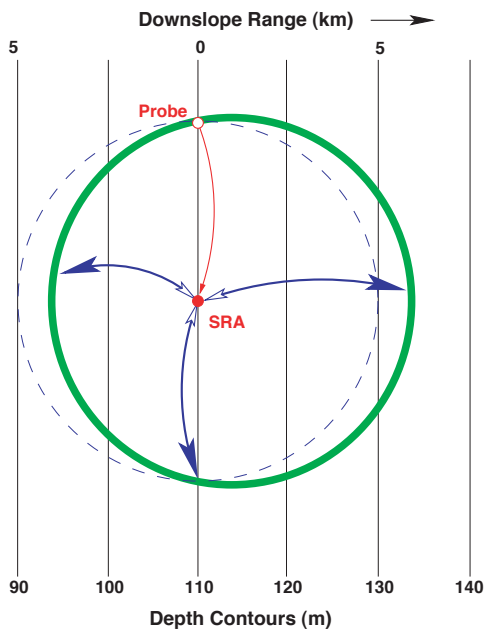


FIGURE 2
Plan view of the ocean bottom for a controlled reverberation experiment. The propagation path from probe source to SRA is in red; the path of the time-reversed back propagation is in blue. Reverberation from the green focal annulus returns along the blue paths and is represented by unfilled arrows.

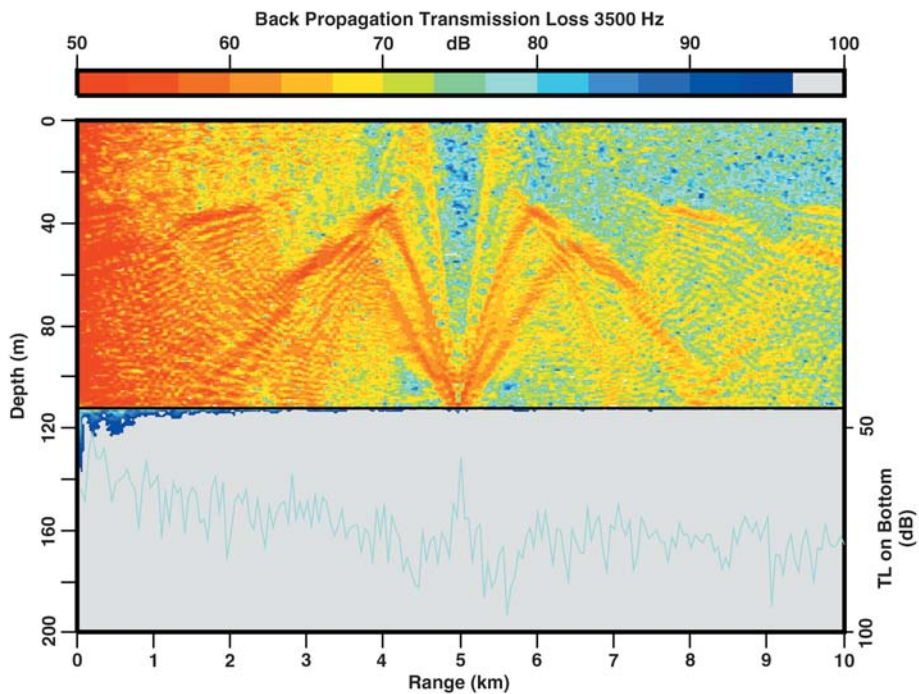


FIGURE 3
Backpropagation from the SRA to the probe source at 5-km range calculated by a parabolic equation acoustic model using an experimentally measured environment. The blue curve gives the acoustic intensity incident on the bottom to reveal a tight focus at the probe source location.

mentally measured channel responses in a matched-filter detector. Channel spreading is more pronounced for signals that have larger bandwidth, lower frequencies, and longer propagation paths; these are also the signals that have potential benefits for active sonar. Conceptually, the matched filter emphasizes the

portions of the spectrum where the signal resides without increasing the magnitude of the noise. It is implemented by filtering a received noisy signal with the time-reversed replica of the expected signal, thus matched filtering can be thought of as a time-reversal technique. To use this conceptual solution, the ex-

pected echo from the target must be known. However, since the echo depends on many unknown target and waveguide parameters, it is necessary to approximate the matched filter by using the incident signal, numerical modeling, or direct measurement.

MGS is a technological approach to finding the matched filter from in situ measurements, and is adaptable to different sonar configurations and designs. The concept is to measure the channel spreading due to propagation by deploying several probe sources in the ocean volume where detection is required. The probe sources emit signals that are then measured with the TRM. The received signals are the one-way responses of the environment at a set of positions that are used to estimate the matched filter.

The program at NRL has focused on the scientific problems associated with this process: How many probe sources are needed to characterize a typical shallow-water environment? How does this number vary with bandwidth, frequency, and range? What is the expected improvement in detection from the use of MGS? We have focused on understanding the processes involved as well as determining a methodology for determining the answers.

Even though acoustic propagation in shallow-water regions is complicated, a large number of MGS is not necessarily required. In the recent TREX-03 experiment, data were taken to determine the number of MGS required for detection of targets at ranges between 2 and 4 km with a band of frequencies from 3 to 3.5 kHz. In this higher frequency, broader bandwidth case, only 10 MGS were required to cover 80% of the received echo. This small number of MGS is sufficient to increase the signal-to-noise ratio by 30 to 40 dB (assuming white Gaussian noise or reverberation). The implication of this result is that for realistic frequencies and bandwidths, a manageable number of probe sources, perhaps as few as five per kilometer, are required to estimate the environmental spreading caused by acoustic propagation in shallow water. Furthermore, a detection algorithm that is based on these in situ environmental estimates can significantly improve detection over noise, and possibly over reverberation also.

BROADBAND TIME-REVERSAL

The Time-Reversal Operator Decomposition (DORT) method is a signal-processing algorithm developed to decouple overlapping time-domain signals due to multiple targets.¹ To construct the time-reversal operator (TRO), a TRM is used to collect the backscattered signal from a collection of targets (Fig. 4). It has been shown previously that the eigenvectors of the TRO correspond to the scattered signals from

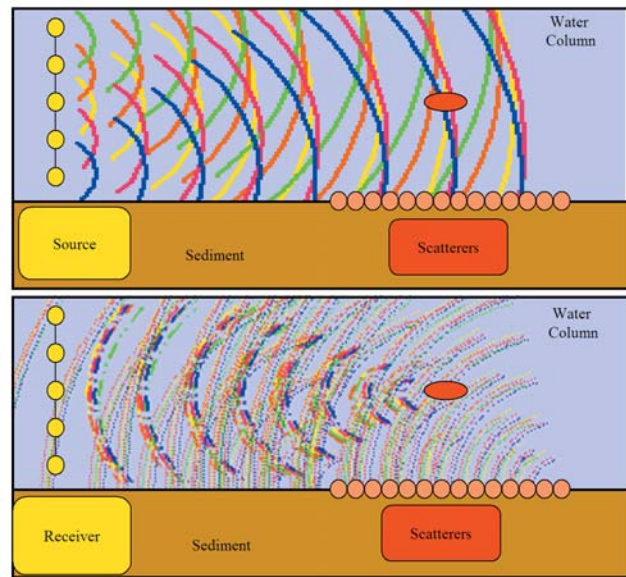


FIGURE 4
The two stages of forming a matrix of data from the scatterers. In the top panel, each source sequentially transmits a signal. After each source transmits, each receiver records the scattered data from each source (bottom panel). The figure shows two kinds of scatterer: one is the scatterer in the middle of the water column; the other is a collection of small scatterers located on the bottom of the water column.

the individual targets in the waveguide. This technique has potential application in the fields of medical ultrasound, communications, and sonar.

In spite of the potential for isolating targets in shallow-water environments, there are several shortcomings of this method that we are addressing at NRL. The first is that a significant amount of time is still required to acquire the data necessary to construct a TRO. This is because a sequence of pings has to be emitted from the TRM and the resulting backscattered signal captured. However, the temporal variability of the ocean, as well as motion of the SRA and scatterers, can significantly affect the measured field during the data acquisition. A second shortcoming of the original method is that it uses narrowband signals. In shallow water, sonar systems are often reverberation limited, i.e., the dominant noise process is scattering from sources such as bottom roughness, bottom inhomogeneities, bubble plumes, and fish. To overcome them, broadband signals are typically used to better detect isolated targets from generally more distributed clutter. Broadband signals also typically contain more clues that can be used to classify the echo as originating from a target or clutter.

We have derived a broadband extension of the DORT algorithm. This method applies conventional DORT processing to the individual frequency components of a broadband signal and then transforms the resulting eigen-channels back into the time domain

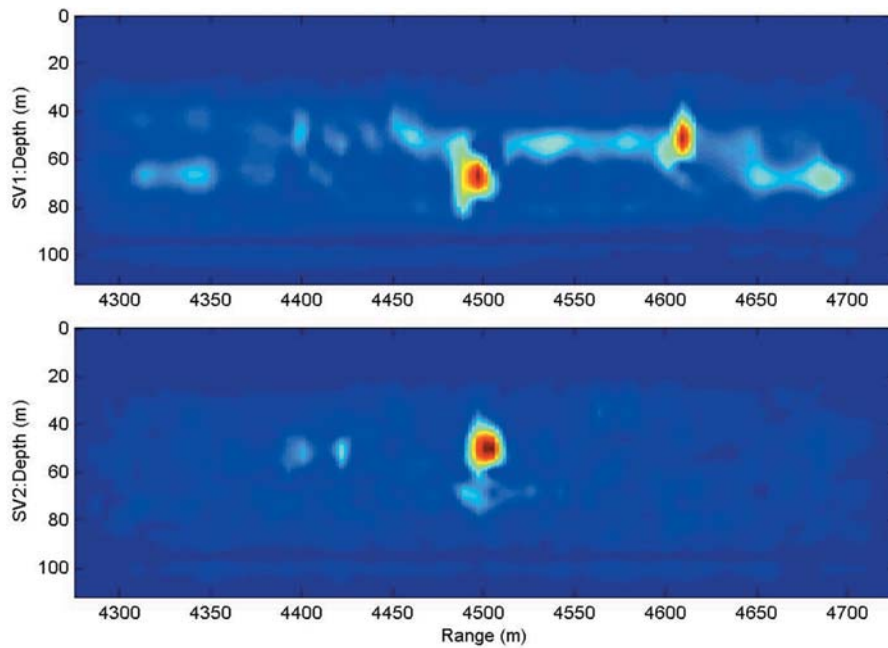


FIGURE 5
 This broadband acoustic image is generated from two eigen-channel outputs of broadband DORT. The upper panel shows the image from the first singular vector and the lower panel shows the image from the second. Several scatterers are in the water column. In the upper panel, two large scatterers are particularly apparent. In the lower panel, a smaller scatterer is isolated from the stronger scatterer at the same range.

where existing broadband signal processing can be applied. We demonstrate this method using a numerical simulation with a probe signal of approximately 100 Hz bandwidth. The scatterers in this problem are positioned at different ranges except for two, which are located at 4500 m but at different depths (50 and 70 m), in order to more stringently test the isolation capability of this technique. Figure 5 shows backpropagation images (the TRM data propagated through the waveguide with a numerical model) generated from the first and second of the eigen-channels. In the upper panel, the first eigen-channel is backpropagated and two strong scatterers are apparent; the other weaker scatterers are not as evident due to the color scale. In the upper panel, only the deeper scatterer at the 4500-m range is imaged. In the lower panel, the second eigen-channel is backpropagated and now the 50-m deep scatterer at the 4500-m range is revealed. There is also a hint of the 70-m deep scatterer present in the second eigen-channel. This is caused by frequency-dependent fading that occurs in shallow-water propagation. Effectively, the fading causes the scatterer at 70-m not to be the strongest at all frequencies, and hence it appears in multiple eigen-channels. This is a well known problem in adaptive beamforming algorithms, notably in the area of teleconferencing with multiple microphones. Methods for overcoming this problem with shallow-water propagation are currently under investigation.

Broadband DORT also has the potential to overcome the problem of taking sequential data in shallow water, and it was tested experimentally during the TREX-03 experiment. The NRL SRA and an echo-repeater were deployed at ranges varying between 1 to 5 km. Linear frequency modulated and pseudorandom noise (PRN) signals in the 3.0-3.5 kHz band were transmitted from subapertures of the array to probe the environment. The PRN signals were designed to be approximately orthogonal to each other so that they could be simultaneously transmitted, with each group of sources having its unique PRN signal. In each case, the echoes from each were recorded from each element of the array. Preliminary results suggest that PRN signals are necessary to implement broadband DORT in shallow water.

REVERBERATION FOCUSING

It is not always possible or practical to position a probe source at a desired focusing location in the ocean. We are investigating time-reversal methods for focusing a TRM in an uncertain environment without placing a probe source.² One idea is to obtain an estimate of the transfer function between a desired focal point on the ocean floor and the SRA by exploiting the boundary reverberation due to a known SRA incident pulse. For this measurement, the SRA will transmit a ping, or series of pings, and then record the resulting reverber-

ant signal on all receiving channels. By filtering the reverberation signal with a time window corresponding to a desired focusing range, a map can be constructed that specifies the amplitude and phase of the SRA elements in order to focus back to the source of the reverberation. Several factors complicate a straightforward application of this approach. First, several scatterers from different depths and azimuths may contribute to a given time window of reverberation data. Secondly, the backscattered signal is typically weak and must be detected from sources of noise in the vicinity of the SRA. To overcome these difficulties, we are implementing broadband probe signals that can be detected with a matched-filtering approach.

During TREX-03, the NRL 64-channel SRA was deployed from a ship that was moored in approximately 80 m of water (only 56 of the 64 elements were in the water). A 1-s incident continuous wave pulse was transmitted from the array, and the resulting reverberation was received on the SRA. The amplitude of the reverberation time series was beamformed; Fig.

6 shows the time series for all beams. The energy summed over all of the array elements is shown in the bottom panel. Because of propagation effects in the waveguide, certain ranges are preferentially ensonified with more energy than other ranges. The peaks in the backscattered energy curve correlate well with the ranges where the incident beam strongly interacts with the bottom. Figure 7 shows the acoustic field that results when a segment of the captured reverberation is time-reversed and propagated through the ocean environment that was measured during this test. The top panel shows the transmission loss in a range-depth plot with a dynamic range of 20 dB where the SRA spans the water column at the origin of the range axis. The plot shows a partial focusing of energy at the bottom at approximately 1250 m from the SRA. The bottom panel of Fig. 7 shows the transmission loss at a depth of 81.5 m, near the sediment interface. At the focusing range, the transmission loss plot shows an enhanced ensonification on the bottom of about 5 dB compared to the neighboring ranges.

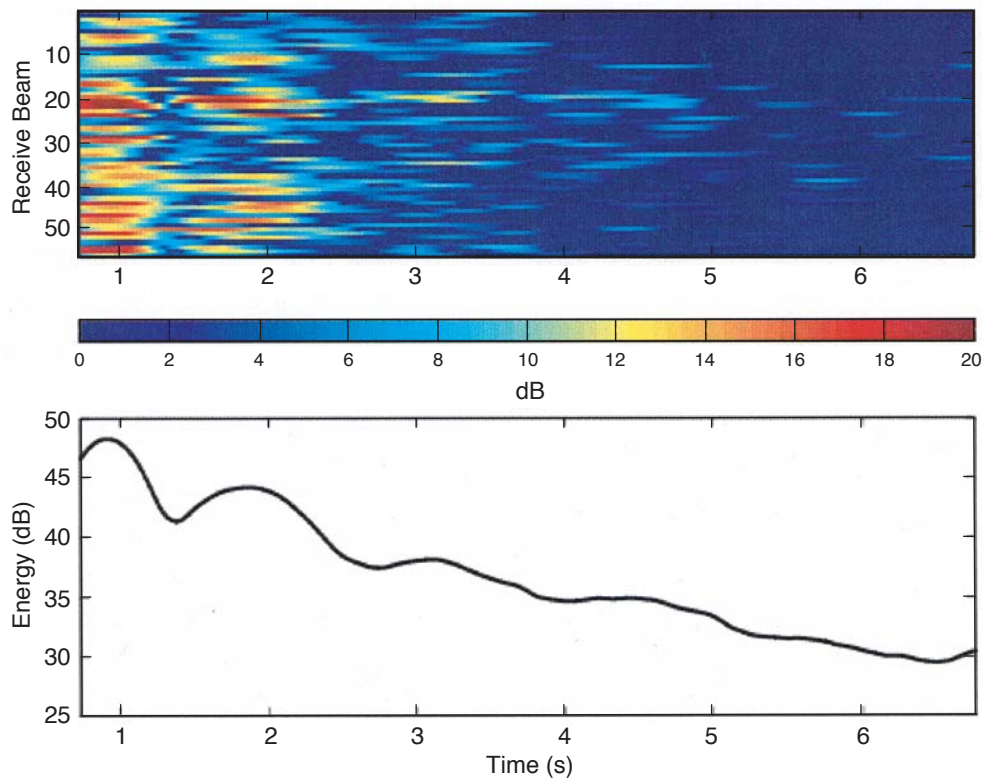


FIGURE 6 Reverberation recorded on SRA after a 1-s CW ping centered at 1427 Hz. The top panel shows the received time series that has been beamformed. The bottom panel is the received energy summed over all array elements. The peaks in the received energy correlate with ranges where the incident beam interacts with the sediment interface.

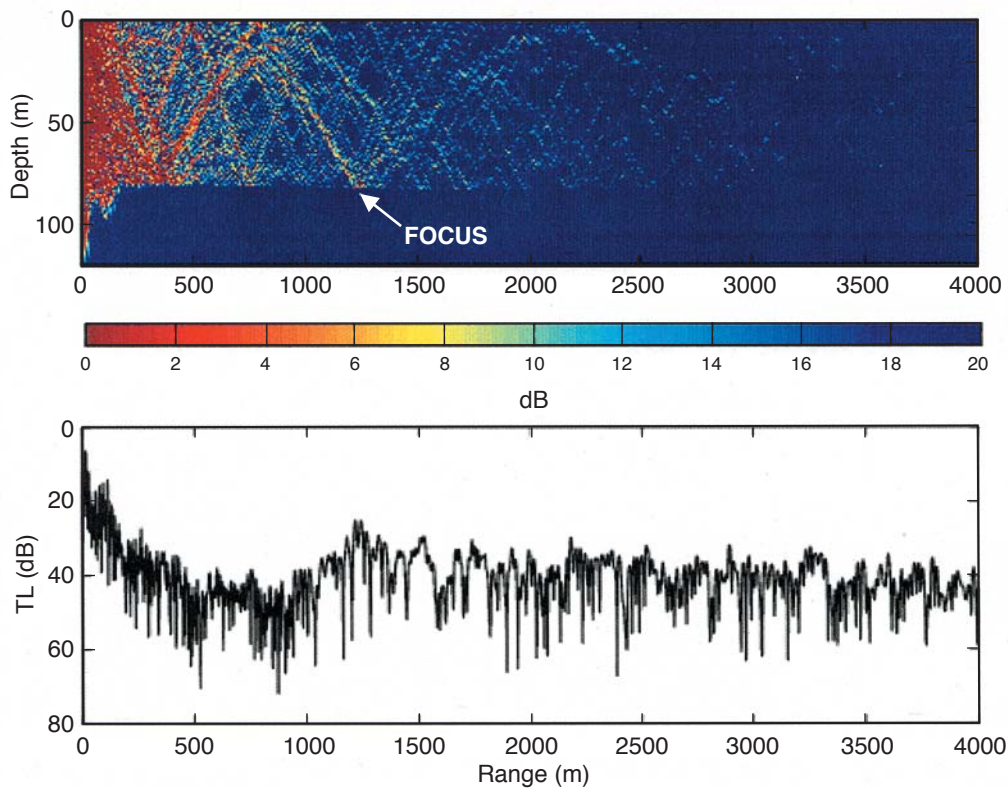


FIGURE 7

Backpropagation of a time-reversed window of the reverberation signal shown in Fig. 6. The time window is approximately 1.87 ± 0.05 s, corresponding to a nominal range from the SRA of approximately 1400 m. The color plot shows the backpropagation of this reverberation segment through the environment that was measured during the experiment. The bottom curve is a plot of the transmission loss near the bottom (81.5-m depth) showing the increased ensonification of approximately 5 dB near the bottom at about 1250 m from the array.

CONCLUSIONS

At NRL, the concept of a time-reversal mirror is being applied to acoustic detection and remote sensing applications in shallow-water ocean environments. These ideas are being tested in at-sea experiments with a unique 64-channel source-receiver array. Time-reversal processing offers potential benefits to Navy systems because it can focus acoustic energy in uncertain environments. Applications of this technology to antisubmarine warfare, wide-area bathymetry mapping, and mine hunting are being developed.

ACKNOWLEDGMENTS

The authors thank E.R. Franchi and J.S. Perkins for their helpful comments in preparing this manuscript.
[Sponsored by ONR]

References

- ¹C. Prada, S. Manneville, D. Spoliansky, and M. Fink, "Decomposition of the Time-Reversal Operator: Detection and Selective Focusing on Two Scatterers," *J. Acoust. Soc. Am.* **99**, 2067-2076 (1996).
- ²J.F. Lingeitch, H.C. Song, and W.A. Kuperman, "Time Reversed Reverberation Focusing in a Waveguide," *J. Acoust. Soc. Am.* **111**, 2609-2614 (2002).

THE AUTHORS



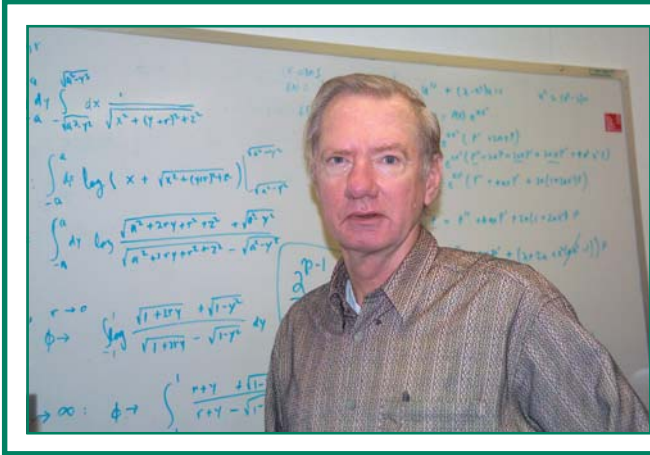
JOSEPH F. LINGEVITCH received his Ph.D. in applied mathematics from Northwestern University in 1995. He joined the NRL Acoustics Division as an NRC post-doctoral fellow in 1995 to work on applications of parabolic equation methods to problems in underwater acoustics. In 1997 he became a research physicist in the Acoustics Division. His research interests include parabolic equation modeling, scattering, atmospheric wave propagation, geo-acoustic inversion, and applications of time-reversal techniques to detection problems. He is a Fellow of the Acoustical Society of America.



CHARLES F. GAUMOND received his B.S. degree in physics from Clarkson University and his M.A. and Ph.D. degrees from the University of Rochester. Since 1979 he has been employed as a research physicist at the Naval Research Laboratory. He has had temporary assignments as a program analyst for the Director of Defense Research and Engineering in the Office of the Secretary of Defense and as a program manager at the Office of Naval Research. His areas of specialization have been ultrasonics, acousto-optics, acoustical imaging, experimental and numerical acoustical scattering, sonar analysis, research and development strategy, time-frequency analysis, passive sonar and active sonar. He is currently the Chairman of the Signal Processing in Acoustics Technical Committee of the Acoustical Society of America.



DAVID M. FROMM received his B.A. degree in mathematics and physics in 1974 from the University of Delaware. He received his M.S. and Ph.D. degree in physics in 1983 and 1990, respectively, from the University of Delaware. Dr. Fromm joined NRL as a research physicist in the Acoustic Systems Branch in 1985. He has specialized in the modeling of underwater acoustic reverberation, developing both ray-theoretic and normal mode implementations of a bistatic reverberation model for active sonar systems. Dr. Fromm has performed the acoustic analysis for several marine mammal incidents involving Navy sonars. His current research efforts concern the application of time-reversal techniques to the active sonar problem to enhance detection and classification, and to mitigate the need for detailed environmental information.



B. EDWARD McDONALD received a Ph.D. in physics from Princeton University in 1970, after which he joined the NRL Plasma Physics Division. From 1970 to 1980, he carried out numerical investigations of ionospheric plasma processes related to high-altitude nuclear weapons effects and naturally occurring plasma turbulence affecting satellite communication. From 1980 to 1990 he developed theory and numerical solution techniques for fluid dynamics and nonlinear acoustics. He joined the Acoustics Division in 1990. Since that time he has developed theory and computer models for prediction and interpretation of ocean processes in surface reverberation, acoustic propagation across major ocean basins, acoustic thermometry of ocean climate, and underwater explosions. From 1997 to 2000 he was Principal Scientist at the NATO Saclant Centre in La Spezia, Italy.



WINDSAT – REMOTE SENSING OF OCEAN SURFACE WINDS

P.W. Gaiser

Remote Sensing Division

The wind vector affects a broad range of naval missions, including strategic ship movement and positioning, aircraft carrier operations, aircraft deployment, effective weapons use, underway replenishment, and littoral operations. Furthermore, accurate wind vector data aid in short-term weather forecasting, the issuing of timely weather warnings, and the gathering of general climatological data. WindSat is a satellite-based multifrequency polarimetric microwave radiometer developed by the Naval Research Laboratory for the U.S. Navy and the National Polar-orbiting Operational Environmental Satellite System (NPOESS) Integrated Program Office (IPO). It is designed to demonstrate the capability of polarimetric microwave radiometry to measure the ocean surface wind vector from space. The sensor provides risk reduction for the development of the Conical Microwave Imager Sounder (CMIS), which is planned to provide wind vector data operationally starting in 2010. WindSat is the primary payload on the Air Force Coriolis satellite, which was launched on 6 January 2003. It is in an 840-km circular Sun-synchronous orbit. It is currently undergoing rigorous calibration and validation to verify mission success.

NAVY NEED FOR WIND INFORMATION

WindSat strives to answer the battlespace environment question, “What’s the wind speed and direction around the carrier strike group?” Winds over the ocean affect nearly every aspect of naval operations, including carrier operations, mission planning for precision guided munitions, surf forecasting for expeditionary forces, and avoidance of nuclear, biological, and chemical clouds. The global ocean surface wind vector (speed and direction) provides essential information for short-term weather forecasts and warnings, nowcasting, and climatology and oceanography studies in both the civilian and military sector. This can lead to improved accuracy in tropical cyclone forecasting and improved ship routing. Carrier post-cruise reports following deployments in the Adriatic Sea stated that the most critical piece of meteorological data was the wind direction. The same reports indicated that wind direction was the least-understood parameter in their environment. Despite this critical need, the Navy has not been able to obtain global wind direction information from space. Space-borne passive microwave sensors, such as the Special Sensor Microwave Imager (SSM/I), operationally provide environmental data such as tropospheric water vapor mass, cloud liquid water mass, sea ice age and concentration, and ocean surface wind speed.¹

One parameter that has not been provided by microwave radiometers is wind direction. However, recent work and advance in polarimetric radiometry suggest that it may be possible to measure the complete ocean surface wind vector (speed and direction) from space-borne microwave radiometer (such as SSM/I) if the instrument is modified to include measurement of the full Stokes vector (the current generation of SSM/I sensors measure only the first two components of the four-element vector).^{2,3}

WindSat is a satellite-based multifrequency polarimetric microwave radiometer developed by the Naval Research Laboratory Remote Sensing Division and the Naval Center for Space Technology for the U.S. Navy and the National Polar-orbiting Operational Environmental Satellite System (NPOESS) Integrated Program Office (IPO). WindSat is designed to demonstrate the viability of using polarimetric microwave radiometry to measure the ocean surface wind vector from space. It is the primary payload on the Air Force Coriolis satellite, which is sponsored jointly by the DoD Space Test Program (STP) and the Navy (SPAWAR PMW-155). WindSat shares this mission with the Solar Mass Ejection Imager (SMEI) developed by the Air Force Research Laboratory (AFRL). A spacecraft developed by Spectrum-Astro of Gilbert, Arizona, supports both payloads. The WindSat/Coriolis mission was launched on a Titan II rocket from Vandenberg

Air Force Base on 6 January 2003. In addition to potentially providing the Navy with badly needed ocean surface wind vector measurements, WindSat provides risk reduction data that the NPOESS will use in the development of the Conical Microwave Imager Sounder (CMIS), which would provide wind vector measurements operationally beginning in the 2009 time frame, building on the pathfinding work of WindSat.

POLARIMETRIC RADIOMETRY BACKGROUND

Microwave radiometry is a well-established technology for remote sensing of the environment. Radiometers such as WindSat measure the microwave emission from the field of view (FOV) of its antenna. Figure 1 illustrates that the received energy is a combination of energy emitted from the surface (ocean), radiation from the atmosphere, and energy from the sky reflected off the surface. The measured quantity is known as the brightness temperature. For the surface emission, it is related to the physical temperature by

$$T_{B,p} = e_p (\cos\theta) T_{\text{phys}},$$

where $T_{B,p}$ is the brightness temperature in polarization p , e is the scene emissivity, T_{phys} is the physical temperature of the scene, and (θ, φ) represent the viewing geometry. By definition, a perfectly absorbing and emitting blackbody has an emissivity of one. Therefore, at thermal equilibrium it has a brightness temperature equal to its physical temperature. All other scenes have an emissivity less than one. The emissivity depends not only on the geometry and polarization, but also on the physical properties of the medium. For sea water, in particular, the emissivity is

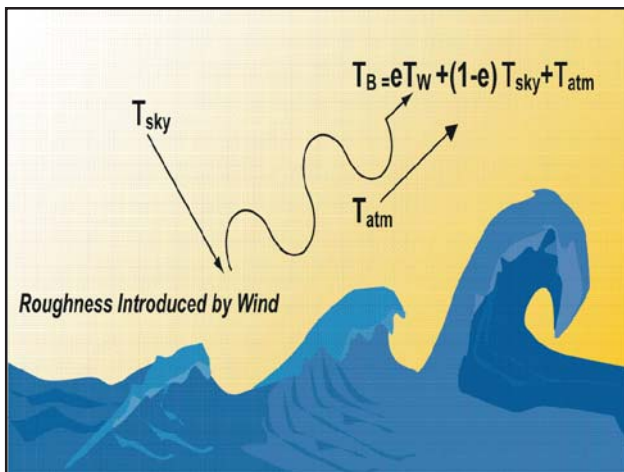


FIGURE 1
Conceptual description of principles of microwave radiometer measurements.

a function of the water temperature, salinity, and the roughness of the medium's surface.

It has long been known that the microwave emission from the ocean surface depends on the wind speed at the surface. As the winds increase, the seas become rougher and the microwave emission increases. However, the wind-driven waves on the ocean surface are not isotropic; their distribution varies with wind direction. Therefore, the intensity of the emission depends not only on the wave structure, but also on the orientation of the wind-driven waves.

WindSat is the first space-borne polarimetric microwave radiometer. As a polarimetric radiometer, WindSat measures not only the principal polarizations (vertical and horizontal), but also the cross-correlation of the vertical and horizontal polarizations. The cross-correlation terms represent the third and fourth parameters of the modified Stokes vector, defined as

$$I_s = \begin{bmatrix} I \\ Q \\ U \\ V \end{bmatrix} = \begin{bmatrix} T_v \\ T_b \\ T_{45} - T_{-45} \\ T_{lc} - T_{rc} \end{bmatrix} = \begin{bmatrix} \langle E_v E_v^* \rangle \\ \langle E_b E_b^* \rangle \\ 2\text{Re}\langle E_v E_b^* \rangle \\ 2\text{Im}\langle E_v E_b^* \rangle \end{bmatrix}.$$

In this definition, T_v , T_b , T_{45} , T_{-45} , T_{lc} , and T_{rc} represent brightness temperatures (radiances) at vertical, horizontal, plus 45°, minus 45°, left-hand circular, and right-hand circular polarizations, respectively. The Stokes vector provides a full characterization of the electromagnetic signature of the ocean surface and the independent information needed to uniquely determine the wind direction.

WINDSAT INSTRUMENT DESCRIPTION

Figure 2 shows the WindSat payload. The radiometer operates in discrete bands at 6.8, 10.7, 18.7, 23.8, and 37.0 GHz. Table 1 provides key design and performance parameters of the system. The 10.7, 18.7, and 37.0 GHz channels are fully polarimetric. The 6.8 channel is dual-polarization (vertical and horizontal), and is more sensitive to sea surface temperature (SST) than to winds. Thus it is used to remove measurement noise due to variations in SST. Similarly, the 23.8 channel has dual-polarization. This frequency responds strongly to water vapor in the atmosphere, which attenuates the signal from the ocean surface. Thus, 23.8 channel data mitigates the effects of the water vapor.

WindSat uses a 1.8-m offset reflector antenna fed by 11 dual-polarized feed horns. The antenna beams view the Earth at incidence angles ranging from 50 to 55°. Table 1 shows the nominal beamwidth and

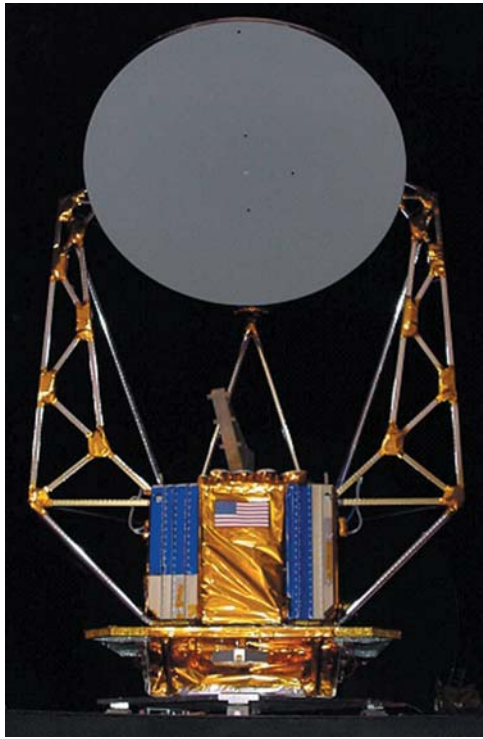


FIGURE 2
WindSat payload in the thermal/vacuum chamber. The cold sky reflector has been removed in this picture.

Table 1. WindSat Configuration

Band (GHz)	Polarization	Bandwidth (MHz)	Earth Incidence Angle (deg)	Horizontal Spatial Resolution (km)
6.8	V, H	125	53.5	40 × 60
10.7	V, H, ±45, L, R	300	49.9	25 × 38
18.7	V, H, ±45, L, R	750	55.3	16 × 27
23.8	V, H	500	53.0	12 × 20
37.0	V, H, ±45, L, R	2000	53.0	8 × 13

resulting surface spatial resolution of each band. The Coriolis satellite orbits Earth at an altitude of 840 km in a Sun-synchronous orbit. The satellite completes just over 14 orbits per day. The orbit and antenna geometry result in a forward-looking swath of approximately 1000 km and an aft-looking swath of about 400 km. The fully integrated WindSat payload stands 10 ft tall and weighs approximately 675 lb.

WINDSAT RADIOMETER MEASUREMENTS

After being powered on on 24 January 2003, the WindSat radiometer achieved thermal stability in less than 36 h, at which time the receiver gains also stabilized. The gains and receiver offsets were adjusted via ground commands to optimize the dynamic range of the receivers. The WindSat calibration and validation (cal/val) team then began rigorous analysis of the system performance and debugging of the ground data processing system (GDPS). One of the first

products from this process was radiometric imagery for all 22 channels. As an example, Fig. 3 shows a brightness temperature image of three consecutive descending passes for the 18.7 GHz +45°-polarization channel collected on 31 March 2003. Several features stand out in the false-color image. The visible structures of bright bands and other regions of locally high brightness temperatures over the ocean are typical of atmospheric variations in water vapor, clouds, and rain. In the North Atlantic, the brightness temperatures in the Labrador Sea and Hudson Bay (colored yellow/green in the image) are higher than the ambient ocean and are typical of sea ice signatures, whereas the cooler brightness temperatures over Greenland are representative of a permanent ice sheet. Over land, there are also noticeable differences in brightness temperatures, which are due to differences in the physical temperature of the terrain, such as between North America (early spring) and equatorial South America. Lastly, in North America, the

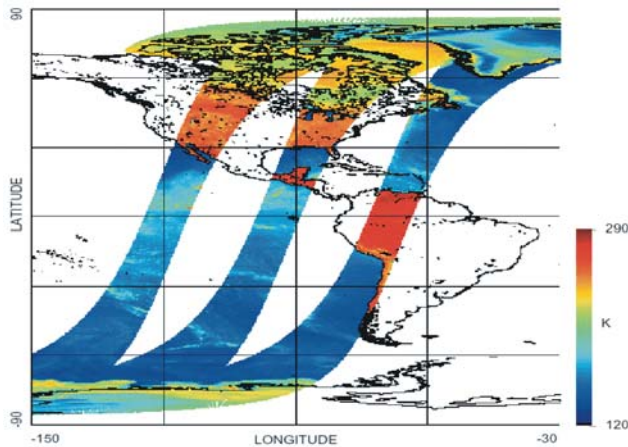
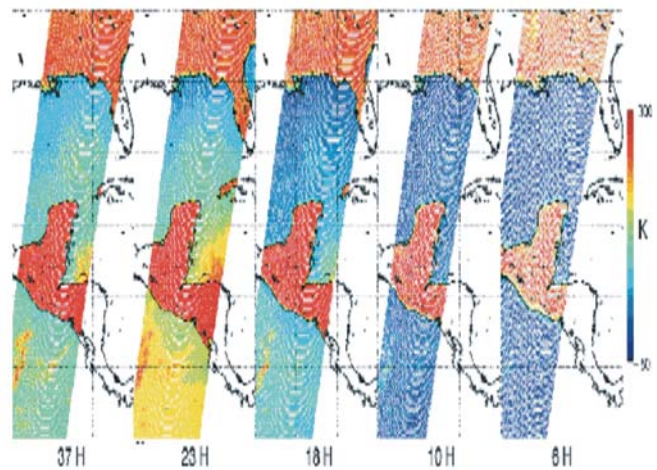


FIGURE 3
WindSat image showing three consecutive descending passes of 18.7, +45 (18P) channel.

FIGURE 4
Composite image showing horizontal polarization at each of five WindSat frequency bands. Area is Yucatan peninsula of Mexico.



brightness temperature decreases with increasing latitude over northern Canada, which is consistent with signatures of snow cover in those regions for this time of year.

Figure 4 highlights a portion of this same pass over Mexico and Central America, showing simultaneous images at horizontal polarization for each of the five WindSat frequencies. In this series of images, one can see how the various frequencies respond differently to the same oceanic and atmospheric conditions, most noticeably in the increased sensitivity to clouds and water vapor (which appear as bright features) in the higher frequency channels.

To illustrate the differences among polarizations at the same frequency, Fig. 5 depicts the 37 GHz imagery at vertical, horizontal, +45° linear, and left-circular polarizations. (For these color scales, differences between left and right circular polarizations are too subtle to be illustrative; the same is true for +45° and -45° linear polarizations, so only one of each pair is shown here.) When comparing these images, it is clear that over the ocean the magnitudes of the +45° and left-circular brightness temperatures lie between the values of the vertical and horizontal polarizations

as is expected, since these polarizations are weighted combinations of vertical and horizontal.

WIND DATA FROM WINDSAT

As part of the WindSat calibration and validation, we have compiled a large set of WindSat data matched with modeled wind fields over the ocean. These wind fields come from the Global Data Assimilation System (GDAS) generated by the NOAA National Center for Environmental Prediction. The GDAS wind fields are generated every 6 h. The matchups are limited to WindSat data collected within 1 h of the analysis. Figure 6 shows WindSat third and fourth Stokes parameters plotted against wind direction. The different colors represent different wind speeds. The signals can be modeled as sinusoidal functions. The third has significant first and second harmonics, whereas the fourth is dominated by the second harmonic. It is also interesting to note that the third and fourth Stokes parameters are odd functions with respect to the wind direction. Vertical and horizontal polarizations also behave sinusoidally, but they are even functions relative to wind direction. These

signatures agree well with model simulations and data collected from airborne polarimetric radiometers.⁴

Figure 6 shows that the peak-to-peak variations change with the wind direction. However, even at the higher winds, the peak-to-peak signal is less than 4 K. Typical 37 GHz vertical polarization brightness temperatures over the ocean are approximately 200 K. Thus, the wind direction signal is a very small. Therefore, the WindSat design emphasized sensitivity and stability in the calibration.

As a more tangible way to look at the wind direction signal, consider Fig. 7, which depicts an image of Hurricane Isabel from the WindSat 18.7 GHz third Stokes parameter channel. The wind circulates around the storm in a counter-clockwise fashion. Comparing the signal in the image with the plots in part (b) of the figure, one can see how the signal changes as the wind direction shifts around the perimeter of the storm. Hurricane Isabel was a Category 5 storm when these data were collected. The intense rain and high levels of clouds and water vapor attenuate the peak-to-peak response of the

WindSat signals. Collecting data at multiple frequencies provides necessary information to account for the effects of the atmosphere and the sea surface temperature.

The objective of the WindSat program is to retrieve the ocean surface wind vector from the WindSat data. The NRL WindSat team is developing algorithms and software that take advantage of the characteristics described earlier. The algorithms must work globally and derive the wind speed and direction to within ± 2 m/s and $\pm 20^\circ$, respectively, over a range of 3 to 25 m/s winds. After successful calibration and validation, all algorithms will be transitioned to the Navy for operational use of WindSat data.

Working in collaboration with other institutions such as the Jet Propulsion Laboratory (JPL) and the National Oceanographic and Atmospheric Administration (NOAA), preliminary wind vector retrievals have been developed. Figure 8 shows an example of these early retrievals in the southern Atlantic where (a) is the retrieved wind vector and (b) is the GDAS wind field for that time. There is very good agreement

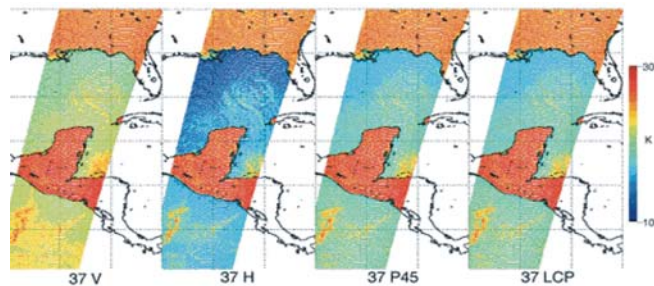


FIGURE 5
Composite image showing 37 GHz brightness temperatures at vertical, horizontal, +45°, and left-circular polarizations.

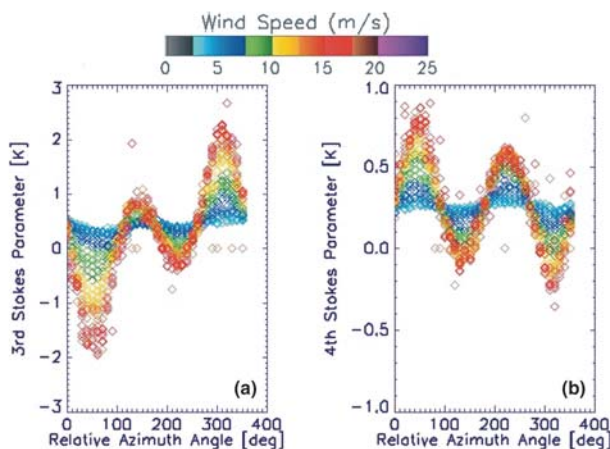


FIGURE 6
Sensitivity of 10.7 GHz third (a) and fourth (b) Stokes parameters to wind direction. The colors represent different wind speed ranges. Wind vector truth data supplied by the NOAA GDAS system. Figure courtesy of NOAA/NESDIS/ORA.

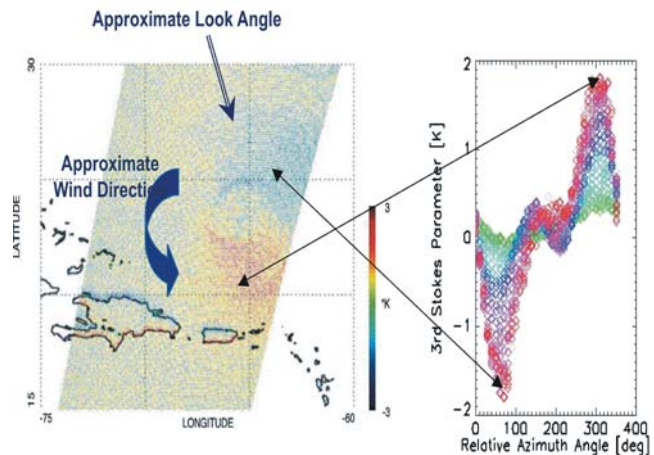


FIGURE 7
Hurricane Isabel on 14 September 2003, as seen by WindSat 18.7 GHz third Stokes parameter. Notice how the signal changes around the circulation pattern of the storm.

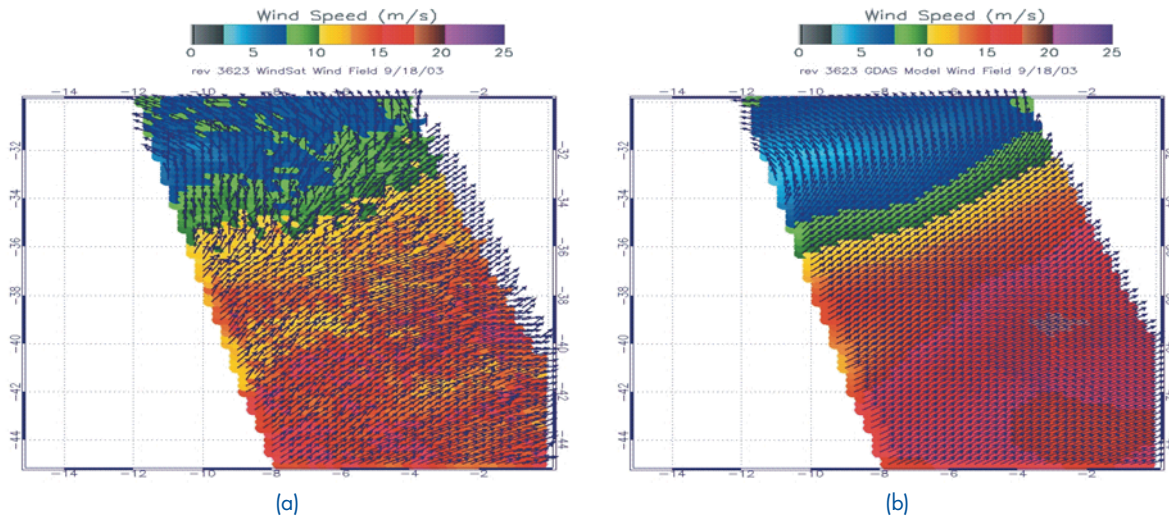


FIGURE 8
 (a) Preliminary wind vector retrieval compared with (b) GDAS analytical wind field. The image is over the southern Atlantic and is based on empirical model developed using WindSat/GDAS matchups. Figure courtesy of NOAA/NESDIS/ORA.

between the two images. Notice in particular the increasing wind speed from north to south. Similar circulation patterns can be seen in the low wind region at the northern edge of the image. While this is only a preliminary retrieval, it demonstrates the vast potential of the WindSat mission.

CONCLUSIONS

As the mission, tactics, and platforms of the Navy continue to evolve, the need for improved battlespace environment intelligence grows. The WindSat mission is designed to satisfy this requirement by providing timely ocean surface wind vector measurements to the warfighter. The WindSat payload is the first space-borne polarimetric microwave radiometer. Early results demonstrate the capability to retrieve the wind speed and direction over the ocean. As the calibration and validation phase of WindSat nears completion, NRL will continue to develop the WindSat capability to get needed information into the hands of the users.

The mission of WindSat does not end there. WindSat data, algorithms, and designs are playing an important role in the development of the NPOESS CMIS, which is the future operational source of environmental data such as ocean winds. Furthermore, the WindSat data are being studied and exploited, not only at NRL but also at many research institutions, to develop new applications for polarimetric microwave radiometer data.

ACKNOWLEDGMENTS

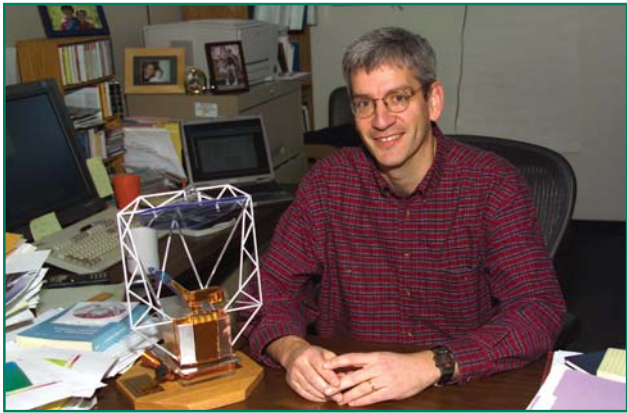
I acknowledge the contributions of the many who helped in the development and exploitation of WindSat. These include David Spencer, Michael Mook, Jerry Golba, Jeff Cleveland, Bill Purdy, and Pattie Klein of the Naval Center for Space Technology. Within the Remote Sensing Division, I thank Elizabeth Twarog, Karen St. Germain, Gene Poe, Don Richardson, Richard Cember, Larry Choy, Craig Smith, Mike Bettenhausen, Al Uliana, and Beverly Gardiner. Lastly, I thank my collaborators at the NOAA/NESDIS Office of Research and Applications: Paul Chang, Nai-Yu Wang, and Tim Mavor, with special thanks to Larry Connor and Zorana Jelenak for building the matchup database and developing the preliminary wind direction retrieval.

[Sponsored by SPAWAR and NPOESS]

References

- ¹ J.P. Hollinger, J.L. Peirce, and G.A. Poe, "SSM/I instrument evaluation," *IEEE Trans. Geosci. Remote Sens.* **28**(5), 781-790, (1990).
- ² S.H. Yueh, W.J. Wilson, F.K. Li, S.Y. Nghiem, and W.B. Ricketts, "Polarimetric Measurements of the Sea Surface Brightness Temperature Using an Aircraft K-band Radiometer," *IEEE Trans. Geosci. and Remote Sens.* **33**(1) 85-92, (1995).
- ³ P. Chang, P. Gaiser, K. St. Germain, and L. Li, "Multi-Frequency Polarimetric Microwave Ocean Wind Direction Retrievals," *Proceedings of the International Geoscience and Remote Sensing Symposium 1997*, Singapore, 1997.
- ⁴ K.M. St. Germain, G.A. Poe, and P.W. Gaiser, "Polarimetric Emission Model of the Sea at Microwave Frequencies and Comparison with Measurements," *Prog. Electromag. Res.* **37**, 2-32 (2002).

THE AUTHOR



PETER W. GAISER received his B.S. degree in electrical engineering from Virginia Tech in 1987. He received his Ph.D. in 1993 from the University of Massachusetts at Amherst, where he studied microwave remote sensing, with emphasis on synthetic aperture interferometric radiometry. He joined NRL in May 1993, where he now heads the Microwave Remote Sensing Section of the Remote Sensing Division. While at NRL, he has been involved in polarimetric radiometry research. His research interests also include instrument design, data collection, and model development specifically for the ocean wind vector measurements from space. Dr. Gaiser also pursues research interest in microwave radiometry for other environmental remote sensing applications and passive millimeter wave imaging. Dr. Gaiser is the principal investigator for the WindSat spaceborne polarimetric microwave radiometer demonstration project.

BACTERIOPHAGE T4 — THE ORIGINAL NANOBOT

Bacteriophage T4 is a virus that infects bacteria. When T4 touches the bacterial surface, its articulated legs bend. When the baseplate makes contact, an enzyme is released, burning a hole through the cell wall. Instantly the stalk shortens and, like a syringe, injects DNA into the bacterium. The DNA takes over the infected host and turns it into an efficient virus factory.



97 Passive Swimmer Detection
S. Stanic, C.K. Kirkendall, A.B. Tveten, and T. Barock

98 Passive Acoustic Ranging by Multimode Waveguide Interferometry
A. Turgut, M.H. Orr, and B.H. Pasewark

PASSIVE SWIMMER DETECTION

S. Stanic
Acoustics Division

C.K. Kirkendall, A.B. Tveten, and T. Barock
Optical Sciences Division

Introduction: Protecting our commercial and military harbor facilities both at home and abroad from underwater threats is a high priority. It is estimated that an explosion or serious attack on one port would almost certainly result in the disruption of regional commerce for as long as 4 months.¹ Technological advances and the increased availability of closed-circuit breathing systems, diver delivery vehicles, and mini-submarines have focused attention on the need for coastal and harbor surveillance, target detection, and target identification systems.

Both military and commercial port facilities are generally located in areas where the water depths range from 10 to 50 m. At these depths, environmental conditions have a strong influence on the performance of all acoustic surveillance and detection systems. Passive detection of underwater threats are subject to background environmental variabilities that will change with location, shipping densities, and time of day. Seasonal changes will also depend on biological activities.

Passive Detections: To demonstrate the ability to passively detect divers who are using open circuit breathing systems, a series of detection measurements were taken in San Diego Bay in the fall of 2002. A number of conventional and fiber optic hydrophone sensors were placed on the harbor bottom and connected via fiber optic cables to an instrumentation van located onshore. The sensors were deployed in 12 m of water, approximately 120 m from shore. Divers entered the water at a distance

of 50 m from the sensors and approached the sensors from several different directions and depths. Figure 1 is a schematic of experiments.

Figure 2 shows the received signals as the diver approached the sensors at a height of approximately 2 m above the bottom. The signals were first detected when the diver came within 24 m, and the levels increased as the diver approached the sensors and passed directly overhead. The signatures were generated by the mechanical operation of the diving equipment. The diver breathing patterns are clearly visible in the acoustic time series collected during the experiments.

Figure 3 is the measured harbor average noise spectra for the times when the diver was in the water. These spectra are similar to those measured by Anderson and Guber in 1971.² The noise levels generated by the diver's regulators are shown, but they are detectable only at the high end of the spectra.

Summary: A field test has shown that it is possible to detect divers equipped with open-circuit breathing sys-

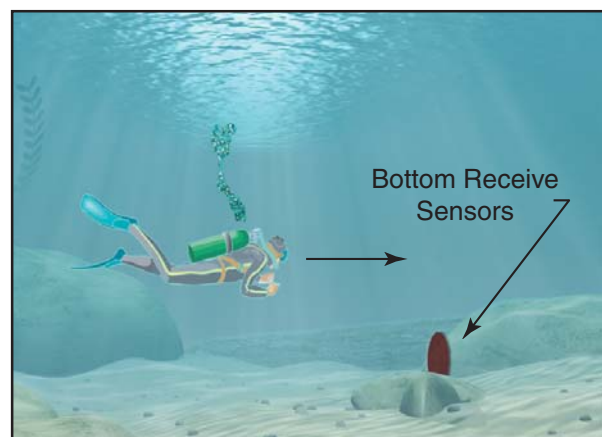


FIGURE 1
Diver and bottom-mounted sensors.

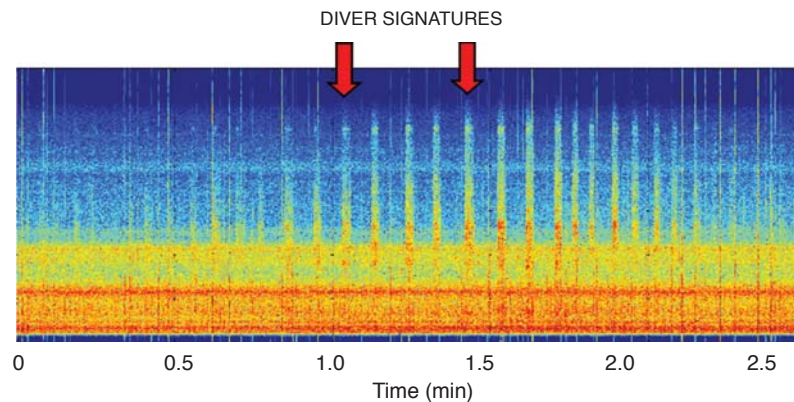
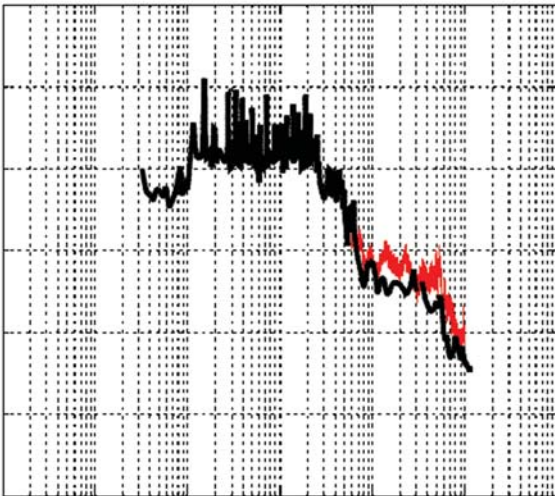


FIGURE 2
Received passive signal as the diver approached and passed over one of the bottom-mounted sensors.



— SCUBA radiation re ~1 m (Stanic/Kirkendall, 2002, unpublished data)
 — San Diego Bay – Ship side noise (Stanic/Kirkendall, 2002, unpublished data)

FIGURE 3
 Harbor noise and diver signature spectra.

tems in the harbor environment by passively detecting the acoustic emission from the dive equipment. Although detections were made using individual hydrophones, additional signal gains can be obtained by using multichannel arrays and conventional array processing. This will increase the detection ranges and provide bearing information.

[Sponsored by CNO]

References

- ¹ www.GovExec.com. March 6, 2002.
- ² A.L. Anderson and G.L. Guber, “Ambient Noise Measurements at 30, 90, and 150 kHz in Five Ports,” *J. Acoust. Soc. Am.* **49**, 928-930 (1971).

PASSIVE ACOUSTIC RANGING BY MULTIMODE WAVEGUIDE INTERFEROMETRY

A. Turgut, M.H. Orr, and B.H. Pasewark
Acoustics Division

Introduction: To achieve the power projection to land mission, the Navy needs the ability to passively estimate the range of submerged targets operating in a dynamic littoral environment. The authors are investigating a passive range estimation technique that may be robust in environmentally variable littoral operating areas. The technique will require the deployment of four lightly populated vertical arrays (2 to 4 hydrophones). Acoustic signals received on the vertical arrays will be used to form “virtual horizontal arrays.” Range ratios (the ratio of the distance from two vertical arrays and the target) esti-

mated from “virtual horizontal arrays” derived from pairs of the four vertical array system will be used to localize a passive target. We have used acoustic data taken in a dynamic littoral setting to demonstrate that accurate range ratios can be estimated from two vertical line arrays (VLAs). The technique hinges on the fact that broadband acoustic signals propagate in the shallow water as modes with slightly different phase speeds and, as a result, create interference structures in both range and frequency.

Passive Acoustic Ranging in Littoral Waters: We combine two techniques to estimate the range ratio of a passive target in littoral waters. The first is to generate a “virtual receiver” by applying holographic array processing¹ to broadband acoustic signals received on two VLAs. The second is the use of a waveguide invariant² parameter to form a “virtual receiver array” from a virtual receiver. Turgut has combined the two techniques and derived an analytical formulation that describes the signal interference structure of the virtual array output.³ The formulation can be used to estimate the range ratio to a target when its signal is received simultaneously on two VLAs. The analytic formula predicts the interference structure for a given range ratio r_1/r_2 . The range ratio is defined as the ratio of r_1 and r_2 , i.e., the range from each vertical line array to the passive target of interest. By using the range ratios extracted from a set of four VLAs, analysis indicates that the absolute range of the target from the receivers can be determined.

Illustration: Figure 4 is a three-dimensional sketch of the geometrical configuration of two VLAs that could be used to construct two “horizontal virtual arrays,” HVA1 and HVA2. We illustrate the use of the Turgut formalism to estimate the range ratio of an acoustic source from two vertical arrays operating in a dynamic littoral ocean waveguide. The data consist of broadband (60-140 Hz) acoustic signals that were projected to two VLAs during the SWARM95 New Jersey Shelf experiment. The source was 15.5 km from the VLA1 and 18 km from the VLA2, i.e., the range ratio is either 0.86 or 1.16. The source depth was 45 m, and water depths at the source location (VLA1 and VLA2) were 72, 70, and 90 m, respectively. Figure 5(a) shows the measured virtual array signal intensity along the VLA1 propagation track. Figure 5(d) shows the measured virtual array signal intensity along the VLA2 propagation track. In Fig. 5(a), the virtual array signal intensity was obtained by shifting the frequency bins of the received acoustic signals on the VLA2 up to ± 11 Hz. Contours of constant virtual array outputs (level curves) were identified by an edge detection algorithm or by a visual marking, as shown in Figs. 5(a) and 5(d). Figures 5(c) and 5(f) show the cost function ϕ defined as the rms value of a least-squares fit between the predicted level curves to the marked level curves. Minimum values of the cost function correspond to a best estimation of range

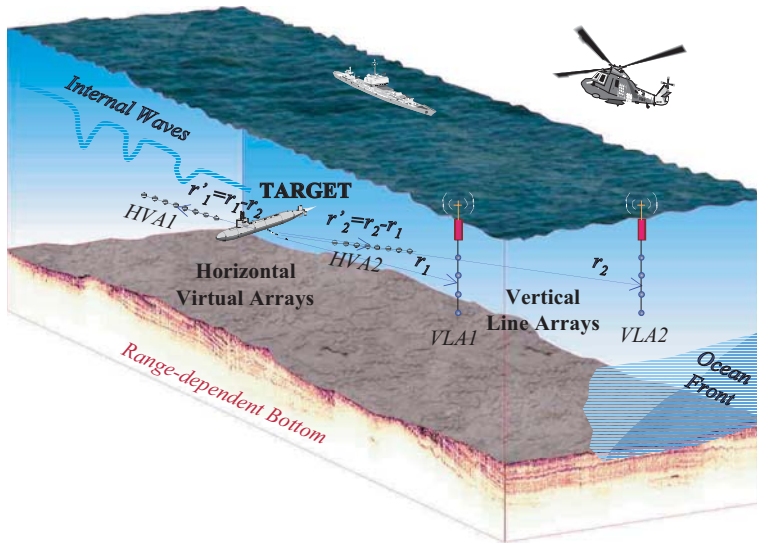


FIGURE 4
Geometrical configuration and construction of two virtual arrays using two VLAs in a complex littoral environment.

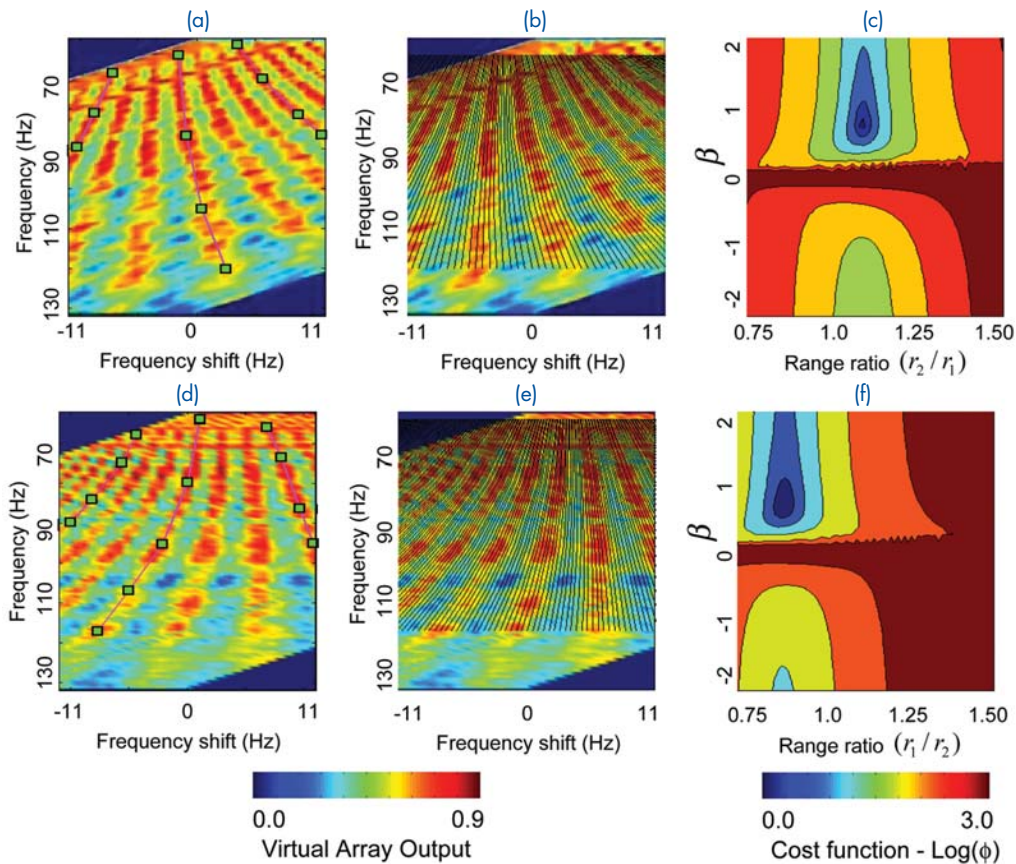


FIGURE 5
Illustration of curve fitting method for estimating range ratios and waveguide invariant β : (a,d) visual marking of the level curves; (b,e) comparison of measured virtual array output and calculated level curves by using estimated parameters; (c,f) cost function ϕ as a function of range ratios and waveguide invariant β .

ratios and the waveguide invariant parameter called beta. The best estimations were $r_2/r_1 = 1.14$, $r_1/r_2 = 0.88$, and $\beta = 0.75$. The estimated range ratios are comparable to the actual range ratios, $r_2/r_1 = 1.16$ and $r_1/r_2 = 0.86$ mentioned earlier. The agreement between the estimated and true range ratios is remarkable, especially considering that two VLAs have different propagation tracks and the environmental parameters are unknown along each track. Figures 5(b) and 5(e) show the levels curves calculated by using the estimated parameters and plotted on the measured virtual array intensity. Excellent agreement was obtained between measured and predicted level curves.

The impact of littoral fluid dynamic-induced waveguide variability on range ratio estimation has also been addressed. Figure 6(a) shows the SWARM95 experimental configuration and observed internal solitary wave (ISW) propagation direction. Figure 6(b) shows the virtual array output when the ISWs were outside the acoustic propagation track. Interference structures can be observed for almost the entire signal bandwidth and estimated parameters match the previously estimated values. Figures 6(c), 6(d), and 6(e) show the results when the ISWs were in the propagation track. Each figure is separated by 30 min. Interference structures seem to be destroyed by ISWs for signal frequencies greater than 100 Hz.

Hz. Even in this case, a passive estimate of the range ratios was still possible for frequencies less than 100 Hz. Based on minor differences observed in the virtual array outputs, and estimated range ratios and β values, we conclude that the range ratio estimation technique is robust, even under highly dynamic oceanographic conditions.

Summary: We outline a robust method to passively estimate the range ratio of a target from two vertical line arrays in the littoral environment. We expect that the technique will allow reliable target range (and bearing) estimation if four vertical arrays are placed in an area of interest.

[Sponsored by ONR]

References

1. A. Al-kurd and R. Porter, "Performance Analysis of the Holographic Array Processing Algorithm, Ocean Acoustic Holography: Using a Reference Source to Remove Oceanographic Variability," *J. Acoust. Soc. Am.* 97(3), 1747-1763 (1995).
2. L.M. Brekhovskikh and Y.P. Lysanov, *Fundamentals of Ocean Acoustics* (New York, Springer, 1991), 2nd edition.
3. A. Turgut, "Method and Apparatus for Passive Acoustic Ranging in Shallow Water," Patent Application, Navy Case # 84,558, 2003.

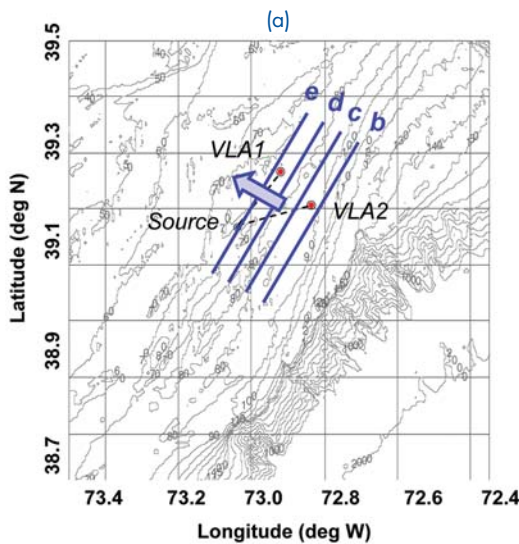
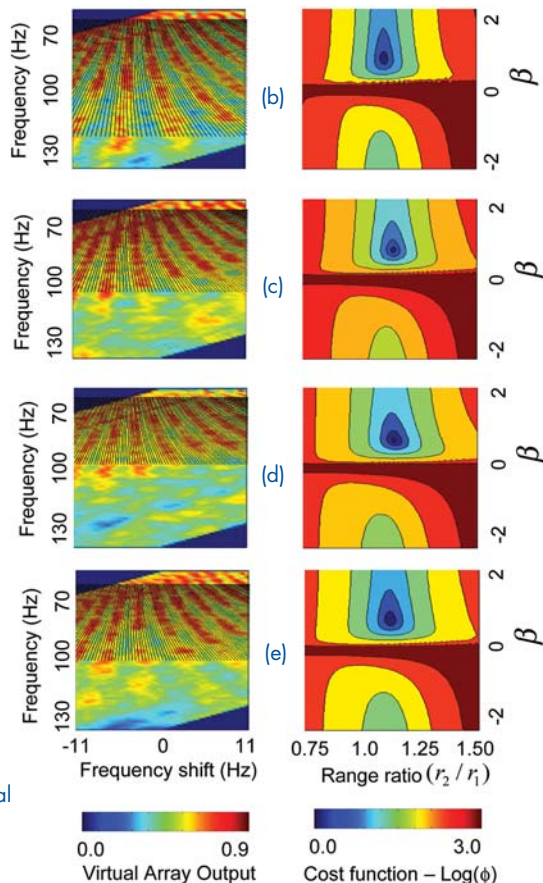
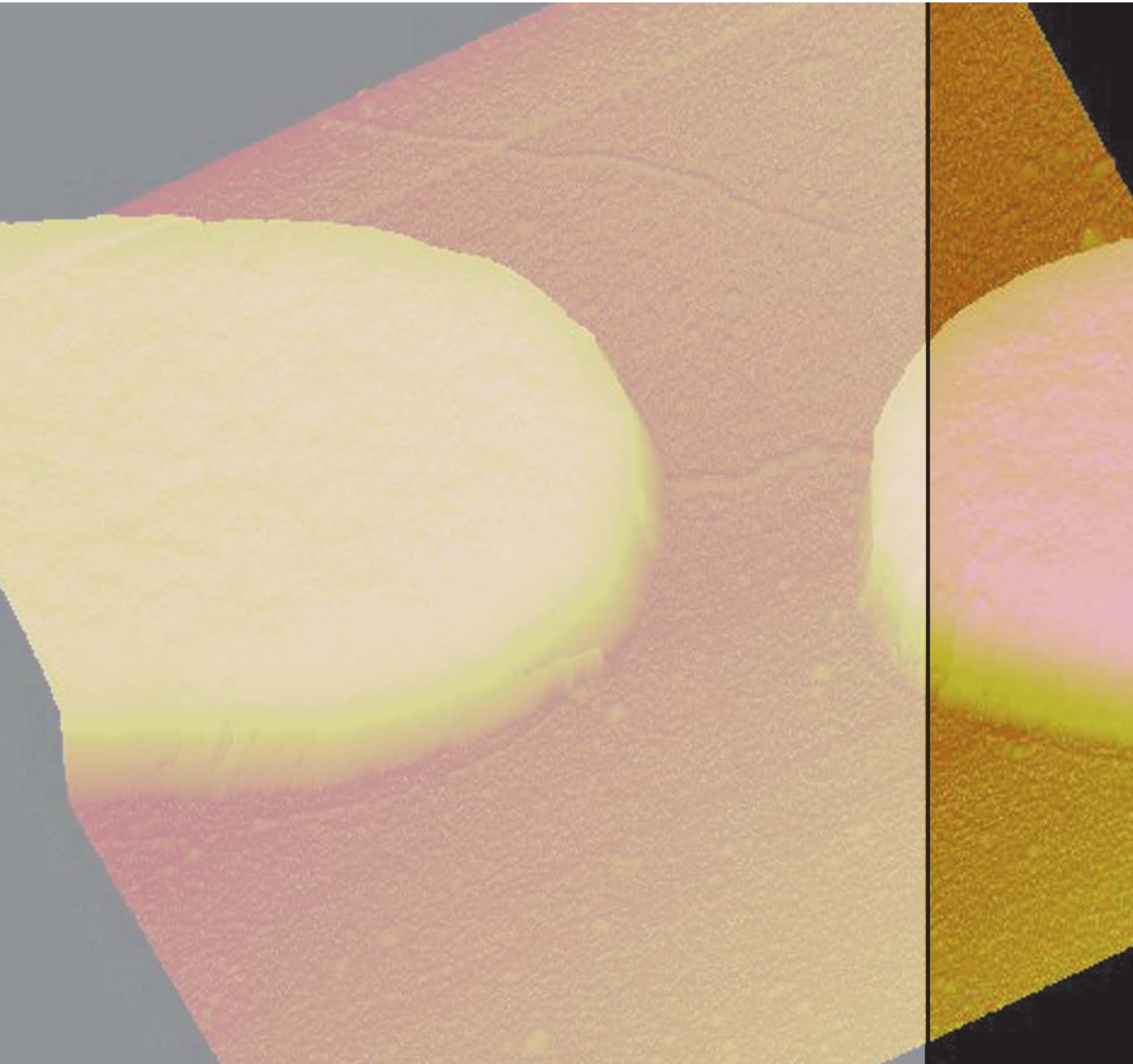


FIGURE 6 Virtual array outputs and calculated cost functions under highly dynamic oceanographic conditions. (a) Experimental configuration and observed ISW geometry; (b) ISWs are not present in the propagation tracks; (c,d,e) ISWs are in the propagation tracks.





CARBON NANOTUBE BUNDLE ATTACHED TO ELECTRODES

Scanning electron micrograph of a carbon nanotube bundle spanning electrodes fabricated from a ferromagnetic nickel alloy. Magnetic fields generated within the device were used to align and accurately place the nanotubes.



103 Real-Time, High-Resolution, Three-Dimensional Cloud and Wind Data
Assimilation Technology for the Battlespace Environment

Q. Zhao, J. Cook, P. Harasti, and J. Strahl

105 NRL Ionosphere Model: SAMI3

J. Huba and G. Joyce

106 The High Frequency Active Auroral Research Program

E.J. Kennedy, P. Rodriguez, and C.A. Selcher

109 Advances in Upper Atmosphere Forecasting: NOGAPS-ALPHA

J.P. McCormack, L. Coy, S.D. Eckermann, D.R. Allen, T. Hogan, and Y.-J. Kim

REAL-TIME, HIGH-RESOLUTION, THREE-DIMENSIONAL CLOUD AND WIND DATA ASSIMILATION TECHNOLOGY FOR THE BATTLESPACE ENVIRONMENT

Q. Zhao,¹ J. Cook, P. Harasti,² and J. Strahl³

¹*Marine Meteorological Division*

²*University Corporation for Atmospheric Research*

³*Science Applications International Corporation*

Introduction: To meet the U.S. Navy's increasing needs for accurate and detailed descriptions and predictions of the 3-D battlespace atmospheric environment, a high-resolution data assimilation system using remotely sensed data is under development at the Marine Meteorological Division of the Naval Research Laboratory. This system fuses remotely sensed data, particularly a combination of radar and satellite data, which possess information about the 3-D dynamical and hydrological structures of the atmosphere with high spatial and temporal resolutions, especially over oceans or in data-denied areas where conventional meteorological information is limited.

Data Assimilation System: The new data assimilation system uses a variational approach, together with advanced data fusion techniques, to retrieve 3-D cloud and wind fields from radar observations, geostationary satellite data, and surface observations in real-time. Also, the data assimilation system has the capability to use data from multiple radars to enlarge data coverage and to improve data resolution and accuracy.

The cloud analysis algorithm uses data fusion technologies to merge brightness temperatures and cloud albedo from geostationary satellite data, radar reflectivity from Doppler radar observations, and cloud observations from surface reports to retrieve 3-D cloud information.¹ The Navy's Coupled Ocean/Atmosphere Mesoscale Prediction System (COAMPSTM)* model forecasts are used as background fields for cloud analyses. Figure 1 gives an example of 3-D clouds produced by this system from a severe storm case on May 10, 2003, when a squall line developed and moved from north to south across the Washington, DC, and Norfolk, Virginia, areas. In this case, data from three radars in the storm area provided very fine structures of the storms that were missing from the background fields, especially at lower levels; satellite data and surface observations gave good estimations of cloud top and base heights.

A variational approach is used to retrieve the 3-D winds from radar observations of radial velocities.² By minimizing a simplified cost function, this method forces

the analysis fields toward radar observations and the first guess fields from model forecasts, and at the same time, applies the radial momentum and mass continuity equations as constraints to ensure that the retrieved wind fields satisfy the dynamic laws that govern atmospheric flow. After wind retrieval, temperature and pressure perturbations are also computed to match the retrieved winds to keep the dynamic balance between the wind and mass fields. Extensive testing of the radar wind retrieval system has been accomplished. Figure 2 gives an example of retrieved horizontal winds from an isolated storm in North Carolina on July 24, 2002. In this case, data from the Doppler radar in Morehead City of North Carolina were used in the analysis. Strong lower level convergence near the storm center that was not apparent in the background fields can be seen clearly in Fig. 2.

Products and Applications: Several environmental parameters critical to Navy warfighters and their missions can be directly derived from the 3-D clouds and winds produced by the data assimilation system. As an example, cloud ceiling derived from the 3-D clouds in Fig. 1 is given in Fig. 3. In this figure, cloud base height less than 1000 m can be seen in several locations with the lowest cloud base height of less than 500 m. Verifications against surface observations show notable improvements in the accuracy of the derived cloud base heights over those from the background fields, especially in convective regions. Experiments have also been conducted to assimilate the retrieved 3-D clouds and winds into the high-resolution COAMPS model, and the results have showed some improvement in short-term theater-scale weather prediction. Verification of the radar radial velocity derived from the first-hour forecasts of 3-D winds with radar data assimilation against radar observations for the storm case in Fig. 1 shows an increase of 0.182 in correlation and a decrease of 1.59 (m/s) in RMS error over the control forecast. The high-resolution winds from both the data assimilation system and the COAMPS model forecast are input into chemical/biological dispersion models, which are used for assessing contamination avoidance and decontamination strategies. The technology was demonstrated during Fleet Battle Experiment – Juliet with products providing up-to-date, detailed information to tactical decision makers about the 3-D atmospheric battlespace conditions. This work, though focused on battlespace environmental applications, establishes a scientific framework for using radar-derived meteorological information in multiple nowcasting and numerical weather prediction applications.

Acknowledgments: The authors thank Dr. Qin Xu of the National Severe Storm Laboratory for his assistance in the system development; and Mike Frost of CSC

*COAMPS is a trademark of the Naval Research Laboratory

FIGURE 1

3-D clouds (with water mixing ratio isosurface of 0.15 g/kg, blue color represents clouds below 700-hPa pressure level) of a severe storm system on the east coast on May 10, 2003, retrieved from radar, satellite and surface observations, and horizontal winds at 500-m level above the ground.

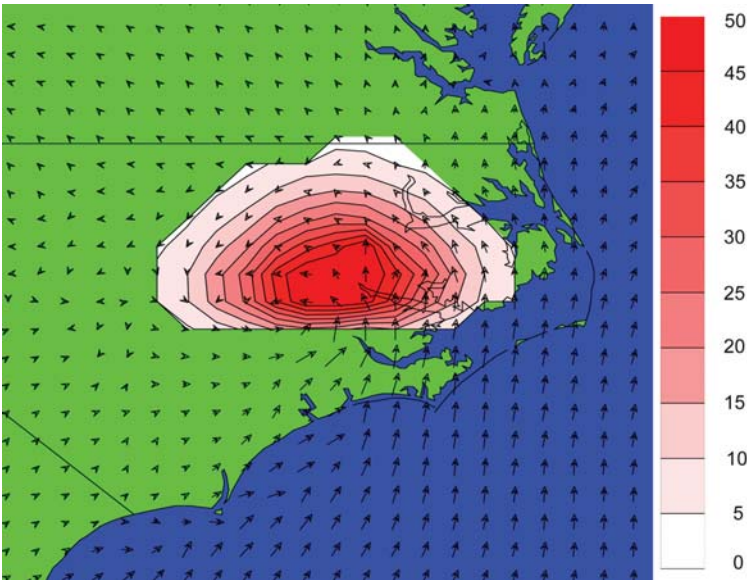
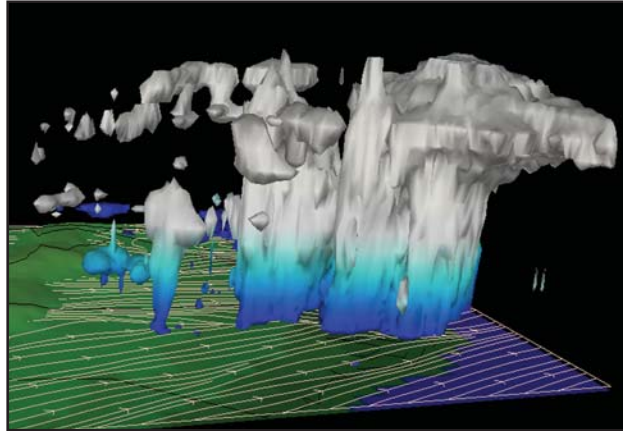
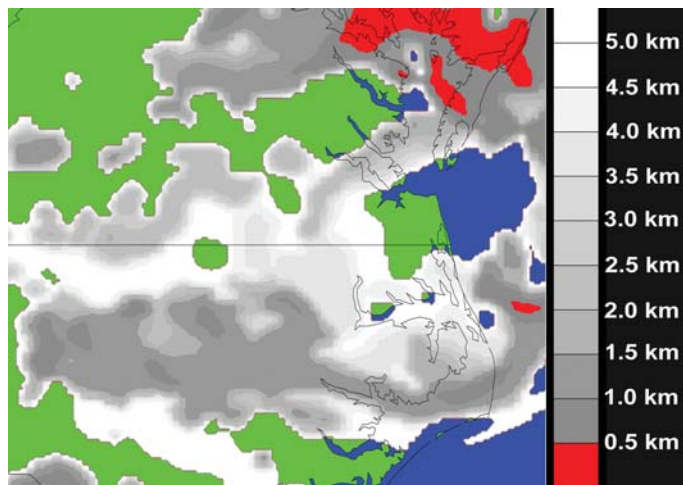


FIGURE 2

Radar observed reflectivity (shaded area, dBZ) of an isolated storm on July 24, 2002, and retrieved horizontal winds (with maximum vector representing 17 m/s) at 750-m level above the ground.

FIGURE 3

Cloud ceiling derived from the 3-D clouds in Fig. 1 with red color indicating regions with cloud base heights less than 500 m.



and Larry Phegley of NRL for their help in acquiring real-time radar and satellite data.

[Sponsored by NRL and ONR]

References

- ¹C.S. Albers, J.A. McGinley, D.L. Birkenheuer, and J.R. Smart, "The Local Analysis and Prediction System (LAPS): Analyses of Clouds, Precipitation, and Temperature," *Wea. and Forecasting*, 11, 273-287 (1996).
- ²Q. Xu, H. Gu, and W. Gu, "A Variational Method for Doppler Radar Data Assimilation," *Preprints, Fifth Symposium on Integrated Observing Systems*, 14-19 January 2001, Albuquerque, New Mexico, Amer. Meteor. Soc., 118-121 (2001).

NRL IONOSPHERE MODEL: SAMI3

J. Huba and G. Joyce
Plasma Physics Division

Introduction: Military systems are relying increasingly on space-based assets for communication and navigation. A critical aspect of the operation of these systems is the nature of the ionosphere. The ionosphere, a partially ionized gas surrounding the Earth in the altitude range 90 km to 1,000 km, can strongly affect the propagation of electromagnetic waves. Under certain circumstances, the ionosphere can severely degrade electromagnetic signals and, for example, interrupt communication links. Thus, it is vital that the ionospheric environment be known, and even forecasted, for reliable military operations.

To meet the Navy's needs in defining the ionospheric environment, we have developed a new three-dimensional model of the low- to mid-latitude ionosphere based on first-principles physics: SAMI3 (Sami3 is Also a Model of the Ionosphere). The model is an outgrowth of the two-dimensional ionosphere model SAMI2¹ that has been successful in understanding both satellite observations² and radar data³.

Ionosphere Model: SAMI3 models the plasma and chemical evolution of seven ion species (H^+ , He^+ , N^+ , O^+ , N_2^+ , NO_2^+ , and O_2^+) in the altitude range 85 km to 20,000 km. The ion temperature equation is solved for three ion species (H^+ , He^+ , and O^+) as well as the electron temperature equation. Ion inertia is included in the ion momentum equation for motion along the geomagnetic field. An offset, tilted dipole geomagnetic field is used, and the plasma is modeled from hemisphere to hemisphere. High altitude boundary conditions are not needed since a complete ionospheric flux tube is modeled. In addition, the $\mathbf{E} \times \mathbf{B}$ drift motion of the plasma is included for both zonal electric fields (vertical drifts) and meridional electric fields (zonal drifts). The neutral com-

position and temperature are specified using the empirical NRLMSISE00 model and the neutral winds using the HWM model. SAMI3 uses a unique, nonorthogonal, nonuniform, fixed grid. The grid is designed to optimize the numerical mesh so that the spatial resolution decreases with increasing altitude. The plasma is transported transverse to the geomagnetic field using a finite volume method in conjunction with the donor cell method. The code is fully parallelized using the Message Passing Interface (MPI) method, which is critical to computational efficiency for large-scale simulations.

Figure 4 shows the vertical total electron content (TEC) contour plot from a typical SAMI3 run. The TEC is the line integrated electron density through the ionosphere; one TEC unit is 10^{16} m^{-2} . This figure illustrates the near-global coverage of SAMI3, which is $\pm 60^\circ$ magnetic latitude. Also, this figure clearly shows the Appleton anomaly: the ionization crests that are approximately $\pm 15^\circ$ from the magnetic equator and denoted by the red contour level.

Aside from being used to model and understand ionospheric morphology, SAMI3 will be used in the tomographic reconstruction of the ionospheric electron density. TEC data can be obtained using a satellite-borne radio beacon and an array of ground receivers. The electron density in the satellite-receiver plane can be obtained from this TEC data using tomographic reconstruction algorithms. However, the accuracy of the reconstructed electron data can depend on the initial "guess" of ionospheric conditions. We can improve the accuracy of this method by using SAMI3 results to provide the initial "guess."

Current Research: Finally, an area of current research involves coupling SAMI3 to other space-environment models. A major concern of modeling space plasma processes is self-consistency. For example, an important input into SAMI3 is the electric field that convects the plasma; in fact, the electric field is responsible for the formation of the Appleton anomaly shown in Fig. 4. However, this electric field is now prescribed in SAMI3 via an empirical model. A better way to obtain the electric field is to solve a potential equation $\nabla \cdot \underline{\underline{\Sigma}} \cdot \nabla \Phi = J_{\parallel}$ where $\underline{\underline{\Sigma}}$ is the ionospheric conductance and J_{\parallel} is the field-aligned current. The Lyon/Fedder/Mobarry (LFM) model of the solar wind/magnetosphere system and the Rice Convection Model (RCM) of the inner magnetosphere solve a potential equation, but they use a simplified or empirical model for the ionospheric conductance and are not fully self-consistent. We are now coupling SAMI3 to both the LFM and RCM models. The basic idea is that SAMI3 will provide the ionospheric conductance needed to solve for the potential Φ . The LFM and RCM will calculate Φ which, in turn, will be used in SAMI3 to calculate the electric field needed to convect

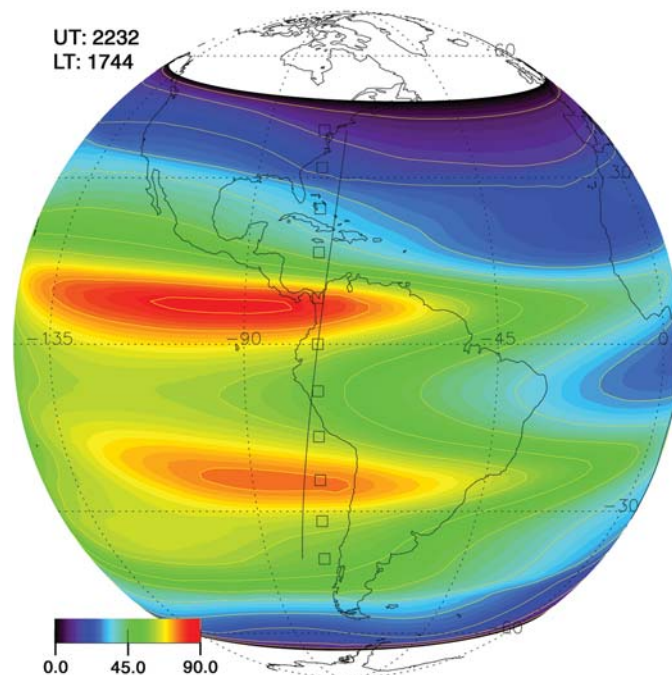


FIGURE 4
Vertical TEC contour plot from a typical SAMI3 run.

the plasma self-consistently. In this way, coupled SAMI3/LFM and SAMI3/RCM models will be a major step forward in modeling the near-Earth space environment.

More information on NRL ionosphere modeling can be found at <http://wwwppd.nrl.navy.mil/sami2-OSP>.

[Sponsored by ONR and NASA]

References

- ¹J.D. Huba, G. Joyce, and J.A. Fedder, "SAMI2 (Sami2 is Another Model of the Ionosphere): A New Low-latitude Ionosphere Model," *J. Geophys. Res.* **105**, 23,035 (2000).
- ²J.D. Huba, K.F. Dymond, G. Joyce, S.A. Budzien, S.E. Thonnard, J.A. Fedder, and R.P. McCoy, "Comparison of O⁺ Density from ARGOS Data Analysis and SAMI2 Model Results," *Geophys. Res. Lett.* **29**(7), 1102, doi:10.1029/2001GL013089, 2002.
- ³J.D. Huba, G. Joyce, and J.A. Fedder, "Simulation Study of Mid-latitude Ionosphere Fluctuations Observed at Millstone Hill," *Geophys. Res. Lett.* **30**(18), 1943, doi:10.1029/2003GL018018, 2003.

THE HIGH FREQUENCY ACTIVE AURORAL RESEARCH PROGRAM

E.J. Kennedy, P. Rodriguez, and C.A. Selcher
Information Technology Division

Introduction: Electromagnetic waves in certain frequency ranges are absorbed or refracted by the ionosphere, an electrically conductive region of the upper atmosphere beginning at an altitude of approximately 80 km. Radio waves of sufficient energy density are capable

of temporarily modifying its electrical and physical properties within a small volume, enabling a new type of interactive research having application to a variety of Navy and DOD missions. The High Frequency Active Auroral Research Program, jointly sponsored by the Office of Naval Research, the Air Force Research Laboratory, and DARPA, is constructing a new interactive ionospheric research facility in Gakona, Alaska, to conduct both basic and applied research in this scientific discipline. We present a description of the major components of the HAARP Gakona Facility including technical detail of its current and planned performance capabilities. We also present some results from three research areas: extremely low and very low frequencies (ELF/VLF) generation, artificial optical emissions, and space research.

Facility Description: The HAARP Gakona Facility is located in a relatively remote region of south central Alaska where a variety of ionospheric conditions may occur, ranging from quiet to mid-latitude to auroral. The major feature of the facility is the high frequency (HF) phased array antenna, currently consisting of 48 elements. When completed in 2006, this array will consist of 180 elements with performance parameters as shown in Table 1.

The facility also includes a suite of 17 on-site scientific and diagnostic instruments including magnetometers, riometers, a digisonde, and three upper atmospheric radars. Work has begun on an incoherent scatter radar. Since becoming operational in March 1999, the HAARP Gakona Facility has been used in 27 research campaigns. Figure 5 is an overhead photo of the facility.

Table 1 — HF Phased Array Antenna Performance Parameters

	Current	2006
Radiated power	960 kW	3,600 kW
Frequency coverage	2.8 to 8.2 MHz	2.8 to 10 MHz
Effective radiated power (ERP)	75 to 83 dBW	86 to 95 dBW
Antenna beamwidth	9° to 32°	4.5° to 15°
Beam slewing	30° from zenith @ all azimuths	
Beam reposition time	15 μ s	



FIGURE 5
Overhead photo of the HAARP Gakona Facility.

Generation of ELF/VLF Waves: Much of the research at the facility is focused on the generation of ELF/VLF because of the value of these frequencies to the Navy for undersea applications. Propagating radio waves in the ELF/VLF frequency range are generated at the lower edge of the ionosphere when high-power HF radio waves modulate the conductivity of the ionospheric D and E layers in the presence of a background or “electrojet” current. The practical utility of this technique for communication systems is dependent on improving the efficiency and reliability of this process. A recent experiment was performed at HAARP to study the scaling of the ionospherically generated ELF signal with power transmitted from the HF array. Results were in excellent agreement with computer simulations confirming that the ELF power increases with the square of the incident HF power. Furthermore, no saturation effects were observed indicating that greater ELF generation efficiency is possible with greater incident power.

Optical Emissions: The interaction of high-power radio waves with the ionospheric can produce faint optical

emissions at specific wavelengths. Recent experiments at the HAARP Gakona Facility investigated the role of the HF beam pointing direction on the production of artificial airglow. The exciting result was that by pointing the HF beam directly along a geomagnetic field line, artificial emissions of greater than 200 Rayleighs (R) at 630.0 nm and greater than 50 R at 557.7 nm could be produced. This intensity was nearly an order of magnitude larger than that produced by heating directly overhead. Weak emissions of approximately 10 R were observed with effective radiated power (ERP) levels as low as 2 MW. These measurements have been repeated in other research campaigns with observations over a wide range of ionospheric conditions.¹ Figure 6 shows the artificially generated emission at 557.7 nm that was obtained using the NRL CCD imager during one of the experiments. (The imager used in this research uses a high resolution, cooled CCD. It was developed by NRL’s Plasma Physics Division and on loan to HAARP for the experiment.)

Lunar Radar Experiment: In another experiment, measurements were made of lunar radar cross-section by

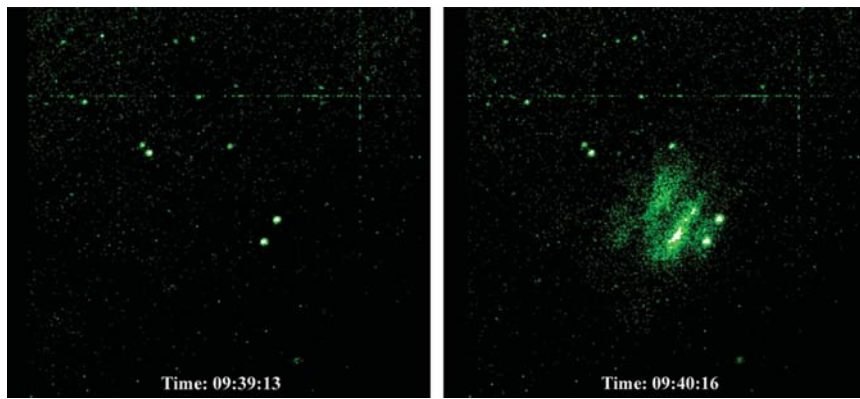


FIGURE 6

Two images of the sky over the HAARP Gakona Facility using the NRL-cooled CCD imager at 557.7 nm. The field of view is approximately 38°. The left-hand image shows the background star field with the HF transmitter off. The right-hand image was taken 63 s later with the HF transmitter on. Structure is evident in the emission region.

transmitting high-power radar pulses directly at the Moon from the HAARP facility and receiving the echo pulses with the WAVES radio receiver onboard the NASA/WIND spacecraft. This is the first time that such a lunar echo experiment has been done using a ground-based radar in combination with a spacecraft, a new approach to space research.² During the two-hour experiment, the WIND satellite was about 40,000 km from the Moon's surface. Figure 7 is a 5-s interval of data showing the direct HAARP pulses (large peaks) and the lunar echo pulses (smaller peaks) received by the WAVES radio receiver. From the ratio of intensities of pairs of direct and echo pulses, we obtain an average lunar radar cross-section of about 15% relative to the geometric cross-section, with maximum values of about 50%. The HAARP transmissions were done at 8.075 MHz, a radio wavelength of 37 m; our measurements extend the spectrum of lunar radar cross-sections to the longest wavelength at which this experiment has been done.

The lunar radar experiment provided evidence of high reflectivity locations on the lunar surface that may be associated with topographical features. This new technique for lunar radar measurements is free of scintillation effects caused by the Earth's ionosphere and provides a relatively clean measurement of the echo. Thus, high

power radars, such as HAARP, can bring an important new tool to lunar research, and future radar experiments with lunar-orbiting spacecraft can provide a new window on lunar topography.

Conclusion: Even though the HAARP facility is only partially complete, research results have already added new knowledge to the field of ionospheric interactions in basic and applied radio science. A primary focus area of the research program addresses communications and surveillance needs of the Navy with the potential to enable new capabilities for undersea applications.

[Sponsored by ONR]

References

- ¹T. Pedersen, M. McCarrick, E. Gerken, C. Selcher, D. Sentman, A. Gurevich, and H.C. Carlson, "Magnetic Zenith Enhancement of Artificial Airglow Production at HAARP," *Geophys. Res. Lett.* 30(4), 1169, doi: 10.1029/2002GLO16096, 2003.
- ²P. Rodriguez, E.J. Kennedy, M.J. Keskinen, C.L. Siefing, Sa. Basu, M. McCarrick, J. Preston, M. Engebretson, M.L. Kaiser, M.D. Desch, K. Goetz, J.-L. Bougeret, and R. Manning, "The WIND-HAARP Experiment: Initial Results of High Power Radiowave Interactions with Space Plasmas," *Geophys. Res. Lett.* 25(3), 257-260 (1998).

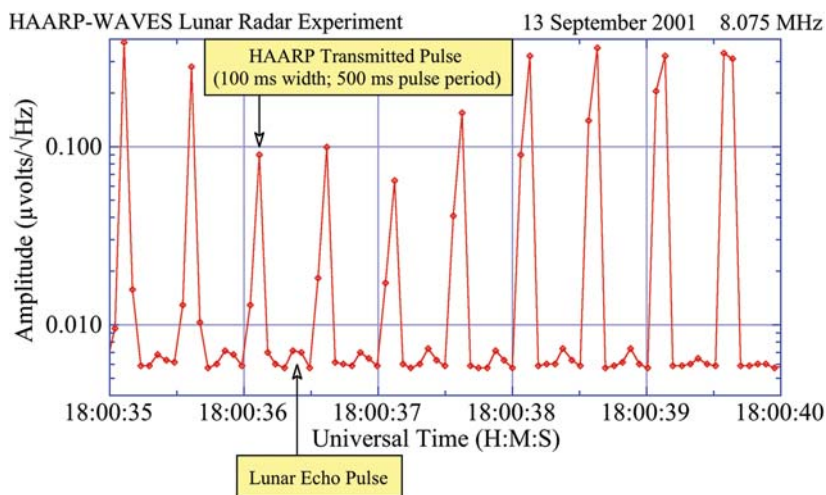


FIGURE 7

Direct and echo radar pulses measured by the WAVES radio receiver. The lunar radar cross-section is calculated from the ratio of direct and echo pulses.

ADVANCES IN UPPER ATMOSPHERE FORECASTING: NOGAPS-ALPHA

J.P. McCormack,¹ L. Coy,¹ S.D. Eckermann,¹ D.R. Allen,² T. Hogan,³ and Y.-J. Kim³

¹Space Science Division

²Remote Sensing Division

³Marine Meteorology Division

Introduction: The Navy Operational Global Atmospheric Prediction System (NOGAPS) provides detailed atmospheric analyses and forecasts for numerous Department of Defense (DOD) applications. The heart of NOGAPS is an atmospheric general-circulation model (GCM) with an operational capability currently extending from the surface to 30 km altitude. NRL scientists from the Space Science, Remote Sensing, and Marine Meteorology Divisions have been working jointly on a multi-year project to develop a new high-altitude version of NOGAPS extending up to 85 km and beyond (Fig. 8). There is a growing recognition in the atmospheric science community that weather disturbances at higher altitudes can penetrate to lower altitudes and influence development of surface weather features. The primary goal of this project is to support all aspects of Naval operations through better prediction of surface conditions as well as tropospheric and upper atmospheric winds, temperature, moisture, and clouds. In particular, the upward extension of the existing model now makes it possible to better understand and predict upper atmospheric disturbances that can affect satellite remote sensing applications, vehicle reentry, high-altitude unmanned aerial vehicle (UAV) performance, and high-altitude dispersal

of explosively injected material. The product of this effort is the NOGAPS-ALPHA (Advanced Level Physics-High Altitude) model.

Implementation and Innovations: NOGAPS-ALPHA is a spectral model with 54 vertical levels from the surface to approximately 85 km on a hybrid sigma-pressure grid. This new vertical grid is terrain-following near the surface, transitioning to constant pressure levels in the lower stratosphere. NOGAPS-ALPHA contains a new radiative transfer scheme and updated climatologies for radiatively active trace species such as ozone and water vapor. NOGAPS-ALPHA also uses new initialization routines for winds and temperatures in the upper stratosphere and mesosphere, beyond the range of current operational analyses. New physical packages have been added describing the effects of sub-grid scale gravity waves on the global atmospheric circulation. In addition, the model now combines global transport calculations of chemical constituents such as stratospheric ozone with an interactive photochemical scheme to describe the time evolution of these constituents over periods of days, weeks, or months. Multi-year model runs have also been performed to verify the performance of the new high-altitude components of the NOGAPS model. These simulations extend to 5 years and were performed on a suite of massively parallel supercomputers made available through the DOD High Performance Computing Modernization Program.

Simulations of the 2002 Ozone Hole: The unprecedented southern hemisphere stratospheric major warming event during September 2002, provides an excellent

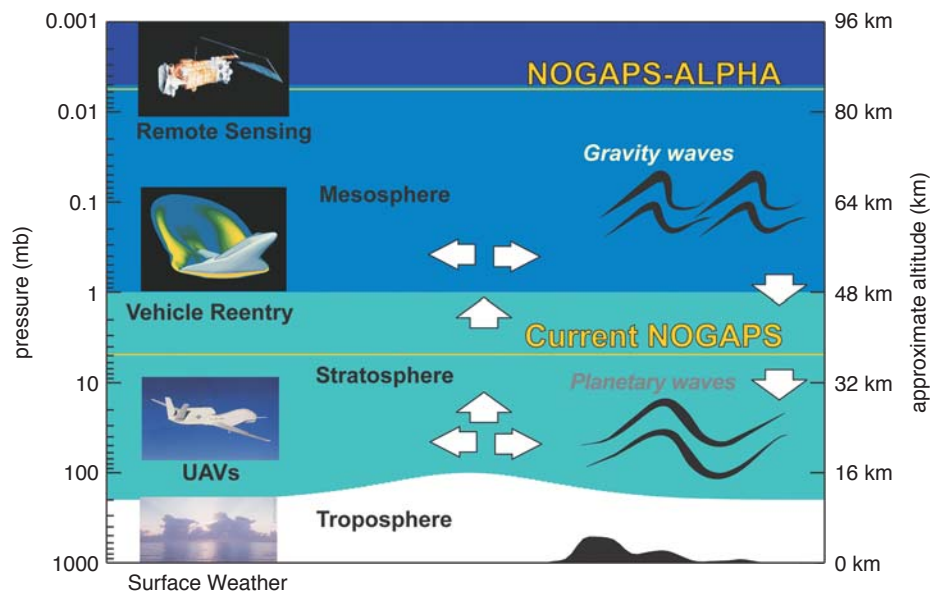


FIGURE 8

The atmospheric regions covered by the current operational version of the NOGAPS model and the newly developed NOGAPS-ALPHA model. Arrows represent wave-induced transport through the troposphere, stratosphere, and mesosphere.

opportunity to showcase the new capabilities of NOGAPS-ALPHA. On September 23, 2002, the Antarctic polar vortex began to split in two following a series of large planetary-scale wave disturbances in the southern hemisphere winter stratosphere (see Fig. 9) that brought unusually warm air over the South Pole. As a result, the size and depth of the springtime ozone hole over Antarctica decreased to its smallest value in over 20 years. This was the first time a stratospheric major warming has occurred over the South Pole since observations began. Figure 9 shows that NOGAPS-ALPHA hindcasts of 10 hPa geopotential height and total ozone column amounts initialized on September 23, 2002, compare well with NASA GEOS 4 meteorological analyses and NASA TOMS total ozone measurements during the period of September 23 to September 27, 2002.

Tracer Transport: With the new NOGAPS-ALPHA model, it is now possible to diagnose global-scale constituent transport throughout the stratosphere. As planetary wave disturbances propagate upwards from the troposphere into the stratosphere and mesosphere, they grow in amplitude until they “break,” resulting in an irreversible transfer of heat and momentum. The resulting motions transport chemical constituents such as ozone and nitrous oxide (N_2O) across regions where the mixing of air is otherwise minimal under quiescent conditions. Figure 10 shows a NOGAPS-ALPHA simulation of the effect of a planetary wave-breaking event on the distribution of N_2O near 32 km altitude, where a large “tongue” of air with high N_2O mixing ratio is stripped out of the lower latitudes and transported poleward into a region of relatively low N_2O mixing ratio.

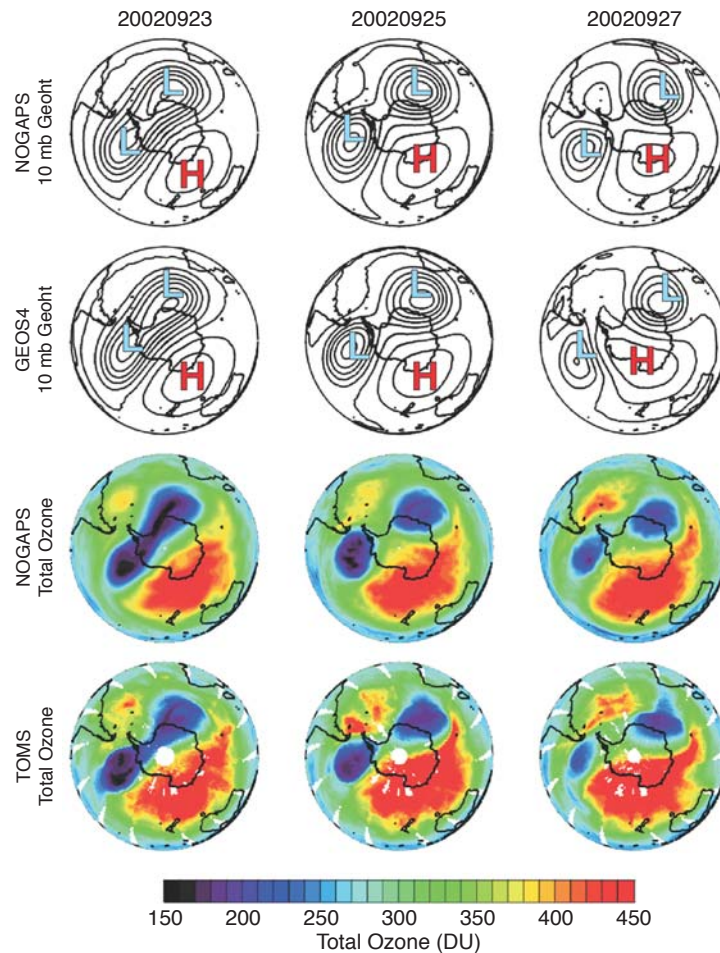


FIGURE 9 NOGAPS-ALPHAS hindcasts of the September 2002, stratospheric major sudden warming and early break-up of the antarctic ozone hole. Also shown are NASA GEOS4 meteorological analyses and TOMS total ozone observations. Total ozone is measured in Dobson Units (DU).

3 January 2002 0:00Z
Forecast Hour +000336

Pressure: 8 hPa (Altitude: ~33 km)

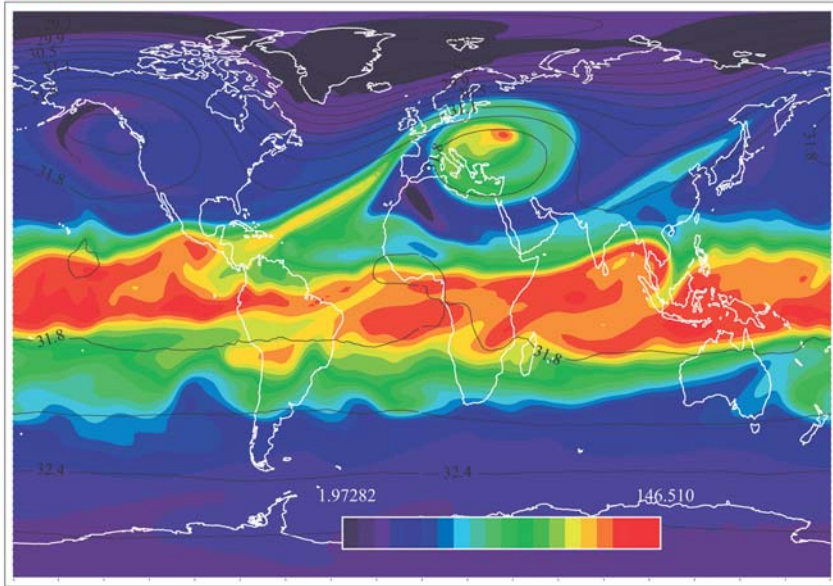


FIGURE 10
NOGAPS-ALPHA simulations of stratospheric N₂O mixing ratio in parts per billion by volume illustrating complex poleward transport of air with high N₂O mixing ratios during a planetary wave-breaking event.

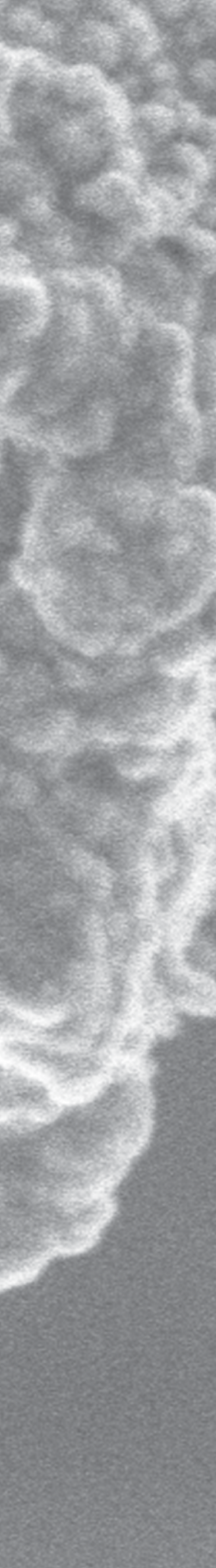
Summary: NOGAPS-ALPHA, a high-altitude version of the Navy's global numerical weather prediction model, now makes it possible to generate both medium-range forecasts (1 to 2 weeks) and multi-year climate simulations from the surface to 85 km altitude. With its state-of-the-art treatment of the physical and dynamical processes coupling the tropospheric, stratospheric, and

mesospheric regions of the atmosphere, NOGAPS-ALPHA opens the door to the next generation in Navy forecasting and analysis capabilities. Linking NOGAPS-ALPHA with the new NRL Atmospheric Variational Data Assimilation Scheme (NAVDAS) is the next step in fully developing and exploiting these new capabilities.

[Sponsored by ONR]

COPPER-PLATED LIPID TUBULES

Scanning electron micrographs of diacetylenic lipid tubules coated electrolessly with copper. The lipid is a modified version of the material found in cell membranes. The tubules are hollow and are 1 to 2 mm in diameter and about 30 mm long. The electroless coating of copper reinforces the tubules and renders them highly electrically conductive. The copper is formed of small grains, 30 to 100 nm in size, grown together to a thickness of about 300 nm, covering both the interior and exterior walls of the tubule.



115 Navy Cyanide Test Kit (NACTEK)

J.R. Deschamps

116 Water-Soluble Carbon Nanotubes

O.-K. Kim, J. Je, J.W. Baldwin, S. Kooi, P.E. Pehrsson, and L.J. Buckley

118 Neuronal Network Biosensor for Environmental Threat Detection

*K.M. Shaffer, S.A. Gray, S.J. Fertig, J.V. Selinger, T.J. O'Shaughnessy,
N.V. Kulagina, D.A. Stenger, and J.J. Pancrazio*

121 Self-Cleaning Catalytic Filters Against Pesticides and Chemical Agents

A. Singh, Y. Lee, and W.J. Dressick

NAVY CYANIDE TEST KIT (NACTEK)

J.R. Deschamps

Laboratory for Structure of Matter

Gap Identified: Naval vessels take on supplies and water when in port. Fleet potable water sources may be in areas where there is no secure water supply. Potable water is screened for a variety of contaminants, but a gap in the testing was identified. There was no field test for cyanide in potable water. This gap is of concern to at least one command of the Naval Operational Forces and resulted in an emergency request for a system to measure the presence of cyanide in potable drinking water.

Solution: A quick and convenient field test-kit based on a colorimetric reaction on paper strips is used to measure the concentration of free cyanide. This is combined with a portable meter with a cyanide specific-ion electrode to confirm negative readings and collect additional evidence when high cyanide concentrations are detected.

To meet the extremely tight time constraints on this project, commercial off-the-shelf (COTS) items were used when available. The final kit must be reliable, portable, and simple for Navy corpsman to use. A test kit must reliably detect cyanide concentrations of 2.0 parts per million (ppm).

Background: Water quality standards and testing methods are provided in the Tri-Service Technical Bulletin, "Sanitary Control and Surveillance of Field Water Supplies." This document defines a concentration of 2.0 ppm as the acceptable level of free cyanide in potable water. This concentration is higher than the acceptable level (0.2 ppm) specified in the "National Primary Drinking Water Regulations" (NPDWR). The difference between these two standards is related to their application. The NPDWR standard limits lifetime exposures, while the Tri-Service standard is limited to consumption of 15 liters of water a day for one year or less.

Technical Issues: A chemical (colorimetric) technique can be used to provide a convenient and rapid means of measuring the free cyanide concentration in

water samples. A portable meter and specific-ion electrode can be used to confirm these measurements. Cyanide specific-ion electrodes have a reported working range of 0.2 to 260 ppm.

Oxidizing agents, sulfides, and fatty acids are known to interfere with some chemical tests for cyanide. The effect of these compounds on a specific ion electrode is not known. Sensitivity to related, less toxic, species (i.e., SCN^- and $\text{Fe}(\text{CN})_6^-$) is also poorly defined. Chloride, bromide, and iodide are reported to interfere with cyanide specific-ion electrodes. The magnitude of this interference needs to be evaluated and limits defined for non-interference.

Results: All of the methods tested are sensitive only to free cyanide. The effect of solutions of cyanide complexes and related ions were evaluated as part of the testing "EM Quant" test strips were selected for rapid assessment of water samples. A positive test results in production of a purple color in the sensitive area of a test strip and can be used to determine free cyanide concentrations between 1 and 30 ppm. Cyanide concentrations greater than 10 ppm turn the test solution pale yellow (Fig. 1). The presence of chloride ions at concentrations up to 300 mM had no effect. Although weakly buffered solutions in the range of pH 4 to 10 had no apparent effect on the color produced well buffered samples where pH's greater than 8 caused a noticeable reduction in the production of purple color. Tests conducted with tap water, SCN^- , and $\text{Fe}(\text{CN})_6^-$ produced no discernable purple color on the test strip.

The response of the ion-selective electrode was log linear between mV and concentration. Since the ion-selective electrode requires the addition of a concentrated alkaline reagent, pH has little effect on this test. Although chloride, bromide, and iodide are reported to interfere with the cyanide ion-selective electrode, concentrations up to 30 mM had only a moderate effect (i.e., 3.5% error or less). The highest concentration of chloride ion tested was 272 mM, which resulted in a measured concentration of cyanide that was 16% less than the expected value.

Summary: A prototype kit was assembled and tested by a Navy corpsman (Fig. 2) within three weeks of the

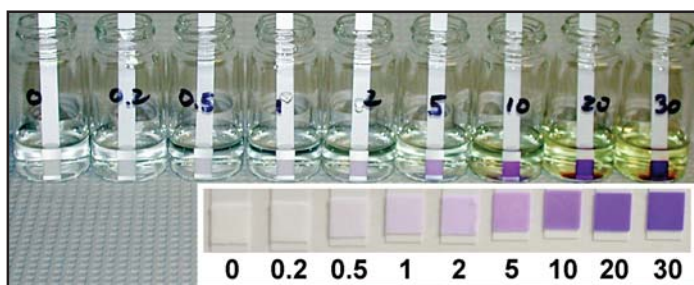


FIGURE 1

The colorimetric test for the presence of cyanide results in a bright purple color in the sensitive area of the test strip. A pale yellow color also develops in the test solution at higher cyanide concentrations. Insert shows color scale used to estimate cyanide concentration.



FIGURE 2
HM2 (SW) Clifton Butler (Naval Readiness Command, Mid-Atlantic) assists in testing the NACTEK protocols. The results from the colorimetric test are confirmed using a selective-ion electrode and test meter.

initial request to NRL. The Naval Cyanide Test Kit (NACTEK) can reliably detect cyanide in water at concentrations of 0.2 ppm or higher, and the initial screening can be completed in less than 1 minute. The use of two different detection technologies minimizes the chance of an inaccurate test that could result in the use cyanide-containing water. Before NACTEK, no field test was available to the Fleet to test potable water supplies for the presence of unacceptable levels of cyanide.

Acknowledgments: Dr. Keith B. Ward (ONR) assisted in producing the technical manuals, and HM2 (SW) Clifton Butler (Naval Readiness Command, Mid-Atlantic) assisted in testing the prototype kit.

[Sponsored by ONR]

WATER-SOLUBLE CARBON NANOTUBES

O.-K. Kim,¹ J. Je,² J.W. Baldwin,^{1,3} S. Kooi,^{1,3} P.E. Pehrsson,¹ and L.J. Buckley¹

¹Chemistry Division

²University of Connecticut (Postdoc)

³NRC Postdoc

Introduction: Single-wall carbon nanotubes (SWNTs, abbreviated as NTs) have been intensively investigated over the last several years because growing interests in their unique chemical and physical properties for molecular electronics¹ and chemical/biological sensors.² However, the widespread use of NTs is severely limited by the difficult nature of processing and handling them in a facile manner because of its insolubility in a process-friendly solvent. One solution for this is the use of polymers, which not only solubilize NTs by encapsula-

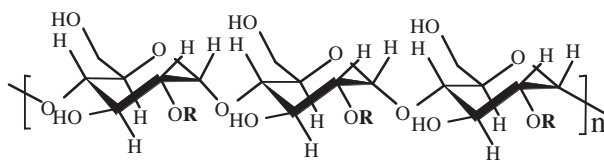
tion but also keep the intrinsic property of NTs intact. However, typical polymers tend to randomly wrap around NT bundles³ in solution unless they have a specific binding interaction that drives individual NTs to be encapsulated.

Approach: Our approach is focused on developing a molecularly controlled process of encapsulation of NTs with water-soluble amylose (a glucose-based natural polymer), whose biocompatibility and functionality are particularly attractive for biological applications. Previously, we have developed expertise⁴ in the supramolecular inclusion of organic molecules with water-soluble amylose. This commonly requires the use of a solvent to permit a loose, interrupted, helical conformation of amylose to allow the molecular inclusion. The solubilization of NTs by amylose requires two important conditions for efficient encapsulation and colloidal stability: a debundled fine dispersion of the NTs, and a strong binding interaction with the amylose. The former can be made by sonication, but the latter requires an optimal solvent condition for the amylose complexation. The following is a unique process that is simple, fast, and efficient to produce a stable colloidal solution of amylose-NTs complexes, with a helically twisted surface morphology.

For solubilization, a small piece of HiPco NT mat is sonicated in water for 15 min; the resulting fine suspension of NTs is treated with amylose in DMSO with additional sonication of a few minutes, during which the suspended NTs are completely dissolved. The colloidal solution is stable over several weeks without separation. This is extremely important for processing the materials into devices in which a colloidal solution enables various solution processing techniques.

The influence of solvent composition on the NT solubilization by amylose was assessed by ultraviolet/visible light absorption at 500 nm (Fig. 3). The inset shows the trend of the solubilization as a function of DMSO volume fraction, which is represented by the absorption. A strong dependence on the solvent composition is indicative of a special binding interaction⁴ between NTs and amylose. The slightly lowered solubility in 100% water is due to the relatively poor solubility of amylose in water, in contrast to its homologs⁵ such as CMA, whose solubilization of NTs is somewhat higher in 100% water.

As shown in Fig. 4, the SEM image (A) shows loosely twisted NTs with a diameter of approximately 30 nm. The atomic force microscope (AFM) gives an enhanced image of the helical twist (C), which reveals a locally intertwined multiple twist (B), which is probably caused by the sonication processing step. This twisted structure discloses a new feature where amylose can encapsulate a large diameter (≥ 1 nm) guest molecule. This is driven by hydrophobic interactions due to the chirality and the linear chain structure.⁵ Raman spectra (Fig. 5) of amylose-encapsulated NTs indicate a small shift ($3\text{--}5\text{ cm}^{-1}$) relative to the pristine NTs in



Amylose: $R = H$
 CMA: $R = CH_2COOH$

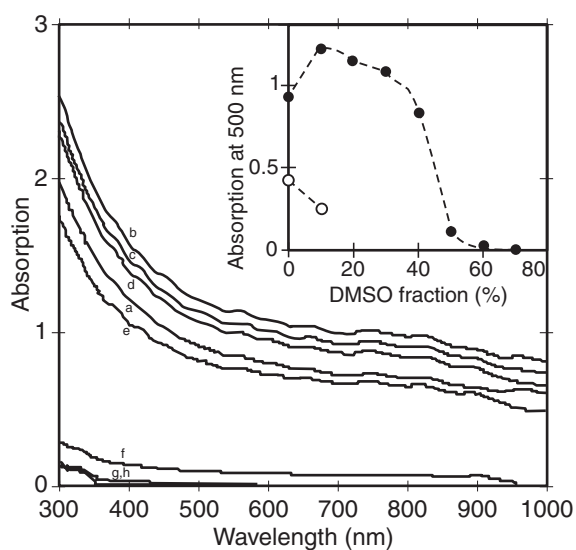


FIGURE 3

Absorption spectra of amylose-encapsulated SWNT prepared in various DMSO-H₂O mixtures: 0 (a), 10 (b), 20 (c), 30 (d), 40 (e), 50 (f), 60 (g), and 70 (h) vol % DMSO. Inset shows the NTs solubilization with (●) or without (○) pre-sonication (published from *J. Am. Chem. Soc.* **125**, 4426 (2003)).

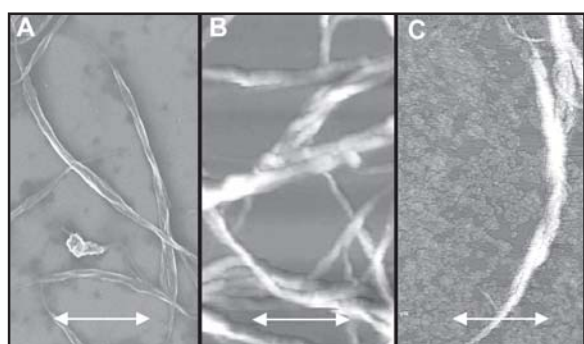


FIGURE 4

SEM (A) and AFM (B and C) images of amylose-encapsulated SWNTs. The markers are (A) 600 nm; (B) 500 nm; and (C) 250 nm (published from *J. Am. Chem. Soc.* **125**, 4426 (2003)).

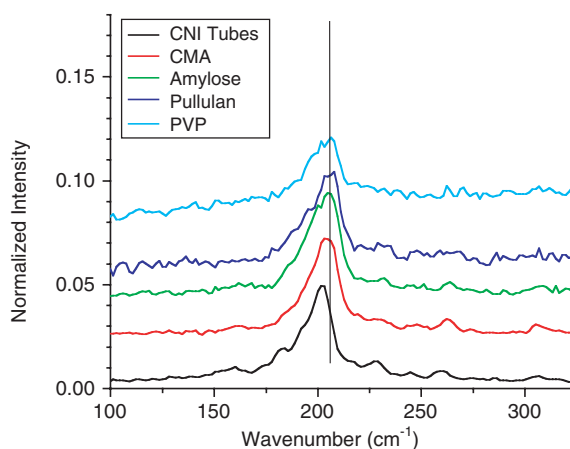


FIGURE 5

Raman spectra of polymer-treated SWNT: radial breathing modes (488 nm source).

the radial breathing mode frequency. This structure is similar to that described⁶ previously for polymer-wrapped NTs and is further evidence of the encapsulated structure.

Summary: In conclusion, a simple, efficient process for solubilization of NTs with amylose in aqueous DMSO has been described. This process requires sonication of the NTs in water and subsequent treatment of the fine NT dispersion with amylose with an additional brief sonication. The best solvent condition is 10-20% DMSO, in which amylose assumes an interrupted loose helix, suggesting that the helical state of amylose is not a prerequisite for amylose encapsulation of NTs. The scanning electron microscope and AFM display images of twisted ribbons showing the encapsulation of NTs by amylose.

[Sponsored by ONR]

References

- ¹T. Rueckes, K. Kim, E. Joslevich, G.Y. Tseng, C.L. Cheung, and C.M. Lieber, "Carbon Nanotube-Based Nonvolatile Random Access Memory for Molecular Computing," *Science* **289**, 94-97 (2002).
- ²R.J. Chen, Y. Zhang, D. Wang, and H. Dai, "Noncovalent Sidewall Functionalization of Single-Walled Carbon Nanotubes for Protein Immobilization," *J. Am. Chem. Soc.* **123**, 3838-3839 (2001).
- ³A. Star, D.W. Steuerman, J.R. Heath, and J.F. Stoddart, "Starved Carbon Nanotubes," *Angew. Chem Int. Ed.* **41**, 2508-2512 (2002).
- ⁴O.-K. Kim, L.-S. Choi, H.Y. Zhang, et al. "Second Harmonic-Generation by Spontaneous Self-Poling of Supramolecular Thin Films of an Amylose-Dye Inclusion Complex," *J. Am. Chem. Soc.* **118**, 12220-12221 (1996).
- ⁵O.-K. Kim, J. Je, J.W. Baldwin, S. Kooi, P.E. Pehrsson, and L.J. Buckley, "Solubilization of Single-Wall Carbon Nanotubes by Supramolecular Encapsulation of Helical Amylose," *J. Am. Chem. Soc.* **125**, 4426-4427 (2003).
- ⁶A.B. Dalton, C. Stephan, J.N. Coleman, et al., "Selective Interaction of a Semiconjugated Organic Polymer with Single-Wall Nanotubes," *J. Phys. Chem. B*, **104**, 10012-10016 (2000).

NEURONAL NETWORK BIOSENSOR FOR ENVIRONMENTAL THREAT DETECTION

K.M. Shaffer,¹ S.A. Gray,¹ S.J. Fertig,² J.V. Selinger,¹ T.J. O'Shaughnessy,¹ N.V. Kulagina,¹ D.A. Stenger,¹ and J.J. Pancrazio¹

¹Center for Bio/Molecular Science and Engineering

²Nova Research, Inc.

Introduction: A critical technology void exists in our ability to detect a broad range of environmental threats ranging from toxic industrial chemicals and materials

through chemical agents. NRL has developed a biosensor system that combines microelectrode array technology with neuronal cell culture techniques to yield physiologically relevant information about a broad set of known and unanticipated threats. Extracellular monitoring of bioelectrical activity from cultured networks grown over microelectrode arrays provides a noninvasive approach that allows long-term monitoring. The biosensor system condenses a large amount of laboratory instrumentation to a portable instrument format that requires only minimal training to operate. We have successfully demonstrated the use of this system in recent field exercises in which detection of toxins in both potable water samples and in sea water was performed. A strong correlation between biosensor sensitivity and lethal dosages of a range of environmental threats is presented, and challenges for the future are discussed.

Neurons on Microelectrode Arrays: The sensing element of the neuronal network biosensor contains mouse spinal cord or frontal cortex neurons grown on substrate-integrated microelectrode arrays (MEAs). The MEAs consist of transparent patterns of indium-tin oxide conductors, 10 mm wide, which are photoetched and passivated with a polysiloxane resin. Laser de-insulation of the resin results in 64 recording sites over an area of 1 mm.² After depositing biological attachment factors on the surface, embryonic neurons are placed over the surface and allowed to grow into mature interconnected networks¹ (Fig. 6(a)). Neurons communicate with one another via action potentials or spikes; changes in spike rate are the fundamental means by which information is transmitted in the nervous system. While spikes are typically monitored by piercing cells with glass or metal microelectrodes (inevitably a destructive process), the MEAs allow noninvasive recording of extracellular spike activity (Fig. 6(b)). Neuroactive compounds, which include many environmental threats, act on neuronal receptors to modulate the spike dynamics. This information is readily monitored by the MEAs, and changes in such activity can be used as a means of detecting neuroactive compounds.

NRL, in collaboration with the University of North Texas, has recently developed a robust method to store and transport living networks, such that living networks can be shipped across the United States via commercial carrier. This success has led to the emergence of a commercial effort (Applied Neuronal Network Dynamics, Inc.) to supply the biological component of the biosensor system. With the availability of the biological component of the sensor to many potential end-users, neuronal networks are uniquely poised to provide broad spectrum threat detection.

The NRL Portable Biosensor: Traditionally, a large quantity of complex laboratory equipment requiring

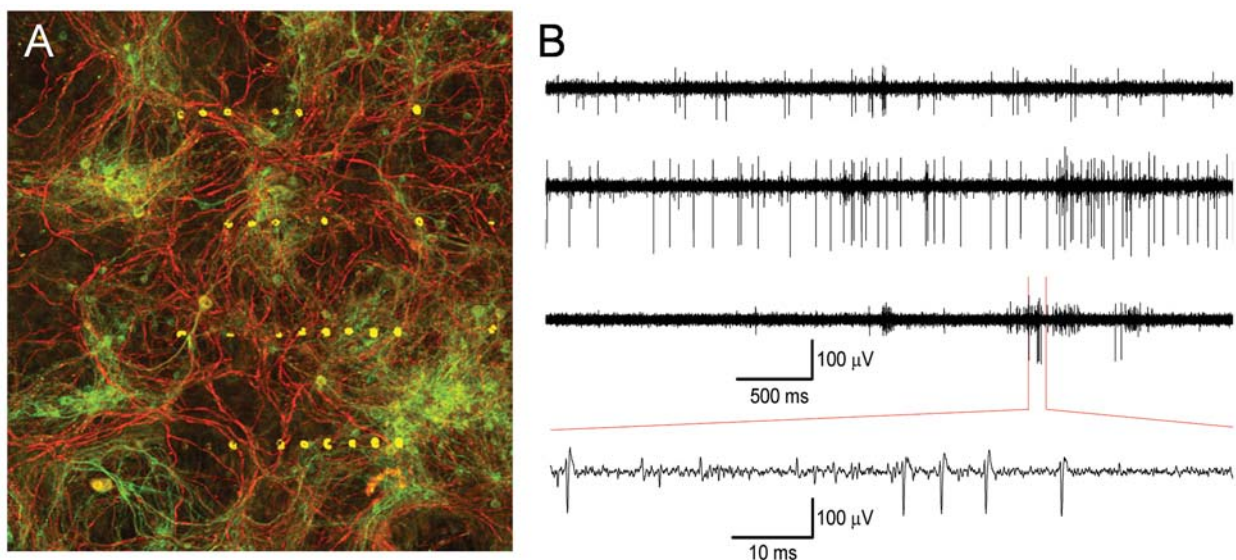


FIGURE 6 Spinal cord neuronal network serving as a biological component for the biosensor system. (A) The dual fluorescence image highlights neuronal features with immunocytochemical techniques where the neuronal axons are shown in red and the cell bodies and dendrites are shown in green. On the microelectrode array substrate, several of the 64 recording sites, which are 10 mm in diameter, fluoresce yellow. (B) Representative extracellular recordings from spinal cord cultures.

both significant space and experienced personnel have been needed to make use of cultured neuronal networks. NRL has developed a portable system that condenses this equipment while reducing the expertise needed to operate it.² The portable biosensor consists of an aluminum case (45 × 30 × 40 cm) containing pumps, valves, and temperature controllers with amplifiers and filters capable of processing microvolt-level extracellular signals (Fig. 7). Each neuronal network on an MEA is enclosed in a stainless steel recording chamber, which maintains the cultures at physiological temperature and provides a means of introducing aqueous phase samples. A high-level user interface for real-time monitoring of neuronal network activity has been developed by NRL.

Sensitivity to Environmental Threats: The neuronal network biosensor has been successfully used to detect a broad spectrum of environmental threats including toxins, organophosphates, and metals. Figure 8(a) shows the rapid response of the neuronal network sensor to saxitoxin, a Schedule 1 chemical agent. The biosensor has been successfully tested off-site from NRL for the blind evaluation of samples at the Eliatox-Oregon workshop held at Oregon-State University in 2002, and more recently for the evaluation of red tide toxins in sea water cultures at the National Oceanic Atmospheric Administration in Charleston, South Carolina. Overall, there is a strong positive correlation ($r = 0.92$) between the sensitivity of the networks versus toxicity for a wide range of environmental threats (Fig. 8(b)). In general, the networks respond to environ-

mental threats at concentrations 2-3 orders of magnitude below that which induces toxicity.

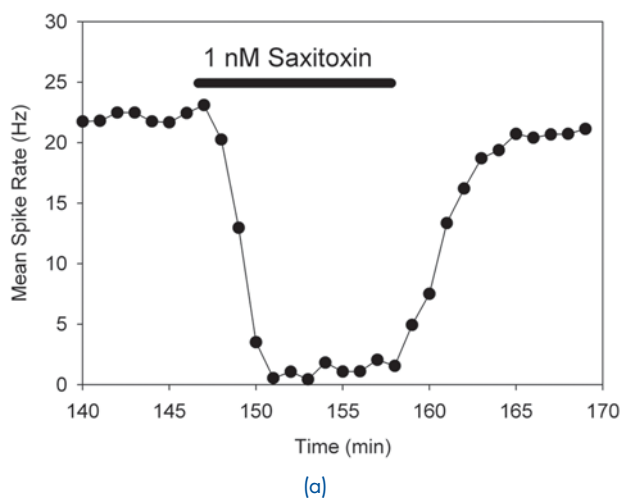
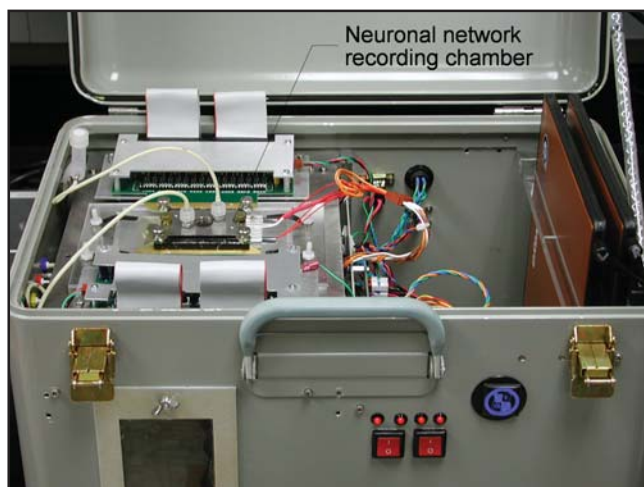
Prospects for Future Development: The neuronal network biosensor monitors a broad range of compounds for toxicity without being specific for any one compound. Alterations in the baseline bioelectrical activity of the neuronal network provide a means of rapidly detecting environmental threats. Future challenges involve the development and validation of statistically robust threat detection algorithms, exploration of cell preservation techniques to enhance shelf-life of the biological component, and the implementation of neural stem cell technology to reduce or eliminate reliance on animal-derived tissue for biosensor use. This biosensor technology can be readily miniaturized and implemented for environmental monitoring, municipal water source security, and homeland defense applications.

[Sponsored by DARPA and ONR]

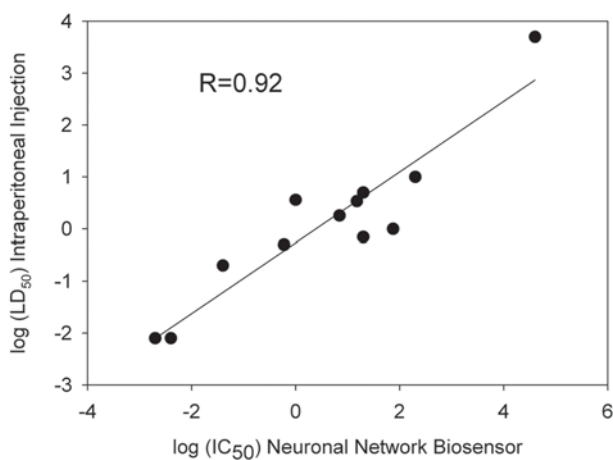
References

- G.W. Gross, A. Harsch, B.K. Rhoades, and W. Gopel, "Odor, Drug, and Toxin Analysis with Neuronal Networks in Vitro: Extracellular Array Recording of Network Responses," *Biosens. Bioelectron.* 12, 373 (1997).
- J.J. Pancrazio, S.A. Gray, Y.S. Shubin, N. Kulagina, D.S. Cuttino, K.M. Shaffer, K. Eisemann, A. Curran, B. Zim, G.W. Gross, and T.J. O'Shaughnessy, "A Portable Microelectrode Array Recording System Incorporating Cultured Neuronal Networks for Neurotoxin Detection," *Biosens. Bioelectron.* 18, 1339 (2003).

FIGURE 7
 Portable neuronal network biosensor. Open case view showing several internal subsystems including the stainless steel chamber containing the neuronal network.



(a)



(b)

FIGURE 8
 (a) Rapid and reversible inhibition of mean spike rate from neuronal network biosensor with exposure to the chemical agent saxitoxin at 1 nM or 0.3 parts per billion. (b) Strong positive correlation between the sensitivity of the neuronal network biosensor represented as log (IC₅₀), concentration that induces a 50% of the maximal modulation, x-axis and the log (LD₅₀), mg/kg dosage of a compound that, when injected, induces lethality in 50% of the mice or rats. Data points compiled from following agents: tetrodotoxin, saxitoxin, botulinum toxin A, cadmium, mercury, arsenic, chloroquine, brevetoxins, trimethylolpropane phosphate, domoic acid, ethyl alcohol, strychnine, and cyanide.

SELF-CLEANING CATALYTIC FILTERS AGAINST PESTICIDES AND CHEMICAL AGENTS

A. Singh, Y. Lee, and W.J. Dressick
Center for BioMolecular Science and Engineering

Introduction: Heightened awareness of the hazards of chemical pollutants and pesticides, coupled with a growing threat of chemical exposure due to accidental spills or terrorist action, poses a challenge to develop countermeasures. Current protection gear (e.g., gloves, masks, and clothing) is based on the removal of environmental toxins using efficient adsorption materials, and/or the use of impermeable barriers to separate toxins from protected targets. Both approaches suffer from problems such as weight, cost, bulkiness, regeneration capabilities, and disposal safety concerns. Therefore, there is an urgent need to develop noncorrosive, environmentally benign, cost-effective, lightweight, robust, self-decontaminating, hazardous material-free systems for handling and neutralizing pesticides and toxins present in air or water.

Focus of Our Research: We are focusing on developing multifunctional thin-film (~8 nm) coatings containing existing catalysts¹ capable of neutralizing toxins on contact. These catalysts include biological species such as enzymes and chemical compounds like metal-amine complexes, both of which can deactivate toxins like pesticides or nerve agents. Both catalyst types have deficiencies and merits. Metal complexes are long lasting, but exhibit low activity. For example, the pesticide methyl parathion (MPT) is slowly hydrolyzed ($k \sim 2.6 \times 10^{-2} \text{ s}^{-1}$) by the stable *bis*-ethylenediamine Cu(II) complex. In

contrast, enzymes such as organophosphorus hydrolase (OPH)¹ rapidly hydrolyze MPT ($k \sim 50 \text{ s}^{-1}$), but lose activity quickly as they denature in the environment. Despite improvements in enzyme stability via genetic alterations, an effective system having both high catalytic activity and stability for protection and threat reduction applications does not yet exist.

Enzyme Stability: Our approach for developing such systems addresses the key question of enzyme stability via enzyme encapsulation in polyelectrolyte (PE) multilayer films. Such films are readily fabricated by sequential adsorption of oppositely charged PEs, such as branched polyethylenimine (BPEI) and polyacrylic acid (PAA), onto substrates like beads or cloth from H₂O via dipcoating or spraycoating methods. This layer-by-layer approach is well established² and, by adjusting PE chemistries, provides an environment that stabilizes enzymes against denaturation while preserving activity. Figure 9(a) shows a structural cross-section of a generalized film of this type. Occasional replacement of a PE layer by a layer of charged nanoparticle adsorbents, metal complexes, or enzymes during film fabrication creates a film with a tunable sandwich structure. Toxins entering such a film initially encounter enzyme layers that rapidly hydrolyze most of the toxin. Underlying layers of metal complexes provide a backup to the enzymes. The innermost adsorbent layers prevent toxin by-products from reaching the protected target. The versatility of the method is shown by the use of beads (e.g., glass or polycyclodextrin (PCD)) in Fig. 9(b) or glass fabrics (e.g., electrospun fiber) in Fig. 9(c) as substrates for PE film deposition.

Figure 10 illustrates an application of our PE-coated beads for filter technologies. PCD microbeads, which adsorb and concentrate MPT for more efficient enzyme hydrolysis, were initially dipcoated with three bilayers of

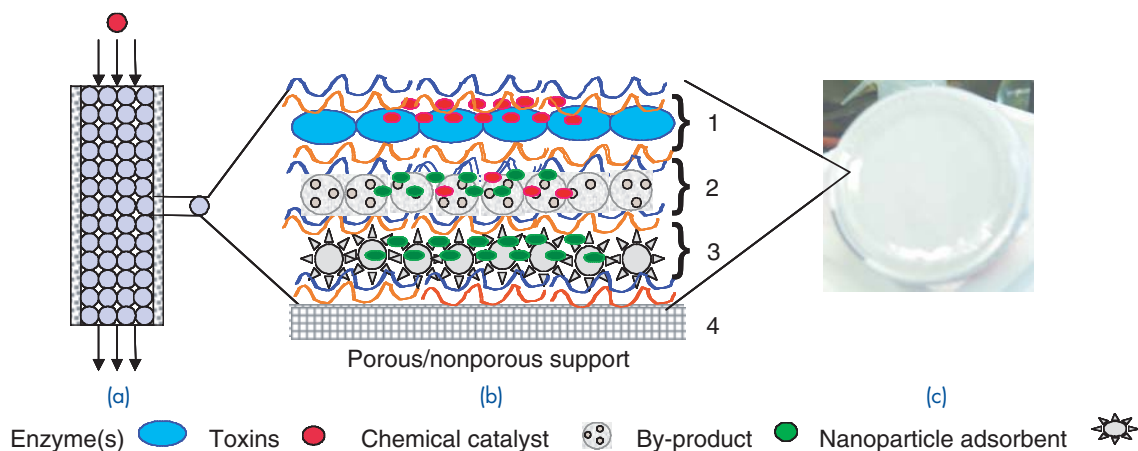


FIGURE 9 Self-cleaning filters against chemical agents: (a) Components and their placement; (b) Filter cartridge schematic; (c) A bioactive surface (electrospun glass fabric).

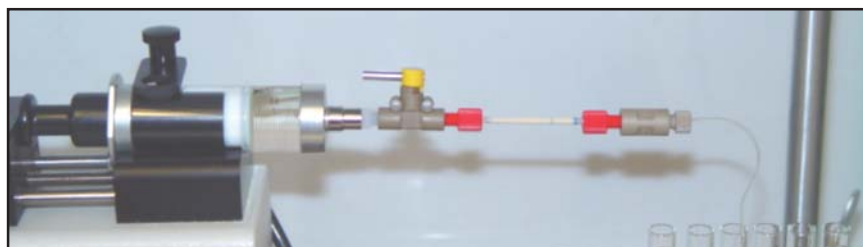


FIGURE 10
Set up for testing catalytic efficiency of beads in flow-through filter system.

BPEI and PAA, then five bilayers of BPEI and OPH enzyme, and finally a capping BPEI layer to form a film of structure PCD-[BPEI/PAA]₃[BPEI/OPH]₅BPEI. These modified beads were packed into the column shown in Fig. 10 and tested as a filter for removal of MPT from water. Under continuous solution flow with a filter residence time of ~114 s, the filter removed >99% of MPT from a 100- μ M MPT input stream for 60 days.

Figure 11 shows the application of the thin PE film layers onto a fiberglass (FG) cloth using a spraycoating method. In this case, a film of structure FG-BPEI/OPH/BPEI containing a single OPH layer was formed. This cloth (~0.1 g piece) was used to hydrolyze 12 fresh 100- μ M MPT solutions during 19 days. The OPH sustained 100% activity during the first two cycles, dropping to ~72% of its initial activity by the third cycle. Activity dropped to ~50% during the second week and ~33% during the third week, which is still excellent for most practical applications. In total, the 12 catalytic cycles led to hydrolysis of ~390- μ M MPT. In contrast, an aqueous solution of OPH denatured and lost >95% activity within ~96 h. Initial results using cotton cloths coated with our PE films suggest that OPH stabilities are comparable or greater than those in FG cloths.

Demonstrated Ability: We have now demonstrated the ability to stabilize enzymes in thin, multilayer PE assemblies while sustaining activity under harsh working environments. This accomplishment, coupled with the ability to deposit films on nearly any substrate, opens the possibility for developing user-friendly, cost-effective, efficient means for chemical agent protection. We are



FIGURE 11
Fabrication of bioactive multilayers by spraycoating on cloth for individual protection.

continuing our research with the goals of incorporating materials capable of both sensing (e.g., indicators of film activity or impending threats) and decontaminating a wider range of threats (e.g., biological), as well as integrating our films into currently used military technologies (e.g., clothes or water filters).

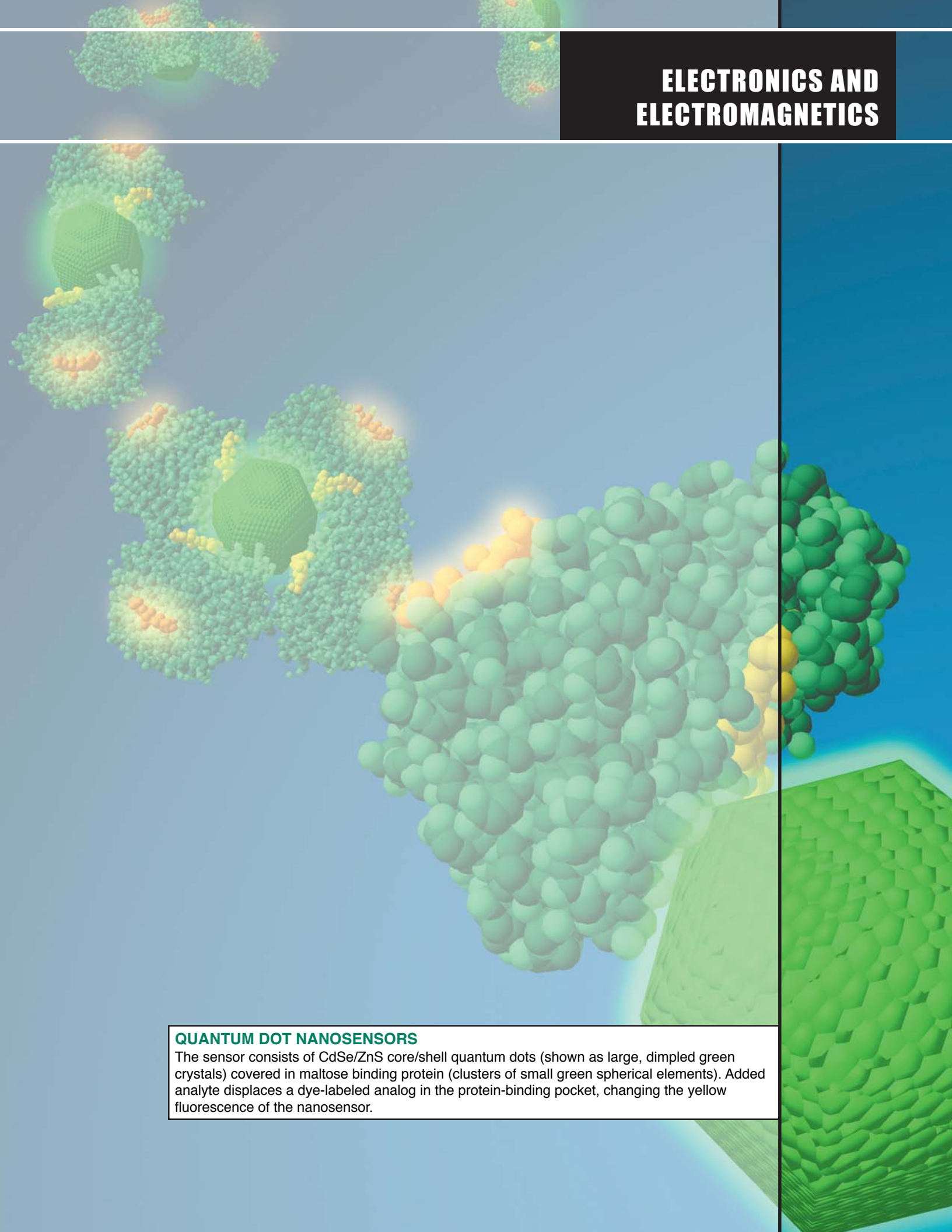
[Sponsored by ONR]

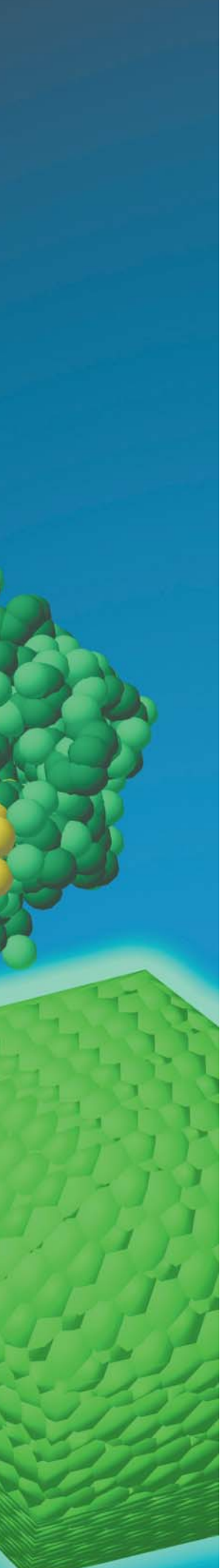
References

- ¹W. Mulbry and W. Rainina, "Biodegradation of Chemical Warfare Agents," *ASM News* **64**, 325-331 (1998).
- ²G. Decher, "Fuzzy Nanoassemblies: Toward Layered Polymeric Multicomposites," *Science* **277**, 1232 (1997).
- ³Y. Lee, I. Stanish, T.C. Chang, V. Rastogi, and A. Singh, "Sustained Enzyme Activity of Organophosphorus Hydrolase in Polymer Encased Multilayer Assemblies," *Langmuir* **19**, 1330-1336 (2003).

QUANTUM DOT NANOSENSORS

The sensor consists of CdSe/ZnS core/shell quantum dots (shown as large, dimpled green crystals) covered in maltose binding protein (clusters of small green spherical elements). Added analyte displaces a dye-labeled analog in the protein-binding pocket, changing the yellow fluorescence of the nanosensor.





125 UHF Delta-Sigma Waveform Generator

R.M. White, B.H. Cantrell, J.P. McConnell, and J.J. Alter

127 Unmanned Aerial Vehicle (UAV) Radar

D.W. Baden, E.M. Kutrzyba, A.P. Desrosiers, J.O. Alatishe, S. Talapatra, and M.G. Parent

129 The NRL 94 GHz High-Power WARLOC Radar as a Cloud Sensor

W.M. Manheimer, A.W. Fliflet, K. St. Germain, G.L. Linde, W.J. Cheung, V. Gregers-Hansen, M.T. Ngo, and B.G. Danly

132 Coupled Quantum Dots for Quantum Computing

T.L. Reinecke, Y. Lyanda-Geller, M. Bayer, and A. Forchel

UHF DELTA-SIGMA WAVEFORM GENERATOR

R.M. White, B.H. Cantrell, J.P. McConnell, and J.J. Alter
Radar Division

Introduction: A laboratory bench model of a UHF delta-sigma waveform generator was developed and tested. The waveform generator, which will eventually consist of only a few components, can generate both high-fidelity transmit waveforms and local oscillator signals for UHF radars. The application would be for digital radars. These radars require a large number of small, inexpensive digital waveform generators that have very good performance but not ultra-high performance because some performance improvement is obtained by paralleling a large number of waveform generators.

Delta-Sigma Background: Conventional digital-to-analog (D/A) conversion methods require a large number of bits for high resolution. Delta-sigma digital-to-analog converters (DACs) use only one bit. However, they can provide the same resolution as a 16-bit (or higher) conventional DAC, at a cost of increased overall system complexity and a higher sampling rate. Although delta-sigma coding circuitry is relatively simple for small signal bandwidths at baseband (namely, audio bandwidths of 20-24 kHz), capturing higher frequencies with large signal bandwidths (which are typically needed for radar transmission waveforms and/or radar local oscillators (LOs)), is much more complex and is still a significant field of research. In the search for low-cost, high-performance frequency generation for digital radar, it is useful to investigate the potential of delta-sigma waveforms since they can provide the high resolution needed by radars.

Creating a Delta-Sigma Waveform Generator: This research involved designing, constructing, and successfully demonstrating a UHF Delta-Sigma Waveform Generator. The waveform generator is DAC hardware only; the actual delta-sigma A/D is encoded through a MATLAB program, and the digital waveforms are then stored in an Agilent Logic Analysis System. Although the delta-sigma encoding produces a single binary bitstream, the code is stored as a 16-bit parallel waveform in the Agilent system because it cannot operate at the high serial bitrate needed (2.5 Gbps). The stored waveforms can then be replayed through the Delta-Sigma Waveform Generator hardware to recreate the analog waveform. The main components of the waveform generator are the Agilent pattern generator, a serializer, and a very high speed flip-flop to buffer the output (Fig. 1). The only other components of the system are the various clock signals required and filters for the analog signal band.

The simplicity of the architecture is the main highlight of this design, showing that high-quality waveforms can be produced with a minimal amount of hardware.

The waveforms tested on this system were a sinusoid and a linear FM, representing a LO and transmission type waveform, respectively. Figure 2 shows typical measurements of these delta-sigma created waveforms (in this figure, the out-of-band noise has not been filtered out). Although some issues with spurious signals must be resolved, the waveform generator produces low noise waveforms. The overall noise profile is difficult to measure accurately because of high frequency PRF lines that appear in the signal band, but created sinusoids have a noise floor as low as -140 dBc/Hz over an 80 MHz bandwidth. Since the waveforms are digitally synthesized in a software A/D process, the frequency and bandwidth are easily variable (up to UHF frequencies, 100 MHz bandwidth).

A slightly different architecture of the UHF Delta-Sigma Waveform Generator was constructed using a field-programmable gate array (FPGA) evaluation board (to store and process waveforms), which produced waveforms nearly as high in quality. This architecture effectively replaces the Agilent pattern generator and the serializer with an FPGA, creating a low-cost design using a small number of parts that can all fit onto a small printed circuit board (Fig. 3, filters and simple complementary transmission line circuitry not shown).

Applications and Significance: This work can be directly applied to waveform and LO synthesis for UHF radar systems. Using a higher delta-sigma sampling rate will allow larger signal bandwidths and/or higher signal center frequencies to be produced. The delta-sigma sampling rate of 2.5 Gbps chosen for this project corresponds to the I/O rate of our current generation of FPGAs. Flip-flops with a much higher sampling rate are already on the market, and the next generation of Xilinx FPGAs will allow us to use a sampling rate of 10 Gbps, which will be suitable for working with L-band or S-band waveforms. Since the circuit can also be easily scaled down to a very small physical size, an ideal application is use in digital phased array radars in which a self-contained exciter circuit is needed at each radiating element. The Delta-Sigma Waveform Generator shows the potential to meet the strict cost requirement of such a system and provide the ultra-high quality waveform needed through paralleling or ensemble averaging.

As this project demonstrates, delta-sigma encoding does not have to be restricted to very low frequencies and small bandwidths. The value of high-speed delta-sigma D/A conversion is that it requires only a small number of relatively low-cost parts to produce a high quality waveform.

[Sponsored by ONR]

•

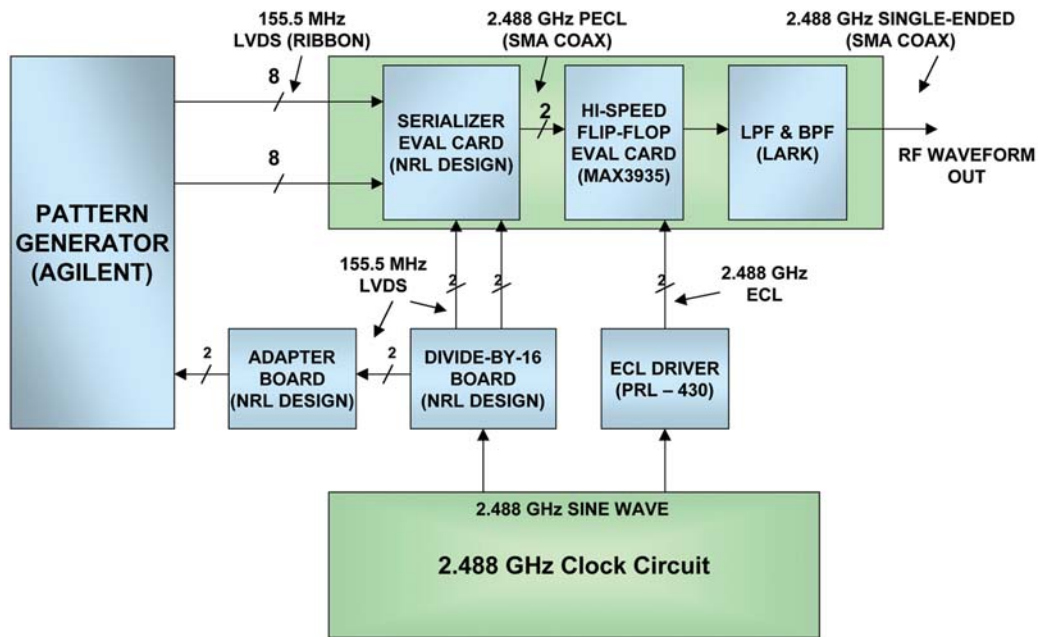
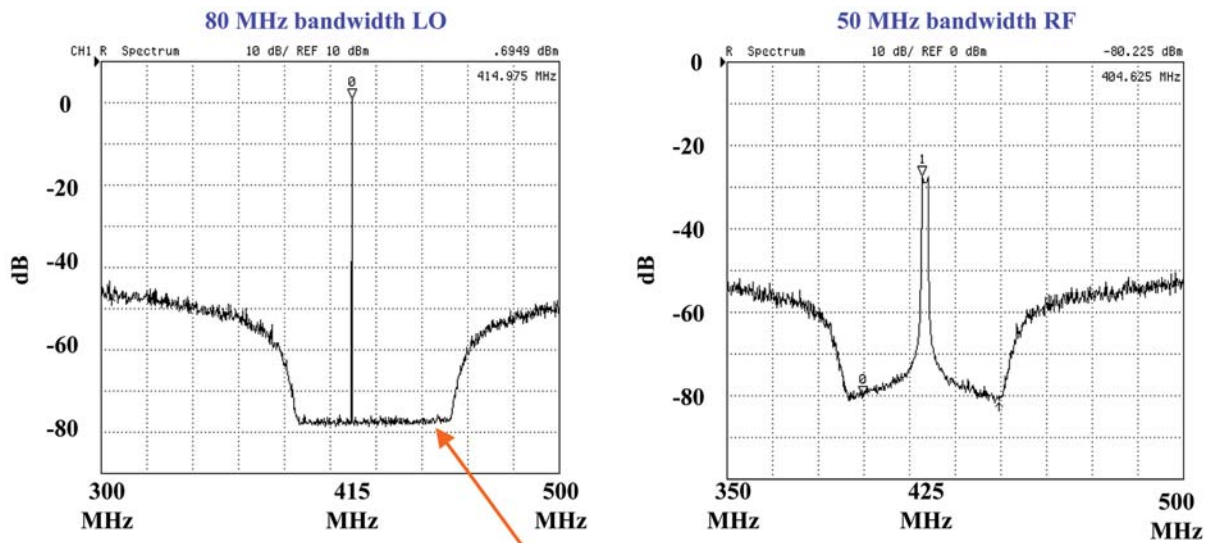


FIGURE 1
UHF delta-sigma waveform generator.



Spectrum analyzer noise floor.
Actual measured noise floor: -140 dBc/Hz.

FIGURE 2
Measured waveform spectra from the UHF delta-sigma waveform generator at 2.5 Gbps sampling rate (signal band is unfiltered).

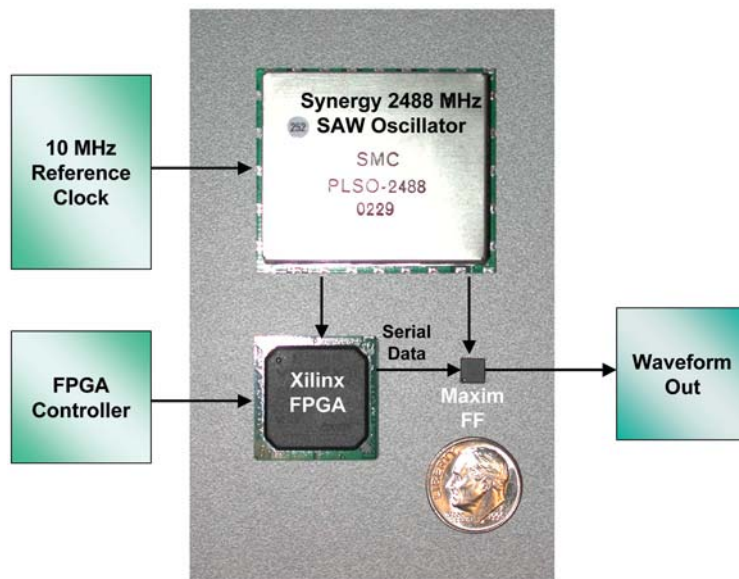


FIGURE 3
Key components of the delta-sigma waveform generator.

UNMANNED AERIAL VEHICLE (UAV) RADAR

D.W. Baden, E.M. Kutrzyba, A.P. Desrosiers,
J.O. Alatishe, S. Talapatra, and M.G. Parent
Radar Division

Introduction: The Unmanned Aerial Vehicle (UAV) Radar project is designing and demonstrating a synthetic aperture radar (SAR) and moving target indicator (MTI) radar to (1) detect and track moving ground vehicles and small boats to a range of 80 nmi, (2) provide a simultaneous SAR ground map, (3) provide targeting quality data for weapons, (4) provide for low false track rates, (5) use low microwave frequencies for foliage penetration, and (6) fit in a Navy vertical take-off UAV. This proof-of-concept program supports the Navy's Tactical Ultra-Light Unmanned Aerial Vehicle Program, sponsored by PMA-263.

Algorithms: The different algorithms that have been analyzed for use with this radar include: Displaced Phase Center Antenna (DPCA), Space Time Adaptive Processing (STAP), and Velocity SAR (VSAR). Data are being collected to verify that Velocity SAR will be the optimal algorithm. VSAR assumes that input data from each antenna element is pulse-compressed, motion-compensated, and is in baseband in-phase and quadrature (I and Q) form. The primary difference between VSAR and standard SAR is that VSAR initially requires the formation of multiple (N) SAR images, one from each antenna in an antenna array, while standard SAR forms just one image from one antenna. To detect moving targets, a

given pixel is processed over all N images, and this process is repeated for every pixel location. For moving targets, the radar echo phase shift from antenna element to antenna element for each range/azimuth pixel location may be detected.^{1,2}

System Hardware: The radar is a low-power (300 W peak, expandable to 1 kW), L-band (1290-1315 MHz) that is capable of detecting small targets out to an unambiguous range of 25 nmi (expandable to 80 nmi). A field-programmable gate array (FPGA)-based digital signal processor (DSP) board is used to generate the low-power transmit waveform at the first intermediate frequency (IF) of 45 MHz. Typical waveforms outputted by the FPGA board include a bandwidth (BW) = 1 to 10 MHz, pulse repetition interval (PRI) = 1 ms (adjustable), and pulse width (PW) = 8 to 67 μ s. The primary waveform will be a linear FM with 67 μ s PW, 1.024 ms PRI, 7.5 MHz BW, and 45 MHz IF chirp.

The receiver subsection consists of 16 IF channels (at 45 MHz center frequency, 10 MHz BW). Radar echo data are acquired/sampled via eight dual-channel Pentek digital receivers, which are housed in a 21-slot VME chassis. Data are transferred from the digital receivers via fiber channel to a RAID (Redundant Array of Inexpensive Disks) for post processing. The acquisition subsystem is capable of collecting 20 s of data per run. The current radar system configuration uses a temporary antenna consisting of six receivers and four transmit ports. The final antenna design will have 24 receive ports but only 16 will be active. Each port contains one vertically half-wavelength dipoled antenna element. The transmit dipoles are half-wavelength spaced in both directions,

while the receive dipoles have a horizontal spacing of a quarter-wavelength.

Field Testing: The platform chosen for this iteration of testing is a truck. The radar system is housed in an 8 × 7 × 7-ft aluminum shelter with the antenna housing secured to the roof. This shelter is secured to the stake-body truck and powered by a 20 kW generator also located aboard the truck. For the initial testing of the radar system last summer, the radar was stationary at NRL's Chesapeake Bay Detachment (CBD), looking toward Tilghman Island. Returns from the newly working radar system at CBD are consistent with radar data collected from other systems. Radar returns have been identified as Tilghman and Sharps Islands and also a large ship that was noted during data collection. The radar system is still maturing as initial testing begins. The system used only three receive channels during the early stages of development. The first test with the moving radar occurred in Hancock, Maryland, on elevated areas overlooking low-lying country roads where the truck could safely and legally travel at 60 mph. Along these country roads, a target was placed at several designated locations traveling at various speeds. As data processing continues, images will be produced with the target in and out of the field of

view. Figure 4 shows preliminary data from the Hancock, Maryland, processing. The radar was also used to collect more data in a similar site at Afton Mountain near Charlottesville, Virginia. The radar system had six receive elements at that time. Figure 5(a) shows a digital orthographic view merged with digital terrain elevation data (DTED) reflectance and shed fan from the transmit area on Interstate Highway I-64 near Afton, Virginia. Figure 5(b) is an image of data collected with the UAV radar. Notice the similarities between the DTED data and the radar data, such as the hook on the left-hand side of the image at 5 statute miles and the mountain ridges from 6 to 10 statute miles (with the area in between hidden because of near-range landscape).

Summary: The data prove that the Radar Division has a new working radar system. As the radar matures and the data are analyzed, the VSAR algorithm will be used to show that the radar will be able to detect a small moving target. The system will be populated with 16 elements in January 2004, and the radar will continue to be tested at the previous test sites. Future plans will be to locate funding to fly a similar system in either a helicopter or small aircraft.

[Sponsored by ONR]

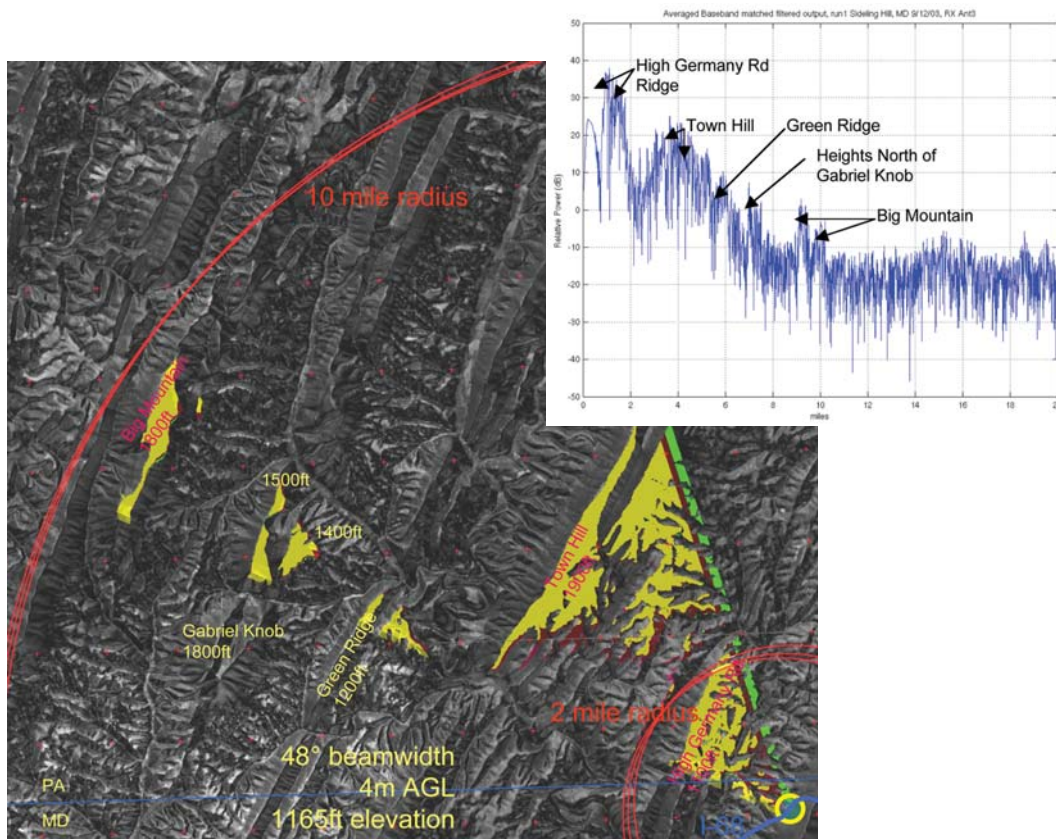


FIGURE 4
Geographic scatters in radar returns.

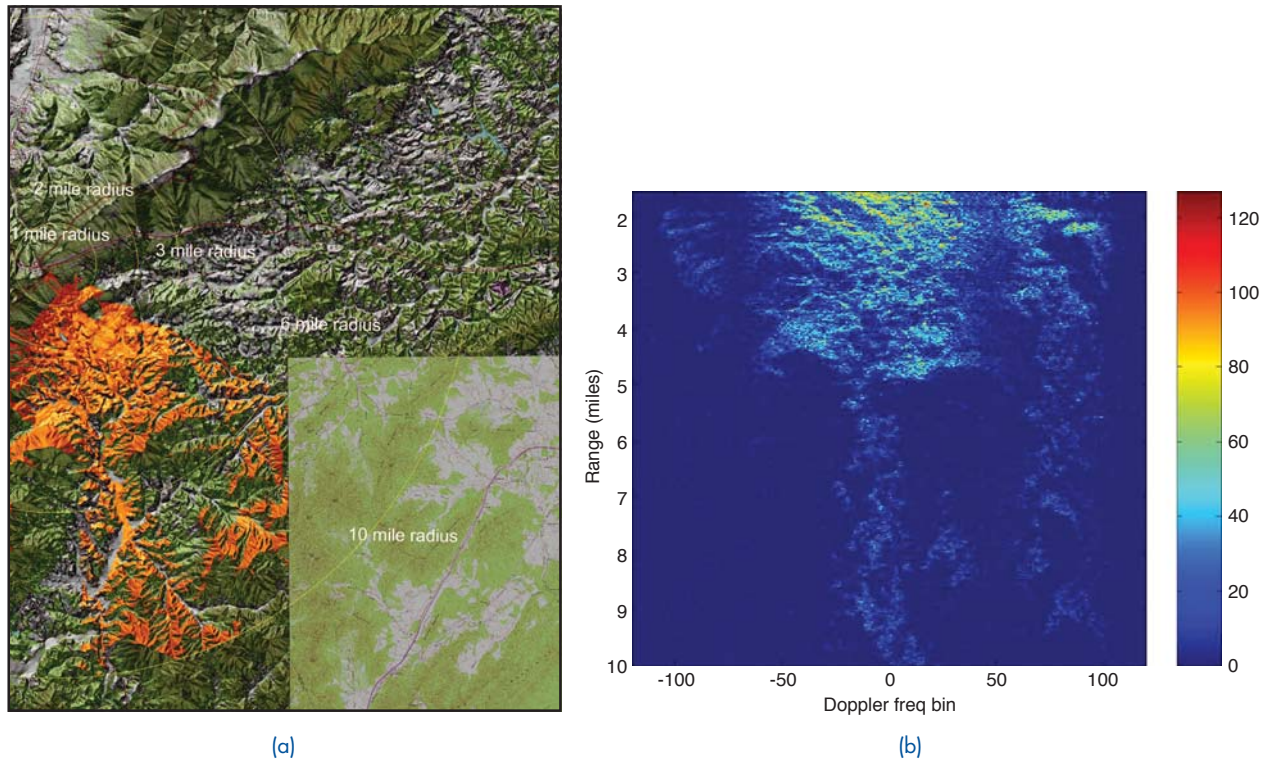


FIGURE 5
 (a) Digital orthographic view merged with DTED reflectance and shed fan from transmit area on Interstate Highway I-64 near Afton, VA. (b) Image of data collected with UAV radar.

References

- ¹M. Picciolo, B. Cantrell, E. Kutrzyba, S. Schutz, M. Parent, J. Alatishe, and S. Talapatra, "UAV Radar," presented at *Military Sensing Symposia (MSS)*, National Institute of Standards and Technologies, Gaithersburg, MD 27-29 November 2001.
- ²B. Friedlander and B. Porat, "VSAR: A High Resolution Radar System for Detection of Moving Targets," *IEEE Proc. Radar, Sonar, Navig.* 34(3) 205-218 (1997).

THE NRL 94 GHZ HIGH-POWER WARLOC RADAR AS A CLOUD SENSOR

W.M. Manheimer,¹ A.W. Fliflet,¹ K. St. Germain,² G.J. Linde,³ W.J. Cheung,³ V. Gregers-Hansen,³ M.T. Ngo,³ and B.G. Danly⁴

¹Plasma Physics Division

²Remote Sensing Division

³Radar Division

⁴Electronics Science and Technology Division

Introduction: NRL has recently set up a high-power 94 GHz radar called WARLOC at its Chesapeake Bay Detachment (CBD) on the western shore of the Chesapeake Bay. The heart of the WARLOC system is a state-of-the-art 94 GHz gyrokystron, developed by a team led

by NRL.¹ The 1.8-m Cassegrain antenna has a 0.1° angular beam width and is mounted on a high-precision pedestal with a 2π steradian solid angle scanning capability. This project was primarily supported to investigate a variety of DOD-related issues, including aircraft identification, precision tracking, and counter stealth. However, the team realized early on that WARLOC could also be an unmatched cloud sensor, and this has been investigated. Radars operating at 94 GHz have been used previously for remotely sensing cloud properties,² but the much higher power and antenna gain of the WARLOC radar give it about 50 dB additional sensitivity. This allows the detection of lower reflectivity clouds at longer ranges, and permits rapid, high-resolution two- and three-dimensional imaging of clouds for the first time.

Because the radar cross section of a cloud droplet of radius r is proportional to r^6/λ ,⁴ where λ is the wavelength, millimeter-wave radars scatter much more strongly from clouds than conventional radars, which normally do not detect clouds. On the other hand, laser radars (lidars) cannot penetrate visibly opaque clouds. Thus millimeter-wave radars are well suited to cloud imaging. While the use of millimeter-wave radars is limited by atmospheric attenuation, there are propagation windows at 35 and 94 GHz; the former having less atmospheric attenuation, the latter enhancing the droplet cross section. The radar reflectivity per unit volume of a cloud is denoted by Z and measures the sixth moment of the

droplet distribution. It is usually expressed in units of mm^6/m^3 , and is often displayed on a logarithmic scale as $\text{dBZ} = 10 \log Z$.

A variety of waveforms have been programmed into WARLOC. One is the short pulse (SP) mode, a 100-ns pulse (15-m range resolution); another is the search radar (SR) mode, which is a much longer pulse, but which is compressed on return to the same 15-m range resolution. The sensitivity is increased by the ratio of the uncompressed to compressed pulse times. Both have been used for cloud imaging, the latter being necessary for weak clouds, long range or high attenuation.

A Millimeter-Wave Cloud Image: A sector of a medium-altitude cirrus cloud was scanned at about 1 p.m. on April 9, 2002.³ On-site measurements showed the temperature at 11 a.m. was 23°C and the relative humidity was 62%. At CBD, the sky was mostly overcast, with low-altitude stratocumulus clouds. However, WARLOC obtained images of the cloud above this. Note that no ground-based laser system could have obtained these data because of the intervening lower level cloud. The radar waveform was a 100 ns, unchirped pulse, and the pulse repetition frequency (PRF) was 500 Hz. This pulse length gives a 15-m range resolution, and the 0.1° beam width gives an angular resolution of about 10 m at a range of 6 km. The cloud data were obtained with the radar pointing in an easterly direction while sweeping upward in the vertical plane between 30° and 50° to the horizontal at a rate of $0.1^\circ/\text{s}$. At this PRF and scanning rate, the radar elevation angle changes by 0.02° during a train of 100 pulses. This is much less than the 0.1° angular width of the antenna

beam, so the 100-pulse train is sampling essentially the sample cloud volume element, and the results can be averaged over this number of pulses.

Figure 6(a) shows a white-on-black false-color plot of dBZ plotted as a function of distance $\mathbf{R} = (X, Y)$ from the radar. The wedge-shaped region is the sector sampled by the radar. The image resolution of about 15 m allows the cloud structure to be seen in extremely fine detail. A horizontal and diagonal vein is apparent in the cloud, as well as filamentary structure throughout the volume and wispy structures emerging from the top. Notice also the intricate structure of the cloud boundary on the bottom left-hand side of the figure. We are quite sure that no other sensor could image the internal structure of a visibly opaque cloud in this kind of detail.

The Cloud Correlation Function: Figure 6(b) shows the 104-pulse-averaged data for Z displayed on a linear scale. The figure shows a speckle pattern overlaid on the cloud structure, indicative of a random process, perhaps fluid turbulence, playing a role. The speckle pattern is all but imperceptible in Fig. 6(a) because of the compression of the logarithmic scale. To investigate this random process, we have calculated the spatial correlation function of Z : $C(\mathbf{r})$. It is a scalar function of a two-dimensional vector \mathbf{r} and is shown in Fig. 7. Notice that it comes to a cusp at zero point separation. The figure shows that the cloud fluctuations are correlated over about 3-4 times longer distance horizontally (x -direction) than vertically (y -direction). Also, the correlation function is quite anisotropic, even at the shortest scale lengths that WARLOC can resolve.

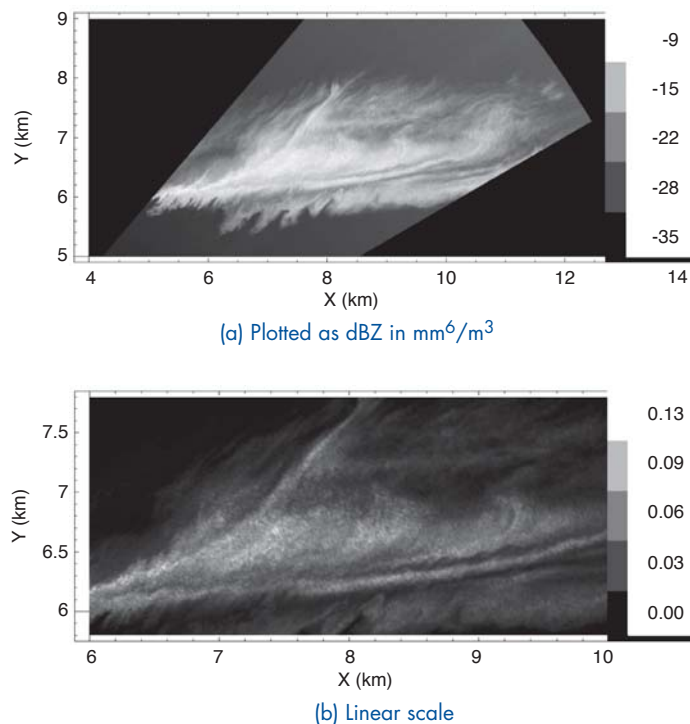


FIGURE 6
A white-on-black false-color plot of the reflectivity factor Z of a cloud scanned on April 9, 2002.

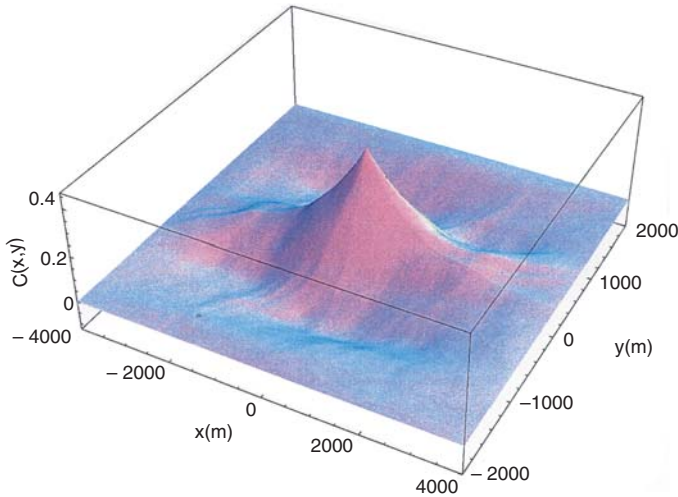


FIGURE 7
Correlation function for the cloud region shown in Fig. 6(b).

It is natural to think that fluid turbulence occurs in clouds. One of the most important results of modern fluid turbulence theory was obtained by Kolmogorov, who predicted that turbulence scale lengths would include an “inertial range” in which eddies would progress from larger to smaller scale lengths without dissipation. The inertial range falls between the long (outer) scale length at which power is injected, and the short (inner) scale length at which power is dissipated by viscous damping. If the turbulence is homogeneous and isotropic, Kolmogorov showed that in the inertial range the correlation function scales as $r^{-2/3}$ where r is the separation between fluid points. The one-dimensional correlation functions $C(x,0)$ and $C(0,y)$, for the horizontal and vertical directions, respectively, are plotted in Fig. 8. Under each plot is another curve illustrating $x^{2/3}$ ($y^{2/3}$) behavior. Clearly, the cusp behavior is characteristic of the Kolmogorov inertial range with one important caveat. The theory is derived under the assumption that the turbulence is at least locally isotropic, whereas the cloud correlation function is anisotropic down the smallest scale lengths we can resolve. Figure 8 also allows us to easily discern the outer scale length, the distance at which the

measured correlation function departs from the $x^{2/3}$ dependence. It is about 1.5 km horizontally and about 0.5 km vertically. Furthermore, the horizontal correlation decreases monotonically, but the vertical correlation shows an interesting wave-like structure probably associated with the process driving the turbulence.

To summarize, the NRL WARLOC radar has demonstrated the ability to image the internal structure of visibly opaque clouds in tremendous detail. These images can provide new multi-dimensional information on cloud turbulence.

[Sponsored by ONR]

References

- ¹ V. Gregers-Hansen, G.J. Linde, W.J. Cheung, B.G. Danly, M.T. Ngo, and R. Myers, “WARLOC: a New 94 GHz High Power Coherent Radar,” *2001 NRL Review*, p. 107.
- ² J.B. Mead, A.L. Pazmany, S.M. Sekelsky, and R.E. McIntosh, *Proc. IEEE* **82**, 1891 (1994).
- ³ W.M. Manheimer, A.W. Fliflet, K. St. Germain, G.J. Linde, W.J. Cheung, V. Gregers-Hansen, M.T. Ngo, and B.G. Danly, “Initial Cloud Images with the NRL High Power 94 GHz WARLOC Radar,” *Geophys. Res. Lett.* **30**, 1103 (2003). •

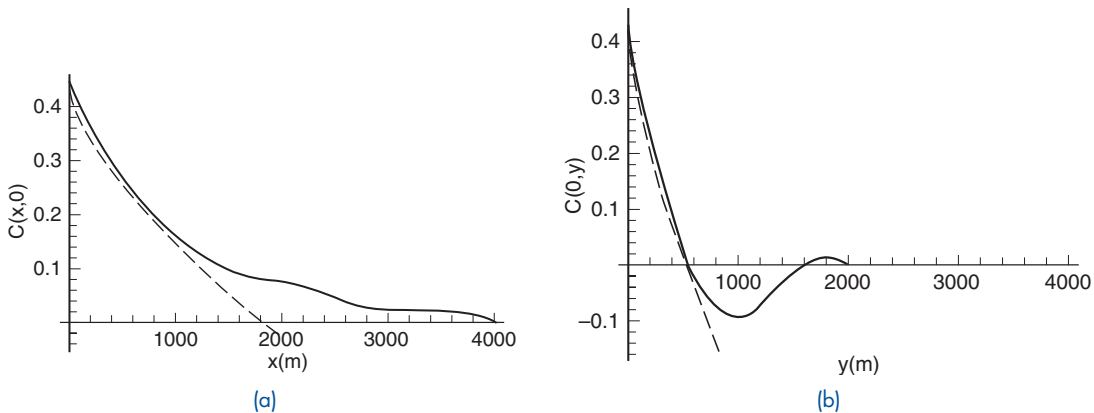


FIGURE 8
The solid curve in (a) shows the correlation function $C(x,0)$, and the dashed curve shows a function proportional to $x^{2/3}$ for comparison. Similar curves for $C(0,y)$ are shown in (b).

COUPLED QUANTUM DOTS FOR QUANTUM COMPUTING

T.L. Reinecke,¹ Y. Lyanda-Geller,¹ M. Bayer,² and A. Forchel³

¹Electronics Science and Technology Division

²University of Dortmund

³University of Wuerzburg

Introduction: In digital computers, information is represented in classical ‘bits’ by either 0 or 1. Quantum information is represented in “quantum bits” with wavefunctions $\Psi = \alpha|0\rangle + \beta|1\rangle$. These bits involve the continuous phase and thus contain much more information than the classical bit. The search for physical implementations for quantum information technologies is a major focus of current multidisciplinary research efforts. Quantum information technology can form the basis for powerful encryption schemes and secure communications, for code breaking through prime number factoring, and for ultra-powerful computation.

The key requirement for these technologies is physical implementations of qu-bits, particularly of the coupled qu-bits for quantum gates. Two qu-bit gates are the bases for manipulation of information in computations. Solid state implementations, particularly those from semiconductors, are especially needed for systems that can be scaled up to large numbers of qu-bits and integrated in current semiconductor technologies. Quan-

tum dots with their sharp optical lines behave like artificial atoms and are of great interest as qu-bits. In them, the two states can be represented either by the two levels of a spin in the dot in a magnetic field or by the presence/absence of an exciton (an optically excited electron-hole pair). Although quantum dot implementations for qu-bits have been widely studied, appropriately coupled quantum dots for two qu-bit gates have not been achieved to date.

Coupled Quantum Dots for Gates: The requirements for coupling between quantum dots to make gates are that the coupling be coherent so that information not be lost during computation, and that the coupling can be turned on and off externally to carry out the information exchange in the gate. In work done jointly between NRL and researchers in Germany,¹ we have demonstrated coupled quantum dots for gates. Single “self-organized” InAs quantum dots were grown by molecular beam epitaxy between GaAs substrates and GaAs overlayers (Fig. 9(a)). InAs dots form at the interface due to strain from the mismatch of the lattice constants of the two materials. Pairs of such quantum dots are formed on closely spaced interfaces. The strain around the two quantum dots causes them to form above one another.

The energies of excited electron-hole pairs in these coupled dots are shown in the lower part of Fig. 9(b) as a function of distance between the dots. The dependence of the energies on separation arises from overlap of the

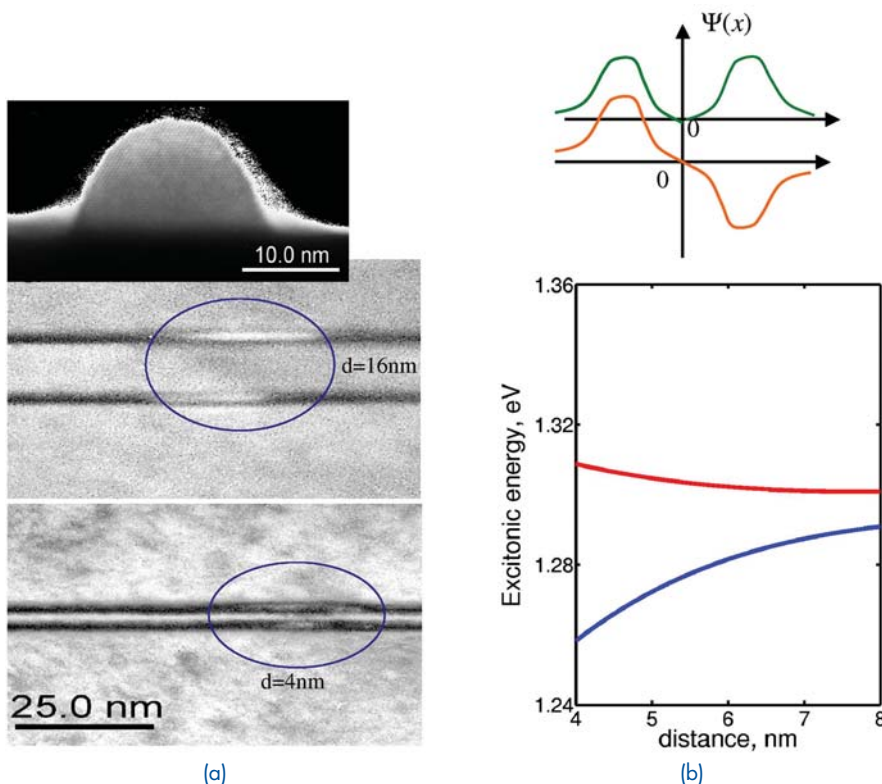


FIGURE 9 Left-hand side shows transmission electron micrographs for an InAs/GaAs quantum dot grown by molecular beam epitaxy and for coupled pairs of quantum dots on adjacent layers. Lower panel on right-hand side gives energies of electron hole pair in coupled pair of quantum dots as a function of distance between them. Upper panel on right-hand side sketches bonding and antibonding wavefunctions of two atoms.

electron and hole wavefunctions in the two dots, and Coulomb interactions between the electron and hole. This distance dependence is similar to the splitting between the bonding and antibonding electron states of a simple molecule, which is sketched in the upper part of Fig. 9(b). Our theoretical results for this distance dependence (Fig. 9(b)) are in agreement with recent photoluminescence experiments on these coupled dot structures. This indicates that the coupling between the dots is quantum mechanical and thus coherent. Additional experimental and theoretical results for the diamagnetic shifts and anticrossings in magneto-optical studies confirm that the coupling is indeed coherent.¹

We have also devised a simple method to control the coupling between these quantum dots with an electric field. This field brings the excitons in the two dots into and out of resonance, as illustrated in the upper part of Fig. 10. The structure is formed into a Schottky diode, with metal films on the top and bottom as illustrated in the bottom of Fig. 10, to apply an electric field to the coupled dots. The right-hand side of Fig. 11 shows calculations of the wavefunctions of an exciton in the coupled dots as functions of the electron and hole coordinates. At zero field, the wavefunction consists of approximately equal parts of an intradot exciton (an electron and hole in the same dot) and interdot excitons. At nonzero field, the wavefunction is composed mainly of one state with electron and hole in different dots. These calculations are

in good quantitative agreement with the photoluminescence data shown in the left-hand side of Fig. 11, which exhibit one feature (intradot exciton) with decreasing in energy and intensity and another (interdot exciton) appearing with increasing field. The observed features result from modifications of the electron and the hole wavefunctions in the two dots, and these results demonstrate that a simple electric field controls their wavefunction mixings.

Conclusions: We have fabricated coupled quantum dot structures from closely spaced self-organized InAs quantum dots, and we have demonstrated that the coupling between the dots is coherent. We also have shown that a simple electric field controls the couplings between carriers in the two dots. Two qu-bit quantum gates will be made from these coupled quantum dots by doping spins into each dot. The gate operations needed in quantum information technologies will be carried by electric field pulses on the coupled dots.

[Sponsored by ONR and DARPA]

Reference

¹M. Bayer, G. Ortner, A. Forchel, Y.B. Lyanda-Geller, T.L. Reinecke, P. Hawrylak, S. Fafard, and Z.R. Wasilewski, "Fine Structure of Excitons in InAs/GaAs Coupled Quantum Dots: A Sensitive Test of Electronic Coupling," *Phys. Rev. Lett.* **90**, 086404 (2003).

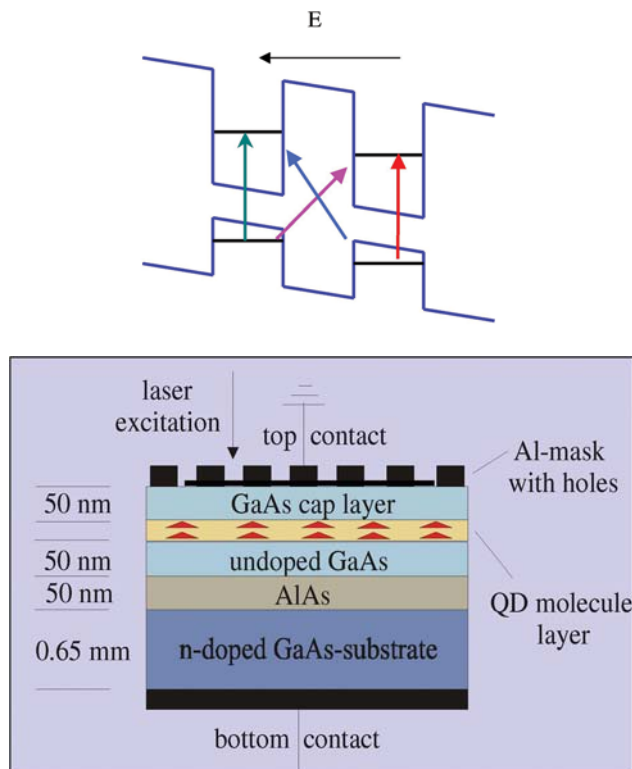


FIGURE 10

Upper panel shows a sketch of excitons in two coupled quantum dots being brought into and out of resonance with an electric field. Lower panel is a sketch of Schottky diode structure in which an electric field is applied to coupled quantum dots.

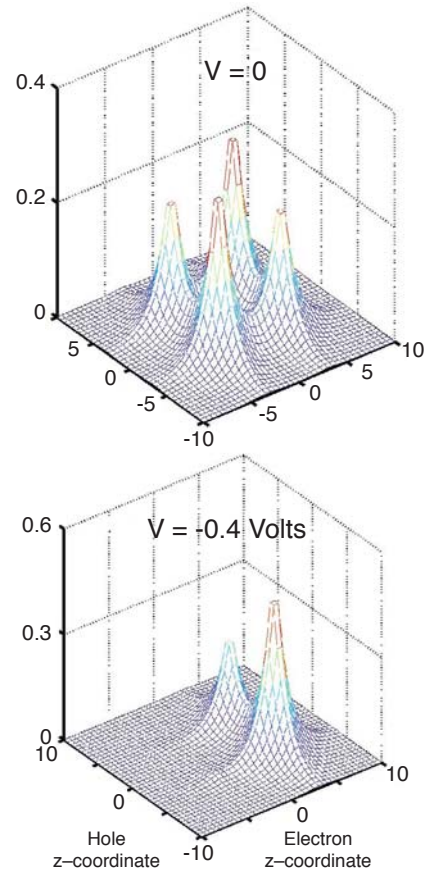
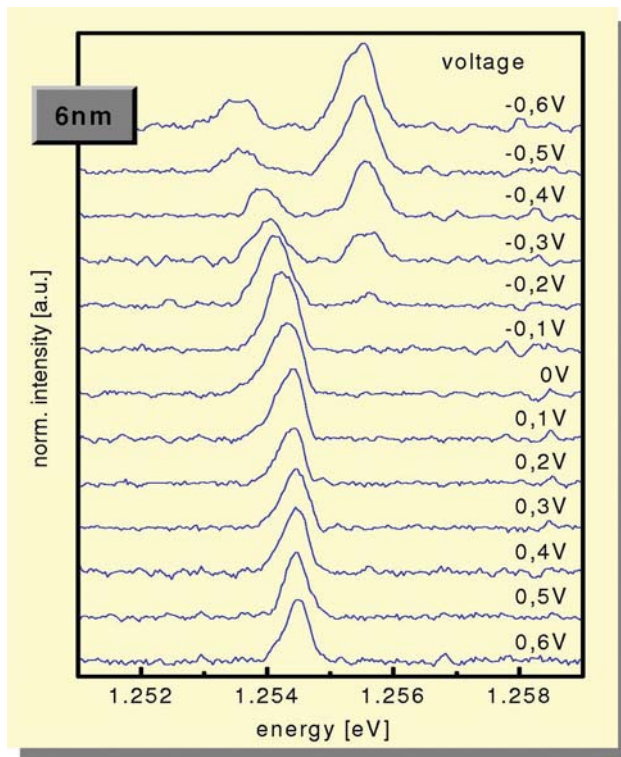
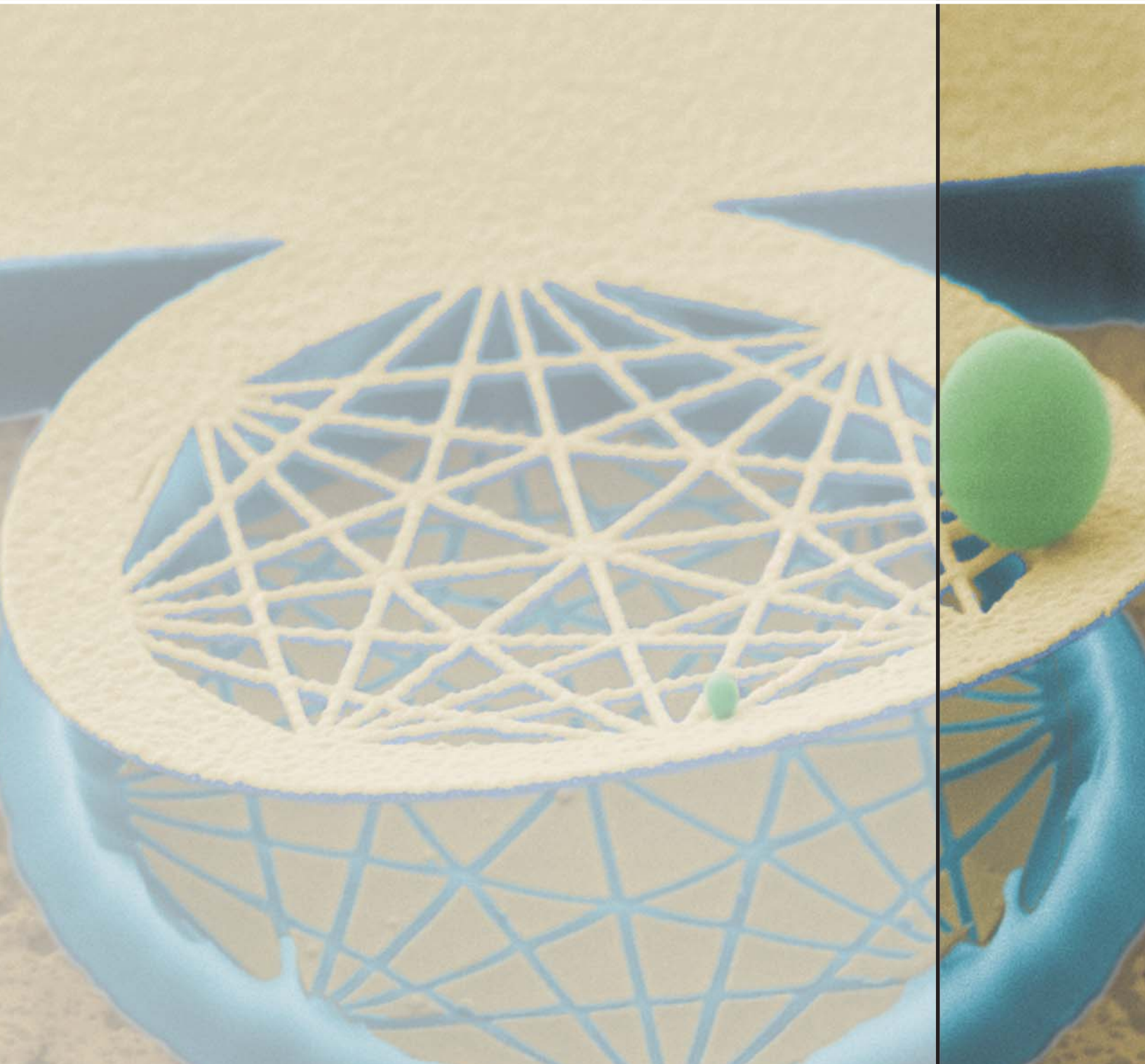


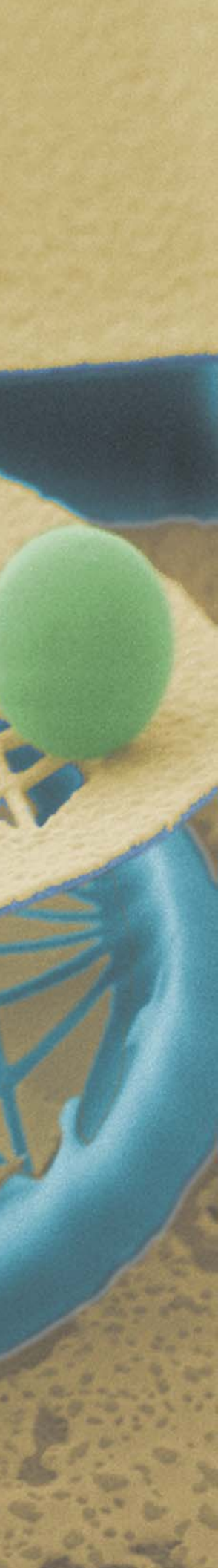
FIGURE 11

Right-hand panel gives wavefunctions of an electron and a hole in a coupled dot structure as functions of electron and hole coordinates for electric field $E = 0$ and $E = 6.2$ V/cm. Left-hand panel gives photoluminescence results for coupled quantum dot structure as a function of electric field. The calculations give a detailed explanation of experiment both for the energies and for the intensities of the features.



NANO DIAMOND TENNIS RACQUET

A color-enhanced scanning electron micrograph of a prototype NEMS resonator fabricated from 30-nm-thick nanocrystalline diamond film and covered by 30 nm of sputtered gold. Because of the 1-mm-diameter particle accidentally on it, we call it our Nano Tennis Racquet. The smaller particle and the “strings” are 80 nm wide.



137 Energy-Aware Broadcasting and Multicasting in Wireless Ad Hoc Networks

J.E. Wieselthier, G.D. Nguyen, and A. Ephremides

140 Netcentric Multi-INT Fusion Targeting Initiative (NCMIFTI)

D.C. Linne von Berg, M.R. Kruer, J.N. Lee, M.D. Duncan, J.G. Howard, F. Olchowski, and R.A. Patten

143 Real-Time Exploitation and Dissemination of Tactical Reconnaissance Imagery During Operation Iraqi Freedom for Ground and Maritime Operations

J.N. Lee, D.C. Linne von Berg, M.D. Duncan, M.R. Kruer, and R.A. Patten

144 Volume Sensor for Shipboard Damage Control

S.L. Rose-Pehrsson, J.C. Owrutsky, D.T. Gottuk, D.A. Steinhurst, C.P. Minor, J.P. Farley, and F.W. Williams

148 Control Algorithms for UUV Teams Using Acoustic Communications

P. McDowell and B. Bourgeois

ENERGY-AWARE BROADCASTING AND MULTICASTING IN WIRELESS AD HOC NETWORKS

J.E. Wieselthier and G.D. Nguyen
Information Technology Division
A. Ephremides
University of Maryland

Energy-Aware Networking: In many military networking applications, battery energy is a precious resource that must be carefully managed. Whereas most energy-related studies have concentrated on improved batteries and low-power electronics, we have approached this problem from the novel perspective of networking techniques. Our primary focus is on an “energy-constrained” mode of operation, under which each node is equipped with batteries that cannot be recharged or replaced. Therefore, nodes whose batteries are depleted are removed, and the network may no longer fulfill its objectives. To address the specific problem of energy-aware tree construction for broadcast (one-to-all) and multicast (one-to-many) communication, we have developed the Broadcast Incremental Power (BIP) and Multicast Incremental Power (MIP) algorithms.¹

Ad Hoc Wireless Networks Are Different: The wireless ad hoc networking environment presents formidable challenges. For example, unlike cellular networks (which have fixed base stations), ad hoc networks have no infrastructure; they do not even have pre-defined links. By increasing RF transmitter power, one can increase communication range; however, this causes increased energy expenditure and interference.

We first assume the use of omnidirectional antennas; thus all nodes within communication range of a transmitting node can receive its transmission. Consider the example shown in Fig. 1, in which a subset of the multicast tree involves Node i , which is transmitting to its neighbors, Node j and Node k . A single transmission at power $P_{i,(j,k)} = \max\{P_{ij}, P_{ik}\}$ is sufficient to reach both of them. We exploit this property, which we refer to as the “wireless multicast advantage,” in our BIP algorithm.

Wired networks are typically designed using a layered protocol stack, in which the functions at each layer (physical, data link, network, etc.) are designed independently. However, a “cross-layer” approach is more appropriate for ad hoc wireless networks. Specifically, our algorithms jointly choose transmission power (which can be different at each node) and tree structure.

The Broadcast Incremental Power (BIP) Algorithm: We assume that the locations of the nodes are known,

and that the power required to support communication between two nodes is equal to r^α , where r is the distance between them and $2 \leq \alpha \leq 4$. We further assume that RF power is continuously variable and under network control. Our goal is the construction of a minimum-energy broadcast tree, rooted at the source node. Since this is an NP-complete problem, heuristics are needed.

Under our BIP algorithm,¹ the first in the literature to address this problem, nodes are added to the tree, one at a time. The node that is added at each step is the one that requires the minimum value of *incremental* power. Let us say that Node i is already transmitting at power level $P(i)$, which is not sufficient to reach Node j . Then the incremental power to reach Node j is $C_{ij} = P_{ij} - P(i)$, where $P_{ij} = r_{ij}^\alpha$ is the total power required to reach Node j . Figure 2 shows the first three steps and final tree structure generated by BIP, where Node 10 is the source node. BIP is easily adapted to multicast operation by pruning the branches of the tree that do not lead to desired destinations, resulting in the Multicast Incremental Power (MIP) algorithm.

Extension of Network Life in Energy-Limited Operation: In situations where energy at the nodes is not renewable (e.g., sensors or individual warriors that cannot replace their batteries), it is helpful to use a cost function that incorporates the residual energy at each node.² Specifically, the incremental cost of Node i transmitting to Node j is defined to be

$$C_{ij} = (P_{ij} - P(i)) \left(\frac{E_i(0)}{E_i(t)} \right)^\beta,$$

where $E_i(0)$ is the initial value of energy at Node i , and $E_i(t)$ is the residual energy at time t . By setting $\beta > 0$, use of nodes with little residual energy is discouraged, and load balancing is thereby achieved. Figure 3 shows that by setting $\beta = 1$, the death of the first node is delayed considerably, thereby extending the network’s useful life.

Further Enhancement Using Directional Antennas: The use of directional antennas can provide energy savings and interference reduction by concentrating RF energy where it is needed. We assume that each node’s beamwidth θ can be chosen, such that $\theta_{\min} \leq \theta \leq 360$. We have considered two basic approaches for broadcasting and multicasting with directional antennas,³ which are described in Fig. 4. This figure shows the evolution of cumulative delivered traffic volume under MIP for the two schemes, for several values of θ_{\min} . In all cases, traffic is delivered at a constant rate until the network dies; this is a consequence of setting $\beta = 1$. As θ_{\min} is reduced, both the network lifetime and traffic volume increase, and D-MIP shows a greater performance advantage over RB-MIP.

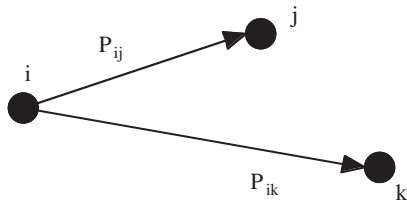


FIGURE 1

The “wireless multicast advantage” associated with omnidirectional antennas: $P_{i,(j,k)} = \max\{P_{ij}, P_{ik}\}$. The two destinations can both be reached using the *maximum* value of power required to reach either of them individually. This situation is quite different from that of wired networks, in which the cost to reach two neighbors is generally the *sum* of the costs to reach them individually.

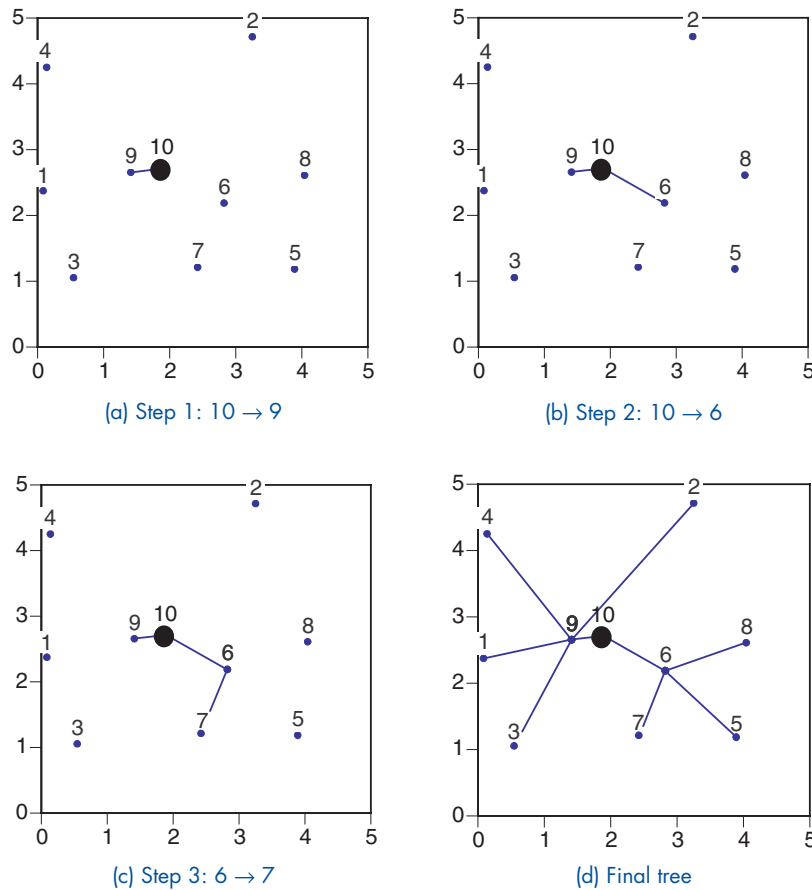


FIGURE 2

Example of tree construction using BIP (first three steps and final tree); $\alpha = 2$. At each step of the algorithm, one node is added to the tree, i.e., the node that can be added using the least value of *incremental power*.

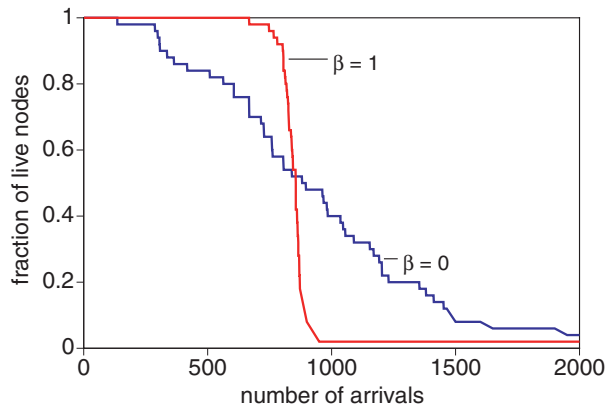
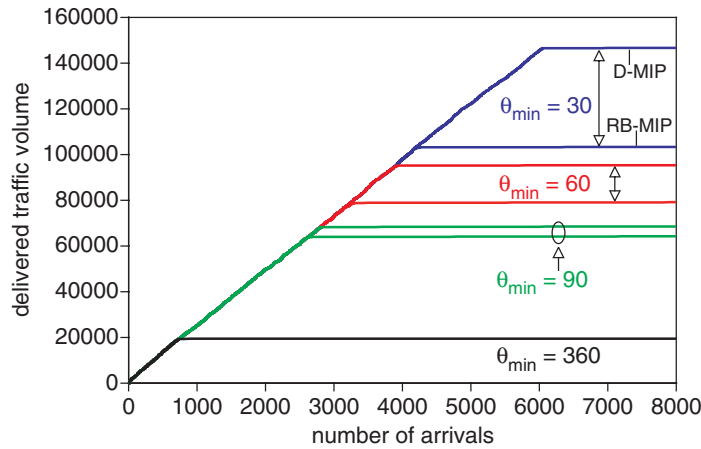


FIGURE 3 Evolution of number of live nodes under MIP for 50-node network. Setting the energy-aware parameter $\beta = 1$ discourages the use of energy-starved nodes, thereby providing load balancing and delaying the death of the first node considerably.



Reduced Beam BIP (RB-BIP) and MIP (RB-MIP)

- Construct the tree by using an algorithm designed for omnidirectional antennas; then reduce each antenna beam to the minimum possible width that can support the tree.

Directional BIP (D-BIP) and MIP (D-MIP)

- Incorporate directional antenna properties into the tree-construction process.

FIGURE 4 Traffic volume vs time for D-MIP and RB-MIP for several values of θ ($\beta = 1$). The use of directional antennas provides significant increase in network lifetime and delivered traffic volume. This improved performance is especially apparent for D-BIP and D-MIP, which exploit the properties of directional antennas as the tree is constructed.

Summary: Our seminal research introduced the problem of energy-aware tree construction for broadcasting and multicasting to the research community. It has stimulated research by many others. We have shown that novel networking techniques, based on cross-layer design, can improve network performance and extend network lifetime. We have also developed distributed versions of our algorithms. Future military ad hoc and sensor networks will benefit from these approaches to support Navy/Marine Corps operations.

[Sponsored by ONR]

References

- J.E. Wieselthier, G.D. Nguyen, and A. Ephremides, "Energy-Efficient Broadcast and Multicast Trees in Wireless Networks," *Mobile Net. Appl. (MONET)* 7(6), 481-492 (2002).
- J.E. Wieselthier, G.D. Nguyen, and A. Ephremides, "Resource Management in Energy-Limited, Bandwidth-Limited, Transceiver Limited Wireless Networks for Session-Based Multicasting," *Comp. Net.* 39(2), 113-131 (2002).
- J.E. Wieselthier, G.D. Nguyen, and A. Ephremides, "Energy-Aware Wireless Networking with Directional Antennas: The Case of Session-Based Broadcasting and Multicasting," *IEEE Trans. Mobile Comp.* 1(3), 176-191 (2002).

NETCENTRIC MULTI-INT FUSION TARGETING INITIATIVE (NCMIFTI)

D.C. Linne von Berg, M.R. Kruer, J.N. Lee, M.D. Duncan, J.G. Howard, F. Olchowski, and R.A. Patten
Optical Sciences Division

Introduction: The NRL Optical Sciences Division has initiated a multiyear effort to develop and demonstrate an airborne netcentric suite of multi-intelligence (multi-INT) sensors and exploitation systems for real-time target detection and targeting product dissemination. The goal of this effort is to develop an airborne real-time intelligence-gathering and targeting system that can be used to detect concealed, camouflaged, and mobile targets. The multi-INT sensor suite includes high-resolution visible/infrared (EO/IR) dual-band cameras, visible-to-near infrared, short-wave, and long-wave infrared (VNIR/SWIR/LWIR) hyperspectral (HSI) sensors, synthetic aperture radar (SAR), electronics intelligence sensors (ELINT), and off-board networked sensors. Other sensors are also being considered for inclusion in the sensor suite to address unique target detection needs. The purpose of integrating a suite of multi-INT sensors on a single platform is to optimally perform real-time fusion of the onboard sensor streams in order to improve the detection probability and reduce the false alarms that occur in reconnaissance systems that use single sensor types on separate platforms, or use independent target-detection algorithms on multiple sensors. In addition to the integration and fusion of the multi-INT sensors, the NCMIFTI effort is establishing an open systems netcentric architecture that will provide a modular “plug and play” capability for additional system components and provide distributed connectivity to multiple sites for remote system control and exploitation.

Netcentric Architecture: The NCMIFTI system consists of two main subsystems, the control and display stations (CADS) and the airborne sensor/avionics/fusion components. The CADS system was developed to be platform-independent and allows for the reuse of the system software on multiple hardware configurations, depending on mission needs. Already demonstrated hardware configurations range from TAC-4 rack VME RaceWay-UNIX based systems for shipboard installation, to ruggedized HMMWV/P-3 systems, to laptop and desktop PC units (Fig. 5). The input and output interfaces to the CADS systems include various tactical control, imagery, and data RF links, multiple tape and solid state recorder interfaces, and Ethernet/ATM network connectivity, in addition to the operator interface. The NCMIFTI avionics components include the multi-INT sensor systems, the system control and sensor fusion processing electronics, and the airborne communication

links. The imagery format used to exchange image information between system components is the standard National Imagery Transmission Format Standard (NITFS 2.1). The data and control interfaces are handled via copper and fiber-based gigabit Ethernet. For sensor systems that currently do not output standard NITFS imagery in Ethernet packets, the Sensor Link Interface Chassis (SLIC) converts the sensor-specific formats into the NCMIFTI standard format. Figure 6 outlines the netcentric architecture for the avionics and airborne control and display stations. This architecture allows for control and screening of the airborne NCMIFTI sensors and processors via the onboard CADS systems and/or from distributed networked CADS systems that may be remotely located.

Initial P-3 Implementation and Real-time Flight Demonstration: The initial configuration of the NCMIFTI system was demonstrated during P-3 flights over Montana and Georgia in July-August 2003 that exercised the real-time fusion targeting and netcentric dissemination capabilities. The demonstrated sensor suite for these flights included a high-resolution dual-band EO/IR camera similar to the F/A-18 SHARP sensor and two HSI sensors (VNIR and SWIR) (Fig. 6). CDL carried compressed sensor data to the ground. CADS systems at several ground sites (Fort Benning, Georgia; SPAWAR, Charleston, South Carolina, and NRL-DC) (Fig. 7) were interconnected via the Defense Research and Educational Network (DREN) to demonstrate real-time netcentric image screening, exploitation, and dissemination. In addition to the facilities that were outfitted with NRL CADS systems, several other sites (e.g. DISA) were secondary recipients of fused targeting products via classified networks. Figure 8 shows the CADS waterfall and situational awareness screens implemented for simultaneous reception and exploitation of the EO/IR and VNIR HSI imagery transmitted from the P-3 and networked to the various distributed exploitation locations. Also shown are fused targeting products, with the HSI detection cues, from two of the P-3s targeting missions (i.e., camouflaged Cessna aircraft and tagged convoy detection).

Summary and Acknowledgments: The initial flight demonstrations of the NCMIFTI project have shown great promise for real-time airborne multi-INT fusion target detection, exploitation, and dissemination. Significant support for these demonstrations was provided by NRL's Center for Computational Science (networking, DREN connectivity), the Space Dynamics Laboratory (CADS, SLIC joint development), the NRL Flight Support Detachment, Smart Logic, Inc., and Platform Systems, Inc. Future NCMIFTI flight demonstrations with long-range oblique HSI, ELINT, and SAR sensors are planned for 2004.

[Sponsored by OSD]

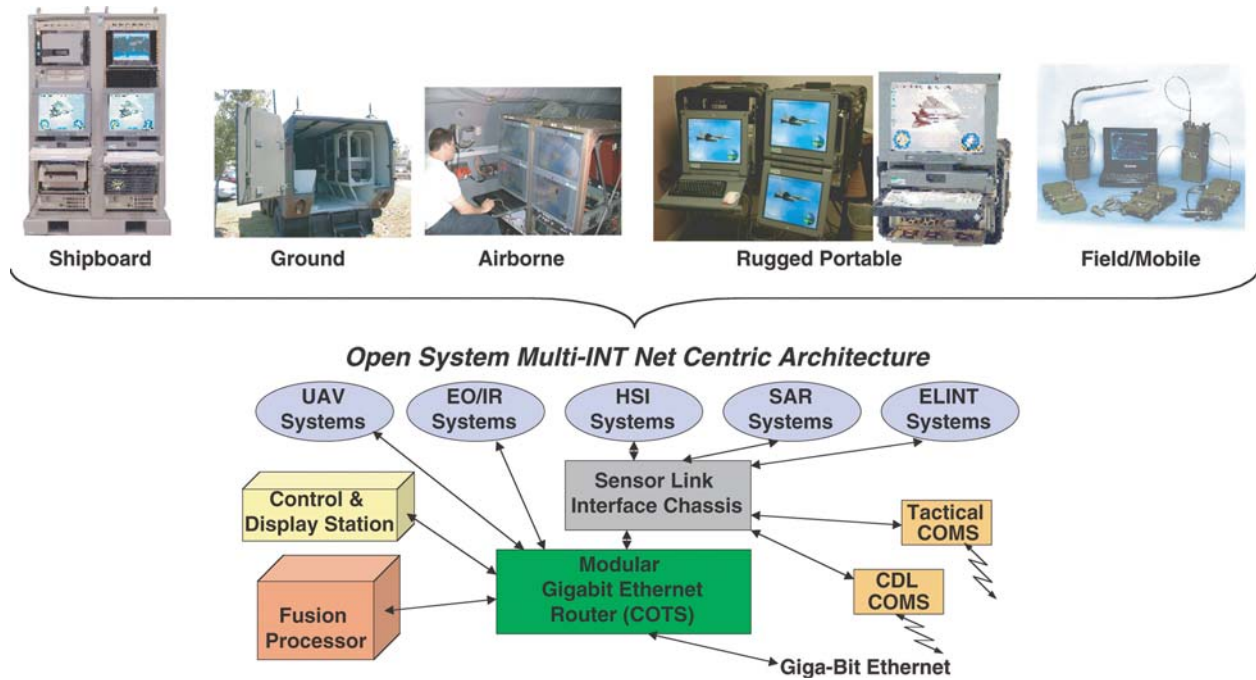


FIGURE 5
Netcentric open system control and display station architecture.

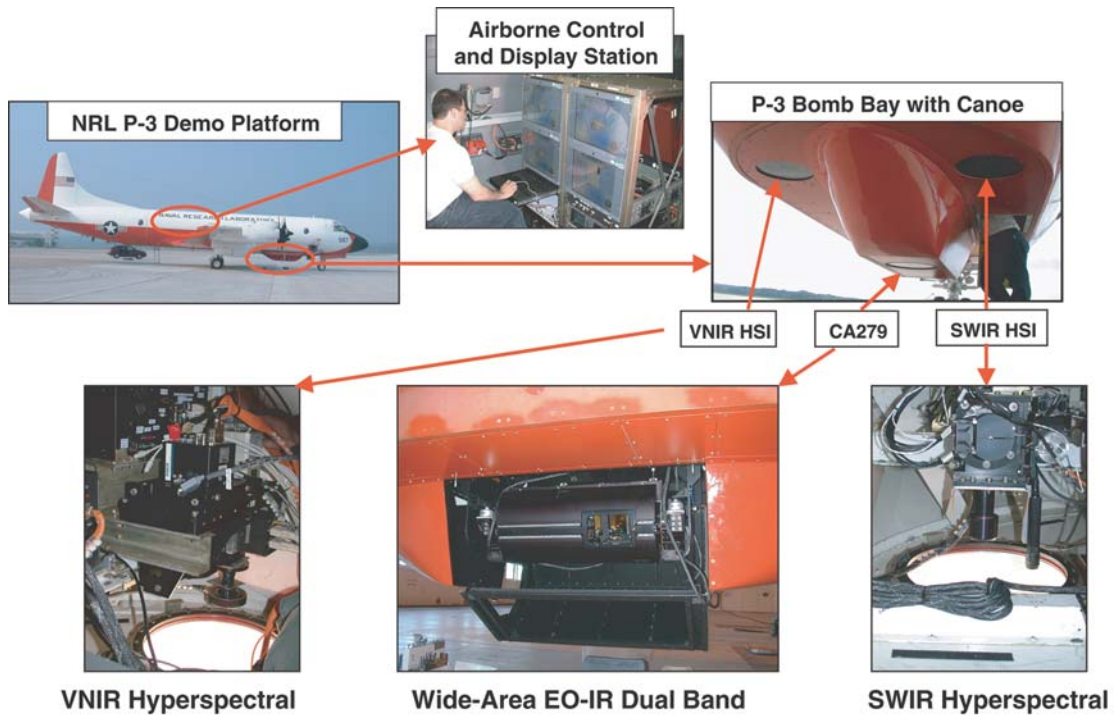


FIGURE 6
August 03 P-3 EO/IR and HSI Payloads—Multi-INT fusion processing for real-time target detection.

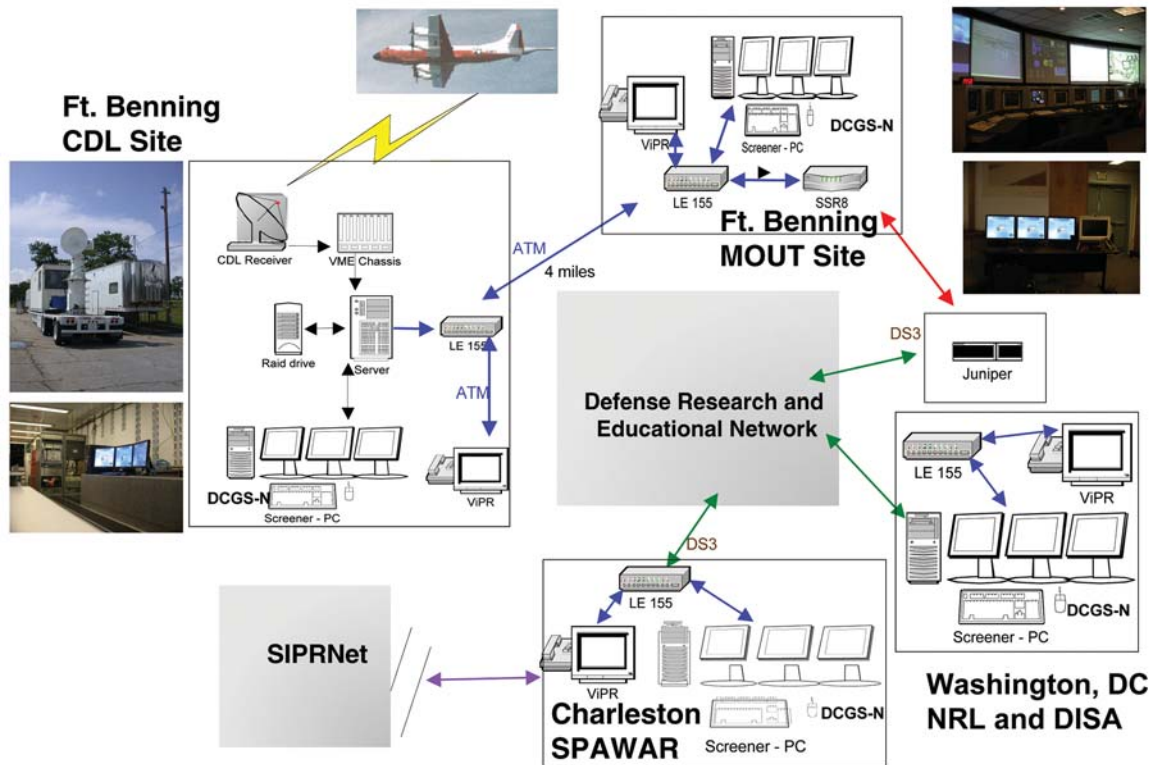


FIGURE 7
Netcentric ground station interconnectivity.

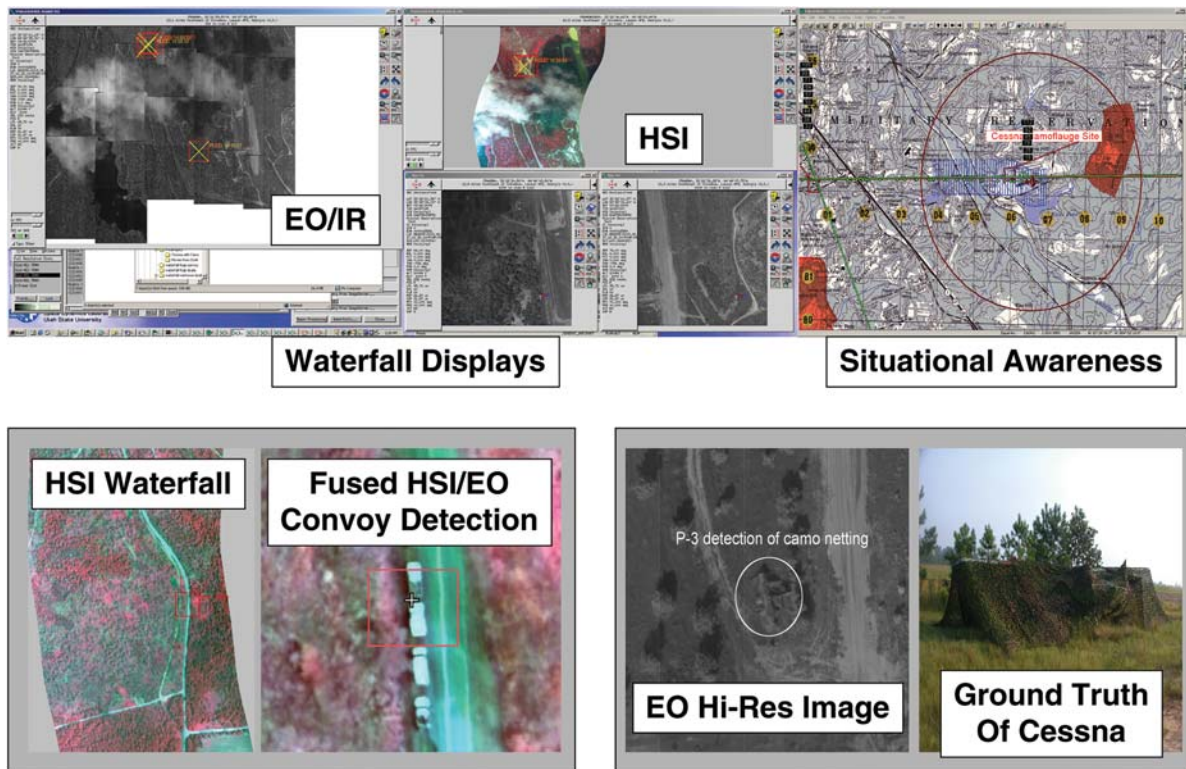


FIGURE 8
Real-time fusion target detection and exploitation.

REAL-TIME EXPLOITATION AND DISSEMINATION OF TACTICAL RECONNAISSANCE IMAGERY DURING OPERATION IRAQI FREEDOM FOR GROUND AND MARITIME OPERATIONS

J.N. Lee, D.C. Linne von Berg, M.D. Duncan,
M.R. Kruer, and R.A. Patten
Optical Sciences Division

Introduction: The technology of reconnaissance, both manned and unmanned, has changed dramatically in the last 15 years. The availability of digital electro-optical cameras has enabled the switch from wet film cameras and enables potential near-real-time transmission of imagery. However, increased focal-plane pixel count and frame rate result in data rates that stress the capability of the highest-bandwidth communication links, even with data compression. Advanced processing hardware and techniques are therefore needed to control data rates and to reduce the timeline for imagery products to reach front-line forces. Such capabilities were demonstrated during Operation Iraqi Freedom (OIF).

Two Reconnaissance Systems: The Navy, in generating strike missions and assessing battle damage, continues to use high-speed, carrier-based, multimission fighter aircraft equipped with reconnaissance pods to rapidly reach target areas, to allow timely retasking, and to obtain up-to-date imagery of large areas under a variety of conditions. In OIF, the Navy used the F-14 wet-film Tactical Airborne Reconnaissance Pod System (TARPS) pod, and also introduced digital reconnaissance systems that offer imaging at other wavelengths, including infrared for day/night operation. The basis for this new Navy capability are two reconnaissance systems developed by NRL—the Full-Capability (F-CAP) version of the Tactical Air Reconnaissance Pod-Completely Digital (TARPS-CD) System¹ for the F-14, and the Shared Airborne Reconnaissance Pod (SHARP) System² for the F-18 Super Hornet. The F-CAP system was deployed with the USS *Harry S. Truman* and Air Wing CVW-3 with F-14 squadron VF-32, while the SHARP system was deployed with the USS *Nimitz* with F-18 squadron VFA-41.

Imagery Upon Demand: During OIF, near-real-time high-resolution images were supplied to ground Special Forces in Northern Iraq using F-CAP capabilities, using the F-14's Fast Tactical Imagery (FTI) radio, the Common Data Link (CDL) capability on the pod and the ship, and other communication channels. This appears to be the first time such forces could obtain “virtually real-time imagery upon demand,” according to unclassified reports. Front-line troops were able to receive targeting-

level imagery without the reported three-to-nine day delay associated with existing image dissemination channels or the set-up times associated with special “stove-piped” dissemination channels from operations centers using imagery obtained from satellites and other aircraft. By using an available voice channel between the F-14 and ground forces, the aircrew used the F-CAP Airborne Image Exploitation System (ARIES)¹ to effect real-time “sensor to shooter” targeting of time-critical targets. ARIES-processed images, along with a voice channel, were transmitted to ground forces equipped with portable FTI receivers. ARIES represents a planned future capability for SHARP.

Crucial Images Transmission: TARPS-CD/F-CAP is a risk-reduction effort for SHARP developed by NRL. Its purpose is to transform the Navy from film to the new digital reconnaissance technologies and demonstrate emerging SHARP capabilities. F-CAP includes a pod built to the SHARP architecture.² It communicates with a carrier-based NRL-built Navy Input station (NAVIS) connected to the ship's CDL. NAVIS receives, displays, manipulates, and exploits imagery and connects to communication channels to disseminate imagery products. The NAVIS ground station has also transitioned into full-rate production as the Navy's Tactical Input Segment (TIS), version 1.5, to support SHARP and other imagery sources. The F-CAP pod is the latest in a series of TARPS-CD technology prototypes that have been evaluated during four Fleet exercises and deployments. The earlier carrier-based F-14 exercises with the TARPS-CD pod demonstrated the system's capability as an organic asset for the carrier group commander to perform reconnaissance and battle damage assessment, to rapidly capture imagery on wide-area missions, and to supply imagery to the carrier in near-real time using the high-bandwidth (>200 Mbps) CDL. However, the limited range and availability of CDL, coupled with the crucial need for rapid image exploitation, established the need to transmit urgently needed images to the user, even at reduced bandwidths. This can be accomplished if the F-14 aircrew is able to select the crucial images and transmit them over the FTI system. The NRL-developed ARIES allows the back-seater (the Radar Intercept Officer/ RIO) aboard the F-14 to use an analog video display to view and select from a stream of still images from the reconnaissance sensor (a very sophisticated and fast high-resolution digital camera). NRL built a low-bandwidth interface to the pod and a cockpit control console, so the RIO can roam, pan, and zoom in on selected images on the back-seat display to highlight target areas for digital capture and transmission by FTI. ARIES overlays key information on the video image, such as latitude and longitude. High-speed computation is done within the pod payload, while low-bandwidth commands and analog

imagery are communicated between pod and cockpit. This architecture could also be used for remote operations with low-bandwidth links from other locations, e.g., from the ground for unmanned aerial vehicle (UAV) payloads.

Event-marked Frames: Figure 9 shows an example of ARIES-transmitted imagery for relocatable targets. During the deployment of the USS *Truman*, F-14 aircrews used the high-coverage rate of F-CAP to perform real-time wide-area maritime reconnaissance and exploitation in the cockpit. Target frames, i.e., images containing a ship, can be “event-marked” by the RIO and re-displayed later. Figure 9(a) shows an array of seven event-marked frames on the RIO’s display. The RIO then zooms into one frame to the desired resolution (Fig. 9(b), with the white dot in the checkerboard indicating the selected frame). The overlay provides the latitude and longitude



(a) Waterfall display of event-marked frames



(b) Zoomed view of upper-left frame of Fig. 9(a)

FIGURE 9
ARIES transmitted imagery.

of the crosshair position, and the notation DEC: 1:4 in Fig. 9(b) indicates that further zoom is available in the video display (1/4 of full resolution is shown). The ARIES software is capable of displaying a wide range of user-selected system parameters as overlays for the final imagery product.

In OIF, the TARPS-CD F-CAP system validated the use of fully digital technology as a superior replacement for wet-film based systems and provided risk reduction for the emerging capabilities of the Navy’s SHARP System for the F-18.

Acknowledgments: The TARPS-CD F-CAP and SHARP prototype developments were led by NRL’s Optical Sciences Division. F-CAP Fleet deployments were managed by NAVAIR PMA-241, and SHARP developments were transitioned to PMA-265. Other Team members were: Recon Optical, Inc.; Smart Logic, Inc.; V-Systems, Inc.; SFA, Inc.; DCS Corp.; Space Dynamics Laboratory; Geologics Corp.; and Raytheon Technical Services Company.

[Sponsored by NAVAIR]

References

- ¹J.N. Lee, D.C. Linne von Berg, M.R. Kruer, and M.D. Duncan, “Demonstration of a High-Rate Tactical Reconnaissance System with Real-time Airborne Image Exploitation,” *2003 NRL Review*, pp. 151-153.
- ²M.D. Duncan, M.R. Kruer, D.C. Linne von Berg, R.A. Patten, and J.N. Lee, “Report on the SHARP Prototype Effort,” NRL/FR-MM/5633-01-10,015, December 17, 2001.

VOLUME SENSOR FOR SHIPBOARD DAMAGE CONTROL

S.L. Rose-Pehrsson,¹ J.C. Owrutsky,¹ D.T. Gottuk,² D.A. Steinhurst,³ C.P. Minor,³ J.P. Farley,¹ and F.W. Williams¹

¹*Chemistry Division*

²*Hughes Associates, Inc.*

³*Nova Research, Inc.*

Introduction: Situational awareness is an important aspect of Damage Control (DC) that requires novel approaches to meet the demands of the Navy environment. Multicriteria point-sensor arrays comprised of smoke detectors and chemical sensors have demonstrated improved response times and superior nuisance source rejection compared to individual point sensors. However, these fire detection systems depend on diffusion of the particles and chemical species to the detector, which results in slow responses to smoldering fires. In addition,

they have difficulty discriminating fire-like nuisance sources, such as welding, grinding steel, and cutting with a torch. Surveillance cameras in ship spaces provide a visible image that can be used to confirm the presence of fire or nuisance sources. Some fire detection companies are investigating video image detection (VID) using machine vision for fire detection in large facilities such as warehouses and tunnels. VID is a new and very attractive approach to fire detection because of the ability to see the entire compartment or volume of a space (i.e., volume sensor). The VID system provides rapid fire detection without requiring the fire effluents to travel to the detector.

Using a multisensory approach, the Naval Research Laboratory is developing a new detection capability for DC in the shipboard environment. The Advanced Volume Sensor Project is an important element of the ONR Future Naval Capabilities program, Advanced Damage

Countermeasures. This program seeks to develop and demonstrate improved DC capabilities to include anticipatory DC response mechanisms to help ensure that the recoverability performance goals for the CVN21 and the DD(X) family of ships can be met with established manning levels and systems. Figure 10 shows the overall concept. Advanced Volume Sensor is a multiyear project to identify, evaluate, and adapt video image detection technologies for improved situational awareness and damage control assessment onboard Navy ships. Various spectral and acoustic signatures are being used in combination with video images and image recognition technologies for the development of a sensor system that is able to provide a broad range of situational awareness for a space. The objective of this project is to develop an affordable, real-time, remote detection system that will identify shipboard DC conditions and provide an alarm for events such as fire, explosions, pipe ruptures, and flooding level.

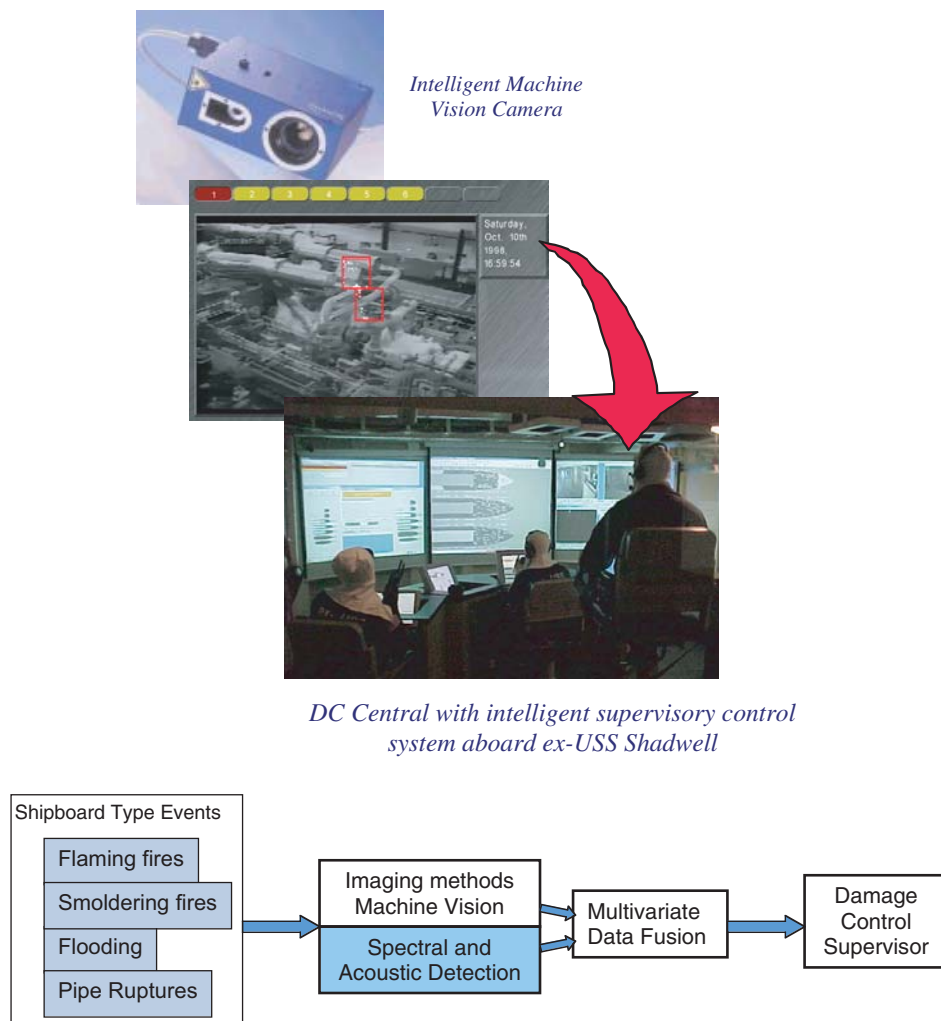


FIGURE 10
Volume sensor concept.

The approach takes advantage of existing and emerging technology in the rapidly growing fields of optics, acoustics, and computer processing. This technology uses conventional surveillance cameras, which are currently being incorporated into new ship designs, and therefore will provide multiple system functions with the same hardware.

Volume Sensor Development: Three commercial video-based fire detection systems have been evaluated onboard the ex-USS *Shadwell*, the Naval Research Laboratory's full-scale fire research facility in Mobile, Alabama. The commercial VID systems were evaluated to assess the state of the art and to determine suitability for shipboard applications.¹ Test results indicated that the VID systems using smoke alarm algorithms could provide equivalent or improved fire detection compared to point-type smoke detectors for most of the conditions evaluated. However, improvements are necessary for robust detection in the small, cluttered spaces characteristic of the Navy environment.^{2,3} For example, these systems cannot detect a fire obscured from the view of the camera.

Methods to enhance the performance of VID for the Navy application and expand the capabilities, such as to include detection of flooding and pipe ruptures, are being developed. The primary areas being investigated are (1) visible image video with improved machine vision algorithms, (2) augmenting visible image video with long wavelength video and spectral sensors, (3) the addition of acoustic sensors, and (4) multivariate algorithm development. The spectral-based component is focused on optical techniques in spectral regions outside the visible region, or otherwise using methods that emphasize spectral discrimination in conjunction with the visible VID techniques. Acoustic signatures are being evaluated for enhanced discrimination of DC events, particularly flooding and pipe ruptures. Advanced algorithms are being applied to the video images to identify the alarm conditions. Multivariate data analysis is being explored to integrate the sensor components and identify a variety of DC events. A novel approach to video database retrieval and archival methods was developed. All of these methods are being evaluated using DC events including fire, flooding and pipe ruptures. The successful components are being integrated into a breadboard system for further optimization of the detection methods. Development of the machine vision and multivariate data analysis methods will be a major emphasis of future work. The intention is to provide a more comprehensive overall volume sensor than would result from video detection alone.

Two distinct approaches to optical detection outside the visible are being pursued.^{4,5} These are long wavelength, nightvision cameras, which provide some degree of both spatial and spectral resolution or discrimination, and single or multiple element narrow spectral band de-

ectors, which are spectrally but not spatially resolved and operate with a wide field of view at specific wavelengths ranging from the mid infrared to the ultraviolet. The primary advantages of long wavelength imaging are the higher contrast for hot objects and more effective detection of reflected flame emission compared to images obtained from cameras operating in the visible region. Our approach exploits the long wavelength response of standard charge coupled device (CCD) arrays used in many cameras (e.g., camcorders and surveillance cameras). A long pass filter transmits light with wavelengths longer than a cutoff, typically in the range 700-900 nm. This increases the contrast for fire, flame, and hot objects, and suppresses the normal video images of the space, thereby effectively providing some degree of thermal imaging. There is more emission from hot objects in this spectral region than in the visible (<600 nm). Testing has demonstrated detection of objects heated to 400°C or higher.

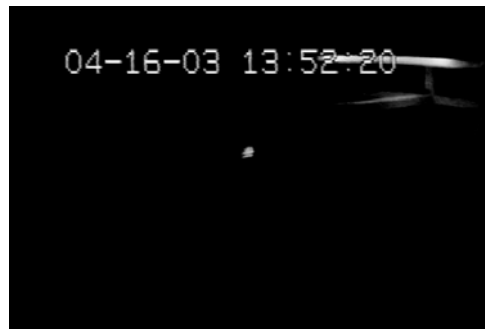
To our knowledge, this is the first use of nightvision videos for indoor fire detection. The approach is a compromise between expensive, spectrally discriminating cameras operating in the mid-infrared (IR) and inexpensive, thermally indifferent visible cameras. Nightvision is particularly useful in several respects: providing high-contrast images and therefore straightforward line-of-sight detection for flames and hot objects, where the latter would include bulkheads that have been heated by obstructed fires (Fig. 11) and identifying obstructed fire and flame based on reflected light (Fig. 12). A simple luminosity-based algorithm has been developed and used to evaluate camera/filter combinations for fire, smoke and nuisance event detection.⁶ The graphical user interface for this algorithm is shown in Fig. 12.

Conclusions: New capabilities for situational awareness for shipboard DC are being developed. Spectral and acoustic signatures combined with video images and machine vision provide event recognition beyond fire detection to include flooding, and pipe ruptures. A state-of-the-art database retrieval and archival method has been developed to facilitate algorithm development and optimization. Machine-vision algorithms with faster responses to fires and fewer false alarms than currently available have been demonstrated. Fire detection has been improved through the development of a low-cost method for long wavelength imaging. Long pass filters applied to the long wavelength CCD response of surveillance cameras increases the contrast to flames and hot objects and extends fire event recognition to fires outside of the field of view of the camera and behind bulkheads. Real-time fire detection with these cameras is possible by using a recently developed algorithm based on luminosity. These techniques have applications beyond shipboard use and could be beneficial in monitoring facilities for homeland security.

[Sponsored by ONR]



(a) Nightvision camera at start of test



(b) Nightvision camera 00:04:39 into test



(c) Nightvision camera 00:12:17 into test



(d) Nightvision camera 00:20:43 into test, effectively the end of the test

FIGURE 11

Long wavelength camera video (nightvision camera) for fire behind the bulkhead. The still images show the compartment before test ignition and at three times during the test.

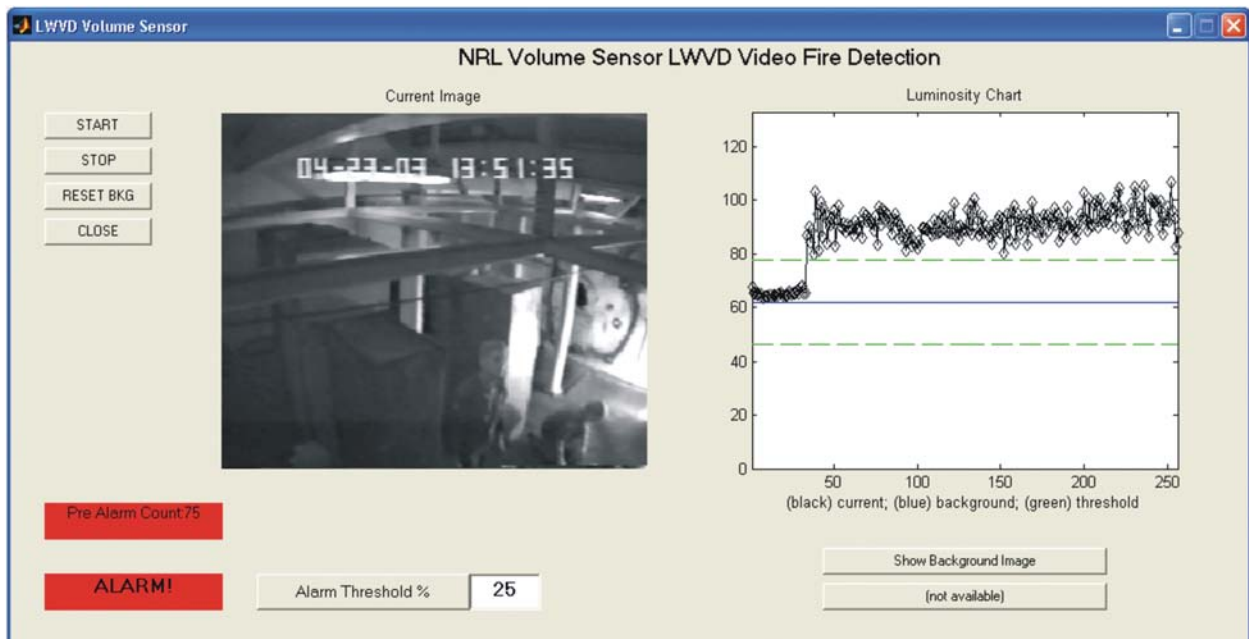


FIGURE 12

NRL graphical user interface for nightvision cameras using the luminosity algorithm for a fire outside the view of the camera.

References

- ¹D.T. Gottuk, M.A. Harrison, J.L. Scheffey, S.L. Rose-Pehrsson, F.W. Williams, and J.P. Farley, "An Initial Evaluation of Video-Based Fire Detection Technologies," NRL Letter Report 6180/0457, December 16, 2002.
- ²M.A. Harrison, D.T. Gottuk, S.L. Rose-Pehrsson, J.C. Owrutsky, F.W. Williams, and J.P. Farley, "Video Image Detection (VID) Systems and Fire Detection Technologies: Preliminary Results from the Magazine Detection System Response Tests," NRL Letter Report 6180/0262, July 21, 2003.
- ³D.T. Gottuk, M.A. Harrison, S.L. Rose-Pehrsson, J.C. Owrutsky, J.P. Farley, and F.W. Williams, "Shipboard Evaluation of Fire Detection Technologies for Volume Sensor Development: Preliminary Results," NRL Letter Report 6180/0282, August 25, 2003.
- ⁴J.C. Owrutsky, D.A. Steinhurst, H.H. Nelson, and F.W. Williams, "Spectral Based Volume Sensor Component," NRL/MR/6110-03-8694, July 30, 2003.
- ⁵D.A. Steinhurst, J.C. Owrutsky, S.L. Rose-Pehrsson, D.T. Gottuk, F.W. Williams, and J.P. Farley, "Spectral-Based Volume Sensor Testbed VS1 Test Series Results ex-USS *Shadwell*, April 20-25, 2003," NRL Letter Report 6110/075, June 27, 2003.
- ⁶D.A. Steinhurst, C.P. Minor, J.C. Owrutsky, S.L. Rose-Pehrsson, D.T. Gottuk, F.W. Williams, and J.P. Farley, "Long Wavelength Video-Based Event Detection, Preliminary Results from the CVNX and VS1 Test Series, ex-USS *Shadwell*, April 7-25, 2003," NRL/MR/6110-03-8733, December 31, 2003. •

CONTROL ALGORITHMS FOR UUV TEAMS USING ACOUSTIC COMMUNICATIONS

P. McDowell and B. Bourgeois
Marine Geosciences Division

Introduction: Interest in the use of multiple unmanned underwater vehicles (UUVs) for military and commercial uses is growing because of the potential benefits to underwater operations such as searching, inspection, and surveying. NRL researchers are developing control, communications, and positioning methods to enable the use of multiple UUV formations. In the undersea environment, traditional methods of communication and navigation (radio and GPS) are ineffective. Properties of seawater make control of UUVs very difficult. Because inertial-based vessel positioning systems typically yield position error growth on the order of 1% of the distance traveled,¹ they are not adequate for formation maneuvering. The only viable alternative underwater for communications and positioning is acoustics, but these systems yield fairly short ranges and very low bandwidths.² A promising approach, which is the focus of this work, is vessel relative positioning and navigation using combined

communication/position acoustic systems. Formation maneuvering based on inter-vessel positioning and navigation has distinct advantages in that it can reduce or eliminate the requirement for pre-deployed positioning systems, and it can be used to increase the sensor footprint in searching and surveying tasks.

To control multiple vehicle formations, classic logic, behavior-based, and neural network controllers have been developed. The formations are fashioned after those observed in nature, most notably lines of ducks and caterpillars. The classic logic control systems used were modeled after Braitenburg machines and served as a baseline capability for comparison. Neural network controllers, which hold the promise of real-time adaptability, were grown using a genetic algorithm and in situ sensor data. Both computer simulations and tests using mobile land robots equipped with frequency multiplexed acoustic communication systems have demonstrated the feasibility of these approaches. Several real-world problems have been tackled, including acoustic sensor directivity and reverberation.

The algorithms in this work are based on the leader/follower paradigm, commonly used in military operations, in which all of the robots in the formation position themselves relative to an assigned lead robot. The overall lead robot is typically controlled by an operator or programmed to do waypoint following. Figure 1 is a conceptual view of a line formation. In this figure, the green robot, whose identification (ID) is 0, is the lead robot. It is followed by the robot whose ID is 1, which is in turn followed by the robot whose ID is 2, and so on. In this illustration, neural networks control the follower robots while an operator maneuvers the lead robot.

Figure 13: The system operates in a passive manner, meaning that the robots do not exchange position or bearing and range information. Instead, each robot, except the leader, steers itself toward an acoustic chirp emitted from the robot in front of it. For example, the leader chirps at frequency range *A*, the robot directly behind it steers in the direction that it perceives is the source of the chirp in frequency range *A*, and at the same time chirps

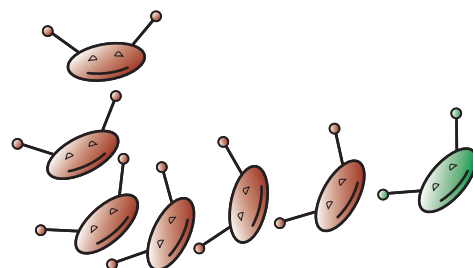


FIGURE 13
Robot line. The green robot is controlled manually. Using their sensors and controllers, the other robots follow.

in frequency range B . The robot behind it steers towards the source of frequency range B and so on.

Figure 14: This figure shows robots in laboratory following each other. As in Fig. 13, the lead robot is controlled manually, and the others follow using sensors and control algorithms. Using the classic logic method, the robot simply steers in the direction of the strongest signal. This method is robust and works well in both simulation and laboratory settings, but it has problems when the source is directly in front or behind. To alleviate this problem, the behavior routine was developed. It alternates between search, seek, and follow modes, depending on whether the signal is getting more or less intense over time. In simulation it works well, but because of reverberation and multipath problems in the laboratory, it is less effective (as illustrated in Fig. 15). The neural network approach relies on a feed-forward neural network trained in a teaching mode to detect the signal direction in relation to the robot. This same network is then used as a controller. Its performance is similar to that of the classic logic technique in both simulation and in laboratory testing.

Figure 15: In concept, this work has shown that formation maneuvering using acoustic sensors is possible in both a simulated environment and in the physical world of the laboratory. It has also shown that the structure of the formation can remain viable without using a centralized controller, or by using external infrastructure-based communications. Since the communications between the robots uses very low bandwidth acoustic methods, this work is relevant to UUV team operations.

[Sponsored by ONR]

References

- ¹J. Kinsey and L. Whitcomb, "Preliminary Experiments with a Calibration Technique for Gyro and Doppler Navigation Sensors for Precision Underwater Navigation," *Proceedings of the 13th International Symposium on Unmanned Untethered Submersible Technology*, Durham, NH, August 2003.
- ²D.B. Kilfoyle and A.B. Baggeroer, "The State of Art in Underwater Acoustic Telemetry," *IEEE J. Ocean. Eng.* 25(1), 4-27 (2000). ●

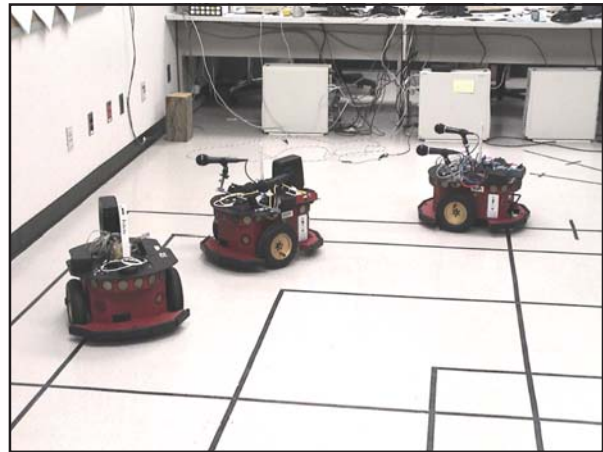


FIGURE 14
A three-robot following test. The lead robot is being operated manually while the second and third robots are using their microphones to track the robots in front of them.

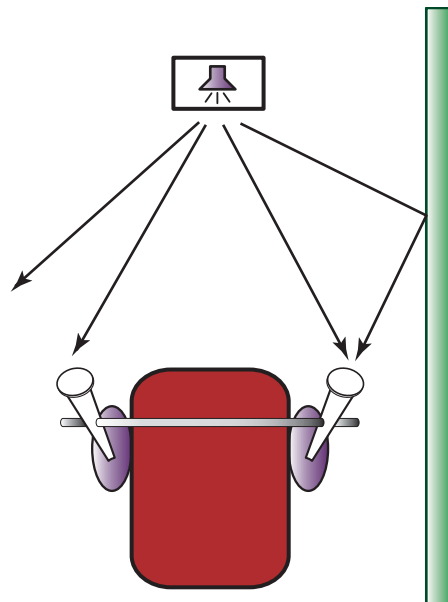
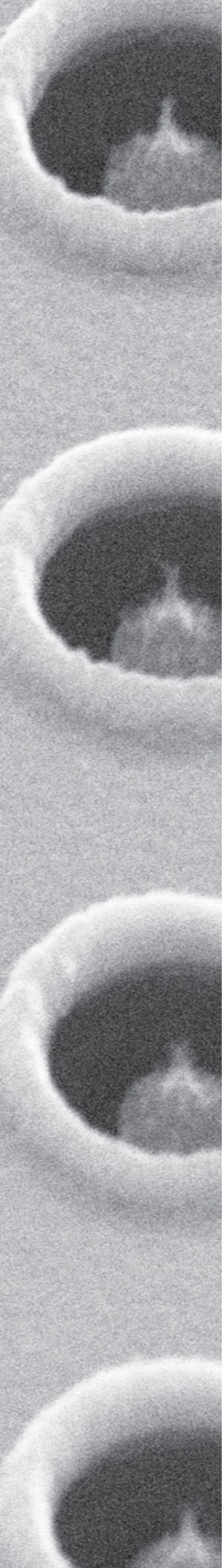


FIGURE 15
The wall is reflecting sound back to the robot that would normally be radiated elsewhere. In this case, the robot may read a higher intensity value on its right side, causing it to errantly turn toward the wall.

CARBON NANOTUBE FIELD EMITTER ARRAY

An array of electron sources consisting of vertically aligned carbon nanotubes grown by chemical vapor deposition on the tops of microgated silicon posts. These NRL-invented nanotube “cold-cathode” devices have demonstrated very low voltage, high current density, and exceptional robustness, enabling many potential applications such as radio frequency amplifiers for communication, electric propulsion for microsattellites, and portable X-ray sources for field medical and security diagnostics.



153 Qualification of Copper Water Heat Pipes for Space Application
K. Cheung

156 GelMan: A Physical Model for Measuring the Response to Blast
K.E. Simmonds, P. Matic, M. Chase, and A. Leung

158 Rapid Prototyping of Conformal Antenna Structures
*A. Piqué, R.C.Y. Auyeung, M.W. Nurnberger, D.J. Wendland, C.B. Arnold,
A.R. Abbott, and L.C. Schuette*

160 Carbon Nanotube Networks: A New Electronic Material
E.S. Snow, J. Novak, M.D. Lay, and E.J.S Houser

QUALIFICATION OF COPPER WATER HEAT PIPES FOR SPACE APPLICATION

K. Cheung
Spacecraft Engineering Department

Introduction: Copper water heat pipes have been extensively used for electronic cooling in laptop computers for several years. Despite its acceptance in terrestrial applications, copper water heat pipes have very limited space flight heritage; publications on space application of copper water heat pipe are rare. The Naval Center for Space Technology (NCST) has implemented this technology in its recently launched low earth orbit (LEO) payload (WindSat) to provide temperature control for its low noise amplifiers (LNAs). The copper water heat pipe is 4 mm in outside diameter and 305 mm in length. Its primary function is to transport heat from the LNAs to the feedbench radiators, where heat rejects into the deep space. As part of the risk mitigation process, a flight qualification test program was established by NCST. This article describes the methodology of the test program, test results, and selected flight data.

Test Program Overview: Figure 1 summarizes the overall sequence of this qualification test program. All of the tests were performed at the component level. These tests were designed to demonstrate that the copper water heat pipes are able to meet the heat transfer performance required by the WindSat program, and that they can withstand the extreme environments experienced during ascent and on-orbit operation. The qualification tests also validated the initial screening technique and procedure,

which served as a standard component-level acceptance test for the flight units.

Initial Screening Test: All heat pipes were visually inspected for dents, cracks, and susceptible solder/epoxy joints. Then, the heat pipes were tested in a group of 20 in a thermal vacuum chamber. End-to-end (evaporator-to-condenser) thermal conductance of each heat pipe was evaluated with the applied heat load and the temperature difference measured. A predetermined heat load (0.75 W) was applied on one end of the heat pipe, and the other end of the heat pipe was attached to a heat sink controlled at 10 °C. T-type thermocouples were placed along the heat pipes to monitor their temperatures. A conductance value between 0.15 W/C and 0.35 W/C is considered acceptable. This is derived from system-level thermal analysis as a conductance requirement to remove waste heat from the LNAs and keep them within their temperature limits (0 °C to 40 °C). After the conductance measurement, the heat pipes were frozen to -30 °C for about 2 h, and then thawed by applying a heat load of 0.75 W on the evaporator end of each heat pipe. Another conductance measurement was then performed to determine whether any degradation in performance resulted from freezing the heat pipe. Statistically, about 50% of the heat pipes passed the initial screening. Most of the failed heat pipes had thermal conductance values fall outside the required range. It is realized that the manufacturing process of these copper water heat pipes is not optimized for flight build quality. The differences in thermal conductance among the heat pipes may suggest inconsistency in the amount of working fluid charged and the presence of noncondensable gas (NCG).

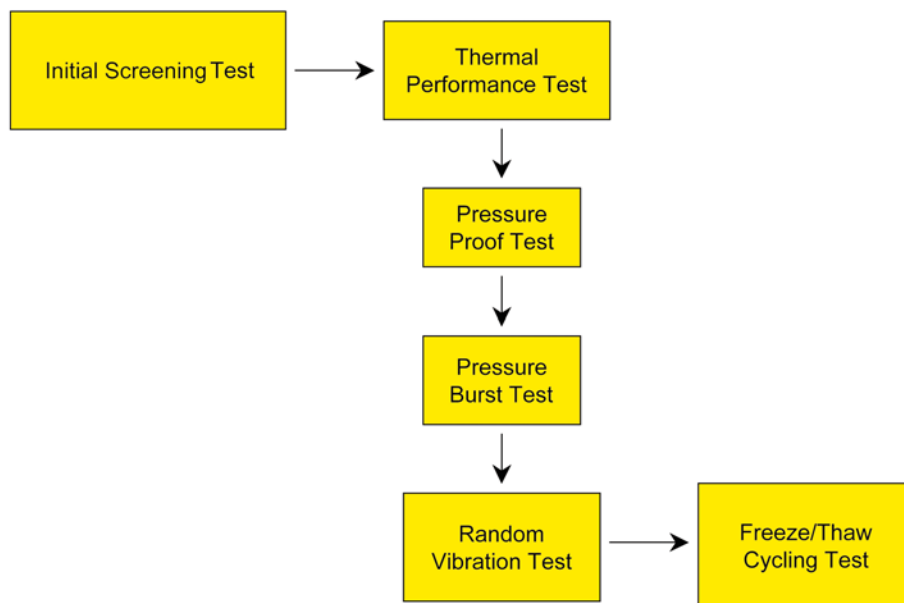


FIGURE 1
Overview of heat pipe qualification test program.

Thermal Performance Test: The purpose of the thermal performance test was to verify heat transport capability and overall thermal conductance of the copper water heat pipe to meet program requirement. In order to provide adequate temperature control for the LNAs, the copper water heat pipe must transport a 0.75 W heat load with an overall thermal conductance between 0.15 W/C and 0.35 W/C. Five heat pipes were selected from the flight lot for this test. They were tested at two sink temperatures (10 °C and 30 °C), and three heat load levels (0.5 W, 0.75 W, and 1.0 W). The heat pipes were oriented vertically, with the condenser end at the bottom. Test results demonstrated that all five heat pipes operated successfully and met the heat transport and thermal conductance requirements.

It is realized that moderate bending of heat pipe is needed for this flight application. Therefore, the second part of this test was to demonstrate that the copper water heat pipe can tolerate moderate bending. The same five qualifying heat pipes were bent, with two 90-deg bends in the middle. The bend radius is about 0.5 in. Thermal performance test was then repeated. Test data did not indicate any degradation in heat transport capability or overall thermal conductance as a result of the bending.

Pressure Proof Test: After the thermal performance test, the same qualifying heat pipes were tested to verify the pressure containment integrity. For the pressure proof test, internal pressures of the heat pipes were raised to two times the maximum design pressure (MDP) by external heating. The MDP for current applications is 47.4 kPa. Upon completion, the thermal performance test was repeated. Test results did not show any degradation in thermal conductance and heat transport performance. In addition, dimensional measurements were made at controlled locations along the heat pipes both before and after the pressure proof test. No significant deformation was found on the controlled locations.

Pressure Burst Test: The purpose of the pressure burst test was to ensure that the heat pipe would not rupture at four times the MDP. Two new heat pipes in straight configuration were selected for this test. Similar to the pressure proof test, the internal pressure of the heat pipe was raised by external heating. Neither heat pipe burst when they reached four times the MDP.

Three-Axis Random Vibration Test: The objective of this test was to verify that the design and workmanship of the heat pipe was adequate to survive launch vibration loads. Both straight and bend configurations were tested. The heat pipe was assembled on to a test fixture, which allowed one end of the heat pipe to be rigidly fixed while the other end was attached to a cantilevered beam having a natural frequency of approximately 60 Hz. The intent of this test setup was to expose the beam

to a conservative simulation of flight-like loading. A three-axis accelerometer was used to measure the response of the cantilevered beam. To document any changes in heat pipe performance, thermal conductance and heat transport capability were measured before and after the random vibration test. All qualifying heat pipe units passed the random vibration test. No physical damage or thermal performance degradation was found on the heat pipes.

Freeze/Thaw Cycling Test: The objective of this test was to determine the survivability of copper water heat pipe under repetitive freeze/thaw cycles. This is an environment that may be seen during flight operation, particularly in the safe hold mode. Five heat pipes were subjected to 100 freeze/thaw cycles, which has been determined to be four times the expected number of freezing that may occur throughout ground operations and flight mission. During the freeze/thaw cycles, the evaporator end of the heat pipe was kept between 3 °C to 11 °C, which simulates the thermostatically controlled heater operation during flight operation. All heat pipes were tested vertically, with the condenser end at the bottom. Figure 2 shows the overall thermal conductance (G) measured between cycles for the five heat pipes tested. It also provides the state of health of the heat pipes throughout the test. Two of the five heat pipes failed after 60 freeze/thaw cycles. Thermal conductance of the failed heat pipe significantly deteriorated. Figure 2 also shows damage at the condenser end of heat pipe due to repetitive freezing and thawing. Frozen water expanded and weakened the copper shell at each cycle until it ruptured. Although the remaining three heat pipes did not fail, similar deformation was found at the condenser end. It is concluded that the copper water heat pipe can only tolerate freezing to some extent. It is not meant to be used in a situation in which the system is routinely exposed below freezing temperature. To minimize such risk, auxiliary heaters were added to the heat pipe system to prevent freezing.

Conclusions: Copper water heat pipe was flight qualified at NRL for the WindSat program. Thermal performance and structural integrity of the heat pipes were demonstrated to satisfy program requirement. Flight temperature data from the last 10 months since launch indicates that the heat pipe system operates reliably without any anomaly. Figure 3 also shows that all 22 LNAs are well within the 0 °C to 40 °C temperature requirement. Temperature gradients among the LNAs are able to keep within 5C throughout the seasons.

Acknowledgments: The author expresses his gratitude to the WindSat team who participated in various parts of this test program.

[Sponsored by ONR]

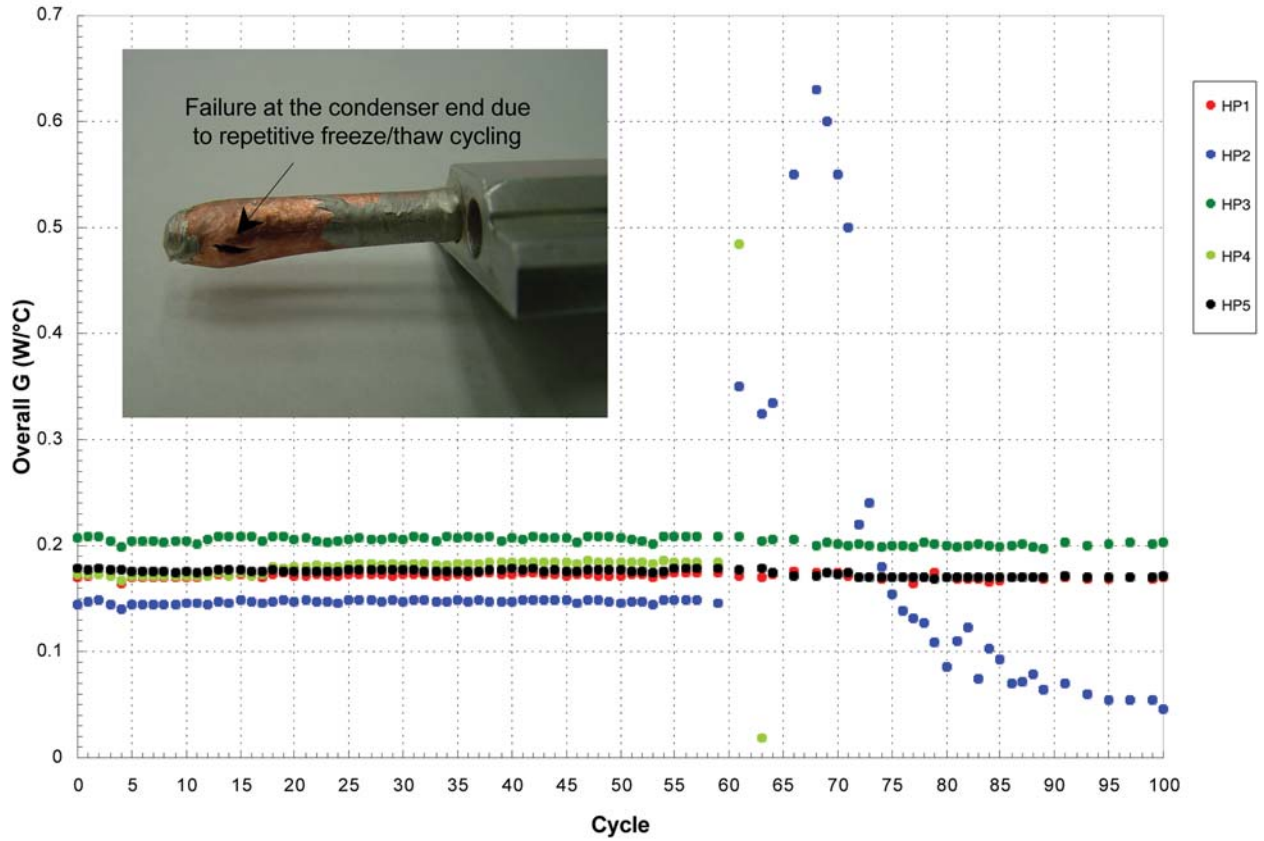


FIGURE 2
Overall thermal conductance measured between freeze/thaw cycles.

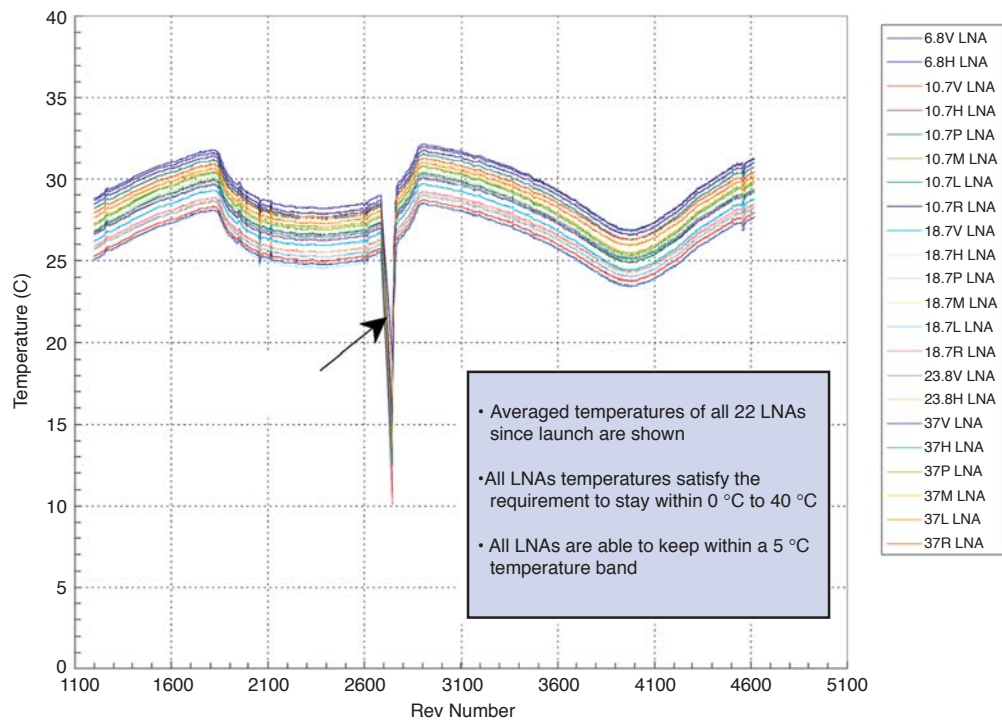


FIGURE 3
On-orbit LNA temperature data.

GELMAN: A PHYSICAL MODEL FOR MEASURING THE RESPONSE TO BLAST

K.E. Simmonds and P. Matic
Materials Science and Technology Division
M. Chase and A. Leung
NOVA Research, Inc.

Introduction: On the battlefield, ground forces are at great risk from nonpenetrating blunt trauma forces and blast dynamics that may cause injury to vital organs. The biodynamics describing the mechanisms of these injuries is not well understood. The objective of NRL's research is to develop tissue surrogate materials that simulate the mechanical and acoustical properties of biological tissues. These are then assembled into an experimental test system of the human thorax, called "GelMan," for assessing blunt forces and blast dynamics. With accurate surrogate systems, we can determine the manner in which the blast wave interacts with the thorax and any protective equipment worn, as well as how distinct pressure time histories and strain rates produce loads on tissues. Beyond the obvious military applications, potential civilian applications include understanding automobile crash injuries, nonlethal projectiles used by law enforcement personnel, and the performance of blast-resistant office structures for protection against terrorist attacks.

GelMan Thoracic Model: The NRL Multifunctional Materials Branch has developed, in coordination with Office of Naval Research (ONR) Medical S&T, the GelMan thoracic model that is instrumented for studying the biodynamics of blunt force trauma. The main objective of this research is to develop a surrogate model with more-accurate material properties and geometries than current thoracic models. One focus is to develop materi-

als that duplicate the acoustical and mechanical responses of biological tissues. By using modified ordnance gelatin, tissue simulant formulations have been developed that have the necessary acoustical and mechanical bulk properties for the human lungs and heart. Figure 4(a) shows the stress/strain relationship measured for the surrogate lung material, actual human lung tissue, and ordnance gelatin. Molds of standard lungs and the heart are used to make anatomically correct organs (Fig. 4(b)) used in the GelMan model.

Impact Experiments: Experimental and finite-element analysis was applied to study the dynamic response of GelMan to low velocity impacts. The experiment was designed to relate impactor velocity, size, and associated frequencies to material damage. The experiment measured displacements, wave propagations, and stress distribution by using embedded accelerometers, pressure sensors, and photoelastic techniques. These measurements provided the basis for understanding the GelMan response to subsequent exposures to vibrations, shock tube pressure pulses, and blasts.

A GelMan finite-element model consisting of cylindrical lungs and surrounding tissue was constructed. The computational model predicted surface and internal displacements as well as stress field distributions similar to those found in experimental drop tests using photoelastic visualization techniques. This computational model will be used for developing and understanding more complex thoracic models.

Shaker Table and Shock Tube Experiments: With the use of the Spacecraft Engineering Division's vibration/shaker table at NRL (Fig. 5(a)), tests were performed on a GelMan with constant peak accelerations of 0.25, 0.50, and 1.00 g, and frequencies from 5 Hz to 1 kHz. In the frequency domain, resonance peaks of accel-

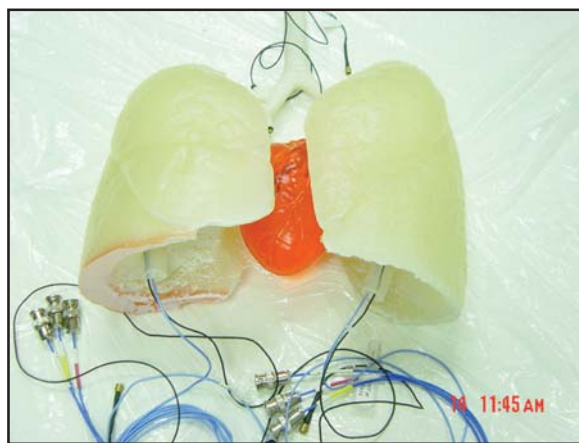
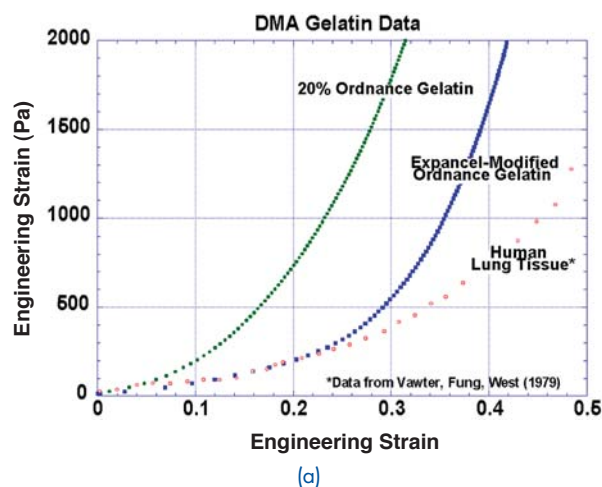


FIGURE 4
(a) Modified gelatin stress/strain properties designed to match lung tissue properties up to 24% strain, which covers the range of interest for lung damage. (b) Instrumented anatomically shaped lung and heart surrogates.

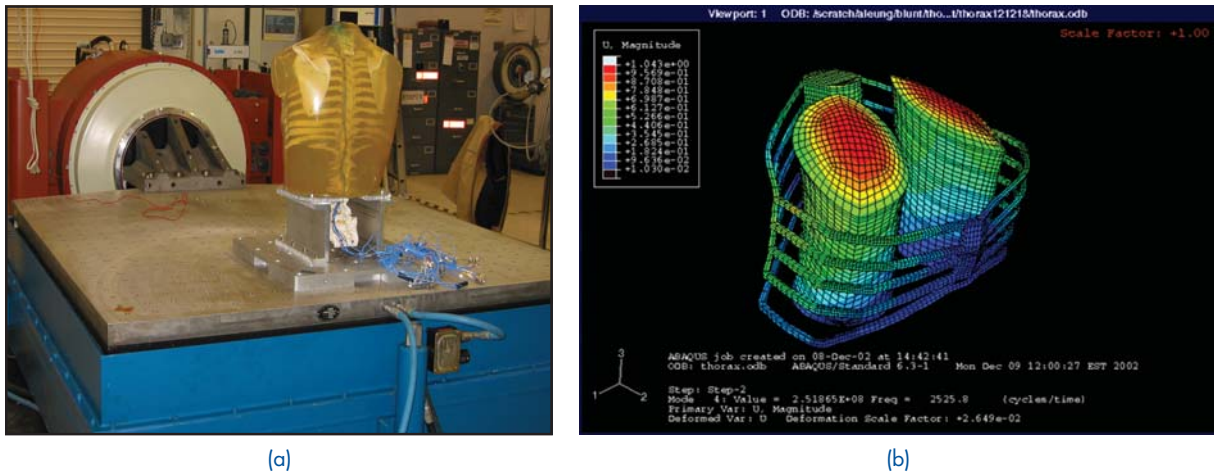


FIGURE 5 (a) Thoracic model during vibration mechanical testing. (b) Finite-element modeling of thoracic model on shaker table.

eration and pressures for the critical components of the complex system were measured for the first four modes of vibrations. The GelMan system was also subjected to dynamic pressure pulse conditions using the shock tube facility at the Walter Reed Army Institute of Research.

A steady-state modal analysis of the GelMan (Fig. 5(b)) was performed to analyze the mechanical vibration characteristics of the thorax; this compared well with measured responses. An advantage of this model is that it provides local stress, strain, pressure, and acceleration data that can be used to develop a damage criterion and optimize sensor locations for the thorax model. These additional shock impulse loading experiments will be used to identify the frequencies and modes of vibration that cause injury to the organs.

Field Trial Experiments: The NRL GelMan thoracic model has been deployed at various blast test sites to measure free field and confined-space responses to blast.

The information from these tests and the shock tube tests will be used to develop transfer functions relating blast waves to the body response.

During one of the free field test series (Fig. 6(a)), GelMan was used to evaluate the effectiveness of body armor (Fig. 6(b)) against blast. Body armor is a soft vest used with and without hard ceramics inserts. These types of body armor systems are designed to provide effective protection against ballistic weapons threat. The free field blast data, in conjunction with shock tube tests (Fig. 6(c)), showed that the soft and combined soft and hard body armor systems do, however, slightly increase the peak lung pressures when subjected to blast. This suggests that future body armor designs should attempt to protect against blast as well as to preserve the ballistic protection capabilities. The GelMan system can be used to guide and evaluate new body armor designs by linking the external ballistic and pressure loads to the internal body dynamics.



FIGURE 6 (a) Blast detonation at test sight. (b) Thoracic model with body armor at test sight. (c) Instrumented thoracic model undergoing shock impulse from pressurized shock tube.

Summary and Significance: The GelMan surrogate provides valuable information useful for warfighter protection by supplementing medical injury models for blasts and resolving the local biodynamic response of tissue that may lead to injury. In the future, this may lead to the development of better armor to protect soldiers and sailors against blunt trauma and blast injuries.

Acknowledgments: The authors acknowledge the assistance of D. Bowers and D. VanDerLoo (Materials Science and Technology Division); the assistance of P. Peffers and B. Haynes (NRL Spacecraft Engineering Department); A. Jurrus (Armed Forces Institute of Pathology) and J. Morris (Walter Reed Army Institute of Research).

[Sponsored by ONR, DTRA, and NATICK]

RAPID PROTOTYPING OF CONFORMAL ANTENNA STRUCTURES

A. Piqué,¹ R.C.Y. Auyeung,¹ M.W. Nurnberger,² D.J. Wendland,³ C.B. Arnold,⁴ A.R. Abbott,³ and L.C. Schuette⁵

¹Materials Science and Technology Division

²Space Systems Development Department

³ITT Industries

⁴Princeton University

⁵Tactical Electronic Warfare Division

Introduction: The size of portable and mobile devices is continuously shrinking. This requires new approaches for integrating the antennas into a system. Frequently, antennas are attached as an afterthought, and often in locations and orientations that expose them to easy damage. An alternative is to implement conformal antenna designs that are integrated in or on the housing of the mobile device. This offers considerable size and

location flexibility in comparison to what can be accomplished by using traditional antenna structures. Conformal antennas exhibit uniquely thin and unobtrusive profiles, reduced sizes, and potentially improved performance, making them well-suited for use in unmanned sensor and distributed autonomous systems. However, the adoption of conformal geometries for antenna designs must be taken into account during the system design process, as it impacts the antenna input impedance and radiation patterns. Therefore, any approach to the development of conformal antennas will benefit from the ability to go through the design, fabrication, and optimization cycle quickly and inexpensively. In particular, the fabrication of conformal antennas can be extremely slow and expensive. Rapid prototyping techniques based on laser machining and laser direct-write offer a unique capability to greatly reduce the time spent in fabricating these structures. When integrated with RF testing hardware, a real-time tuning capability can be implemented that further shortens the development cycle from weeks to hours.

The term “direct-write” refers to any technique or process capable of removing, depositing, dispensing, or processing different types of materials over various surfaces following a preset pattern or layout.¹ The ability to accomplish both pattern and material transfer processes simultaneously opens the door for the development and manufacture of next-generation commercial and defense microelectronic systems. The potential offered by direct-write techniques lies in their ability to transfer and/or process most materials over any surface with extreme precision, resulting in a functional structure or working device. Direct-write technologies do not compete with photolithography for size and scale, but rather add a complementary tool for specific applications requiring conformal patterning, rapid turnaround and/or pattern iteration. Among those techniques, laser direct-write offers several advantages for the rapid prototyping of conformal antenna structures. Figure 7 shows the laser direct-write

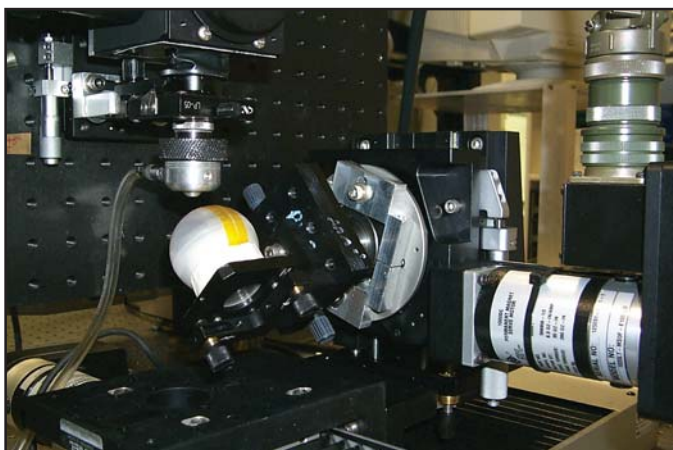


FIGURE 7
Laser direct-write set up adapted for laser micromachining of conformal antenna patterns.

system used for performing 3-D laser micromachining and laser deposition on spherical surfaces of lightweight substrates compatible with conformal antenna designs.

Technical Approach: Because of its durability and robustness, a spherical fiberglass dome was chosen as the substrate for the implementation of a conformal GPS antenna (1575 MHz) design. The integration of the antenna and matching structure onto the surface of the dome required a slot-based design to give a broad, circularly polarized radiation pattern for operation over a wide range of orientations. The fiberglass domes were coated with an $\sim 100\ \mu\text{m}$ thick conductive silver epoxy layer from which the conformal crossed-slot antenna and the coplanar waveguide (CPW) feeds (Fig. 8) were generated by laser micromachining. The degree of roughness present in the surface of the fiberglass dome affected the uniformity by which the depth and width of the laser micromachined trenches could be controlled. To correct for these variations, individual components of the antenna design were tested and then tuned by laser machining the required matching elements (inductive loading on the antenna slots, series stubs on the CPW).

The crossed slots are fed by using two CPW transmission lines oriented 45 deg from the slots. CPW is used because it requires only one conductor plane and because its radiation loss can be minimized by the appropriate choice of dimensions and the use of air-bridges. The tuning stubs are implemented using series CPW shorted stubs placed inside the center conductor of the CPW feed line. The laser processing is critical to this approach, since it allows the implementation of these stubs with high precision in the very limited space available and conformal to the surface. The CPW lines transition to female right-angle connectors that are mounted below the equator inside the dome, allowing connection to measurement equipment or to the 90-deg hybrid and low noise amplifier (LNA).

The initial design of the antenna was validated using a 3-D finite-element modeling software package.² Figure 9 shows both the simulated geometry as well as a sample set of radiation patterns. The patterns are typical of a curved or drooping crossed dipole, and show both good gain and polarization performance over greater than one hemisphere, allowing for greater variability in device orientation. A major challenge in the development of conformal antennas on composites is the lack of knowledge of material parameters. In these simulations, the material properties and dimensions were estimated to give a first-order solution. In the actual fabrication of the antenna, the design and manufacturing steps are planned to allow tuning and deduction of the material parameters as the machining progresses. The rapid prototyping ability discussed here is critical to this approach, as it allows quick and frequent machine/measure cycles that would be nearly impossible with other techniques.

Summary: Laser direct-write is a valuable technique for the rapidly prototyping conformal antennas on arbitrary surfaces. A conformal antenna consisting of two orthogonal crossed slots, designed for operation at 1575 MHz, was laser micromachined on a fiberglass dome coated with a silver conductive layer. The feed network for this antenna, containing two CPW transmission lines and matching circuits, was also laser micromachined. The individual elements of the design are functional and show the expected performance. The fully integrated package, including hybrids and LNA, is expected to be completed and tested in the near future.

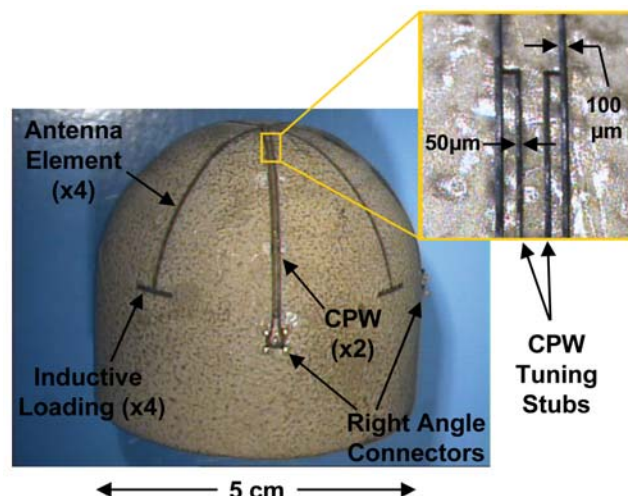
[Sponsored by ONR]

References

- ¹A. Piqué and D.B. Chrisey, editors, *Direct-Write Technologies for Rapid Prototyping Applications* (Academic Press, San Diego, CA, 2002).
- ²HFSS Version 9.0, Ansoft Corp., Pittsburgh, PA.

FIGURE 8

A prototype crossed-slot GPS conformal antenna made by laser direct-write on a metal-coated fiberglass dome; inset shows a section of the tuning stubs for the CPW.



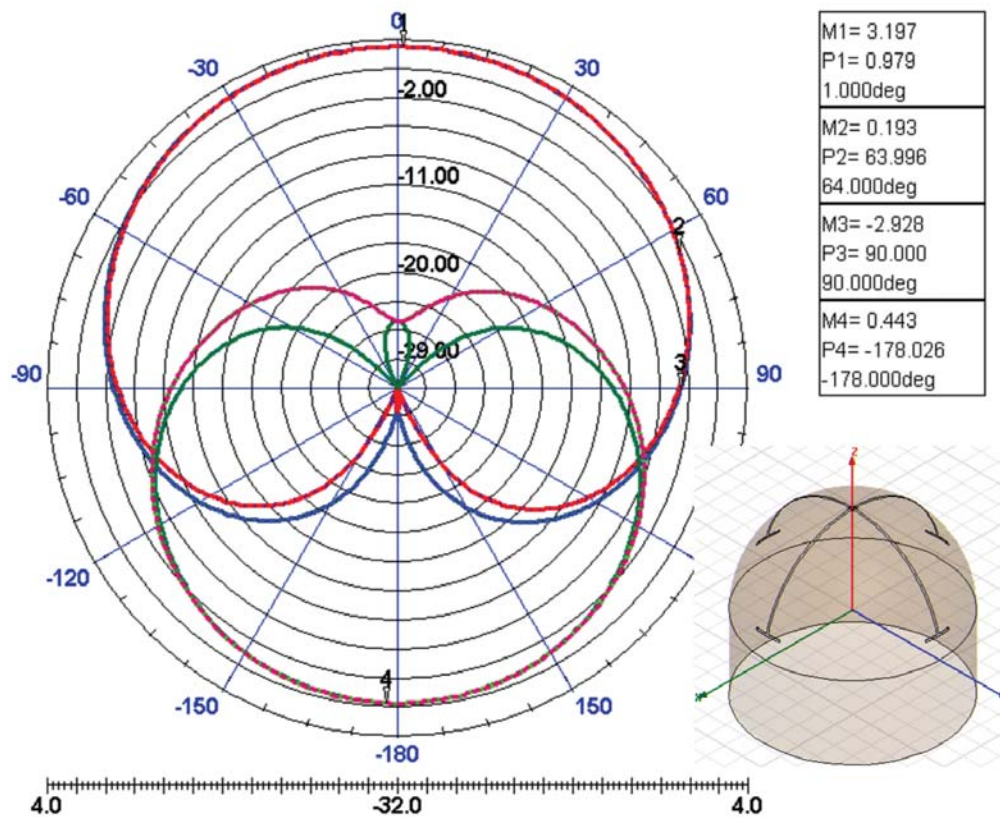


FIGURE 9 Co- and cross-polarization radiation patterns ($\phi = 0, 90$ cuts) for the loaded crossed slots on the spherical dome shown in the inset.²

CARBON NANOTUBE NETWORKS: A NEW ELECTRONIC MATERIAL

E.S. Snow, J. Novak, and M.D. Lay
Electronics Science and Technology Division
 E.J. Houser
Materials Science and Technology Division

Background: Single-wall carbon nanotubes (SWNTs) are unique electronic structures. They are one-dimensional wires composed entirely of surface atoms yet exhibit transport properties superior to bulk single-crystalline silicon (Si). This high electron mobility makes them an ideal candidate for electronic device applications, while their virtually infinite surface-to-volume ratio offers extraordinary sensitivity for chemical and biological sensor applications. However, a major obstacle presently preventing their commercial and/or military implementation in new classes of electronic devices is the lack of a technique for the controlled assembly of large numbers of SWNTs with precisely controlled position and orientation. Until this obstacle is overcome or circumvented, SWNT-based devices and sensors will remain

in the realm of impressive laboratory curiosities without real-world applications.

At NRL we have developed an approach to realizing SWNT electronic applications that circumvents the assembly problem stated above by using a random network of SWNTs (Fig. 10). We have recently discovered that such carbon nanotube networks (CNNs) form an electrically conducting thin film, and that this network is conducting because of the high-quality electrical contact formed between intersecting nanotubes.¹ We have found that the electronic properties of CNNs can range from semiconducting to metallic, depending on the network density. Devices fabricated from such networks circumvent the requirement of precise position and structural control because the devices display the averaged properties of many randomly distributed interconnected SWNTs.

An additional feature of CNNs is that they can be processed into devices using conventional fabrication technology without affecting their electrical properties. Thus, CNNs retain the interesting electronic properties of individual SWNTs while providing the processing capabilities of conventional electronic materials. This combination of features opens up a wide range of electronic

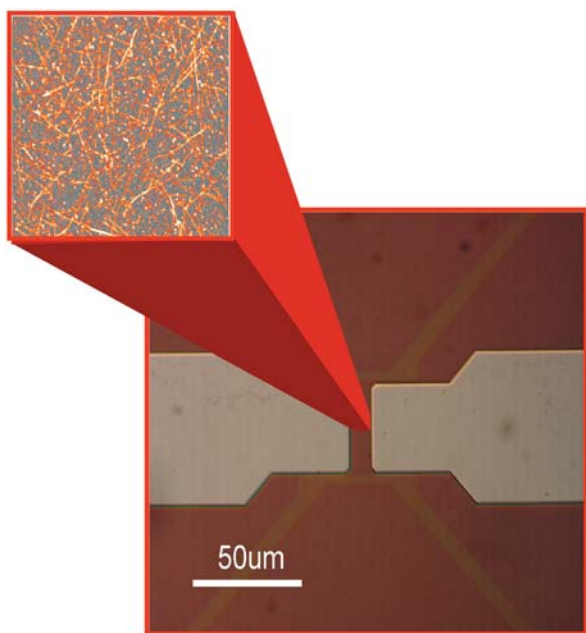


FIGURE 10
Optical image of a CNN device; inset shows an atomic force microscope image of the CNN that electrically connects the two electrodes.

and sensor applications, two of which (macroelectronics and chemical detection) are described below.

Chemical Detection: Because they are composed entirely of surface atoms, the electrical resistance of SWNTs is extremely sensitive to the physisorption of certain chemical vapors. In addition, the otherwise chemical inertness of SWNTs makes them very robust for operating in harsh environments. Consequently, SWNTs offer the potential for a new class of chemical sensors.

In such sensors, the adsorption of an analyte molecule with electron donor or acceptor properties results in a charge transfer between the analyte and the SWNT that changes its electrical resistance. Because many chemical warfare agents and toxic industrial chemicals have strong electron transfer properties, CNN-based devices can serve as highly sensitive chemical sensors for defense and homeland security applications.

At NRL we have performed preliminary experiments to test the viability of CNN chemical detectors, with a focus on achieving high levels of sensitivity and chemical specificity. Our initial experiments have established that SWNT network devices are capable of detecting nerve agents with sub-ppb sensitivity.² In these experiments, we fabricated CNN-based chemical sensors and used these devices to detect dimethyl methylphosphonate (DMMP), a nerve agent simulant (Fig. 11). In order to obtain a chemically specific response, we have combined the CNNs with chemoselective polymers recently developed at NRL. This combination has the potential to provide

highly sensitive, low-power chemical detectors for chemical warfare agents and toxic industrial chemicals.

Macroelectronics: An important emerging area of technology is macroelectronics. Macroelectronics has the goal of providing inexpensive electronics on polymeric substrates. Such electronics will be “printed” onto large-area polymeric films by using fabrication techniques more analogous to text and imaging printing than conventional semiconductor microfabrication technology. Applications of such macroelectronics include light-weight flexible displays, inexpensive RF identification, and smart materials or clothing. Conventional semiconductors are not suitable for such applications, because such materials require a crystalline substrate and are too expensive. Consequently, a large investment has been made in developing organic semiconductors that can be deposited at room temperature onto a wide range of substrates. This effort has achieved only moderate success because of the low-quality electron transport found in organic semiconductors.

CNNs provide a promising new material for macroelectronic applications because of the high-quality electron transport intrinsic to SWNTs and because CNNs can be deposited at room temperature onto polymeric and many other substrates. We have demonstrated thin-film transistors fabricated using CNNs that have an electron mobility more than an order of magnitude larger than the mobility found in organic semiconductors (Fig. 12). Consequently, with further development CNNs should provide a low-cost electronic material for flexible, unbreakable displays and inexpensive macroelectronics.

Future Work: The promising results of our initial research indicate that CNNs can serve as a new electronic material for a variety of applications such as macro-

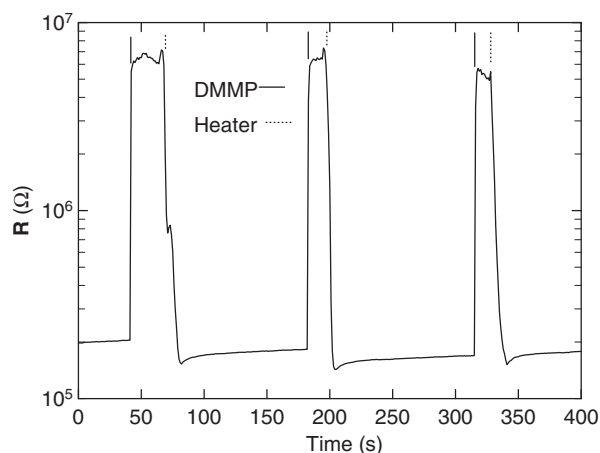


FIGURE 11
Response of a CNN sensor to doses of DMMP, a chemical simulant for nerve agents. The resistance of the CNN increases upon exposure and is refreshed by heating the device.

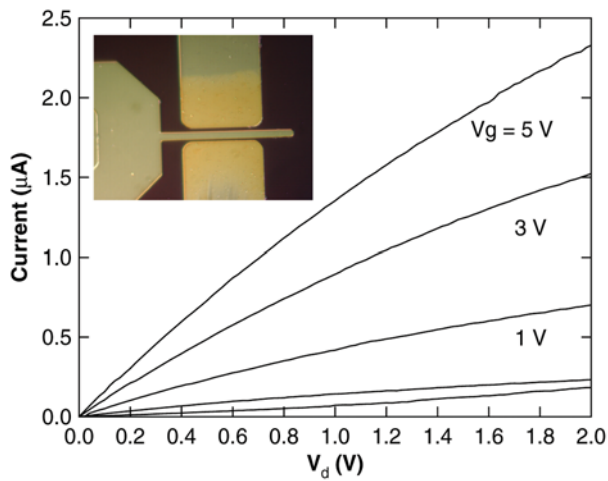


FIGURE 12 Transistor characteristics for a CNN thin-film transistor; the inset is an optical image of the source, drain, and gate electrodes of the device.

electronics and chemical sensing where submicron device size is not required. In such applications, the larger device size averages the properties of many individual SWNTs, yielding good device-to-device reproducibility. Future work includes improving the transistor performance by using chemical separation techniques to purify SWNTs based on electronic type, chemical functionalization of the SWNTs to further enhance the sensitivity and chemical specificity of the sensors, and exploring additional CNN applications such as biosensing.

[Sponsored by ONR]

References

- ¹E.S. Snow, J.P. Novak, P.M. Campbell, and D. Park, "Random Networks of Single-Wall Carbon Nanotubes as an Electronic Material," *Appl. Phys. Lett.* **82**, 2145-2147 (2003).
- ²J.P. Novak, E.S. Snow, E.J. Houser, D. Park, J.L. Stepnowoski, and R.A. McGill, "Nerve Agent Detection Using Networks of Single-Wall Carbon Nanotubes," *Appl. Phys. Lett.* **83**, 4026-4028 (2003).

SPIRAL GROWTH AT THREADING DISLOCATIONS

The surface of a 4-mm-thick GaSb film grown on a GaAs(001) substrate by molecular beam epitaxy. The image, with a field of view of approximately 1mm, reveals the nanometer-scale morphology of the spiral-like structures that grow around threading dislocations in the film (caused by the film's 7% lattice mismatch with the substrate). Each threading dislocation creates a 0.3-nm-height "step" where it emerges at the surface.



165 Drag Coefficient, Surface Roughness, and Reference Wind Speed

P.A. Hwang

167 An Approach for Coupling Diverse Geophysical and Dynamical Models

J.D. Dykes, R.A. Allard, C.A. Blain, B. Estrade, T. Keen, L. Smedstad, A. Wallcraft, M. Bettencourt, and G. Peggion

170 Airborne Sea-Surface Topography in an Absolute Reference Frame:
Applications to Coastal Oceanography

J. Brozena, V. Childers, and G. Jacobs

172 New Observations of Hydroxyl from the Space Shuttle by NRL's
SHIMMER

J.G. Cardon, C.R. Englert, M.H. Stevens, R.R. Conway, J.M. Harlander, and F.L. Roesler

DRAG COEFFICIENT, SURFACE ROUGHNESS, AND REFERENCE WIND SPEED

P.A. Hwang
Oceanography Division

Introduction: Drag coefficient (C_D) and surface roughness (z_0) are important parameters for quantifying air-sea momentum and energy exchanges. In almost all earlier analyses of C_D and z_0 , the reference wind speed at 10-m elevation (U_{10}) is used. Although the adoption of U_{10} in the analyses provides a consistent reference level of wind measurements (compared to earlier reports using “mast height” or “anemometer height”), the dynamical significance of the 10-m elevation in the marine boundary layer is not clear. From a heuristic point of view, surface waves are the ocean surface roughness, and the air-sea interaction processes are influenced by wave conditions. Because the influence of surface waves decays exponentially, with wavelength serving as the vertical length scale, the dynamically meaningful reference elevation should be λ , the characteristic wavelength of the peak component of surface wave spectrum.

Wavelength Scaling: For a logarithmic wind profile,

$$U(z) = \frac{u_*}{\kappa} \ln \frac{z}{z_0}, \quad (1)$$

where U is the wind speed, u_* the wind friction velocity, κ the von Kármán constant (0.4), z the vertical elevation,

and z_0 the dynamic roughness, the drag coefficient referenced to wind speed at the elevation equal to one-half of the surface wavelength, $C_{\lambda/2} = u_*^2 / U_{\lambda/2}^2$ is

$$C_{\lambda/2} = \kappa^2 \left(\ln \frac{\pi}{k_p z_0} \right)^{-2}. \quad (2)$$

Equation (2) suggests that a natural expression of the dimensionless surface roughness is $k_p z_0$,

$$k_p z_0 = \pi \exp \left(-\kappa C_{\lambda/2}^{-0.5} \right). \quad (3)$$

Analysis of several field experiments with wind-sea dominated wave conditions¹ yields

$$C_{\lambda/2} = A_c \omega_{**}^{a_c}, \quad (4)$$

with $A_c = 1.22 \times 10^{-2}$, $a_c = 0.704$, where $\omega_{**} = u_* \omega_p / g$ is the dimensionless frequency of the air-sea coupled system, g the gravitational acceleration, and ω_p the frequency of peak spectral component (Fig. 1(a)). Although the data scatter is large, the result is a substantial improvement over C_{10} (Fig. 1(b-d)). Figure 1 illustrates convincingly that $C_{\lambda/2}$ is indeed superior to C_{10} for accounting for the surface wave effects on the wind stress over the ocean surface.

Figure 2(a) shows the dimensionless roughness $k_p z_0$. The measurements from different sources collapse very nicely following the wavelength scaling function (Eq. (3)). The surface roughness is also frequently expressed in

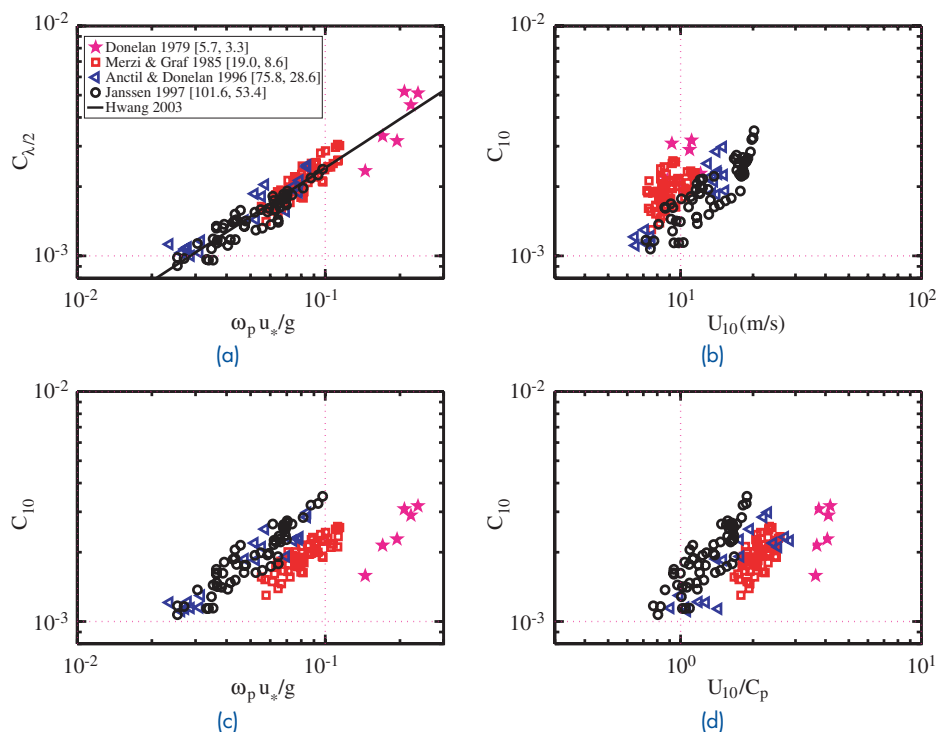


FIGURE 1
Drag coefficient based on (a) wavelength scaling,¹ $C_{\lambda/2}(\omega_{**})$, and 10-m scaling: (b) $C_{10}(U_{10})$, (c) $C_{10}(\omega_{**})$, and (d) $C_{10}(U_{10}/C_p)$, where C_p is the phase speed of the peak component of wave spectrum. The data scatter in C_{10} expressions is considerably worse than that of the $C_{\lambda/2}$ expression. The solid curve is Eq. (4).

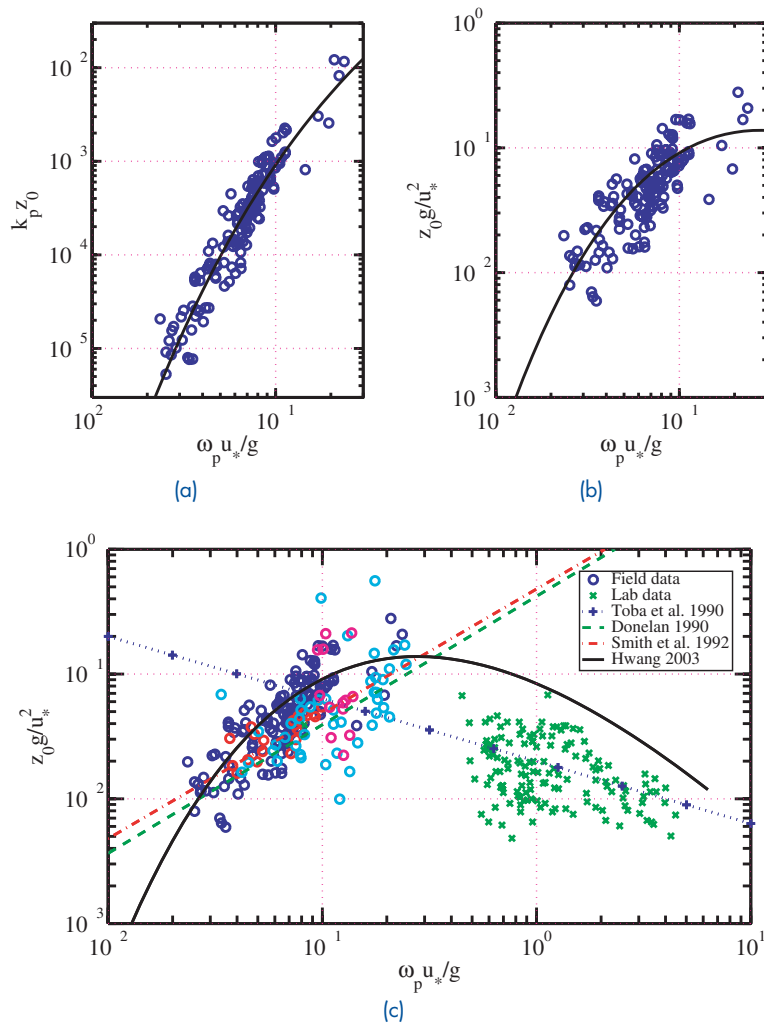


FIGURE 2 Dimensionless roughness in terms of (a) $k_p z_0(\omega_{**})$, and (b) $z_{0*} = z_0 g / u_*^2$; the curve represents Eq. (4) applied to Eqs. (3) and (5). (c) Same as (b) but includes additional field and laboratory data in the comparison. Empirical relations from several earlier studies² are also shown in this figure.

terms of the Charnock parameter, $z_{0*} = z_0 g / u_*^2$, which can be obtained from applying the dispersion relation of surface waves to Eq. (3),¹

$$z_{0*} = \pi \tanh kb \omega_{**}^{-2} \exp \left[-\kappa (A_c \omega_{**}^{a_c})^{-0.5} \right]. \quad (5)$$

The Charnock parameter increases with ω_{**} in the frequency range of the field data (Fig. 2(b)). The parameterization function (Eq. (5)) predicts that the dependence of $z_{0*}(\omega_{**})$ reverses to a decreasing trend at $\omega_{**} > \sim 0.25$ and z_{0*} approaches ω_{**}^2 asymptotically at very large ω_{**} . The inverse relationship of $z_{0*}(\omega_{**})$ at high ω_{**} range has been observed in laboratory measurements² (Fig. 2(c)). It is noted that the apparently different behavior of z_{0*} with ω_{**} shown in Fig. 2(c) had generated considerable controversies in the air-sea research community, as is evident from the large number of empirical (and contradicting) relations of $z_{0*}(\omega_{**})$ that have been proposed in the literature.² The present analysis predicts correctly the increasing trend of

$z_{0*}(\omega_{**})$ in the low-frequency region and the decreasing trend in the high-frequency region.

Conclusions: Quantification of the drag coefficient and surface roughness is critically influenced by the choice of the reference wind speed. It is shown that when the scaling wind speed is referenced to the surface waves, the experimental data of drag coefficient and surface roughness can be collapsed into simple clusters. The analysis yields strong evidence that surface waves are the roughness element of the ocean surface and that they exert significant influences on air-sea momentum exchanges. The results also have important implications on ocean remote sensing applications.

[Sponsored by ONR]

References

- ¹P.A. Hwang, "Influence of Wavelength on the Parameterization of Drag Coefficient and Surface Roughness," *J. Oceanogr.* (in press).
- ²I.S.F. Jones and Y. Toba (eds.), *Wind Stress Over the Ocean* (Cambridge University Press, Cambridge, UK, 2001).

AN APPROACH FOR COUPLING DIVERSE GEOPHYSICAL AND DYNAMICAL MODELS

J.D. Dykes, R.A. Allard, C.A. Blain, B. Estrade, T. Keen, L. Smedstad, and A. Wallcraft
Oceanography Division

M. Bettencourt
Center of Higher Learning/University of Southern Mississippi

G. Peggion
University of New Orleans

Introduction: Successful military operations in littoral waters rely on timely analyses and forecasts of a diverse range of environmental variables associated with geophysical and dynamical processes. The complex, interdependent processes of the littoral environment are captured using separate numerical models that simulate circulation and sediment dynamics driven by wind, waves, tides, and buoyancy over spatial scales that extend over kilometers to meters. Typically, meteorological and oceanographic models run in a loosely coupled fashion, each model sequentially provides information to the other through a cascade of individual forecasts. Data between models are exchanged via written files, with each model responsible for handling differences in grid structure, desired quantities, and/or file formats. For this case, model interdependence is usually limited to one-way and the time to forecast depends on all models.

Ideally, we would like to process various computations simultaneously and exchange information as needed without regard to variations in computational grids or file formats. One could envision providing the ability to connect any model to a common server capable of handling any grid configuration and providing the computed information to any other model in the needed form. This methodology has now become possible with the advent of the Model Coupling Environmental Library (MCEL). The implementation of MCEL for model coupling provides the following benefits: (1) allows one-way or two-way model interaction; (2) assumes the burden of handling grids of different structure; and (3) requires minimal intrusion in existing code. Other benefits include a reduction in development time for a coupled model system and more efficient computations due to the parallel, distributed construct of the MCEL.

Under the recent High Performance Simulation of Littoral Environments (HFSole) Challenge Project, we configured two applications to provide a rigorous test for MCEL-based model coupling. Success is defined as the appropriate and accurate transfer of information from one model to another and improved efficiency as com-

pared to file-based, sequential coupling. All models in the coupled model suite have been individually validated via model-data comparisons. The results demonstrate enormous potential for the MCEL to revolutionize the simulation of complex environments having diverse, interdependent processes by facilitating the coupling of models that represent these processes.

Description of Tests: Two applications designed to investigate the MCEL performance involved the coupling of five geophysical and dynamical models. The first model, the Hybrid Coordinate Ocean Model (HYCOM), captures the large-scale wind and thermodynamic-driven ocean circulation using a structured horizontal grid and a unique hybrid vertical gridding strategy. HYCOM simulations provide open-ocean forcing for the shelf-scale ocean circulation simulated by the Navy Coastal Ocean Model (NCOM), also a wind and thermodynamic-driven ocean circulation model. Results from the NCOM model in turn provide water-level forcing for the Advanced Circulation model (ADCIRC), a hydrodynamic model that is particularly well-suited for simulating tide and surge dynamics in the coastal areas at very high resolution. ADCIRC computations occur over an unstructured triangular finite-element mesh. Currents and water elevations from ADCIRC then drive a shallow-water wave model, the Simulating Waves Nearshore (SWAN) model in the nearshore. The Littoral Sediment Optical Model (LSOM), a sediment transport and water clarity model developed at NRL, is also focused on very shallow coastal waters, receiving wave information from SWAN and currents from the ADCIRC model.

The two domains for which the coupled model system is applied are the Mississippi Bight in the northeast Gulf of Mexico and the Spanish coastal waters, both shown in Fig. 3. One-way coupling is depicted in the conceptual diagram of Fig. 4, which highlights the connections between each model and the role of the MCEL server in facilitating coupling. To ensure portability of the coupled model system and the MCEL server, the applications are run on three different high-performance computer architectures at two DOD Major Shared Resource Centers.

Results: We are able to validate the coupled model computations using the MCEL server by comparing to identical file-based coupling applications. One would expect that connection to the server would result in minimal degradation of accuracy; indeed this is observed with errors limited only by model precision. We found across computational platforms differences on the order of machine precision, an excellent indication of the robustness of MCEL. Significant improvement in computational time is realized using the MCEL server for the five-model coupled system. The typical coupled model application

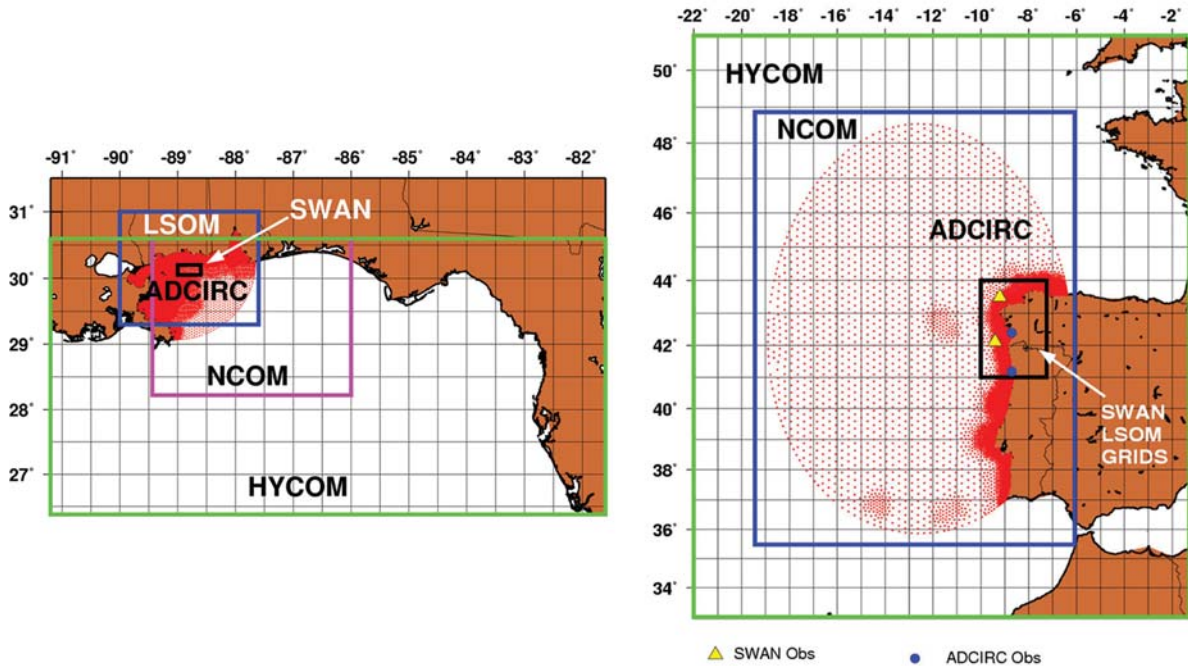


FIGURE 3 Five models running over domains of varying size and structure are connected to the MCEL server, which handles the interpolation of gridded fields regardless of domain diversity.

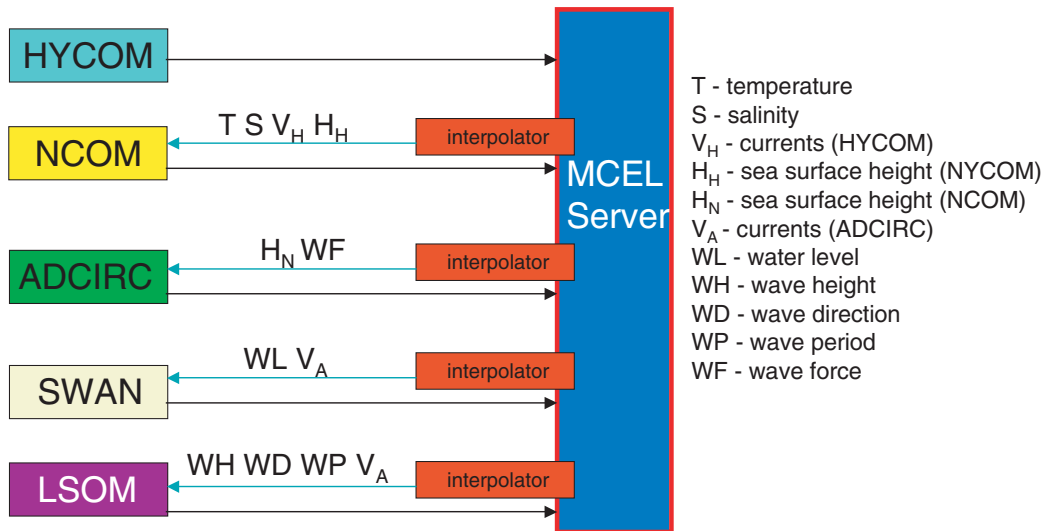


FIGURE 4 These participating models were connected to the MCEL server. The black arrows depict the flow of data as model output to the server. The green arrows show the flow of certain interpolated parameters, as required by the receiving model.

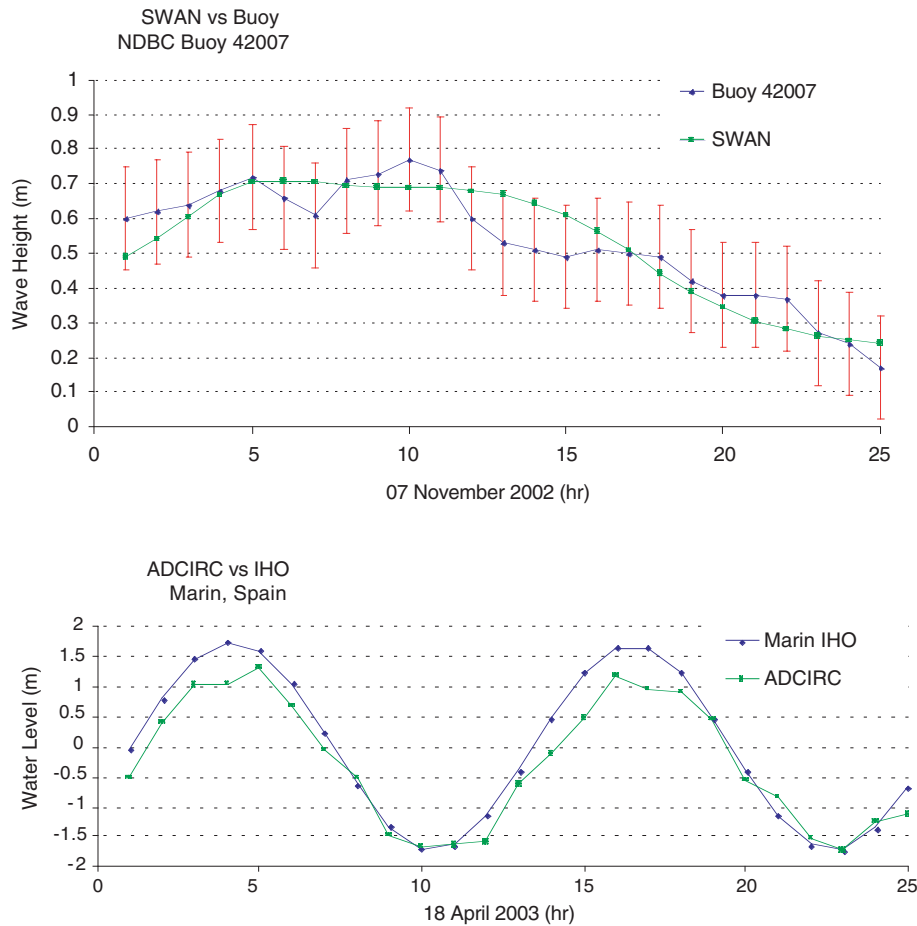


FIGURE 5
 Sample comparisons between model output and observational data gave the assurance that, under these test conditions, the models are functioning as they were originally designed. The error bars in the SWAN vs buoy comparison are ± 0.15 m.

on the IBM SP4 experienced a reduction of more than 33% when using the MCEL server. Validation of the coupled model system is accomplished by comparison to available observations. Figure 5 shows sample comparisons for ADCIRC and SWAN vs buoy data. Reasonable representations of observed dynamics further reinforce the validity of the MCEL approach for model coupling.

Conclusions: The efficiency, portability and accuracy of the MCEL approach for model coupling has been demonstrated. MCEL connects geophysical and dynamical models that represent a range of processes and spatial scales and handles a diversity of grid structures. MCEL requires minimal intervention within existing model codes, which facilitates its ease of use. The potential of the MCEL server is unlimited. Increasingly complex coupled processes are capable of being represented by numerical models today. The MCEL server releases researchers from the mechanics of model coupling, allow-

ing their focus to turn to the unknowns of coupled processes.

Acknowledgments: The HFSoLE Portfolio was funded under the Common High Performance Software Support Initiative (CHSSI) of the Department of Defense (DOD) High Performance Computing Modernization Program (HPCMP). Special thanks to Mr. Carl Szczechowski of NAVOCEANO for serving as an independent reviewer of the MCEL coupled model system.

[Sponsored by ONR]

Reference

¹R. Allard, A. Wallcraft, C.A. Blain, M. Cobb, L. Smedstad, P. Hogan, T. Keen, S. Howington, C. Berger, J.M. Smith, and M. Bettencourt, "Providing the Warfighter Information Superiority in Littoral Waters," *High Performance Computing Contributions to DOD Mission Success 2002*, March 2003, pp. 78-80.

AIRBORNE SEA-SURFACE TOPOGRAPHY IN AN ABSOLUTE REFERENCE FRAME: APPLICATIONS TO COASTAL OCEANOGRAPHY

J. Brozena,¹ V. Childers,¹ and G. Jacobs²

¹*Marine Geosciences Division*

²*Oceanography Division*

Introduction: Water-level measurements are fundamental to Navy operations. Data from tide gages, satellite altimetry, and bottom pressure-gage/inverted echo sounders are assimilated into tide and circulation models to produce nowcasts and forecasts of parameters of interest (e.g., currents, acoustic propagation, and navigability of harbors and channels). Unfortunately, highly dynamic coastal ocean processes occur at temporal and spatial scales that cannot be captured by the available water level measurement systems. Additionally, there is no universal vertical datum that allows measurements from the different types of systems to be directly combined as heights. Instead, the delta or change in water level over time at a given location is the quantity generally assimilated into models. These time-derivatives of height are very useful, but they lack the information contained in the long-period average heights from mean currents, nonstandard water density, and wind set-up effects.

Airborne Measurement Techniques: NRL has been developing airborne measurement techniques, altimetry and gravity, to determine sea-surface height and residual height anomaly at the short time and space scales required for littoral regions. In our method, a precise radar altimeter measures the distance to the sea-surface beneath the aircraft. We combine these ranges with extremely accurate (cm-level) interferometric-mode Global Positioning System (GPS) estimates of the aircraft height above the reference ellipsoid. This produces sea-surface height profiles that are similar to conventional satellite altimetry. However, the airborne method is not restricted by the inherent orbital limitations in sampling in which there is a trade-off between sub-satellite track spacing and revisit times. Airborne altimetry may also be collected in close proximity to the coast where land within the large illuminated footprint of the satellite-borne radar corrupts the data.

We have also developed a methodology for providing a high-resolution geoid reference surface or vertical datum that can be used for any of the water-level measurement systems. The geoid is an equipotential surface of gravity that would approximate mean sea level (msl) if the ocean were motionless. The fit between the equipotential surface and sea level can be global or local. Our method involves calculating a precise local geoid from historical marine and terrestrial gravity data in the region

augmented with airborne gravity data collected simultaneously with the airborne altimetry profiles. We then determine any offsets of the local geoid from GPS surveyed tide gages along the shoreline and with conventional altimetric mean sea-surface models away from shore. A gravitational geoid was calculated for the northern Gulf of Mexico to serve as a test msl reference surface. The local geoid and calibrated offsets provide a means to connect airborne, satellite, and tide-gage observations in an absolute (WGS-84) framework. It is also possible to transfer precise absolute vertical coordinates to bottom-moored water-level instrumentation by simultaneous collection of water levels from the bottom instruments and the airborne, GPS-referenced altimeter.

Flight Testing: In May 2003 we performed a series of 10 altimetry flights over the northern Gulf of Mexico near the mouth of the Mississippi River. The experiment was designed to test the accuracy and resolution of the airborne measurements while examining the temporal and spatial variability of the coastal sea-surface heights and related water-column temperature anomalies. Airborne expendable bathythermograph (AXBT) probes were dropped regularly to acquire the temperature data. Internal cross-over statistics and crossings of a GPS-surveyed tide gage indicate sea-surface topography accuracy of better than 5 cm rms.

We were fortunate to have a large warm-core eddy pinned against the slope in the test area throughout the experiment. The eddy showed a topographic relief of about 1 m (including a low, moat-like structure around the boundary of the eddy) and created a highly dynamic environment with coherent and rapidly varying sea-surface height anomalies across the region (Fig. 6). The AXBT data collected at the same time show wave-like temperature and topographic anomalies propagating up the continental slope (Fig. 7). Time and space scales of these features are hours to days and tens to a few hundred kilometers. The airborne altimetry revealed the structure and temporal evolution of the eddy and its interaction with the bottom topography of the slope in much greater detail than would be possible with space-borne altimeters. The airborne method also allowed the collection in situ water column measurements.

Uses: The new measurement capability can be used to improve our understanding of the littoral environment. Since the airborne altimeter and GPS equipment is relatively small and light, there is also good potential to utilize this method on unmanned airborne vehicles for access to denied areas of Navy interest. The high-resolution geoid msl reference used for this program is an initial step in providing a unified vertical datum for integrating water-level measurements of all types. This should help to improve the resolution and accuracy of the next generation of ocean circulation and tide models.

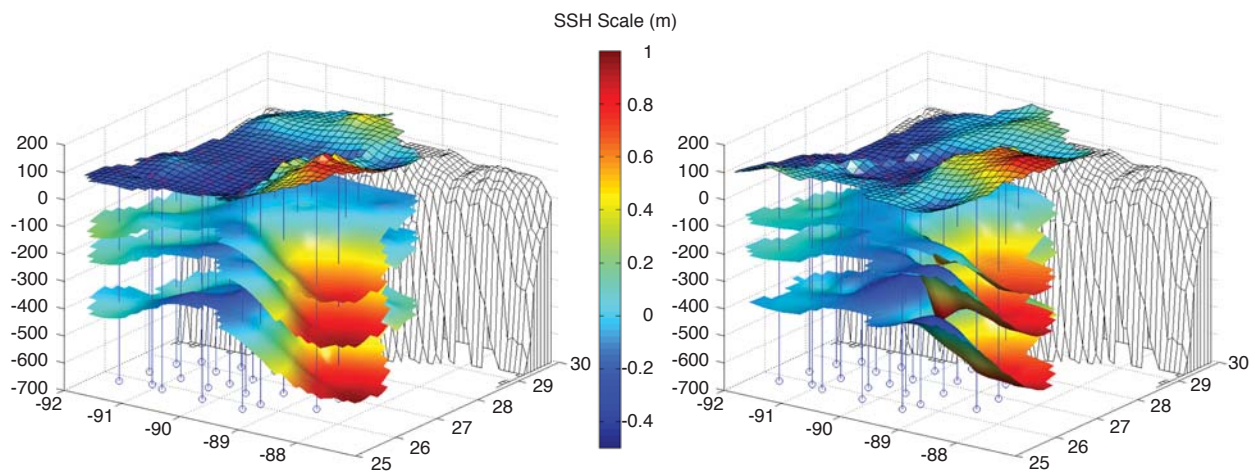


FIGURE 6

Sea-surface height anomalies from a sequence of eight of the altimetry reflights. The contour interval is 5 cm. Black triangles show the locations of the MMS bottom-moored pressure gage/inverted echo sounders that will provide ground-truth when the data are retrieved. One side of the large warm-core eddy and the bounding, moat-like topographic low are visible in the figures over the entire 16-day period. Also prominent is a coastal high near the mouth of the Mississippi river that waxes and wanes over the period.

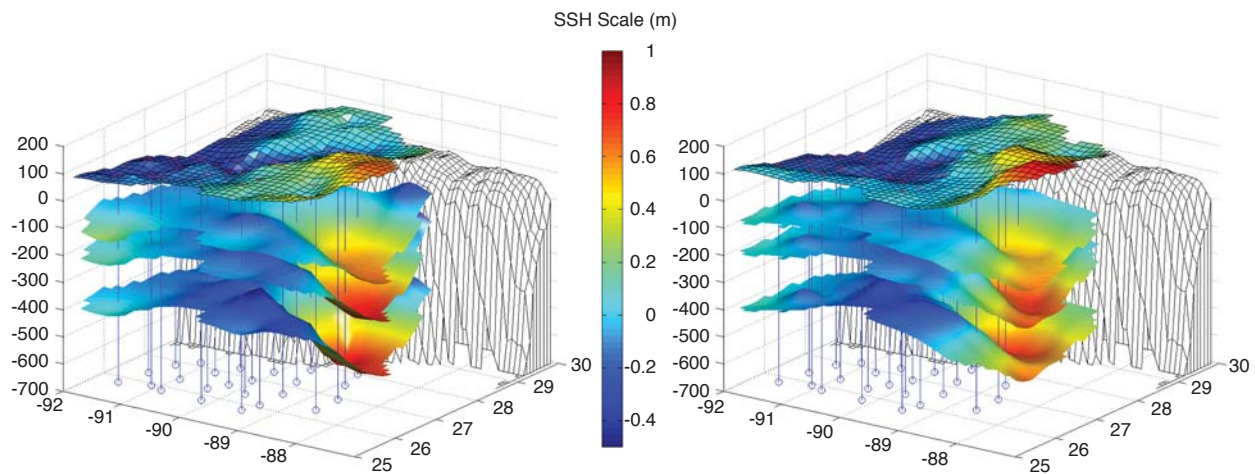


FIGURE 7

Sea-surface height anomaly overlaid to the 20, 15, and 10 °C isotherms (interpolated from the AXBT data) from every other flight of Fig. 6. Bathymetry of the continental slope is shown behind the surfaces, and the blue symbols and vertical blue lines show the position of the MMS bottom moorings. The eddy and bounding moat are again clearly seen. When animated, the entire data sequence clearly shows wavelike features in the topography and isotherms propagating shoreward and up the slope.

Acknowledgments: The Naval Oceanographic Office provided the 600 AXBT buoys deployed for this experiment. Our thanks to the Navy P-3 crew from the NRL Military Operations and Flight Support Detachment for an excellent job of flying and maintaining the aircraft.

[Sponsored by ONR]

NEW OBSERVATIONS OF HYDROXYL FROM THE SPACE SHUTTLE BY NRL'S SHIMMER

J.G. Cardon,¹ C.R. Englert,¹ M.H. Stevens,¹
R.R. Conway,¹ J.M. Harlander,² and F.L. Roesler³

¹Space Science Division

²St. Cloud State University

³University of Wisconsin, Madison

Introduction: Remote sensing from space uniquely enables global observation of hydroxyl (OH) by ultraviolet (UV) solar resonance fluorescence in the Earth's middle atmosphere. An understanding of the photochemistry of OH in the middle atmosphere (20-90 km altitude) is a primary focus of the Upper Atmospheric Physics Branch. Measuring the vertical distribution of OH is invaluable to understanding middle atmospheric chemistry including ozone destruction, the Polar Mesospheric Cloud phenomenon, and the water budget. Despite its importance, OH remains one of the least measured atmospheric constituents.

The observation of OH solar resonance fluorescence in the middle atmosphere requires high spectral resolution to separate the relatively bright and spectrally complex solar scattered background from the relatively weak OH emission features near 308 nm. NRL's MAHRSI instrument¹ provided the first global measurements of mesospheric OH during two Shuttle missions in the 1990s. However, the size and weight of conventional grating spectrometers like MAHRSI renders them impractical for future long-duration space flight opportunities. As an alternative, the Spatial Heterodyne IMager for MEsospheric Radicals (SHIMMER),² which is based on a breakthrough interferometric technique called spatial heterodyne spectroscopy (SHS), has been designed to make OH measurements similar to MAHRSI's while requiring far fewer spacecraft resources. SHIMMER flew on the Space Shuttle Atlantis mission STS-112 in October 2002. It has the advantages of high throughput, high spectral resolution, small size, and low mass, all in a rugged instrument with no moving optical components. The Shuttle flight successfully demonstrated, for the first time, the suitability of SHS for spaceflight applications.

The SHS Concept: SHS is similar to a Fourier transform spectrometer (FTS), with the mirrors in the Michelson interferometer arms replaced by fixed, tilted gratings equidistant from the beamsplitter. Diffraction at the gratings results in a wavenumber-dependent tilt of the wavefronts recombining at the beamsplitter, and interference of the tilted wavefronts creates Fizeau fringes at the instrument's fixed charge coupled device (CCD) detector (Fig. 8). The Fourier transform of the interferogram produced at the CCD yields the incident spectrum. The angle and groove density of the gratings is selected so that for a chosen wavelength, the beams retro-reflect along the optical axis, thus producing no interference fringes. Incident light at wavelengths close to this (heterodyne) wavelength produces fringes that are sampled at the CCD. When viewing the Earth's limb from space, the scene is imaged on the gratings and the gratings are imaged on the CCD, with the dispersion plane parallel to the horizon. Limb scanning is avoided since the detector

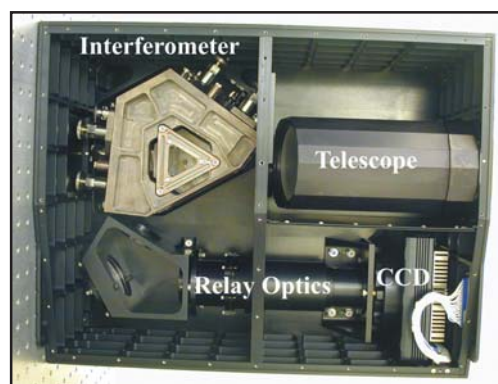
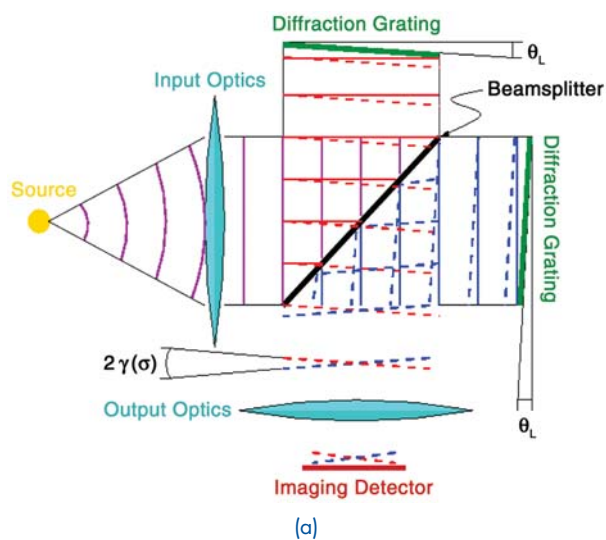


FIGURE 8
(a) SHS conceptual diagram and (b) the SHIMMER instrument.

simultaneously records interferograms in each horizontal row of the CCD corresponding to discrete altitudes.

The SHIMMER Instrument: Figure 8 includes a photograph of SHIMMER. The spectral resolution (0.0059 nm), passband (307-310 nm), field-of-view ($2.3^\circ \times 2.3^\circ$), and sensitivity requirements of SHIMMER were determined using previous successful MAHRSI OH measurements. The telescope focuses the limb on the gratings, imaging altitudes along the columns of the CCD while producing interferograms along the rows. The interferometer uses a nonpolarizing beamsplitter, a pair of field-widening prisms, and a pair of 1200 l/mm gratings. Relay optics focus the plane of the gratings on the CCD. The interferometric elements are mounted in the triangular Vascomax steel structure, allowing very precise and stable positioning of the prisms and gratings relative to the beamsplitter.

Measurement Results: Figure 9 shows an important measurement result for the SHS proof-of-concept. Since SHIMMER images the entire altitude range of interest simultaneously, and since the UV signal varies greatly over this range, minimization of scattered light in the instrument is critical. The triangles show the profile imaged by SHIMMER, and the dashed line shows the profile measured by MAHRSI (with its narrow field-of-view scanning up and down the limb). The figure demonstrates that SHIMMER succeeded in accurately imaging the profile. The highest spectral resolution mesospheric OH resonance fluorescence spectra ever measured were retrieved from the data (Fig. 10). Work in progress indicates that the radiance and noise evident in the spectrum

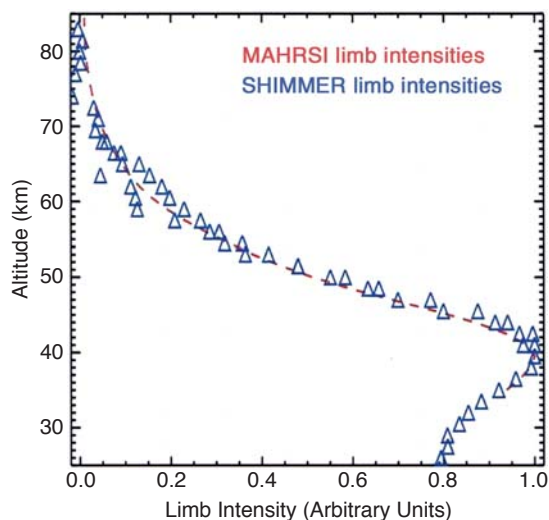


FIGURE 9
Limb altitude intensity profile (peaks normalized to 41 km).

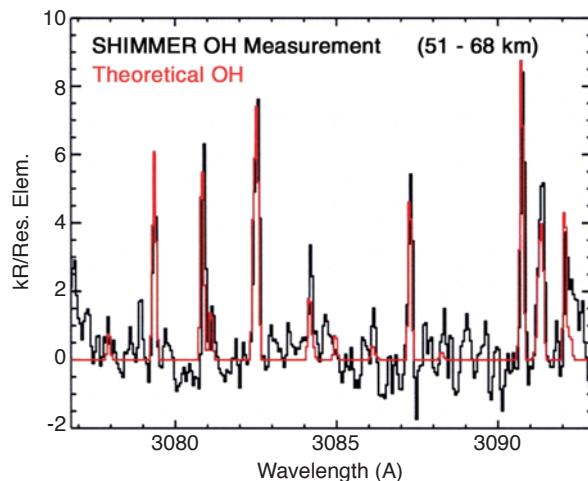


FIGURE 10
Hydroxyl spectrum (51-68 km).

are near expectations. Because of operational and limb viewing constraints, only 36 s of OH data were acquired. Nonetheless, the retrieval unambiguously demonstrates that SHIMMER accurately measured the UV emission from the limb at high spectral resolution.

Summary: Data from the STS-112 mission demonstrate that SHIMMER met its design goals. It produced high spectral resolution solar and OH spectra over a broad altitude range without the use of any moving optical components. The mesospheric OH measurements provide an important supplement to those made by the much larger and heavier MAHRSI instrument, and the mission has provided a successful and invaluable proof-of-concept of the innovative new SHS technology for space-based remote sensing.

Acknowledgments: The mission's success was made possible by the dedicated efforts of R. Feldman, J. Moser, L. Marlin, C. Brown, and the integration and operations team at the DOD Space Test Program Shuttle and ISS Payload Office. This research was supported by grants from the National Science Foundation, the Low Cost Access to Space Program of NASA's Office of Space Science, and the U.S. DOD Space Test Program.

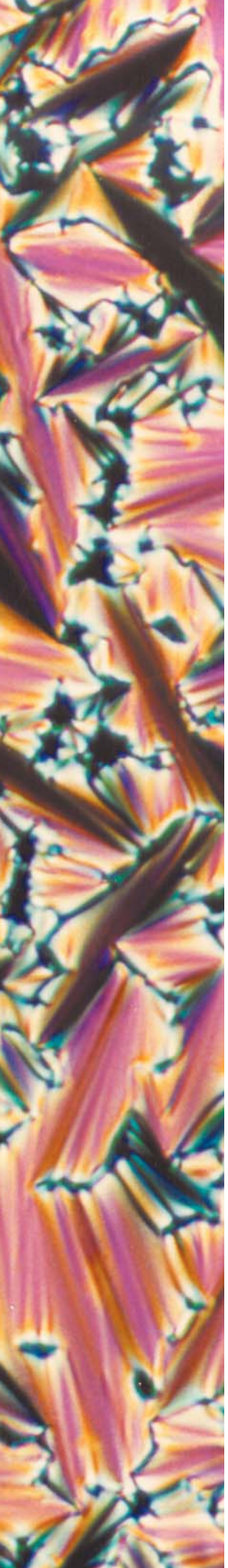
[Sponsored by ONR]

References

- ¹R.R. Conway, M.H. Stevens, C.M. Brown, J.G. Cardon, S.E. Zasadil, and G.H. Mount, "The Middle Atmosphere High Resolution Spectrograph Investigation," *J. Geophys. Res.* **104**, 16327-16348 (1999).
- ²J.M. Harlander, F.L. Roesler, J.G. Cardon, C.R. Englert, and R.R. Conway, "SHIMMER: a Spatial Heterodyne Spectrometer for Remote Sensing of Earth's Middle Atmosphere," *Appl. Opt.* **41**, 1343-1352 (2002).

FERROELECTRIC LIQUID CRYSTAL

This picture shows a texture smectic A mesophase of a ferroelectric side-chain liquid crystal at 145 °C. The cell (4 mm thick) containing the sample is placed between crossed polarizers. The bistable electro-optic effect is achieved by applying an external electric field across the cell that switches the molecules from one tilt direction to the other as the field is reversed. This material exhibits a switching time of ~600 ms at room temperature to ~150 ms at 140 °C. Potential applications include display devices (e.g., flat TV screens), transducers, pyroelectric detectors, and nonlinear optic devices suitable for optical computers.



177 Development of the Fiber Optic Wide Aperture Array: From Initial Development to Production

A. Dandridge, A.B. Tveten, and C.K. Kirkendall

179 High-Resolution Distributed Fiber Optic Sensing

C.K. Kirkendall, R.E. Bartolo, A.B. Tveten, and A. Dandridge

DEVELOPMENT OF THE FIBER OPTIC WIDE APERTURE ARRAY: FROM INITIAL DEVELOPMENT TO PRODUCTION

A. Dandridge, A.B. Tveten, and C.K. Kirkendall
Optical Sciences Division

Introduction (1986-1990): In the late 1970s, NRL began the development of fiber optic sensors for Navy surveillance applications.¹ The initial thrust was fiber optic acoustic sensors for towed arrays. The basic approach used a passive fiber interferometer to measure acoustically induced fiber strains (using techniques of fiber strain amplification) while the interrogating laser and processing electronics were located remotely from the fiber sensor array. While the technology for remote interrogation and multiplexing of fiber sensors was proceeding for towed arrays, the use of fiber optic sensors for hull-mounted arrays was being considered. By the late 1980s, NRL became actively involved in developing both fiber optic hydrophone designs, multiplexing approaches, and laser sources for the hull-mounted hydrophone systems. Initial work concentrated on both low-frequency (12×12 in.) and midfrequency hydrophones (less than 5×5 in.). By the late 1980s, however, it became clear that the most likely transition path was the development of a midfrequency range, area-averaging hydrophone to form a lightweight version of the Navy's Wide Aperture Array (WAA) hydrophone system for fast attack submarines (the Lightweight Wide Aperture Array, LWAA). The system provided major weight savings and allowed for

easier and less costly technology-refresh by moving all the electronics and active optics inboard. Figure 1 shows the system concept.

Technical challenges included designing an area-averaging fiber hydrophone with a flat response, more than an order of magnitude higher in frequency than existing designs. This was achieved by incorporating two, fiber-wrapped, air-backed metal mandrels whose acoustic responsivity was optimized for the operational hydrostatic environment. A second challenge was to provide a low noise interrogation/multiplexing approach to accommodate reliability requirements, minimize the number of fibers needed to interrogate the array, and allow sufficient bandwidth for high frequency, wide dynamic range signals. This was accomplished by using a lithium niobate phase modulator to produce the phase carrier and a modified FM-phase generated carrier interrogation/multiplexing approach. Finally, to meet the stringent noise requirements of the system, NRL identified a neodymium YAG solid state laser operating in the $1.3\text{-}\mu\text{m}$ band. Unlike the semiconductor laser being used at the time for fiber sensor interrogation, which missed the noise floor by ~ 25 dB, the fast roll-off with frequency of the FM noise of this Nd:YAG source allowed the noise floor to be met with usable margin.

The Prototype System (1990-1993): After NRL had demonstrated each of these basic building blocks of the system (and performed preliminary flow noise testing of the two-mandrel fiber hydrophone²) a contract was awarded to Litton Guidance and Control Systems (now Northrop Grumman) to build a 49-channel prototype array for flow noise testing at Lake Pend Oreille, Idaho,

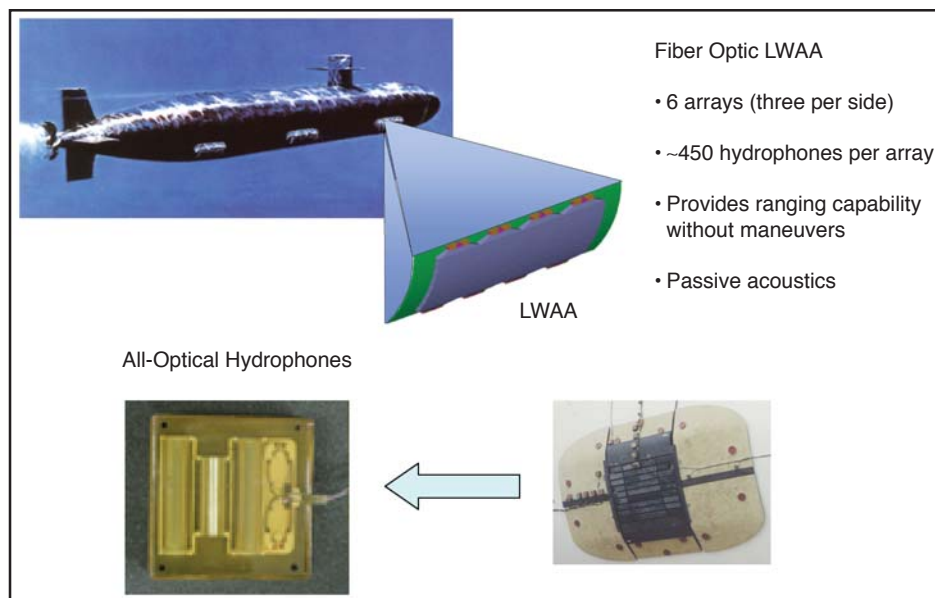


FIGURE 1
System concept.

and acoustic/vibration testing at Seneca Lake, New York. This effort was funded by an Advanced Technology Demonstration (ATD) program sponsored by the Naval Sea Systems Command. During this period, NRL (and the Naval Undersea Warfare Center (NUWC), which had responsibility for the mechanics of the array) worked closely with the contractor to ensure that this subarray would meet all the Navy's stringent specifications. This required moving to a five-mandrel design. This often required NRL to perform a number of important tests (in 1991 and 1992) to demonstrate specific technology approaches to the team that would have to be followed if the ATD were to be successful. One particular area where NRL played a major role was in defining critical performance parameters of the demodulator. Figure 2 shows an example of NRL improvements to the performance of the demodulator during flow noise testing. These tests also allowed NRL to demonstrate improvements to the baseline system, some of which would be used in the preproduction and production systems. In 1993, the prototype ATD array performed all the required tests successfully, which paved the way to the next stage of development.

Advanced Development (1994-1999): After the successful completion of ATD, Litton was tasked with designing the system with production in mind. One of the major changes was going to a two-mandrel, air-backed polycarbonate mandrel hydrophone. Fortunately, NRL

had already demonstrated this basic design three years previously and we were able to verify the flow noise performance without incurring another costly flow noise test. NRL also played a major role in keeping the program on track after the contractor lost key personnel during the telecommunications boom. On numerous occasions, only NRL had the detailed system design knowledge to overcome numerous technical challenges that had to be overcome to allow the system to meet performance specifications in all acoustic/pressure environments.

Production System (2000 and On): Much of the production phase involved packaging the required components and required modifications of the hydrophone to ease manufacturability. During this phase, NRL's participation was much reduced; however, we still played a significant role in qualifying hydrophones built with optimized construction techniques. We also continued optimizing the various algorithms required for low noise demodulation of interferometric signals. In August 2003, the lead ship of the Navy's latest class of attack submarine, the USS *Virginia*, was christened (Fig. 3). The sonar suite of this vessel includes the Fiber Optic Wide Aperture Array, the first fiber optic surveillance grade acoustic sensor system on an operational platform. The current system still uses the basic hydrophone concept, interrogation/multiplexing, and laser proposed by NRL in the late 1980s.

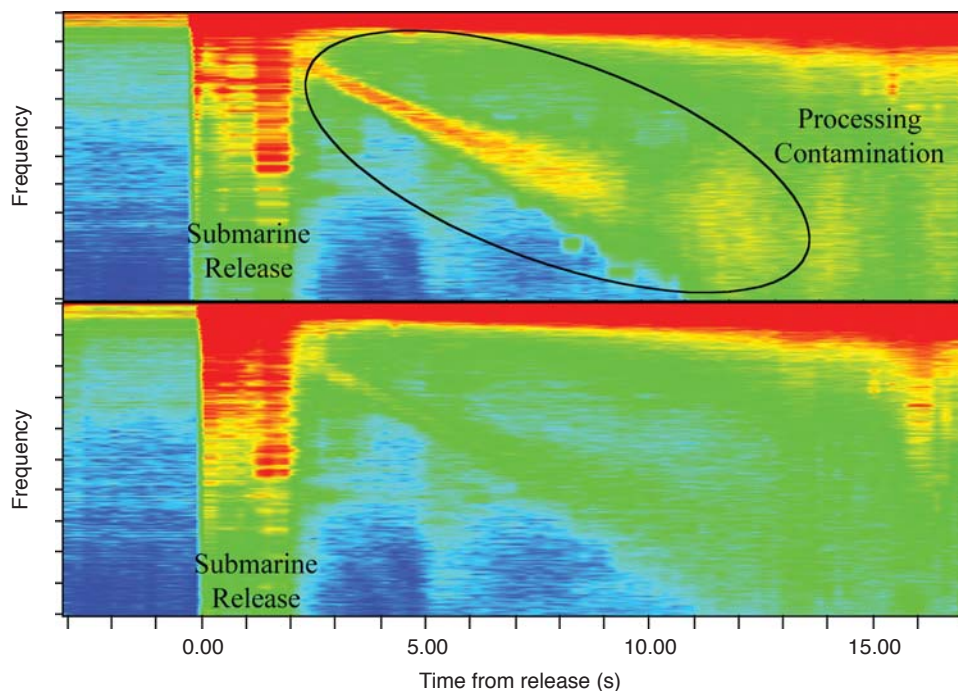


FIGURE 2 Improved noise performance with NRL processing under “pop-up” conditions. Upper figure: conventional fiber optic processing, lower figure: NRL processing, contamination reduced by up to 20 dB.

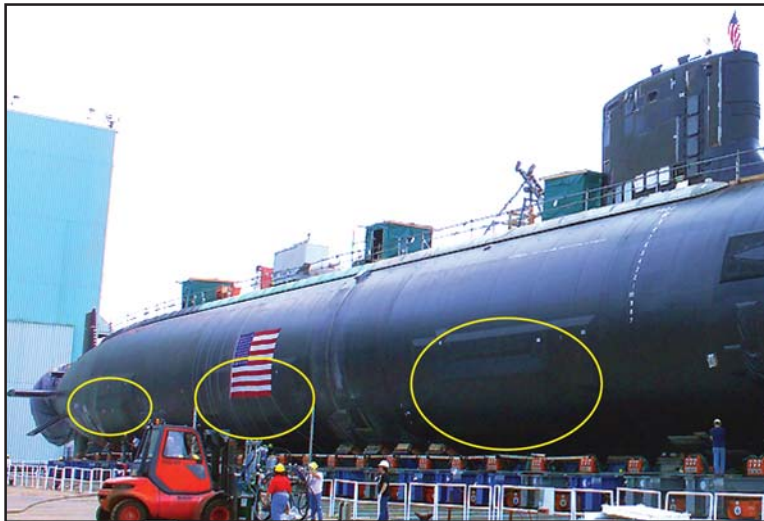


FIGURE 3
USS Virginia, hull array patches circled.

Acknowledgments: The authors acknowledge the help and support of Gary Cogdell of NRL and Aileen Sansone, previously of NRL, and Roger Maple, previously at NUWC. The authors also acknowledge the work of the Northrop Grumman team who made this system a reality.

[Sponsored by NAVSEA]

References

- ¹A. Dandridge and G.B. Cogdell, "Navy Applications of Fiber Optic Sensors," *IEEE Lightwave Comm. Syst.* 2, 81-89, (1991).
- ²A. Dandridge, A.B. Tveten, and A.M. Sansone, "Flow Noise Performance of Air-backed Plastic Mandrel Hydrophones on the KAMLOOPS Buoyant Test Vehicle," *JUA(USN)* 50, 601-625 (2000).

HIGH-RESOLUTION DISTRIBUTED FIBER OPTIC SENSING

C.K. Kirkendall,¹ R.E. Bartolo,² A.B. Tveten,¹ and A. Dandridge¹

¹*Optical Sciences Division*

²*SFA Incorporated*

Introduction: Fiber optic sensing has several key advantages over conventional sensing approaches. These advantages include lower cost and high reliability, and the sensors are electrically passive. High-performance fiber optic sensors are typically based on interferometric techniques that can detect extremely small changes in the phase of the light that has traveled through different paths. Fiber optic sensing technology is naturally evol-

ing toward simpler transducers and optical architectures. Figure 4(a) shows notional optical architecture for a time-division multiplexed (TDM) sensor array using Michelson interferometers. Each sensor channel in the TDM architecture (shown in gray) requires three fiber optic couplers, two mirrors, an optical delay coil, and at least eight optical splices (not shown) to connect the individual components. Although the component costs are reasonable, the touch labor required to assemble each sensor increases the cost. In-line configurations, like that shown in Fig. 4(b), significantly reduce the component count and the required assembly time. In this configuration, the optical delay coil is merged with the sensor coil and each channel shares a mirror with the adjacent channel. While a significant improvement, touch labor is still required to make at least two optical splices per channel. Replacing the coupler-mirror components in Fig. 4(b) with fiber Bragg gratings (FBGs) further simplifies the architecture. The FBG, a wavelength-specific mirror, is written directly into the optical fiber and requires no external components or splices. With FBG mirrors, the architecture reduces to that shown in Fig. 4(c) in which the optical fiber in the system is a single continuous length of fiber. This allows automated manufacturing techniques to be applied, which significantly reduces the cost of the system. The next step in this evolution is to eliminate the FBGs and use inherent properties of the optical fiber to form the mirrors between the sensors, as shown in Fig. 4(d). This promises the lowest cost since no optical components are required and no special processes need to be applied to the fiber. In this architecture, the mirrors are "virtual" and can be formed anywhere in the fiber, allowing the array design to be dynamic with variable sensor location and aperture. This allows truly unique capabilities for an adaptive array that can be dy-

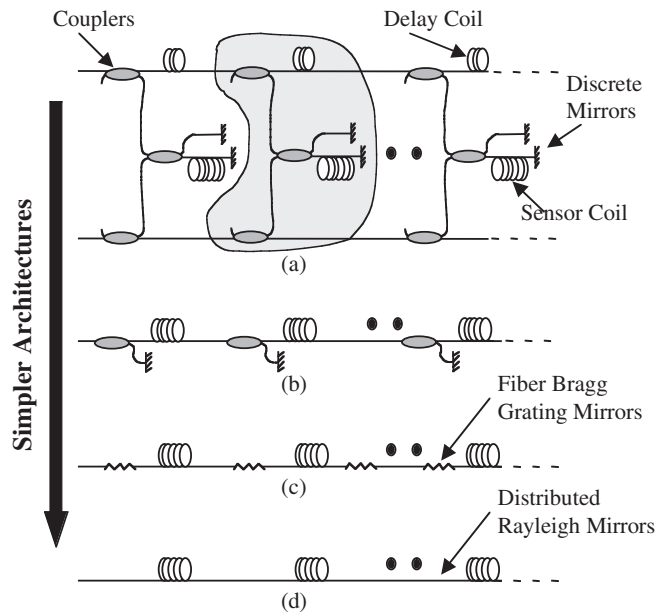


FIGURE 4 The trend toward simpler fiber optic multiplexing architectures; from discrete coupler based interferometers (a), to in-line Michelson configurations (b, c) with fewer components, to Rayleigh based architectures (d) which use inherent properties of the fiber itself and require no additional optical components.

namically optimized to detect and track a particular target or reject a strong interfering signal.

Concept: This vision can be realized by using the inherent backscattered signal in an optical fiber that results from random fluctuations in the index of refraction. This is the same principle used in optical time domain reflectometry (OTDR) in which the Rayleigh backscattered signal is examined for attenuation variations or breaks over a length of optical fiber. In our approach, instead of using the amplitude of the Rayleigh signal, we extract the phase information from the backscattered signal.^{1,2} The phase of the backscattered signal is extremely sensitive to path length variations, and length changes as small as 20 pico-meters can be detected with this approach. Depending on the aperture, this corresponds to strains in the 0.2 to 10 pico-strain range, which is an extremely sensitive strain sensor. Figure 5 shows a simplified block diagram using a receiving interferometer. Here, a pulse of light is passed through an optical circulator to interrogate a length of fiber. As the probe pulse travels through the sensing fiber, light is scattered back toward the circulator. The circulator routes this backscattered signal to a receiving interferometer with a path mismatch of ΔL between the two arms. The receiving interferometer delays the return signal by different amounts such that the backscattered light from two different sections of sensing fiber interfere at the output of the interferometer. The phase information from the

backscattered signal can be extracted by monitoring the interference pattern. For each input pulse into the sensing fiber, the output of the receiving interferometer is a continuum of interference signals over a spatial aperture of $\Delta L/2$. The physical location of the scattered signal is encoded in the time-of-flight of the return signal. Different locations in the sensing fiber can be monitored by selecting a different time slice in the return signal. For this configuration, the spatial aperture is set by the path difference in the receiving interferometer, which is fixed. It is relatively straightforward to reconfigure the electro-optics system to support a truly variable aperture on a pulse-to-pulse basis.

Results and Applications: To demonstrate the sensitivity and spatial accuracy of this approach, a 180-m test fiber was interrogated. The test fiber contained three independently modulated 30-m segments, each separated by 10 m. Figure 6 shows the spectral output as a function of distance. The three 30-m sections are modulated at different frequencies, and the modulation on the third segment has been attenuated by 30 dB. These drive levels correspond to strains of ~200 nano-strain and 6 nano-strain, respectively.

We have applied this interrogation technique to a number of applications—from high-performance acoustic arrays to high-spatial-resolution structural monitoring applications. The unique capabilities of this interrogation approach make it very useful in many application areas.

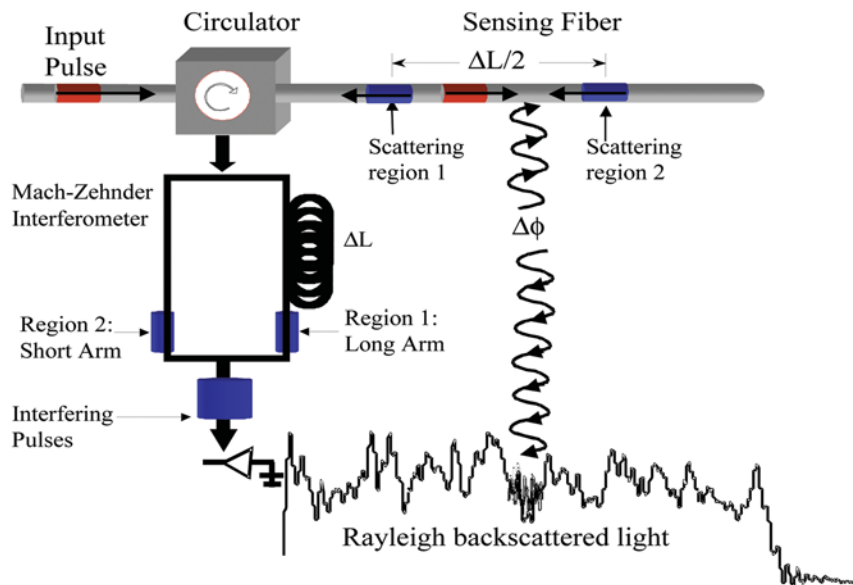


FIGURE 5
Example Rayleigh backscatter interrogation system block diagram.

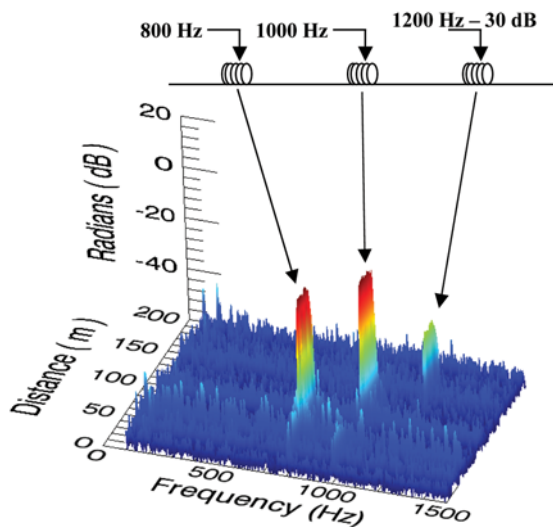


FIGURE 6
Interrogation system output of a 180-m long test fiber with three 30-m fiber segments separated by 10 m each and modulated at 800, 1000, and 1200 Hz, respectively. The last 30-m segments modulation amplitude is reduced by 30 dB.

We have recently applied this technology to the characterization and demodulation of coated fiber sensors. This is an enabling technology for coated fiber sensors systems that apply specialized coatings directly to the optical fiber to increase the coupling from the desired measurand to the optical fiber. Coated fiber sensors represent the lowest cost sensor technology in which a coating is simply extruded on a continuous piece of optical fiber.

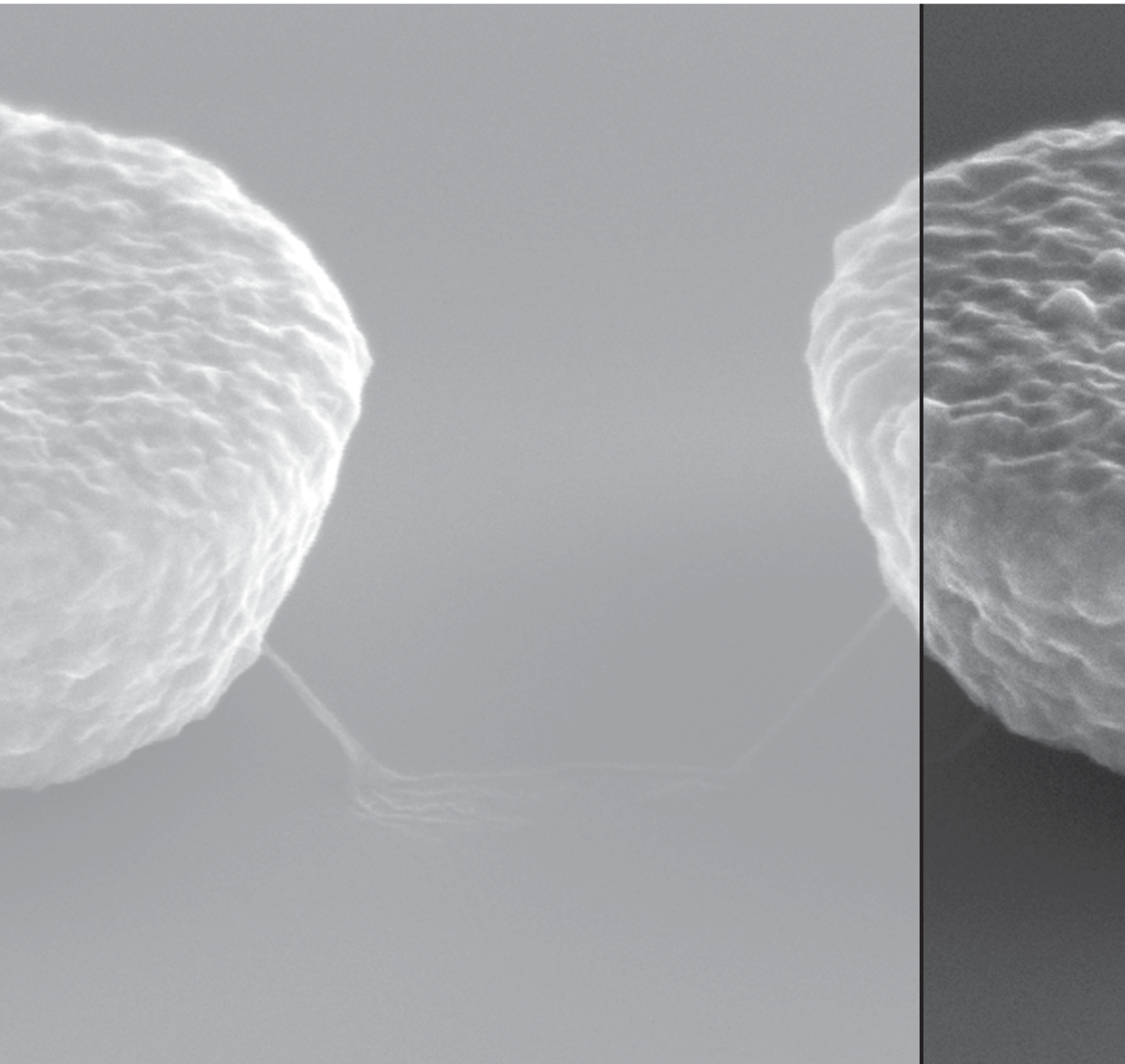
The Rayleigh scattering approach has been demonstrated over several kilometers, and 10- to 20-km segments appear to be achievable. Long sensing lengths combined with the high strain and spatial resolution

makes this an attractive and cost-effective sensing approach for many homeland security applications.

[Sponsored by ASTO and ONR]

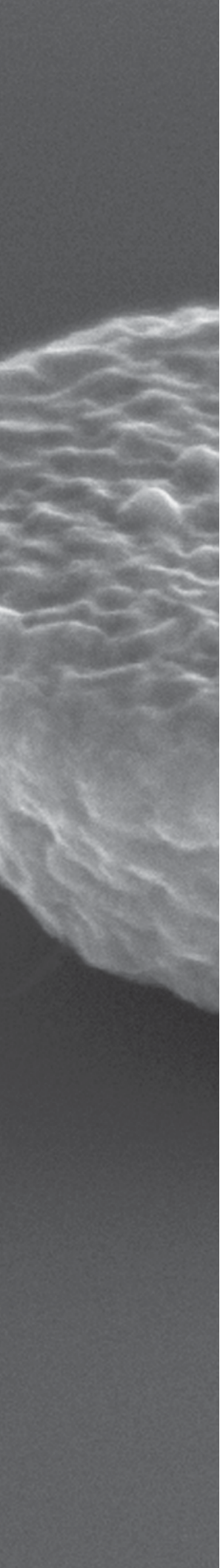
References

- ¹M.D. Mermelstein, A. Tveten, C.K. Kirkendall, and A. Dandridge, "Double-Pulse Heterodyne Rayleigh Backscattering in an Acoustically Driven Single-Mode Optical Fiber," NRL-FR-9932, 1999
- ²M.D. Mermelstein, R. Posey, G.A. Johnson, and S.T. Vohra, "Rayleigh Scattering Optical Frequency Correlation in a Single-mode Optical Fiber," *Opt. Lett.* 26, 58-60 (2001). •



CARBON NANOTUBE BUNDLE ATTACHED TO ELECTRODES

Scanning electron micrograph of a carbon nanotube bundle spanning electrodes fabricated from a ferromagnetic nickel alloy. Magnetic fields generated within the device were used to align and accurately place the nanotubes.



185 Unattended Ground Sensor Network

J. Heyer and L.C. Schuette

186 Measurement of Ocean Wave Spectra and Surface Slopes by
Polarimetric SAR

D.L. Schuler and J.S. Lee

188 The Lowest Frequency Detection of the Black Hole at the Center
of Our Galaxy

M.E. Nord, T.J.W. Lazio, N.E. Kassim, W.M. Goss, and N. Duric

191 High-Resolution Infrared Ocean Imagery

G.O. Marmorino, G.B. Smith, and G.J. Lindemann

UNATTENDED GROUND SENSOR NETWORK

J. Heyer and L.C. Schuette
Tactical Electronic Warfare Division

Introduction: NRL's Tactical Electronic Warfare Division (TEWD) scientists are exploring a novel unattended ground sensor network, the Adaptive Reactive Sensor and Effector Network and Insertion Capability (ARSENIC). The system is a heterogeneous mixture of unattended ground sensors and effectors that provide an adaptive distributed system with the ability to detect signals of interest and influence the environment. Key considerations for our unmanned ground sensor and effector network include size, mission duration, delivery method, precise and covert emplacement, probability of detection, sensor ruggedization, network communications, and detection classification. Additional issues include reach-back communications, antennas, and data visualization. Results of this research will be directly applicable to parties interested in countering threat radar, Weapons of Mass Destruction (WMD), and vehicle and/or infantry movements.

Unmanned Delivery: Unattended ground sensor networks have typically been deployed by "putting boots on the ground," or from manned aircraft. NRL has significant experience with unmanned air vehicles (UAVs) and UAV payloads—thus the desire to capitalize on these efforts to use an unmanned asset to provide precise and covert placement. As currently designed, the ARSENIC network is composed of 48 physically identical nodes deployed from a Finder Unmanned Air Vehicle (Fig. 1). Finder was developed by TEWD and is currently deployed from a Predator (MQ-1L) aircraft, shown in Fig. 2 carrying two Finder UAVs. The Finder was chosen because it provides a 400 km combat radius and a precision



FIGURE 1
Finder unmanned air vehicle.



FIGURE 2
Finder aircraft on wing stations of Predator unmanned aircraft.

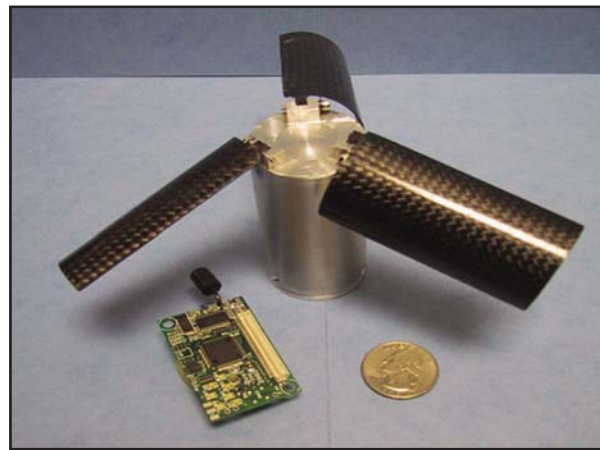


FIGURE 3
Prototype device using MJU-27B flare form factor.

emplacement delivery system. In the absence of satellite communications, Finder can also operate as an airborne tactical relay. The unattended node (Fig. 3) is configured in an MJU-27B form factor. The MJU-27B is a common chaff or flare round carried by U.S. Naval aircraft, such as the F/A-18 Hornet. (Also shown is a small circuit board that incorporates an integrated CPU and Local Area Network (LAN) radio and battery.) A U.S. quarter is shown for comparison. After being dropped from the Predator, the Finder UAV will fly a pre-programmed route. When the area of interest is reached, the ARSENIC nodes will be deployed from the Finder and the wings will extend, causing the node to spiral down.

Electronics: The electronics package includes a Texas Instruments MSP430F149 ultra-low power microcontroller, which provides limited computational ability, and a ChipCon CC1000 UHF transceiver, which provides a low-power communication network capability. Also shown in Fig. 3 is a lithium sulphur dioxide (LiSO₂) battery. An electronic warfare payload is incorporated into the node. The EW payload provides a jamming capability designed to work against radars and communication networks. Efforts are underway to in-

crease the mission duration by increasing the battery size while maintaining the same overall size and weight of the node.

Uses: The primary use of the ARSENIC system is to covertly deny the use of enemy radars and or communication equipment in tactically relevant areas. Because of the up-close placement, the power levels required can be extremely low. The ARSENIC system provides an established delivery system, volume, computational ability, and power bus for other sensors. Future efforts will involve creating a true multimodal network. The ARSENIC node is sufficiently large and of a robust design to incorporate infrared, chemical, seismic, or acoustic sensors. This would prove useful for covertly characterizing traffic on a road or on a mountain path. A heterogeneous network of ARSENIC nodes could be seeded along a road to provide multispectral in situ assessment.

Data Visualization: A critical piece of an unmanned sensor and effector system is the command and control infrastructure. TEWD scientists have developed a radio frequency (RF) tactical decision aid called Builder. Builder is a PC-based tool for visualizing RF energy in a geospatial manner. Builder provides the operator an assessment of the internode communications and of the ability of the jammers to effect threat assets based on geometry and radiated power levels. The ARSENIC network uses the Builder Radio Frequency Tactical Decision Aid to assist both in the placement of the nodes and for visualizing the data reports back from the nodes.

[Sponsored by ONR]

MEASUREMENT OF OCEAN WAVE SPECTRA AND SURFACE SLOPES BY POLARIMETRIC SAR

D.L. Schuler and J.S. Lee
Remote Sensing Division

Introduction: New methods that use the capabilities of fully polarimetric synthetic aperture radar (SAR) image data to measure ocean wave slopes and wave spectra have been developed. The methods have been tested by using aircraft-platform NASA/AIRSAR data obtained during flights over California coastal waters. Independent techniques have been developed to measure slopes in the SAR azimuth (flight) direction and the (orthogonal) range direction. Wave spectra measured using these new methods compare favorably with spectra developed using conventional intensity-based radar methods, and also with in situ National Data Buoy Center (NDBC) buoy data.

SAR instruments have traditionally operated by using a single polarization to measure wave-induced back-

scatter cross-section modulations. The backscatter measurements require a parametrically complex modulation transfer function (MTF) to relate cross-section values to physical wave properties, such as slopes or wave spectra.

In the Fourier-transform domain, orthogonal slope information is used to estimate a complete directional ocean wave slope spectrum. The advantage of using the new SAR algorithms is that a nearly direct physical measurement of the slope is made that does not require the use of a nonlinear, complex MTF.

A method¹ that senses modulations of polarization orientation angle is used to measure wave slopes in the azimuth direction. Slope magnitudes smaller than 1° are measurable. An eigenvector/eigenvalue decomposition parameter Alpha is used to measure wave slopes in the range direction.² Waves in the range direction cause modulation of the local incidence angle that, in turn, modulates the value of Alpha. From these azimuth and range slope pairs, a complete directional wave slope spectrum can be measured.

Ocean Slope Measurements: The wave-induced modulation in the orientation angle is directly related to the surface slope in the azimuth direction. To a lesser extent, the modulation is also dependent on the slope in the range direction and the incidence angle ϕ . The average incidence angle for each image pixel is known from the flight geometry, and the range slope is determined using an algorithm that relates Alpha modulation to the slopes of long waves propagating in the range direction. Combining the measurements of azimuth and range slopes provides complete ocean wave slope information in any direction. The RMS slopes determined using these new techniques agreed well with values calculated from the NDBC buoy data.

Wave Spectra (Azimuth Direction): NASA/JPL/AIRSAR data at L-band imaging a coastal area in northern California was used to determine how well the azimuth component of an ocean wave spectrum could be measured using orientation angle modulation. Figure 4(a) is an L-band, VV-polarization (pol), false color-coded image that shows the imaged area and the measurement test site. A wave system with an estimated dominant wavelength of 156 m is propagating through the site with a wave direction of 320°. Figure 4(b) shows an orientation angle wave spectra of this wave system vs wavenumber ($2\pi/(\text{wavelength})$) plotted radially. The white rings are located at 50-m wavelength intervals. The dominant wave, corresponding to a wavelength of 156 m, can be determined from this spectrum.

Figure 5(a) shows modulations in the polarization orientation angle induced by azimuth traveling ocean waves; Fig. 5(b) is a histogram of the orientation angles. The range of orientation angles was ± 4 deg.

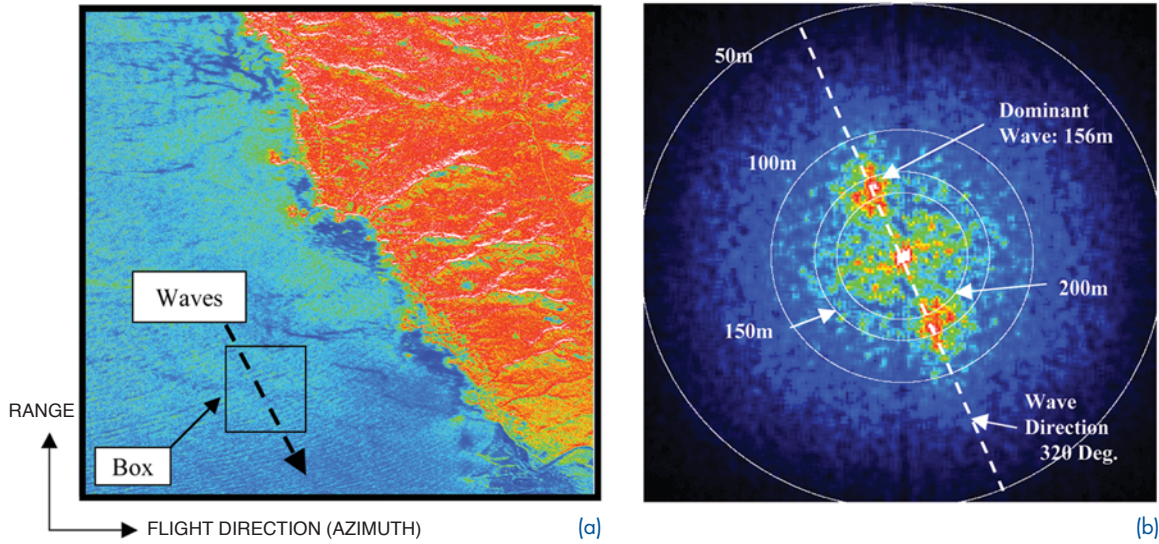


FIGURE 4
 (a) An L-band, VV-pol, AIRSAR image showing ocean waves propagating through the study area box. (b) Orientation angle spectra vs wavenumber for azimuth direction waves propagating in the study area. The dominant wave is propagating at a heading of 320°.

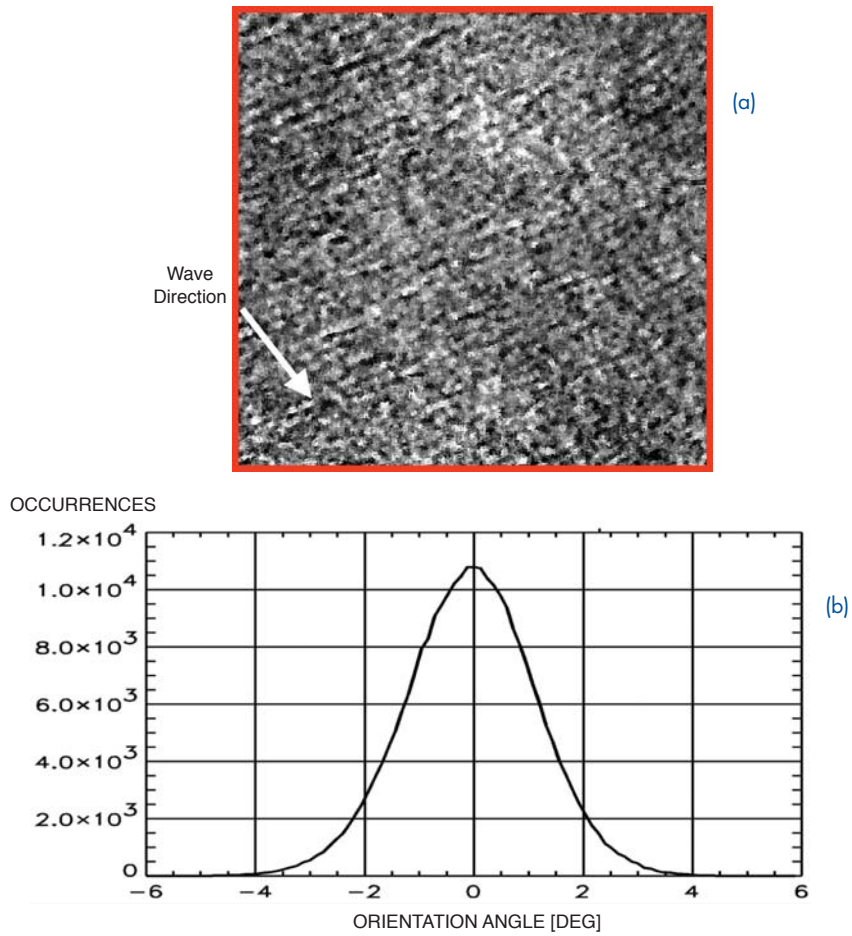


FIGURE 5
 (a) Modulations in the orientation angle image; (b) histogram of the distribution of orientation angle values.

Figure 6(a) presents a profile through the orientation angle spectrum made in the direction (320°) of maximum wave spectral energy. Figure 6(b) is a similarly directed profile, but it represents a conventional VV-pol image SAR intensity spectrum. It is apparent that the orientation angle spectrum has a much higher dominant wave spectral peak/background ratio than the SAR intensity spectrum.

Wave Spectra (Range Direction): A new concept has been investigated for SAR measurements of ocean slopes in the range direction. This concept was developed as a means of circumventing some of the difficulties associated with conventional backscatter intensity-based methods.

The Alpha parameter, developed from the Cloude-Pottier polarimetric decomposition theorem,² has useful properties for measuring slopes and slope spectra in the range direction. In the range direction, Alpha is sensitive to wave-induced modulations in the local incidence angle ϕ . In the azimuth direction, it is roll-invariant and, thus,

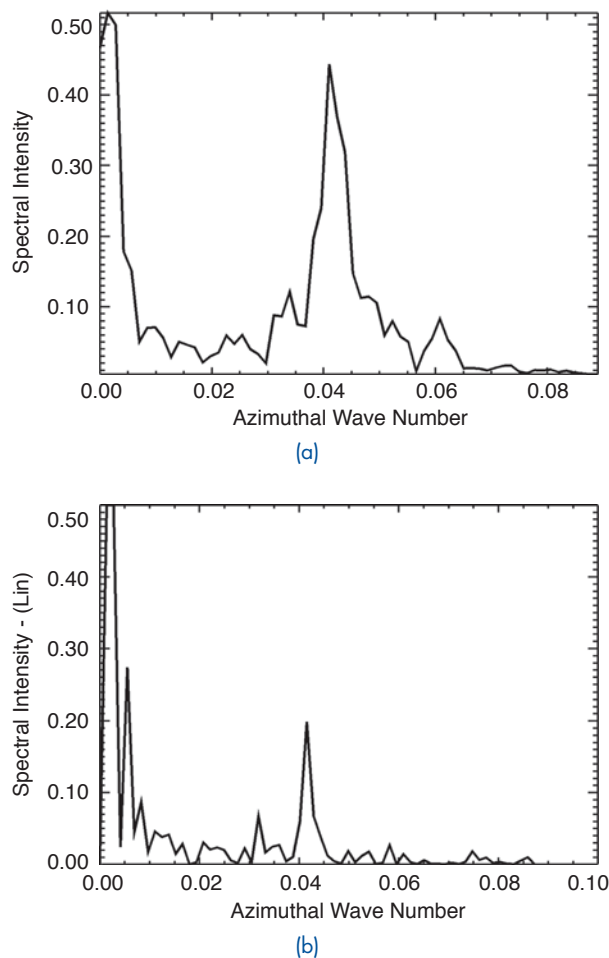


FIGURE 6
(a) Plots of spectral intensity vs wavenumber for wave-induced orientation angle modulations, and (b) for conventional VV-pol intensity modulations.

insensitive to azimuth slopes. Thus, the orthogonal slope measurement variables are well decoupled.

The wave spectra of range traveling waves can be determined using the Alpha parameter. A spectral profile was developed using the Alpha parameter technique, and a dominant wave was measured having a wavelength of 154 m and a propagation direction of 315° . The dominant wavelengths and wave directions determined from the wave spectra agreed well with NDBC buoy data.

Summary: New methods have been investigated that are capable of accurately measuring ocean slope distributions and wave spectra in both the range and azimuth directions. The new measurements are sensitive and provide nearly direct measurements of ocean slopes.

Using aircraft/satellite platforms, this new Navy remote sensing capability will provide large-area measurements of sea state in support of U.S. Navy Fleet operations.

[Sponsored by ONR]

References

- ¹D.L. Schuler, J.S. Lee, T.L. Ainsworth, and M.R. Grunes, "Terrain Topography Measurement using Multi-pass Polarimetric Synthetic Aperture Radar Data," *Radio Science*, 35(3), pp. 813-832 (2002).
- ²E. Pottier, "Unsupervised Classification Scheme and Topography Derivation of POLSAR Data on the $\ll H/A/\alpha \gg$ Polarimetric Decomposition Theorem," *Proc. of the 4th International Workshop on Radar Polarimetry*, IRESTE, Nantes, France, pp. 535-548, 1998.

THE LOWEST FREQUENCY DETECTION OF THE BLACK HOLE AT THE CENTER OF OUR GALAXY

M.E. Nord,^{1,2} T. J.W. Lazio,¹ N.E. Kassim,¹ W.M. Goss,³ and N. Duric²

¹Remote Sensing Division

²Physics and Astronomy Department, University of New Mexico

³National Radio Astronomy Observatory

Introduction: Early radio observations revealed that the central region of our Galaxy is radio bright and located in the constellation of Sagittarius. Subsequent observations showed that this region, known as Sagittarius A, is a complex of radio sources including a supernova remnant, several ionized hydrogen regions, and a radio point source known as Sagittarius A*. Studies of stellar and gas motions in the vicinity of Sagittarius A* strongly suggest the presence of roughly three million solar masses of dark mass in a region less than the size of the solar sys-

tem. This dark mass is now considered to be the black hole at the center of our Milky Way Galaxy.

Mass accreting onto the black hole is heated to great temperatures and is the source of the radiation coming from Sagittarius A*. This radiation has been detected at many frequencies in the radio regime (1 to 230 GHz) and recently in the near infrared and X-ray bands. However, one of the mysteries surrounding this object is its overall lack of emission, which suggests that either the black hole is not accreting at the rate expected, the accretion process creates radiation inefficiently, or both. Detecting Sagittarius A* at the widest range of frequencies will help elucidate the nature of its radiation processes.

Until recently, radio observations at frequencies below 1 GHz were severely limited by the Earth's ionosphere. However, recent work at NRL in conjunction with work at the National Radio Astronomy Observatory¹ has allowed for data-adaptive ionospheric compensation, and allowed this area of the radio spectrum to be observed with high spatial resolution.

Methodology: The Galactic Center region was imaged at the radio frequency of 330 MHz with the National Radio Astronomy Observatory's Very Large Array radio interferometer. Previous observations at similar radio frequencies had not detected Sagittarius A*. These nondetections were attributed to an ionized hydrogen region, known as Sagittarius A West, blocking emission from Sagittarius A* at frequencies below ~1 GHz. However, when imaging of the region was completed, a region of emission was observed at the location of Sagittarius A* (Fig. 7).

The region around the black hole thought to emit radio signals is less than 10 light-hours (the distance light travels in 10 hours, roughly 10^{10} km) in diameter (~0.5 mrad at a distance of 25,000 light years). However, density fluctuations in the interstellar plasma along the line of sight produce scattering that causes the observed size of the radio-emitting region to be much larger, with the size rising as the inverse square of the observation wavelength. When the 330 MHz size of Sagittarius A* is ex-

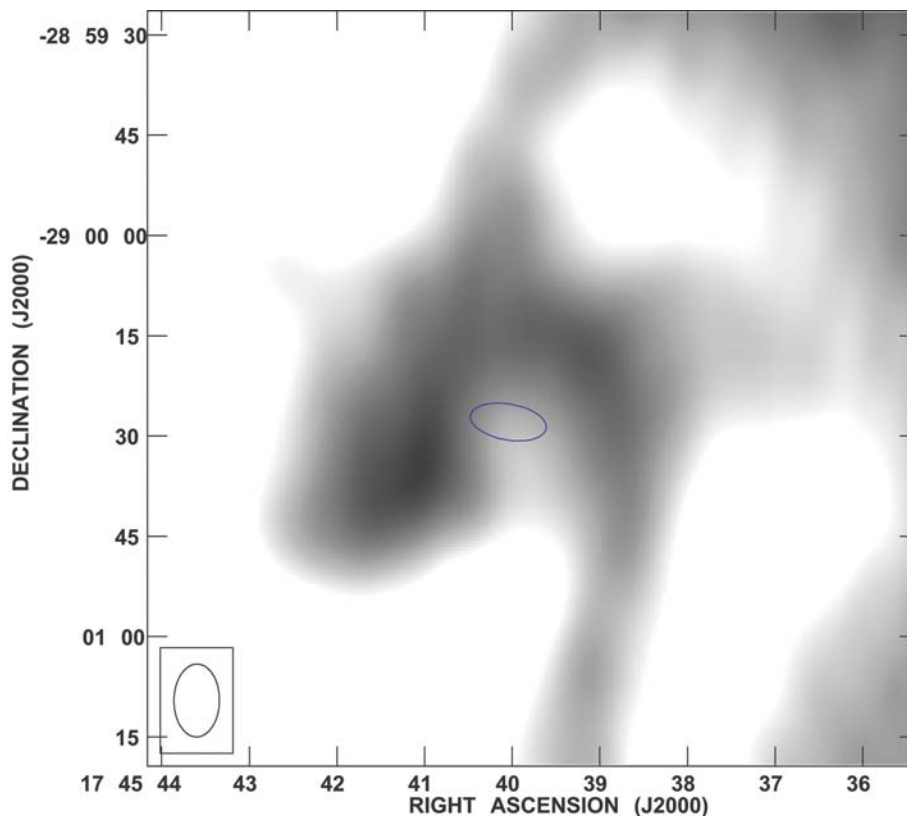


FIGURE 7

Image of the region surrounding Sagittarius A*. White areas indicate high brightness due to the background supernova remnant Sagittarius A East, dark regions indicate low brightness due to absorption by the ionized hydrogen region, Sagittarius A West. The blue oval in the center is the location and size of Sagittarius A* as extrapolated from higher frequency measurements. Note that a local maximum in 330 MHz intensity occurs at this location. The oval in the lower left represents the resolution element of the interferometer (33 by 53 μ rad). The image is roughly 0.5 mrad on a side.

trapolated from measurements at higher frequencies in this way, the expected 330 MHz size and shape agree well with the size and shape of the emission region in Fig. 7. Figure 8 demonstrates that the integrated brightness of the source also agrees well with measurements at higher frequencies. We therefore conclude that we have detected Sagittarius A* at 330 MHz; this is the lowest frequency at which it has ever been detected.

Interpretation: Little theoretical work has gone into modeling the emission of Sagittarius A* at frequencies below 1 GHz; the source was considered unobservable in this frequency regime. However, this detection does suggest several interesting properties of the region surrounding the black hole. As shown in Fig. 8, the integrated 330 MHz emission is what is expected from extrapolations from higher frequencies. Significant absorption from the Sagittarius A West ionized hydrogen region is seen along lines of sight near the source. Therefore, it is surprising that Sagittarius A* is detected at all at 330 MHz, much less at the level expected from extrapolations from higher frequencies. Although it is possible that the intrinsic brightness of Sagittarius A* is rising to offset partial absorption, we feel that the observation is best explained simply by the lack of any significant absorption along the line of sight.

The lack of absorption could be modeled in at least two ways. Either the absorbing medium is inherently clumped, with the line of sight to the black hole having low absorption by chance, or the black hole itself is responsible for evacuating the plasma in its immediate en-

viron. Unfortunately, our data cannot differentiate between these two possibilities, but both possibilities are of interest to understanding the environs of Sagittarius A*.

This detection also contains information about high-energy particles in the vicinity of the black hole. The radio emission of Sagittarius A* is synchrotron in origin; high-energy electrons spiraling around magnetic fields radiate according to their energy and the strength of the magnetic fields. This 330 MHz emission comes from electrons with lower energy than the higher frequency detections, probing the lower end of the high-energy particle spectrum.

Conclusions: We have used the Very Large Array radio interferometer to image the radio source associated with the black hole at the center of our Galaxy at the lowest radio frequency at which it has ever been detected. This detection was unexpected. Emission from the source was expected to be absorbed by intervening ionized gas at frequencies below ~1 GHz. The detection suggests that the line of sight to the black hole is relatively free of obscuring plasma, and it probes the high-energy particle spectrum of the region surrounding the black hole.

[Sponsored by ONR]

References

- ¹M. Nord, T.J.W. Lazio, and N.E. Kassim, "Imaging the Galactic Center at 74 MHz: Viewing Our Galaxy through the Last Electromagnetic Window," *NRL Review*, 2002.
- ²M. Nord, T.J.W. Lazio, N.E. Kassim, W.M. Goss, and N.E. Duric, "Detection of Sagittarius A* at 330 MHz with the Very Large Array," *Astrophys. J. Ltrs.*, accepted for publication. •

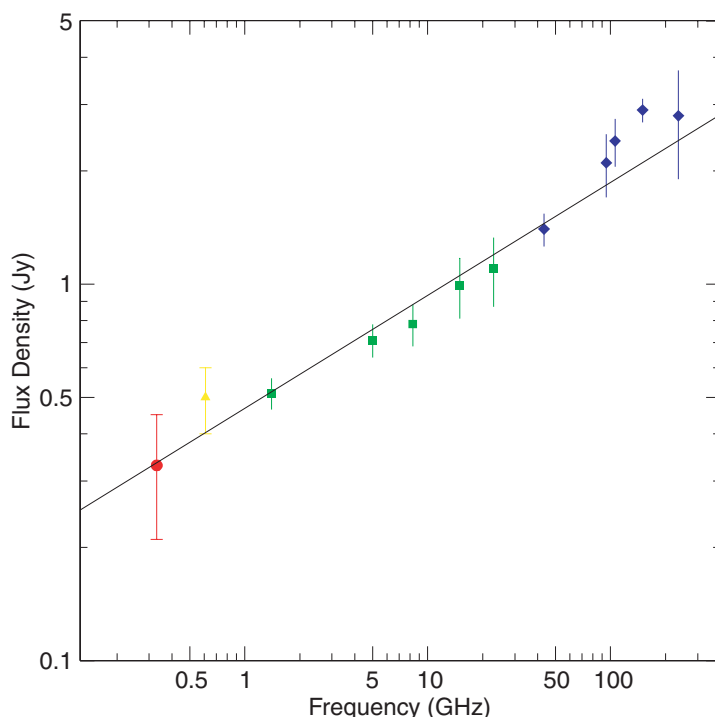


FIGURE 8

Radio spectrum of Sagittarius A*. The red point is this detection; the yellow point is a recent 610 MHz detection; green represents the radio regime; and blue is the sub-millimeter regime.² For reference, the solid line indicates a power law spectrum with a spectral index of 0.3. The integrated emission is on the abscissa and is in units of Janskys (Jy), with one Jansky being equal to $10^{-26} \text{ W M}^{-2} \text{ Hz}^{-1}$.

HIGH-RESOLUTION INFRARED OCEAN IMAGERY

G.O. Marmorino, G.B. Smith, and G.J. Lindemann
Remote Sensing Division

Introduction: When viewed in the infrared at meter-scale resolution, a normally bland ocean surface becomes covered with complex and fascinating patterns of intersecting dark streaks and elongated bright patches that reveal the underlying small-scale circulation of the ocean. Remarkably, because of the presence of a millimeter-thick ‘cool skin,’ these patterns are expected to occur, even if the underlying water has a uniform temperature. Understanding such patterns can lead to more realistic models of ocean currents, horizontal dispersion and vertical mixing, air-sea exchange processes, and acoustic propagation.

Physics of the Ocean Cool Skin: At small scales, it is hypothesized that infrared imagery reveals horizontal variations in currents through their interaction with the water’s cool skin. The cool skin is a thin thermal boundary layer through which heat flows upward by molecular conduction to match the atmospheric flux (i.e., the sum of the evaporative, radiant, and sensible heat transfers). This requires the surface temperature to be typically a few tenths of a degree less than that of the bulk water lying beneath. In areas where surface currents diverge, the cool skin is horizontally stretched and so it thins, resulting in a slight increase in surface temperature to maintain the heat flux; likewise, where surface currents converge, the cool skin is compressed and so it thickens, resulting in a slight decrease in surface temperature. Details of this conceptual model are being tested through comparisons of computer simulations and laboratory measurements.¹ For an upward heat flux of approximately 100 W/m^2 and low levels of ambient turbulence, the predicted temperature fluctuations due to horizontal straining are of the order of 0.1°C .

Aircraft Sampling: To see if these predicted fluctuations in surface temperature could be visualized, measurements were made using a digital, midrange infrared camera having a resolution of 0.02°C . The camera was deployed aboard a small, manned aircraft and oriented to view at nadir. Sampling was done in December 2002, over the inner West Florida continental shelf and near the mouth of Tampa Bay. Altitude was about 200 m, giving a surface resolution of 0.4 m. A variety of hydrodynamic phenomena were observed, including surface-penetrating turbulence, breaking waves, wakes, Langmuir circulation, and internal waves. The latter two, having been analyzed in detail, are described below.

Langmuir Cells: Under moderate winds, the imagery shows long, dark (cool) streaks that reveal a set of

counter-rotating cells called Langmuir circulation (Fig. 9). Surface convergences form between successive pairs of cells and are responsible for the cool streaks in the imagery. The spacing of the streaks in Fig. 9 is 10 to 20 m, but the water depth was only 3 m. This gives each cell an unusually large width-to-height aspect of about 2.5. Theoretical work² suggests Langmuir cells can become unstable through “pairing” of adjacent cells, resulting in adjacent streaks merging and individual streaks terminating. Evidence for this predicted behavior is clear in the infrared imagery (two circled areas). Such detailed structures persisted over several minutes and drifted with the downwind surface current.

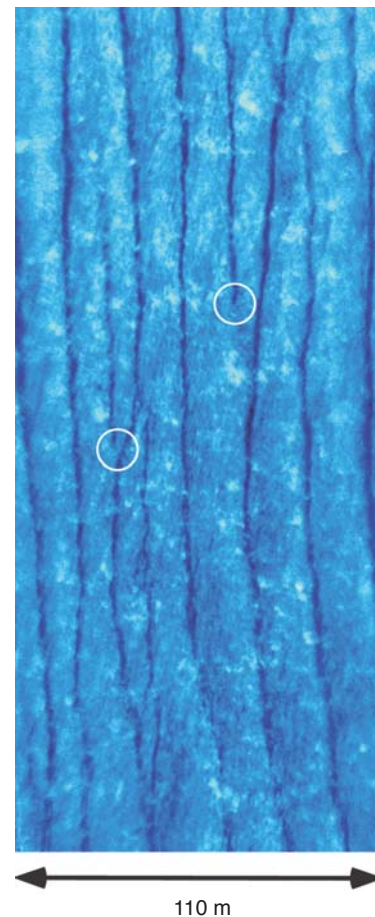


FIGURE 9 Nighttime infrared image showing long dark streaks caused by Langmuir cells. The streaks are about 0.2°C cooler than the ambient surface water. A wind of about 5 m/s was blowing from top to bottom, approximately parallel to the streaks. Upper circle highlights where one streak terminates; lower, where two other streaks merge. Such details persisted between successive aircraft passes and drifted downwind. Bright (warm) spots occurring throughout the image represent small-scale breaking waves.

Internal Waves: Under winds too low to generate Langmuir cells and surface waves, the imagery shows a pattern of both dark and bright bands (Fig. 10). These arise from the alternately converging and diverging surface currents of a group of about six internal waves. The left-most dark band is the leading edge of the group, which propagated seaward (toward the left) during late flood tide. In this case, the spacing of the dark bands (about 15 m) gives the wavelength of the internal waves. The temperature fluctuations induced by the internal waves are about 0.15°C , which is consistent with expectations. Fine structure within some bright bands may be caused by instabilities generated by vertical current shear within the waves themselves. Temperature variability on such scales would degrade acoustic signal coherence, for example.

Summary: High-resolution infrared imagery of the ocean surface has been obtained under low to moderate winds. The examples of Langmuir circulation and internal waves illustrate the effects of hydrodynamic straining of the cool skin. The infrared images are able to provide new and detailed views of such phenomena. Such views are not easily obtained with other imaging sensors, such as microwave radars that rely on backscatter from a wind-roughened sea surface. The imagery has raised some intriguing questions: Do the wide Langmuir cells result from interaction with the bottom? Can in-water measurements be made to confirm that internal wave instabilities are being imaged? Under what conditions does the imagery begin to reveal structures within the atmospheric boundary layer? These questions will be explored in follow-up studies.

Acknowledgments: The aircraft sampling was made possible through an interagency agreement with the National Oceanic and Atmospheric Administration.

[Sponsored by ONR]

References

- ¹R.I. Leighton, G.B. Smith, and R.A. Handler, "Direct Numerical Simulations of Free Convection Beneath an Air-water Interface at Low Rayleigh Numbers," *Phys. Fluids* 15, 3181-3193 (2003).
- ²S.A. Thorpe, "The Breakup of Langmuir Circulation and the Instability of an Array of Vortices," *J. Phys. Oceanogr.* 22, 350-360 (1992). •

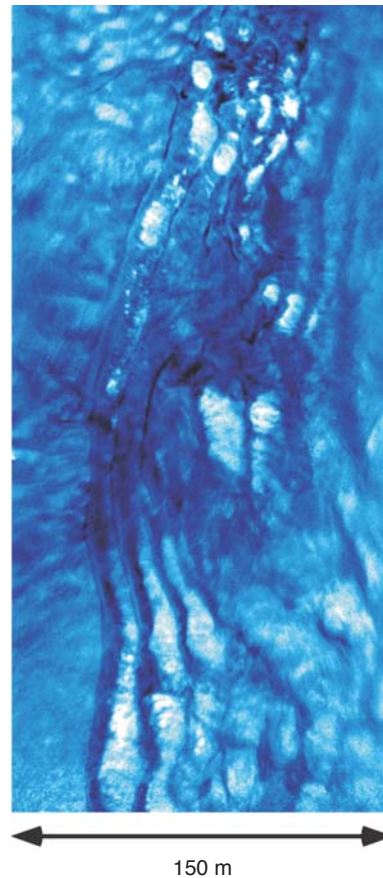
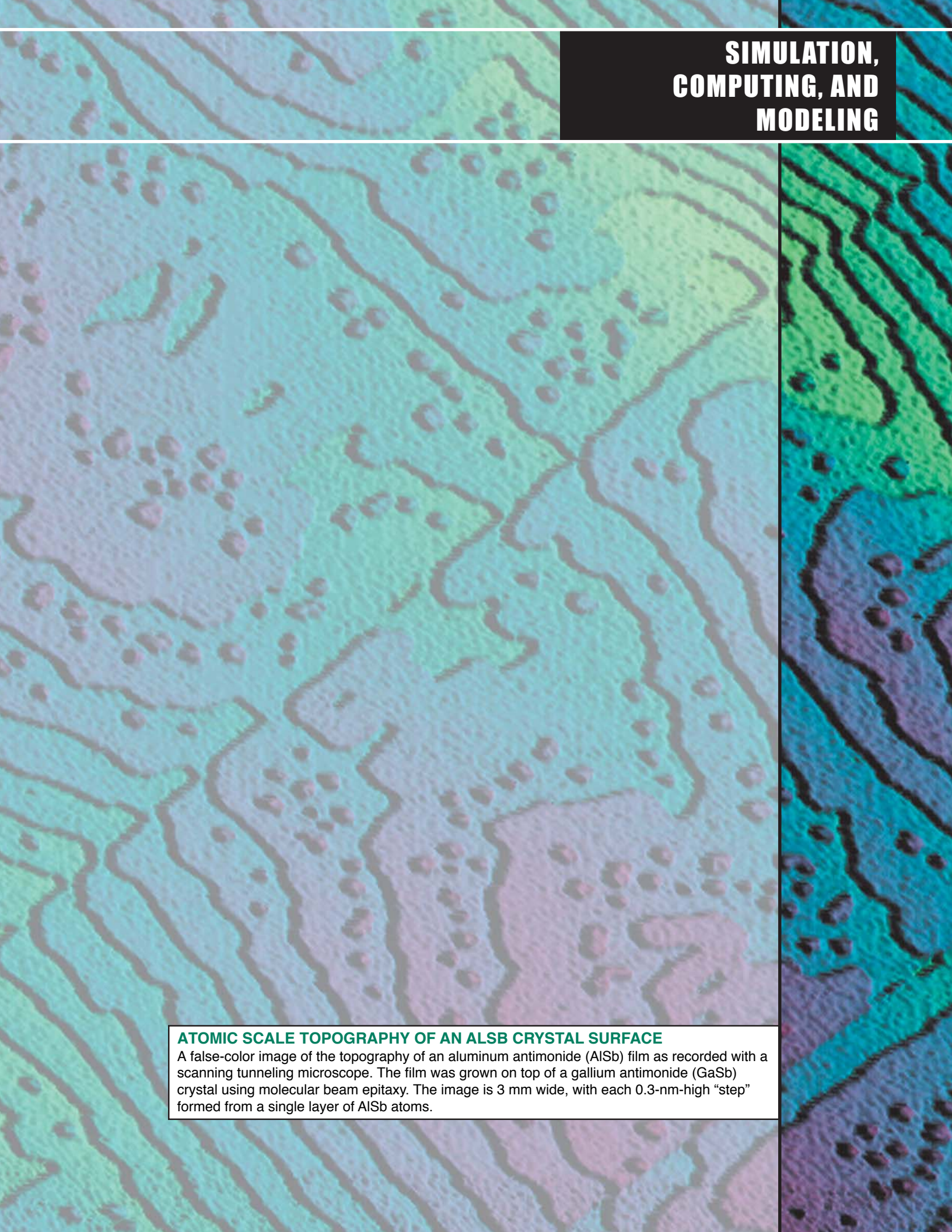


FIGURE 10

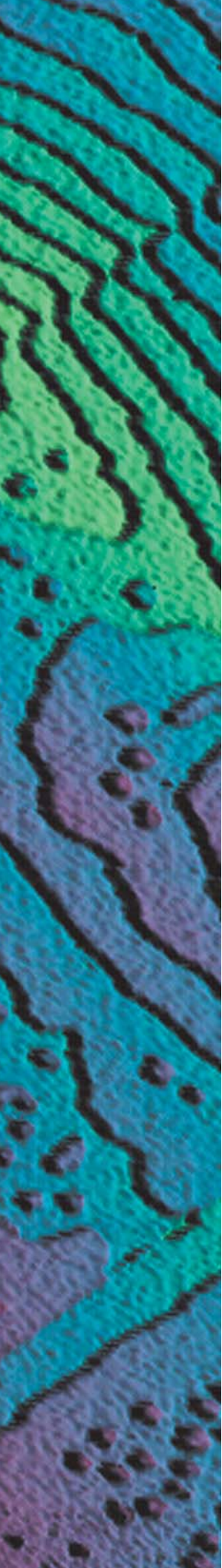
Daytime infrared image showing a group of about six internal waves—the dark and bright bands oriented top to bottom. The left-most dark band is the leading edge of the group, which is propagating toward the left-hand edge of the image. The distance between the more prominent dark bands is 15 m. Winds were light (about 1 m/s). The temperature variations in the image are about $\pm 0.15^{\circ}\text{C}$.



SIMULATION, COMPUTING, AND MODELING

ATOMIC SCALE TOPOGRAPHY OF AN ALSB CRYSTAL SURFACE

A false-color image of the topography of an aluminum antimonide (AlSb) film as recorded with a scanning tunneling microscope. The film was grown on top of a gallium antimonide (GaSb) crystal using molecular beam epitaxy. The image is 3 mm wide, with each 0.3-nm-high “step” formed from a single layer of AlSb atoms.



195 Human System Interface Assessment of the Sonar Workstation
During the USS *Nicholson* Integrated Undersea Warfare Sea Test

J.A. Ballas and B. McClimens

197 Autonomous Navigation Control of UAVs Using Genetic
Programming

C.K. Oh, G. Cowart, and J. Ridder

199 Electronics and Physics of Left-Handed Materials and Circuits

C.M. Krowne

201 Real-Time Wave, Tide, and Surf Prediction

R.A. Allard, J. Christiansen, T. Taxon, S. Williams, and D. Wakeham

HUMAN SYSTEM INTERFACE ASSESSMENT OF THE SONAR WORKSTATION DURING THE USS NICHOLSON INTEGRATED UNDERSEA WARFARE SEA TEST

J.A. Ballas and B. McClimens
Information Technology Division

Introduction: Future Naval surface combatants ships will have to do more with fewer people, and the Navy is addressing this challenge in several ways. The Naval Sea Systems Command (NAVSEA) has recently established the Human Systems Integration (HSI) Directorate (SEA 03) to certify that “ships and systems delivered to the Fleet enhance Sailor performance; optimize manpower, personnel and training; and promote personnel safety, survivability, and quality of service.” Such certification will occur only if HSI is considered throughout the design and development process, within each subsystem. In order to ensure superior capability in undersea warfare, even with reduced manning, NAVSEA’s Integrated Undersea Warfare for the 21st Century (IUSW-21) project supported the development and testing of an advanced sonar system, including a workstation with four touch screens and automation of sonar search, detection, localization, and classification, and intelligent interface capability.¹ The major participants (and their responsibilities) in the IUSW-21 project were the Naval Undersea Warfare Division-Newport (sea-test planning, management, and analysis), the Lockheed Martin Corporation (sonar processing subsystem), and the Raytheon Company (data fusion and workstation automation). NRL’s Naval Center for Applied Research in Artificial Intelligence was

brought into the project to develop and execute a plan to assess the operation of the workstation during the sea test aboard the USS *Nicholson*. The test occurred off the east coast of the United States during September-October 2002 in two phases. During the first phase, an echo-repeater was towed by another vessel to serve as a simulated target. In the second phase, a real target was deployed.

IUSW-21 System and Workstation: The technologies tested under the IUSW-21 program included several methods of transmitting and receiving sonar signals and new methods for data fusion. Additionally, methods of adapting the sonar signal to the environment were explored and tested. The IUSW-21 program also addressed ways to reduce manning by developing technologies that would enable a single operator (vice the four or more that are required in current surface sonar operations) to control the sonar system, interpret the information, and develop an integrated assessment of the underwater tactical situation. The single-operator workstation design included both new concepts in workstation design as well as new concepts in automating sonar watchstanding. Figure 1 shows the workstation deployed on the USS *Nicholson*. The overall design was developed by SPAWAR² with Office of Naval Research funding. The IUSW-21 sea test was the first operational use of this design, and it was therefore very important to obtain empirical data on its usage. The major features of the design are the three main displays and a User Interaction Panel (UIP) just in front of the operator that was used to interact with the automated sensor fusion system and to configure the displays. A keyboard and trackball were also available. The assignment of information to the three main displays was one of the primary design decisions in implementing the design. For the IUSW-21, the left dis-



FIGURE 1
Single-operator sonar workstation deployed on USS *Nicholson* for the IUSW-21 sea test.

play was used for the top-level geosituation (geosit) (TLG), which shows the overall sonar situation integrated with other tactical information. The center display had the Secondary Geosit (SG), which can show amplifying geo-information about a sonar track, such as data histories that are being fused together. The left display was used for drill down information such as sonar acoustic. The initial IUSW-21 design had the TLG in the center, with the SG on the right and the drill-down on the left. However, because there are occasions when two drill-down displays might be needed simultaneously, and because the TLG would always be present, the design taken to sea put the TLG on the right. This allowed placement of the two drill-down displays adjacent to each other on the left and center.

Workstation Operation Evaluation: During the sea test, the operation of the workstation was observed and recorded in real time using a personal digital assistant (PDA) with a transparent overlay that had the events to be observed, and a software application that time-stamped the stylus entries. The observer watched the operator and touched the event areas on the PDA overlay as they were observed. This method of observation and recording was used in lieu of computer recording because it provided an opportunity to record more events than keystrokes and was more flexible. Three categories of events were observed and recorded: (1) Where the operator is looking; (2) What the operator is doing manually; and (3) What is happening on the workstation screens. Twenty hours of workstation operation were observed, and 30,744 entries were made during 40 separate test events. In addition to observing the workstation operation, the operators were asked to complete subjective workload questionnaires. This article covers only the workstation operation.

Results: Time Spent Viewing Specific Displays and Eye Movement between Displays—Figure 2 summarizes usage of the three main displays and the User Interaction Panel (UIP) for the first phase of the test, and Fig. 3 summarizes the second phase. Overall, the operators were primarily engaged in the Top Level Geosit display, as intended, especially in the second phase of the test. There was also a decrease in time spent viewing the UIP in the second phase. This reflected less interaction with the automation control, as well as less manual configuration of the displays. There were other differences in the usage of the workstation between the two phases. These differences were due to the adoption of a strategy in the second phase of searching tactically salient areas (i.e., where they thought the target was located). This search involved looking at certain sensor information on the center display and acoustic information on the left display associated with the tactically salient areas. This strategy re-

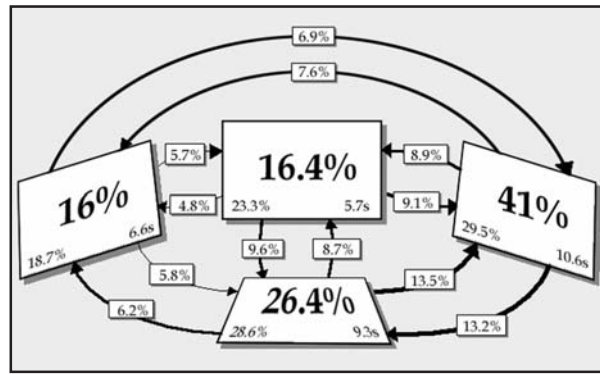


FIGURE 2 Usage of the four displays in Phase 1 of the sea test. The large percentages show the overall amount of time viewing a display. The arrows indicate the eye/head transitions between displays, as a percentage of all transitions. The smaller percentages indicate the total percentage of transitions to a display, and the last number is the average amount of time for each look to a display in seconds.

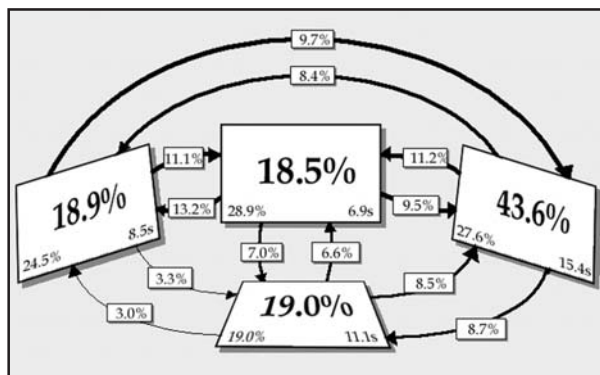


FIGURE 3 Usage of the four displays in Phase 2 of the sea test when an actual target was present.

quired more looks between the center and left displays, and longer average times on the right display.

User Interface Panel Interaction—The time spent looking at the UIP was highly correlated ($r = 0.88$) with the number of manual interactions with the panel (Fig. 4). Reducing the number of manual operations or simplifying them would have the direct effect of reducing the time needed to spend on the UIP and free up time for the main displays.

Impact: These empirical results (as well as the subjective workload results) have been incorporated into both Raytheon³ and NUWC⁴ reports of the sea test. On the basis of this work, recommendations were made to the DD(X) IUSW team at Raytheon, and a Cooperative Research and Development Agreement (CRADA) between

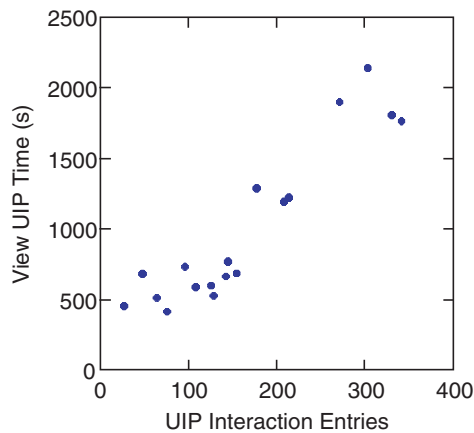


FIGURE 4
Correlation between the time spent on the User Interaction Panel and the number of manual interactions with the panel.

NRL and Raytheon was executed to support collaboration on the next design of the sonar workstation. The recommendations included suggestions about how to improve the effectiveness of the UIP as well as ways to simplify and improve the operator's interaction with the automation. Raytheon is simplifying the UIP design and placing some of the user controls on the main displays in the next version of the workstation being developed for the DD(X).⁵

Acknowledgments: Bob Miyamoto of the Applied Physics Laboratory was instrumental in identifying the opportunity for HSI analysis of the IUSW-21 workstation. Execution of the plan and analysis of the results were supported by the Raytheon Company.

[Sponsored by ONR and Raytheon]

References

- ¹W.L. Hatcher, M. Kurnow, and I. Rozenfeld, "Lessons Learned from the At-Sea Testing of IUSW-21 Single Operator Workstation," in *Proceedings of the 2003 Human Systems Integration Symposium*, June 23-25, 2003, American Society of Naval Engineers.
- ²G. Osga, K. van Orden, N. Campbell, D. Kellmeyer, and D. Lulue, "Design and Evaluation of Warfighter Task Support Methods in a Multi-Modal Watchstation," Technical Report 1874, SPAWAR Systems Center San Diego, CA, May 2002.
- ³Raytheon Company, "IUSW-21 Advanced Development Model, Final Report," Raytheon Document Number G786477, November 26, 2002.
- ⁴Naval Undersea Warfare Command, "IUSW-21 Advanced Development Model FY2002 Sea Test Report," NUWC-NPT Technical Memorandum, 03-021, Naval Undersea Warfare Center, Newport, RI, June 2, 2003.
- ⁵Raytheon Company, "DD(X) Sense Segment Integrated Undersea Warfare (IUSW) Engineering Development Model (EDM) IUSW Control (UC) Human Computer Interface (HCI) Display Definition Document, Release 5," July 23, 2003.

AUTONOMOUS NAVIGATION CONTROL OF UAVS USING GENETIC PROGRAMMING

C.K. Oh and G. Cowart
Tactical Electronic Warfare Division
J. Ridder
SoSACorp

Introduction: An autonomous navigation capability is required for unmanned air vehicles (UAVs) used in electronic warfare applications. Because the electronic battlefield is dynamic, UAVs will need to move reactively to threat locations in ways that cannot be preprogrammed. We have created a new approach that satisfies both the autonomy and optimization needs of UAV navigation by using an artificial intelligence technique. This new approach is quite distinct from current preprogrammed waypoint navigation methods. Genetic programming (GP)¹ is used to create an algorithm that uses noisy and relatively crude input sensor data to generate roll-angle commands for UAV flight control.

Genetic Programming: GP is a computation technique to evolve near-optimized computer programs that produce some desired output when presented with particular input. GP is based on LISP-like expressions¹ and operates on tree data structures. In GP, populations of hundreds or thousands of computer programs are genetically bred. This breeding is done using the Darwinian principle of survival and reproduction of the fittest, along with a genetic recombination (crossover) operation appropriate for mating computer programs. Figure 5 is a flowchart for a GP evolutionary computational process. The inputs to the GP are function and terminal sets. A fitness function evaluates each member (program) of the population over each cycle of the computation. To evolve a successful program (rule tree), function sets, terminal sets, and fitness measures must be designed that are appropriate and effective for the specific application.

Electronic Warfare Simulation Environment: The simulation environment is a square, 100 nmi on each side. The simulator gives the UAV a random initial position in the middle half of the southern edge of the environment and the radar site a random position within the environment. The navigation controller receives only two pieces of information as input: the amplitude and the angle of arrival (AoA) of incoming radar signals. The navigation controller then changes the desired roll angle of the UAV control surface based on the GP-developed control algorithm. For this first stage of research, a stationary, continuously emitting radar is used as the signal source. To increase the robustness of the system, only the

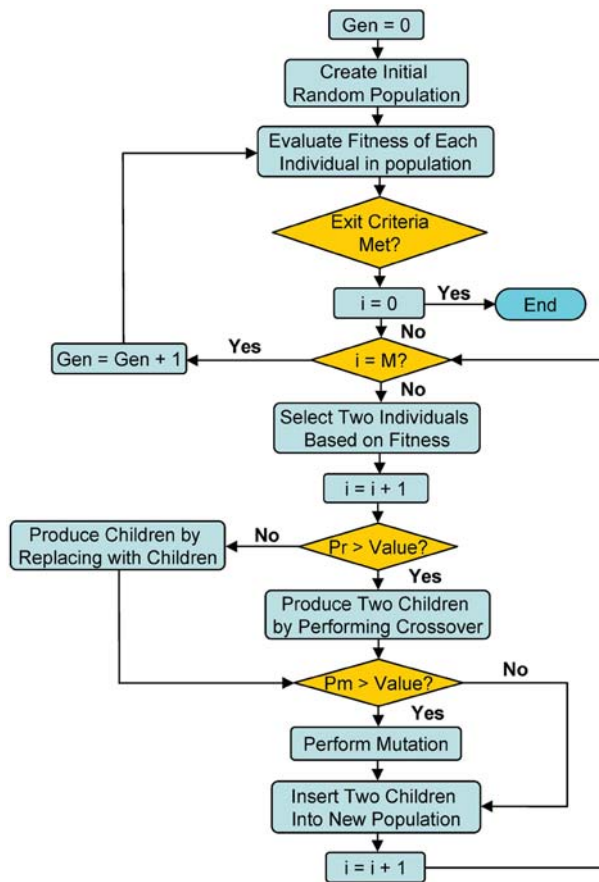


FIGURE 5 Flowchart of GP computational procedure. Index i refers to an individual in the population of size M . The variable Gen is the number of the current generation. The Pr and Pm are crossover and mutational rate, respectively.

sidelobes of the radar emissions are modeled. Gaussian noise is added to the radar signal. Also, the simulation models an imprecise AoA. The main goal of the controller is to autonomously move the UAV to the vicinity of the radar as quickly and efficiently as possible and then circle around the radar.

Evolving UAV Navigation Control Logic: There are two sensor inputs: amplitude of the incoming radar signal and its angle of arrival. The UAV is modeled to have a GPS onboard, therefore position information is available. Additionally, the slope of the signal amplitude is made available. A function set was constructed with nearly 30 members, most of which are common operators (+, >, *IfThen*, etc.) typical of GP experiments, and some are specific to this problem such as $AoA > 0$ or $AmplitudeSlope < 0$. When turning, six actions (terminal sets) are available. Turns may be hard (10° changes in the roll angle) or shallow (2° changes) in left and right. The *WingsLevel* terminal sets the roll angle to 0° , and the *NoChange* terminal keeps the roll angle the same. The fitness measure to optimize the flight path is to minimize

the distance between the UAV and the radar. Because of the intensive computational power required to evolve rule sets by GP, all evolutionary computations were done on a Beowulf cluster parallel computer with 92 2.4 GHz Pentium 4 processors.

New Autonomous UAV Navigation Controller: Figure 6 shows best, worst, and average fitness profiles over 500 generations. Figure 7 shows the UAV flight paths of UAV for an evolved controller when using the near-optimal control logic generated by GP. The evolved controllers were able to overcome a noisy environment and inaccurate sensor data in tracking and locating a radar site. A significant aspect of the research was developing the right function and terminal sets for the problem as well as fitness measures that would generate a realistic control command rule set for realizable UAV navigation.

Summary: In simulation using GP, we were able to evolve navigation controllers for UAVs capable of flying to a target radar while using inaccurate sensor inputs in a noisy environment. We selected realistic flight parameters

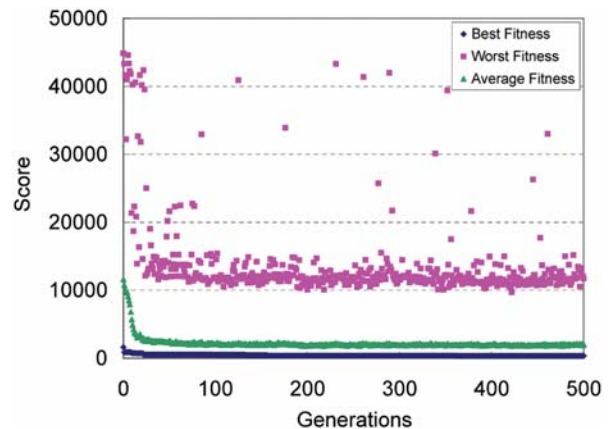


FIGURE 6 Fitness score profiles over 500 generations. Average fitness score is calculated over 500 individuals.

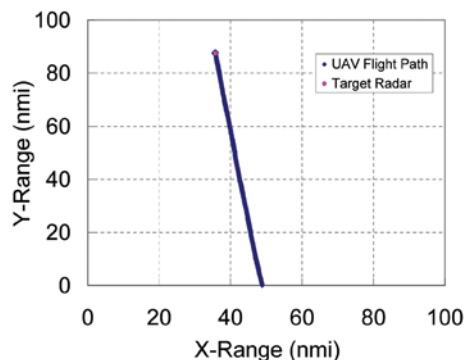


FIGURE 7 UAV flight path from (49, 0) to the target radar located at (46, 88).

and sensor inputs to aid the transference of the controllers evolved in simulation to real UAVs. The next stage is to demonstrate the method in hardware by having a UAV autonomously navigate under the command of GP evolved control logic.

[Sponsored by ONR]

Reference

¹J. Koza, *Genetic Programming* (MIT Press, Cambridge, MA, 1992).

ELECTRONICS AND PHYSICS OF LEFT-HANDED MATERIALS AND CIRCUITS

C.M. Krowne

Electronics Science and Technology Division

Introduction: The use of left-handed materials in the construction of components for physics instruments or electronic devices is an extremely new area to blossom. The materials display a different property of matter compared to ordinary matter in regard to the way in which electromagnetic waves propagate or travel through them. In ordinary matter, the energy flow or power goes in the same direction as the phase front or phase motion of the wave. This is not unlike what one would see if a pebble were dropped in a pond of water and the ripples observed. Power flow of the ripples or of an electromagnetic wave can be represented by a vector, called the Poynting vector \mathbf{P} and the phase front by another vector \mathbf{k} . At any given location we can say that $\mathbf{P} \cdot \mathbf{k} > 0$, where the dot indicates the multiplication of two vectors, called the dot product.

Left-Handed Physics: Left-handed materials do not produce positive dot products between the power and phase vectors. Rather they have $\mathbf{P} \cdot \mathbf{k} < 0$, in seeming contradiction to what we understand to be normal behavior. However, there is nothing fundamental that dictates, based on Maxwell's equations, that the product must always be positive. Since it is known that the Poynting vector is equal to the cross-product of the electric \mathbf{E} and magnetic \mathbf{H} fields, or $\mathbf{E} \times \mathbf{H}$, in normal matter it can be demonstrated that \mathbf{E} , \mathbf{H} , and \mathbf{k} form a right-handed system (Fig. 8(a)). Clearly, if \mathbf{k} points oppositely to \mathbf{P} , the triad \mathbf{E} , \mathbf{H} , and \mathbf{k} must form a left-handed system (Fig. 8(b)). And this is how the term "left-handed materials" arose. Left-handed material is sometimes abbreviated as LHM. Similarly, for ordinary matter, or right-handed material, we can use RHM. Left-handed materials have also been variously referred to as negative index of refraction materials (NIM or NIRM), negative phase velocity materials (NPV or NPVM), backward wave materials (BWM), negative permittivity and perme-

ability materials or double negative materials (DNM or NM).

Prior Research: Interest in left-handed media (LHM) originally arose because of its purported ability, in combination with right-handed (RHM) or ordinary media, to allow unusual focusing of waves, with possible applications in subwavelength control of optical imaging and negative index of refraction (NIR) behavior leading to new radar uses. Definite proof of NIR has occurred in several laboratories in the last two years, and there is little question that focusing possibilities exist in the much lower frequency microwave/millimeter wavelength regimes compared to the optical regime.¹ One of the unusual properties of the LHM in conjunction with RHM is the ability to take diverging or parallel rays of light and focus them with a flat plate of LHM. A convex lens will now cause rays of light hitting it from a source to diverge, but a concave lens will focus the light rays. These unusual behaviors of LHM were pointed out more than 35 years ago in the Russian physics literature.² However, the possibility of backward wave behavior has been known since the 1950s and is available in both the American and British physics and electronics literature. So for nearly half a century, something has been known about LHM. The earliest work involved backward wave propagation in traveling wave tubes³ or microwave or millimeter wave devices and models using nonreciprocal materials or higher order modes.

Electronic Devices: In contrast to the imaging and radar applications stemming from LHM, potential electronic uses may also exist because new physics of propagation in left-handed media occur in structures compatible with integrated circuits,⁴ such as seen in Fig. 9. By treating the LHM as intrinsic with microscopic properties that may be described by constitutive relations relating the displacement field or electric flux density \mathbf{D} and electric field intensity \mathbf{E} , $\mathbf{D} = \epsilon\mathbf{E}$, and relating the magnetic flux density \mathbf{B} to magnetic field intensity \mathbf{H} , $\mathbf{B} = \mu\mathbf{H}$, the electromagnetic fields within guided wave structures used in integrated circuits can be studied. Completely new dispersion diagrams (ω vs k) and electromagnetic field configurations have been found,⁵ as shown in Fig. 10 at 10 GHz.⁶ It has been proven that propagation in these structures enables regions of forward and backward waves to exist. Such new propagation behavior is in agreement with recent macroscopic realizations using lumped/distributed circuit elements to make backward wave circuits.⁷

Microwave Applications: These circuits show that various transmission lines, couplers, and other circuit elements with different or improved characteristics can be made. It is expected that the same could be done for filters, producing devices with new properties or improved

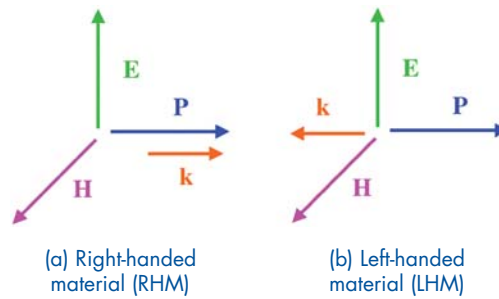


FIGURE 8
Orientation of the Electric \mathbf{E} , magnetic \mathbf{H} , power \mathbf{P} , and phase \mathbf{k} vectors.

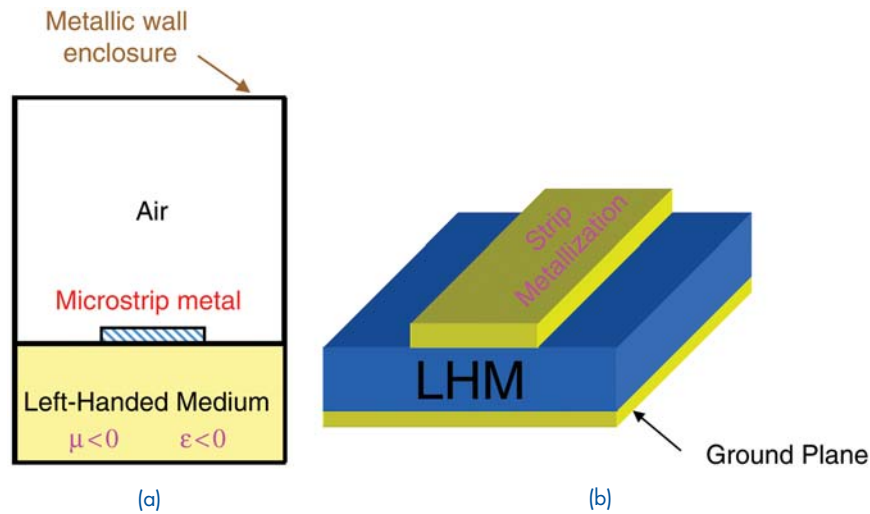


FIGURE 9
Single microstrip structure using a DNM or LHM substrate. (a) Cross-sectional drawing with a DNM substrate having negative ϵ and μ to get the left-handed property, with a perfect conductor enclosing the device. (b) Perspective drawing without the encumbrance of the enclosing walls.

characteristics, taking advantage of the propagation and evanescent frequency bands existing in the dispersion diagram. Additionally, the new electromagnetic field distributions strongly imply that improved isolators and circulators could be constructed using LHM in combination with nonreciprocal materials based on carrier cyclotron motion or spin precession. New control components using reciprocal media are also possible, by teaming LHM with ferroelectric materials, for example.

[Sponsored by ONR]

References

- ¹R.A. Shelby, D.R. Smith, and S. Schultz, "Experimental Verification of a Negative Index of Refraction," *Science* **292**, 77-79 (2001).
- ²V.G. Veselago, "The Electrodynamics of Substances with Simultaneous Negative Values of ϵ and m ," *Soviet Physics USPEKHI*, **10**(4), 509-514 (Jan.-Feb. 1968).

- ³H.R. Johnson, "Backward Wave Oscillators," *Proc. IRE*, 684-697 (1955).
- ⁴C.M. Krowne and M. Daniel, "Electronic Aspects of Propagation in Left-Handed Guided Wave Structures: Electromagnetic-Media Interactions," *IEEE Int. Micro. Symp. Dig.* **1**, 309-312 (2003).
- ⁵C.M. Krowne, "Physics of Propagation in Left-Handed Guided Wave Structures at Microwave and Millimeter Wave Frequencies," *Cornell Univ. Archive* arXiv.org/abs/physics/0305004, May 5, 2003. To be published *Phys. Rev. Letts.*, 2004.
- ⁶C.M. Krowne, "Electromagnetic Field Theory and Numerically Generated Results for Propagation in Left-Handed Guided Wave Single Microstrip Structures," *IEEE Trans. Micro. Th. Tech.*, **51**(12) 2269-2283 (2003).
- ⁷C. Caloz and T. Itoh, "Novel Microwave Devices and Structures Based on the Transmission Line Approach of Meta-Materials," *IEEE MTT-S Int. Micro. Dig.* **1**, 195-198 (2003).

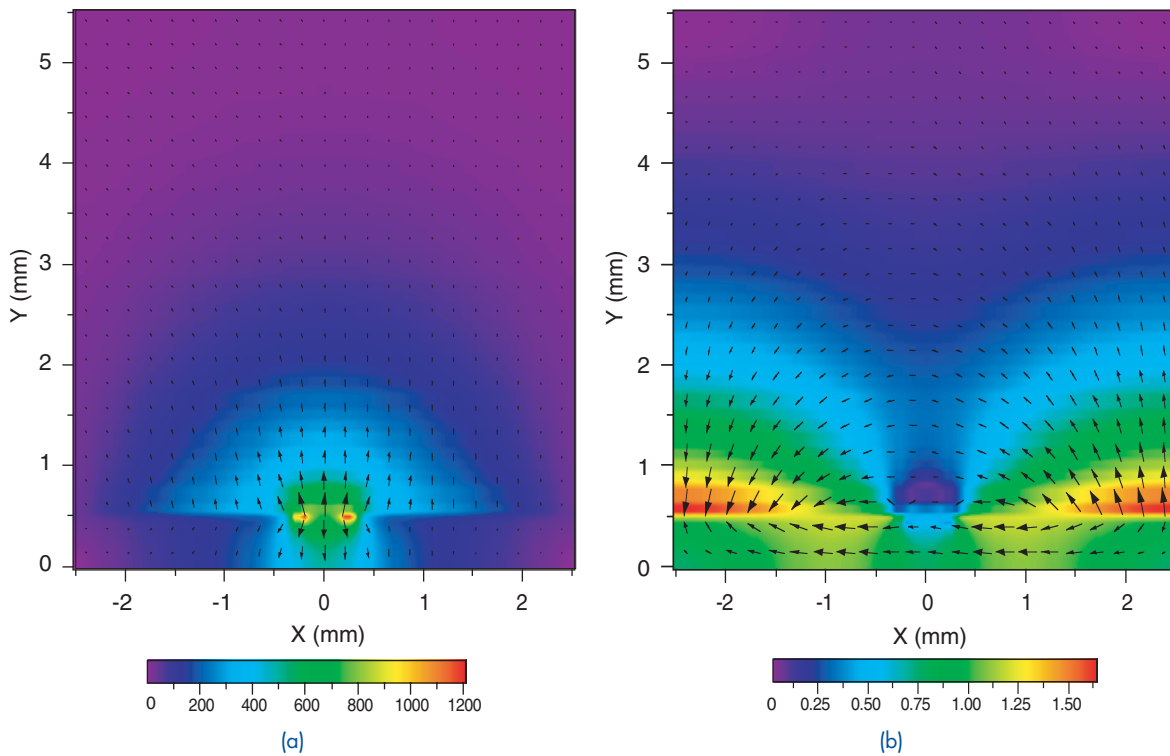


FIGURE 10
 (a) Magnitude plot of the electric field E distribution, with an overlaid arrow plot giving the electric field vector \mathbf{E} at 10 GHz.
 (b) Magnitude plot of the magnetic field H distribution, with an overlaid arrow plot giving the magnetic field vector \mathbf{H} at 10 GHz.

REAL-TIME WAVE, TIDE, AND SURF PREDICTION

R.A. Allard,¹ J. Christiansen,² T. Taxon,² S. Williams,³ and D. Wakeham⁴

¹*Oceanography Division*

²*Argonne National Laboratory*

³*Anteon, Inc.*

⁴*Neptune Sciences, Inc.*

Introduction: As the U.S. Navy and Marine Corps are increasingly required to operate within the littorals, there is a need to quickly set up ocean prediction models to support military planning and operations. Amphibious landings, mine countermeasures, and Special Forces operations are often required on hostile beaches. What are the expected longshore currents at a specific time on a specific beach? Will the predicted sea state prevent landing craft from operating within 48 hours? What is the ideal time for ingress/egress due to tides and currents? The Distributed Integrated Ocean Prediction System (DIOPS) provides the capability to quickly set up and perform wave, tide, and surf predictions for any worldwide location, provided adequate bathymetry is available.¹

DIOPS Models: The backbone of DIOPS is the Simulating Waves Nearshore (SWAN) wave model used to predict nearshore wave conditions. SWAN includes wind-generated wave growth, the effects of refraction, shoaling, and dissipation. SWAN can receive wave energy (spectra) on its lateral boundaries from a deep-water wave model such as WAM (a DIOPS component) or WaveWatch III from the Fleet Numerical Oceanographic and Meteorology Command.

PCTIDES is a globally relocatable tidal-prediction model containing a 2-D barotropic ocean model. A 0.25° resolution global tide model, Finite Element Solutions 99 (FES99),² is used to provide tidal conditions on open boundaries. Surface winds, pressures, and/or astronomical tides are used to force the model. Additionally, a database containing more than 4200 stations from the International Hydrographic Office can be assimilated into the model solution.

The Navy Standard Surf Model (NSSM) is the primary software for U.S. Navy operational surf forecasting. NSSM receives boundary conditions just outside the surf zone from SWAN and utilizes water levels from PCTIDES to adjust the beach profile. One-dimensional surf calculations are performed for each transect, perpendicular to the beach. Outputs include surf zone width, longshore current, breaker type (spilling, plunging, or surging), and the

Modified Surf Index (MSI) that characterizes overall surf conditions used in operational planning.

DIOPS Architecture: The Dynamic Information Architecture System (DIAS), developed by Argonne National Laboratory, is the DIOPS software object framework that allows these models to work together in various context-dependent scenarios within the same simulation. DIAS is a flexible, extensible, object-oriented framework for developing and maintaining complex simulations. The object-based DIOPS framework decomposes the maritime environment from the deep ocean to the shore into classes of software objects, each with its own spatially distributed sets of attributes, and with dynamic behaviors that are implemented by the appropriate ocean physics models. The DIAS software architecture underlying DIOPS enforces the stricture that models may communicate only with domain objects, and never directly with each other. This makes it relatively easy to add or swap models without recoding. Figure 11 shows the relationship of DIOPS model components in the offshore, nearshore, and surf zone.

The DIOPS Graphical User Interface, developed by Anteon, is divided into three functional areas using “window pane” technology. Although a standard windowing concept, this technology was leveraged from the Navy Integrated Tactical Environmental Subsystem (NITES) II Object Oriented Redesign (OOR). The DIOPS display is divided into the Task Area, Chart Area, and the

Analysis Area. The operator can click and drag the windowpane to make one area larger and another smaller, but portions of each remain visible: no hidden windows. Figure 12 shows the PCTIDES model configuration for an area in the Ligurian Sea.

Real-time Exercise Support: DIOPS has been running at the Naval Pacific Meteorology and Oceanography Center (NPMOC) in San Diego, where a beta-test site was established since 2001. DIOPS has supported numerous military and NATO exercises, including Millennium Challenge '02 (California), Strong Resolve 2002 (Baltic Sea), Operation Iraqi Freedom '03, and most recently, Northern Lights '03 (NL03) in Luce Bay, Scotland. Figure 13(a) depicts wave conditions on September 17, 2003 in support of NL03. Figure 13(b) shows a comparison of PCTIDES water levels (top) and nested SWAN wave height (bottom) compared to in situ measurements.

Summary: DIOPS is a relocatable wave, tide, and surf prediction system capable of operating on UNIX or PC platforms. DIOPS development is geared toward operation by junior enlisted personnel. The entire suite of models can be run at a Meteorologic and Oceanographic Command regional center with the ingestion of atmospheric forcing fields such as winds, sea-level pressure, and available bathymetry. Future efforts will link DIOPS with the Delft3D modeling system, using bathymetry

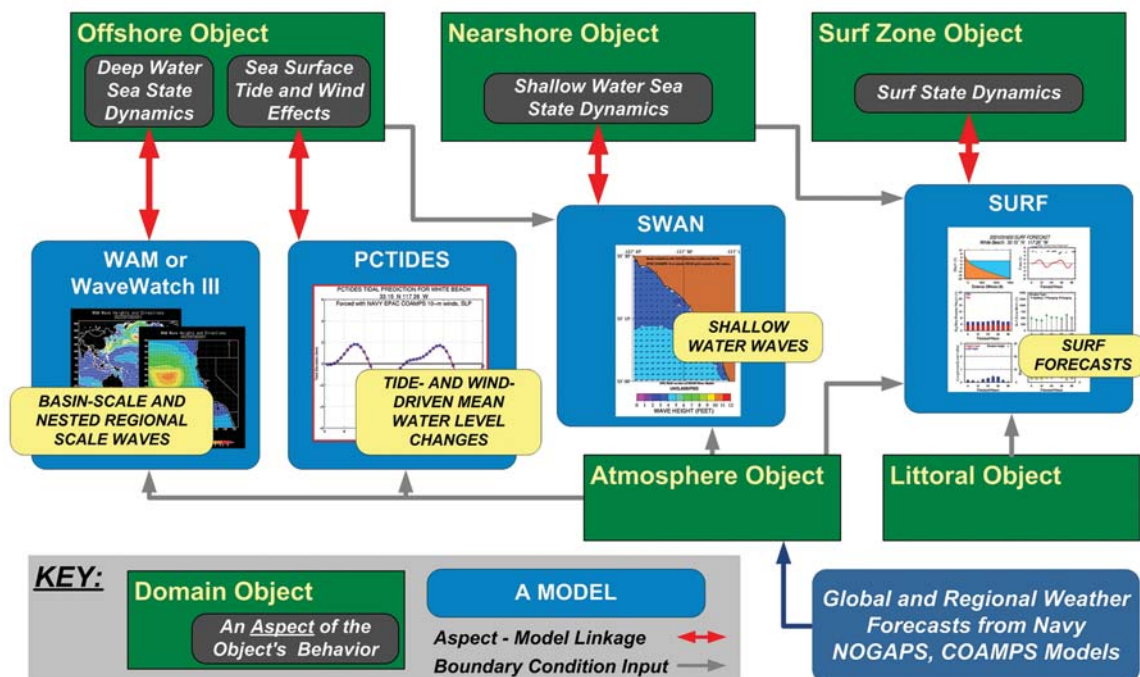


FIGURE 11 DIOPS domain object interactions between offshore, nearshore, and the surf zone.

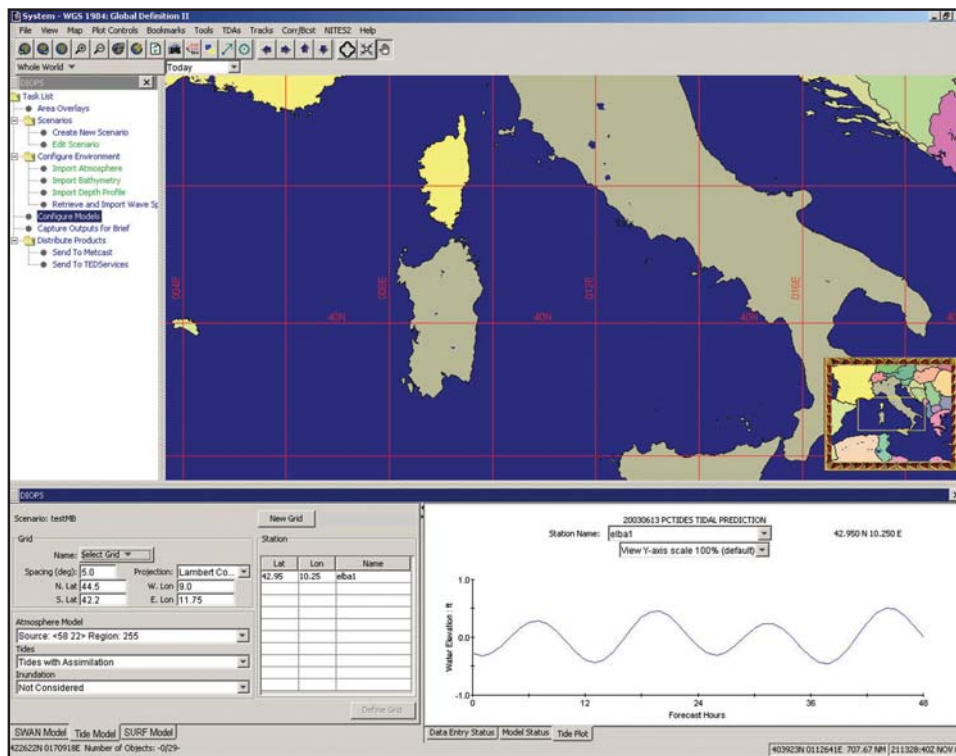


FIGURE 12
PCTIDES model configuration for the Ligurian Sea.

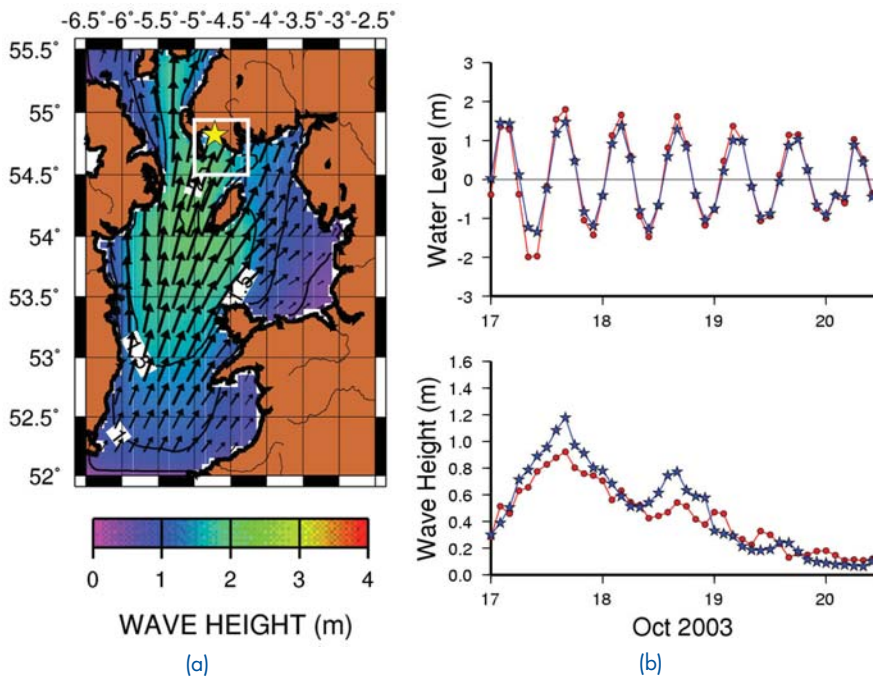


FIGURE 13
(a) SWAN wave prediction for September 17, 2003. Arrows show direction to which waves are moving. White box denotes high-resolution SWAN model nest. Yellow star indicates location where measurement data are available. (b) Time-series of (top) water levels and (bottom) wave heights at a location in Luce Bay, Scotland (yellow star). Red line denotes observation, blue line represents model prediction.

from unmanned underwater vehicles to predict rip currents and 2-D surf conditions. A webservices architecture will also be developed.

Acknowledgments: The authors acknowledge Dr. Daniel Conley at the SACLANT Undersea Research Centre for providing the NL03 data.

[Sponsored by ONR and SPAWAR]

References

- ¹R. Allard, J. Christiansen, T. Taxon, S. Williams, and S. Williams, "The Distributed Integrated Ocean Prediction System (DIOPS), in *Proceedings of the MTS/IEEE Oceans 2002*, Biloxi, MS, October 28-31, 2002, pp. 680-684.
- ²F. Lefevre, C. LeProvost, F. Lyard, and E.J.O. Schrama, "FES98 and FES99: Two New Versions of the FES Global Tide Finite Element Solutions," Topex Poseidon Science Working Team 2000 (SWT 2000) meeting poster (2000).



FLEXING OF A CARBON NANOTUBE

NRL molecular dynamics simulation of the 90-ps oscillation of a 30-nm-long multiwall carbon nanotube composed of over 12,000 atoms. The nanotube consists of an inner semiconducting chiral tubule with radii of 0.69 nm and 1.03 nm, respectively. The initial conditions for the simulation were obtained by bending and relaxing the tube past the point it buckled and then releasing one of its ends.



207 Tactical Microsatellite Experiment (TacSat-1)

M. Hurley

209 The Microelectronics and Photonics Test Bed (MPTB): The First Six Years

K.A. Clark, M.S. Johnson, and A.B. Campbell

212 Rapid Satellite Payload Development for TacSat-1

C.M. Huffine

TACTICAL MICROSATELLITE EXPERIMENT (TACSAT-1)

M. Hurley

Spacecraft Engineering Department

Introduction: The DOD's Office of Force Transformation (OFT) and the Naval Research Laboratory are working on the development of and experimentation with a tactical microsatellite system, with emphasis on producing operationally relevant capabilities. Touchstones of this system include: quick response, Joint Task Force (JTF) organic, selectable payloads, coverage for military conflicts and opportunities at any location on Earth, and an unmanned aerial vehicle (UAV) class of cost. This system ultimately integrates space assets into the forces such that the JTF Commander can call up the assets by deciding the payload capability needed, the area of interest, the area for direct downlink, and the date to call-up the assets. Once deployed, the space assets are directly tasked via the SIPRNET, which is also used to distribute the collected data and products.

TacSat-1 has several payloads that provide capabilities for cross-platform missions, specific emitter identification, and visible and infrared (IR) imaging. TacSat-1 is currently under construction and is scheduled for an early 2004 launch, a schedule that is less than 1 year from the sponsor's go-ahead. To meet this timeline and the challenging budget, many different technical and programmatic approaches are being implemented. This article provides a top-level overview of the experiment and some approaches being used to perform the experiment.

Background: During the second half of 2002, NRL studied the tactical application of space assets. Relatively new technologies and processes in the areas of microsatellites, affordable and quick-response launch vehicles, and the classified SIPRNET (Secret Internet Protocol Router Network) make tactical use of space assets possible in the relatively near term. OFT agreed with the core findings of the study and decided to start an Operationally Responsive Space Initiative consisting of a series of experiments. TacSat-1 is the first experiment in this OFT initiative. The TacSat-1 experiment received go-ahead on May 7, 2003 and is scheduled to launch within 1 year of this date.

TacSat-1 Objectives: One of the objectives of TacSat-1, as well as the broader initiative, is to make space assets and their capabilities available to operational users. Additionally, OFT intends for the TacSat-1 experiment to generate policies where concepts and technology co-evolve, ultimately ensuring that space-based assets emerge as an organic part of the JTF.

The overarching objective of this experiment is to provide and launch an operationally relevant micro-satellite (Fig. 1), with the ability to task and disseminate data through existing operational networks (SIPRNET), in less than 1 year and for less than \$15 million (to include launch costs). Additionally, this experiment will explore concept-technology pairings that develop near-term paths for the tactical use of space in four key areas.

In the area of micro-satellite design and processing, the TacSat-1 schedule and low cost are pushing intelligent applications of standard processes as well as new design and test approaches. One of the new approaches includes utilization of unmanned aerial vehicle (UAV) components within a hermetically sealed, fan-cooled chassis, to help them survive and operate in space.

The TacSat-1 experiment will provide one data point in the area of responsive, on-demand space lift. The experiment uses a new, commercial launch vehicle (the Falcon Launch Vehicle) being developed by Space Exploration technologies with private capital to compete within dynamic market conditions. During the TacSat-1 launch preparation, tailored DOD approaches to mission assurance and risk mitigation are being developed to be appropriate for the rapid cycle times and low-cost class of micro-satellites missions.

The TacSat-1 space element will be used in operational experiments, showing a way for space assets to become an organic part of the JTF. Direct tasking and data dissemination are being performed both real-time from aircraft and time-latent (based on orbital positioning) via the SIPRNET (Fig. 2).

Finally, TacSat-1 will help the development of space professionals and the processes needed for responsive space. An important aspect of this is the strong government-industry team implementing TacSat-1. This largely in-place team allows the entire experiment to be defined

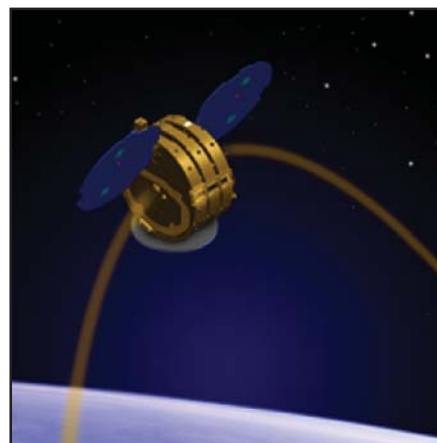


FIGURE 1
TacSat-1 spacecraft.

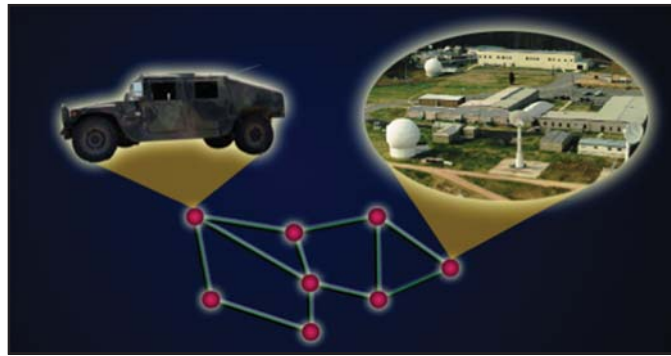


FIGURE 2
Blossom Point ground station connected to tactical users via SIPRNET.

and implemented faster than most contracts can be put in place. This government-industry team approach also helps to spread the knowledge gained from TacSat-1 into industry as well as within the government.

Payload Capabilities: TacSat-1 payloads will provide several experimental capabilities. Machine-to-machine collaboration between air and space assets (Fig. 3) for geo-location is one of the payload capabilities. This capability has the potential to path-find future national capabilities and concepts of operation (CONOPS). This payload is a deviation of NRL's Spacecraft Engineering Department payload development that has been done for the Navy TENCAP (Tactical Exploitation of National Capabilities) and a CONOP extended from an ONR program.

A specific emitter identification (SEI) payload is another capability. This payload is a Tactical Electronic Warfare Division (TEW) development that has been re-packaged for space. Both the SEI and cross-platform mission payload also leverage the TEW Low Cost Receivers (LCR-100) design, which is an enabling micro-satellite technology because of its impressive capability yet small size, weight, and power.

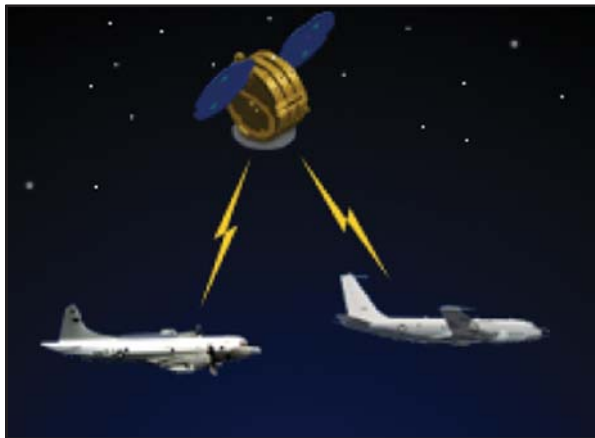


FIGURE 3
Space-to-air asset collaboration.

Two imaging cameras have been included to provide intuitive data for the SIPRNET tasking and data dissemination part of the experiment. One camera is an infrared camera (Fig. 4) that uses a microbolometer FPA, which does not require cryogenic cooling, thereby significantly reducing complexity (size, weight and power). This IR camera is a product of an Army Night Vision Laboratory development and was recommended for flight by TEW. The IR camera collects in the 7.5 to 12- μm range and will provide 850-m resolution. A visible camera is also installed and will provide 70-m resolution.

Key Partnerships: Many partnerships have been made to achieve this experiment within the schedule and cost. Some of the key partnerships and roles are discussed here. The Naval Research Laboratory is the program manager, integrator of the micro-satellite, and responsible for the TacSat-1 mission design and implementation. Air Force Space Command, Space and Missile Center (SMC) is providing mission oversight for the booster, and the 30th Space Wing is providing the launch facility and launch services, and operates the Western Range in support of the launch. TacSat-1 capitalizes on NASA's Virtual Mission Operations Center (VMOC) for SIPRNET payload tasking and data dissemination. VMOC is also being adopted, and experimented with, by the Air Force Space Battlelaboratory and the Army Space & Missile Defense Command Battle Laboratory for a spacecraft/



FIGURE 4
IR omega camera by Indigo.

NIPRNET (Nonclassified Internet Protocol Router Network) interface. The Blossom Point Ground Station is providing satellite command and control as well as SIPRNET-based payload tasking and data dissemination using a tailored version of VMOC. The NRO Office of Space Launch is providing the payload processing facility at Vandenberg Air Force Base. Regional Combatant Commanders are providing operational experimentation and coordination. The SpaceX Corporation is on contract for the launch of TacSat-1 aboard the inaugural flight of their Falcon Launch Vehicle (Fig. 5).

The result is an impressive team of organizations all working to ensure the success of the TacSat-1 experiment.

[Sponsored by OFT]



FIGURE 5
Falcon launch vehicle.

THE MICROELECTRONICS AND PHOTONICS TEST BED (MPTB): THE FIRST SIX YEARS

K.A. Clark,¹ M.S. Johnson,² and A.B. Campbell³

¹Space Systems Development Department

²Spacecraft Engineering Department

³Electronics Science and Technology Division

Introduction: One of the biggest challenges for satellite engineers is designing microelectronics and photonics subsystems that will operate reliably and survive the effects of the natural space radiation. These effects are the result of both total-dose and displacement-damage radiation and single-event phenomena due to cosmic rays, electrons, and protons. Total-dose and displacement-damage radiation can degrade electronics and photonics

devices over time. Single-event phenomena can be either destructive or nondestructive. An example of destructive phenomena is a single-event latchup, in which a single particle causes a silicon-controlled rectifier-like regenerative process that can result in burnout of the device.

Nondestructive phenomena include bit-flips in random access memories that are transient and can be corrected using well-known fault-tolerant techniques. To address these radiation effects, the satellite engineer has two options: use electronics and photonics devices that are specifically hardened against the effects of radiation, or use fault-tolerant techniques with commercial devices that have been shown to be tolerant of the radiation. The radiation tolerance level can be measured by performing ground testing with radioactive sources, such as Co⁶⁰, and accelerator particle beams to simulate the space radiation environment. Because of the differences between what can be simulated on Earth and what is actually seen in space, a more accurate approach to measure the tolerance is to fly the microelectronic and photonic devices in a space-based test bed.

MPTB Description: NRL developed the Microelectronics and Photonics Test Bed (MPTB) to directly measure the effects of space radiation on microelectronic and photonic devices while simultaneously measuring the radiation environment. Tied to this was an extensive ground-test program in which the same devices that were flown were also tested with radioactive sources and particle accelerators. This way, both the radiation tolerance in space and our ability to test and model this tolerance can be evaluated with ground testing. MPTB is a secondary satellite payload that does not pose a risk to the primary mission of the satellite. It is flying in a highly elliptical orbit (HEO). This orbit allows it to sample a variety of environments, including the electron and proton belts as well as the region beyond Earth's magnetosphere near geosynchronous altitudes. Functional and characteristic changes in the devices caused by total-dose and displacement radiation damage and single-event phenomena are measured and telemetered to the ground for analysis. Figure 6 is a block diagram of MPTB. It consists of a redundant core electronics unit (CEU) and three experiment panels, each with eight experiment daughterboard slots. Figure 7 is a photograph of the experiment panels during integration and test. The CEU provides the interface to the host vehicle and is the master controller of MPTB. Each experiment panel provides digital, analog, and power interfaces and low-level control to the daughterboards. Each daughterboard contains an individual microelectronic or photonic device experiment. Because of the severe radiation environment, the CEU and experiment panels needed to be designed to be tolerant of both total-dose radiation and single-event phenomena so as not to compromise the experiments.

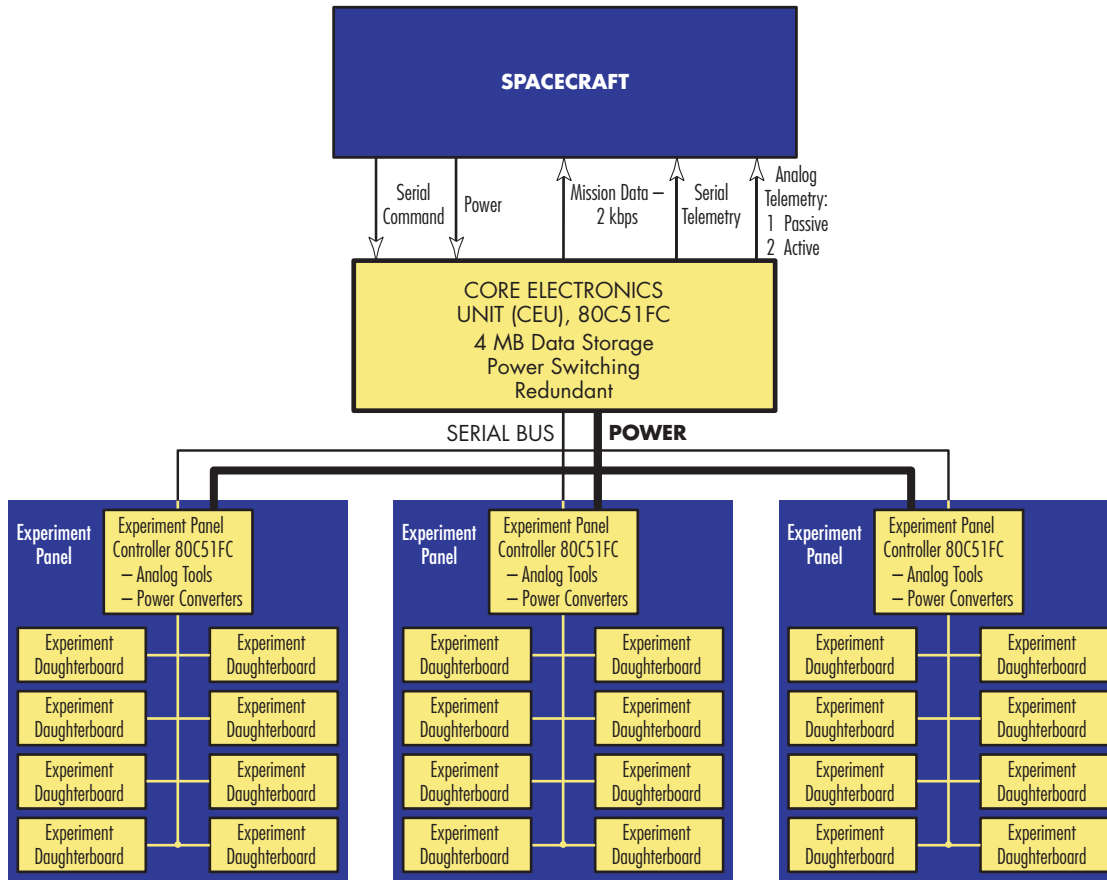


FIGURE 6
MTPB block diagram.

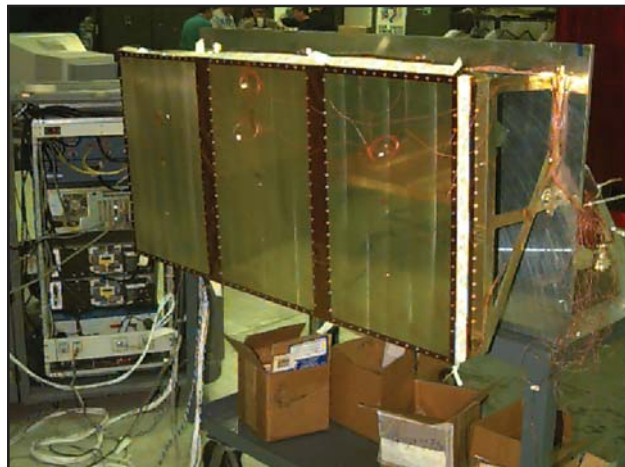


FIGURE 7
Experiment panels during integration and test.

On-orbit operations of MPTB began in November 1997. To support these operations, NRL developed the MPTB Ground Processing Architecture. This architecture consists of the front end processor at the host vehicle's remote ground facility and the MPTB control site at the Blossom Point Field Site. A week's worth of daily command load files are generated at Blossom Point and sent to the remote ground facility, where they are transmitted daily to the satellite. Experiment data are downlinked to the front end processor at the remote ground facility and sent back to Blossom Point, where operations personnel monitor data from MPTB in real time to verify that the experiments are operating within tolerances. Data are postprocessed and transferred to NRL for collection and distribution by the Solid State Devices Branch of the Electronics Science and Technology Division (Code 6810).

On-Orbit Data Highlights: The experiments hosted on MPTB included commercial random-access memories, analog-to-digital converters, analog integrated circuits, microprocessors, indium phosphide high-speed test circuits, fiber-optic data busses, field programmable gate arrays, opto-isolators, and radiation environment monitors. The experimenters included scientists and engineers from industry, government laboratories, academia, and non-US space agencies. MPTB has provided approximately 15 gigabytes of data to the radiation effects community, more on-orbit data than any other radiation effects experiment. This has resulted in 47 publications, with more on the way. Some of the highlights from the on-orbit data include a row-upset anomaly in a dynamic random access memory (DRAM), enhanced low-dose rate sensitivity (ELDRS) of bipolar transistors, and the effect of solar activity on the proton spectrum in MPTB's orbit.

The NRL-developed DRAM Memory Stack Experiment observed a row-upset anomaly in an IBM LUNAES 16-Mbit DRAM on June 23, 1999. The anomaly resulted in 1024 simultaneous bit errors. This was the first time such an anomaly had been reported on-orbit. The most likely cause of the anomaly was a single-event upset in the delay circuit portion of the refresh circuitry that cleared all the memory cells for that particular row.

The objective of the NAVSEA/Crane-developed linear bipolar transistor experiment is to investigate enhanced low-dose rate sensitivity (ELDRS) of bipolar transistors. The ELDRS phenomena can result in greater degradation of bipolar transistors at the space radiation dose rate than at the higher dose rate used in ground testing. Various temperature and dose-rate combinations were performed in ground radiation testing to model this effect. The on-orbit data demonstrated that the degradation is indeed enhanced at the space dose-rate levels and also showed that the design margin for a proposed elevated temperature modeling approach is not sufficient.¹

The objective of the UK Ministry of Defence-sponsored Cosmic Ray Environment Dosimeter (CREDO) experiment is to measure the flux of protons with energies greater than 38 MeV and the linear energy transfer spectra of cosmic rays in the 100-20,000 MeV/(g-cm²) range. The experiment itself consists of two diode-based particle telescopes and accompanying measurement electronics. The flux measurements are read every few minutes to allow a precise temporal correlation between the environment and single-event phenomena observed on other experiments. For example, based on the CREDO proton flux measurements, it was determined that the row-upset anomaly described above occurred as MPTB was flying through the proton belts. Figure 8 shows the effect that a solar event has on the total proton flux. Prior

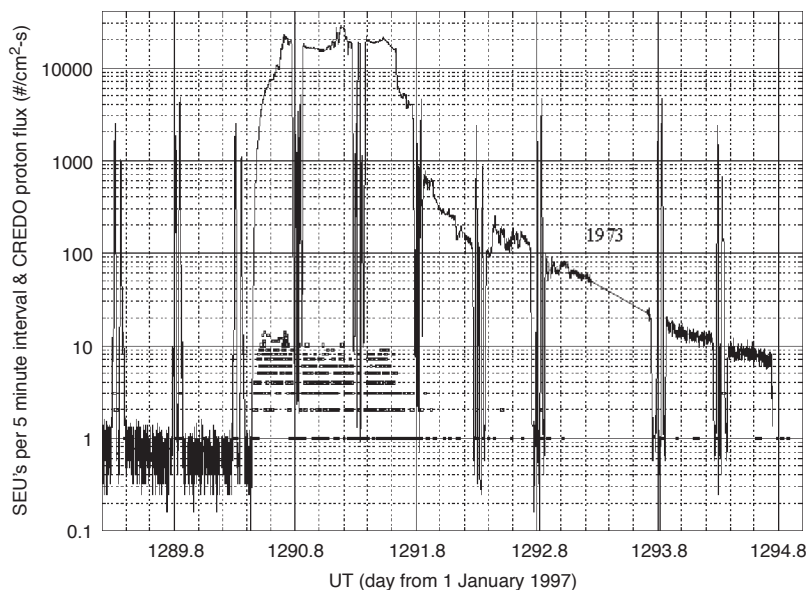


FIGURE 8
CREDO-measured proton flux during July 14, 2000 solar event.

to day 1290, the proton flux peaks twice per orbit as MPTB passes through the proton belts. As a result of the solar event on July 14, 2000 (day 1290) the proton flux during the entire orbit increases significantly,² which also increases the total number of single-event upsets (SEUs) observed on MPTB. This shows that the radiation environment in a highly elliptical orbit is not only variable due to proton-belt passes, but also because of changes due to solar events.

Summary: The NRL-developed MPTB has proven to be a well-designed, reliable, on-orbit experiment. During its first six years of operation, it has provided the worldwide radiation effects community with an enormous amount of on-orbit data that have resulted in a better understanding of radiation effects phenomena and the natural radiation environment in space.

[Sponsored by DTRA and SPAWAR]

References

- ¹J.L. Titus, D. Emily, J.F. Krieg, T. Turflinger, R.L. Pease, and A.B. Campbell, "Enhanced Low Dose Rate Sensitivity (ELDRS) of Linear Circuits in a Space Environment," *IEEE Trans. Nucl. Sci.* 46(6), 1608-1615 (1999).
- ²C.S. Dyer, P.R. Truscott, C. Sanderson, C. Watson, C.L. Peerless, P. Knight, R. Mugford, T. Cousins, and R. Noulty, "Radiation Environment from CREAM and CREDO During the Approach to Solar Maximum," *IEEE Trans. Nucl. Sci.* 47(6), 2208-2217 (2000). •

RAPID SATELLITE PAYLOAD DEVELOPMENT FOR TACSAT-1

C.M. Huffine
Space Systems Development Department

Introduction: The Department of Defense (DOD) Office of Force Transformation (OFT) approached the Naval Research Laboratory with an opportunity to build and launch a microsatellite that would provide operationally responsive access to, and near-term tactical exploitation of space.¹ A key challenge posed to the Laboratory by OFT was to build this operational capability in less than 1 year from the approval to proceed (ATP) to an on-orbit utility. One of the objectives of TacSat-1, as well as the broader initiative, is to make space assets and their capabilities available to operational users. Additionally, OFT intends for the TacSat-1 experiment to generate policies in which concepts and technology co-evolve, ultimately ensuring that space-based assets emerge as an organic part of the Joint Task Force. Bringing this first "tactical satellite" vision together required the development of new partnerships and methods, and the leveraging of existing hardware, software, and facilities.

Copperfield-2, an existing sensor system developed for flight on the Global Hawk unmanned aerial vehicle (UAV), became the cornerstone of the TacSat-1 payload infrastructure.

Changing Paradigms: TacSat-1 sought to investigate flawed and limited interactions where failure is a significant data point. As a result, the initiative is exploring and taking advantage of emerging concepts that will broaden the technology base and provide incentives to a new space cadre, all of which seek to mitigate risk averse behavior. In order to execute the initiative successfully, risk was appropriately managed, commensurate with the level of cost and time associated with the development and testing process. "Traditional" satellite programs often manage risk with very stringent requirements for reliability, parts screening, and documentation, resulting in significant increases in cost and time and inflexibility in addressing today's threats. TacSat-1 has intentionally taken many risks, both in its conceptual application and with its UAV components, all combined to produce high payoff. Commercial parts are being used throughout the spacecraft. Mechanical build processes are being changed and streamlined to meet a significantly truncated schedule. Payload software development is leveraging open-standard protocols and tools wherever possible in order to provide for the highest amount of re-use and adaptation. Finally, the bus infrastructure for TacSat-1 builds on Orbcomm hardware, taking advantage of a proven and paid-for space heritage.

Payload Adaptation and TACSAT-1 Implementation: The core payload component, Copperfield-2, provides two key functions for the satellite. First, it is itself a sensor system that receives signals of interest and provides for machine-to-machine collaboration between air and

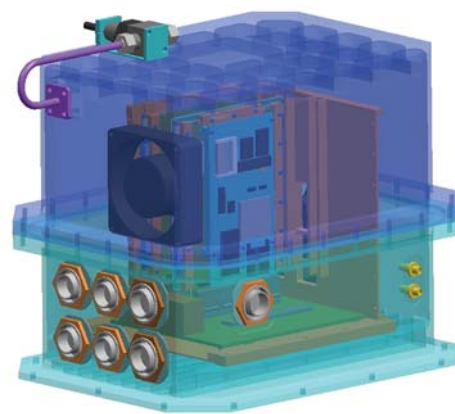


FIGURE 9
This three-dimensional CAD rendering shows the payload environmental enclosure, which enables convection-cooled components to operate in a space environment.

space assets for geo-location. Secondly, it serves as a general-purpose computer system and provides storage and data handling. A module designed specifically for TacSat, called the high-speed interface (HSI), provides conversion from the TCP/IP payload communication protocol, to the proprietary OX.25-based communications that the Orbcomm bus provides.

TCP/IP-based systems provide tremendous flexibility and standardized communications between various devices. The Copperfield-2 system sponsor is striving to provide TCP/IP-enabled payload elements that allow for the ultimate in flexibility — payloads and ground stations can be placed virtually anywhere routable via TCP/IP packets. Another OFT goal is to eventually provide an entirely TCP/IP-based satellite system so that classical integration challenges can be eliminated and so that speed of development and launch are not held hostage to newly created interfaces.

Copperfield-2 was designed from the ground up to provide a modular payload infrastructure that can be adapted to changing needs and requirements. This capability is used in the TacSat-1 program; the addition of support hardware for the visible camera, via the PCI bus allowed the “frame grabber” card to be used by the general-purpose processor, and the frame grabber card manufacturer’s driver to be used with minimal modifications. This capability reduced the development timeline significantly, and allowed insertion of a new camera and frame-grabber card well into the program.

While hardware allows the physical interconnection of payload components, the most “custom” part of the satellite development is putting together the payload control software. All of the Copperfield payload components with processors run on the Linux operating system. Much of the payload software was implemented through the use of BASH (Bourne again shell) scripts operating on the various processors. This allows the special binary “drivers” (either real operating system drivers or user-space programs), which provide control to the other payload elements, to be small command-line utilities that can be completely tested in their limited functionality.

By utilizing the BASH scripting language and leveraging GNU utilities that come with Linux software distributions, software components that have been well tested and had tremendous peer review are re-used and provide the core functionality. Custom software components that are required to interface with specific hardware or software can be of limited scope. Linux and the GNU utilities provide the glue logic that binds the payload together.

Summary: Few satellite programs have the latitude or the ability to take risks that the TacSat-1 initiative provides. In this context, the TacSat-1 program allows innovative leveraging of both government and commercial off-the-shelf hardware components, as well as novel approaches to creating payload software which provides for maximum flexibility and standards-based operation. The modular nature of the Copperfield-2 allowed rapid hardware integration, proving the concept of a modular payload that scales from UAV applications to a spacecraft application. In the same vein, the very simplistic UAV payload software requirements were significantly expanded for TacSat-1, extending the role of standards-based open-source software such that it provides a modular software infrastructure suitable for flexible command and control of the TacSat-1 payload and for uses other than space.

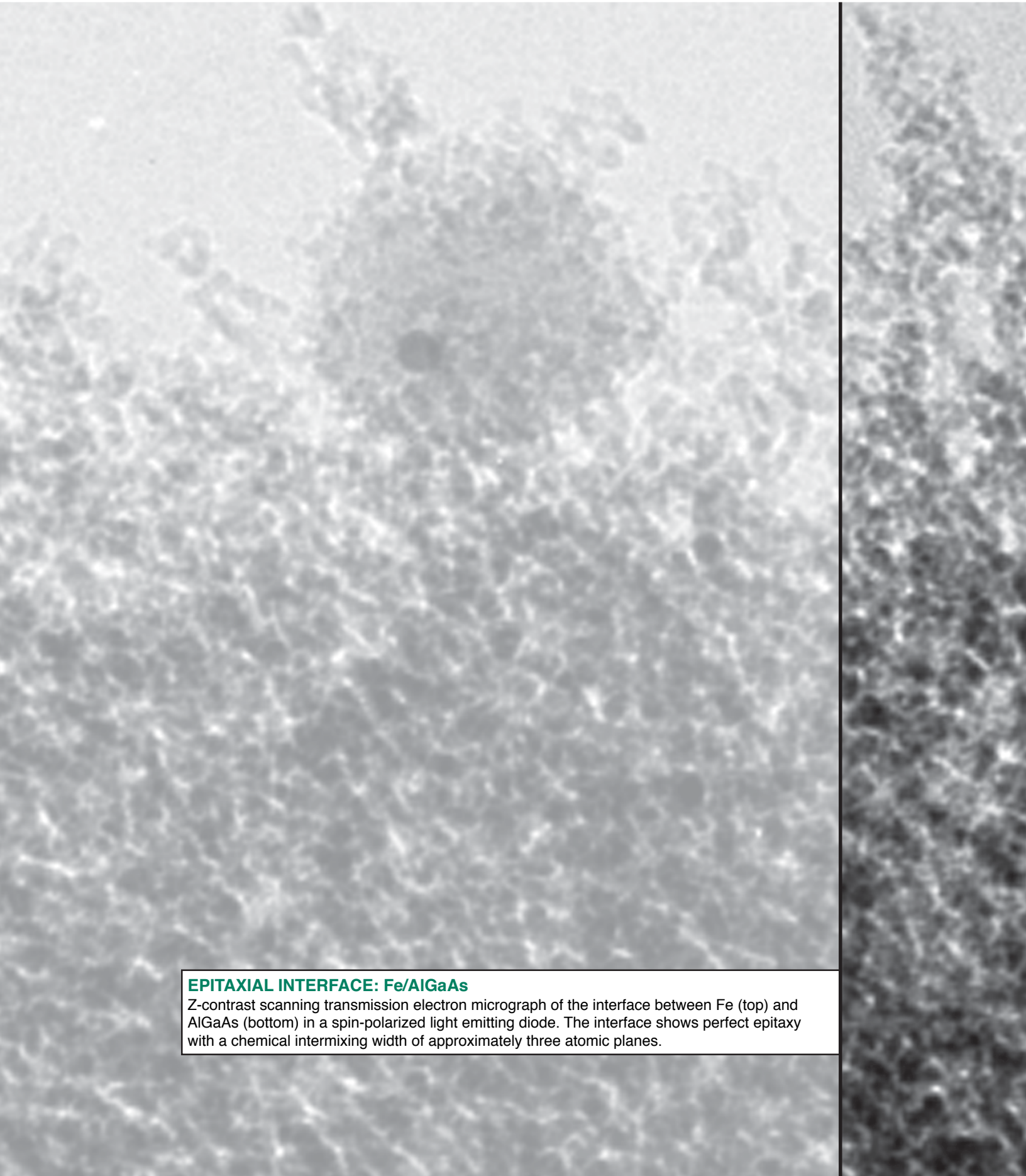
Acknowledgments: The author acknowledges the contributions to this effort by Stuart Nicholson, Eric Karlin, and Mike Steininger of SGSS, Inc.; Brian Micek of Titan Corp.; Chris Gembaroski, Don Kremer, and the Copperfield-2 team at Aeronix, Inc.; Jeff Angielski for the PTR Group; and the Copperfield-2 UAV payload sponsor, LCDR Michael Carlan, USN.

[Sponsored by OFT]

Reference

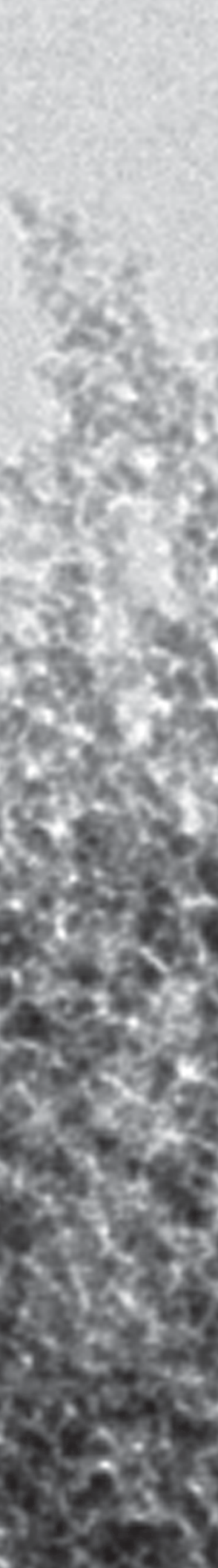
¹Office of Force Transformation, “TACSAT-1 Fact Sheet,” OFT, November 2003. •

SPECIAL AWARDS AND RECOGNITION



EPITAXIAL INTERFACE: Fe/AlGaAs

Z-contrast scanning transmission electron micrograph of the interface between Fe (top) and AlGaAs (bottom) in a spin-polarized light emitting diode. The interface shows perfect epitaxy with a chemical intermixing width of approximately three atomic planes.



217 Special Awards and Recognition

234 Alan Berman Publication and Edison Patent Awards

SPECIAL AWARDS & RECOGNITION

NRL is proud of its many distinguished scientists, engineers, and support staff. Here we feature some who have received awards from prestigious institutions, the Department of the Navy, and NRL.

awards from outside of NRL

ELECTED TO THE NATIONAL ACADEMY OF SCIENCES

Dr. Judith Lean

Space Science Division

The National Academy of Sciences is a private organization of scientists and engineers dedicated to the furtherance of science and its use for the general welfare. It was established in 1863 by a congressional act of incorporation (signed by Abraham Lincoln), which calls on the Academy to act as an official adviser to the federal government, upon request, in any matter of science or technology. Election to membership in the Academy is considered one of the highest honors that can be accorded a U.S. scientist or engineer. Dr. Lean was elected in recognition of her "distinguished and continuing achievements in original research." Dr. Lean's research focuses on the mechanisms, measurements, and modeling of variations in the Sun's radiative output at all wavelengths, and the effects of this variability on the Earth's global climate and space weather.



ELECTED TO THE NATIONAL ACADEMY OF ENGINEERING

Dr. Elaine Oran

Laboratory for Computational Physics and Fluid Dynamics

Election to the National Academy of Engineering is among the highest professional distinctions accorded an engineer. Academy membership honors those who have made "important contributions to engineering theory and practice, including significant contributions to the literature of engineering theory and practice," and those who have demonstrated accomplishment in "the pioneering of new fields of engineering, making major advancements in traditional fields of engineering, or developing/implementing innovative approaches to engineering education." Dr. Oran was recognized for her "work in unifying engineering, scientific, and mathematical disciplines into a computational methodology to solve challenging aerospace combustion problems." She is known for her pioneering applications of numerical simulations for solving problems in fluid dynamics and reacting flows.





2003 PRESIDENTIAL RANK OF DISTINGUISHED SENIOR PROFESSIONAL

Dr. Fran Ligler

Center for Bio/Molecular Science and Engineering

The Presidential Rank Awards were established to recognize a select group of career Senior Executives who have demonstrated exceptional performance over an extended period of time. Nominees are outstanding leaders and must consistently demonstrate strength, integrity, industry, and a relentless commitment to public service. Through their personal conduct and their results-oriented program management, they will have established and maintained a high degree of public confidence and trust. Dr. Ligler has pioneered the development of ultrasensitive antibody-based detection systems for biological and chemical detection. Her work has had a profound impact upon the development of biosensor-based detection of Biological Warfare (BW) agents over the past 15 years, leading to significant improvements in the Nation's capability for early and accurate detection. Since 1986, she has made the Naval Research Laboratory one of the world's leaders in the invention, development, and field testing of portable biosensors for the rapid, on-site analysis of complex samples. She has concentrated on developing the technology to make it generic in application with increased capability, manufacturability, and ease of use. She has demonstrated applications of these biosensors for identification of BW agents, monitoring of environmental pollutants, food safety analysis, diagnosis of infectious disease, screening for drug abuse, and detection of explosives. Four biosensor systems invented and developed by Dr. Ligler are now commercially available, and several major corporations are working to integrate them into BW defense, environmental monitoring, and food safety systems.



2003 PRESIDENTIAL RANK OF MERITORIOUS SENIOR PROFESSIONAL

Dr. John Reintjes

Optical Sciences Division

The Presidential Rank Awards were established to recognize a select group of career Senior Executives who have demonstrated exceptional performance over an extended period of time. Nominees are outstanding leaders and must consistently demonstrate strength, integrity, industry, and a relentless commitment to public service. Through their personal conduct and their results-oriented program management, they will have established and maintained a high degree of public confidence and trust. Dr. Reintjes invented a new technology, LaserNet Fines (LNF) to provide an automated and quantitative measure of the status of mechanical systems. Based on optical imaging of debris particles in flowing fluid and real-time computer classification with artificial neural networks, LNF will reduce unexpected down time, improve productivity, and prevent many catastrophic failures of Army, Navy, and Air Force aircraft, Navy ships and submarines, and Army and Marine Corps land and amphibious vehicles. Applications in private industry include commercial airlines, electric power industry, commercial shipping, off-shore oil drilling and off-road construction equipment.

2003 PRESIDENTIAL RANK OF MERITORIOUS SENIOR PROFESSIONAL

Dr. Edward Franchi

Acoustics Division

The Presidential Rank Awards were established to recognize a select group of career Senior Executives who have demonstrated exceptional performance over an extended period of time. Nominees are outstanding leaders and must consistently demonstrate strength, integrity, industry, and a relentless commitment to public service. Through their personal conduct and their results-oriented program management, they will have established and maintained a high degree of public confidence and trust. During his distinguished tenure as the Naval Research Laboratory's Acoustic Division Superintendent and earlier as Associate Technical Director at Naval Oceanographic Research and Development Activity/Naval Oceanographic and Atmospheric Research Laboratory, Dr. Franchi has created and led an internationally recognized research and development organization with renowned acousticians, cutting edge science and technology programs, and a long record of achievements to meet the challenges of the 21st century Navy.



DOCTOR HONORIS CAUSA

Drs. Isabella and Jerome Karle

Laboratory for Structure of Matter

The Jagiellonian University, a 600-year-old academic institution in Krakow, Poland, granted the title of Doctor Honoris Causa to Drs. Isabella and Jerome Karle for their vast contributions to modern crystallography, chemistry, solid state physics, and molecular biology. Speaking for the Jagiellonian University, Dr. Stanislaw Hodorowicz, Vice Rector for Research, called the celebration, "a tribute to the value of the life and work of outstanding people and distinguished scientists." The receipt of an honorary degree in Europe is often different than it is in the United States. In Krakow, it entails a special ceremony, in an ancient but well-preserved historical area of the university with the pomp and circumstance characteristic of an ancient and renowned university.





NATIONAL INVENTORS HALL OF FAME INDUCTEE

Dr. George Carruthers

Space Science Division

To commemorate the centennial of the Wright Brothers' first powered flight, the 31st annual induction of the National Inventors Hall of Fame recognized pioneers in the aviation and aerospace industries. Dr. Carruthers was inducted in recognition of his invention of the far-ultraviolet electrographic camera. The Far Ultraviolet Camera and Spectrograph, sent to the Moon on the Apollo 16 mission, was based on the far-ultraviolet electrographic camera that he invented to give scientists fresh, revealing images of Earth and space. A pioneer in ultraviolet astronomy, Dr. Carruthers' invention was first used in sounding rocket flights in 1966, and made the first detection of molecular hydrogen in deep space in a 1970 flight. The camera used in the Apollo 16 mission produced about 200 photos revealing new features of Earth's far-outer atmosphere, as well as deep-space objects from the perspective of the lunar surface. It also produced new far-ultraviolet images of stars, nebulas, and galaxies, as well as new views of the Earth.



SIGMA XI 2003 PURE SCIENCE AWARD

Dr. Jerry Meyer

Optical Sciences Division

Dr. Meyer was recognized for his contributions to the physics of narrow-gap quantum heterostructures and quantum-well lasers for the infrared. The award specifically notes Dr. Meyer "as one of the world's leading theoretical authorities on quantum-engineered heterostructure material properties, quantum-well design via wavefunction engineering, and novel device concepts. His widely imitated type-II 'W' laser is considered a major breakthrough in mid-IR opto-electronics." Dr. Meyer's work on semiconductor optical and transport phenomena has included pioneering studies of "dynamic screening" in bipolar plasmas, multi-ion screening in doped materials, and a superlattice transport theory that smoothly bridges the gap between three-dimensional bulk systems and two-dimensional quantum wells.



SIGMA XI 2003 APPLIED SCIENCE AWARD

Ms. Anne Kusterbeck

Center for Bio/Molecular Science and Engineering

Ms. Kusterbeck was recognized for "successfully developing and transitioning flow immunosensor technology, from basic concept to commercial instruments, for use by the Navy and the Nation for environmental monitoring, law enforcement, workplace safety, and homeland security." Ms. Kusterbeck's work on developing the technology and later commercializing instruments for explosives and drugs of abuse has had a significant impact on Navy and Environmental Protection Agency programs for environmental monitoring of explosives, as well as on drug screening for law enforcement agencies and workplace communities. The commercial biosensor that uses the flow immunosensor technology was named a "Top 100 Technology of 2002" by *Popular Science* magazine.

SIGMA XI 2003 YOUNG INVESTIGATOR AWARD

Dr. Rhonda Stroud

Materials Science and Engineering Division

Dr. Stroud was recognized for her work on quasicrystals, colossal magnetoresistance, and transmission electron microscopy of nanoscale materials. Dr. Graham Hubler, head of the Surface Modification Branch, said, "In her relatively short research career, Dr. Stroud has distinguished herself as one of the top young materials physicists, and demonstrated valuable leadership skills here at NRL." Her thesis work at Washington University led to the discovery of the first stable Ti-based quasicrystal. This discovery spawned research in hydrogen and deuterium loaded quasicrystals, for basic studies of the structure of interstitial spaces in quasicrystals, and for application as hydrogen storage media.



NAVY SUPERIOR CIVILIAN SERVICE AWARD

Dr. John Lee

Optical Sciences Division

Dr. Lee was presented the Navy Superior Civilian Service Award for his leadership role in the development and demonstration of the Prototype SHARED Reconnaissance Pod (SHARP) digital reconnaissance technology, which has had a major impact on efforts to improve capabilities of future tactical reconnaissance systems. According to the citation, "Dr. Lee's leadership and hard work was instrumental in the success of the demonstration flight of the Prototype SHARP Pod and the NRL P-3 aircraft with a Prototype SHARP payload. He provided the leadership that was essential to the success of major hardware and software development tasks. His direct participation in the system integration and testing contributed materially to the timely success of the Prototype demonstration and his willingness to devote time far in excess of normal working hours provided an example of dedication that motivated the entire team."



NAVY SUPERIOR CIVILIAN SERVICE AWARD

Mr. Dale Linne von Berg

Optical Sciences Division

Mr. Linne von Berg received the Navy Superior Civilian Service Award for "his exceptional performance in the development and demonstration of the SHARED Reconnaissance Pod (SHARP) Prototype program." He was cited "as a motivating force for introducing into the Prototype SHARP effort standards for data compression, image format, and interfaces for the Ground Control Station (GCS)." Mr. Linne von Berg was the key leader in the development of the SHARP reconnaissance management system (RMS) and the NAVIS GCS that was used for the Pentagon demonstration and initial testing of the engineering and manufacturing development (EMD) pods.





TECHNICAL COOPERATION PROGRAM (TTCP) ACHIEVEMENT AWARD

Dr. Robert Brady and Mr. Gregory Nichols

Chemistry Division and Tactical Electronic Warfare Division

The Technical Cooperation Program (TTCP) is an international consortium dedicated to fostering collaborative research efforts in defense science involving Australia, Canada, New Zealand, the United Kingdom, and the United States. Dr. Brady was cited for “the development of ship exterior coatings that reflect a large proportion of incident solar energy while maintaining all the desirable physical, chemical, and environmental properties of existing paints.” Mr. Nichols was cited for “making a significant contribution in extending specific emitter identification capabilities to military radars with non-magnetron transmitters which represent the vast majority of modern military radar designs.”



2003 FEDERAL LABORATORY CONSORTIUM (FLC) AWARD FOR EXCELLENCE IN TECHNOLOGY TRANSFER

Dr. Jeffrey Bowles

Remote Sensing Division



This award recognizes employees for outstanding work that has led to the successful transfer of technology developed at a Federal laboratory. Dr. Bowles was recognized for his “successful transfer of ORASIS, a software application used for the analysis and compression of hyperspectral images.” ORASIS is based on algorithms developed and patented by NRL. Hyperspectral images are composite images made up of multiple pictures of a “scene” taken at different wavelengths. This technology mathematically identifies constituent components and maps their abundances within the image. The technology greatly enhances the contrast of military targets and helps to automate the processing of the images and is, therefore, of great interest to meet Department of Defense surveillance needs. The Earth image products from ORASIS will be used for oil, gas, and mineral exploration; environmental assessment; crop analysis for optimizing irrigation and fertilization; and military remote sensing.

2001 PRESIDENT OF THE AVS SCIENCE AND TECHNOLOGY SOCIETY

Mr. Bruce Sartwell

Chemistry Division

The AVS Science and Technology Society is a nonprofit organization, which promotes communication, dissemination of knowledge, recommended practices, research, and education in the use of vacuum and other controlled environments to develop new materials, process technology, devices, and related understanding of material properties for the betterment of humanity. The Naval Research Laboratory was recognized for its support of Mr. Sartwell in his role as the 2001 President of the AVS Science and Technology Society. Each year the AVS sends a plaque to the institution where the year's President is employed, expressing its appreciation for their support. The citation reads: "Presented to the Naval Research Laboratory, in appreciation for the support of Bruce D. Sartwell, elected President of the AVS Science and Technology Society, 2001."



JEROME KRUGER AWARD IN CORROSION SCIENCE

Dr. Ed McCafferty

Chemistry Division

The award is named for Jerome Kruger, Professor Emeritus at Johns Hopkins University and an internationally known corrosion scientist. Dr. McCafferty was cited "for his distinguished contributions to the understanding of surface chemistry, the passivity of metal surfaces, surface modification, modeling, corrosion inhibitors, and adhesion science."

ROBERT T. FOLEY AWARD OF THE NATIONAL CAPITAL SECTION OF THE ELECTROCHEMICAL SOCIETY

The award is named for the late Robert T. Foley, long-time Professor of Chemistry at American University, noted corrosion scientist and supporter of the Electrochemical Society. Dr. McCafferty received the award for his work in corrosion science and education, and for his activities in the Electrochemical Society. Dr. McCafferty has been an adjunct faculty member first at The George Washington University, where he has taught a graduate course on the "Environmental Effects on Materials," and at Mary Washington College, where he taught undergraduate general chemistry.





2003 GEORGE KIMBELL BURGESS MEMORIAL AWARD

Dr. Ashraf Imam

Materials Science and Technology Division

The George Kimbell Burgess Memorial Award was established in 1941, by the Washington DC Chapter of the American Society for Metals as a tribute to Dr. Burgess in appreciation of his outstanding contributions to the science of metallurgy. This award is the highest award for scientific achievement given by the DC Chapter in recognition of outstanding achievement in research or administration to a member of the ASM Washington DC Chapter who has made original contributions in the field of metallurgy, materials, or mechanics or who demonstrates outstanding leadership in those fields within the five-year period prior to the award. Dr. Imam serves as a team leader in pursuing basic research on material structure-property relationship with emphasis on titanium alloy development, kinetics of transformation in solid phase, small-angle neutron scattering, acoustic damping, Ni-base superalloy, Al-Li alloy, titanium aluminide, and microalloying of steel.



ACHIEVEMENT IN TECHNICAL INGENUITY AWARD

Dr. Bruce Gaber, Dr. Fran Ligler, and Ms. Anne Kusterbeck

Center for Bio/Molecular Science and Engineering

The Impact Test System, a patented NRL technology licensed to LifePoint, Inc. of California, was recognized with an Achievement in Technical Ingenuity Award. The Impact Test System is a noninvasive drug and alcohol testing system that can process results in under five minutes. The technology is based on NRL's flow immunosensor, a biosensor for small molecules. The system can detect up to nine drugs and alcohol from one laboratory-quality saliva sample. Other advantages include its portability, low cost of operation, rapid response, and blood test accuracy

using only saliva. Potential users include law enforcement agencies, industrial workplaces, and medical emergency rooms.



2003 DISTINGUISHED ALUMNI AWARD FROM THE UNIVERSITY OF WISCONSIN-MADISON

Dr. Peter Vogt

Marine Geosciences Division

Dr. Vogt was recognized for his "distinguished scholarly achievements in marine geophysics and marine geology, including fundamental contributions to our understanding of plate tectonic processes." Along with his coworkers, he has studied marine geology and geophysics in almost all the oceans, and has spent more than three years total on a variety of research vessels, mostly as the chief (or co-chief) scientist.

2002 INTERNATIONAL PUBLIC MANAGEMENT ASSOCIATION (IPMA) LEADING EDGE AWARD

Demonstration Project Team – Ms. Betty Duffield, Ms. Janet Deschak, Ms. Lynda Heater, Ms. Linda Owens, Ms. Paula Scholten, Mr. Michael Vonk, Mr. Darryl Schenk, and Ms. Barbara Cain
Human Resources Office



The International Public Management Association recognized eight NRL team members for their significant accomplishments in human resource management for the further development and final implementation of the NRL Personnel Management Demonstration Project. Accomplishments were based on a Human Resources (HR) program that can be shown to support and enhance the mission of the agency, the use of innovative technology in business solutions, achievement of considerable cost reduction, evidence of substantial improvement in quality of work, efficiency, and customer service, and demonstration of ability to act as “change agent.” These accomplishments resulted in an achievement that can be recognized as significant by other professionals in human resources.

2002 COMMUNICATOR AWARDS' CRYSTAL AWARD FOR EXCELLENCE

Ms. Carol Hambric, Ms. Linda Greenway, and Mr. James Marshall
Former Technical Information Division



The Communicator Awards is an international awards competition that recognizes outstanding work in the communications field. The prestigious Award of Excellence is presented to entrants whose ability to communicate is among the best in the field. The former Technical Information Division's multimedia office was presented the award for its “A Tour of NRL” CD-ROM. NRL's award is one of 17 U.S. Government agency award winners. Most winners of this award were production companies.

2002 TELLY AWARDS

Ms. Carol Hambric, Ms. Linda Greenway, and Mr. James Marshall

The Telly Awards were founded in 1980 to showcase and give recognition to excellence in non-network television, cable commercials, and film and video production. Over the past 23 years, the Telly Awards have become a well-known and highly respected, national competition. Entries to the Telly do not compete against each other; rather, they compete against a high standard of excellence. The Telly is one of the most sought after awards in the TV, commercial, and video industry. The former Technical Information Division's multimedia team was presented with two bronze Telly Awards in the Corporate and Miscellaneous categories for its “A Tour of NRL” CD-ROM.





FEDERAL AND ARMED FORCES LIBRARIES ROUND TABLE (FAFLRT) OF THE AMERICAN LIBRARY ASSOCIATION (ALA) DISTINGUISHED SERVICE AWARD

Mr. James King

Ruth H. Hooker Research Library

The Federal and Armed Forces Libraries Round Table of the American Library Association promotes: library and information service and the library and information profession in the Federal and Armed Forces communities; appropriate utilization of federal and armed forces library and information resources and facilities; and an environment for the stimulation of research and development relating to the planning, development, and operation of federal and armed forces libraries. This award recognizes Mr. King's outstanding and sustained contributions to FAFLRT as its official web master and discussion list coordinator. Maintaining both a web site and a discussion list are time consuming responsibilities – one that Mr. King has willingly assumed in an efficient and professional manner. As web master, Mr. King has made many improvements to FAFLRT's web presence and facilitated the sharing of information among its active membership. He also serves on several professional and scientific society boards advising on information technology issues.

awards from within NRL



E.O. HULBURT SCIENCE AWARD

Dr. David Singh

Materials Science & Technology Division

This award is NRL's highest civilian honor for scientific achievement. Dr. Singh was recognized for his "outstanding contributions to the development and application of first principles methods in materials science, and for imaginative approaches in understanding and discovery of novel materials for Navy use." Dr. Singh is an expert on density functional based methods, particularly the linearized augmented planewave (LAPW) method and its extensions, on which he has written the only book, as well as the planewave-pseudopotential methods. His expertise in these methods, his abilities in applying them, and his insights in condensed matter physics, have allowed him to make very substantial contributions to the scientific activity of the Center for Computational Materials Science and the community at large.

NAVY MERITORIOUS CIVILIAN SERVICE AWARD

Dr. Brenda Little

Oceanography Division

The Meritorious Civilian Service Award is the third highest award bestowed by the Navy to its civilian employees. Dr. Little's award recognized her sustained innovative role and outstanding transitional impact in the field of marine molecular processes. She was cited for "her meritorious achievements and dedication to the United States Navy and the Naval Research Laboratory while serving as the senior scientist for Marine Molecular Processes. Dr. Little's pioneering innovations and advancements in electron microscopy, biomineralization, and corrosion mechanisms have made great strides in furthering the United States Navy as a world leader in identifying and understanding microbiologically influenced corrosion."



NAVY MERITORIOUS CIVILIAN SERVICE AWARD

Dr. John Harding

Oceanography Division

The Meritorious Civilian Service Award is the third highest award bestowed by the Navy to its civilian employees. This award is presented for extraordinary service, specific achievements and/or accomplishments, or heroism in a life-threatening situation. Dr. Harding was recognized for "his meritorious achievement and dedication to the United States Navy and the Naval Research Laboratory while serving as the head of the Ocean Dynamics and Prediction Branch since 1995. Because of Dr. Harding's dedication and vision, the Branch is a world leader in global ocean modeling and prediction, and continues to be at the forefront of important research relevant to the operational missions of the United States Navy."



NAVY MERITORIOUS CIVILIAN SERVICE AWARD

Mr. Charles Steenbuck

Navy Office of General Counsel

The Meritorious Civilian Service Award is the third highest award bestowed by the Navy to its civilian employees. According to the citation, Mr. Steenbuck was recognized for "exemplary service and dedication to the Naval Research Laboratory, the Navy Office of General Counsel, and the Department of the Navy. Mr. Steenbuck has demonstrated extraordinary leadership, resourcefulness, and responsiveness over the past decade, during which his efforts sustained and advanced the Office of Counsel's ability to provide the highest quality legal services in support of the Navy's research mission. He particularly distinguished himself through his coordinating of NRL's response to an FBI subpoena related to the high-profile anthrax investigations; leading the successful defense against a protest challenging the acquisition of advanced Improved Data Modems needed by U.S. forces deployed to Iraq; playing a key role in establishing memoranda of agreement for homeland mediary agreement between NRL and George Mason University; and coordinating NRL's use of authority granted under Section 246 of the National Defense Authorization Act of 1999 to find innovative ways of supporting technology between NRL and universities and non-government entities."





NAVY MERITORIOUS CIVILIAN SERVICE AWARD

Dr. Richard Colton

Chemistry Division

The Meritorious Civilian Service Award is the third highest award bestowed by the Navy to its civilian employees. Dr. Colton was recognized for being a role model for leadership, dedication and service, and productivity. According to the citation, Dr. Colton has “made important contributions as a scientist, technologist, and manager. Over 120 papers in refereed journals and over 4,600 citations to those papers measure his impact in science. For his outstanding science record, the American Chemical Society of Washington recognized him in 1992 with the Hillebrand Prize. His science discoveries have led to six patents and the evolving commercialization of instrumentation measuring surface nanomechanics and of chemical/biological sensors utilizing binding forces to discriminate against false alarms. As Surface Chemistry Branch Head over the past five years, he has inspired an effort that produces more than one-third of the division archival productivity and one half of its invited talks to professional society conferences. In addition, he has made significant contributions to the NRL response to Team Tango, the Nanoscience Institute, and the Invention Evaluation Board.”



NAVY MERITORIOUS CIVILIAN SERVICE AWARD

Dr. Anthony Dandridge

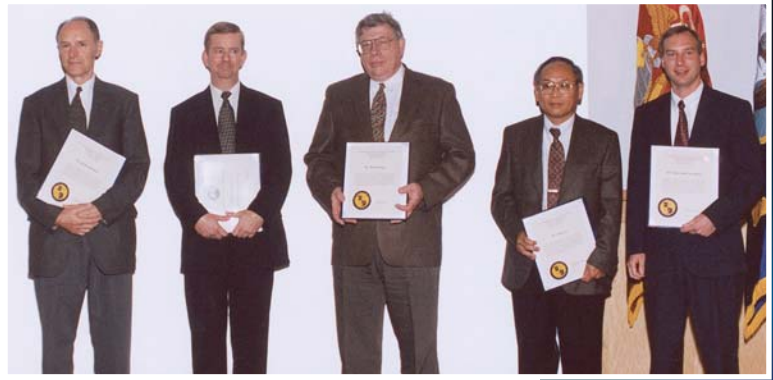
Optical Sciences Division

The Meritorious Civilian Service Award is the third highest award bestowed by the Navy to its civilian employees. Dr. Dandridge was cited for his exceptional performance in the transition of the fiber-optic planar array from the initial 6.2 hydrophone and electro-optic system development, through 6.3 and 6.4 to production for the Virginia-class attack submarines. According to the citation, “Dr. Dandridge provided the multiplexing architecture, the hydrophone design, optical source, interrogation approach, and demodulation approach for this system. He played a major role in the overall design, as well as determining a number of critical performance parameters of the system. He designed and performed a number of the critical tests, which verified his performance predictions and helped define the system as it now is. Dr. Dandridge holds a number of patents pertaining to the key elements in the system.” Dr. Dandridge’s contributions in the area of hull array development also provided the basis for the development of a number of other fiber-optic acoustic sensor systems.

NRL AWARD OF MERIT FOR GROUP ACHIEVEMENT

Drs. Raymond Patten, Michael Duncan, Melvin Kruer, John Lee, and Mr. Dale Linne von Berg
Optical Sciences Division

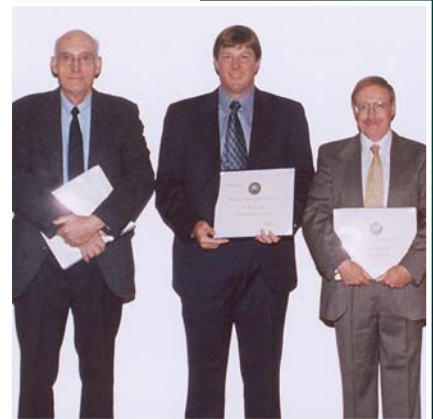
NRL researchers were cited for their outstanding achievements in the SHARed Reconnaissance Pod (SHARP) Prototype program. According to the citation, "The SHARP Prototype program successfully demonstrated real-time reconnaissance operations of the SHARP Prototype system on an F/A-18 aircraft and of the SHARP Prototype payload on a P-3 in coordinated flights, with each aircraft down-linking imagery to a NAVIS ground station and displaying that imagery in real time to an audience at the Pentagon, on August 28, 2001. As a consequence of the Prototype program, the SHARP program has continued into the EMD phase and is on schedule to meet the ambitious operational deployment plans for SHARP. The individuals recognized were outstanding in their technical accomplishments, leadership in the testing and integration efforts, and their planning, management, and execution of a complex program involving multiple organizations and diverse interests."



NRL AWARD OF MERIT FOR GROUP ACHIEVEMENT

Dr. Alan Tveten, Mr. Clay Kirkendall, Dr. Anthony Dandridge, and Mr. Gary Cogdell (not shown)
Optical Sciences Division

According to the citation, "During the past fifteen years, personnel from the Optical Techniques Branch and the Fiber-Optics Technology Program Office have successfully led the Navy's effort to transition fiber-optic sensor technology from 6.1 Basic Research to the Fleet. The research team managed all phases of development from the initial discovery and invention performed under the Office of Naval Research sponsorship to the engineering and manufacturing development phase currently in progress. These systems include the fiber-optic light-weight wide-aperture array (LWAA), the all-optical deployable system (AODS), and the fiber-optic TB-29 towed array."



NRL AWARD OF MERIT FOR GROUP ACHIEVEMENT

Dr. Donald Forester, Dr. Scott Browning, Dr. Frank Klemm, Dr. Gary Roan, Dr. Don Northam, Mr. Richard Gurney, Dr. Ann Mera, Dr. Joel Schnur, Dr. Paul Schoen, Dr. Dan Zabetakis, Dr. Alok Singh, Mr. Ronald Price, and Ms. Anne Kusterbeck

Systems Directorate, Center for Bio/Molecular Science and Engineering, Chemistry Division, and Tactical Electronic Warfare Division

According to the citation, "This team developed a radar-absorbing panel for antenna isolation in the NULKA decoy that weighs less than half as much as the coating it replaces. The reduction in weight allows longer dwell time and improvements in performance for the decoy. The work required a collaboration across NRL and involved a combination of chemical synthesis, biophysics, metal chemistry, polymer chemistry, surface chemistry, materials science, microwave engineering, and technical program management, a tour de force of scientific disciplines. This combination of talents nurtured the development of a new radar absorber from the observation of unusual microcylinders in a biomembrane constituent, through their transformation to a robust metallic powder, to their incorporation in an artificial dielectric composite, to their testing as a radar absorber."



COMMANDING OFFICER'S AWARD FOR EXCELLENCE IN MISSION SUPPORT

Small Purchase Section

Supply Division

The NRL Award for Excellence in Mission Support is given in recognition of significant contributions not involving the sciences and engineering. It constitutes the highest NRL award that may be given for such contributions. The Small Purchase Section was presented this award for its sustained, outstanding performance for the NRL research community by procuring required materials, supplies, and services for the entire Laboratory. In FY02, this group awarded \$49.4M worth of acquisitions that fell within the purview of the simplified acquisition thresholds, using an average of 4.4 days for each procurement. The individuals recognized were outstanding in their accomplishments by continuing to provide many of the tools necessary for the NRL community to achieve their mission goals.

COMMANDING OFFICER'S AWARD FOR EXCELLENCE IN SECRETARIAL SUPPORT

Ms. Lynda Kelly
Radar Division

Ms. Kelly was cited for her "efficiency, initiative, dedication, professionalism, and outstanding personal contributions to her branch and division, providing a positive impact on their efficient and smooth operation." The basis for her nomination is the major role Ms. Kelly has played in three areas: conference organization and management; management of the branch budget; and performance above and beyond expected secretarial duties. Her accomplishments include her invaluable work in organizing and managing the international AMEREM 2002 Symposium, hosted by both NRL and the U.S. Naval Academy in Annapolis, MD, in June 2002. She followed this by applying her management skills in support of the First Tri-Service Waveform Diversity Workshop, hosted by NRL and attended by 100 senior researchers and midlevel managers, representing a number of DOD organizations.



THE 2003 NRL REVIEW ARTICLE AWARDS

Awards for *NRL Review* articles recognize authors who submit outstanding research articles for this publication. The articles are judged on the relevance of the work to the Navy and DOD, readability to the college-graduate level, clearness and conciseness of writing, and the effective use of graphics that are interesting and informative. The following awards were presented for articles that appeared in the *2003 NRL Review*.

FEATURED RESEARCH ARTICLE

"Filamentation and Propagation of Ultra-short, Intense Laser Pulses in Air," Dr. Antonio Ting, Dr. Daniel Gordon, Dr. Richard Hubbard, Dr. Joseph Peñano, and Dr. Phillip Sprangle (Plasma Physics Division)



Flanked between CAPT David Schubert and Dr. John Montgomery, from left to right, are Drs. Antonio Ting, Joseph Peñano, Daniel Gordon, and Richard Hubbard. (Dr. Phillip Sprangle not pictured.)

DIRECTORATE AWARDS FOR SCIENTIFIC ARTICLES

SYSTEMS DIRECTORATE

"Tactical Aircraft Directed Infrared Countermeasures System Overview," Mr. Kenneth Sarkady, Dr. Hugo Romero, Mr. David Cordray, Dr. James Lynn, and Mr. Roger Mabe (Optical Sciences Division)



Left to right: CAPT David Schubert, Mr. Roger Mabe, Dr. James Lynn, Mr. Kenneth Sarkady, Dr. Hugo Romero, and Dr. John Montgomery. (Mr. David Cordray not pictured.)

MATERIALS SCIENCE AND COMPONENT TECHNOLOGY DIRECTORATE

"A New Ferromagnetic Semiconductor: Mn_xGe_{1-x} ," Mr. Aubrey Hanbicki, Dr. Berend Jonker, Dr. Steven Erwin, Dr. Carl Hellberg, and Dr. George Spanos (Materials Science and Technology Division)



Left to right: CAPT David Schubert, Dr. Carl Hellberg, Dr. Steven Erwin, Mr. Aubrey Hanbicki, Dr. Berend Jonker, and Dr. John Montgomery. (Dr. George Spanos not pictured.)

OCEAN AND ATMOSPHERIC SCIENCE AND TECHNOLOGY DIRECTORATE

"Through-The-Sensors Concepts to Refresh the Environmental Picture," Mr. William Avera, Mr. Michael Harris, Mr. Donald Walter, Mr. Leonard Bibee, and Mr. Douglas Lambert (Marine Geosciences Division)



Left to right: CAPT David Schubert, Mr. Michael Harris, Mr. William Avera, and Dr. John Montgomery. (Mr. Donald Walter, Mr. Leonard Bibee, and Mr. Douglas Lambert not pictured.)

NAVAL CENTER FOR SPACE TECHNOLOGY

"Free-Space High-Speed Laser Communication Link Across the Chesapeake Bay," Mr. Christopher Moore, Ms. Michele Suite, Mr. Michael Vilcheck, Mr. Walter Smith III, Mr. William Scharph, Ms. Anne Reed (Space Systems Development Department), Dr. William Rabinovich, Dr. Jeffrey Koplou, and Dr. Sean Moore (Optical Sciences Division)



Left to right: CAPT David Schubert, Ms. Anne Reed, Dr. William Rabinovich, Mr. Christopher Moore, Ms. Michele Suite, Dr. Sean Moore, Mr. Walter Smith III, Mr. William Scharph, and Dr. John Montgomery. (Mr. Michael Vilcheck and Dr. Jeffrey Koplou not pictured.)

ALAN BERMAN RESEARCH PUBLICATION AND EDISON (PATENT) AWARDS

The Annual Research Publications Awards Dinner (ARPAD) was established in 1968 to recognize the authors of the best NRL publications each year. These awards not only honor individuals for superior scientific accomplishments in the field of naval research, but also seek to promote continued excellence in research and in its documentation. In 1982, the name of this award was changed to the Alan Berman Research Publication Awards in honor of its founder.

Of the 258 papers considered for 2003 awards, 35 were selected for recognition. They represent 158 authors. The names of the authors with the titles and abstracts of their publications are listed under their respective research divisions.

NRL also recognizes patents as part of its annual publication awards program. The NRL Edison (Patent) Awards were established in January 1991 to recognize NRL employees for outstanding patents issued to NRL by the U.S. Patent and Trademark Office during the preceding calendar year. The awards recognize significant NRL contributions to science and engineering as demonstrated by the patent process that are perceived to have the greatest potential benefit to the country. Of the 63 patents considered for 2003, 3 were selected representing 7 inventors and 3 patent attorneys. They are listed under the NRL Edison (Patent) Awards.

PUBLICATION AWARDS

SIGNATURE TECHNOLOGY OFFICE

Electromagnetic Waves Focused by a Negative-Index Planar Lens
P.F. Loschialpo, D.L. Smith, D.W. Forester, F.J. Rachford, and J. Schelleng

RADAR DIVISION

Accurate and Efficient Numerical Integration of Weakly Singular Integrals
in Galerkin EFIE Solutions
Douglas J. Taylor

Micro-Doppler Phenomenon and Radar Signature
Victor C. Chen and André P. des Rosiers

INFORMATION TECHNOLOGY DIVISION

Resolving Multiple Occluded Layers in Augmented Reality
*Mark A. Livingston, J. Edward Swan II, Dennis Brown, Joseph L. Gabbard, Deborah Hix,
Tobias H. Höllerer, Simon J. Julier, and Yohan Baillot*

Preparing to Resume an Interrupted Task: Effects of Prospective
Goal Encoding and Retrospective Rehearsal
J. Gregory Trafton, Derek P. Brock, Erik M. Altmann, and Farilee E. Mintz

OPTICAL SCIENCES DIVISION

Joint Subspace Detection in Hyperspectral Sensing
Alan Schaum and A. Stocker

Air-Included Polymer Coatings for Enhanced Sensitivity of
Fiber-Optic Acoustic Sensors
*James H. Cole, Alan Tveten, Clay Kirkendall, Anthony Dandridge,
Sara Motley, and Jacek Jarzynski*

TACTICAL ELECTRONIC WARFARE DIVISION

A Multiple Hypothesis Correlation Algorithm for Advanced Multi-Sensor,
Multi-Platform Integration in CEC
Edward N. Khoury and Ronald E. Helmick

CHEMISTRY DIVISION

Step Structure and Surface Morphology of Hydrogen-terminated Silicon: (001) to (114)
Arnaldo R. Laracuente and Lloyd J. Whitman

DC-ARM Final Demonstration Report
*Frederick W. Williams, John P. Farley, Patricia A. Tatem, Arthur F. Durkin,
Xuan H. Nguyen, Ariam C. Luers, Daniel T. Gottuk, Hung V. Pham,
Joseph L. Scheffey, Jennifer T. Wong, Ryan Downs, and Eric Runnerstrom*

MATERIALS SCIENCE AND TECHNOLOGY DIVISION

Self-Doping of Gold Chains on Silicon: A New Structural Model for Si(111)-(5×2)-Au
Steven C. Erwin

Laser Deposition of Polymer and Biomaterial Films
*D.B. Chrisey, A. Pique, R.A. McGill, J.S. Horwitz, B.R. Ringeisen,
D.M. Bubb, and P.K. Wu*

LABORATORY FOR COMPUTATIONAL PHYSICS AND FLUID DYNAMICS

Partial Fuel Filling in Pulse Detonation Engines
C. Li and K. Kailasanath

Thermonuclear Supernovae: Simulations of the Deflagration Stage
and Their Implications
*Vadim N. Gamezo, Alexei M. Khokhlov, Elaine S. Oran, Robert O. Rosenberg,
and Almadena A. Chtchelkanova*

PLASMA PHYSICS DIVISION

Laboratory Investigation of Boundary Layer Processes Due to
Strong Spatial Inhomogeneity
W.E. Amatucci, G. Ganguli, D.N. Walker, G. Gatling, T. McCulloch, and M. Balkey

Eliminating the Transit-Time Instability in Large-Area Electron-Beam Diodes
M. Friedman, Y. Chan, S. Obenschain, J.D. Sethian, and S.B. Swanekamp

ELECTRONICS SCIENCE AND TECHNOLOGY DIVISION

Three-Dimensional Mapping of Single-Event Effects Using Two-Photon Absorption

Dale McMorrow, Joseph S. Melinger, William T. Lotshaw, Stephen Buchner, Younes Boulghassoul, Lloyd W. Massengill, and Ronald L. Pease

A Micro-Air-Vehicle Jammer Payload

Walter Kruppa, Chrisen Rauscher, Francis J. Kub, and M. Ziya Gun

CENTER FOR BIO/MOLECULAR SCIENCE AND ENGINEERING

Nematic Elastomer Fiber Actuator

Jawad Naciri, Banaballi R. Ratna, Amritha Srinivasan, Nikolay Nikolov, Hong Jeon, and Patrick Keller

Conductance Scaling of Molecular Wires in Parallel

James G. Kushmerick, Jawad Naciri, Ranganathan Shashidhar, and John C. Yang

ACOUSTICS DIVISION

Nonlinear Internal Waves in the South China Sea: Observation of the Conversion of Depression Internal Waves to Elevation Internal Waves

Marshall H. Orr and Peter C. Mignerey

Fast Fourier Transform and Singular Value Decomposition Formulations for Patch Nearfield Acoustical Holography

Earl G. Williams, Brian H. Houston, and Peter C. Herdic

REMOTE SENSING DIVISION

Improving the Performance of Classifiers in High-Dimensional Remote Sensing Applications: An Adaptive Resampling Strategy for Error-Prone Exemplars (ARESEPE)

Charles M. Bachmann

Angular Diameters of Stars from the Mark III Optical Interferometer

D. Mozurkewich, J.T. Armstrong, R.B. Hindsley, A. Quirrenbach, C.A. Hummel, D.J. Hutter, K.J. Johnston, A.R. Hajian, N.M. Elias II, D.F. Buscher, and R.S. Simon

OCEANOGRAPHY DIVISION

The NRL Layered Global Ocean Model (NLOM) with an Embedded Mixed Layer Sub-Model: Formulation and Tuning

Alan J. Wallcraft, Harley E. Hurlburt, A. Birol Kara, and Peter A. Rochford

Ocean-Acoustic Solitary Wave Studies and Predictions

A.C. Warn-Varnas, Zack Hallock, S.A. Chin-Bing, D.B. King, and J.A. Hawkins

MARINE GEOSCIENCES DIVISION

Comparison of Optical and Radar Measurements of Surf and Swash Zone Velocity Fields

Jack A. Puleo, K. Todd Holland, Gordon Farquharson, and Stephen J. Frasier

Geographical Data Interchange Using XML-Enabled Technology
within the GIDB™ System

*Ruth Wilson, Frank McCreedy, Roy Ladner, Kevin Shaw, Fred Petry, David Olivier,
Maria Cobb, Todd Lovitt, and Mahdi Abdelguerfi*

MARINE METEOROLOGY DIVISION

Coupled Ocean-Atmosphere Nested Modeling of the Adriatic Sea
During Winter and Spring 2001

*Julie Pullen, James D. Doyle, Richard Hodur, Jeffrey W. Book, Henry Perkins,
Andrea Ogston, and Richard Signell*

A High-Resolution Numerical Study of the Asian Dust Storms of April 2001

*Ming Liu, Douglas L. Westphal, Shigong Wang, Atsushi Shimizu,
Nobuo Sugimoto, Jun Zhou, and Yan Chen*

SPACE SCIENCE DIVISION

Evolving Active Region Loops Observed with the *Transition Region and
Coronal Explorer: II. Time-Dependent Hydrodynamic Simulations*

Harry P. Warren, John T. Mariska, and Amy R. Winebarger

The Influence of the 11-Year Solar Cycle on the Quasi-Biennial Oscillation

John P. McCormack

SPACE SYSTEMS DEVELOPMENT DEPARTMENT

Modeling Single-Event Effects in a Complex Digital Device

*Kenneth A. Clark, Dale McMorrow, Alan A. Ross, Herschel H. Loomis,
Todd R. Weatherford, Douglas J. Fouts, and Stephen P. Buchner*

Time of Day Management for Satellite Communications

Rachel Evans and Joseph A. White

SPACECRAFT ENGINEERING DEPARTMENT

Orbit Propagation with Lie Transfer Maps in the Perturbed Kepler Problem

Liam Healy

NRL EDISON (PATENT) AWARDS

OPTICAL SCIENCES DIVISION

Helical Fiber Amplifier

Jeffrey Koplou, Lewis Goldberg, Daby Kliner, and Dorothy I. Becker

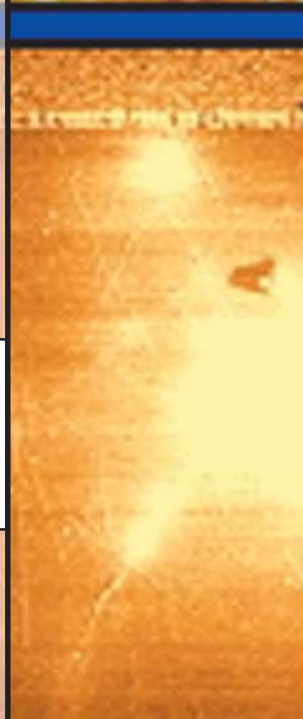
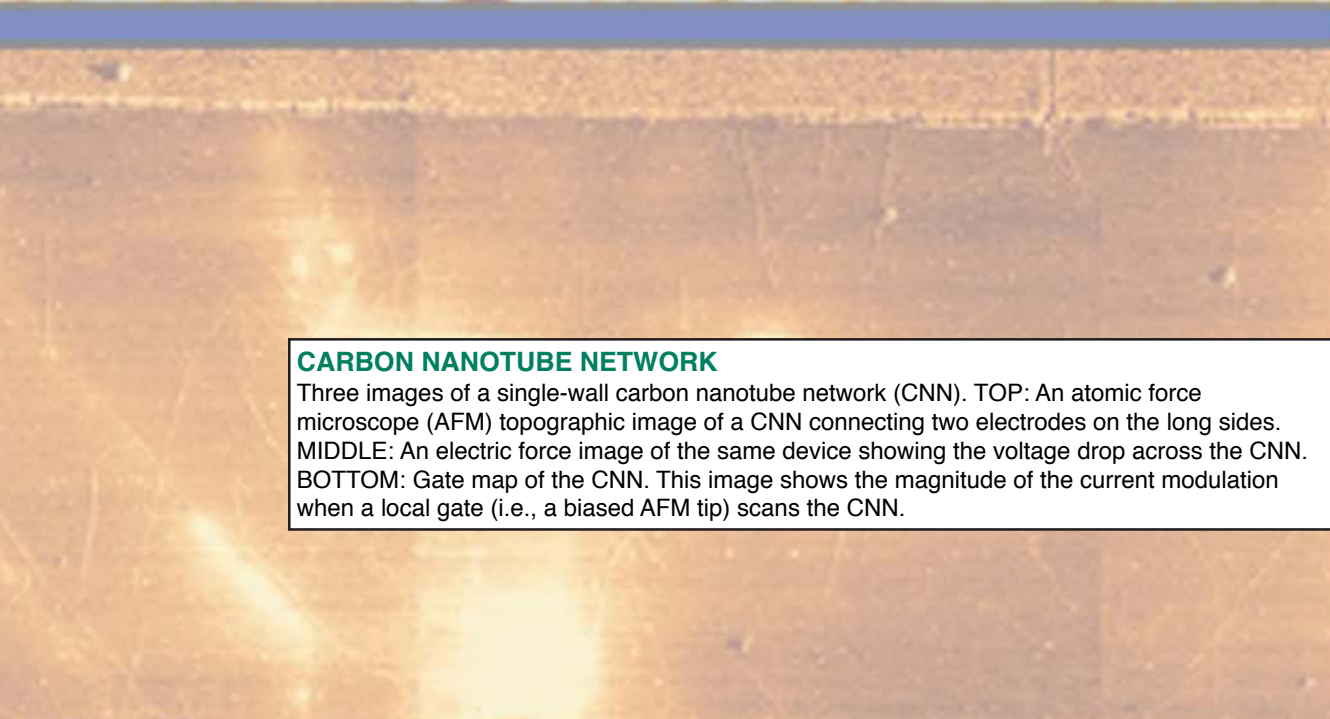
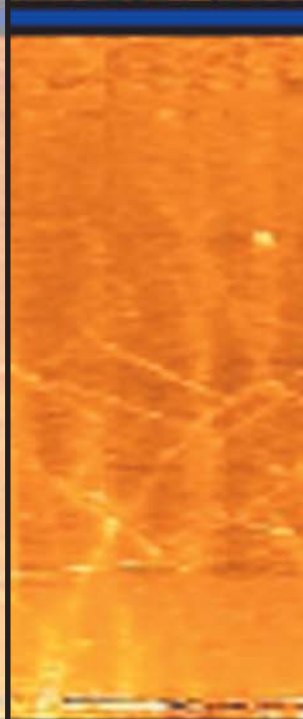
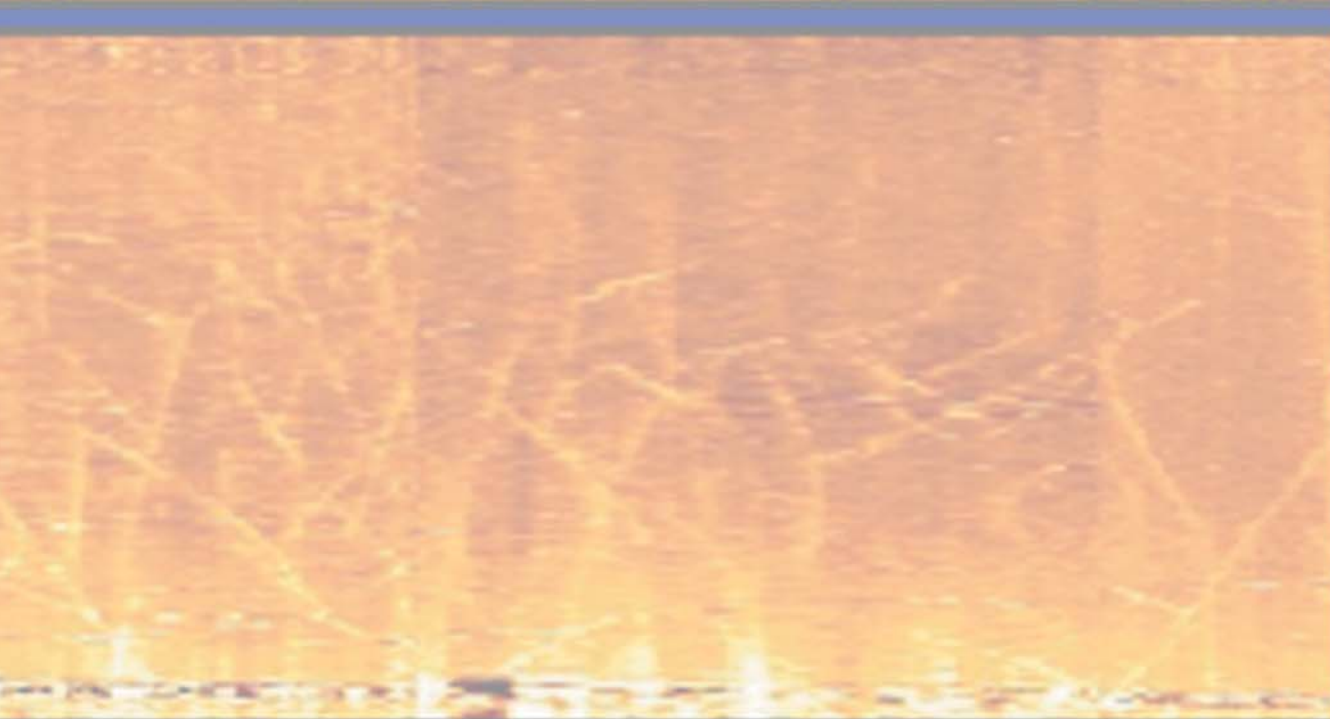
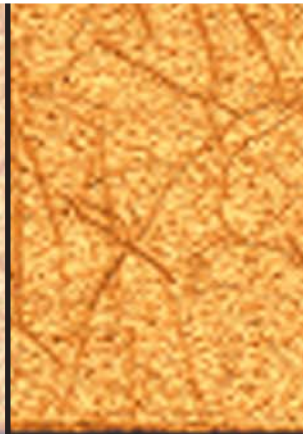
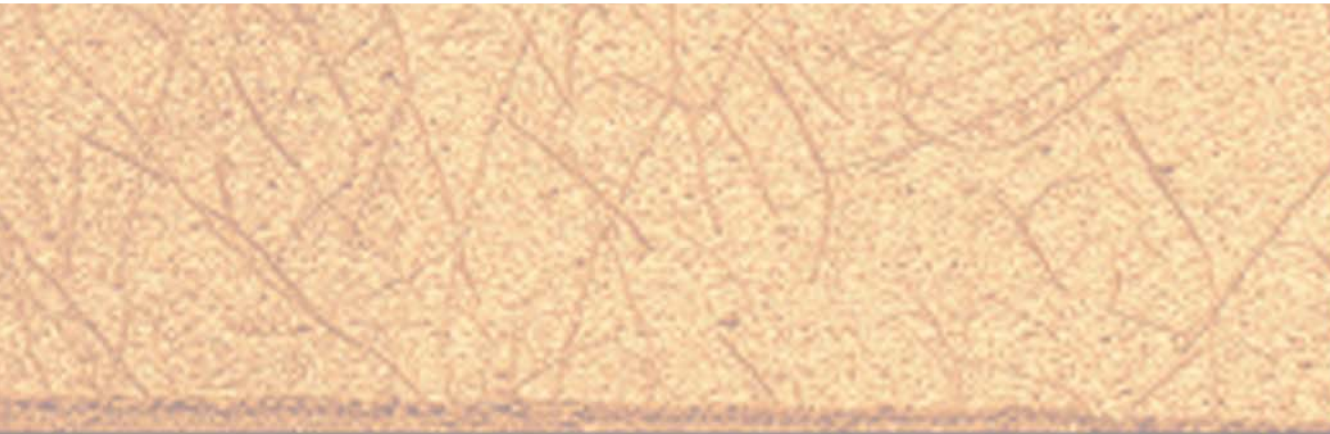
Method of Patterning Electrically Conductive Polymers

Zakya Kafafi, Woohong Kim, and Stephen Hunnius

MATERIALS SCIENCE AND TECHNOLOGY DIVISION

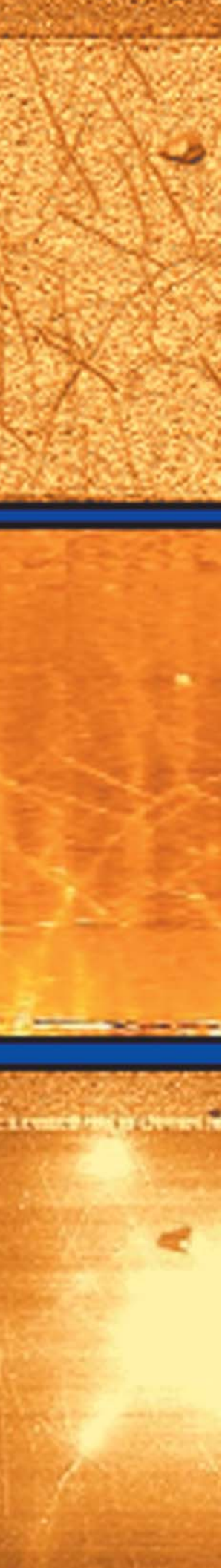
Linear Chemoselective Carbosilane Polymers and Methods for Use in
Analytical and Purification Applications

R. Andrew McGill, Eric J. Houser, and Rebecca Forman



CARBON NANOTUBE NETWORK

Three images of a single-wall carbon nanotube network (CNN). TOP: An atomic force microscope (AFM) topographic image of a CNN connecting two electrodes on the long sides. MIDDLE: An electric force image of the same device showing the voltage drop across the CNN. BOTTOM: Gate map of the CNN. This image shows the magnitude of the current modulation when a local gate (i.e., a biased AFM tip) scans the CNN.



241 Programs for NRL Employees — Graduate Programs, Continuing Education, Professional Development, Equal Employment Opportunity (EEO) Programs, and Other Activities

244 Programs for Non-NRL Employees — Recent Ph.D., Faculty Member, and College Graduate Programs, Professional Appointments, College Student Programs, and High School Student Programs

PROGRAMS FOR NRL EMPLOYEES

The Human Resources Office, Personnel Operations Branch, continues to support and provide traditional and alternative methods of training for employees. During 2003, NRL employees were encouraged to develop their skills by attending training to enhance their job performance in order to continue to meet the future needs of NRL as well as their own goals for growth.

One common study procedure is for employees to work full time at the Laboratory while taking job-related scientific courses at universities and schools in the Washington area. The training ranges from a single course to full graduate and postgraduate programs. Tuition for training is paid by NRL. The formal programs offered by NRL are described here.

GRADUATE PROGRAMS

- The **Advanced Graduate Research Program** (formerly the Sabbatical Study Program, which began in 1964) enables selected professional employees to devote full time to research or pursue work in their own or a related field for one year at an institution or research facility of their choice without the loss of regular salary, leave, or fringe benefits. NRL pays all travel and moving expenses for the employee and dependents. Criteria for eligibility include professional stature consistent with the applicant's opportunities and experience, a satisfactory program of study, and acceptance by the facility selected by the applicant. The program is open to paraprofessional employees (and above) who have completed 6 years of Federal Service, 4 of which have been at NRL.

- The **Edison Memorial Graduate Training Program** enables employees to pursue advanced studies in their fields at local universities. Participants in this program work 24 hours each workweek and pursue their studies during the other 16 hours. The criteria for eligibility include a minimum of one year of service at NRL, a bachelor's or master's degree in an appropriate field, and professional standing in keeping with the candidate's opportunities and experience.

- To be eligible for the **Select Graduate Training Program**, employees must have a college degree in an appropriate field and must have demonstrated ability and aptitude for advanced training. Students accepted into this program devote a full academic year to graduate study. While attending school, they receive one-half of their salary, and NRL pays for tuition and laboratory expenses.

- The **Naval Postgraduate School (NPS)**, located in Monterey, California, provides graduate programs to enhance the technical preparation of Naval officers and civilian employees who serve the Navy in the fields of science, engineering, operations analysis, and management. It awards a master of arts degree in national security affairs and a master of science degree in many technical disciplines.

NRL employees desiring to pursue graduate studies at NPS may apply for a maximum of six quarters away from NRL, with thesis work accomplished at NRL. Specific programs are described in the NPS catalog. Participants will continue to receive full pay and benefits during the period of study.

- In addition to NRL and university offerings, application may be made to a number of noteworthy programs and fellowships. Examples of such opportunities are the **Capitol Hill Workshops**, the **Legislative Fellowship (LEGIS) program**, the **Federal Executive Institute (FEI)**, the **Fellowship in Congressional Operations**, and the **Executive Leadership Program for Mid-Level Employees**. These and other programs are announced from time to time, as schedules are published.

- Research conducted at NRL may be used as **thesis material for an advanced degree**. This original research is supervised by a qualified employee of NRL who is approved by the graduate school. The candidate should have completed the required course work and should have satisfied the language, residence, and other requirements of the graduate school from which the degree is sought. NRL provides space, research facilities, and supervision but



NRL WISE Network members and supporters gather to celebrate recent accomplishments of NRL women scientists and goals.

leaves decisions on academic policy to the cooperating schools.

CONTINUING EDUCATION

- **Undergraduate and graduate courses** offered at local colleges and universities are subsidized by NRL for employees interested in improving their skills and keeping abreast of current developments in their fields. These courses are also available at a number of DOD installations in the Washington, DC, area.

- NRL offers **short courses** to all employees in a number of fields of interest including technical subjects, computer operation, and supervisory and management techniques. Laboratory employees may attend these courses at nongovernment facilities as well. Interagency courses in management, personnel, finance, supervisory development, and clerical skills are also available.

For further information on any of the above programs, contact the Employee Relations and Development Branch (Code 1850) at (202) 404-8314.

- The **Scientist-to-Sea Program (STSP)** provides increased opportunities for Navy R&D laboratory/center personnel to go to sea to gain first-hand insight into operational factors affecting system design, performance, and operations on a variety of ships. NRL is a participant of this ONR program. For further information contact the Administrative Office of the Systems Directorate (Code 5002) Dorene Ernst or Troy Mayo at (202) 767-3314.

PROFESSIONAL DEVELOPMENT

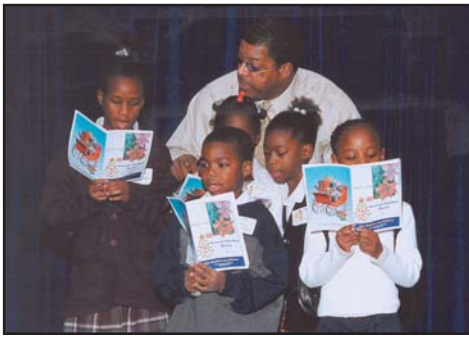
NRL has several programs, professional society chapters, and informal clubs that enhance the professional growth of employees. Some of these are listed below.

- The **Counseling Referral Service (C/RS)** helps employees to achieve optimal job performance through counseling and resolution of problems such as family, stress and anxiety, behavioral, emotional, and alcohol- or drug-related problems that may adversely impact job performance.

C/RS provides confidential assessments and short-term counseling, training workshops, and referrals to additional resources in the community. (Contact Dr. Ralph Surette at (202) 767-6857.)

- The **NRL Women in Science and Engineering (WISE) Network** was formed in 1997 through the merger of the NRL chapter of WISE and the Women in Science and Technology Network. Luncheon meetings and seminars are held to discuss scientific research areas, career opportunities, and career-building strategies. The group also sponsors projects to promote the professional success of the NRL S&T community and improve the NRL working environment. Membership is open to all S&T professionals. (Contact Dr. Rhonda Stroud at (202) 404-4143 or Dr. Ellen Goldman at (202) 404-6052.)

- **Sigma Xi**, the scientific research society, encourages and acknowledges original investigation in pure and applied science. As an honor society for research scientists, individuals who have demonstrated the ability to perform original research are elected to membership in local chapters. The NRL Edison Chapter, comprising approximately 400 members, recognizes original research by presenting awards annually in pure and applied science to outstanding NRL staff members. The chapter also sponsors lectures at NRL on a wide range of scientific topics for the entire NRL community. These lectures are delivered by scientists from all over the nation and the world. The highlight of the Sigma Xi lecture series is the Edison Memorial Lecture, traditionally featuring a distinguished scientist. (Contact Dr. Steve Hellberg at (202) 767-3934.)



The Community Outreach Program hosted its 36th annual holiday party for neighborhood children representing four local District of Columbia elementary schools in Ward 8.

- The **NRL Mentor Program** was established to provide an innovative approach to professional and career training and an environment for personal and professional growth. It is open to permanent NRL employees in all job series and at all sites. Mentorees are matched with successful, experienced colleagues having more technical and/or managerial experience who can provide them with the knowledge and skills needed to maximize their contribution to the success of their immediate organization, to NRL, to the Navy, and to their chosen career fields. The ultimate goal of the program is to increase job productivity, creativity, and satisfaction through better communication, understanding, and training. NRL Instruction 12400.1A provides policy and procedures for the program. (Contact Ms. Dawn Brown at (202) 767-2957.)

- Employees interested in developing effective self-expression, listening, thinking, and leadership potential are invited to join either of two NRL chapters of **Toastmasters International**. Members of these clubs, who possess diverse career backgrounds and talents, meet two to four times a month in an effort to learn to communicate not by rules but by practice in an atmosphere of understanding and helpful fellowship. NRL's Commanding Officer and Director of Research endorse Toastmasters as an official training medium at NRL. (Contact Kathleen Parrish at (202) 404-4963 for more information.)

EQUAL EMPLOYMENT OPPORTUNITY (EEO) PROGRAMS

Equal employment opportunity is a fundamental NRL policy for all employees regardless of race, color, national origin, sex, religion, age, or disability. The NRL EEO Office is a service organization whose major functions include counseling employ-

ees in an effort to resolve employee/management conflicts, processing formal discrimination complaints, providing EEO training, and managing NRL's affirmative employment recruitment program. The NRL EEO Office is also responsible for sponsoring special-emphasis programs to promote awareness and increase sensitivity and appreciation of the issues or the history relating to females, individuals with disabilities, and minorities. (Contact the NRL Deputy EEO Officer at (202) 767-5264 for additional information on any of our programs or services.)

OTHER ACTIVITIES

- The **Community Outreach Program** traditionally has used its extensive resources to foster programs that provide benefits to students and other community citizens. Volunteer employees assist with and judge science fairs, give lectures, tutor, mentor, coach, and serve as classroom resource teachers. The program also sponsors African American History Month art and essay contests for local schools, student tours of NRL, a student Toastmasters Youth Leadership Program, an annual holiday party for neighborhood children, and other programs that support the local community. Also through this program, NRL has active partnerships with four District of Columbia public schools. (Contact Mr. Dom Panciarelli at (202) 767-2541.)

- Other programs that enhance the development of NRL employees include four computer user groups (**IBM PC**, **Mac**, **NeXT**, and **Sun**) and the **Amateur Radio Club**. The **Recreation Club** encourages wide interest in sports for employees with its many facilities and programs, such as a heated indoor pool; basketball and volleyball court; weight room; table tennis; hot tub; five martial arts disciplines; aerobics classes; water walking and exercise; and sports leagues. Sportswear, NRL and seasonal paraphernalia, and discount tickets to amusement parks are available at the Rec Club office. The **Showboaters** theater group has been "in the dark" for a number of years. Regrouping is needed. Showboaters is looking for dedicated persons with all sorts of talent for membership. Presently, stage properties are stored at the Chesapeake Bay Detachment until the nonprofit drama group can form a new foundation and relocate to a stage elsewhere on the Lab. Traditionally, the NRL Showboaters performed two major productions each year (in Building 222) in addition to occasional performances at Laboratory functions and benefits for local charities. Membership is always open and is not limited to NRL employees. (Contact Barbarajo Cox at (202) 404-4998.)

PROGRAMS FOR NON-NRL EMPLOYEES

Several programs have been established for non-NRL professionals. These programs encourage and support the participation of visiting scientists and engineers in research of interest to the Laboratory. Some of the programs may serve as stepping-stones to federal careers in science and technology. Their objective is to enhance the quality of the Laboratory's research activities through working associations and interchanges with highly capable scientists and engineers and to provide opportunities for outside scientists and engineers to work in the Navy laboratory environment. Along with enhancing the Laboratory's research, these programs acquaint participants with Navy capabilities and concerns and provide a path to full-time employment.

RECENT PH.D., FACULTY MEMBER, AND COLLEGE GRADUATE PROGRAMS

- The **National Research Council (NRC) Cooperative Research Associateship Program** selects associates who conduct research at NRL in their chosen fields in collaboration with NRL scientists and engineers. The tenure period is two years (renewable for a possible third year).
- The **NRL/ASEE Postdoctoral Fellowship Program**, administered by the American Society for Engineering Education (ASEE), aims to increase the involvement of highly trained scientists and engineers in disciplines necessary to meet the evolving needs of naval technology. Appointments are for one year (renewable for a second and possible third year).
- The **Naval Research Enterprise Intern Program (NREIP)** program has been initiated as a two-year demonstration effort involving 69 NROTC colleges and universities. The Office of Naval Research (ONR) is offering summer appointments at Navy laboratories to current sophomores, juniors, seniors, and graduate students from participating schools. Associated Western Universities (AWU) is handling the administration of the application process through a website. Electronic applications are sent for evaluation to the point of contact at the Navy

laboratory identified by the applicant. ONR will provide directly to the student a stipend of \$3,000 to undergraduates and \$4,000 to graduate students, plus \$2,000 for travel and living expenses.

- The American Society for Engineering Education also administers the **Navy/ASEE Summer Faculty Research and Sabbatical Leave Program** for university faculty members to work for 10 weeks (or longer, for those eligible for sabbatical leave) with professional peers in participating Navy laboratories on research of mutual interest.
- The **NRL/United States Naval Academy (USNA) Cooperative Program for Scientific Interchange** allows faculty members of the U.S. Naval Academy to participate in NRL research. This collaboration benefits the Academy by providing the opportunity for USNA faculty members to work on research of a more practical or applied nature. In turn, NRL's research program is strengthened by the available scientific and engineering expertise of the USNA faculty.

- The **National Defense Science and Engineering Graduate Fellowship Program** helps U.S. citizens obtain advanced training in disciplines of science and engineering critical to the U.S. Navy. The three-year program awards fellowships to recent outstanding graduates to support their study and research leading to doctoral degrees in specified disciplines such as electrical engineering, computer sciences, material sciences, applied physics, and ocean engineering. Award recipients are encouraged to continue their study and research in a Navy laboratory during the summer.

For further information about the above six programs, contact Ms. Lesley Renfro at (202) 404-7450.

PROFESSIONAL APPOINTMENTS

- **Faculty Member Appointments** use the special skills and abilities of faculty members for short periods to fill positions of a scientific, engineering, professional, or analytical nature.

- **Consultants and experts** are employed because they are outstanding in their fields of specialization or because they possess ability of a rare nature and could not normally be employed as regular civil servants.

- **Intergovernmental Personnel Act Appointments** temporarily assign personnel from state or local governments or educational institutions to the Federal Government (or vice versa) to improve public services rendered by all levels of government.

COLLEGE STUDENT PROGRAMS

The student programs are tailored to undergraduate and graduate students to provide employment opportunities and work experience in naval research. These programs are designed to attract applicants for student and full professional employment in fields such as engineering, physics, mathematics, and computer sciences. The student employment programs are designed to help students and educational institutions gain a better understanding of NRL's research, its challenges, and its opportunities. Employment programs for college students include the following:

- The **Student Career Experience Program** (formerly known as the Cooperative Education Program) employs students in study-related occupations. The program is conducted in accordance with a planned schedule and a working agreement among NRL, the educational institution, and the student. Primary focus is on the pursuit of bachelors degrees in engineering, computer science, or the physical sciences.

- The **Student Temporary Employment Program (STEP)** enables students to earn a salary while

continuing their studies and offers them valuable work experience.

- The **Summer Employment Program** employs students for the summer in paraprofessional and technician positions in engineering, physical sciences, computer sciences, and mathematics.

- The **Student Volunteer Program** helps students gain valuable experience by allowing them to voluntarily perform educationally related work at NRL.

For additional information on these undergraduate and graduate college student programs, contact Code 1810 at (202) 767-8313.

HIGH SCHOOL STUDENT PROGRAMS

- The **DOD Science & Engineering Apprentice Program (SEAP)** employs high school juniors, seniors, and college students to serve for eight weeks as junior research associates. Under the direction of a mentor, students gain a better understanding of research, its challenges, and its opportunities through participation in scientific programs. Criteria for eligibility are based on science and mathematics courses completed and grades achieved; scientific motivation, curiosity, and capacity for sustained hard work; a desire for a technical career; teacher recommendations; and achievement test scores. The NRL Program is the lead program and the largest in DOD.

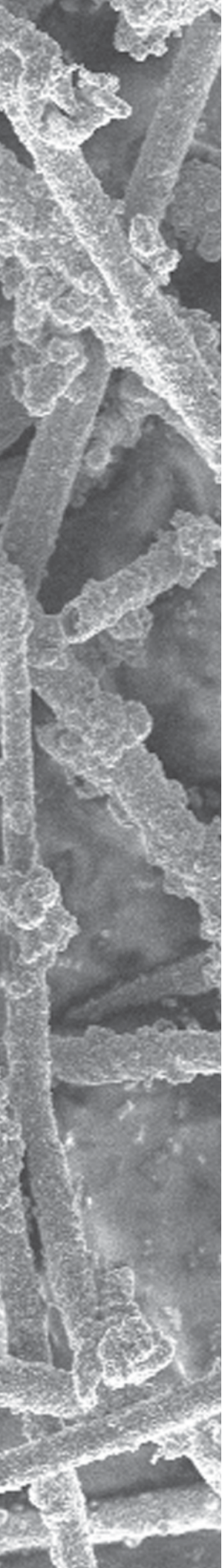
For additional information, contact Dawn Brown (Code 1850) at (202) 767-2957.

The image is a scanning electron micrograph (SEM) showing a dense network of interconnected, elongated, and somewhat irregular tubular structures. These tubules are coated with a fine, granular texture, which is the electrolessly deposited copper. The tubules vary in orientation, some running parallel to each other while others cross at various angles. The overall appearance is that of a complex, porous, and interconnected network of thin, hollow tubes.

GENERAL INFORMATION

COPPER-PLATED LIPID TUBULES

Scanning electron micrographs of diacetylenic lipid tubules coated electrolessly with copper. The lipid is a modified version of the material found in cell membranes. The tubules are hollow, and are 1 to 2 μm in diameter and about 30 μm long. The electroless coating of copper reinforces the tubules and renders them highly electrically conductive. The copper is formed of small grains, 30 to 100 nm in size, grown together to a thickness of about 300 nm, covering both the interior and exterior walls of the tubule.



249 Technical Output

250 Key Personnel

251 Contributions by Division, Laboratories, and Departments

254 Subject Index

257 Author Index

258 Employment Opportunities

TECHNICAL OUTPUT

The Navy continues to be a pioneer in initiating new developments and a leader in applying these advancements to military requirements. The primary method of informing the scientific and engineering community of the advances made at NRL is through the Laboratory's technical output—reports, articles in scientific journals, contributions to books, papers presented to scientific societies and topical conferences, patents, and inventions.

The figures for calendar year 2003 presented below represent the output of NRL facilities in Washington, D.C.; Bay St. Louis, Mississippi; and Monterey, California.

In addition to the output listed, NRL scientists made more than 711 oral presentations during 2003.

Type of Contribution	Unclassified	Classified	Total
Articles in periodicals, chapters in books, and papers in published proceedings	1084	0	1084
NRL Formal Reports	17	2	19
NRL Memorandum Reports	77	1	78
Books	5	0	5
Patents granted			63
Statutory Invention Registrations (SIRs)			2

*This is a provisional total based on information available to the Ruth H. Hooker Research Library on February 26, 2004. Additional publications carrying a 2003 publication date are anticipated.

KEY PERSONNEL

Area Code (202) unless otherwise listed
 Personnel Locator - 767-3200
 DSN-297 or 754

Code	Office		Phone Number
EXECUTIVE DIRECTORATE			
1000	Commanding Officer	CAPT D.M. Schubert, USN	767-3403
1000.1	Inspector General	CAPT C.W. Fowler, USN	767-3621
1001	Director of Research	Dr. J.A. Montgomery	767-3301
1001.1	Executive Assistant	Mr. D. DeYoung	767-2445
1002	Chief Staff Officer	CAPT C.W. Fowler, USN	767-3621
1004	Head, Technology Transfer	Mr. P.A. Regeon (Acting)	404-8411
1006	Head, Office of Program Administration and Policy Development	Mrs. L. McDonald	767-3091
1008	Office of Counsel	Mr. J. McCutcheon	767-2244
1030	Public Affairs Officer	Mr. R. Thompson	767-2541
1200	Head, Command Support Division	CAPT C.W. Fowler, USN	767-0793
1220	Head, Security	Ms. M.S. Overton	767-2922
1400	Head, Military Support Division	CDR J.L. Buckles, USN	767-2273
1600	Officer-in-Charge, Flight Support Detachment	CDR T.M. Munns, USN	301-342-3751
1800	Director, Human Resources Office	Ms. B.A. Duffield	767-3421
1830	Deputy EEO Officer	Ms. D. Erwin	767-5264
3005	Deputy for Small Business	Ms. M. Nicholl	767-6263
3540	Head, Safety Branch	Mr. K.J. Pawlovich	404-4471
BUSINESS OPERATIONS DIRECTORATE			
3000	Associate Director of Research	Mr. D. Therning	767-2371
3200	Head, Contracting Division	Mr. J.C. Ely	767-5227
3300	Comptroller, Financial Management Division	Mr. S.A. Birk	767-3405
3400	Supply Officer	Ms. C. Hartman	767-3446
3500	Director, Research and Development Services Division	Mr. S. Harrison	767-3697
SYSTEMS DIRECTORATE			
5000	Associate Director of Research	Dr. R.A. LeFande	767-3324
5300	Superintendent, Radar Division	Dr. P.K. Hughes II	404-2700
5500	Superintendent, Information Technology Division	Dr. J.D. McLean (Acting)	767-2903
5600	Superintendent, Optical Sciences Division	Dr. T.G. Giallorenzi	767-3171
5700	Superintendent, Tactical Electronic Warfare Division	Dr. F. Klemm	767-6278
MATERIALS SCIENCE AND COMPONENT TECHNOLOGY DIRECTORATE			
6000	Associate Director of Research	Dr. B.B. Rath	767-3566
6030	Head, Laboratory for Structure of Matter	Dr. J. Karle	767-2665
6100	Superintendent, Chemistry Division	Dr. J.S. Murday	767-3026
6300	Superintendent, Materials Science and Technology Division	Dr. D.U. Gubser	767-2926
6400	Director, Lab. for Computational Physics and Fluid Dynamics	Dr. J.P. Boris	767-3055
6700	Superintendent, Plasma Physics Division	Dr. S. Ossakow	767-2723
6800	Superintendent, Electronics Science and Technology Division	Dr. G.M. Borsuk	767-3525
6900	Director, Center for Bio/Molecular Science and Engineering	Dr. J.M. Schnur	404-6000
OCEAN AND ATMOSPHERIC SCIENCE AND TECHNOLOGY DIRECTORATE			
7000	Associate Director of Research	Dr. E.O. Hartwig	404-8690
7100	Superintendent, Acoustics Division	Dr. E.R. Franchi	767-3482
7200	Superintendent, Remote Sensing Division	Dr. L.J. Rickard (Acting)	767-3391
7300	Superintendent, Oceanography Division	Mr. S. Payne (Acting)	228-688-5507
7400	Superintendent, Marine Geosciences Division	Dr. H.C. Eppert, Jr.	228-688-4650
7500	Superintendent, Marine Meteorology Division	Dr. S.W. Chang	831-656-4721
7600	Superintendent, Space Science Division	Dr. H. Gursky	767-6343
NAVAL CENTER FOR SPACE TECHNOLOGY			
8000	Director	Mr. P.G. Wilhelm	767-6547
8100	Superintendent, Space Systems Development Department	Mr. R.E. Eisenhauer	767-0410
8200	Superintendent, Spacecraft Engineering Department	Mr. H.E. Senasack, Jr.	767-6411

CONTRIBUTIONS BY DIVISIONS, LABORATORIES, AND DEPARTMENTS

Radar Division

- 125 UHF Delta-Sigma Waveform Generator
*R.M. White, B.H. Cantrell, J.P. McConnell,
and J.J. Alter*
- 127 Unmanned Aerial Vehicle (UAV) Radar
*D.W. Baden, E.M. Kutrzyba, A.P.
Desrosiers, J.O. Alatishe, S. Talapatra, and
M.G. Parent*
- 129 The NRL 94 GHz High-Power WARLOC
Radar as a Cloud Sensor
*W.M. Manheimer, A.W. Fliflet, K. St.
Germain, G.L. Linde, W.J. Cheung, V.
Gregers-Hansen, M.T. Ngo, and B.G. Danly*

Information Technology Division

- 106 The High Frequency Active Auroral Research
Program
*E.J. Kennedy, P. Rodriguez, and C.A.
Selcher*
- 137 Energy-Aware Broadcasting and Multicasting
in Wireless Ad Hoc Networks
*J.E. Wieselthier, G.D. Nguyen, and A.
Ephremides*
- 195 Human System Interface Assessment of the
Sonar Workstation During the USS *Nicholson*
Integrated Undersea Warfare Sea Test
J.A. Ballas and B. McClimens

Optical Sciences Division

- 97 Passive Swimmer Detection
*S. Stanic, C.K. Kirkendall, A.B. Tveten, and
T. Barock*
- 140 Netcentric Multi-INT Fusion Targeting
Initiative (NCMIFTI)
*D.C. Linne von Berg, M.R. Kruer, J.N. Lee,
M.D. Duncan, J.G. Howard, F. Olchowski,
and R.A. Patten*
- 143 Real-Time Exploitation and Dissemination of
Tactical Reconnaissance Imagery During

Operation Iraqi Freedom for Ground and
Maritime Operations

*J.N. Lee, D.C. Linne von Berg, M.D.
Duncan, M.R. Kruer, and R.A. Patten*

- 177 Development of the Fiber Optic Wide
Aperture Array: From Initial Development
to Production
*A. Dandridge, A.B. Tveten, and C.K.
Kirkendall*

- 179 High Resolution Distributed Fiber Optic
Sensing
*C.K. Kirkendall, R.E. Bartolo, A.B. Tveten,
and A. Dandridge*

Tactical Electronic Warfare Division

- 158 Rapid Prototyping of Conformal Antenna
Structures
*A. Piqué, R.C.Y. Auyeung, M.W.
Nurnberger, D.J. Wendland, C.B. Arnold,
A.R. Abbott, and L.C. Schuette*
- 185 Unattended Ground Sensor Network
J. Heyer and L.C. Schuette
- 197 Autonomous Navigation Control of UAVs
Using Genetic Programming
C.K. Oh, G. Cowart, and J. Ridder

Laboratory for Structure of Matter

- 115 Navy Cyanide Test Kit (NACTEK)
J.R. Deschamps

Chemistry Division

- 116 Water-Soluble Carbon Nanotubes
*O.-K. Kim, J. Je, J.W. Baldwin, S. Kooi, P.E.
Pehrsson, and L.J. Buckley*
- 144 Volume Sensor for Shipboard Damage
Control
*S.L. Rose-Pehrsson, J.C. Owrutsky, D.T.
Gottuk, D.A. Steinhurst, C.P. Minor, J.P.
Farley, and F.W. Williams*

Materials Science and Technology Division

- 51 New Horizons in Cathodic Protection Design
V.G. DeGiorgi, E.A. Hogan, and S.A. Wimmer
- 156 GelMan: A Physical Model for Measuring the Response to Blast
K.E. Simmonds, P. Matic, M. Chase, and A. Leung
- 158 Rapid Prototyping of Conformal Antenna Structures
A. Piqué, R.C.Y. Auyeung, M.W. Nurnberger, D.J. Wendland, C.B. Arnold, A.R. Abbott, and L.C. Schuette
- 160 Carbon Nanotube Networks: A New Electronic Material
E.S. Snow, J.P. Novak, M.D. Lay, and E.J. Houser

Plasma Physics Division

- 59 Propagation of High-Energy Lasers in a Maritime Atmosphere
P. Sprangle, J. Peñano, A. Ting, and B. Hafizi
- 105 NRL Ionosphere Model: SAMI3
J. Huba and G. Joyce
- 129 The NRL 94 GHz High-Power WARLOC Radar as a Cloud Sensor
W.M. Manheimer, A.W. Fliflet, K. St. Germain, G.L. Linde, W.J. Cheung, V. Gregers-Hansen, M.T. Ngo, and B.G. Danly

Electronics Science and Technology Division

- 69 Fabrication of a Fast Turn-off Transistor by Wafer Bonding
K.D. Hobart, F.J. Kub, and J.M. Neilson
- 129 The NRL 94 GHz High-Power WARLOC Radar as a Cloud Sensor
W.M. Manheimer, A.W. Fliflet, K. St. Germain, G.L. Linde, W.J. Cheung, V. Gregers-Hansen, M.T. Ngo, and B.G. Danly
- 132 Coupled Quantum Dots for Quantum Computing
T.L. Reinecke, Y. Lyanda-Geller, M. Bayer, and A. Forchel

- 160 Carbon Nanotube Networks: A New Electronic Material
E.S. Snow, J.P. Novak, M.D. Lay, and E.J. Houser
- 199 Electronics and Physics of Left-Handed Materials and Circuits
C.M. Krowne
- 209 The Microelectronics and Photonics Test Bed (MPTB): The First Six Years
K.A. Clark, M.S. Johnson, and A.B. Campbell

Center for Bio/Molecular Science and Engineering

- 118 Neuronal Network Biosensor for Environmental Threat Detection
K.M. Shaffer, S.A. Gray, S.J. Fertig, J.V. Selinger, T.J. O'Shaughnessy, N.V. Kulagina, D.A. Stenger, and J.J. Pancrazio
- 121 Self-Cleaning Catalytic Filters Against Pesticides and Chemical Agents
A. Singh, Y. Lee, and W.J. Dressick

Acoustics Division

- 77 Applications of Time-Reversal to Underwater Acoustics
J.F. Lingeitch, C.F. Gaumont, D.M. Fromm, and B.E. McDonald
- 97 Passive Swimmer Detection
S. Stanic, C.K. Kirkendall, A.B. Tveten, and T. Barock
- 98 Passive Acoustic Ranging by Multimode Waveguide Interferometry
A. Turgut, M.H. Orr, and B.H. Pasewark

Remote Sensing Division

- 87 WindSat – Remote Sensing of Ocean Surface Winds
P.W. Gaiser
- 109 Advances in Upper Atmosphere Forecasting: NOGAPS-ALPHA
J.P. McCormack, L. Coy, S.D. Eckermann, D.R. Allen, T. Hogan, and Y.-J. Kim
- 129 The NRL 94 GHz High-Power WARLOC Radar as a Cloud Sensor
W.M. Manheimer, A.W. Fliflet, K. St. Germain, G.L. Linde, W.J. Cheung, V. Gregers-Hansen, M.T. Ngo, and B.G. Danly

- 186 Measurement of Ocean Wave Spectra and Surface Slopes by Polarimetric SAR
D.L. Schuler and J.S. Lee
- 188 The Lowest Frequency Detection of the Black Hole at the Center of Our Galaxy
M.E. Nord, T.J.W. Lazio, N.E. Kassim, W.M. Goss, and N. Duric
- 191 High-Resolution Infrared Ocean Imagery
G.O. Marmorino, G.B. Smith, and G.J. Lindemann

Oceanography Division

- 165 Drag Coefficient, Surface Roughness, and Reference Wind Speed
P.A. Hwang
- 167 An Approach for Coupling Diverse Geophysical and Dynamical Models
J.D. Dykes, R.A. Allard, C.A. Blain, B. Estrade, T. Keen, L. Smedstad, A. Wallcraft, M. Bettencourt, and G. Peggion
- 170 Airborne Sea-Surface Topography in an Absolute Reference Frame: Applications to Coastal Oceanography
J. Brozena, V. Childers, and G. Jacobs
- 201 Real-Time Wave, Tide, and Surf Prediction
R.A. Allard, J. Christiansen, T. Taxon, S. Williams, and D. Wakeham

Marine Geosciences Division

- 148 Control Algorithms for UUV Teams Using Acoustic Communications
P. McDowell and B. Bourgeois
- 170 Airborne Sea-Surface Topography in an Absolute Reference Frame: Applications to Coastal Oceanography
J.M. Brozena, V. Childers, and G. Jacobs

Marine Meteorology Division

- 103 Real-Time, High-Resolution, Three-Dimensional Cloud and Wind Data Assimilation Technology for the Battlespace Environment
Q. Zhao, J. Cook, P. Harasti, and J. Strahl

- 109 Advances in Upper Atmosphere Forecasting: NOGAPS-ALPHA
J.P. McCormack, L. Coy, S.D. Eckermann, D.R. Allen, T. Hogan, and Y.-J. Kim

Space Science Division

- 109 Advances in Upper Atmosphere Forecasting: NOGAPS-ALPHA
J.P. McCormack, L. Coy, S.D. Eckermann, D.R. Allen, T. Hogan, and Y.-J. Kim
- 172 New Observations of Hydroxyl from the Space Shuttle by NRL's SHIMMER
J.G. Cardon, C.R. Englert, M.H. Stevens, R.R. Conway, J.M. Harlander, and F.L. Roesler

Space Systems Development Department

- 158 Rapid Prototyping of Conformal Antenna Structures
A. Piqué, R.C.Y. Auyeung, M.W. Nurnberger, D.J. Wendland, C.B. Arnold, A.R. Abbott, and L.C. Schuette
- 209 The Microelectronics and Photonics Test Bed (MPTB): The First Six Years
K.A. Clark, M.S. Johnson, and A.B. Campbell
- 212 Rapid Satellite Payload Development for TacSat-1
C.M. Huffine

Spacecraft Engineering Department

- 153 Qualification of Copper Water Heat Pipes for Space Application
K. Cheung
- 207 Tactical Microsatellite Experiment (TacSat-1)
M. Hurley
- 209 The Microelectronics and Photonics Test Bed (MPTB): The First Six Years
K.A. Clark, M.S. Johnson, and A.B. Campbell

SUBJECT INDEX

- 3 kJ KrF laser facility (Nike), 31
- 3 MV Tandem Pelletron Accelerator Facility, 29
- Acoustic positioning, 148
- Acoustic Seafloor Characterization System (ASCS), 37
- Acoustics Division, 32
- Acoustics, 45, 77, 177, 179
- Ad hoc networks, 137
- Administrative Services Branch, 40
- Advanced Graduate Research Program, 241
- Advanced Multifunction Radio Frequency Concept (AMRFC) Testbed Facility, 46
- Advanced Research and Global Observation Satellite (ARGOS), 39
- Airborne Geographical Sensor Suite (ACSS), 41
- Airborne infrared imagery, 191
- Airborne measurement techniques, 170
- Airborne Polarimetric Microwave Imaging Radiometer (APMIR), 36
- Aircraft 153442, 46
- Aircraft 154587, 46
- Amateur Radio Club, 243
- Ambient noise, 97
- Amphibious operations, 201
- ARIES, 143
- ATDnet, 24
- Audio Laboratory, 25
- Autonomous and optimized control logic, 197
- Backward wave devices, 199
- BAMEX, 46
- Bergen Data Center, 38, 42
- Bio-catalytic coatings, 121
- Biomaterial development, 32
- Biomolecular interactions/sensing, 116
- Biosensor, 118
- Black Hole, 188
- Blunt trauma force, 156
- Boundary element, 51
- Bow Echo and Mesoscale Convective Vortices Experiment (BAMEX), 41
- Bragg Crystal Spectrometer (BCS), 38
- Capitol Hill Workshops, 241
- Carbon nanotubes, 19, 160
- Cathodic protection, 51
- Center for Bio/Molecular Science and Engineering, 32
- Chemical analysis facilities, 28
- Chemical protection, 121
- Chemical sensor, 160
- Chemical testing, 115
- Chemical/biological warfare defense, 32
- Chemistry Division, 28, 44
- Chesapeake Bay Detachment (CBD), 24, 41
- Class-10 clean room, 46
- Class-1000 clean room, 32
- Cloud radar, 129
- CMIS, 36
- Coated fiber, 179
- College student programs, 245
- Colored dissolved organic matter (CDOM), 36
- Common Data Link (CDL), 46
- Community Outreach Program, 23, 243
- Compact Antenna Range, 24
- Compound Semiconductor Processing Facility (CSPF), 31, 45, 47
- Computational Electromagnetics (CEM) Facility, 24
- Computational modeling, 51
- Conformal antennas, 158
- Contaminant Transport Analyst, 18
- Continuing education, 242
- Cool skin, 191
- Cooperative Aircraft Identification system, 24
- Cooperative Engagement Capability (CEC), 41
- Corporate Facilities Investment Plan (CFIP) 43
- Corrosion, 51
- Counseling Referral Service, 242
- Coupled Ocean/Atmosphere Mesoscale Prediction System-On Scene (COAMPS-OS³), 42
- Coupling, 167
- Cray MTA, 47
- Credit Union, 23
- Crossed-wire tunnel junction, 19
- CT scanner, 38, 46
- CT-Analyst, 18
- Cyanide, 115
- Daley Supercomputer Resource Center, 38, 42
- Data assimilation, 103
- Deep-Towed Acoustic Geophysical system (DTAGS), 37
- Defense Research and Engineering Network (DREN), 25
- Delta-Sigma DAC, 125
- Detection, 97
- Digital acquisition buoy systems (DABS), 34
- Digital frequency synthesis, 125
- Digital Holographic Imaging System, 33
- Digital Library, 41
- Digital Processing Facility, 27
- Digital radar, 125
- Distributed Center (DC), 44
- Diver, 97
- DOD Science & Engineering Apprentice Program (SEAP), 245
- Drag coefficient, 165
- Edison Memorial Graduate Training Program, 241
- Electra Doppler Radar (ELDORA), 46
- Electra, 47
- Electron Microscopy Facility, 38
- Electronic warfare, 185
- Electronics and electromagnets, 209
- Electronics Science and Technology Division, 47
- Electronics Science and Technology, 31, 45
- ELF, 106
- Emittance Measurements Facility, 27
- Energy awareness, 137
- Environment, 167
- Epicenter, 31, 47
- Equal Employment Opportunity (EEO) programs, 243
- Executive Leadership Program for Mid-Level Employees, 241
- Exhibits/Multimedia Office, 40
- Extreme Ultraviolet Imaging Telescope (EIT), 39
- ex-USS *Shadwell* (LSD-15), 43
- Federal Executive and Professional Association, 23
- Federal Executive Institute (FEI), 241
- Fellowship in Congressional Operations, 241
- Fiber optics, 177, 179
- Finite-element model, 156
- Fire detection, 144
- Fleet Battle Experiments, 26
- Fleet Numerical Meteorology and Oceanography Center (FNMOC), 38, 42
- Flight qualification, 153
- Flight Support Detachment (NRL FSD), 23, 41, 46
- Focal-Plane Evaluation Facility, 26
- Force Protection/Homeland Defense (FP/HD), 44
- Free-Surface Hydrodynamics Laboratory, 36
- Frequency generation, 125
- Galactic Center region, 188
- GAMBLE II, 30
- Gas hydrates, 21
- GCM, 109
- GelMan, 156

Genetic programming, 197
 Geoid, 170
 Geospatial Information Data Base (GIDB), 38
 Geostationary Satellite/Radar Processing Center, 38, 42
 Global Imaging of the Ionosphere (GIMI), 39
 GPS, 158
 Graduate Programs, 241
 Head-mounted displays (HMDs), 26
 Heat pipe, 153
 High energy laser propagation, 59
 High Gain High Sensitivity (HGHS), 47
 High Performance Computing Modernization Program (HPCMP), 44
 High performance computing, 167
 High Probability of Intercept-Precision Direction Finding (HPOI-PDF), 46
 High school students program, 245
 High voltage devices, 69
 High-definition TV (HDTV), 25
 High-Resolution Airglow and Auroral Spectroscopy (HIRAAS), 39
 HOBILabs Hydrosat, 36
 Human Resources Office, 241
 Human system integration, 195
 Human-computer interaction, 195
 Hydroxyl, 172
 Immersive Room, 26
 Immersive Simulation Laboratory, 25
 In Situ Sediment Acoustic Measurement System (ISSAMS), 37
 InfoNet, 44
 Information Security Engineering Laboratory, 25
 Information Technology Division, 24, 47
 Center for Computational Science (CCS), 44
 InfoWeb, 41, 44
 InfraLynx, 19
 Infrared Test Chamber, 27
 Institute for Nanoscience, 23, 44
 Integrated Communications Testing (ICT) Laboratory, 25, 47
 Integrated Electronic Warfare System (IEWs), 41
 Intelligent control, 148
 Internal waves, 191
 Inverse synthetic aperture radar (ISAR), 24
 Ion Implantation Facility, 29
 Ionosphere, 105, 106
 IR Missile-Seeker Evaluation Facility, 26
 JOC Line of Sight Communications system, 18
 John C. Stennis Space Center (SSC), 42
 Joint Operations Center (JOC), 18
 Joint Typhoon Warning Center, 38
 JTF WARNET, 26
 Laboratory for Advanced Materials Synthesis (LAMS), 31, 45
 Laboratory for Computational Physics and Fluid Dynamics (LCP & FD), 30
 Laboratory for Structure of Matter, 27
 Langmuir circulation, 191
 Large Area Plasma Processing System (LAPPS) facility, 30, 45
 Large-Angle Spectrometric Coronagraph (LASCO), 39, 46
 Large-Optic, High-Precision Tracker system, 27
 Laser direct-write, 158
 Laser Facilities, 29
 Launch vehicle, 207
 Left-handed materials, 199
 Legislative Fellowship (LEGIS) program, 241
 Linux, 212
 Littoral environments, 98, 167
 Low Frequency Array (LOFAR), 45
 Machine vision, 144
 Microelectronics, 160
 Magneto mobile robot, 19
 Major Shared Resource Center (MSRC), 42
 Marine Corrosion Test Facility, 28
 Marine Geosciences Division, 37, 42, 46
 Marine Meteorology Division (NRL-MRY), 38, 42
 Maritime atmosphere, 59
 Master Environmental Laboratory, 42
 Material Synthesis and Processing, 29
 Materials Science and Technology, 29
 Materials synthesis/property measurement facility, 28
 Mercury pulsed-power generator, 47
 Meteorological analysis, 103
 Meteorological/oceanographic (METOC), 38
 Meteorology, 109
 Methane hydrates, 21
 Microsatellites, 207
 Microwave radiometer, 87
 Middle Atmosphere High Resolution Spectrograph Investigation (MAHRSI), 20
 Midway Research Center (MRC), 43
 Mobile Ad Hoc Networking (MANET), 26
 Modeling, 105, 109
 Models, 167
 Molecular Beam Epitaxy, 29
 Molecular electronics, 116
 Moving Map Composer Facility, 38
 Moving target indicator, 127
 Multi-Threaded Architecture (MTA), 25
 Nanoelectronics Processing Facility (NPF), 45
 Nanometer measurement/manipulation facility, 28
 Nanoscience Research Institute, 44
 Nanostructures, 133
 NASA's Space Shuttle, 20
 National Defense Science and Engineering Graduate Fellowship Program, 244
 National Polar-orbiting Operational Environmental Satellite System, 20
 National Radio Astronomy Observatory's Very Large Array (VLA), 45
 National Research Council (NRC) Cooperative Research Associateship Program, 244
 National Weather Service Forecast Office (NWSFO), 42
 Naval Center for Space Technology (NCST), 39, 43
 Naval Fleet/Force Technology Innovation Office, 27
 Naval Postgraduate School (NPS) Annex, 42, 241
 Naval Research Enterprise Intern Program (NREIP), 244
 NAVIS (Navy Input Station), 18
 Navy Integrated Tactical Environmental System (NITES), 42
 Navy Prototype Optical Interferometer (NPOI), 36
 Navy Technology Center for Safety and Survivability, 42
 Navy/ASEE Summer Faculty Research and Sabbatical Leave Program, 244
 Nearfield scanning optical microscope (NSOM), 33
 Negative index of refraction, 199
 Neuron, 118
 NEWAVE facility, 26
 NICE.net, 25
 Night vision, 144
 NOGAPS, 109
 NP-3D EW flying laboratory, 27
 NRL Mentor Program, 243
 NRL/ASEE Postdoctoral Fellowship Program, 244
 NRL/United States Naval Academy (USNA) Cooperative Program for Scientific Interchange, 244
 NULKA, 20
 Ocean Research Laboratory, 45
 Ocean Science and Technology, 186
 Ocean wave spectra and slopes, 186
 Ocean winds, 87

Oceanography Division, 37, 42
 OFT, 212
 Operation Iraqi Freedom (OIF), 18, 143
 Optical Calibration Facility, 36
 Optical fire detection, 144
 Optical Real-time Adaptive Spectral Identification System (ORASIS), 21
 Optical Sciences Division, 26
 Oriented Scintillation Spectrometer Experiment (OSSE), 38
 P-3 aircraft, 24
 P-3 Orion turboprop, 43
 Passive acoustic ranging, 98
 Payload, 212
 Pharos III, 30
 Phased array antenna, 106
 Photographic services, 40
 Physical Property Measurement, 29
 Physical scale modeling, 51
 Plasma Physics Division, 30, 45
 Plasma Physics, 47
 Polarimetric SAR, 186
 Polarimetric, 87
 Potable water, 115
 Power Device Characterization Facility (PDCF), 31
 Power electronics, 69
 Power switching transistors, 69
 Professional appointments, 244
 Professional development, 242
 Profiling Optics Package, 36
 Publication services, 40
 Quantum computing, 133
 Quantum dot, 133
 Radar Division, 23
 Radar Imaging Facility, 24
 Radar Signature Calculation Facility, 24
 Radar Test Bed Facility, 24
 Radar, 103
 Rapid prototyping, 158
 Real-time imagery exploitation, 140
 Real-time networking, 140
 Reconnaissance sensors, 140, 143
 Recreation Club, 23, 243
 Remote Sensing Division, 34, 45
 Remote sensing from space, 172
 Remote Sensing, 186, 188
 Response Workbench, 26
 Robotics Laboratory, 25
 Ruth H. Hooker Research Library, 40, 44
 Sagittarius A*, 188
 Salt Water Tank Facility, 33, 45
 Satellite technology, 209
 Satellite, 103, 212
 SCI Origin 2000, 30
 Scientist-to-Sea Program, 242
 Sea WiFS, 37
 Seabird CDT36
 Select Graduate Training Program, 241
 Self-cleaning filter, 121
 Semiconductors, 133
 Sensing, 177, 179
 SGI Altix, 25, 47
 SGI Origin3800, 25, 44, 47
 Shared Airborne Reconnaissance Pod (SHARP), 18
 SHIMMER, 172
 Ship Motion Simulator (SMS), 26, 41
 Showboaters, 23, 243
 Sigma Xi, 22, 242
 Silicon Carbide Processing Laboratory (SCPL), 45, 47
 SIPRNET, 207
 Situational awareness, 144
 Software Definable Radio (SDR)-Pathfinder, 19
 Solar Coronagraph Optical Test Chamber (SCOTCH), 46
 Solar Heliospheric Observatory satellite, 39
 Solar Ultraviolet Spectral Irradiance Monitor (SUSIM), 38
 Sonar, 195
 Space Research, 209
 Space Science Division, 38, 46
 Space Solar Cell Characterization Facility (SSCCF), 31, 47
 Space, 105, 212
 Spatial heterodyne spectroscopy (SHS), 172
 SSMIS, 36
 Stennis Space Center (NRL-SSC), 42
 Student Career Experience Program, 22, 245
 Student Temporary Employment Program (STEP), 245
 Student Volunteer Program, 245
 Summer Employment Program, 245
 Surface roughness, 165
 Surrogate, 156
 Synchrotron Radiation Facility, 28
 Synthetic aperture radar, 127
 Table-Top Terawatt (T³) laser, 30, 47
 Tactical Air Reconnaissance Pod System-Completely Digital (TARPS-CD), 18
 Tactical Electronic Warfare (TEW) Division, 27
 Tactical Oceanography Simulation Laboratory (TOSL), 34
 Tactical Oceanography Wide Area Network (TOWAN), 34
 Tactical, 207
 Target detection, 140
 Technical Information Services Branch, 40
 Technology transfer, 21
 Thin-Film Preparation Facilities, 29
 Thoracic model, 156
 Three-dimensional tissue, 19
 Time reversal, 77
 Tissue simulants, 156
 Toastmasters International, 23, 243
 Toastmasters Youth Leadership Program, 23
 TORPEDO Ultra v.2, 41, 44
 Toxin, 118
 Trace Element Accelerator Mass Spectrometry (TEAMS), 29
 Two-photon absorption/optical limiting, 116
 UAV navigation, 197
 UAV radar, 127
 UHF Delta Sigma Waveform Generator, 125
 Ultrafast Laser Facility (ULF), 31
 Ultra-loss, Fiber-Optic Waveguide Facility, 26
 Ultrawideband Synthetic Aperture Radar (NUSAR), 45
 Unattended networks, 185
 Unconventional Stellar Aspect (USA), 39
 Undersea communication, 106
 Underwater vessel formations, 148
 Upper Atmosphere Research Satellite (UARS), 38
 Upper atmosphere, 109
 Vacuum Electronics Fabrication Facility (VEFF), 31
 Vacuum Ultraviolet Space Instrument Test Facility, 46
 Velocity SAR (VSAR), 127
 Very Large Array radio telescope, 20
 Video image detection, 144
 Video services, 40
 Virtual Reality (VR) Laboratory, 26
 Wafer Banding Facility (WBF), 31
 Wall clock, 167
 WARLOC, 24, 129
 Water-level measurements, 170
 Wave, tide, and surf prediction, 201
 Waveguide invariant, 98
 Wavelength, 165
 WETLabs Super MODAPS, 36
 WETLabs WetStar, 36
 Wind stress, 165
 WindSat, 20, 36, 153
 Wireless networks, 137
 Women in Science and Engineering (WISE) Network, 22, 242

AUTHOR INDEX

- Abbott, A.R., 158
Alatishe, J.O., 127
Allard, R.A., 167, 201
Allen, D.R., 109
Alter, J.J., 125
Arnold, C.B., 158
Auyeung, R.C.Y., 158
Baden, D.W., 127
Baldwin, J.W., 116
Ballas, J.A., 195
Barock, T., 97
Bartolo, R.E., 179
Bayer, M., 132
Bettencourt, M., 167
Blain, C.A., 167
Bourgeois, B., 148
Brozena, J.M., 170
Buckley, L.J., 116
Campbell, A.B., 209
Cantrell, B.H., 125
Cardon, J.G., 172
Chase, M., 156
Cheung, K., 153
Cheung, W.J., 129
Childers, V., 170
Christiansen, J., 201
Clark, K.A., 209
Conway, R.R., 172
Cook, J., 103
Cowart, G.A., 197
Coy, L., 109
Dandridge, A., 177, 179
Danly, B.G., 129
DeGiorgi, V.G., 51
Deschamps, J.R., 115
Desrosiers, A.P., 127
Dressick, W.J., 121
Duncan, M.D., 140, 143
Duric, N., 188
Dykes, J.D., 167
Eckermann, S.D., 109
Englert, C.R., 172
Ephremides, A., 137
Estrade, B., 167
Farley, J.P., 144
Fertig, S.J., 118
Fliflet, A.W., 129
Forchel, A., 132
Fromm, D.M., 77
Gaiser, P.W., 87
Gaumont, C.F., 77
Goss, W.M., 188
Gottuk, D.T., 144
Gray, S.A., 118
Gregers-Hansen, V., 129
Hafizi, B., 59
Harasti, P., 103
Harlander, J.M., 172
Heyer, J., 185
Hobart, K.D., 69
Hogan, E.A., 51
Hogan, T., 109
Houser, E.J., 160
Howard, J.G., 140
Huba, J., 105
Huffine, C.M., 212
Hurley, M., 207
Hwang, P.A., 165
Jacobs, G., 170
Je, J., 116
Johnson, M.S., 209
Joyce, G., 105
Kassim, N.E., 188
Keen, T., 167
Kennedy, E.J., 106
Kim, O.-K., 116
Kim, Y.-J., 109
Kirkendall, C.K., 97, 177, 179
Kooi, S., 116
Krowne, C.M., 199
Kruer, M.R., 140, 143
Kub, F.J., 69
Kulagina, N.V., 118
Kutrzyba, E.M., 127
Lay, M.D., 160
Lazio, T.J.W., 188
Lee, J.N., 140, 143
Lee, J.S., 186
Lee, Y., 121
Leung, A., 156
Linde, G.J., 129
Lindemann, G.J., 191
Lingevitch, J.F., 77
Linne von Berg, D.C., 140, 143
Lyanda-Geller, Y., 132
Manheimer, W.M., 129
Marmorino, G.O., 191
Matic, P., 156
McClimens, B., 195
McConnell, J.P., 125
McCormack, J.P., 109
McDonald, B.E., 77
McDowell, P.M., 148
Minor, C.P., 144
Neilson, J.M., 69
Ngo, M.T., 129
Nguyen, G.D., 137
Nord, M.E., 188
Novak, J.P., 160
Nurnberger, M.W., 158
O'Shaughnessy, T.J., 118
Oh, C.K., 197
Olchowski, F., 140
Orr, M.H., 98
Owrutsky, J.C., 144
Pancrazio, J.J., 118
Parent, M.G., 127
Pasewark, B.H., 98
Patten, R.A., 140, 143
Peggion, G., 167
Pehrsson, P.E., 116
Peñano, J., 59
Piqué, A., 158
Reinecke, T.L., 132
Ridder, J., 197
Rodriguez, P., 106
Roesler, F.L., 172
Rose-Pehrsson, S.L., 144
Schuette, L.C., 158, 185
Schuler, D.L., 186
Selcher, C.A., 106
Selinger, J.V., 118
Shaffer, K.M., 118
Simmonds, K.E., 156
Singh, A., 121
Smedstad, L., 167
Smith, G.B., 191
Snow, E.S., 160
Sprangle, P., 59
St. Germain, K., 129
Stanic, S., 97
Steinhurst, D.A., 144
Stenger, D.A., 118
Stevens, M.H., 172
Strahl, J., 103
Talapatra, S., 127
Taxon, T., 201
Ting, A., 59
Turgut, A., 98
Tveten, A.B., 97, 177, 179
Wakeham, D., 201
Wallcraft, A., 167
Wendland, D.J., 158
White, R.M., 125
Wieseltheier, J.E., 137
Williams, F.W., 144
Williams, S., 201
Wimmer, S.A., 51
Zhao, Q., 103

EMPLOYMENT ^{NRL} OPPORTUNITIES

NRL offers a wide variety of challenging positions that involve the full range of work, from basic and applied research to equipment development. The nature of the research and development conducted at NRL requires professionals with experience. Typically there is a continuing need for electronics, mechanical, aerospace, materials engineers, metallurgists, computer scientists, and oceanographers with bachelor's and/or advanced degrees and physical and computer scientists with Ph.D. degrees.



Chemists. Chemists are recruited to work in the areas of combustion, polymer science, bioengineering and molecular engineering, surface science, materials, synthesis, nanostructures, corrosion, fiber optics, electro-optics, microelectronics, electron-device technology, and laser physics.

Physicists. Physics graduates may concentrate on such fields as materials, solid-state physics, fiber optics, electro-optics, microelectronics, vacuum science, plasma physics, fluid mechanics, signal processing, ocean acoustics, information processing, artificial intelligence, electron-device technology, radio-wave propagation, laser physics, ultraviolet/X-ray/gamma-ray technology, electronic warfare, electromagnetic interaction, communications systems, radio frequency/microwave/millimeter wave/infrared technology, computational physics, radio and high energy astronomy, solar physics, and space physics.

Biologists. Biologists conduct research in areas that include bio-sensor development, tissue engineering, molecular biology, genetic engineering, proteomics, and environmental monitoring.

Oceanographers, Meteorologists, and Marine Geophysicists. These employees work in the areas of ocean and atmospheric dynamics, air-sea interaction, upper-ocean dynamics, oceanographic bio-optical modeling, oceanic and atmospheric numerical modeling and prediction, data assimilation and data fusion, retrieval and application of remote sensing data, benthic processes, aerogeophysics, marine sedimentary processes, advanced mapping techniques, atmospheric physics, and remote sensing. Oceanographers and marine geophysicists are located in Washington, D.C., and the Stennis Space Center, Bay St. Louis, Mississippi. Meteorologists are located in Washington, D.C., and Monterey, California.

for
**Highly Innovative, Motivated,
and Creative Personnel**

Electronics Engineers and Computer Scientists. These employees may work in the areas of communications systems, electromagnetic scattering, electronics instrumentation, electronic warfare systems, radio frequency/microwave/millimeter wave/infrared technology, radar systems, laser physics technology, radio-wave propagation, electron device technology, spacecraft design, artificial intelligence, information processing, signal processing, plasma physics, vacuum science, microelectronics, electro-optics, fiber optics, solid state, software engineering, computer design/architecture, ocean acoustics, stress analysis, and expert systems.



Mechanical and Aerospace Engineers. These employees may work in areas of spacecraft design, remote sensing, propulsion, experimental and computational fluid mechanics, experimental structural mechanics, solid mechanics, elastic/plastic fracture mechanics, materials, finite-element methods, nondestructive evaluation, characterization of fracture resistance of structural alloys, combustion, CAD/CAM, and multi-functional material response.

Materials Scientists/Engineers. These employees are recruited to work on materials, microstructure characterization, electronic ceramics, solid-state physics, fiber optics, electro-optics, microelectronics, fracture mechanics, vacuum science, laser physics and joining technology, and radio frequency/microwave/millimeter wave/infrared technology.



For more information on current vacancy listings,
visit <http://hroffice.nrl.navy.mil/>

NAVAL RESEARCH LABORATORY

4555 Overlook Ave., SW ♦ Washington, DC 20375-5320

LOCATION OF NRL IN THE CAPITAL AREA



Quick Reference Telephone Numbers

	NRL Washington	NRL- SSC	NRL- Monterey	NRL CBD	NRL FSD Patuxent River
Hotline	(202) 767-6543	(202) 767-6543	(202) 767-6543	(202) 767-6543	(202) 767-6543
Personnel Locator	(202) 767-3200	(228) 688-3390	(831) 656-4316	(410) 257-4000	(301) 342-3751
DSN	297- or 754-	828	878	—	342
Direct-in-Dialing	767- or 404-	688	656	257	342
Public Affairs	(202) 767-2541	(228) 688-5328	(202) 767-2541	—	(202) 767-2541

Additional telephone numbers are listed on page 250.

NAVAL RESEARCH LABORATORY

Lifetime Achievement Award



DR. BHAKTA B. RATH

On January 21, 2004, Dr. Rath was recognized for his immeasurable contribution to the fields of Materials Science and Engineering, his mentoring of basic research at NRL, and his creativity in applying emerging technologies to national security and to the needs of the Fleet. His internationally recognized research program advancements include harnessing material behavior and chemical/biological processes to reduce Navy environmental problems; sensors based on coupling electronics to cellular function, immunoassays, and gene chips; explosive detection; survivability/lethality improvements through fire-resistant materials and automated damage control for reduced manning; computational methods to predict material properties; and high-temperature superconductors for power production and transmission. Dr. Rath's persistence and foresight were influential in the establishment of the Institute for Nanoscience at NRL (dedicated October 2003). Dr. Rath's efforts to rapidly transition scientific discoveries into Naval/DOD technology have resulted in such innovations as the Surface Acoustic Wave miniaturized chemical sensor; several different coating technologies with special properties; damage control hardware and doctrine; and a mobility fuel quality control specification that saves the Navy an estimated \$25 million yearly.

www.nrl.navy.mil

